THE EFFECT OF MONOMER SEQUENCE ON THE PROPERTIES AND DEVICE PERFORMANCE OF CONJUGATED ORGANIC SEMICONDUCTORS

by

Shaopeng Zhang

Bachelor of Science in Chemistry, Lanzhou University, 2010

Submitted to the Graduate Faculty of the

Dietrich School of Arts and Sciences in partial fulfillment

of the requirements for the degree of

Doctor of Philosophy in Chemistry

University of Pittsburgh

2017

UNIVERSITY OF PITTSBURGH

Dietrich School of Arts and Sciences

This dissertation was presented

by

Shaopeng Zhang

It was defended on

March 31st, 2017

and approved by

Geoffrey R. Hutchison, Associate Professor, Chemistry

Alexander Star, Professor, Chemistry

John A. Keith, Assistant Professor, Chemical & Petroleum Engineering

Dissertation Advisor: Tara Y. Meyer, Associate Professor, Chemistry

THE EFFECT OF MONOMER SEQUENCE ON THE PROPERTIES AND DEVICE PERFORMANCE OF CONJUGATED ORGANIC SEMICONDUCTORS

Shaopeng Zhang, PhD

University of Pittsburgh, 2017

Although sequence effect can potentially be a powerful tool to tune the photophysical properties of conjugated oligomers and copolymers prepared from donor and acceptor monomers, nearly all research to date focuses on the alternating structure. Little is known about the properties of other sequences and sequence has not been exploited as a tool for tuning these materials for specific applications. In order to explore this potentially powerful tool, a series of sequenced phenylene-vinylene oligomers was synthesized and investigated both experimentally and computationally. Using Horner-Wadsworth-Emmons (HWE) chemistry, dimers, trimers, tetramers, pentamers, and hexamers were prepared from two building block monomers, a relatively electron-poor unsubstituted *p*-phenylene-vinylene and an electron-rich dialkoxy-substituted *p*-phenylene-vinylene. UV-Vis absorption/emission spectra and cyclic voltammetry demonstrated that the optoelectronic properties of these oligomers depended significantly on sequence.

To further understand the influence of monomer sequence on the properties and solar cell performance of donor-acceptor conjugated oligomers, a library of dimers, trimers, and tetramers were prepared from phenylene and benzothiadiazole monomers linked by vinylene groups. Optical and electrochemical studies established the influence of sequence on both the λ_{max} and redox potentials of this series of structurally related oligomers. The effect of end groups (cyano, bromo, and alkyl) was also demonstrated to be important for the properties of these oligomers. Bulk heterojunction (BHJ) solar cells fabricated with selected tetramers as the donor exhibited power conversion efficiencies that varied by a factor of three as a function of sequence.

The sequence effect on donor-acceptor conjugated polymers was also studied. Two trimeric isomers, comprising dialkoxy phenylene vinylene, benzothiadiazole vinylene, and alkyl endgroups with terminal olefins, were synthesized. Sequence effects were evident in the optical/electrochemical properties and thermal properties. The trimers were used as macromonomers in an ADMET polymerization to give sequenced polymers. The optical and electrochemical properties were similar to those of their trimer precursors—sequence effects were still evident.

These results suggest that sequence control is important for tuning optoelectronic properties and photovoltaic performance of these structurally related conjugated oligomers. The polymerization of oligomeric sequences is a practical approach for the incorporation of sequence into polymers.

TABLE OF CONTENTS

LIST OF TABLES

LIST OF FIGURES

SYMBOLS AND ABBREVIATIONS

Å	angstrom
A	electron-accepting unit
A	unsubstituted phenylene vinylene unit
Abs	absorption
ADMET	acyclic diene metathesis
AFM	atomic force micscope
AIBN	azobis(isobutyronitrile)
aq	aqueous
Ar	aryl
B	dialkoxy-substituted phenylene vinylene
B	benzothiadiazole unit
BBN	borabicyclo[3.3.1]nonane
BHJ	bulk heterojunction
Br	bromine
brine	saturated aqueous NaCl
^{n}Bu	*n*-butyl
^{t}Bu	*tert*-butyl
C8	α-olefinic alkyl group
^{o}C	degrees Celsius
calcd	calculated
cm	centimeter

CN	Cyano
CV	cyclic voltammetry/voltammogram
d	day
d	doublet (NMR signal)
δ	chemical shift
D	electron-donating unit
DCE	1,2-dichloroethane
DCM	dichloromethane
dd	doublet of doublets (NMR signal)
ddt	doublet of doublets of triplets (NMR signal)
DFT	density functional theory
DIBAL-H	diisobutylaluminum hydride
DMF	*N*,*N*-dimethylformamide
DPV	differential pulse voltammetry/voltammograms
DSC	differential scanning calorimetry
dt	doublet of triplets (NMR signal)
e	an electron, fundamental unit of charge
ε	extinction coefficient, molar absorptivity
E	energy
E_{HOMO}	HOMO energy
E_{LUMO}	LUMO energy
ΔE	energy difference

ΔE_d	energy difference between the LUMO of a polymer donor and the LUMO of a fullerene acceptor
ΔE_{gap}	HOMO-LUMO gap or bandgap
ΔE_{off}	offset energy between the HOMO of a polymer donor and the LUMO of a fullerene acceptor
EI	electron impact ionization
em	emission
eq	equivalent
ESI	electrospray ionization
Et	ethyl
Et_2O	diethyl ether
EtOAc	ethyl acetate
eV	electron volt
FF	fill factor
g	gram
h	hour
η	power conversion efficiency
HOMO	highest occupied molecular orbital
HRMS	high resolution mass spectrometry
HWE	Horner-Wadsworth-Emmons
Hz	hertz
I	irradiance
ITO	indium tin oxide

J	coupling constant (NMR signal)
J	current density
J_{SC}	short-circuit current density
kDa	kilodalton
λ	wavelength
λ_{max}	wavelength at maximum absorption or emission
L	liter
LUMO	lowest unoccupied molecular orbital
μ_h	hole mobility
M	molar (moles per liter)
M^+	molecular ion
mA	milliamp
Me	methyl
MeCN	acetonitrile
MeOH	methanol
meV	millielectron volt
mg	milligram
MHz	megahertz
min	minute
mL	milliliter
μL	microliter
μm	micrometer
mmol	millimole

μmol	micromole
M_n	number average molecular weight
mol	mole
MP	melting point
MS	mass spectrometry
mult	multiplet (NMR signal)
M_w	weight average molecular weight
m/z	mass/charge ratio
NBS	*N*-bromosuccinimide
nm	nanometer
NMR	nuclear magnetic resonance
OAc	acetate
OLED	organic light-emitting diode
OPV	oligo(phenylene-vinylene)
p	para
P	power
P	dialkoxy-substituted phenylene vinylene
$PC_{61}BM$	phenyl-C_{61}-butyric acid methyl ester
PDI	polydispersity index
PEDOT	poly(ethylenedioxythiophene)
pent	pentet (NMR signal)
Ph	phenyl
Ph_2O	diphenyl ether

Phos	dimethyl phosphonate
PhMe	toluene
PLA	poly(lactic acid)
PLGA	poly(lactic-*co*-glycolic acid)
pm	picometer
ppm	parts per million
PPV	poly(*p*-phenylene-vinylene)
psi	pounds per square inch
PSS	polystyrene sulfonate
q	quartet (NMR signal)
quat	quaternary carbon
RAFT	reversible addition-fragmentation transfer
ROMP	ring-opening metathesis polymerization
ROP	ring-opening polymerization
rt	room temperature
s	second
s	singlet (NMR signal)
sat	saturated
SEC	size exclusion chromatography
t	triplet (NMR signal)
T	temperature
T_c	crystallization transition temperature
T_g	glass transition temperature

T_m	melting transition temperature
TBAB	tetrabutylammonium bromide
THF	tetrahydrofuran
TLC	thin-layer chromatography
TOF	time of flight
tt	triplet of triplets (NMR signal)
UV/VIS	ultraviolet/visible
V	volt (unit)
V	voltage (potential difference)
V_{OC}	open-circuit voltage
E_{ox}	oxidation potential
E_{red}	reduction potential

PREFACE

I went to Lanzhou University for my undergraduate and started my polymer research there. After spending two years in Prof. Mingzhu Liu's lab working on hydrogels, I found myself very interested in materials research. I am deeply grateful to the Chemistry Department of University of Pittsburgh for offering me the opportunity to continue my studies in the US. At Pitt, I joined Prof. Tara Meyer's group. Tara is the best advisor I could imagine for my PhD study. She always has creative thoughts on projects and my research has benefited greatly from her input. My learning has not been limited to research. She offered me significant help in adapting to life in the US including learning American culture, improving my writing and communication skills, teaching undergraduates, and professional networking. She helped me to mature from a student to a professional chemist.

My fellow students in the Meyer group have also contributed to my research and I also consider them to be good friends. I inherited my first research project from Dr. Ben Norris. With the foundation he built, we made some great contributions. Dr. Ryan Stayshich, Dr. Jian Li, Dr. Ryan Weiss and Dr. Percay Calvo-Marzal were also in the lab when I joined the group. They offered me guidance and help as I was just getting started. My more recent colleagues, Jeff Auletta, Emily Barker, Jamie Nowalk, Jordan Swisher, Mike Washington, Dr. Amy Short, and Colin Ladd have worked side-by-side with me in the past few years, giving me advice and offering their support in so many ways.

I am very fortunate to collaborate closely with some talented researchers. Throughout my Ph.D., I have had the privilege of working with Prof. Geoffrey Hutchison. I consider him to be

my co-advisor as he worked with me at every stage of my research from the initial idea to the manuscript writing. His expertise in conjugated polymers and computational simulation significantly improved the quality of our research. I would like to thank his group members as well. Ilana Kanal and Dr. Casey Campbell carried out key computational work; Chris Marvin taught me AFM; Stephen Owens offered his thoughts in our meetings. Our external collaborators outside Pitt Chemistry department also contributed a significant part of my graduate study. I particularly thank Prof. Wei You and Nicole Bauer from UNC, who helped me on the device fabrication and characterization and Dr. Angela Bischof and Dr. Ben Lear from Penn State who carried out extensive spectroscopic studies on one of our conjugated dimers.

I want to thank Professors Geoffrey Hutchison, Alexander Star and John Keith for serving on my dissertation defense committee. I would also thank Profs. Nat Rosi and Jennifer Laaser for serving on my proposal committee and for many helpful suggestions. I want to thank Professor Haitao Liu for all his guidance over the past year as my proposal mentor.

In the end, I want to thank my wife Yujie Wang and my parents in China for their support through my PhD study. It is their love that drives me to overcome all the challenges in research and in life. I also want to thank my colleagues and friends in the department particularly Chong Liu who was also my roommate for three years.

Being able to live outside China for several years in my life is an experience that I dreamed about since high school. I was always very interested in understanding the differences in how people live and think in a foreign country. Despite the difficulties in learning English—ordering at Subway was a big challenge when I first arrived—I have grown to like Pittsburgh very much. This is a nice city with friendly people and I enjoy everything about it.

1.0 INTRODUCTION

1.1 OVERVIEW

Sequence effects on properties of donor-acceptor type conjugated organic semiconductors can potentially be utilized for high performance electronics design. Discovering sequence-related properties and establishing sequence-property correlations are necessary for rationale molecular engineering. In this dissertation, oligomers with complex sequence were synthesized via an efficient iterative strategy which precisely controls the monomer placement. Sequence-property correlations were established by characterizing the large library of sequenced oliogmers. Polymers that incorporated these sequenced oligomers were prepared and the retention of photophysical properties was demonstrated.

1.2 SEQUENCE CONTROLLED POLYMERS

Nature refines the properties of biopolymers by exploiting not only composition, but also monomer sequence. Proteins, in which functionality depends directly on sequence are the prototype for this behavior. The photosynthetic pathway, for example, accomplishes multiple functions including optical absorption, energy transfer, electron transfer, and chemical

transformation using a multi-component system comprised largely of macromolecules whose properties are determined by the sequence of the same basic set of building blocks.[1] In contrast with Nature's masterful exploitation of sequence, our ability to tune polymer properties with the monomer sequence is very limited. Conventional synthetic polymers typically consist of simple monomer sequences: alternating, random and block. The lack of synthetic methods for the preparation of sequence-defined polymers on a large scale has, moreover, also limited our understanding of sequence-property relationships.[2-4] In recent years, however, the potential importance of monomer sequence control is has attracted significant new research effort to this field and there have been an increasing number of reports of new polymeric systems with well-controlled monomer sequences.[2, 4-12]

1.2.1 Synthesis

The control of sequence in copolymers can be accomplished by an increasing variety of synthetic techniques, and many different classes of sequence-controlled polymers can be prepared. Sequence can be present in the main chain or in the side chains and can take the form of periodic, multi-block, gradient or complex sequences that mimic those seen in biopolymers (**Figure 1**).[2-4, 8] Depending on the target structure, a wide variety of synthesis techniques have been reported. Sequenced copolymers have been prepared, for example, by convergent/divergent assembly of precise oligomers, sequential polycondensation, acyclic diene metathesis, controlled free-radical polymerizations, solid-phase synthesis and template synthesis (**Figure 2**). [2-5, 8, 10, 12-15]

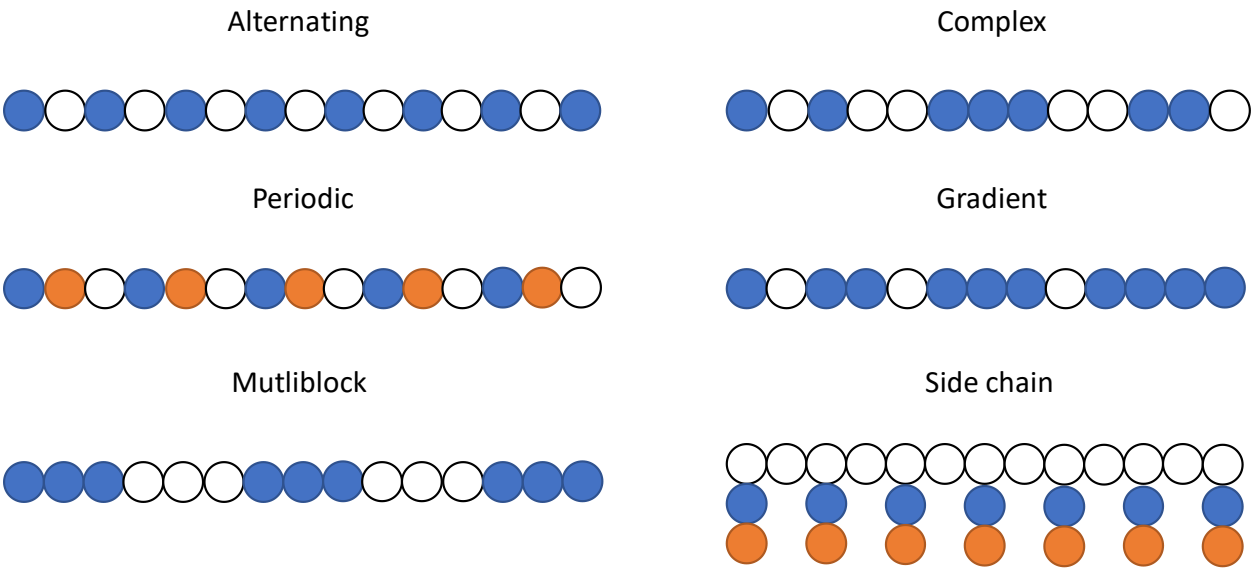

Figure 1. Examples of sequenced polymers.

Periodic sequenced polymers have defined sequence repeating units throughout the polymer main chain, e.g., $(AB)_n$ or $(ABC)_n$. This class of polymer is generally prepared by a step-growth polymerization of sequenced oligomers. Meyer and coworkers, for example, reported the segmer assembly polymerization method for poly(lactic-*co*-glycolic acid) (PLGA) periodic sequenced polymers.[5] Sequenced segmers (LG, LLG) with carboxylic acid and alcohol bifunctional endgroups were assembled to polymers via step-growth polycondensation. The high sequence fidelity of these materials was characterized and verified by the MALDI study.[16] In a more recent paper, entropy-driven ring-opening metathesis polymerization (ED-ROMP) was developed to synthesize a new PLGA materials.[15] The semi-living polymerization nature of ED-ROMP provides molecular weight control in the sequenced polymer synthesis.

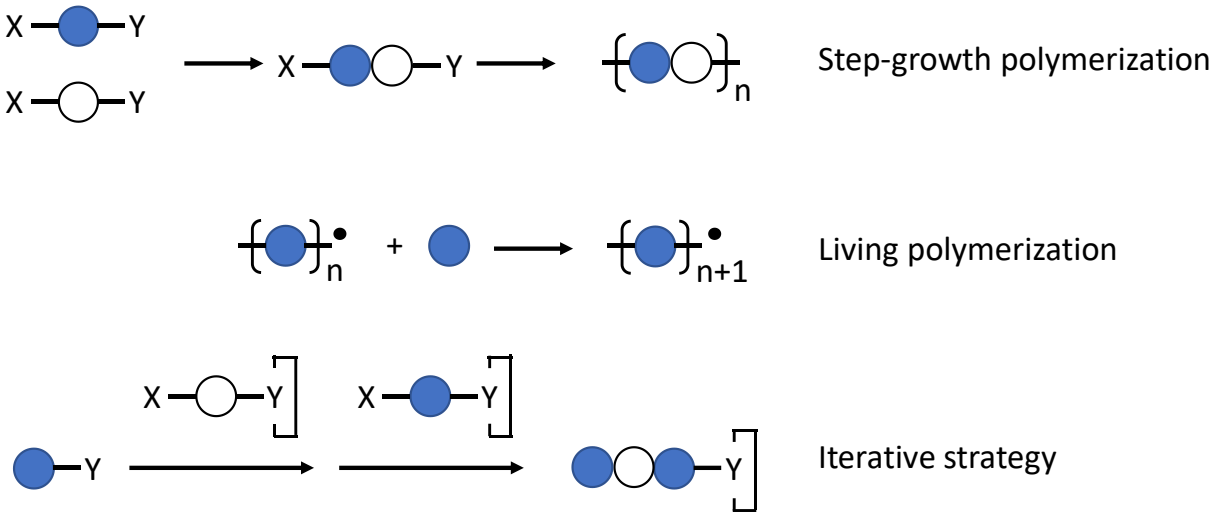

Figure 2. Common synthetic approaches for sequence-controlled polymers.

In the current work, we will focus, however, on the complex sequences with unique, non-periodic structures. This type of structure maximizes the potential of sequence diversity and is typically prepared by an iterative synthesis strategy.[2, 4, 10-13, 17] Monomers are added to the polymer chain one-by-one to offer precise control over sequence along the backbone. Both DNA and solid-phase peptide synthesis exploit this method. Although precise, this approach requires significant synthetic work, high yielding reactions, mild conditions and easy purification protocols to be successfully implemented. Despite these challenges, several iterative systems have been developed for the preparation of non-biological polymers with complex sequences. Such an iterative sequence-controlled propagation can be accomplished using controlled radical polymerizations[11,13] or orthogonal chemoselective reactions.[9, 12, 14, 17-19] Lutz and coworkers have, for example, reported solid-phase synthesis routes to sequenced poly(triazole amide)s, poly(alokoxyamine amide)s and poly(phosphodiester)s using orthogonal chemoselective reactions.[9, 14, 17-18] Using these strategies Lutz has shown that sequenced copolymers can be used to encode information.

1.2.2 Properties

As discussed earlier, the connection of sequence to properties outside of biological macromolecules is not a well-developed area. That being said, there are some reports that offer insight into structure/function in these materials. If we consider first properties that are intrinsic to isolated chains, the sequence itself can be regarded as a property in that the sequence, as Lutz and coworkers reported, can be used to encode information. Polymer hydrophobicity has also been shown to be sequence-related. In a work reported by Sleiman and coworkers, polymers with the same monomer ratios and chain lengths exhibited large differences in hydrophobicity when the structure was changed from alternating to multi-block to diblock.[19] Other single-molecule properties like molecular redox potentials and emission/absorption properties measured in dilute solution phase are also deeply influenced by the monomer sequence. Studies on these properties are part of this dissertation work and will be discussed in more detail later.

Sequence can also be shown to affect interchain interactions like polymer self-assembly. Sequence recognition and sequence-specific binding are both manifestations of this property. Gong and coworkers, for example, reported that hydrogen-bonded bimolecular duplexes with perfectly matched hydrogen donor-acceptor pairs showed much stronger association than ones with mismatched pairs, i.e. hydrogen bond donor-donor or hydrogen bond acceptor-acceptor.[20] Thus, the molecular recognition for these duplex was found to be highly selectively and sequence dependent, which made it a powerful tool for cross metathesis template.

Polymer bulk properties including glass transition temperature (T_g), crystallinity, degradation, and mechanical properties that are important to applications are also affected by sequence. In the Meyer group study of sequenced poly(α-hydroxy acid)s, for example, interesting T_g effects have been observed. In a periodic copolymer system comprising L, G and C (caprolactic

acid) units, they found that $(GLC)_n$ exhibited a T_g which was 8 ^oC higher than that of $(LGC)_n$.[6] Sequence was also correlated with crystallinity; $(LGC)_n$ was amorphous while $(GLC)_n$ was semi-crystalline with a T_m of 37 ^oC. They have also found that hydrolytic degradation is sequence-dependent. Microparticles made from sequenced PLGA with a 1:1 LG ratio, $(LG)_n$, showed a more controlled hydrolytic degradation than the random analogues with identical compositions. Moreover, the molecular weight for the sequenced PLGA decreases nearly linearly while the random exhibits an exponential loss of molecular weight at a much earlier time point.[21] In compression-molded cylindrical constructs made from PLGA, the erosion mechanism are also found to be different between sequenced polymers vs random polymers.[22] Sequenced PLGA constructs exhibit many characteristics that are consistent with surface erosion while the random PLGA degraded by a bulk mechanism.

1.3 SEMICONDUCTING ORGANIC MOLECULES

Organic semiconductors have attracted increasing attentions recently because of their widespread use in scientific and technological areas. Thin film, organic electronic devices, which can be fabricated by low-cost, solution processing methods over large areas and on flexible substrates are one of the most promising technologies. Major applications of organic electronic devices involve organic solar cells, organic field effect transistors, organic light-emitting displays, photocatalytic systems, polymer batteries and supercapacitors.[23-30] Impressive scientific and technological progress has been achieved in these applications. For example, OLEDs are viewed as competitive candidates for the next generation large-size high-resolution displays and solid-state lighting panels. Now OLEDs are becoming commercially available and are moving from

being laboratory curiosities to a part of everyday life. The organic solar cell is a more important application as identifying sources of clean and renewable energy is one of the most challenging issues of the 21st century. Devices based on semiconducting organic materials are predicted to have a theoretical efficiency that approaches 10-15%.[31-33] Since the pioneer work by Tang in 1980s,[34] efficiencies of organic solar cells have been significantly improved, going from 1% to above 10%.[35-36]

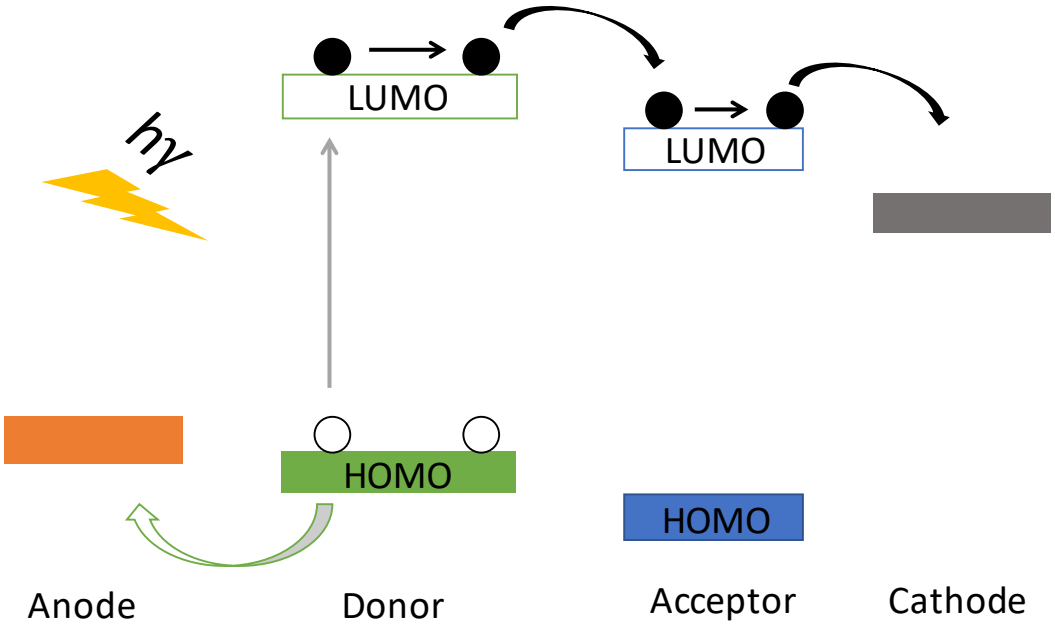

Figure 3. Current generating mechanism for organic solar cell.

A typical organic solar cell includes a donor (*p*-type semiconductor) layer and an acceptor (*n*-type semiconductor) layer. The mechanism may be briefly described as follows (**Figure 3**). First, photons are absorbed by the photo-active donor layer to form excitons (tightly bound electron hole pair). The exciton then diffuses to the D-A interface and dissociates to form charge transfer state or so-called polaron pair. Free charge carriers are subsequently generated from fully dissociated charge transfer states. Due to the limited exciton diffusion length, modern solar cells adapt a bulk heterojunction structure at the donor-acceptor interface. Such structure is made from

co-deposition of a blend donor and acceptor materials and offers a large interface to improve the power conversion efficiency (PCE).

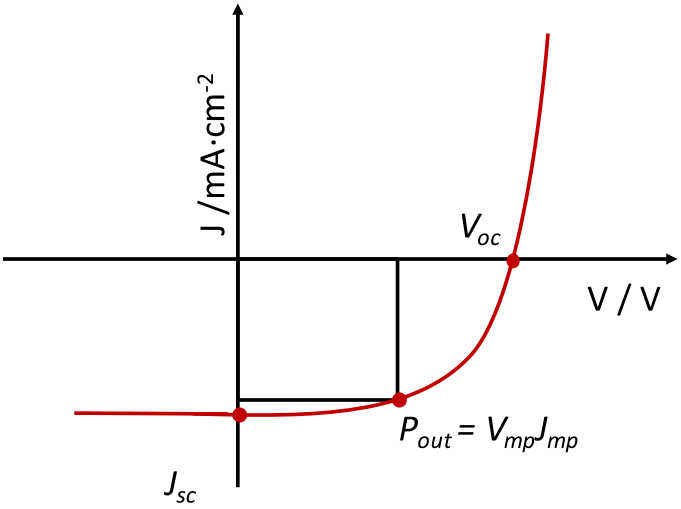

Solar cell power conversion efficiency

$$\eta = \frac{P_{out}}{P_{in}} = \frac{V_{oc}J_{sc}FF}{P_{in}}$$

$$\mathrm{FF} = \frac{V_{mp}J_{mp}}{V_{oc}J_{sc}}$$

Figure 4. Current-voltage (*J-V*) characteristics of a typical solar cell. V_{oc}: open-circuit voltage; J_{sc}: short-circuit current density; *FF*: fill factor; Voltage and current at maximium power output are V_{mp} and J_{mp} respectively.

Power conversion efficiencies, the ratio of maximum power output to input, are represented and directly measured by the current-voltage curves (**Figure 4**). The maximum power output is a product of V_{oc}, J_{sc} and *FF*. V_{oc} is the open-circuit voltage which is the maximum photo-voltage measured in a solar cell. The difference between the donor layer material HOMO level and the acceptor layer material LUMO level is found to significantly influence the V_{oc}. J_{sc} represents the maximum current measured in a solar cell. A large J_{sc} means that more absorbed photons that can be exploited by the solar cell as long as no saturation effects occur. The surface area of the photoactive layer, device thickness, material light absorption properties and charge-transport process are all important factors for high J_{sc}. The fill factor, which represents the quality of the solar cell and related to fraction of charge carriers generated to that reach the electrodes, is defined

as the ratio of the maximum power output to the product of V_{oc} and J_{sc}. Charge transport processes and charge recombination determine the fill factor.

There are multiple factors can affect the efficiency of a solar cell ranging from material properties to the device engineering and fabrication. Research in this document will focus on the material properties of the photo-active donor layer. Ideal materials should have light absorption profile with high solar spectrum coverage and molar absorption coefficient. The HOMO/LUMO energy level should be properly adjusted for high *Voc* and *FF*. Besides, many other factors like charge carrier mobility, material stability and phase segregation power are very important as well.

Controlling multiple parameters for a high efficiency solar cell device is one of the most challenging problems in this field. Fortunately, conjugated organic materials benefits from their rich diversity and ease of tailoring key properties.[23, 37-39] One of the fundamental strategies used to engineer the desired optoelectronic properties of photovoltaic materials is the donor-acceptor strategy.[40-42] Electron-rich (donor or D) and electron-poor (acceptor or A) monomers are copolymerized to give materials with hybrid properties of the respective homopolymers. It is important to note that the "donor (D) monomer" in this context is different from the "donor layer" mentioned above in that the donor layer which absorbs incoming light is often composed of a polymer incorporating both D and A monomers. The HOMO and LUMO energy levels of the DA copolymers are direct related to the HOMO level of the donor unit and the LUMO energy of level the acceptor unit, respectively. Therefore, the copolymer band gap is usually narrower than homopolymers and can be tuned at the molecular level (**Figure 5**).[43] Based on this donor-acceptor strategy, significant progress has been made. Other strategies include developing new sophisticated repeat units, tailoring side-chains, fluorinating the backbone and introducing heteroatoms.[24, 35, 43-45]

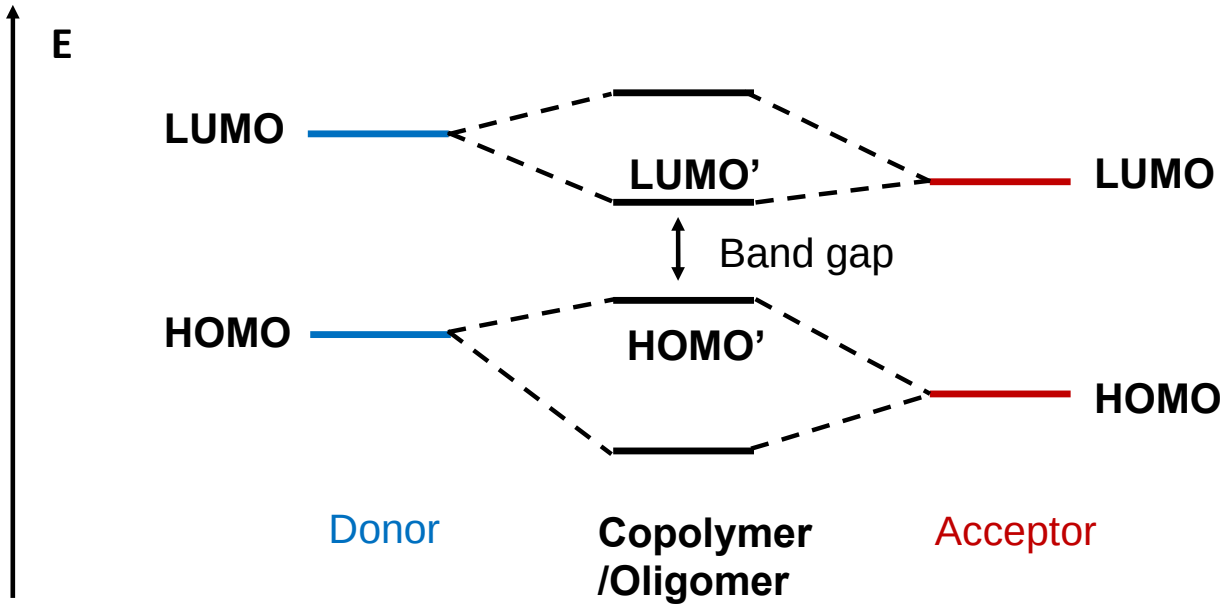

Figure 5. Band gap reduction using a donor-acceptor strategy.

Significant effort has been devoted to discovering new donor and acceptor units as the properties of these polymer largely depend on the repeating unit selection.[35, 46-48] In recent years, many new monomers have been developed as well as different combinations of the donor and acceptor units in polymers. In the **Figure 6**, some of the most common units that give high power conversion efficiencies are listed.

The role of side chains in conjugated molecules is also known to be a significant contributor to their properties and performance.[35, 49] First, side chains are critical for solubilizing the polymer/oligomer as the insoluble nature of backbone with strong π-π interaction. The increased solubility is indispensable for industrial processibility and improving the polymer synthesis. It has also been found that side chains can affect the donor-acceptor layer interface in a solar cell. On the other hand, bulky side chains may provide so much steric hindrance that the coplanarity of the backbone or interchain interaction necessary for charge transport are disturbed. The balance

between good solubility, charge-transport and device efficiencies must be carefully examined and optimized. Chain length, substitution position, branch point, heteroatoms on the side chain, chemical entity (alkyl or conjugated) are common ways to tune the side chain effect.

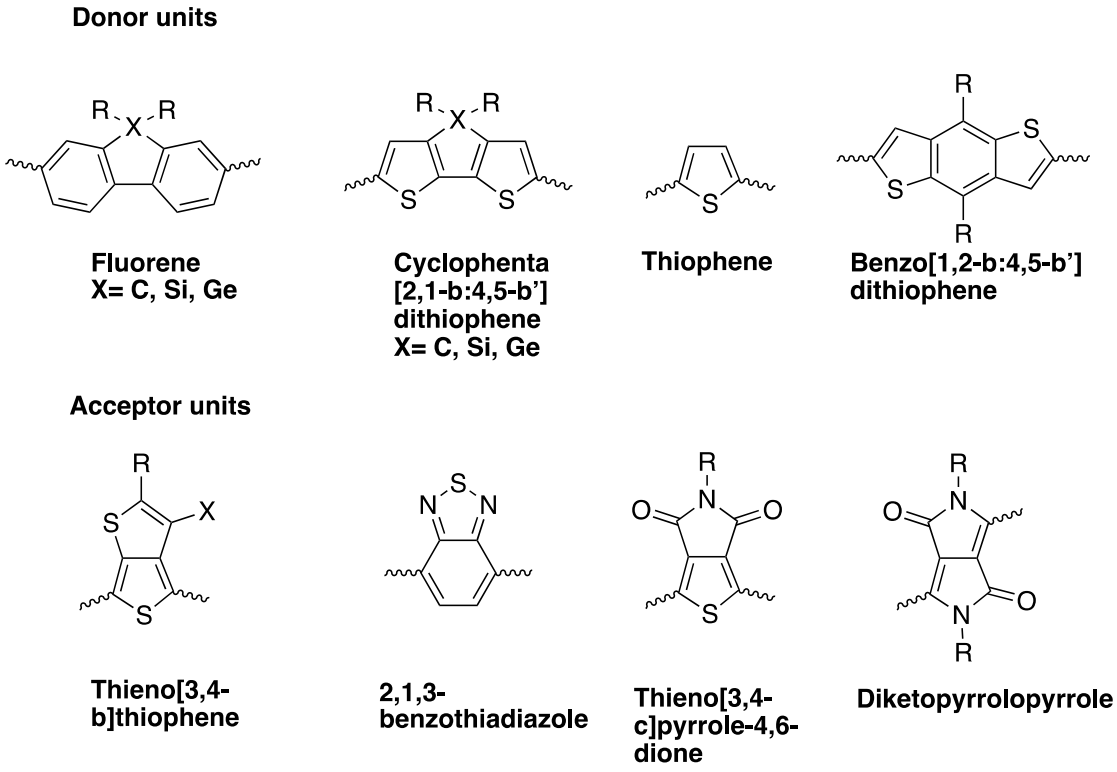

Figure 6. Structures of common donor and acceptor units.

Other substituents on the main chain can also be used to tune the properties of conjugated molecules. Some of the substituents that have strongly impact on the molecule physical and electronic properties include fluorine, cyano or heteroatoms (such as S, Se, Si and Ge). The PCE of solar cell device therefore can also be improved via this approach. The working mechanism behind these substituents are specific in each case. The general strategy of fluorine substitution is often called the "fluorination effect."[50-52] The strong electronegative nature of the fluorine lowers both the HOMO and LUMO energy level of the conjugated molecules without introducing steric hindrance. Intra- and intermolecular F-H and F-S interactions are also widely exploited to improve the conjugation. These interactions allow for more favorable packing and coplanarity of the

backbone. The substitution of a heteroatom for another heavier one from the same group also affects molecular electronic properties. A typical example is replacing thiophene with selenophene to modify HOMO-LUMO levels or even charge carrier mobilities.[50, 53-54] The bridging atom that covalently links two aromatic rings in a donor unit (not aromatically) is normally carbon. Replacing it by Si or Ge in many cases improves the HOMO-LUMO energy level, crystallinity, solubility and change transportation.[53, 55-56]

Polymer and small molecule semiconductors are both considered promising candidates for organic solar cell donor materials. In general polymer systems attract majority of attentions for its higher efficiency and improved film mechanical qualities.[35, 37] Indeed, the highest performance organic solar cell was reported using a polymeric system with a PCE of 11.5%.[36] Research on small molecule semiconductors is quickly expanding due to their unique advantages. Unlike polymers, small molecular structures can be precisely controlled and interpreted. Solar cells fabricated with small molecule donors can benefit from excellent batch to batch reproducibility, facile purification and eliminated chain-end defects.[24-25, 28, 44, 57-58]

1.4 SEQUENCE EFFECTS IN ORGANIC SEMICONDUCTORS

Even though sequence has been found to be useful in tuning material properties of non-conjugated polymers, it is still underexploited in semiconducting organic materials. The lack of research in this area is somewhat puzzling, however, since the molecular properties of conjugated organic semiconductors must necessarily depend on sequence. Important factors for high performance materials, for example, dipole moment, side chain interaction, molecular orbitals, coplanarity, etc. are all strongly influenced by monomer sequence. Bulk properties like

crystallinity, charge transport, melting point, which are built on the molecular properties, may also be sequence controlled. Understanding the structure-property relationship from the monomer sequence perspective will provide a powerful tool to tune material properties for the high performance electronic device.

Though most research on conjugated molecules focus on donor-acceptor unit design, side chain engineering and substituent effects, there are a few interesting examples of sequence effects in the literature (**Figure 7**). The Beaujuge group reported three small-molecule semiconductors (SM1-3) with well-defined sequence as the donor materials for solar cells.[59] These benzodithiophene based molecules have the same building units and end groups but different sequences. The donor unit is fixed in the center and acceptors units are either directly appended to it (SM1), or separated by one (SM2) or two (SM3) thiophene units. The HOMO-LUMO band gap, optical properties, molecular packing and charge transport are all dramatically different from SM1 to SM3. Solar cells fabricated with these molecules as the donor layer show PCE from 2.0% to 6.6%. Du and Liang also reported conjugated small molecules with similar sequence design respectively.[60-61] Two sequenced molecules **BDT-TT-BT** and **BDT-BT-TT**, in Du's work, showed distinct phase separation with $PC_{71}BM$ in the photo-active layer.[60] Liang and co-workers synthesized $BDT(BTTh_2)_2$ and $BDT(ThBTTh)_2$. The power conversion efficiency for solar cells fabricated with these two sequenced molecules are largely different, 4.53% vs 1.58%.[61]

Sequence effects have also been reported for conjugated polymers. Palermo reported a series of thiophene and selenophene copolymers with narrow molecular weight distributions and defined end-groups.[62] The gradient copolymer exhibited intermediate properties comparing with block and random polymers. The sequence effect is particularly apparent in the film morphology which is an important factor in organic electronics. Tsai also reported sequenced polymers consist

of group 16 heterocycles, furan, thiophene, and selenophene.[63] The optical gap and redox potentials can be precisely controlled by changing sequence. Though the AFM topology does not significantly change with sequence, the molecular stacking clearly relies on the polymer sequence. The π-stacking distance can be tuned from 3.7-4.0 Å and the lamellar spacing can be tuned from 15.8 to 15.2 Å by changing the sequence.

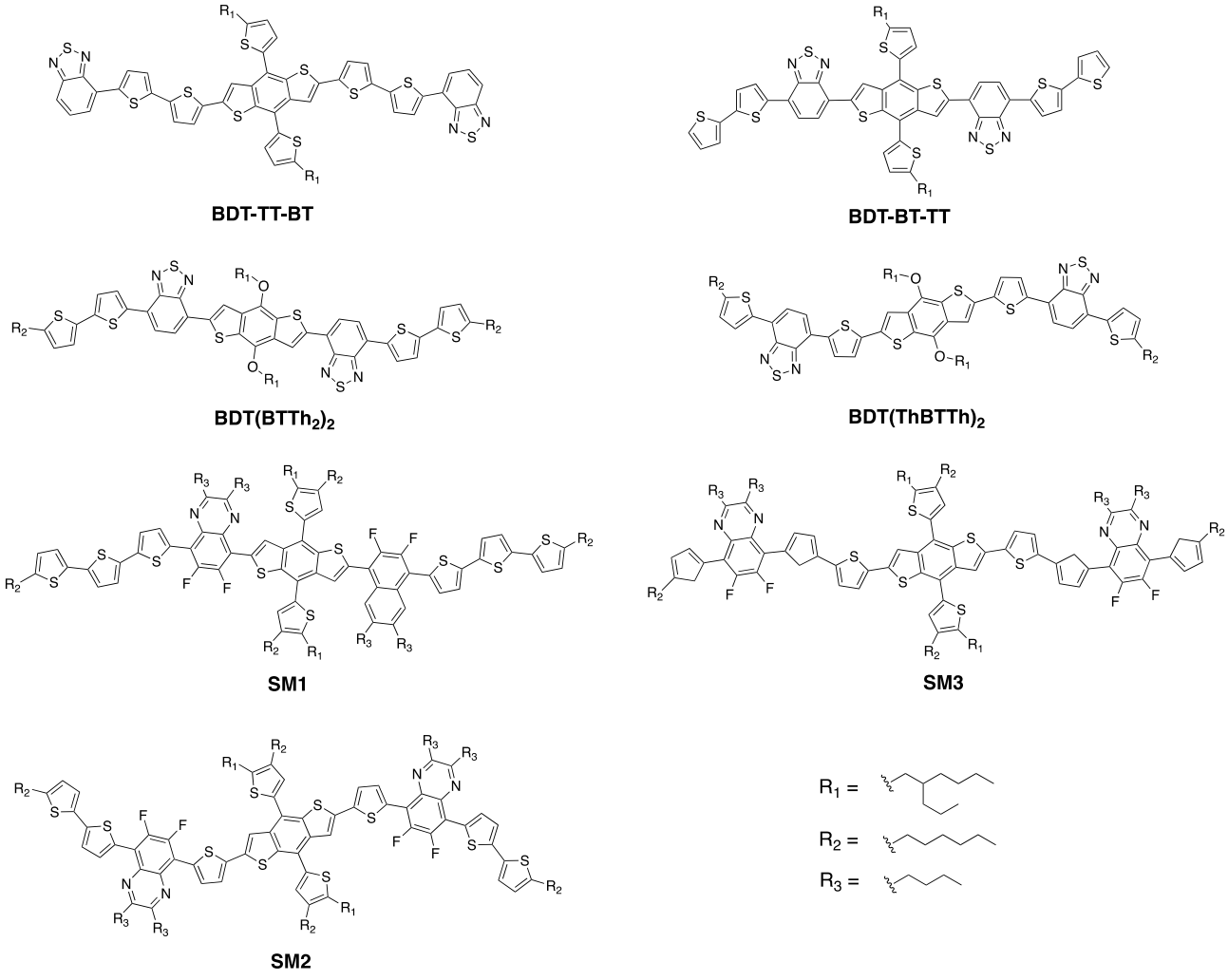

Figure 7. Sequence controlled conjugated oligomers reported in the literature. [59-61]

1.5 OBJECTIVES OF THE CURRENT PROJECT

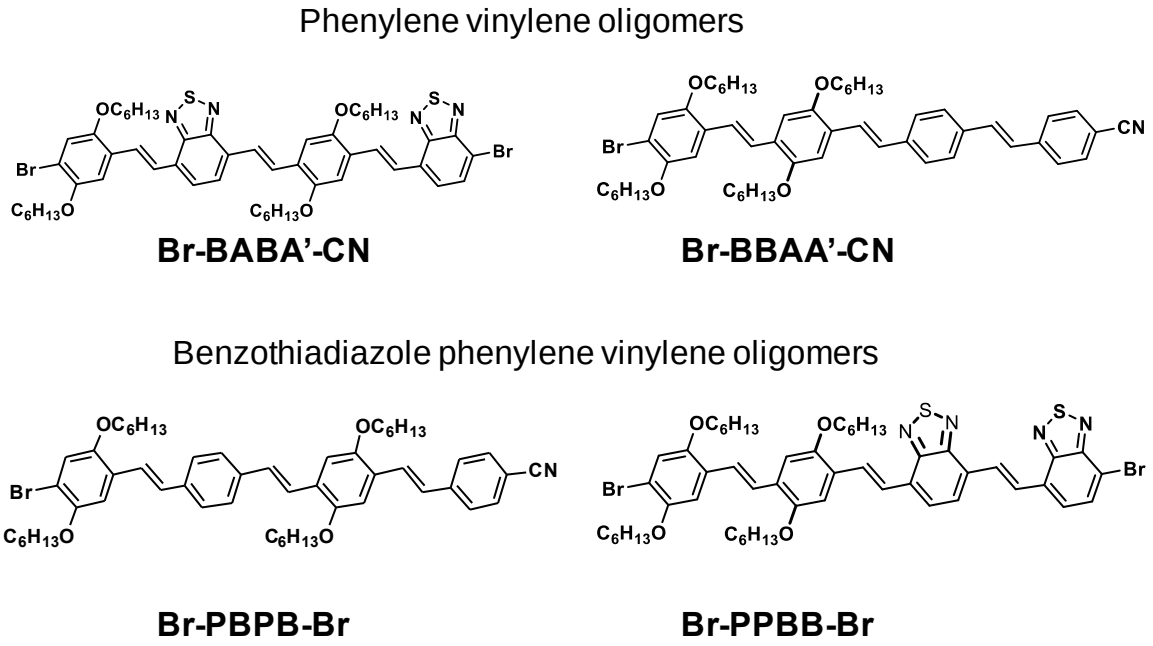

Figure 8. Examples of sequenced oligomers discussed in this dissertation.

In this dissertation, the donor-acceptor monomer sequence effect in conjugated oligomers and polymers bearing conjugated segments was investigated. With a large library of synthesized sequenced molecules (**Figure 8**), properties including HOMO and LUMO energy level, optical properties, film morphology, charge transport, melting point, and solar cell efficiency were characterized to understand the sequence effects. These experiments were supported and enhanced throughout by calculations performed by Professor Hutchison and coworkers who modelled the sequence effects.

In the second chapter, sequence effects on phenylene vinylene oligomers are described. Oligomers from dimers to hexamers were prepared from two monomers—dialkoxy substituted phenylene vinylene and unsubstituted phenylene vinylene. Both the optical and electronic properties of these oligomers were found to depend on the sequence. The experimental results and

computational simulations were found to be in good agreement and demonstrated to offer predictive power.

In the third chapter, the preparation and characterization of oligomers that incorporate the widely-used benzothiadiazole acceptor unit are described. In addition to differences in optical properties, solar cells fabricated with these oligomers by our collaborators, Wei You and Nicole Bauer, showed significant sequence-based differences in the power conversion efficiency.

In the fourth chapter, the incorporation of selected sequenced oligomers into polymeric chains is described. Film properties were demonstrated to improve while photophysical properties were retained.

1.6 REFERNCE

1. Blankenship, R. E.; Tiede, D. M.; Barber, J.; Brudvig, G. W.; Fleming, G.; Ghirardi, M.; Gunner, M. R.; Junge, W.; Kramer, D. M.; Melis, A.; Moore, T. A.; Moser, C. C.; Nocera, D. G.; Nozik, A. J.; Ort, D. R.; Parson, W. W.; Prince, R. C.; Sayre, R. T., Comparing Photosynthetic and Photovoltaic Efficiencies and Recognizing the Potential for Improvement. *Science* **2011,** *332* (6031), 805-809.

2. Lutz, J.-F.; Ouchi, M.; Liu, D. R.; Sawamoto, M., Sequence-controlled polymers. *Science* **2013,** *341* (6146), 1238149.

3. Lutz, J.-F., Aperiodic Copolymers. *ACS Macro Letters* **2014,** *3* (10), 1020-1023.

4. Lutz, J.-F.; Lehn, J.-M.; Meijer, E. W.; Matyjaszewski, K., From precision polymers to complex materials and systems. *Nature Reviews Materials* **2016,** *1*, 16024.

5. Stayshich, R. M.; Meyer, T. Y., New Insights into Poly(lactic-co-glycolic acid) Microstructure: Using Repeating Sequence Copolymers To Decipher Complex NMR and Thermal Behavior. *Journal of the American Chemical Society* **2010,** *132* (31), 10920-10934.

6. Weiss, R. M.; Jones, E. M.; Shafer, D. E.; Stayshich, R. M.; Meyer, T. Y., Synthesis of repeating sequence copolymers of lactic, glycolic, and caprolactic acids. *Journal of Polymer Science Part A: Polymer Chemistry* **2011,** *49* (8), 1847-1855.

7. Colquhoun, H.; Lutz, J.-F. Information-containing macromolecules. Nature Research, 2014.

8. Mutlu, H.; Lutz, J.-F., Reading Polymers: Sequencing of Natural and Synthetic Macromolecules. *Angewandte Chemie International Edition* **2014,** *53* (48), 13010-13019.

9. Al Ouahabi, A.; Charles, L.; Lutz, J.-F., Synthesis of Non-Natural Sequence-Encoded Polymers Using Phosphoramidite Chemistry. *Journal of the American Chemical Society* **2015,** *137* (16), 5629-5635.

10. Amir, F.; Jia, Z.; Monteiro, M. J., Sequence Control of Macromers via Iterative Sequential and Exponential Growth. *Journal of the American Chemical Society* **2016,** *138* (51), 16600-16603.

11. Soejima, T.; Satoh, K.; Kamigaito, M., Main-Chain and Side-Chain Sequence-Regulated Vinyl Copolymers by Iterative Atom Transfer Radical Additions and 1:1 or 2:1 Alternating Radical Copolymerization. *Journal of the American Chemical Society* **2016,** *138* (3), 944-954.

12. Zhang, S.; Hutchison, G. R.; Meyer, T. Y., Sequence Effects in Conjugated Donor–Acceptor Trimers and Polymers. *Macromolecular Rapid Communications* **2016,** *37* (11), 882-887.

13. Hibi, Y.; Ouchi, M.; Sawamoto, M., A strategy for sequence control in vinyl polymers via iterative controlled radical cyclization. *Nature Communications* **2016,** *7*, 11064.

14. Al Ouahabi, A.; Kotera, M.; Charles, L.; Lutz, J.-F., Synthesis of Monodisperse Sequence-Coded Polymers with Chain Lengths above DP100. *ACS Macro Letters* **2015,** *4* (10), 1077-1080.

15. Weiss, R. M.; Short, A. L.; Meyer, T. Y., Sequence-Controlled Copolymers Prepared via Entropy-Driven Ring-Opening Metathesis Polymerization. *ACS Macro Letters* **2015,** *4* (9), 1039-1043.

16. Weiss, R. M.; Li, J.; Liu, H. H.; Washington, M. A.; Giesen, J. A.; Grayson, S. M.; Meyer, T. Y., Determining Sequence Fidelity in Repeating Sequence Poly(lactic-co-glycolic acid)s. *Macromolecules* **2017,** *50* (2), 550-560.

17. Trinh, T. T.; Oswald, L.; Chan-Seng, D.; Lutz, J.-F., Synthesis of Molecularly Encoded Oligomers Using a Chemoselective "AB + CD" Iterative Approach. *Macromolecular Rapid Communications* **2014,** *35* (2), 141-145.

18. Roy, R. K.; Meszynska, A.; Laure, C.; Charles, L.; Verchin, C.; Lutz, J.-F., Design and synthesis of digitally encoded polymers that can be decoded and erased. *Nature Communications* **2015,** *6*, 7237.

19. Edwardson, T. G. W.; Carneiro, K. M. M.; Serpell, C. J.; Sleiman, H. F., An Efficient and Modular Route to Sequence-Defined Polymers Appended to DNA. *Angewandte Chemie International Edition* **2014,** *53* (18), 4567-4571.

20. Zeng, H.; Ickes, H.; Flowers, R. A.; Gong, B., Sequence Specificity of Hydrogen-Bonded Molecular Duplexes. *The Journal of Organic Chemistry* **2001,** *66* (10), 3574-3583.

21. Li, J.; Stayshich, R. M.; Meyer, T. Y., Exploiting sequence to control the hydrolysis behavior of biodegradable PLGA copolymers. *Journal of the American Chemical Society* **2011,** *133* (18), 6910-6913.

22. Washington, M. A.; Swiner, D. J.; Bell, K. R.; Fedorchak, M. V.; Little, S. R.; Meyer, T. Y., The impact of monomer sequence and stereochemistry on the swelling and erosion of biodegradable poly(lactic-co-glycolic acid) matrices. *Biomaterials* **2017,** *117*, 66-76.

23. Facchetti, A., π-Conjugated Polymers for Organic Electronics and Photovoltaic Cell Applications. *Chemistry of Materials* **2011,** *23*, 733-758.

24. Mishra, A.; Bäuerle, P., Small Molecule Organic Semiconductors on the Move: Promises for Future Solar Energy Technology. *Angewandte Chemie International Edition* **2012,** *51* (9), 2020-2067.

25. Chen, Y.; Wan, X.; Long, G., High Performance Photovoltaic Applications Using Solution-Processed Small Molecules. *Accounts of Chemical Research* **2013,** *46* (11), 2645-2655.

26. Wang, C.; Dong, H.; Hu, W.; Liu, Y.; Zhu, D., Semiconducting π-Conjugated Systems in Field-Effect Transistors: A Material Odyssey of Organic Electronics. *Chemical Reviews* **2011**.

27. Rochat, S.; Swager, T. M., Conjugated Amplifying Polymers for Optical Sensing Applications. *ACS Applied Materials & Interfaces* **2013,** *5* (11), 4488-4502.

28. Duan, L.; Hou, L.; Lee, T.-W.; Qiao, J.; Zhang, D.; Dong, G.; Wang, L.; Qiu, Y., Solution processable small molecules for organic light-emitting diodes. *Journal of Materials Chemistry* **2010,** *20* (31), 6392-6407.

29. Zhang, L.; Colella, N. S.; Cherniawski, B. P.; Mannsfeld, S. C. B.; Briseno, A. L., Oligothiophene Semiconductors: Synthesis, Characterization, and Applications for Organic Devices. *ACS Applied Materials & Interfaces* **2014,** *6* (8), 5327-5343.

30. Ellinger, S.; Graham, K. R.; Shi, P.; Farley, R. T.; Steckler, T. T.; Brookins, R. N.; Taranekar, P.; Mei, J.; Padilha, L. A.; Ensley, T. R.; Hu, H.; Webster, S.; Hagan, D. J.; Van Stryland, E. W.; Schanze, K. S.; Reynolds, J. R., Donor–Acceptor–Donor-based π-Conjugated Oligomers for Nonlinear Optics and Near-IR Emission. *Chemistry of Materials* **2011,** *23* (17), 3805-3817.

31. Nunzi, J.-M., Organic photovoltaic materials and devices. *Comptes Rendus Physique* **2002,** *3* (4), 523-542.

32. Scharber, M. C.; Mühlbacher, D.; Koppe, M.; Denk, P.; Waldauf, C.; Heeger, A. J.; Brabec, C. J., Design Rules for Donors in Bulk-Heterojunction Solar Cells—Towards 10 % Energy-Conversion Efficiency. *Advanced Materials* **2006,** *18* (6), 789-794.

33. Dennler, G.; Scharber, M. C.; Ameri, T.; Denk, P.; Forberich, K.; Waldauf, C.; Brabec, C. J., Design Rules for Donors in Bulk-Heterojunction Tandem Solar Cells Towards 15 % Energy-Conversion Efficiency. *Advanced Materials* **2008,** *20* (3), 579-583.

34. Tang, C. W., Two-layer organic photovoltaic cell. *Applied Physics Letters* **1986,** *48* (2), 183-185.

35. Lu, L.; Zheng, T.; Wu, Q.; Schneider, A. M.; Zhao, D.; Yu, L., Recent Advances in Bulk Heterojunction Polymer Solar Cells. *Chemical Reviews* **2015,** *115* (23), 12666-12731.

36. Zhao, J.; Li, Y.; Yang, G.; Jiang, K.; Lin, H.; Ade, H.; Ma, W.; Yan, H., Efficient organic solar cells processed from hydrocarbon solvents. *Nature Energy* **2016,** *1*, 15027.

37. Henson, Z. B.; Mullen, K.; Bazan, G. C., Design strategies for organic semiconductors beyond the molecular formula. *Nature Chemistry* **2012,** *4* (9), 699-704.

38. Grimsdale, A. C.; Chan, K. L.; Martin, R. E.; Jokisz, P. G.; Holmes, A. B., Synthesis of Light-Emitting Conjugated Polymers for Applications in Electroluminescent Devices. *Chemical Reviews* **2009,** *109* (3), 897-1091.

39. Yassar, A.; Miozzo, L.; Gironda, R.; Horowitz, G., Rod–coil and all-conjugated block copolymers for photovoltaic applications. *Progress in Polymer Science* **2013,** *38* (5), 791-844.

40. Heeger, A. J., Semiconducting polymers: the Third Generation. *Chemical Society Reviews* **2010,** *39* (7), 2354-2371.

41. Facchetti, A., π-Conjugated Polymers for Organic Electronics and Photovoltaic Cell Applications. *Chemistry of Materials* **2011,** *23*, 733-758.

42. Carsten, B.; Szarko, J. M.; Son, H. J.; Wang, W.; Lu, L.; He, F.; Rolczynski, B. S.; Lou, S. J.; Chen, L. X.; Yu, L., Examining the Effect of the Dipole Moment on Charge Separation in Donor–Acceptor Polymers for Organic Photovoltaic Applications. *Journal of the American Chemical Society* **2011,** *133* (50), 20468-20475.

43. Brédas, J.-L.; Norton, J. E.; Cornil, J.; Coropceanu, V., Molecular Understanding of Organic Solar Cells: The Challenges. *Accounts of Chemical Research* **2009,** *42* (11), 1691-1699.

44. Hedley, G. J.; Ruseckas, A.; Samuel, I. D. W., Light Harvesting for Organic Photovoltaics. *Chemical Reviews* **2017,** *117* (2), 796-837.

45. Xiao, S.; Zhang, Q.; You, W., Molecular Engineering of Conjugated Polymers for Solar Cells: An Updated Report. *Advanced Materials* **2016**.

46. Etxebarria, I.; Ajuria, J.; Pacios, R., Solution-processable polymeric solar cells: a review on materials, strategies and cell architectures to overcome 10%. *Organic Electronics* **2015,** *19*, 34-60.

47. Yao, H.; Ye, L.; Zhang, H.; Li, S.; Zhang, S.; Hou, J., Molecular Design of Benzodithiophene-Based Organic Photovoltaic Materials. *Chemical Reviews* **2016,** *116* (12), 7397-7457.

48. Collins, S. D.; Ran, N. A.; Heiber, M. C.; Nguyen, T. Q., Small is Powerful: Recent Progress in Solution-Processed Small Molecule Solar Cells. *Advanced Energy Materials* **2017**.

49. Mei, J.; Bao, Z., Side Chain Engineering in Solution-Processable Conjugated Polymers. *Chemistry of Materials* **2014,** *26* (1), 604-615.

50. Reichenbächer, K.; Süss, H. I.; Hulliger, J., Fluorine in crystal engineering—"the little atom that could". *Chemical Society Reviews* **2005,** *34* (1), 22-30.

51. Son, H. J.; Wang, W.; Xu, T.; Liang, Y.; Wu, Y.; Li, G.; Yu, L., Synthesis of fluorinated polythienothiophene-co-benzodithiophenes and effect of fluorination on the photovoltaic properties. *Journal of the American Chemical Society* **2011,** *133* (6), 1885-1894.

52. Wang, Y.; Parkin, S. R.; Gierschner, J.; Watson, M. D., Highly fluorinated benzobisbenzothiophenes. *Organic letters* **2008,** *10* (15), 3307-3310.

53. Dou, L.; Chang, W. H.; Gao, J.; Chen, C. C.; You, J.; Yang, Y., A selenium-substituted low-bandgap polymer with versatile photovoltaic applications. *Advanced Materials* **2013,** *25* (6), 825-831.

54. Intemann, J. J.; Yao, K.; Yip, H.-L.; Xu, Y.-X.; Li, Y.-X.; Liang, P.-W.; Ding, F.-Z.; Li, X.; Jen, A. K.-Y., Molecular weight effect on the absorption, charge carrier mobility, and photovoltaic performance of an indacenodiselenophene-based ladder-type polymer. *Chemistry of Materials* **2013,** *25* (15), 3188-3195.

55. Amb, C. M.; Chen, S.; Graham, K. R.; Subbiah, J.; Small, C. E.; So, F.; Reynolds, J. R., Dithienogermole as a fused electron donor in bulk heterojunction solar cells. *Journal of the American Chemical Society* **2011,** *133* (26), 10062-10065.

56. Coffin, R. C.; Peet, J.; Rogers, J.; Bazan, G. C., Streamlined microwave-assisted preparation of narrow-bandgap conjugated polymers for high-performance bulk heterojunction solar cells. *Nature Chemistry* **2009,** *1* (8), 657-661.

57. Zhang, H.; Tong, X.; Zhao, Y., Diverse Thermoresponsive Behaviors of Uncharged UCST Block Copolymer Micelles in Physiological Medium. *Langmuir* **2014,** *30* (38), 11433-11441.

58. Roncali, J.; Leriche, P.; Blanchard, P., Molecular Materials for Organic Photovoltaics: Small is Beautiful. *Advanced Materials* **2014,** *26* (23), 3821-3838.

59. Wang, K.; Liang, R.-Z.; Wolf, J.; Saleem, Q.; Babics, M.; Wucher, P.; Abdelsamie, M.; Amassian, A.; Hansen, M. R.; Beaujuge, P. M., Donor and Acceptor Unit Sequences Influence Material Performance in Benzo[1,2-b:4,5-b′]dithiophene–6,7-Difluoroquinoxaline Small Molecule Donors for BHJ Solar Cells. *Advanced Functional Materials* **2016,** *26* (39), 7103-7114.

60. Du, J.; Fortney, A.; Washington, K. E.; Bulumulla, C.; Huang, P.; Dissanayake, D.; Biewer, M. C.; Kowalewski, T.; Stefan, M. C., Systematic Investigation of Benzodithiophene-Benzothiadiazole Isomers for Organic Photovoltaics. *ACS Applied Materials & Interfaces* **2016,** *8* (48), 33025-33033.

61. Liang, L.; Wang, J.-T.; Xiang, X.; Ling, J.; Zhao, F.-G.; Li, W.-S., Influence of moiety sequence on the performance of small molecular photovoltaic materials. *Journal of Materials Chemistry A* **2014,** *2* (37), 15396-15405.

62. Palermo, E. F.; McNeil, A. J., Impact of Copolymer Sequence on Solid-State Properties for Random, Gradient and Block Copolymers containing Thiophene and Selenophene. *Macromolecules* **2012,** *45* (15), 5948-5955.

63. Tsai, C.-H.; Fortney, A.; Qiu, Y.; Gil, R. R.; Yaron, D.; Kowalewski, T.; Noonan, K. J. T., Conjugated Polymers with Repeated Sequences of Group 16 Heterocycles Synthesized through Catalyst-Transfer Polycondensation. *Journal of the American Chemical Society* **2016,** *138* (21), 6798-6804.

2.0 SEQUENCE EFFECTS ON ELECTRONIC AND OPTICAL PROPERTIES OF CONJUGATED OLIGMERS COMPRISING PHENYLENE VINYLENES

2.1 OVERVIEW

Although sequence must necessarily affect the photophysical properties of oligomers and copolymers prepared from donor and acceptor monomers, little is known as nearly all the donor/acceptor materials have an alternating structure. A series of sequenced *para*-phenylene-vinylene (PV) oligomers was synthesized and investigated both experimentally and computationally.

In order to provide the full picture of our discoveries, the work of several coworkers will be included in this document. These contributions will be highlighted as they are discussed. Dr. Ben Norris is particularly acknowledged for his contribution to the synthesis development and characterization for part of oligomers and Prof. Hutchison and Dr. Casey Campbell for their computational work. The majority of the work presented in this chapter was previously published in Norris, B. N.; Zhang, S.; Campbell, C. M.; Auletta, J. T.; Calvo-Marzal, P.; Hutchison, G. R.; Meyer, T. Y., Sequence Matters: Modulating Electronic and Optical Properties of Conjugated Oligomers via Tailored Sequence. *Macromolecules* **2013**, 46 (4), 1384-1392. [1]

The following naming conventions are employed in this chapter: 1) unsubstituted *para*-phenylene units are designated **A**; 2) dialkoxy-substituted units are designated **B**; 3) **A'** and **B'** are used for *para*-phenylene units bearing the conjugated cyano endgroup; and 4) oligomers are labeled dimer, trimer etc. based on the number of phenyl units (rather than complete phenylene-vinylene units) to avoid the use of the more exact but cumbersome #.5-mer terminology.

2.2 INTRODUCTION

Nature refines the properties of biopolymers, not just by composition, but also by orchestration of monomer sequence. For example, the photosynthetic pathway exhibits optical absorption, energy transfer, electron transfer, and chemical transformation motifs all within a self-assembled package.[2] In stark contrast, efforts to synthesize organic solar cells focus almost solely on chemical variation of monomer structure, seeking to derive optimal optical, energetic, and charge transfer properties using a very limited number of patterns.[3-5] Organic photovoltaics promise to significantly reduce the cost of solar electrical generation, so optimization of the material should be driven by sequence as well as composition. Here we demonstrate by combined synthesis, computational design, and optical and electrochemical characterization that altering the sequence of widely studied conjugated phenylene-vinylene oligomers can significantly modulate both optical and redox properties. We show that neither long block nor alternating sequences will likely yield optimal properties for photovoltaics.

Third generation photovoltaic polymers rely on the donor-acceptor approach in which electron-poor acceptor and electron-rich donor monomers are copolymerized in an effort to engineer the desired optoelectronic properties as a hybrid of the properties of the respective homopolymers.[3-10] Although alternating and random copolymers/oligomers containing a variety of donor and acceptor monomers have been prepared,[3, 11-14] no systematic effort has been made to determine the effect of the donor-acceptor sequence on the optoelectronic properties. For example, units that encode sequence in some form are nearly always symmetric[15-21] and there are only a few studies that include more than two examples of materials that have complex sequences[22] or are isomeric but sequentially diverse.[23-24]

Recent results from Prof. Hutchison group suggest that monomer sequence can have as much influence on properties of relevance to photovoltaics as the identities and ratios of the monomers. They developed a genetic algorithm for surveying the structure space of conjugated oligomers assembled from various donor-acceptor dimers and computationally predicted the power-conversion efficiencies of photovoltaic cells.[25] Oligomers with complex sequences of dimers exhibited surprisingly large differences in optoelectronic properties and photovoltaic efficiencies.

The power of sequence to control oligomer and polymer properties in applications other than photovoltaics is increasingly being investigated.[26-28] Our group has, for example, examined the effects of sequence on the properties of poly(lactic-*co*-glycolic acid)s and poly(fluorene-*co*-methylene)s.[29-34] The power of sequence to control the properties of oligomers and polymers can also be seen in the metal-catalyzed control of stereochemistry in polyolefins,[35] polylactides,[12, 18] and other monomers;[36] convergent/divergent assembly of precise oligomers,[37] sequential polycondensation,[38] acyclic diene metathesis,[39] controlled free-radical polymerizations,[40-43] and template synthesis of sequences.[44]

This chapter focuses on a model study, combining synthesis and characterization of sequenced oligomers and computational design that demonstrates the power of sequence to control optoelectronic properties. The interplay between the experimental and theoretical work is synergistic throughout. Experimental results from the synthesis of a library of easily prepared shorter oligomers were used to verify the computational approach. The experimental trends and calculations were then exploited to design targeted hexamers. Computational screening of the sequences proved critical as the longer oligomers are synthetically complex and difficult to survey experimentally due to the exponential increase in possible combinations with oligomer length.

2.3 RESULTS

2.3.1 Synthesis of Sequenced Oligomers

Oligo(phenylene-vinylene)s (OPVs) were targeted for this sequence study because these oligomers are well-known to have varied, substituent-dependent optoelectronic properties.[10, 24] A variety of methods for preparation of OPVs have been reported by our group and other researchers.[22, 24, 45-47] The approach selected for this study was developed by Dr. Ben Norris and was a modification of the synthesis by Jørgensen and Krebs[48] featuring alternating Horner-Wadsworth-Emmons (HWE) olefinations of a *p*-cyanobenzyl phosphonate monomer with an oligomer aldehyde followed by DIBAL-H reduction to yield a new reactive aldehyde. The key differences in our approach are the iterative coupling of single phenylene units, rather than dimeric units, which allows for the synthesis of any length oligomers with precise sequence control. Also, worth noting is the study carried out by Dr. Ben Norris in which he compared the use of nitrile-terminated units to acetals.[49] He found that the nitrile route led to increased *E*-selectivity of the HWE reaction and improved purification efficiency.

Four different monomers **Br-A-CHO**, **P-A-CN**, **P-B-CHO** and **P-B-CN** were synthesized and used as building blocks for all oligomers. **Br-A-CHO** and **Br-B-CHO** are used only as the beginning units of each sequenced oligomer. Depending on the monomer sequence targeted, either **P-A-CN** or **P-B-CN** was used in the HWE reaction for chain propagation. **Br-A-CHO** is commercially available, for all other monomers, synthesis details are described in the experimental section. Oligomers with aldehyde endgroups are only considered as synthesis intermediates and were not fully characterized.

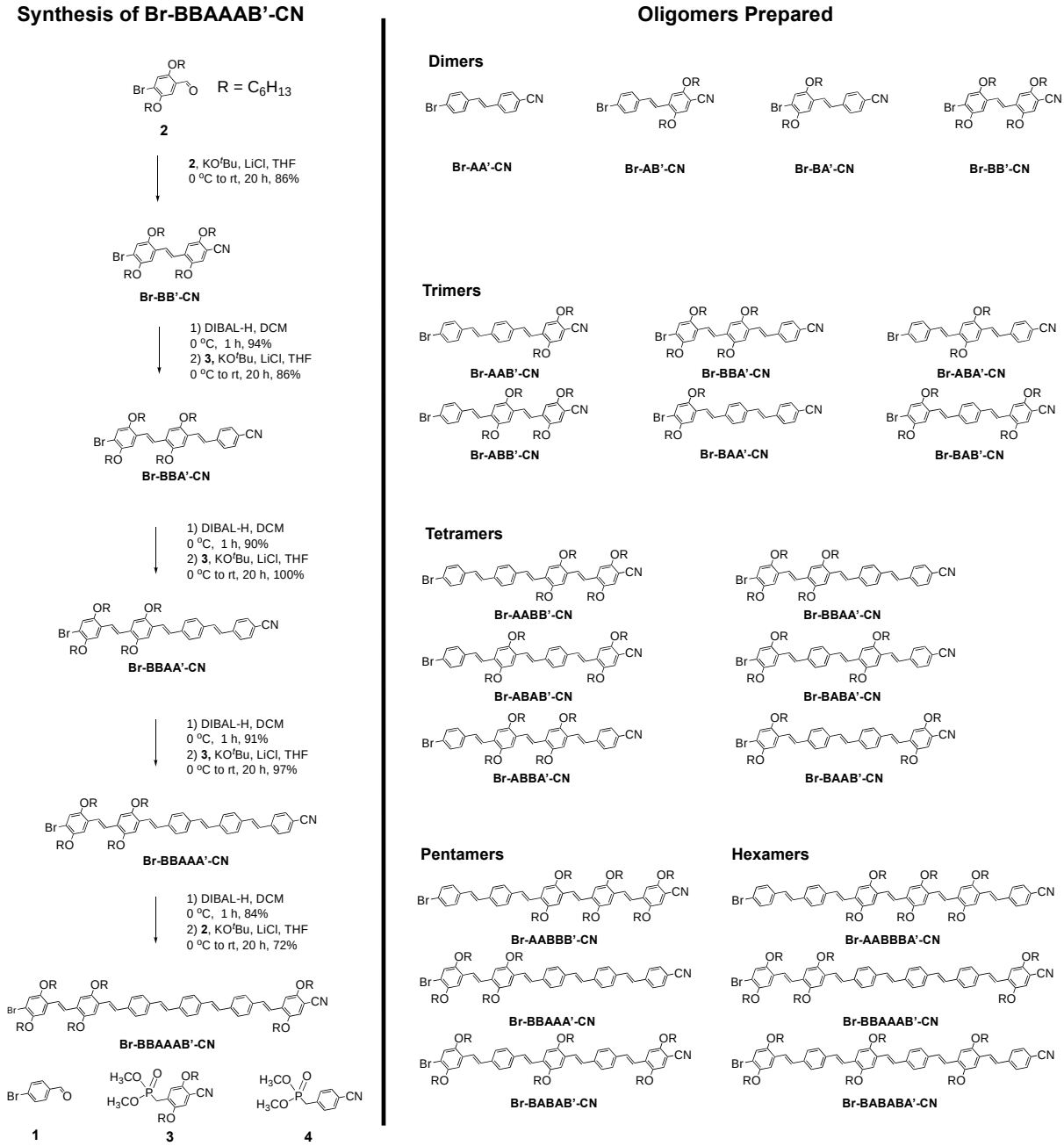

Figure 9. Synthetic approach to sequenced oligomers.

Table 1. Sequenced oligophenylene vinylenes synthesized and characterized in this study.

Oligomer	Yield[a]	*E*:*Z*[b]
Br-AA'-CN	85%[c]	>20:1[d]
Br-AB'-CN	92%[c]	20:1
Br-BA'-CN	96%[c]	20:1
Br-BB'-CN	96%[c]	9:1
Br-AAB'-CN	78%	20:1
Br-BAA'-CN	93%	20:1
Br-BAB'-CN	89%	20:1
Br-ABA'-CN	87%	9:1
Br-ABB'-CN	82%	8:1
Br-BBA'-CN	79%	8:1
Br-BAAB'-CN	83%	>20:1[d]
Br-ABAB'-CN	71%	>20:1[d]
Br-BABA'-CN	85%	>20:1[d]
Br-BBAA'-CN	98%	>20:1[d]
Br-AABB'-CN	80%	20:1
Br-ABBA'-CN	73%	>20:1[d]
Br-AABBB'-CN	59%	10:1
Br-BABAB'-CN	90%	>20:1[d]
Br-BBAAA'-CN	88%	>20:1[d]
Br-AABBBA'-CN	66%	9:1
Br-BABABA'-CN	74%	>20:1[d]
Br-BBAAAB'-CN	60%	>20:1[d]

[a]yield over two steps from relevant previous oligomer (e.g. **Br-BBAA'-CN** was prepared from **Br-BBA'-CN**), unless noted; [b]estimated from ^{1}H NMR spectra.; [c]yield over one step from **Br-A-CHO** (1) or **Br-B-CHO** (2); [d]no peaks for Z isomers were observed.

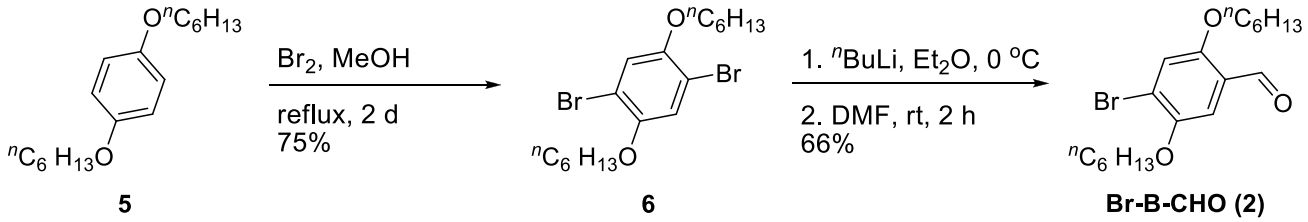

Figure 10. Synthesis of **Br-B-CHO.**

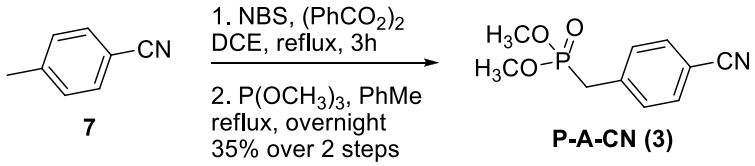

Figure 11. Synthesis of **P-A-CN.**

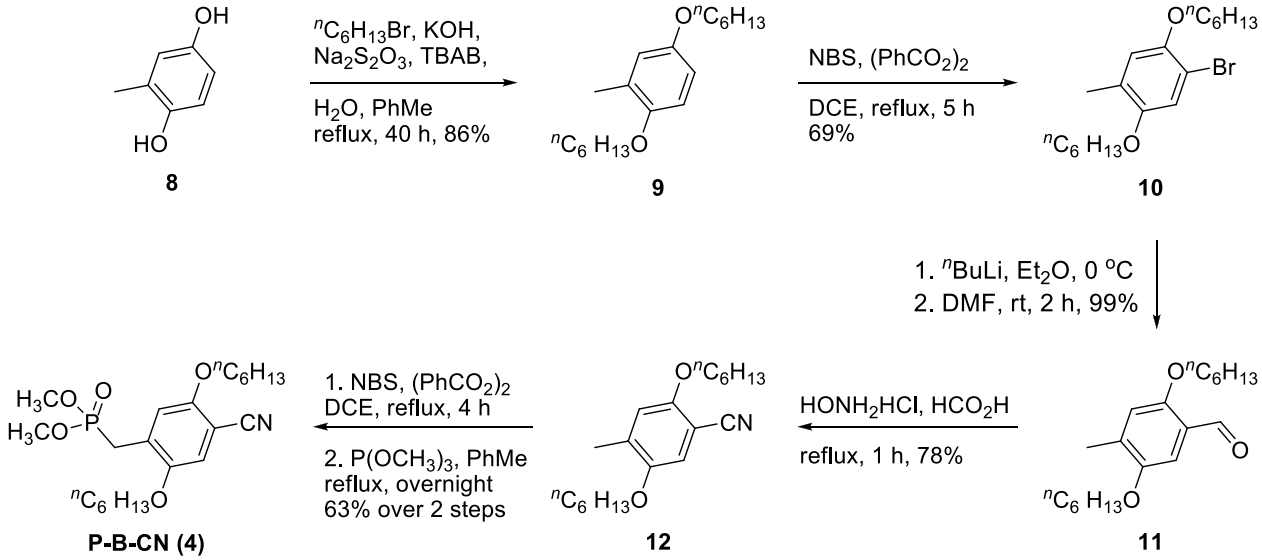

Figure 12. Synthesis of **P-B-CN.**

Four dimers, **Br-AA'-CN**, **Br-AB'-CN**, **Br-BA'-CN**, and **Br-BB'-CN** were prepared by this procedure in high yields and *E*-selectivities (**Table 1**). The nitrile group of each dimer could then be reduced with DIBAL-H to produce an aldehyde endgroup that allowed for subsequent

HWE reactions to increase chain length. By repeating successive cycles of nitrile reduction and HWE coupling a total of 22 sequenced oligomers were prepared: 4 dimers, 6 trimers, 6 tetramers, 3 pentamers, and 3 hexamers (**Figure 9**). To provide an example, the synthesis of hexamer **Br-BBAAAB'-CN** was started by HWE coupling reaction between **Br-B-CHO** with **P-B-CN** using KO^{t}Bu as base stirred at room temperature overnight to give **Br-BB'-CN** with a yield of 86%. Purified **Br-BB'-CN** was treated by DIBAL-H in dry methylene chloride to restore the reactive CHO group for next coupling reaction. **Br-BB'-CHO** was synthesized with 94% yield. Then **Br-BB'-CHO** was used to repeat the procedure above: HWE coupling with **Br-A-CN** with the same conditions and then treated with DIBAL-H to synthesize next reactive aldehyede **Br-BBA'-CHO**. By reapeating this procedure, **Br-BBAAAB'-CN** was successfully synthesized with high yield. The yield over two reactions from **Br-BB'-CN** to **Br-BBA'CN** was 78%, from **Br-BBA'-CN** to **Br-BBAA'-CN** was 98%, from **Br-BBAA'-CN** to **Br-BBAAA'-CN** was 88% and from **Br-BBAAA'-CN** to **Br-BBAAAB'-CN** was 60%.

All HWE reactions and DIBAL-H reductions used to prepare the trimers and tetramers proceeded in good to excellent yields. The yields of the pentamers and hexamers were lower in some cases due to the decreased solubility of the longer oligomers. All oligomers were prepared with high (> 8:1) *E*:*Z*-selectivity, with the lowest selectivity observed for those oligomers with two or more adjacent **B** units. In many cases, the *Z*-isomers were not observable by NMR after purification which suggests an upper limit of 3-5% contamination. In order to facilitate further elaboration of the oligomers, including the possibility of incorporating them into polymeric materials in the future, each OPV was prepared with a bromide group on one terminus and a nitrile on the other.

2.3.2 Computational Approach

All computational experiments in this chapter were conducted by Dr. Casey Campbell and Prof. Hutchison. These results are an indispensable part of the current study, and are thus included in this chapter. Computational methods offer an easy mechanism to screen optoelectronic properties of π-conjugated materials.[50-55] While density functional theory (DFT)-computed orbital eigenvalues are non-physical,[56-57] numerous studies have found a high degree of correlation between these energies and vertical ionization potentials and electron affinities[58-59] as well as accurate predictions of optical band gaps.[50] For solution electrochemistry, the redox potentials can be determined based on the free energy change,[60-61] such as the adiabatic difference in total energy between the neutral and charged systems (ΔSCF). In many cases, systematic deviations reflect a linear free energy relationship[62] between computed and experimental properties, which can be captured simply by linear regression. This regression also corrects for other errors, such as differences in computed and experimental conformations.

Since our objective was to reliably and accurately screen for targeted properties of sequenced oligomers, the regression techniques were extended by use of a "consensus model" to minimize both systematic and random errors, i.e., to improve accuracy and correlation. The consensus model employed here combines two different computational predictions of an experimental property using multivariate regression, e.g., oxidation potential. For redox potentials, DFT eigenvalues and adiabatic total energy differences (ΔSCF) were used, and for optical absorption energies and oscillator strengths, ZINDO and time-dependent DFT (TDDFT) methods were combined.

The computational method was originally developed and calibrated using optical and electrochemical data from sequenced 2-, 3-, and 4-mers. The method was then used to predict the properties of all possible hexamer sequences with a 1:1 A:B ratio (**Table 2**). Using these data, three hexamers with specifically targeted behavior, **Br-AABBBA'-CN**, **Br-BBAAAB'-CN** and **Br-BABABA'-CN**, were selected for synthesis. Prior to discussing the computational results/predictions in more detail, however, the characterization data for all oligomers are presented.

2.3.3 Optical Spectroscopy

The optical spectra of the oligomers vary significantly with sequence (**Table 2**, **Figure 13**, and Appendix A for all spectra). With increasing oligomer length, from trimers (383-412 nm), tetramers (408-437 nm), pentamers (427-449 nm) to hexamers (430-462 nm), the absorption maxima shift to longer wavelengths. This shift is consistent with an increased conjugation length. Overall, the absorption maxima of the trimer, tetramer and hexamer series vary over a range of ~30 nm and the optical HOMO-LUMO gaps, estimated at the onset of absorption, vary over a range ~0.25 eV.

Sequence can be seen to affect the absorption maxima and optical HOMO-LUMO gaps of the trimers. The three trimers, **Br-BAA'-CN**, **Br-ABA'-CN** and **Br-AAB'-CN,** each of which comprises one **B** unit and two **A** units, exhibit absorption maxima ranging from 383-406 nm. A 23 nm difference in absorption maxima and 0.21 eV in optical band gap were observed. For these three trimers, the emission maxima in both solution (433-477 nm) and thin film (507-514 nm) follow a similar trend to $\lambda_{\max}^{\mathrm{abs}}$. There is, however, a noticeable red shift from solution state to in the solid state that is consistent with aggregation.[63-64]

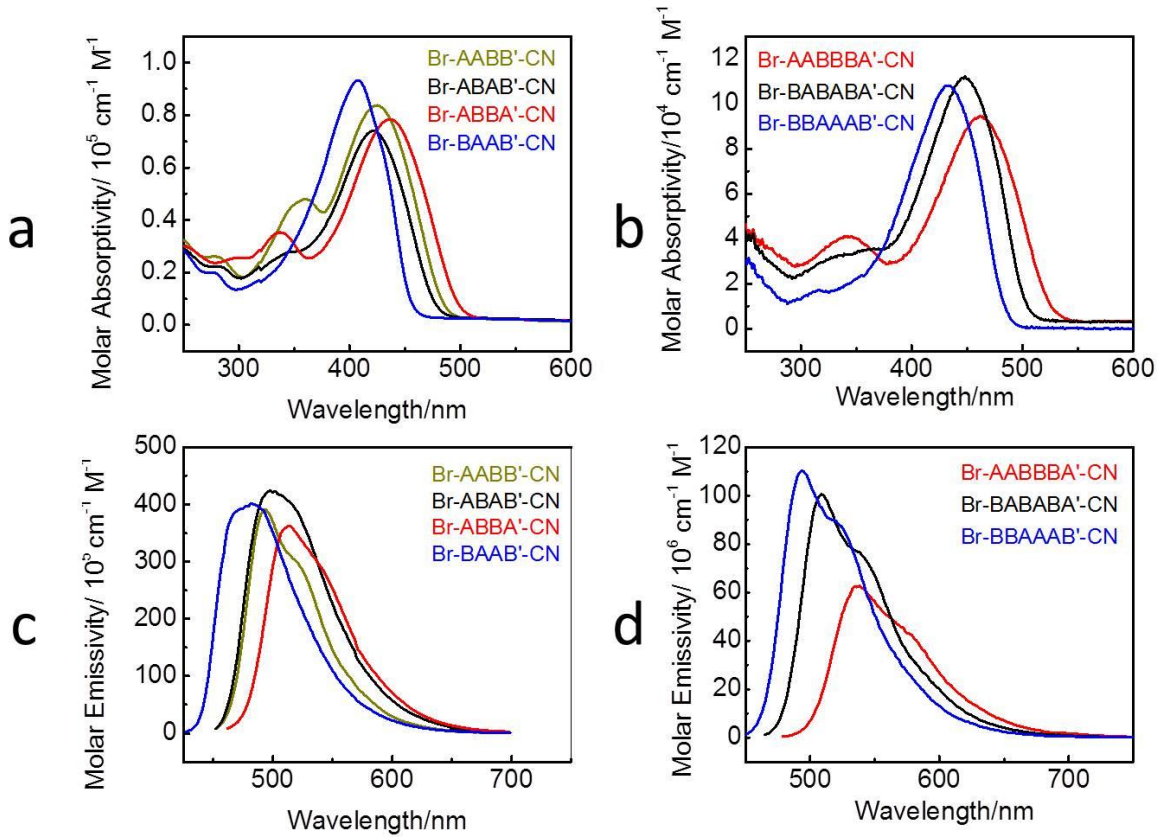

Figure 13. Absorption and emission spectra in $CHCl_3$: (a) absorption spectra for selected tetramers; (b) absorption spectra for hexamers; (c) emission spectra for selected tetramers; and (d) emission spectra for hexamers.

The absorption spectra of **Br-ABBA'-CN**, **Br-BAAB'-CN**, and a representative alternating (**Br-BABA'-CN**) and blocky (**Br-AABB'-CN**) sequence are presented in **Figure 13**. Among the tetramers, the sequence with the smallest band gap is **Br-ABBA'-CN** (2.47 eV), while the complementary sequence, **Br-BAAB'-CN** (2.72 eV)**,** exhibits the largest. The alternating sequences (**Br-ABAB'-CN** and **Br-BABA'-CN**) and the blocky sequences (**Br-AABB'-CN** and **Br-BBAA'-CN**) are intermediate (~2.56 eV). The effect of *Z*-isomer contamination on the optical spectra is negligible, as the materials were prepared with high *E*-selectivity (*vide infra*).

Sequence also impacts the absorption profile of the oligomers. Several sequences exhibit a well-separated higher energy absorption band. These tended to be sequences with **AA** or **BB** blocks, for example **Br-BBAA'-CN** or **Br-ABBA'-CN**, among the tetramers. While the longer

wavelength absorptions are primarily π-π* transitions delocalized across the entire oligomer, the higher energy, weaker absorptions likely derive from excitations between **BB** and **AA** blocks. These peaks, which were also found in the computational results, arise from shorter geometric distances and, thus exhibit smaller transition dipole moments.

The range of band gaps for the pentamer series is smaller (0.13 eV) than that of tetramers. Two pentamers, **Br-AABBB'-CN** and **Br-BABAB'-CN,** which differ only in their monomer sequence, exhibit an optical bandgap variance of 0.1 eV. A larger sequence effect on optical properties was observed, however, for the hexamers. These oligomers exhibited optical band gaps that differed by 0.24 eV, similar to the tetramer series. Consistently, the absorption maxima of hexamers exhibited a reasonably large range (32 nm). The sequence **Br-AABBBA'-CN** exhibits the smallest band gap (2.29 eV) and largest absorption maxima (462 nm), while the complementary sequence **Br-BBAAAB'-CN** has the largest optical band gap (2.53 eV) and smallest absorption maxima (430 nm). The alternating hexamer **Br-BABABA'-CN** exhibits intermediate properties (Optical band gap 2.46 eV and absorption maxima 509 nm). It is important to point out that these results match order predicted from computational model (*vide supra*).

Table 2. Optical properties of sequenced OPVs.

Oligomer	λ_{max}^{abs} [a] / nm	ε [b] / 10^{-3} cm^{-1}M^{-1}	λ_{max}^{em} [a] / nm	λ_{max}^{em} [c] / nm	ΔE_{gap}^{opt} [d] /eV
Br-AA'-CN	327	54.5	379	463	3.44
Br-BA'-CN	309, 362	28.1, 29.2	450	460	2.97
Br-AB'-CN	316, 364	29.4, 24.9	418	443	2.99
Br-BB'-CN	303, 380	16.9, 26.6	450	519	2.89
Br-AAB'-CN	385	93.2	433	507	2.86
Br-BAA'-CN	383	73.2	476	497	2.84
Br-BAB'-CN	396	72.4	474	504	2.77
Br-ABA'-CN	334, 406	37.9, 50.2	477	514	2.65
Br-ABB'-CN	329, 412	34.0, 53.8	478	524	2.63
Br-BBA'-CN	333, 412	29.4, 53.9	488	522	2.62
Br-BAAB'-CN	408	93.3	485	512	2.72
Br-ABAB'-CN	422	73.9	499	549	2.58
Br-BABA'-CN	425	89.9	492	534	2.56
Br-BBAA'-CN	366, 424	41.4, 86.2	515	553	2.56
Br-AABB'-CN	360, 425	47.9, 83.7	492	547	2.55
Br-ABBA'-CN	337, 437	35.3, 78.3	511	541	2.47
Br-AABBB'-CN	351,449	35.5, 90.7	522	578	2.43
Br-BABAB'-CN	435	97.7	508	557	2.52
Br-BBAAA'-CN	427	78.1	500	583	2.56
Br-AABBBA'-CN	342,462	40.8, 94.0	538	616	2.29
Br-BABABA'-CN	448	112.2	509	580	2.46
Br-BBAAAB'-CN	430	108	494	566	2.53

[a] Measured in ~10^{-6} M chloroform solution [b] Calculated at $\boldsymbol{\lambda_{max}^{abs}}$; [c] Thin film, cast from chloroform solution; [d] Determined at the onset of the absorption spectrum.

2.3.4 Electrochemistry

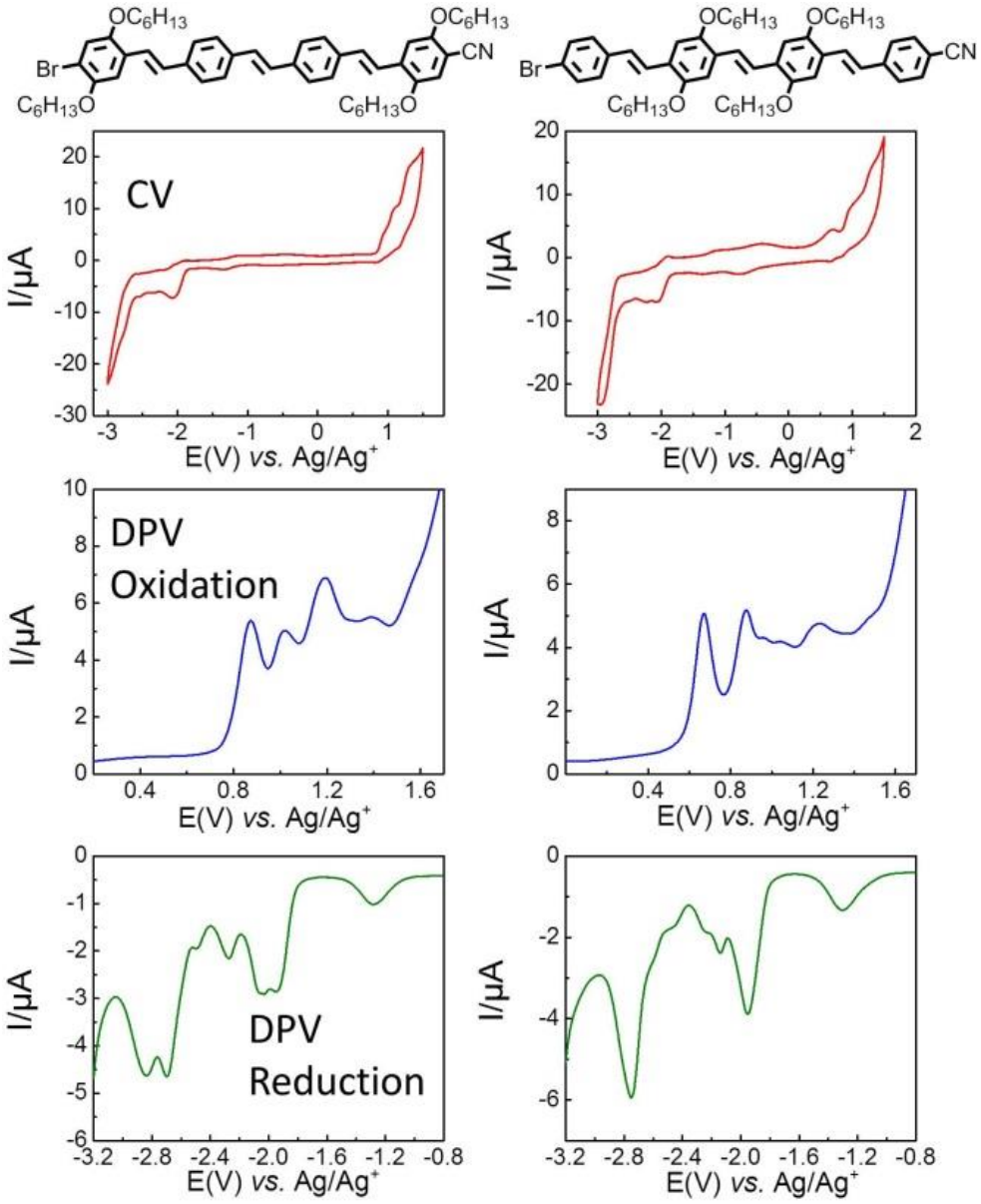

Figure 14. Cyclic voltammograms and differential pulse voltammograms of **Br-BAAB'-CN** and **Br-ABBA'-CN** in THF.

Table 3. Electrochemical properties of sequenced OPVs.

Oligomer	E_{peak}^{ox} [a] / V	E_{peak}^{red} [a] / V	ΔE_{gap}^{ec} [b] / eV
Br-AA'-CN	1.45	-1.93	3.38
Br-BA'-CN	1.06	-1.96	3.02
Br-AB'-CN	1.23	-1.94	3.17
Br-BB'-CN	1.06	-2.17	3.23
Br-AAB'-CN	1.06	-1.94	3.00
Br-BAA'-CN	0.95	-1.93	2.88
Br-BAB'-CN	0.97	-1.97	2.94
Br-ABA'-CN	0.84	-1.92	2.76
Br-ABB'-CN	0.81	-1.93	2.74
Br-BBA'-CN	0.78	-1.94	2.72
Br-BAAB'-CN	0.87	–1.94	2.81
Br-ABAB'-CN	0.69	-2.02	2.71
Br-BABA'-CN	0.69	-1.98	2.67
Br-BBAA'-CN	0.65	-1.99	2.64
Br-AABB'-CN	0.70	-1.99	2.69
Br-ABBA'-CN	0.67	-1.95	2.62
Br-AABBB'-CN	0.63	–1.97	2.60
Br-BABAB'-CN	0.70	–1.96	2.66
Br-BBAAA'-CN	0.69	–1.96	2.65
Br-AABBBA'-CN	0.54	–1.92	2.46
Br-BABABA'-CN	0.64	–1.94	2.58
Br-BBAAAB'-CN	0.67	-1.99	2.66

[a]Potential vs. Ag/Ag^{+}, 240 μM in 0.1 M Bu_4NPF_6 in THF; [b]Determined as $\boldsymbol{\Delta E_{gap}^{ec} = e(E_{peak}^{ox} - E_{peak}^{red})}$;

The electrochemistry of the oligomers is also strongly dependent on sequence (**Figure 14**, **Table 3** and Appendix A for the complete data set). Similar to the optical band gaps, with

increasing oligomer length and increased conjugation lengths, the electrochemical band gap for trimers (2.72-3.00 eV), tetramers (2.62-2.81 eV), pentamers (2.60-2.65 eV) to pentamers (2.46-2.66 eV) also decreased.

All oligomers with sequences containing multiple **B** units exhibit multiple oxidation peaks in their differential pulse voltammograms (DPVs). The first oxidation potentials of the oligomers demonstrate clear dependence on sequence and follow similar trends to the absorption maxima. The number of oxidation peaks and the shapes of the oxidation profiles clearly demonstrate sequence dependence as well, although there is not an obvious trend. The reduction potentials show little dependence on sequence, composition, or conjugation length. With few exceptions, the first reduction potential is at ca. –1.90 V vs. Ag/Ag^+, likely due to reduction of the cyano group.

For the trimer series with 2:1 **A** to **B** ratio, **Br-AAB'-CN**, **Br-BAA'-CN**, and **Br-ABA'-CN**, the first oxidation peak show a range from 0.84 eV to 1.06 eV with a difference of 0.22 eV due to sequence. For the trimer series with a 1:2 **A** to **B** ratio, **Br-BAB'-CN**. **Br-ABB'-CN** and **Br-BBA'-CN**, the first oxidation peaks also exhibited a difference of 0.19 eV.

For the tetramer series, the first oxidation potentials vary over a range of ~200 mV in THF, with **Br-BAAB'-CN** exhibiting the highest first oxidation potential, and the complementary **Br-ABBA'-CN** exhibiting a much lower oxidation potential (0.87 and 0.67 V vs. Ag/Ag^+, respectively). The alternating and blocky sequenced tetramers fall in between, with one exception; **Br-BBAA'-CN** exhibits the least positive first oxidation potential.

Since the first reduction potentials exhibit minimal variation, the differences in magnitude of the electrochemical HOMO-LUMO gaps, $\Delta E_{\mathrm{gap}}^{\mathrm{ec}}$, are related to the first oxidation potentials. The trend based on sequence effects for electrochemical band gaps as well as the variation for each oligomer series (i.e., trimers, tetramers) match that we observed on optical HOMO-LUMO gaps.

However, in contrast to the optical band gaps, the electrochemical gaps exhibit greater variation as a function of endgroup identity. In four out of five examples of inverse sequences (for example, **Br-ABB'-CN** vs. **Br-BBA'-CN)**, the optical bandgaps are similar despite notable changes in the electrochemical band gap. Generally, it was observed that when the **Br** group was attached to the **B** unit (**B**-first as written) the electrochemical gaps were smaller than the **A**-first isomers. A high degree of correlation was otherwise observed between electrochemical and spectroscopic gaps (R^2 = 0.92).

We find a similar trend in the redox potentials of the hexamers as was found in the optical spectroscopy. The sequence **Br-AABBBA'-CN** exhibits the lowest oxidation potential (0.54 V) and smallest $\Delta E_{\mathrm{gap}}^{\mathrm{ec}}$(2.46 eV), while the complementary sequence **Br-BBAAAB'-CN** has the highest oxidation potential (0.67 V) and largest $\Delta E_{\mathrm{gap}}^{\mathrm{ec}}$(2.66 eV). The alternating hexamer **Br-BABABA'-CN** exhibits intermediate properties. The range of gaps is 0.2 eV, in close agreement with the spectroscopic range of 0.24 eV.

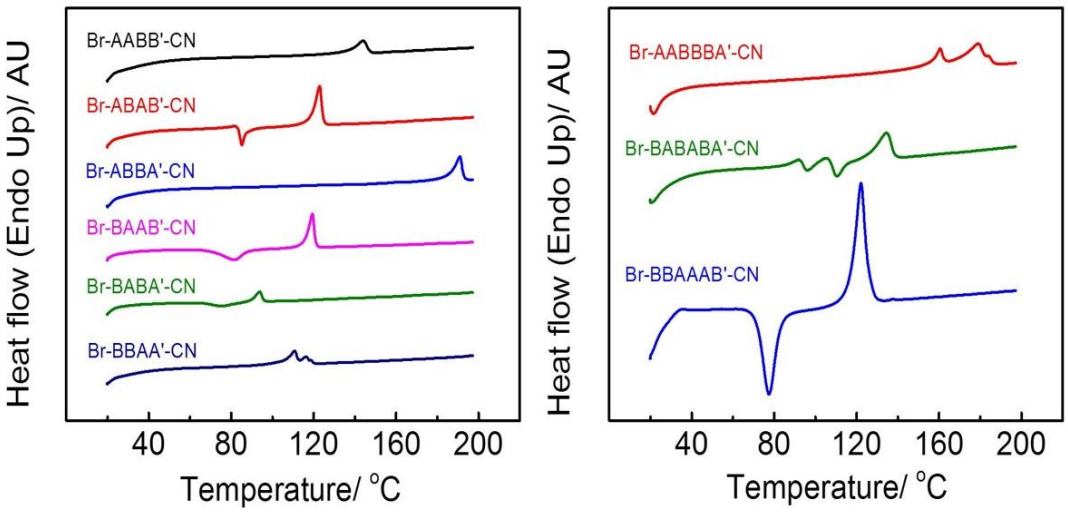

Figure 15. DSC thermograms of all six sequenced tetramers and all three sequenced hexamers.

2.3.5 Thermal Properties

Table 4. Thermal properties of the sequenced OPVs

Oligomer	T_{iso} [a] / °C	T_{LC}[a] / °C	T_C[b] / °C
Br-AA'-CN	197	—	151, 167
Br-BA'-CN	83.2	—	30.6
Br-AB'-CN	74.7[c]	—	—
Br-BB'-CN	96.3	—	68.8
Br-AAB'-CN	105	—	41.6
Br-BAA'-CN	125[c]	—	—
Br-BAB'-CN	104	—	77.8
Br-ABA'-CN	185	64.8[c]	79.5, 85.3, 92.7
Br-ABB'-CN	114	—	43.2
Br-BBA'-CN	109	—	—
Br-BAAB'-CN	119	81.2	—
Br-ABAB'-CN	123	85.0	41.7
Br-BABA'-CN	94	75.4	—
Br-BBAA'-CN	116	111,	57.5
Br-AABB'-CN	144	66.3[c]	114, 121
Br-ABBA'-CN	191	—	124
Br-AABBB'-CN	169	160	156
Br-BABAB'-CN	130	110	106
Br-BBAAA'-CN	171	86.2[c]	153
Br-AABBBA'-CN	184	178, 161	165,169
Br-BABABA'-CN	134	92,105	55.3
Br-BBAAAB'-CN	122	—	—

[a] Exothermic transition observed on second heating scan; [b] Exothermic transition observed on second cooling scan; [c] Transition observed in first scan only

Although not targeted for computational prediction in this investigation, the thermal properties of the prepared oligomers were also acquired and found to depend on sequence (**Figure 15, Table 4**). All oligomers were crystalline with melting points (T_{iso}) ranging from 80-170 °C and most exhibited clear crystallization exotherms (T_c) during differential scanning calorimetry (DSC).

Oligomers with two unsubstituted terminal **A** monomers, **Br-AA'-CN**, **Br-ABA'-CN**, **Br-ABBA'-CN**, and **Br-AABBBA'-CN** exhibited higher temperature melting transitions than other sequences of the same length. Multiple melting transitions observed for several of the longer oligomers are consistent with the existence of liquid crystalline phases with narrow ranges of stability.

Table 5. Computed first oxidation and reduction peak potentials and optical excitation energies $\boldsymbol{\Delta E_{gap}^{comp}}$ of sequenced OPVs from consensus models.

Oligomer	Predicted E_{ox}/V	Predicted E_{red}/V	$\Delta E_{\text{gap}}^{\text{comp}}$ / eV
Br-AA'-CN	1.43	-1.97	3.41
Br-BA'-CN	1.13	-1.99	3.12
Br-AB'-CN	1.21	-1.99	3.20
Br-BB'-CN	1.03	-2.00	3.03
Br-AAB'-CN	1.01	-1.97	2.97
Br-BAA'-CN	0.96	-1.97	2.93
Br-BAB'-CN	0.88	-1.98	2.85
Br-ABA'-CN	0.89	-1.96	2.85
Br-ABB'-CN	0.84	-1.99	2.82
Br-BBA'-CN	0.81	-1.97	2.78
Br-BAAB'-CN	0.80	-1.96	2.76
Br-ABAB'-CN	0.75	-1.95	2.70
Br-BABA'-CN	0.72	-1.95	2.67
Br-BBAA'-CN	0.73	-1.95	2.67
Br-AABB'-CN	0.76	-1.96	2.72
Br-ABBA'-CN	0.69	-1.96	2.65
Br-AABBB'-CN	0.62	-1.97	2.58
Br-BABAB'-CN	0.65	-1.96	2.61
Br-BBAAA'-CN	0.66	-1.94	2.61
Br-AABBBA'-CN	0.54	-1.97	2.51
Br-BABABA'-CN	0.61	-1.95	2.56
Br-BBAAAB'-CN	0.62	-1.96	2.59

2.3.6 Comparison of Computed and Experimental Data

As stated above, the computational consensus models were calibrated by the experimental results on the 2-, 3-, and 4-mers. In general, computed properties (**Table 5**) show only small residual errors compared to their experimental counterparts. The main exception is the predicted LUMO energies or ΔSCF(-) values, compared to the electrochemical first reduction potentials, which are largely dominated by the localized cyano reduction. DFT calculations predict, incorrectly, that the LUMOs are strongly delocalized across the entire oligomer.

The mean unsigned errors (MUE) between computed and experimental parameters after the linear regression analysis were found to be very low, as illustrated in **Figure 16**, with ~0.04 eV MUE for oxidation potentials (R^2 = 0.96), ~0.04 eV MUE for reduction potentials, ~0.07 eV MUE for optical excitation energies (R^2 = 0.89), and ~10% MUE for optical absorption extinction coefficients (R^2 = 0.94). The high degree of agreement is not surprising because the sequenced oligomers define a closely analogous series, and the consensus technique minimizes systematic and random errors.

Based on these consensus models, The properties of all 20 sequenced hexamers *prior to their synthesis* (**Table 16**) were predicted, and found distinct differences, despite the subtle variation in electronic structure of the **B** and **A** monomers. **Br-AABBBA'-CN** was predicted to exhibit the lowest HOMO energy and one of the smallest optical band gaps, while the complementary sequence **Br-BBAAAB'-CN** had a higher HOMO energy and gap. The conventional alternating sequences **Br-ABABAB'-CN** and **Br-BABABA'-CN** fell in between. As observed experimentally, these predictions proved relatively correct, although the difference in the experimental band gaps between hexamers was larger than that predicted. The calculated

difference in predicted gaps spanned a range of only 0.05 eV, while the experimental gaps spanned 0.2 and 0.24 eV for optical and electrochemical data, respectively.

There are several possible explanations for this difference. It is well-known that using TDDFT with conventional functionals underestimates band gaps in longer oligomers due to incorrect asymptotic behavior. For this reason, when screening the hexamers, ZINDO calculations were solely used. Also, such behavior has been observed previously and attributed to differences in computed and experimental conformations.[65-66] The calculations were performed on a low energy conformation, tending towards planarity in longer oligomers, not a solution ensemble of different conformations with shorter effective conjugation lengths.[66] This effect likely explains the smaller range in predicted band gaps in the hexamers, compared with experiment. Still, sequence determines both the orbital overlap and partial charge transfer between **B** and **A** monomers involved in the electronic excitations, and also dictates conformation in solution.[32]

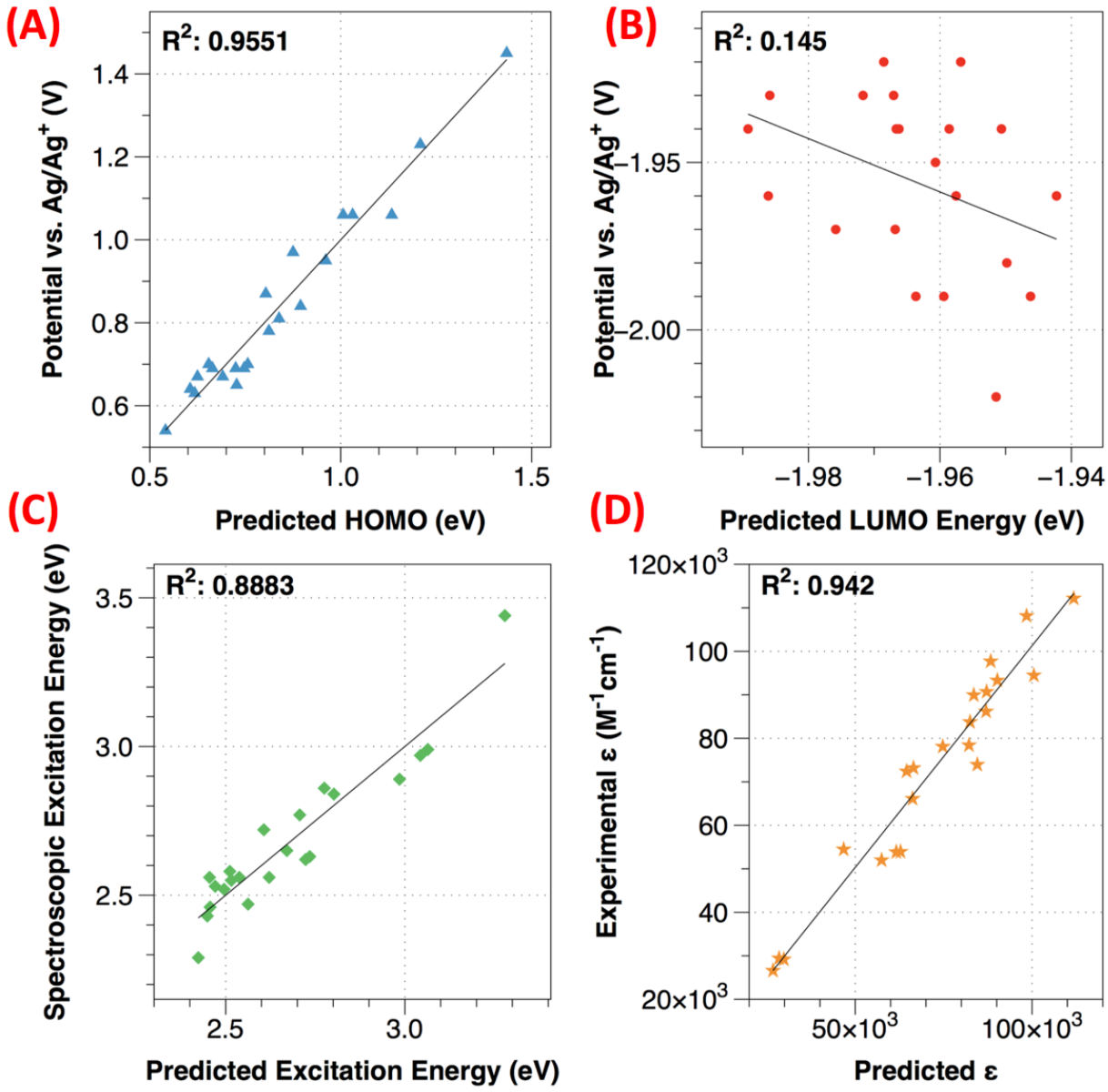

Figure 16. Correlations between computed (a) first oxidation potential, (b) first reduction potential, (c) optical excitation energies ΔE_{gap}^{comp}, and (d) extinction coefficients with their experimental counterparts. Note that for all predicted properties, a consensus model of two predictors was used.

2.4 DISCUSSION

Using an iterative strategy, we prepared multiple unsymmetric *para*-phenylene-vinylene oligomers with good *E*:*Z* selectivity that differ only in sequence. The product oligomers bear functional endgroups that allow for further elaboration including potential inclusion as units in a repeating sequence copolymer. Characterization of these oligomers establishes that the optical absorption and emission energies and intensities, first oxidation potentials, and thermal properties were all modulated by sequence.

The computational approach predicted the sequence-based optoelectronic properties of the conjugated oligomers with outstanding agreement. We were able, as a result, to selectively prepare longer oligomers with targeted characteristics. In particular, we both predicted and confirmed by synthesis that the oxidation potentials and optical excitation energies would exhibit the following trend: **Br-AABBBA'-CN** < **Br-BABABA'-CN** < **Br-BBAAAB'-CN**.

As discussed above, to facilitate synthesis and for future incorporation into polymers, we used Br– and –CN endgroups. One might suppose, that given the subtle difference in electronic structure between **A** and **B** monomers, the variation in optoelectronic properties is due *solely* to endgroup effects (e.g., the electron-withdrawing ability of CN on **A**' and **B**') and not to sequence effects. Instead, sequence generally dominated over endgroup effects except with the first reduction potential, which was dictated by the terminal cyano group. To further elucidate these effects, calculations were performed on tetramers and hexamers, both with, and without Br– and –CN endgroups. While some variations in the exact pattern of sequence effects are found, suggesting both sequence and endgroups have influence, the range of computed HOMO energies and gaps was retained (i.e., a span of 0.15 eV and 0.23 eV for tetramers, with and without endgroups, respectively).

Evidence that sequence effects generally dominate over endgroups can also be seen through the comparison of the optical spectra of specific compounds. The trimers **Br-ABA'-CN** and **Br-BBA'-CN** have almost identical optical band gaps (2.65 eV and 2.62 eV, respectively). When these trimers are extended with **B** and **A** monomers to form **Br-ABAB'-CN** and **Br-BBAA'-CN**, however, their band gaps narrow but remain nearly identical despite the addition of different endgroups. The tetramers **Br-ABAB'-CN** and **Br-AABB'-CN** have similar spectra (band gaps of 2.58 eV and 2.55 eV, respectively) while **Br-BAAB'-CN** shows a much higher optical band gap (2.72 eV) despite the fact that all three tetramers have the same **B'-CN** endgroup. In another example, the pentamers **Br-AABBB'-CN** and **Br-BABAB'-CN** have the same **B'-CN** endgroup and exhibit an optical gap difference of 0.09 eV. When these pentamers are extended to hexamers by adding an additional **A'-CN** unit to give **Br-AABBBA'-CN** and **Br-BABABA'-CN** the optical gap difference almost *doubles* to 0.17 eV, a clear indication that retaining identical endgroups is not sufficient to determine gaps.

The primary trend observed across all properties and the computational results, is that the alternating sequences e.g., **ABABAB** or **BABABA**, are generally neither the highest nor lowest in any category. A secondary widespread trend is that the oligomers that bear **A** monomers in both the first and last positions tend to exhibit smaller HOMO-LUMO gaps, less positive first oxidation potentials, and higher melting points. We also find that among absorption intensities (ε), sequences that bear **B** monomers in both the first and last positions (e.g., **Br-BAAB'-CN** or **Br-BABAB'-CN**) exhibit larger extinction coefficients than their counterparts. Although we find these trends, it is important to acknowledge that the use of complex sequences can lead to synergistic effects, and thus unique "outliers." The use of accurate, reliable computational screening methods makes the identification of these unique sequences practical.

2.5 CONCLUSIONS

This initial study is particularly promising despite the highly similar electronic characteristics of the two monomers. Despite the modest differences in the monomers, relative to true donor-acceptor pairs, we find a measurable difference in the sequenced oligomers across a wide range of characteristics. Sequence effect on the widely adapted systems with greater variation between donor and acceptor monomers are also studied and presented in the next chapter.

Control of sequence provides an entirely new dimension for optimization of conjugated materials. In parallel with the extremely productive strategy of creating novel monomers, sequence engineering offers a pathway to tailor targeted properties using existing, synthetically accessible monomers. Finally, the future correlation of sequence with other properties of interest, e.g., hole mobility, film morphology, and interfacial organization, should allow for the rational design of materials from known monomers that can satisfy the multiplicity of criteria that are necessary for the performance of these materials in real-world photovoltaic applications.

2.6 EXPERIMENTAL

2.6.1 Materials

Unless otherwise noted all compounds were purchased from Aldrich. Anhydrous DMF, ^{n}BuLi (1.6 M in hexanes), and DIBAL-H (1.0 M in hexanes) were dispensed using air-sensitive techniques. NBS was purchased from Alfa Aesar. Benzoyl peroxide and NBS were stored at -20 °C. KO^{t}Bu was stored in a desiccator over anhydrous $CaSO_4$. LiCl was purchased from Fisher

Scientific and dried at 120 °C for at least 24 h. Anhydrous diethyl ether for lithiation reactions was opened immediately prior to use. Reagent grade THF was used for most reactions; notably the HWE reactions used reagent grade THF. DCM for reactions was purified by distillation from CaH_2 or by passing through a column of alumina. All other reagents and solvents were used as received. Column chromatography was carried out on standard grade silica gel (60 Å pore size, 40-63 μm particle size), which was purchased and used as received. Hexanes, dichloromethane, and ethyl acetate used for column chromatography were purchased and used as received. Melting points for all compounds were determined by DSC and are found in the main text in Table 4, listed as T_{iso}.

2.6.2 Synthesis

General HWE procedure. Aldehyde (**Br-A-CHO, Br-B-CHO**, or **OPV-CHO**) (1 eq.), 4-cyanobenzylphosphonate (**P-A-CN** or **P-B-CN**) (1.5 eq), and LiCl (2.3 eq) were dissolved in THF (12 mL per mmol aldehyde) and cooled to 0 ^{o}C under N_2. KO^{t}Bu (2.3 eq) was added portion-wise over 5 minutes, and the reactions were allowed to come to RT overnight with stirring. The reaction mixtures were poured into saturated aqueous NH_4Cl (2.5 mL per mL THF). The aqueous layers were extracted thrice with EtOAc or CH_2Cl_2 (equal volume). The combined organic layers were dried over $MgSO_4$, and the solvent was removed *in vacuo*. The residues were purified by column chromatography. Yields and spectroscopic data for specific oligomers can be found in the supporting information.

General DIBAL-H reduction procedure. OPV nitriles (1 eq.) were dissolved in dry dichloromethane (5 mL per mmol nitrile) and cooled to 0 ^{O}C. DIBAL-H (1.0 M in hexanes, 1.1 eq) was added dropwise. The reaction mixtures were stirred at 0 $^{\circ}$C for 1 h. Wet silica (0.4 mL

H_2O and 1.3 g SiO_2 per mmol nitrile) was added and the mixture was stirred at 0 °C for 1 h. Then, K_2CO_3 (0.5 g per mmol nitrile) and $MgSO_4$ (0.5 g per mmol nitrile) were added. The mixtures were filtered and the solids washed with dichloromethane. The combined filtrate and washes were reduced in volume *in vacuo*, and the residues were purified by column chromatography, except as noted. Yields and spectroscopic data for specific oligomers can be found in the supporting information.

2.6.3 Spectroscopy

NMR Spectroscopy. ^{1}H (300 and 400 MHz) and ^{13}C (75, 100 and 150 MHz) NMR spectra were recorded on Bruker spectrometers. Chemical shifts were referenced to residual ^{1}H or ^{13}C signals in deuterated solvents (7.27 and 77.0 ppm, respectively, for $CHCl_3$ and 5.32 and 54.0 ppm, respectively, for CH_2Cl_2).

Mass Spectrometry. HRMS were recorded on EI-quadrupole or ESI-TOF instruments in the Mass Spectrometry Facility of the University of Pittsburgh.

Optical Spectroscopy. UV/VIS absorption spectra were recorded in $CHCl_3$ on a Perkin Elmer Lambda 9 UV/VIS/NIR spectrometer. Solution ($CHCl_3$) and film emission spectra were recorded on a Varian Cary Eclipse fluorimeter. Films were drop cast on quartz slides from $CHCl_3$.

Thermal Analysis. DSC was performed on a Perkin Elmer Pyris 6 with a heating and cooling rate of 10 °C/min.

2.6.4 Electrochemistry

Cyclic voltammetry (CV) and differential pulse voltammetry (DPV) were recorded on a CHI Electrochemical Workstation Model 430a (Austin, TX). Data were collected using a three electrode system consisting of a glassy carbon disk (3 mm dia.) as working electrode, a non-aqueous Ag/Ag^+ reference electrode (1 mM $AgNO_3$ in acetonitrile), and a Pt-wire as auxiliary electrode in 0.1 M Bu_4NPF_6 in THF freshly distilled from sodium. CV were recorded at 100 mV/s. DPV parameters were as follows: scan rate of 25 mV/s, pulse amplitude 0.05 V and pulse period 0.16 s.

2.6.5 Synthesis of Monomers

Although some of the starting materials and a selection of the oligomers have been previously reported by others, the exact synthesis used and characterization data for all compounds is included herein.

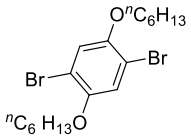

6

1,4-dibromo-2,5-bis(hexyloxy)benzene (6). This compound has been previously synthesized using a procedure in CCl_4,[67] which we were unwilling to handle and unable to acquire in the amounts necessary for our needs. A new procedure using methanol is described. Bromine (70.0 mL, 1.36 mol) was added dropwise to methanol (650 mL) at 0° C. **5** (75.0 g, 269 mmol) was added and the mixture was refluxed for 48 h. The reaction mixture was extracted with hexanes (4x

250 mL). The combined organic layers were washed with 20% aq. $NaHSO_3$ (2x 200 mL), water (200 mL), and brine (200 mL). The solution was dried over $MgSO_4$, and the solvent was removed in vacuo. The residue was recrystallized (9:1 methanol:CH_2Cl_2) to give the title compound as a white solid (88.5 g, 75%). ^{1}H NMR ($CDCl_3$, 300 MHz) δ 0.93 (6H, t, J = 6.8 Hz), 1.30-1.40 (8H, mult), 1.40-1.55 (4H, mult), 1.81 (4H, tt J = 6.8, 6.4 Hz), 3.95 (4H, t, J = 6.4 Hz), 7.09 (2H, s) ppm. ^{13}C NMR ($CDCl_3$) δ 14.00 (CH_3), 22.56 (CH_2), 25.59 (CH_2), 29.06 (CH_2), 31.46 (CH_2), 70.26 (OCH_2), 111.09 (ArBr quat), 118.41 (Ar CH), 150.04 (ArO quat) ppm. HRMS calcd. for $C_{18}H_{28}O_2Br_2$: 434.0456 g/mol. Found: 434.0450 g/mol.

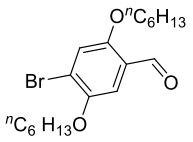

Br-B-CHO (2)

4-bromo-2,5-bis(hexyloxy)benzaldehyde (2 or **Br-B-CHO).** This compound has been previously reported, but the described synthesis by Li, *et al.*,[68] was unsuitable for scale-up. We modified the methods of Peng, *et al.*,[69] which were used to produce a similar compound. Two batches of **6** (34.9 g, 80.0 mmol each) were each dissolved in Et_2O (150 mL) and cooled to 0 °C under N_2. ^{n}BuLi (1.6 M in hexanes, 50 mL, 80 mmol) diluted with 100 mL Et_2O was added to each batch dropwise over 30 min. Anhydrous DMF (10.0 mL, 130 mmol) in Et_2O (35 mL) was added rapidly to each batch. The mixtures were removed from the cold bath and stirred at room temperature for 2 h. The reactions were quenched into water (300 mL). The aqueous layers were extracted with ether (3x100 mL). The organic layers were washed with brine (100 mL) and dried over $MgSO_4$. The solvent was removed *in vacuo*. The residues of both batches were combined and recrystallized from hexanes and then methanol to give the title compound as a while solid (40.5 g, 66%). ^{1}H NMR ($CDCl_3$, 300 MHz) δ 0.80-0.95 (6H,mult), 1.30-1.40 (8H, mult), 1.40-1.55 (4H,

mult), 1.75-1.90 (mult, 4H), 4.00 (2H, t, J = 6.4 Hz), 4.02 (2H, t, J = 6.4 Hz), 7.22 (1H, s), 7.30 (1H, s), 10.41 (1H, s) ppm. ^{13}CNMR ($CDCl_3$) δ 13.95 (CH_3), 13.97 (CH_3), 22.51 (CH_2), 22.53 (CH_2), 25.57 (CH_2), 25.62 (CH_2), 28.94 (CH_2), 28.98 (CH_2), 31.42 (CH_2), 69.76 (OCH_2), 69.76 (OCH_2), 110.52 (Ar CH), 118.39 (Ar CH), 120.89 (ArBr quat), 124.20 (Ar quat), 149.80 (ArO quat), 155.71 (ArO quat), 188.86 (CHO) ppm. HRMS calcd. for $C_{19}H_{29}O_3Br$: 384.1300 g/mol. Found: 384.1298 g/mol

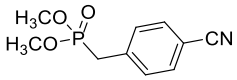

P-A-CN (3)

4-(dimethoxyphosphorylmethyl)benzonitrile (3 or **P-A-CN).** p-Tolunitrile (**7**) (25.0 mL, 209 mmol) was added to 1,2-dicloroethane (400 mL) in a round-bottom flask with stirring. NBS (18.8 g, 105 mmol), and benzoyl peroxide (2.55 g, 10.5 mmol) were added, and the mixture was refluxed until the orange color disappeared (1.5 h). NBS (18.8 g, 105 mmol), and benzoyl peroxide (2.55 g, 10.5 mmol) were added, and the mixture was refluxed again for 1.5 h. The reaction mixture was allowed to stand overnight. The succinimide precipitate was removed by filtration. The filtrate was washed successively with water (200 mL), sat. aq. $NaHCO_3$ (200 mL), and brine (200 mL). The organic solution was dried over $MgSO_4$, and the solvent was removed *in vacuo*. The crude product was dissolved in toluene (100 mL). Trimethyl phosphite (60.0 mL, 508 mmol) was added, and the mixture was refluxed overnight. The solvent was removed *in vacuo*, and the crude product was purified by column chromatography (silica gel, 4:1 CH_2Cl_2:acetone) and then by recrystallization (1:1 ethyl acetate:hexanes) to give the title compound as an off-white crystalline solid (16.7 g, 35% over 2 steps). MP 79.0-81.0 ^oC. ^{1}H NMR ($CDCl_3$) δ 3.17 (2H, d, $^2J_{H-P}$ = 22.4), 3.66 (6H, d, $^3J_{H-P}$ = 11.2 Hz), 7.37 (2H, dd, J_{H-H} = 8.4 Hz, J_{H-P} = 2.0 Hz), 7.58 (d, 2H, J_{H-H} = 8.0

Hz) ppm. ^{13}CNMR ($CDCl_3$, 300 MHz) δ 32.92 (d, $^1J_{C-P}$ = 137 Hz, CH_2), 52.82 (d, $^2J_{C-P}$ = 7 Hz, OCH_3), 110.84 (d, $^5J_{C-P}$ = 3 Hz, Ar quat), 118.45 (d, $^6J_{C-P}$ = 2 Hz, CN), 130.31 (d, $^3J_{C-P}$ = 6 Hz, Ar CH), 132.14 (d, $^4J_{C-P}$ = 3 Hz, Ar CH), 137.02 (d, $^2J_{C-P}$ = 10 Hz, Ar quat) ppm. MS (EI) 225 (M^+), 129, 116, 109 (base) m/z. HRMS calcd for $C_{10}H_{12}NO_3P$: 225.0556 g/mol. Found: 225.0555 g/mol.

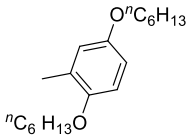

9

2-methyl-1,4-bis(hexyloxy)benzene (9). Based on our previous methods,[47] KOH (40.0 g, 713 mmol) and $Na_2S_2O_3$ (86.0 g, 346 mmol) were dissolved in water (200 mL) in a 1 L round-bottom flask and cooled on ice. 2-Methylhydroquinone (**8**) (42.8 g, 345 mmol), TBAB (5.0 g, 16 mmol), 1-bromohexane (100 mL, 712 mmol), and PhMe (100 mL) were added the order listed. The mixture was refluxed with vigorous stirring for 40 h. The aqueous layer was extracted with PhMe (2x 100 mL). The combined organic layers were washed with water (100 mL) and brine (100 mL) and dried over $MgSO_4$. The solvent was removed *in vacuo*. The residue was purified by column chromatography (silica gel, 17:3 hexanes:CH_2Cl_2) to give the title compound as a yellow liquid (86.3 g, 86%). ^{1}H NMR ($CDCl_3$) δ 0.90-1.00 (6H, mult), 1.30-1.45 (8H, mult), 1.45-1.60 (4H, mult), 1.75-1.90 (4H, mult), 3.94 (2H, t, *J* = 6.4 Hz), 3.95 (2H, t, *J* = 6.4 Hz), 6.71 (1H, dd, *J* = 9.0 Hz, 3.0 Hz), 6.77 (1H, d, *J* =9.0 Hz), 6.79 (1H, d, *J* = 3.0 Hz) ppm. ^{13}C NMR ($CDCl_3$) δ 13.99 (CH_3), 16.34 (CH_3), 22.60 (CH_2), 25.75 (CH_2), 25.83 (CH_2), 29.39 (CH_2), 29.45 (CH_2), 31.59 (CH_2), 31.61 (CH_2), 68.41 (OCH_2), 68.68 (OCH_2), 111.46 (Ar CH), 112.11 (Ar CH), 117.56 (Ar CH), 128 (Ar quat), 151.39 (ArO quat), 152.78 (ArO quat) ppm. MS(EI): 292 (M^+), 234, 221, 208,

165, 150, 124 (base), 107, 95, 84, 77, 67, 55 m/z. HRMS calcd for $C_{19}H_{32}O_2$: 292.2402 g/mol. Found: 292.2406 g/mol.

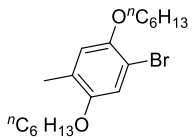

10

1-bromo-2,5-bis(hexyloxy)-4-methylbenzene (10). 9 (37.5 g, 128 mmol) was dissolved in 1,2-dichloroethane (375 mL). NBS (23.0 g, 129 mmol) and benzoyl peroxide (1.56 g, 6.44 mmol) were added and the mixture was refluxed for 5h. Hexanes (100 mL) was added to precipitate succinimide. The filtrate was washed with water (3x 100 mL), sat. aq. NaHCO3 (100 mL), and brine (100 mL). The solution was dried over MgSO4, and the solvent was removed in vacuo. The residue was recrystallized from methanol to give the title compound as a white solid (33.0 g, 69%). ^{1}H NMR ($CDCl_3$) δ 0.90-1.00 (6H, mult), 1.30-1.40 (8H, mult), 1.45-155 (4H, mult), 1.75-1.90 (4H, mult), 2.19 (3H, s), 3.90 (2H, t, J = 6.4 Hz), 3.96 (2H, t, J = 6.4 Hz), 6.76 (1H, s), 6.99 (1H, s) ppm. ^{13}C NMR ($CDCl_3$, 300 MHz) δ 13.98 (CH_3), 14.00 (CH_3), 16.22 (CH_3), 22.58 (CH_2), 25.65 (CH_2), 25.74 (CH_2), 29.26 (CH_2), 29.29 (CH_2), 31.52 (CH_2), 68.84 (OCH_2), 70.28 (OCH_2), 108.88 (ArBr quat), 116.28 (Ar CH), 116.90 (Ar CH), 126.28 (Ar quat), 149.15 (ArO quat), 151.72 (ArO quat) ppm. MS (EI): 372 (M^{+2}), 370 (M^+), 288, 286, 204, 202 (base), 164, 124, 94, 84, 77, 69 m/z. HRMS calcd for $C_{19}H_{31}O_2Br$: 370.1507 g/mol. Found: 370.1500 g/mol.

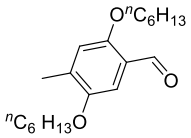

11

2,5-bis(hexyloxy)-4-methylbenzaldehyde (11). Based on the methods of Peng, *et al.*,[69] **10** (30.0 g, 80.1 mmol) was dissolved in Et_2O (150 mL) and cooled to 0 ^oC under N_2. ^{n}BuLi (1.6 M in hexanes, 55 mL, 88 mmol) diluted with 100 mL Et_2O was added dropwise over 30 min. DMF (10.0 mL, 130 mmol) in Et_2O (35 mL) was added rapidly. The mixture was removed from the cold bath and stirred at room temperature for 2 h. The reaction was quenched by pouring into water (300 mL). The aqueous layer was extracted with ether (3x 100 mL). The organic layers were washed with brine (100 mL) and dried over $MgSO_4$. The solvent was removed *in vacuo*. The residue was purified by column chromatography (silica gel, 19:1 hexanes:EtOAc) to give the title compound as an off-white solid (25.7 g, 99%). ^{1}H NMR ($CDCl_3$, 300 MHz) δ 0.85-0.95 (6H, mult), 1.30-1.40 (8H, mult), 1.40-150 (4H, mult), 1.75-1.85 (4H, mult), 2.27 (3H, s), 3.94 (2H, t, J = 6.4 Hz), 4.01 (2H, t, J = 6.4 Hz), 6.79 (1H, s), 7.22 (1H, s), 10.41 (1H, s) ppm. ^{13}C NMR ($CDCl_3$) δ 13.95 (CH_3), 17.21 (CH_3), 22.53 (CH_2), 22.55 (CH_2), 25.69 (CH_2), 25.72 (CH_2), 29.16 (CH_2), 31.47 (CH_2), 31.49 (CH_2), 68.40 (OCH_2), 69.10 (OCH_2), 108.19 (Ar CH), 115.58 (Ar CH), 122.96 (Ar quat), 136.71 (Ar quat), 151.32 (ArO quat), 156.12 (ArO quat), 189.31 (CHO) ppm. MS (EI): 320 (M^+), 292, 236, 152 (base), 124, 91, 84 m/z. HRMS calcd for $C_{20}H_{32}O_3$: 320.2351 g/mol. Found: 320.2349 g/mol.

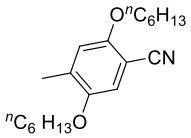

12

2,5-bis(hexyloxy)-4-methylbenzonitrile (12). Based on the methods of Olah,[70] **11** (23.3 g, 73.6 mmol) and hydroxylamine hydrochloride (6.57 g, 94.5 mmol) were added to formic acid (100 mL) in a round-bottom flask and refluxed for 1 h. The dark mixture was poured into ice water (200 mL). The aqueous mixture was extracted with ether (3x50 mL). The combined organic layers were washed with brine (50 mL) and dried over $MgSO_4$. The solvent was removed *in vacuo*, and the residue was purified by column chromatography (silica gel, 99:1 hexanes:EtOAc) to give the title compound as an orange liquid (17.1 g, 78%). ^{1}H NMR ($CDCl_3$, 300 MHz) δ 0.85-0.95 (6H, mult), 1.30-1.40 (8H, mult), 1.40-150 (4H, mult), 1.75-1.85 (4H, mult), 2.24 (3H, s), 3.87 (2H, t, J = 6.4 Hz), 3.98 (2H, t, J = 6.4 Hz), 6.75 (1H, s), 6.88 (1H, s) ppm. ^{13}C NMR ($CDCl_3$) δ 13.87 (CH_3), 16.99 (CH_3), 22.43 (CH_2), 22.46 (CH_2), 25.43 (CH_2), 25.62 (CH_2), 28.94 (CH_2), 29.03 (CH_2), 31.38 (CH_2), 31.40 (CH_2), 68.63 (OCH_2), 69.44 (OCH_2), 98.53 (CN quat), 114.41 (Ar CH), 115.33 (Ar CH), 116.83 (Ar quat), 134.64 (Ar quat), 150.76 (ArO quat), 154.97 (ArO quat) ppm. . HRMS calcd for $C_{20}H_{32}NO_2$: 318.2433 g/mol. Found: 318.2435 g/mol.

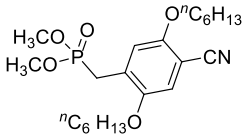

P-B-CN (4)

2,5-bis(hexyloxy)-4-(dimethoxyphosphorylmethyl) benzonitrile (4 or **P-B-CN). 12** (13.8 g, 43.5 mmol) was dissolved in 1,2-dichloroethane (70 mL). NBS (3.90 g, 43.8 mmol), and benzoyl peroxide (0.540 g, 4.45 mmol) were added, and the mixture was refluxed until the orange color disappeared (2 h). NBS (3.90 g, 43.8 mmol), and benzoyl peroxide (0.540 g, 4.45 mmol)

were added, and the mixture was refluxed for a second 2 h. After standing undisturbed overnight, the reaction mixture was filtered through a plug of silica and the solvent was removed *in vacuo*. The crude product was dissolved in PhMe (30 mL). Trimethyl phosphite (16.0 mL, 136 mmol) was added, and the mixture was refluxed overnight. The solvent was removed *in vacuo*, and the crude product was purified by column chromatography (silica gel, 1:1 hexanes:EtOAc) to give the title compound as a viscous orange liquid (11.7 g, 63% over 2 steps). ^{1}H NMR ($CDCl_3$, 300 MHz) δ 0.80-0.90 (6H, mult), 1.25-1.35 (8H, mult), 1.40-150 (4H, mult), 1.70-1.80 (4H, mult), 3.24 (2H, d, $^{2}J_{H-P}$ =22.4 Hz), 3.66 (6H, d $^{3}J_{H-P}$ = 11.2 Hz), 3.89 (2H, t, J = 6.4 Hz), 3.98 (2H, t, J = 6.4 Hz), 6.94 (1H, s), 6.96 (1H, d $^{4}J_{H-P}$ = 2.8 Hz) ppm. ^{13}C NMR ($CDCl_3$) δ 13.83 (CH_3), 22.37 (CH_2), 22.41 (CH_2), 25.35 (CH_2), 25.50 (CH_2), 26.14 (d, $^{1}J_{C-P}$ = 138 Hz, CH_2) 28.78 (CH_2), 28.97 (CH_2), 31.33 (CH_2), 31.34 (CH_2), 52.69 (d, $^{2}J_{C-P}$ = 7 Hz, OCH_3) 69.08 (OCH_2), 69.45 (OCH_2), 100.24 (d, $^{6}J_{C-P}$ = 3 Hz, CN quat), 115.36 (d, $^{4}J_{C-P}$ = 3 Hz, Ar CH), 115.33 (d, $^{3}J_{C-P}$ = 5 Hz, Ar CH), 116.31 (d, $^{5}J_{C-P}$ = 2 Hz, Ar quat), 127.36 (d, $^{2}J_{C-P}$ = 9 Hz, Ar quat), 150.06 (d, $^{3}J_{C-P}$ = 7 Hz, ArO quat), 154.75 (d, $^{4}J_{C-P}$ = 3 Hz, ArO quat) ppm. . HRMS calcd for $C_{22}H_{36}NO_5P^{+}Na$: 448.2229 g/mol. Found: 448.2237 g/mol.

2.6.6 Synthesis of Oligomers

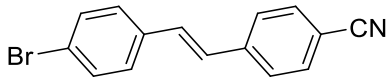

4-(4-bromostyryl)benzonitrile (Br-AA'-CN). This compound has been previously prepared by HWE reactions,[71] but not from 4-bromobenzaldehyde and **P-A'-CN**. According to the general HWE procedure, 4-bromobenzaldehyde (**1**) (2.00 g, 10.8 mmol) , and **P-A'-CN** (**3**) (3.90 g, 16.2 mmol), and LiCl (1.40 g, 32.9 mmol) were dissolved in THF (100 mL) and cooled to 0 ºC

under N_2. KOtBu (3.60 g, 32.1 mmol) was added portionwise over 5 minutes, and the reaction was allowed to come to rt overnight with stirring. After workup, column chromatography (silica gel, 1:1 hexanes:DCM) gave the title compound as a white solid (2.60 g, 9.20 mmol, 85%)). ^{1}H NMR (CD_2Cl_2, 400 MHz) δ 7.11 (1H, d, *J* = 16.4 Hz, *trans* CH=CH), 7.18 (1H, d, *J* = 16.4 Hz, *trans* CH=CH), 7.42 (2H, d, *J* = 8.8 Hz, *p*-C_6H_4), 7.52 (2H, d, *J* = 8.8 Hz, *p*-C_6H_4), 7.59 (2H, d, *J* = 8.4 Hz, *p*-C_6H_4), 7.65 (2H, d, *J* = 8.4 Hz, *p*-C_6H_4) ppm. ^{13}C NMR (CD_2Cl_2, 100 MHz) δ 111.39 (Ar quat), 119.41 (CN), 122.81 (ArBr quat), 127.45 (Ar CH), 127.99 (vinylene CH), 128.92 (Ar CH), 131.39 (vinylene CH), 132.46 (Ar CH), 133.06 (Ar CH), 135.97 (Ar quat), 141.96 (Ar quat) ppm. MS (EI) 285 (M+2), 283 (M^+), 204, 203 (base), 177, 176, 151, 127, 103 m/z. HRMS calcd for $C_{15}H_{10}NBr$ 282.9995 g/mol. Found: 282.9997 g/mol.

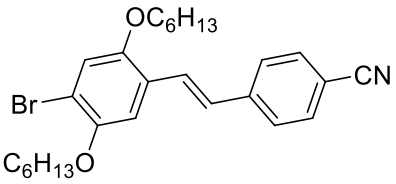

4-(4-bromo-2,5-bishexyloxystyryl)benzonitrile (Br-BA'-CN). According to the general HWE procedure, **Br-B-CHO** (**2**) (1.272 g, 3.30 mmol), **P-A'-CN** (**2**) (1.115 g, 4.95 mmol), and LiCl (321 mg, 7.57 mmol) were dissolved in THF (40 mL) and cooled to 0 °C under N_2. KO^{t}Bu (850 mg, 7.57 mmol) was added portionwise over 5 minutes, and the reaction was allowed to come to rt overnight with stirring. After workup, column chromatography (silica gel, 4:1 hexanes:DCM) gave the title compound as a pale yellow solid (1.480 g, 96%). ^{1}H NMR (CD_2Cl_2, 400 MHz) δ 0.85-1.00 (6H, mult), 1.30-1.45 (8H, mult), 1.45-1.55 (4H, mult), 1.70-1.80 (4H, mult), 3.97 (2H, t, *J* = 6.4 Hz, OCH_2), 4.03 (2H, t, *J* = 6.4 Hz, OCH_2), 7.13 (1H, s), 7.13 (1H, s), 7.16 (1H, d, *J* =

16.4 Hz, *trans* CH=CH), 7.52 (1H, d, *J* = 16.4 Hz, *trans* CH=CH), 7.60 (2H, d, *J* = 8.4 Hz, *p*-C_6H_4), 7.64 (2H, d, *J* = 8.4 Hz, *p*-C_6H_4) ppm. ^{13}C NMR (CD_2Cl_2, 100 MHz) δ 14.36 (CH_3), 14.39 (CH_3), 23.18 (CH_2), 26.24 (CH_2), 26.39 (CH_2), 29.76 (CH_2), 29.81 (CH_2), 32.11 (CH_2), 70.18 (OCH_2), 70.72 (OCH_2), 111.04 (ArBr quat), 112.12 (Ar CH), 113.40 (Ar quat) 118.35 (Ar CH), 119.35 (CN), 125.93 (Ar quat), 127.15 (vinylene CH), 127.36 (Ar CH), 127.88 (vinylene CH), 133.03 (Ar CH), 142.75 (Ar quat), 150.34 (ArO quat), 151.95 (ArO quat) ppm.

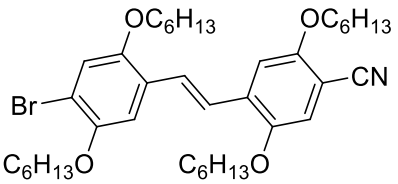

4-(4-bromo-2,5-bishexyloxystyryl)-2,5-bishexyloxybenzonitrile (Br-BB'-CN). According to the general HWE procedure, Br-B-CHO (2) (1.272 g, 3.30 mmol), P-B'-CN (4) (2.106 g, 4.95 mmol), and LiCl (321 mg, 7.57 mmol) were dissolved in THF (40 mL) and cooled to 0 ^{o}C under N_2. KO^{t}Bu (850 mg, 7.57 mmol) was added portionwise over 5 minutes, and the reaction was allowed to come to rt overnight with stirring. After workup, column chromatography (silica gel, 4:1 hexanes:DCM) gave the title compound as a bright yellow solid (2.240 g, 96%). ^{1}H NMR (CD_2Cl_2, 400 MHz) δ 0.85-1.00 (12H, mult), 1.30-1.45 (16H, mult), 1.45-1.55 (8H, mult), 1.70-1.80 (8H, mult), 3.97 (4H, t, *J* = 6.4 Hz, OCH_2), 4.02 (2H, t, *J* = 6.4 Hz, OCH_2), 4.10 (2H, t, *J* = 6.4 Hz, OCH_2), 7.04 (1H, s), 7.13 (1H, s), 7.15 (1H, s), 7.18 (1H, s), 7.45 (1H, d, *J* = 16.8 Hz, *trans* CH=CH), 7.51 (1H, d, *J* = 16.8 Hz, *trans* CH=CH) ppm. ^{13}C NMR (CD_2Cl_2, 100 MHz) δ 14.38 (CH_3), 14.397 (CH_3), 23.16 (CH_2), 23.19 (CH_2), 23.21 (CH_2), 26.13 (CH_2), 26.26 (CH_2), 26.37 (CH_2), 29.64 (CH_2), 29.72 (CH_2), 29.79 (CH_2), 29.84 (CH_2), 32.09 (CH_2), 32.13 (CH_2), 70.04 (OCH_2), 70.11 (OCH_2), 70.18 (OCH_2), 70.69 (OCH_2), 100.82 (Ar quat), 110.73 (Ar CH),

112.26 (Ar CH), 113.06 (ArBr quat), 116.97 (Ar CH), 117.25 (CN), 118.28 (Ar CH), 123.56 (vinylene CH), 126.69 (Ar quat), 127.16 (vinylene CH), 133.66 (Ar quat), 150.34 (ArO quat), 150.73 (ArO quat), 151.89 (ArO quat), 155.70 (ArO quat) ppm. MS (EI): 685 (M+2, base), 683 (M^+), 605, 349, 347, 267, 205, 85 m/z. HRMS calcd for $C_{39}H_{58}NO_4Br$: 683.3549 g/mol. Found: 683.3540 g/mol.

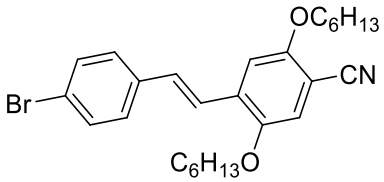

4-(4-bromostyryl)-2,5-bishexyloxybenzonitrile (Br-AB'-CN). According to the general HWE procedure, 4-bromobenzaldehyde (**1**) (611 mg, 3.30 mmol), **P-B'-CN** (**4**) (2.106 g, 4.95 mmol), and LiCl (321 mg, 7.57 mmol) were dissolved in THF (40 mL) and cooled to 0 °C under N_2. KO^{t}Bu (850 mg, 7.57 mmol) was added portionwise over 5 minutes, and the reaction was allowed to come to rt overnight with stirring. After workup, column chromatography (silica gel, 9:1 hexanes:$CHCl_3$) gave the title compound as a pale yellow solid (1.414 g, 92%). ^{1}H NMR (CD_2Cl_2, 400 MHz) δ 0.85-1.00 (6H, mult), 1.30-1.45 (8H, mult), 1.45-1.55 (4H, mult), 1.70-1.80 (4H, mult), 3.97 (2H, t, *J* = 6.4 Hz, OCH_2), 4.09 (2H, t, *J* = 6.4 Hz, OCH_2), 7.04 (1H, s), 7.158 (1H, s), 7.18 (1H, d, *J* = 17.2 Hz, *trans* CH=CH), 7.43 (2H, d, *J* = 8.0 Hz, *p*-C_6H_4), 7.44 (1H, d, *J* = 17.2 Hz, *trans* CH=CH), 7.51 (2H, d, *J* = 8.0 Hz, *p*-C_6H_4) ppm. ^{13}C NMR (CD_2Cl_2, 100 MHz) δ 14.36 (CH_3), 14.37 (CH_3), 23.15 (CH_2), 23.18 (CH_2), 26.11 (CH_2), 26.36 (CH_2), 29.61 (CH_2), 29.68 (CH_2), 32.07 (CH_2), 32.10 (CH_2), 70.11 (OCH_2), 70.24 (OCH_2), 101.18 (Ar quat), 110.76 (Ar CH), 117.04 (Ar CH), 117.15 (CN), 122.50 (ArBr quat), 123.60 (vinylene CH), 128.87 (Ar CH), 132.34 (vinylene CH), 132.43 (Ar CH), 132.81 (Ar quat), 136.69 (Ar quat), 150.79 (ArO quat), 155.66 (ArO quat) ppm.

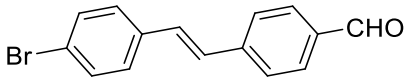

4-(4-bromostyryl)benzaldehyde (Br-AA'-CHO). This compound has been prepared before by Heck[72] and HWE[73] reactions. Our methodology greatly increases yield. According to the general DIBAL-H procedure, **Br-AA'-CN** (448 mg, 1.80 mmol) was dissolved in DCM (10 mL) and cooled to 0 ^{O}C. DIBAL-H (1.0M in hexanes, 1.9 mL, 1.9 mmol) was added dropwise. After workup, the solvent was removed *in vacuo* to give the title compound as a white solid (423 mg, 93%). ^{1}H NMR (CD_2Cl_2, 400 MHz) δ 7.17 (1H, d, *J* = 16.4 Hz, *trans* CH=CH), 7.24 (1H, d, *J* = 16.4 Hz, *trans* CH=CH), 7.45 (2H, d, *J* = 8.4 Hz, *p*-C_6H_4), 7.53 (2H, d, *J* = 8.4 Hz, *p*-C_6H_4), 7.68 (2H, d, *J* = 8.4 Hz, *p*-C_6H_4), 7.87 (2H, d, *J* = 8.4 Hz, *p*-C_6H_4), 9.99 (1H, s, CHO) ppm. ^{13}C NMR (CD_2Cl_2, 100 MHz) δ 122.62 (ArBr quat), 127.52 (vinylene CH), 128.61 (Ar CH), 128.93 (vinylene CH), 130.63 (vinylene CH), 131.20 (Ar CH), 132.47 (Ar CH), 136.20 (Ar quat), 136.20 (Ar quat), 143.49 (Ar quat), 191.97 (CHO) ppm. MS (EI) 288 (M+2), 286 (M^+), 178 (base), 152, 131, 107, 102, 89, 84, 76, 57 m/z. HRMS calcd for $C_{15}H_{11}BrO$: 285.9984 g/mol. Found: 285.9993 g/mol.

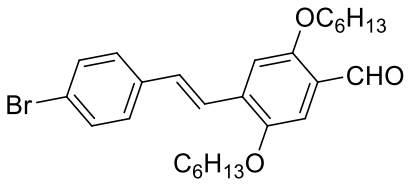

4-(4-bromostyryl)-2,5-bishexyloxybenzaldehyde (Br-AB'-CHO). According to the general DIBAL-H procedure, **Br-AB'-CN** (2.154 g, 4.446 mmol) was dissolved in DCM (25 mL) and cooled to 0 ^{O}C. DIBAL-H (1.0M in hexanes, 4.5 mL, 4.5 mmol) was added dropwise. After workup, column chromatography (silica gel, 3:2 hexanes:DCM) gave the title compound as a yellow oil that crystallized on standing (2.095 g, 95%). ^{1}H NMR (CD_2Cl_2, 400 MHz) δ 0.85-1.00 (6H, mult), 1.30-1.45 (8H, mult), 1.45-1.55 (4H, mult), 1.70-1.80 (4H, mult), 4.02 (2H, t, *J* = 6.4

Hz, OCH_2), 4.12 (2H, t, *J* = 6.4 Hz, OCH_2), 7.20 (1H, s), 7.30 (1H, s), 7.22 (1H, d, *J* = 16.4 Hz, *trans* CH=CH), 7.44 (2H, d, *J* = 8.4 Hz, *p*-C_6H_4), 7.49 (1H, d, *J* = 16.4 Hz, *trans* CH=CH), 7.51 (2H, d, *J* = 8.4 Hz, *p*-C_6H_4), 10.43 (1h, s, CHO) ppm. ^{13}C NMR (CD_2Cl_2, 100 MHz) δ 14.37 (CH_3), 23.17 (CH_2), 23.19 (CH_2), 26.32 (CH_2), 26.42 (CH_2), 29.76 (CH_2), 29.78 (CH_2), 32.13 (CH_2), 32.14 (CH_2), 69.75 (OCH_2), 69.85 (OCH_2), 110.50 (Ar CH), 111.26 (Ar CH), 122.38 (ArBr quat), 124.14 (vinylene CH), 125.06 (Ar quat), 128.86 (Ar CH), 131.28 (vinylene CH), 132.40 (Ar CH), 134.13 (Ar quat), 136.89 (Ar quat), 151.33 (ArO quat), 156.68 (ArO quat), 189.25 (CHO) ppm. MS (EI): 488 (M+2), 486 (M^+, base), 402, 374, 320, 318, 234, 206, 181, 165, 152, 119 m/z. HRMS calcd for $C_{27}H_{35}O_3Br$: 486.1770 g/mol. Found: 486.1763 g/mol.

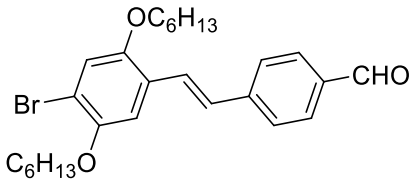

4-(4-bromo-2,5-bishexyloxystyryl)benzaldehyde (Br-BA'-CHO). According to the general DIBAL-H procedure, **Br-BA'-CN** (2.560 g, 5.28 mmol) was dissolved in DCM (30 mL) and cooled to 0 ^{O}C. DIBAL-H (1.0M in hexanes, 5.3 mL, 5.3 mmol) was added dropwise. After workup, column chromatography (silica gel, 3:2 hexanes:DCM) gave the title compound as a yellow solid (2.420 g, 94%). ^{1}H NMR (CD_2Cl_2, 400 MHz) δ 0.85-1.00 (6H, mult), 1.30-1.45 (8H, mult), 1.45-1.55 (4H, mult), 1.70-1.80 (4H, mult), 3.98 (2H, t, *J* = 6.4 Hz, OCH_2), 4.04 (2H, t, *J* = 6.4 Hz, OCH_2), 7.13 (1H, s), 7.16 (1H, s), 7.21 (1H, d, *J* = 16.4 Hz, *trans* CH=CH), 7.57 (1H, d, *J* = 16.4 Hz, *trans* CH=CH), 7.68 (2H, d, *J* = 8.4 Hz, *p*-C_6H_4), 7.86 (2H, d, *J* = 8.4 Hz, *p*-C_6H_4), 9.98 (1H, s, CHO) ppm. ^{13}C NMR (CD_2Cl_2, 100 MHz) δ 14.37 (CH_3), 14.39 (CH_3), 23.19 (CH_2), 26.25 (CH_2), 26.41 (CH_2), 29.79 (CH_2), 29.83 (CH_2), 32.13 (CH_2), 70.20 (OCH_2), 70.73 (OCH_2), 112.10

(Ar CH), 113.25 (ArBr quat), 118.36 (Ar CH), 126.19 (Ar quat), 126.93 (vinylene CH), 127.41 (Ar CH), 128.46 (vinylene CH), 130.62 (Ar CH), 135.96 (Ar quat), 144.27 (Ar quat), 150.35 (ArO quat), 151.95 (ArO quat), 191.95 (CHO) ppm.

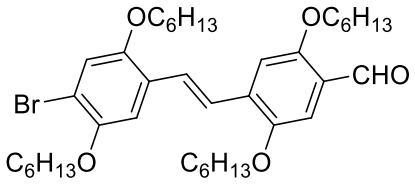

4-(4-bromo-2,5-bishexyloxystyryl)-2,5-bishexyloxybenzaldehyde (Br-BB'-CHO). According to the general DIBAL-H procedure, **Br-BB-CN** (2.00 g, 2.92 mmol) was dissolved in DCM (20 mL) and cooled to 0 ^{O}C. DIBAL-H (1.0M in hexanes, 3.0 mL, 3.0 mmol) was added dropwise. After workup, column chromatography (silica gel, 4:1 hexanes:DCM) gave the title compound as a yellow solid (1.843 g, 92%). ^{1}H NMR (CD_2Cl_2, 400 MHz) δ 0.85-1.00 (12H, mult), 1.30-1.45 (16H, mult), 1.45-1.55 (8H, mult), 1.70-1.80 (8H, mult), 3.98 (2H, t, *J* = 6.4 Hz, OCH_2), 4.03 (2H, t, *J* = 6.4 Hz, OCH_2), 4.04 (2H, t, *J* = 6.4 Hz, OCH_2), 4.11 (2H, t, *J* = 6.4 Hz, OCH_2), 7.13 (1H, s), 7.17 (1H, s), 7.23 (1H, s), 7.30 (1H, s), 7.50 (1H, d, *J* = 16.8 Hz, *trans* CH=CH), 7.58 (1H, d, *J* = 16.8 Hz, *trans* CH=CH), 10.43 (1H, s, CHO) ppm. ^{13}C NMR (CD_2Cl_2, 100 MHz) δ 14.40 (CH_3), 23.19 (CH_2), 23.24 (CH_2), 26.28 (CH_2), 26.35 (CH_2), 26.40 (CH_2), 29.42 (CH_2), 29.81 (CH_2), 29.83 (CH_2), 29.85 (CH_2), 32.14 (CH_2), 32.17 (CH_2), 32.18 (CH_2), 69.68 (OCH_2), 69.78 (OCH_2), 70.13 (OCH_2), 70.68 (OCH_2), 110.41 (Ar CH), 111.17 (Ar CH), 112.19 (Ar CH), 112.94 (ArBr quat), 118.29 (Ar CH), 124.05 (vinylene CH), 124.84 (Ar quat), 126.92 (Ar quat), 127.07 (vinylene CH), 135.02 (Ar quat), 150.35 (ArO quat), 151.28 (ArO quat), 151.89 (ArO quat), 156.75 (ArO quat), 189.25 (CHO) ppm. MS (ESI): 711 (M+Na+2, base), 709 (M+Na), 631, 527, 365 m/z. HRMS calcd for $C_{39}H_{59}O_5Br$+Na: 709.3444 g/mol. Found: 709.3455 g/mol.

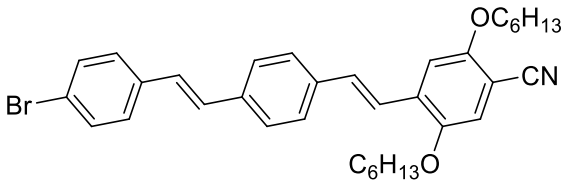

4-(4-(4-bromostyryl)styryl)-2,5-bishexyloxybenzonitrile (Br-AAB'-CN). According to the general HWE procedure, **Br-AA'-CHO** (700 mg, 2.44 mmol), **P-B'-CN** (**4**) (1.557 g, 3.66 mmol), and LiCl (237 mg, 5.59 mmol) were dissolved in THF (30 mL) and cooled to 0 °C under N_2. KO^{t}Bu (627 mg, 5.59 mmol) was added portionwise over 5 minutes, and the reaction was allowed to come to rt overnight with stirring. After workup, column chromatography (silica gel, 7:3 hexanes:DCM) gave the title compound as a yellow solid (1.166 g, 84%). ^{1}H NMR (CD_2Cl_2, 400 MHz) δ 0.93 (6H, t, *J* = 7.0 Hz), 1.30-1.40 (8H, mult), 1.50-1.60 (4H, mult), 1.86 (4H, pent, *J* = 7.3 Hz), 3.98 (2H, t, *J* = 6.4 Hz, OCH_2), 4.11 (2H, t, *J* = 6.4 Hz, OCH_2), 7.05 (1H, s), 7.09 (1H, d, *J* = 16.4 Hz, *trans* CH=CH), 7.14 (1H, d, *J* = 16.4 Hz, *trans* CH=CH), 7.19 (1H, s), 7.25 (1H, d, *J* = 16.4 Hz, *trans* CH=CH), 7.42 (2H, d, *J* = 8.8 Hz, *p*-C_6H_4), 7.48 (1H, d, *J* = 16.4 Hz, *trans* CH=CH), 7.50 (2H, d, *J* = 8.8 Hz, *p*-C_6H_4), 7.53 (2H, d, *J* = 8.8 Hz, *p*-C_6H_4), 7.56 (2H, d, *J* = 8.8 Hz, *p*-C_6H_4) ppm. ^{13}C NMR (CD_2Cl_2, 100 MHz) δ 14.38 (CH_3), 23.16 (CH_2), 23.18 (CH_2), 26.13 (CH_2), 26.39 (CH_2), 29.64 (CH_2), 29.73 (CH_2), 32.09 (CH_2), 32.13 (CH_2), 70.15 (OCH_2), 70.27 (OCH_2), 100.95 (ArCN quat), 110.66 (Ar CH), 117.07 (Ar CH), 117.23 (CN), 121.89 (ArBr quat), 122.83 (vinylene CH), 127.52 (Ar CH), 127.81 (Ar CH), 128.13 (vinylene CH), 128.60 (Ar CH), 129.35 (vinylene CH), 132.16 (vinylene CH), 132.36 (Ar CH), 133.22 (Ar quat), 136.86 (Ar quat), 137.28 (Ar quat), 137.59 (Ar quat), 150.80 (ArO quat), 155.72 (ArO quat) ppm. MS (ES): 587 (M+2), 585 (M^+), 419, 420, 251, 228, 181, 169, 131, 119, 100, 69 (base), 55 m/z. HRMS calcd for $C_{35}H_{40}NO_2Br$: 585.2242 g/mol. Found: 585.2240 g/mol.

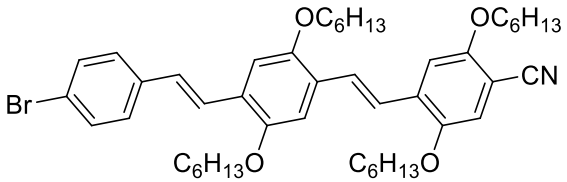

4-(4-(4-bromostyryl)-2,5-bishexyloxystyryl)-2,5-bishexyloxybenzonitrile (Br-ABB'-CN). According to the general HWE procedure, **Br-AB'-CHO** (850 mg, 1.74 mmol), **P-B'-CN** (**4**) (1.11 g, 2.61 mmol), and LiCl (170 mg, 4.01 mmol) were dissolved in THF (25 mL) and cooled to 0 ^{o}C under N_2. KO^{t}Bu (450 mg, 4.01 mmol) was added portionwise over 5 minutes, and the reaction was allowed to come to rt overnight with stirring. After workup, column chromatography (silica gel, 4:1 hexanes:DCM) gave the title compound as a yellow solid (1.181 g, 86%). %). ^{1}H NMR (CD_2Cl_2, 400 MHz) δ 0.85-0.95 (12H, mult), 1.30-1.45 (16H, mult), 1.45-1.60 (8H, mult), 1.80-1.95 (8H, mult), 3.98 (2H, t, *J* = 6.4 Hz, OCH_2), 4.05 (2H, t, *J* = 6.4 Hz, OCH_2), 4.07 (2H, t, *J* = 6.4 Hz, OCH_2), 4.10 (2H, t, *J* = 6.4 Hz, OCH_2), 7.04 (1H, s), 7.13 (1H, d, *J* = 16.4 Hz, *trans* CH=CH), 7.14 (1H, s), 7.15 (1H, s), 7.20 (1H, s), 7.42 (2H, d, *J* = 8.4 Hz, *p*-C_6H_4), 7.46-7.51 (4H, mult) 7.59 (1H d, *J* = 16.8 Hz, *trans* CH=CH) ppm. ^{13}C NMR (CD_2Cl_2, 100 MHz) δ 14.37 (CH_3), 14.39 (CH_3), 23.16 (CH_2), 23.23 (CH_2), 23.25 (CH_2), 26.15 (CH_2), 26.39 (CH_2), 26.48 (CH_2), 26.54 (CH_2), 29.66 (CH_2), 29.75 (CH_2), 30.00 (CH_2), 32.10 (CH_2), 32.16 (CH_2), 32.16 (CH_2), 69.96 (OCH_2), 70.02 (OCH_2), 70.08 (OCH_2), 70.19 (OCH_2), 100.64 (ArCN quat), 110.59 (Ar CH), 110.91 (Ar CH), 111.31 (Ar CH), 117.07 (Ar CH), 117.32 (CN), 121.62 (ArBr quat), 122.99 (vinylene CH), 124.59 (vinylene CH), 127.22 (Ar quat), 127.50 (vinylene CH), 127.70 (Ar quat), 128.33 (vinylene CH), 128.56 (Ar CH), 132.31 (Ar CH) 133.97 (Ar quat), 137.50 (Ar quat), 150.74 (ArO quat), 151.66 (ArO quat), 151.94 (ArO quat), 155.72 (ArO quat) ppm. MS (ESI): 810

(M+Na+2, base), 808 (M+Na), 788, 786, 776, 685 (base)\m/z. HRMS calcd for $C_{47}H_{64}NO_4Br$+Na: 808.3916 g/mol. Found: 808.3965 g/mol.

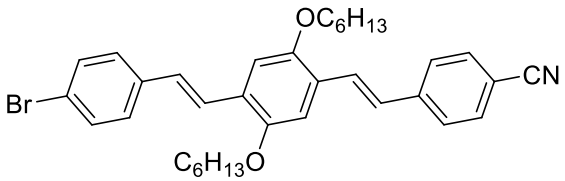

4-(4-(4-bromostyryl)-2,5-bishexyloxystyryl)benzonitrile (Br-ABA'-CN). According to the general HWE procedure, **Br-AB'-CHO** (850 mg, 1.74 mmol), **P-A'-CN** (**3**) (588 mg, 2.61 mmol), and LiCl (170 mg, 4.01 mmol) were dissolved in THF (25 mL) and cooled to 0 ^oC under N_2. KO^{t}Bu (450 mg, 4.01 mmol) was added portionwise over 5 minutes, and the reaction was allowed to come to rt overnight with stirring. After workup, column chromatography (silica gel, 2:3 hexanes:DCM) gave the title compound as a yellow solid (950 mg, 92%). ^1H NMR (CD_2Cl_2, 400 MHz) δ 0.93 (6H, t, *J* = 7.0 Hz), 1.30-1.45 (8H, mult), 1.45-1.60 (4H, mult), 1.86 (4H, pent, *J* = 6.7 Hz), 4.06 (2H, t, *J* = 6.4 Hz, OCH_2), 4.07 (2H, t, *J* = 6.4 Hz, OCH_2), 7.13 (1H, d, *J* = 16.4 Hz, *trans* CH=CH), 7.135 (1H, s), 7.138 (1H, s), 7.18 (1H, d, *J* = 16.4 Hz, *trans* CH=CH), 7.42 (2H, d, *J* = 8.4 Hz, *p*-C_6H_4), 7.48 (1H, d, *J* = 16.4 Hz, *trans* CH=CH), 7.50 (2H, d, *J* = 8.4 Hz, *p*-C_6H_4), 7.61 (1H, d, *J* = 16.4 Hz, *trans* CH=CH), 7.61 (2H, d, *J* = 8.8 Hz, *p*-C_6H_4), 7.65 (2H, d, *J* = 8.8 Hz, *p*-C_6H_4) ppm. ^{13}C NMR (CD_2Cl_2, 100 MHz) δ 14.39 (CH_3), 23.23 (CH_2), 26.51 (CH_2), 29.98 (CH_2), 32.20 (CH_2), 70.02 (OCH_2), 70.06 (OCH_2), 110.83 (ArCN quat), 110.95 (Ar CH), 111.23 (Ar CH), 119.61 (CN), 121.66 (ArBr quat), 124.55 (vinylene CH), 126.44 (Ar quat), 127.57 (Ar CH), 127.39 (vinylene CH), 127.57 (vinylene CH), 127.98 (Ar quat) 128.48 (vinylene CH), 128.58 (Ar CH), 132.30 (vinylene CH), 133.02 (Ar CH), 137.45 (Ar quat), 143.03 (Ar quat), 151.64 (ArO quat), 152.02 (ArO quat) ppm. MS (ES): 587 (M+2), 585 (M^+), 485, 483, 419, 417,

401, 317, 315, 290, 235, 206, 169, 152, 131, 116, 85, 69, 55 (base) m/z. HRMS calcd for $C_{35}H_{40}NO_2Br$: 585.2242 g/mol. Found: 585.2237 g/mol.

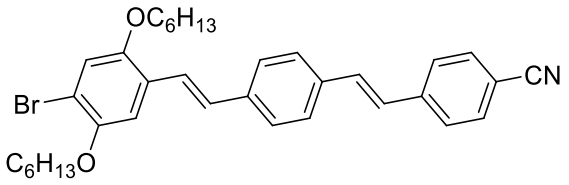

4-(4-(4-bromo-2,5-bishexyloxystyryl)styryl)benzonitrile (Br-BAA'-CN). According to the general HWE procedure, **Br-BA'-CHO** (1.10 g, 2.26 mmol), **P-A'-CN** (**3**) (761 mg, 3.38 mmol), and LiCl (220 mg, 4.01 mmol) were dissolved in THF (40 mL) and cooled to 0 ^oC under N_2. KO^{t}Bu (583 mg, 5.19 mmol) was added portionwise over 5 minutes, and the reaction was allowed to come to rt overnight with stirring. After workup, column chromatography (silica gel, 2:3 hexanes:DCM) gave the title compound as a yellow solid (1.305 g, 99%). ^1H NMR (CD_2Cl_2, 400 MHz) δ 0.93 (6H, t, *J* = 6.4 Hz), 1.30-1.45 (8H, mult), 1.50-1.60 (4H, mult), 1.83 (2H, pent, *J* = 6.8 Hz), 1.85 (2H, pent, *J* = 6.8 Hz), 3.97 (2H, t, *J* = 6.4 Hz, OCH_2), 4.04 (2H, t, *J* = 6.4 Hz, OCH_2), 7.12 (1H, s), 7.14 (1H, d, *J* = 16.0 Hz, *trans* CH=CH), 7.16 (1H, s), 7.16 (1H, d, *J* = 16.4 Hz, *trans* CH=CH), 7.25 (1H, d, *J* = 16.0 Hz, *trans* CH=CH), 7.46 (1H, d, *J* = 16.4 Hz, *trans* CH=CH), 7.55 (4H, br s, *p*-C_6H_4), 7.61 (2H, d, *J* = 8.8 Hz, *p*-C_6H_4), 7.65 (2H, d, *J* = 8.8 Hz, *p*-C_6H_4) ppm. ^{13}C NMR (CD_2Cl_2, 100 MHz) δ 14.39 (CH_3), 23.21 (CH_2), 26.26 (CH_2), 26.42 (CH_2), 29.84 (CH_2), 29.86 (CH_2), 32.14 (CH_2), 32.15 (CH_2), 70.22 (OCH_2), 70.74 (OCH_2), 110.10 (ArCN quat), 110.93 (Ar CH), 112.41 (ArBr quat), 118.35 (Ar CH), 119.52 (CN), 123.97 (vinylene CH), 126.87 (Ar quat), 127.06 (vinylene CH), 127.38 (Ar CH), 127.47 (Ar CH), 127.85 (Ar CH), 129.15 (vinylene CH), 132.34 (vinylene CH), 133.06 (Ar CH), 136.27 (Ar quat), 138.62 (Ar quat), 142.40 (Ar quat), 150.38 (ArO quat), 151.73 (ArO quat) ppm. MS (ESI): 610 (M+Na+2), 608

(M+Na), 527, 365 (base)\m/z. HRMS calcd for $C_{35}H40NO_2Br$+Na: 608.2140 g/mol. Found: 608.2094 g/mol.

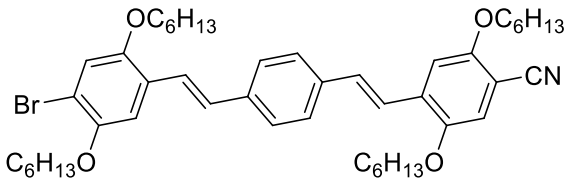

4-(4-(4-bromo-2,5-bishexyloxystyryl)styryl)-2,5-bishexyloxystyrylbenzonitrile (Br-BAB'-CN). According to the general HWE procedure, **Br-BA'-CHO** (1.10 g, 2.26 mmol), **P-B'-CN** (**4**) (1.44 g, 3.38 mmol), and LiCl (220 mg, 4.01 mmol) were dissolved in THF (30 mL) and cooled to 0 ^oC under N_2. KO^{t}Bu (583 mg, 5.19 mmol) was added portionwise over 5 minutes, and the reaction was allowed to come to rt overnight with stirring. After workup, column chromatography (silica gel, 7:3 hexanes:DCM) gave the title compound as a yellow solid (1.687 g, 95%). ^1H NMR (CD_2Cl_2, 400 MHz) δ 0.85-0.95 (12H, mult), 1.30-1.45 (16H, mult), 1.45-1.60 (8H, mult), 1.80-1.95 (8H, mult), 3.97 (2H, t, *J* = 6.4 Hz, OCH_2), 3.98 (2H, t, *J* = 6.4 Hz, OCH_2), 4.04 (2H, t, *J* = 6.4 Hz, OCH_2), 4.11 (2H, t, *J* = 6.4 Hz, OCH_2), 7.04 (1H, s), 7.12 (1H, s), 7.16 (1H, d, *J* = 16.4 Hz, *trans* CH=CH), 7.16(1H, s), 7.19 (1H, s), 7.25 (1H, d, *J* = 16.4 Hz, *trans* CH=CH), 7.46 (1H, d, *J* = 16.4 Hz, *trans* CH=CH), 7.48 (1H, d, *J* = 16.4 Hz, *trans* CH=CH), 7.55 (4H, br s, *p*-C_6H_4) ppm. ^{13}C NMR (CD_2Cl_2, 100 MHz) δ 14.39 (CH_3), 23.18 (CH_2), 23.21 (CH_2), 26.14 (CH_2), 26.27 (CH_2), 26.41 (CH_2), 26.44 (CH_2), 29.66 (CH_2), 29.74 (CH_2), 29.86 (CH_2), 29.87 (CH_2), 32.11 (CH_2), 32.15 (CH_2), 32.17 (CH_2), 70.15 (OCH_2), 70.23 (OCH_2), 70.26 (OCH_2), 70.75 (OCH_2), 100.88 (ArCN quat), 110.60 (Ar CH), 111.89 (Ar CH), 112.35 (ArBr quat), 117.05 (Ar CH), 117.25 (CN), 118.35 (Ar CH), 122.60 (vinylene CH), 123.77 (vinylene CH), 126.92 (Ar quat), 127.45 (Ar CH), 127.79 (Ar CH), 129.21 (vinylene CH), 133.27 (vinylene CH) 133.27 (Ar

quat), 136.99 (Ar quat), 138.36 (Ar quat), 150.38 (ArO quat), 150.78 (ArO quat), 151.72 (ArO quat), 155.73 (ArO quat) ppm. MS (ESI): 810 (M+Na+2), 808 (M+Na), 788, 786, 711, 709, 691, 527 (base)\m/z. HRMS calcd for $C_{47}H_{64}NO_4Br$+Na: 808.3916 g/mol. Found: 808.4011 g/mol.

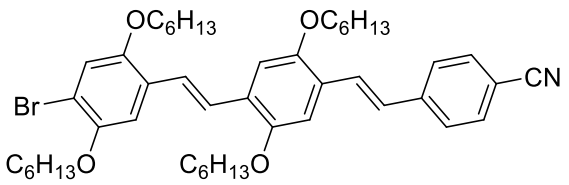

4-(4-(4-bromo-2,5-bishexyloxystyryl)-2,5-bishexyloxystyrylstyryl)benzonitrile (Br-BBA'-CN). According to the general HWE procedure, **Br-BB'-CHO** (1.64 g, 2.39 mmol), **P-A'-CN** (**3**) (807 mg, 3.58 mmol), were dissolved in THF (30 mL) and cooled to 0 ^{o}C under N_2. KO^{t}Bu (618 mg, 5.50 mmol) was added portionwise over 5 minutes, and the reaction was allowed to come to rt overnight with stirring. After workup, column chromatography (silica gel, 1:1 hexanes:DCM) gave the title compound as a yellow solid (1.610 g, 86%). ^{1}H NMR (CD_2Cl_2, 400 MHz) δ 0.85-0.95 (12H, mult), 1.30-1.45 (16H, mult), 1.45-1.60 (8H, mult), 1.80-1.95 (8H, mult), 3.98 (2H, t, *J* = 6.4 Hz, OCH_2), 4.04 (2H, t, *J* = 6.4 Hz, OCH_2), 4.06 (2H, t, *J* = 6.4 Hz, OCH_2), 4.07 (2H, t, *J* = 6.4 Hz, OCH_2), 7.11 (1H, s), 7.14 (1H, s), 7.17 (1H, s), 7.18 (1H, d, *J* = 16.4 Hz, *trans* CH=CH), 7.18 (1H, s), 7.45 (1H, d, *J* = 16.8 Hz, *trans* CH=CH), 7.50 (1H, d, *J* = 16.8 Hz, *trans* CH=CH), 7.62 (1H, d, *J* = 16.4 Hz, *trans* CH=CH), 7.62 (2H, d, *J* = 8.8 Hz, *p*-C_6H_4), 7.65 (2H, d, *J* = 8.8 Hz, *p*-C_6H_4) ppm. ^{13}C NMR (CD_2Cl_2, 100 MHz) δ 14.40 (CH_3), 14.42 (CH_3), 14.43 (CH_3), 23.20 (CH_2), 23.24 (CH_2), 23.26 (CH_2), 26.29 (CH_2), 26.42 (CH_2), 26.50 (CH_2), 26.54 (CH_2), 29.88 (CH_2), 30.00 (CH_2), 30.02 (CH_2), 32.15 (CH_2), 32.19 (CH_2), 32.21 (CH_2), 32.24 (CH_2), 69.97 (OCH_2), 70.00 (OCH_2), 70.15 (OCH_2), 70.69 (OCH_2), 110.78 (Ar CH), 110.95 (Ar CH), 111.17 (ArCN quat), 111.95 (Ar CH), 112.13 (ArBr quat), 118.28 (Ar CH), 119.62 (CN), 124.15 (vinylene

CH), 124.42 (vinylene CH), 126.14 (Ar quat), 127.21 (vinylene CH), 127.30 (Ar CH), 127.55 (Ar quat), 127.64 (vinylene CH), 128.81 (Ar quat), 133.03 (Ar CH), 143.10 (Ar quat), 150.37 (ArO quat), 151.58 (ArO quat), 151.68 (ArO quat), 152.05 (ArO quat) ppm. MS (ESI): 810 (M+Na+2), 808 (M+Na), 788, 786, 711, 709, 691, 527 (base)\m/z. HRMS calcd for $C_{47}H_{64}NO_4Br$+Na: 808.3916 g/mol. Found: 808.4011 g/mol. MS (ESI): 810 (M+Na+2), 808 (M+Na), 786, 776, 707, 527, 365 (base)\m/z. HRMS calcd for $C_{47}H_{64}NO_4Br$+Na: 808.3916 g/mol. Found: 808.3856 g/mol.

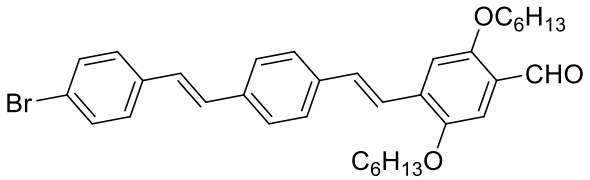

4-(4-(4-bromostyryl)styryl)-2,5-bishexyloxybenzaldehyde (Br-AAB'-CHO). According to the general DIBAL-H procedure, **Br-AAB'-CN** (375 mg, 0.635 mmol) was dissolved in DCM (5 mL) and cooled to 0 ^{O}C. DIBAL-H (1.0M in hexanes, 0.75 mL, 0.75 mmol) was added dropwise. After workup, column chromatography (silica gel, 7:3 hexanes:DCM) gave the title compound as a yellow solid (308 mg, 82%). ^{1}H NMR (CD_2Cl_2, 400 MHz) δ 0.93 (6H, t, *J* = 7.0 Hz), 1.30-1.40 (8H, mult), 1.50-1.60 (4H, mult), 1.86 (4H, pent, *J* = 7.1 Hz), 4.04 (2H, t, *J* = 6.4 Hz, OCH_2), 4.12 (2H, t, *J* = 6.4 Hz, OCH_2), 7.09 (1H, d, *J* = 16.4 Hz, *trans* CH=CH), 7.14 (1H, d, *J* = 16.4 Hz, *trans* CH=CH), 7.22 (1H, s), 7.28 (1H, d, *J* = 16.4 Hz, *trans* CH=CH), 7.30 (1H, s), 7.41 (2H, d, *J* = 8.8 Hz, *p*-C_6H_4), 7.50 (2H, d, *J* = 8.8 Hz, *p*-C_6H_4), 7.53 (1H, d, *J* = 16.4 Hz, *trans* CH=CH), 7.54 (2H, d, *J* = 8.8 Hz, *p*-C_6H_4), 7.57 (2H, d, *J* = 8.4 Hz, *p*-C_6H_4), 10.44 (1H, s, CHO) ppm. ^{13}C NMR (CD_2Cl_2, 100 MHz) δ 14.39 (CH_3), 23.16 (CH_2), 23.18 (CH_2), 23.21 (CH_2), 26.33 (CH_2), 26.44 (CH_2), 29.79 (CH_2), 32.13 (CH_2), 32.17 (CH_2), 69.76 (OCH_2), 69.84 (OCH_2), 110.47 (Ar CH), 111.07 (Ar CH), 121.85 (ArBr quat), 123.35 (vinylene CH), 124.89 (Ar

quat), 127.51 (Ar CH), 127.79 (Ar CH), 128.03 (vinylene CH), 128.58 (Ar CH), 129.37 (vinylene CH), 132.11 (vinylene CH), 132.34 (Ar CH), 133.53 (Ar quat), 136.87 (Ar quat), 137.47 (Ar quat), 151.32 (ArO quat), 156.73 (ArO quat) 189.24 (CHO) ppm. MS (ES): 590 (M+2), 588 (M^+), 420, 288, 286, 178 (base), 152, 131, 102, 90, 77, 69, 55 m/z. HRMS calcd for $C_{35}H_{41}O_3Br$: 588.2239 g/mol. Found: 588.2239 g/mol.

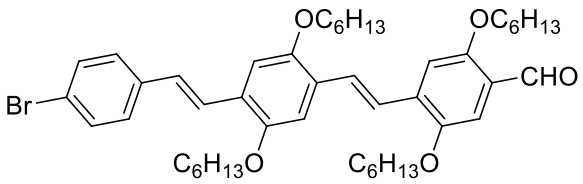

4-(4-(4-bromostyryl)-2,5-bishexyloxystyryl)-2,5-bishexyloxybenzaldehyde (Br-ABB'-CHO). According to the general DIBAL-H procedure, **Br-ABB'-CN** (500 mg, 0.635 mmol) was dissolved in DCM (5 mL) and cooled to 0 ^{O}C. DIBAL-H (1.0M in hexanes, 0.75 mL, 0.75 mmol) was added dropwise. After workup, column chromatography (silica gel, 7:3 hexanes:DCM) gave the title compound as a yellow solid (409 mg, 82%). ^{1}H NMR (CD_2Cl_2, 400 MHz) δ 0.85-0.95 (12H, mult), 1.30-1.45 (16H, mult), 1.45-1.60 (8H, mult), 1.80-1.95 (8H, mult), 4.05 (2H, t, *J* = 6.4 Hz, OCH_2), 4.06 (2H, t, *J* = 6.4 Hz, OCH_2), 4.07 (2H, t, *J* = 6.4 Hz, OCH_2), 7.04 (1H, s), 4.14 (2H, t, *J* = 6.4 Hz, OCH_2), 7.13 (1H, d, *J* = 16.4 Hz, *trans* CH=CH), 7.15 (1H, s), 7.17 (1H, s), 7.25 (1H, s), 7.30 (1H, s), 7.43 (2H, d, *J* = 8.4 Hz, *p*-C_6H_4), 7.50 (2H, d, *J* = 8.4 Hz, *p*-C_6H_4), 7.50 (1H d, *J* = 16.4 Hz, *trans* CH=CH), 7.53 (1H d, *J* = 16.8 Hz, *trans* CH=CH), 7.63 (1H d, *J* = 16.8 Hz, *trans* CH=CH), 10.43 (1H, s, CHO) ppm. ^{13}C NMR (CD_2Cl_2, 100 MHz) δ 14.38 (CH_3), 14.41 (CH_3), 23.18 (CH_2), 23.24 (CH_2), 23.26 (CH_2), 26.35 (CH_2), 26.44 (CH_2), 26.50 (CH_2), 26.53 (CH_2), 29.81 (CH_2), 30.00 (CH_2), 32.14 (CH_2), 32.19 (CH_2), 32.20 (CH_2), 32.23 (CH_2), 69.70 (OCH_2), 69.78 (OCH_2), 69.96 (OCH_2), 69.99 (OCH_2), 110.40 (Ar CH), 110.90 (Ar CH), 110.99

(Ar CH), 111.22 (Ar CH), 121.59 (ArBr quat), 123.49 (vinylene CH), 124.61 (vinylene CH), 124.72 (Ar quat), 127.43 (Ar quat), 127.43 (vinylene CH), 127.57 (Ar quat), 128.24 (vinylene CH), 128.55 (Ar CH), 132.30 (Ar CH) 135.31 (Ar quat), 137.51 (Ar quat), 151.27 (ArO quat), 151.67 (ArO quat), 151.92 (ArO quat), 156.79 (ArO quat), 189.25 (CHO) ppm.

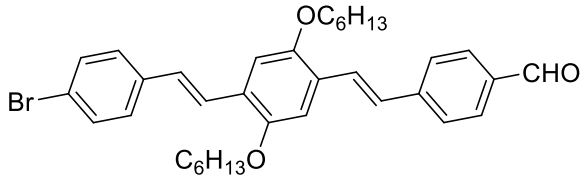

4-(4-(4-bromostyryl)-2,5-bishexyloxystyryl)benzaldehyde (Br-ABA'-CHO). According to the general DIBAL-H procedure, **Br-ABA'-CN** (375 mg, 0.635 mmol) was dissolved in DCM (5 mL) and cooled to 0 ^{O}C. DIBAL-H (1.0M in hexanes, 0.75 mL, 0.75 mmol) was added dropwise. After workup, column chromatography (silica gel, 2:3 hexanes:DCM) gave the title compound as a yellow solid (302 mg, 81%). ^{1}H NMR (CD_2Cl_2, 400 MHz) δ 0.94 (6H, t, *J* = 6.8 Hz), 1.30-1.45 (8H, mult), 1.45-1.60 (4H, mult), 1.80-1.95 (4H, mult), 4.06 (2H, t, *J* = 6.4 Hz, OCH_2), 4.07 (2H, t, *J* = 6.4 Hz, OCH_2), 7.13 (1H, d, *J* = 16.4 Hz, *trans* CH=CH), 7.14 (1H, s), 7.15 (1H, s), 7.23 (1H, d, *J* = 16.8 Hz, *trans* CH=CH), 7.42 (2H, d, *J* = 8.4 Hz, *p*-C_6H_4), 7.49 (1H, d, *J* = 16.4 Hz, *trans* CH=CH), 7.50 (2H, d, *J* = 8.4 Hz, *p*-C_6H_4), 7.60 (1H, d, *J* = 16.8 Hz, *trans* CH=CH), 7.69 (2H, d, *J* = 8.4 Hz, *p*-C_6H_4), 7.86 (2H, d, *J* = 8.4 Hz, *p*-C_6H_4), 9.98 (CHO) ppm. ^{13}C NMR (CD_2Cl_2, 100 MHz) δ 14.41 (CH_3), 23.24 (CH_2), 26.53 (CH_2), 30.00 (CH_2), 32.21 (CH_2), 70.04 (OCH_2), 110.93 (Ar CH), 111.16 (Ar CH), 121.63 (ArBr quat), 124.57 (vinylene CH), 126.69 (Ar quat), 127.36 (Ar CH), 127.36 (vinylene CH), 127.84 (Ar quat), 127.96 (vinylene CH), 128.38 (vinylene CH), 128.57 (Ar CH), 130.62 (Ar CH), 132.30 (Ar CH), 135.83 (Ar quat), 137.47 (Ar quat) 144.56 (Ar quat), 151.65 (ArO quat), 152.00 (ArO quat), 191.94 (CHO) ppm.

MS (ES): 590 (M+2), 588 (M^+), 504, 476, 420, 422, 340, 265, 149, 131, 127, 91, 85, 69 (base) m/z. HRMS calcd for $C_{35}H_{41}O_3Br$: 588.2239 g/mol. Found: 588.2231 g/mol.

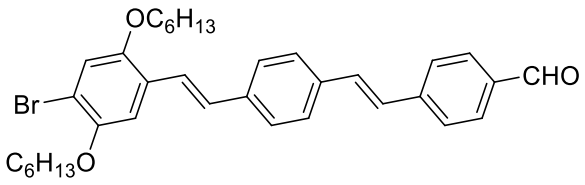

4-(4-(4-bromo-2,5-bishexyloxystyryl)styryl)benzaldehyde (Br-BAA'-CHO). According to the general DIBAL-H procedure, **Br-BAA'-CN** (375 mg, 0.635 mmol) was dissolved in DCM (5 mL) and cooled to 0 ^{O}C. DIBAL-H (1.0M in hexanes, 0.75 mL, 0.75 mmol) was added dropwise. After workup, column chromatography (silica gel, 7:3 hexanes:DCM) gave the title compound as a yellow solid (348 mg, 93%). ^{1}H NMR (CD_2Cl_2, 400 MHz) δ 0.95 (6H, t, *J* = 6.0 Hz), 1.30-1.45 (8H, mult), 1.50-1.60 (4H, mult), 1.83 (2H, pent, *J* = 6.8 Hz), 1.85 (2H, pent, *J* = 6.8 Hz), 3.97 (2H, t, *J* = 6.4 Hz, OCH_2), 4.04 (2H, t, *J* = 6.4 Hz, OCH_2), 7.12 (1H, s), 7.16 (1H, d, *J* = 16.8 Hz, *trans* CH=CH), 7.16 (1H, s), 7.19 (1H, d, *J* = 16.4 Hz, *trans* CH=CH), 7.29 (1H, d, *J* = 16.4 Hz, *trans* CH=CH), 7.46 (1H, d, *J* = 16.8 Hz, *trans* CH=CH), 7.56 (4H, br s, *p*-C_6H_4), 7.68 (2H, d, *J* = 8.4 Hz, *p*-C_6H_4), 7.87 (2H, d, *J* = 8.4 Hz, *p*-C_6H_4), 9.98 (1H, s, CHO) ppm. ^{13}C NMR (CD_2Cl_2, 100 MHz) δ 14.40 (CH_3), 23.20 (CH_2), 23.22 (CH_2), 26.26 (CH_2), 26.42 (CH_2), 29.84 (CH_2), 29.86 (CH_2), 32.14 (CH_2), 32.15 (CH_2), 70.20 (OCH_2), 70.72 (OCH_2), 111.88 (Ar CH), 112.35 (ArBr quat), 118.32 (Ar CH), 123.87 (vinylene CH), 126.87 (Ar quat), 127.41 (Ar CH), 127.46 (Ar CH), 127.63 (vinylene CH), 127.83 (Ar CH), 129.18 (vinylene CH), 130.63 (Ar CH), 132.34 (vinylene CH), 135.98 (Ar quat), 136.49 (Ar quat), 138.49 (Ar quat),143.89 (Ar quat), 150.35 (ArO quat), 151.70 (ArO quat), 191.92 (CHO) ppm. MS (ES): 590 (M+2), 588 (M^+),

422, 420, 221, 181, 131, 119, 100, 85, 69 (base) m/z. HRMS calcd for $C_{35}H_{41}O_3Br$: 588.2239 g/mol. Found: 588.2230 g/mol.

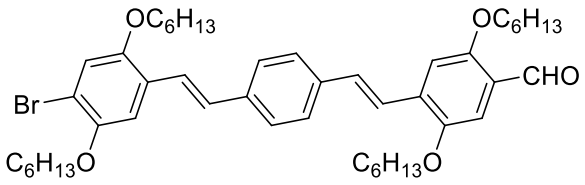

4-(4-(4-bromo-2,5-bishexyloxystyryl)styryl)-2,5-bishexyloxystyrylbenzaldehyde (Br-BAB'-CHO). According to the general DIBAL-H procedure, **Br-BAB'-CN** (500 mg, 0.635 mmol) was dissolved in DCM (5 mL) and cooled to 0 ^{O}C. DIBAL-H (1.0M in hexanes, 0.75 mL, 0.75 mmol) was added dropwise. After workup, column chromatography (silica gel, 2:3 hexanes:DCM) gave the title compound as a yellow solid (426 mg, 85%). ^{1}H NMR (CD_2Cl_2, 400 MHz) δ 0.85-0.95 (12H, mult), 1.30-1.45 (16H, mult), 1.45-1.60 (8H, mult), 1.80-1.95 (8H, mult), 3.97 (2H, t, *J* = 6.4 Hz, OCH_2), 4.04 (4H, t, *J* = 6.4 Hz, OCH_2), 4.12 (2H, t, *J* = 6.4 Hz, OCH_2), 7.12 (1H, s), 7.16 (1H, s), 7.17 (1H, d, *J* = 16.4 Hz, *trans* CH=CH), 7.23 (1H, s), 7.29 (1H, d, *J* = 16.4 Hz, *trans* CH=CH), 7.31 (1H, s), 7.46 (1H, d, *J* = 16.4 Hz, *trans* CH=CH), 7.53 (1H, d, *J* = 16.4 Hz, *trans* CH=CH), 7.56 (4H, br s, *p*-C_6H_4), 10.44 ppm (1H, s, CHO) ppm. ^{13}C NMR (CD_2Cl_2, 100 MHz) δ 14.41 (CH_3), 23.23 (CH_2), 26.29 (CH_2), 26.36 (CH_2), 26.45 (CH_2), 26.47 (CH_2), 29.83 (CH_2), 29.87 (CH_2), 32.16 (CH_2), 32.18 (CH_2), 32.20 (CH_2), 69.78 (OCH_2), 69.85 (OCH_2), 70.22 (OCH_2), 70.73 (OCH_2), 110.49 (Ar CH), 111.03 (Ar CH), 111.97 (Ar CH), 112.32 (ArBr quat), 118.35 (Ar CH), 123.16 (vinylene CH), 123.70 (vinylene CH), 124.88 (Ar quat) 126.95 (Ar quat), 127.44 (Ar CH), 127.78 (Ar CH), 129.25 (vinylene CH), 133.20 (vinylene CH) 134.61 (Ar quat), 137.21 (Ar quat), 138.26 (Ar quat), 150.38 (ArO quat), 151.33 (ArO quat), 151.71 (ArO quat),

156.76 (ArO quat), 189.22 (CHO) ppm. MS (ESI): 813 (M+Na+2), 811 (M+Na), 527, 365 (base)\m/z. HRMS calcd for $C_{47}H_{64}NO_4Br$+Na: 811.3913 g/mol. Found: 811.3898 g/mol.

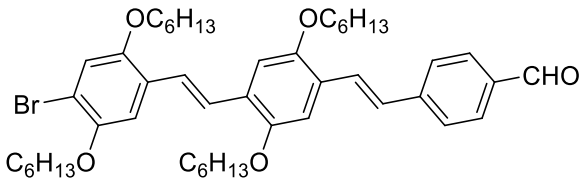

4-(4-(4-bromo-2,5-bishexyloxystyryl)-2,5-bishexyloxystyrylstyryl)benzaldehyde (Br-BBA'-CHO). According to the general DIBAL-H procedure, **Br-BBA'-CN** (500 mg, 0.635 mmol) was dissolved in DCM (5 mL) and cooled to 0 ^{O}C. DIBAL-H (1.0M in hexanes, 0.75 mL, 0.75 mmol) was added dropwise. After workup, column chromatography (silica gel, 7:3 hexanes:DCM) gave the title compound as a yellow solid (490 mg, 98%). ^{1}H NMR (CD_2Cl_2, 400 MHz) δ 0.85-0.95 (12H, mult), 1.30-1.45 (16H, mult), 1.45-1.60 (8H, mult), 1.80-1.95 (8H, mult), 3.98 (2H, t, *J* = 6.4 Hz, OCH_2), 4.04 (2H, t, *J* = 6.4 Hz, OCH_2), 4.07 (2H, t, *J* = 6.4 Hz, OCH_2), 4.08 (2H, t, *J* = 6.4 Hz, OCH_2), 7.11 (1H, s), 7.16 (1H, s), 7.17 (1H, s), 7.18 (1H, s), 7.24 (1H, d, *J* = 16.4 Hz, *trans* CH=CH), 7.45 (1H, d, *J* = 16.8 Hz, *trans* CH=CH), 7.50 (1H, d, *J* = 16.8 Hz, *trans* CH=CH), 7.67 (1H, d, *J* = 16.4 Hz, *trans* CH=CH), 7.69 (2H, d, *J* = 8.0 Hz, *p*-C_6H_4), 7.86 (2H, d, *J* = 8.0 Hz, *p*-C_6H_4), 9.98 (1H, s, CHO) ppm. ^{13}C NMR (CD_2Cl_2, 100 MHz) δ 14.42 (CH_3), 23.20 (CH_2), 23.24 (CH_2), 23.26 (CH_2), 26.28 (CH_2), 26.41 (CH_2), 26.50 (CH_2), 26.55 (CH_2), 29.87 (CH_2), 30.02 (CH_2), 32.15 (CH_2), 32.18 (CH_2), 32.22 (CH_2), 32.23 (CH_2), 70.00 (OCH_2), 70.16 (OCH_2), 70.69 (OCH_2), 110.97 (Ar CH), 111.15 (Ar CH), 111.94 (Ar CH), 112.10 (ArBr quat), 118.29 (Ar CH), 124.07 (vinylene CH), 124.45 (vinylene CH), 126.41 (Ar quat), 127.43 (vinylene CH), 127.34 (Ar CH), 127.59 (Ar quat), 127.81 (vinylene CH), 128.68 (Ar quat), 130.63 (Ar CH), 144.63 (Ar quat), 150.37 (ArO quat), 151.59 (ArO quat), 151.67 (ArO quat), 152.05

(ArO quat), 191.94 (CHO) ppm. MS (ESI): 813 (M+Na+2), 811 (M+Na), 776, 711, 709, 691, 527, 365 (base) m/z. HRMS calcd for $C_{47}H_{65}O_5Br$+Na: 811.3913 g/mol. Found: 811.3935 g/mol.

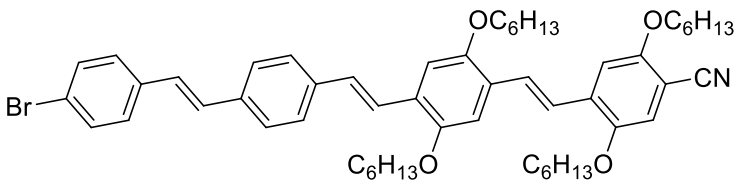

4-(4-(4-(4-bromostyryl)styryl)-2,5-bishexyloxystyryl)-2,5-bishexyloxybenzonitrile (Br-AABB'-CN). According to the general HWE procedure, **Br-AAB'-CHO** (200 mg, 0.341 mmol), **P-B'-CN** (**4**) (220 mg, 0.517 mmol), and LiCl (34.0 mg, 0.802 mmol) were dissolved in THF (5 mL) and cooled to 0 ^oC under N_2. KO^{t}Bu (88.0 mg, 0.784 mmol) was added portionwise over 5 minutes, and the reaction was allowed to come to rt overnight with stirring. After workup, column chromatography (silica gel, 13:7 hexanes:DCM) gave the title compound as an orange solid (293 mg, 97%). ^{1}H NMR (CD_2Cl_2, 400 MHz) δ 0.85-1.00 (12H, mult), 1.30-1.45 (16H, mult), 1.45-1.60 (8H, mult), 1.80-1.95 (8H, mult), 3.99 (2H, t, *J* = 6.4 Hz, OCH_2), 4.06 (2H, t, *J* = 6.4 Hz, OCH_2), 4.08 (2H, t, *J* = 6.4 Hz, OCH_2), 4.11 (2H, t, *J* = 6.4 Hz, OCH_2), 7.04 (1H, s), 7.08 (1H, d, *J* = 16.4 Hz, *trans* CH=CH), 7.14 (1H, d, *J* = 16.4 Hz, *trans* CH=CH), 7.16 (1H, s), 7.17 (1H, s), 7.20 (1H, d, *J* = 16.4 Hz, *trans* CH=CH), 7.21 (1H, s) 7.42 (2H, d, *J* = 8.4 Hz, *p*-C_6H_4), 7.47-7.57 (8H, mult), 7.60 (1H, d, *J* = 16.4 Hz, *trans* CH=CH) ppm. ^{13}C NMR (CD_2Cl_2, 100 MHz) δ 14.38 (CH_3), 14.42 (CH_3), 23.17 (CH_2), 23.23 (CH_2), 23.25 (CH_2), 23.27 (CH_2), 26.15 (CH_2), 26.39 (CH_2), 26.50 (CH_2), 26.55 (CH_2), 29.66 (CH_2), 29.76 (CH_2), 30.01 (CH_2), 30.03 (CH_2), 32.10 (CH_2), 32.17 (CH_2), 32.23 (CH_2), 69.92 (OCH_2), 70.01 (OCH_2), 70.05 (OCH_2), 70.16 (OCH_2), 100.56 (ArCN, quat), 110.51 (Ar CH), 110.74 (Ar CH), 111.28 (Ar CH), 116.95 (Ar CH), 117.34 (CN), 121.73 (ArBr quat), 122.82 (vinylene CH), 123.84 (vinylene CH), 126.98 (Ar quat),

127.43 (Ar CH), 128.43 (Ar CH), 128.52 (vinylene CH), 127.63 (vinylene CH), 128.05 (Ar quat), 128.05 (Ar CH), 128.55 (vinylene CH), 129.51 (vinylene CH), 132.32 (Ar CH), 133.98 (Ar quat), 136.83 (Ar quat), 136.97 (Ar quat), 138.11 (Ar quat), 150.72 (ArO quat), 151.63 (ArO quat), 151.96 (ArO quat), 155.72 (ArO quat) ppm. HRMS calc. for $C_{55}H_{71}NO_4Br$: 888.4566 g/mol. Found: 888.4554 g/mol.

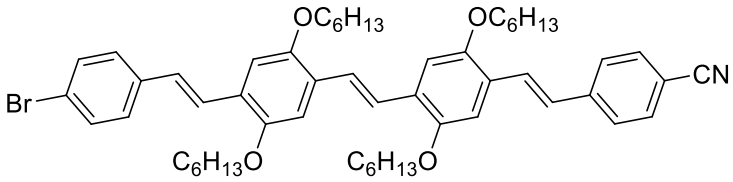

4-(4-(4-(4-bromostyryl)-2,5-bishexyloxystyryl)-2,5-bishexyloxystyryl)benzonitrile (Br-ABBA'-CN). According to the general HWE procedure, **Br-ABB'-CHO** (300 mg, 0.380 mmol), **P-A'-CN** (**3**) (130 mg, 0.577 mmol), and LiCl (37.0 mg, 0.873 mmol) were dissolved in THF (40 mL) and cooled to 0 °C under N_2. KO^{t}Bu (98.0 mg, 0.873 mmol) was added portionwise over 5 minutes, and the reaction was allowed to come to rt overnight with stirring. After workup, column chromatography (silica gel, 4:1 hexanes:DCM) gave the title compound as an orange solid (300 mg, 89%). ^{1}H NMR (CD_2Cl_2, 400 MHz) δ 0.85-1.00 (12H, mult), 1.30-1.45 (16H, mult), 1.45-1.60 (8H, mult), 1.80-1.95 (8H, mult), 4.05-4.10 (8H, mult), 7.11-7.19 (6H, mult), 7.42 (2H, d, J = 8.4 Hz, *p*-C_6H_4), 7.48-7.52 (5H, mult), 7.61-7.66 (5H, mult) ppm. ^{13}C NMR (CD_2Cl_2, 100 MHz) δ 13.83 (CH_3), 13.87 (CH_3), 22.67 (CH_2), 22.70 (CH_2), 25.95 (CH_2), 25.98 (CH_2), 29.44 (CH_2), 29.47 (CH_2), 31.65 (CH_2), 31.68 (CH_2), 69.38 (OCH_2), 69.42 (OCH_2), 69.46 (OCH_2), 110.18 (ArCN, quat), 110.21 (Ar CH), 110.32 (Ar CH), 110.36 (Ar CH), 110.35 (Ar CH), 119.07 (CN), 120.91 (ArBr quat), 123.33 (vinylene CH), 123.93 (vinylene CH), 126.73 (Ar CH quat), 126.83 (Ar quat), 126.99 (vinylene CH), 127.41 (Ar quat), 127.53 (Ar quat), 127.96 (vinylene

CH), 128.01 (vinylene CH), 128.51 (Ar quat), 131.71 (Ar CH), 132.47 (Ar CH), 136.88 (Ar quat), 137.04 (Ar quat), 151.07 (ArO quat), 151.16 (ArO quat), 151.45 (ArO quat), 151.51 (ArO quat) ppm. HRMS calc. for $C_{55}H_{71}NO_4Br$: 888.4566 g/mol. Found: 888.4586 g/mol.

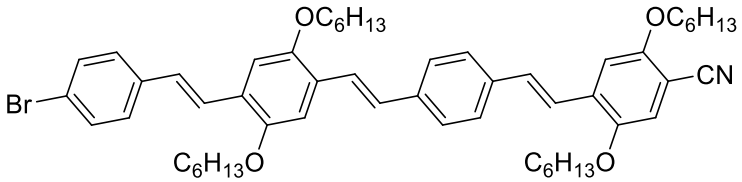

4-(4-(4-(4-bromostyryl)-2,5-bishexyloxystyryl)styryl)-2,5-bishexyloxybenzonitrile (Br-ABAB'-CN). According to the general HWE procedure, **Br-ABA'-CHO** (200 mg, 0.341 mmol), **P-B'-CN** (**4**) (220 mg, 0.517 mmol), and LiCl (34.0 mg, 0.802 mmol) were dissolved in THF (5 mL) and cooled to 0 °C under N_2. KO^{t}Bu (88.0 mg, 0.784 mmol) was added portionwise over 5 minutes, and the reaction was allowed to come to rt overnight with stirring. After workup, column chromatography (silica gel, 2:3 hexanes:DCM) gave the title compound as an orange solid (268 mg, 88%). ^{1}H NMR (CD_2Cl_2, 400 MHz) δ 0.85-1.00 (12H, mult), 1.30-1.45 (16H, mult), 1.45-1.60 (8H, mult), 1.80-1.95 (8H, mult), 3.99 (2H, t, *J* = 6.4 Hz, OCH_2), 4.07 (4H, t, *J* = 6.4 Hz, OCH_2), 4.11 (2H, t, *J* = 6.4 Hz, OCH_2), 7.05 (1H, s), 7.05 (1H, d, *J* = 16.4 Hz, *trans* CH=CH), 7.15 (1H, s), 7.16 (1H, s), 7.19 (1H, s), 7.19 (1H, d, *J* = 16.4 Hz, *trans* CH=CH), 7.26 (1H, d, *J* = 16.4 Hz, *trans* CH=CH), 7.42 (2H, d, *J* = 8.4 Hz, *p*-C_6H_4), 7.48 (1H, d, *J* = 16.4 Hz, *trans* CH=CH), 7.49 (1H, d, *J* = 16.4 Hz, *trans* CH=CH), 7.49 (2H, d, *J* = 8.4 Hz, *p*-C_6H_4), 7.50 (1H, d, *J* = 16.4 Hz, *trans* CH=CH), 7.56 (4H, br s, *p*-C_6H_4), ppm. ^{13}C NMR (CD_2Cl_2, 100 MHz) δ 14.39 (CH_3), 14.41 (CH_3), 23.17 (CH_2), 23.20 (CH_2), 23.25 (CH_2), 26.13 (CH_2), 26.40 (CH_2), 26.54 (CH_2), 29.64 (CH_2), 29.74 (CH_2), 30.02 (CH_2), 30.04 (CH_2), 32.10 (CH_2), 32.15 (CH_2), 32.22 (CH_2), 32.23 (CH_2), 70.04 (OCH_2), 70.05 (OCH_2), 70.13 (OCH_2), 70.23 (OCH_2), 100.81 (ArCN, quat),

110.54 (Ar CH), 110.85 (Ar CH), 110.97 (Ar CH), 117.03 (Ar CH), 117.27 (CN), 121.50 (ArBr quat), 122.47 (vinylene CH), 124.17 (vinylene CH), 124.67 (vinylene CH), 127.05 (Ar quat), 127.41 (Ar CH), 127.78 (Ar CH), 127.96 (vinylene CH), 128.52 (Ar CH), 128.75 (vinylene CH), 132.27 (Ar CH, 133.29 (Ar quat), 136.83 (Ar quat), 137.57 (Ar quat), 138.60 (Ar quat), 150.76 (ArO quat), 151.71 (ArO quat), 151.72 (ArO quat), 155.71 (ArO quat) ppm. HRMS calc. for $C_{55}H_{71}NO_4Br$: 888.4566 g/mol. Found: 888.4570 g/mol.

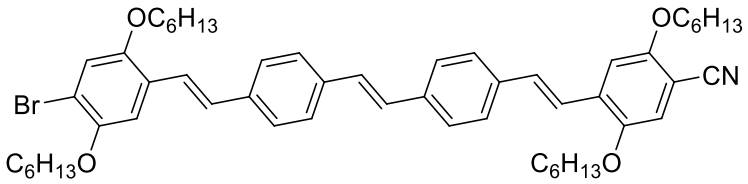

4-(4-(4-(4-bromo-2,5-bishexyloxystyryl)styryl)styryl)-2,5-bishexyloxybenzonitrile (Br-BAAB'-CN). According to the general HWE procedure, **Br-BAA'-CHO** (200 mg, 0.341 mmol), **P-B'-CN** (**4**) (220 mg, 0.517 mmol), and LiCl (34.0 mg, 0.802 mmol) were dissolved in THF (5 mL) and cooled to 0 ^{o}C under N_2. KO^{t}Bu (88.0 mg, 0784 mmol) was added portionwise over 5 minutes, and the reaction was allowed to come to rt overnight with stirring. After workup, column chromatography (silica gel, 7:3 hexanes:DCM) gave the title compound as an orange solid (270 mg, 89%). ^{1}H NMR (CD_2Cl_2, 400 MHz) δ 0.85-1.00 (12H, mult), 1.30-1.45 (16H, mult), 1.45-1.60 (8H, mult), 1.80-1.95 (8H, mult), 3.97 (2H, t, *J* = 6.4 Hz, OCH_2), 3.99 (2H, t, *J* = 6.4 Hz, OCH_2), 4.04 (2H, t, *J* = 6.4 Hz, OCH_2), 4.11 (2H, t, *J* = 6.4 Hz, OCH_2), 7.04 (1H, s), 7.11 (1H, s), 7.16 (1H, d, *J* = 16.4 Hz, *trans* CH=CH), 7.16 (1H, s), 7.17 (2H, br s, *trans* CH=CH), 7.19 (1H, s), 7.25 (1H, d, *J* = 16.4 Hz, *trans* CH=CH), 7.44 (1H, d, *J* = 16.4 Hz, *trans* CH=CH), 7.48 (1H, d, *J* = 16.4 Hz, *trans* CH=CH), 7.54 (4H, br s, *p*-C_6H_4), 7.56 (4H, br s, *p*-C_6H_4) ppm. ^{13}C NMR (CD_2Cl_2, 100 MHz) δ 14.40 (CH_3), 23.17 (CH_2), 23.21 (CH_2), 23.22 (CH_2), 26.13 (CH_2), 26.27

(CH_2), 26.40 (CH_2), 26.43 (CH_2), 29.65 (CH_2), 29.73 (CH_2), 29.85 (CH_2), 29.86 (CH_2), 32.10 (CH_2), 32.15 (CH_2), 32.17 (CH_2), 70.13 (OCH_2), 70.22 (OCH_2), 70.24 (OCH_2), 70.72 (OCH_2), 100.85 (ArCN, quat), 110.59 (Ar CH), 111.85 (Ar CH), 112.21 (ArBr quat), 117.02 (Ar CH), 117.26 (CN), 118.32 (Ar CH), 122.63 (vinylene CH), 122.43 (vinylene CH), 127.05 (Ar quat), 127.44 (Ar CH), 127.80 (Ar CH), 128.43 (vinylene CH), 129.04 (vinylene CH), 129.32 (vinylene CH), 132.21 (vinylene CH), 133.24 (Ar quat), 137.02 (Ar quat), 137.16 (Ar quat), 137.81 (Ar quat), 137.98 (Ar quat), 150.36 (ArO quat), 150.77 (ArO quat), 151.67 (ArO quat), 155.71 (ArO quat) ppm. HRMS calc. for $C_{55}H_{71}NO_4Br$: 888.4566 g/mol. Found: 888.4552 g/mol.

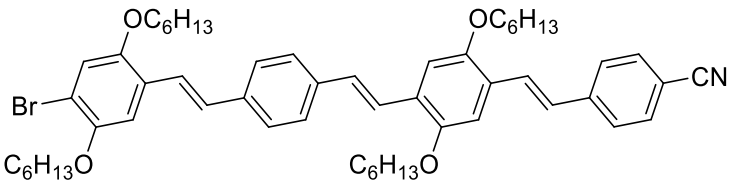

4-(4-(4-(4-bromo-2,5-bishexyloxystyryl)styryl)-2,5-bishexyloxystyryl)benzonitrile (Br-BABA'-CN). According to the general HWE procedure, **Br-BAB'-CHO** (300 mg, 0.380 mmol), **P-A'-CN** (3) (130 mg, 0.577 mmol), and LiCl (37.0 mg, 0.873 mmol) were dissolved in THF (5 mL) and cooled to 0 °C under N_2. KO^{t}Bu (98.0 mg, 0.873 mmol) was added portionwise over 5 minutes, and the reaction was allowed to come to rt overnight with stirring. After workup, column chromatography (silica gel, 1:1 hexanes:DCM) gave the title compound as an orange solid (337 mg, 100%). ^{1}H NMR (CD_2Cl_2, 400 MHz) δ 0.85-1.00 (12H, mult), 1.30-1.45 (16H, mult), 1.45-1.60 (8H, mult), 1.80-1.95 (8H, mult), 3.97 (2H, t, *J* = 6.4 Hz, OCH_2), 4.04 (2H, t, *J* = 6.4 Hz, OCH_2), 4.07 (2H, t, *J* = 6.4 Hz, OCH_2), 4.08 (2H, t, *J* = 6.4 Hz, OCH_2), 7.11 (1H, s), 7.14 (1H, s), 7.16 (1H, d, *J* = 16.4 Hz, *trans* CH=CH), 7.17 (1H, s), 7.18 (1H, d, *J* = 16.4 Hz, *trans* CH=CH), 7.18 (1H, s), 7.20 (1H, d, *J* = 16.4 Hz, *trans* CH=CH), 7.44 (1H, d, *J* = 16.4 Hz, *trans* CH=CH),

7.53 (1H, d, J = 16.4 Hz, *trans* CH=CH), 7.55 (4H, br s, *p*-C_6H_4), 7.62 (2H, s, J = 8.8 Hz, *p*-C_6H_4), 7.62 (1H, d, J = 16.4 Hz, *trans* CH=CH), 7.65 (2H, s, J = 8.8 Hz, *p*-C_6H_4) ppm. ^{13}C NMR (CD_2Cl_2, 100 MHz) δ 14.40 (CH_3), 23.21 (CH_2), 23.25 (CH_2), 26.27 (CH_2), 26.43 (CH_2), 26.53 (CH_2), 26.54 (CH_2), 29.86 (CH_2), 29.99 (CH_2), 30.03 (CH_2), 32.14 (CH_2), 32.17 (CH_2), 32.21 (CH_2), 32.23 (CH_2), 70.00 (OCH_2), 70.08 (OCH_2), 70.22 (OCH_2), 70.71 (OCH_2), 110.75 (Ar CH), 111.21 (Ar CH), 111.81 (Ar CH), 112.15 (ArBr quat, ArCN quat), 118.33 (Ar CH), 119.62 (CN), 123.28 (vinylene CH), 123.57 (vinylene CH), 126.16 (Ar quat), 127.03 (Ar quat), 127.21 (vinylene CH), 127.30 (Ar CH), 127.40 (Ar CH), 127.43 (Ar CH), 127.61 (vinylene CH), 128.41 (Ar quat), 129.36 (vinylene CH), 133.02 (Ar CH), 137.62 (Ar quat), 137.77 (Ar quat), 150.36 (ArO quat), 151.60 (ArO quat), 151.66 (ArO quat), 152.06 (ArO quat) ppm. HRMS calc. for $C_{55}H_{71}NO_4Br$: 888.4566 g/mol. Found: 888.4586 g/mol.

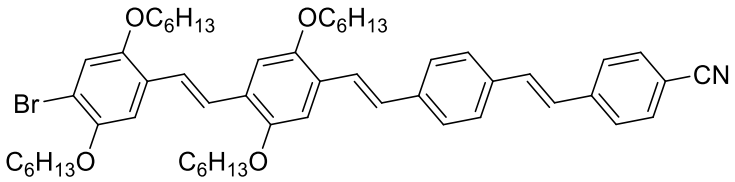

4-(4-(4-(4-bromo-2,5-bishexyloxystyryl)-2,5-bishexyloxystyryl)styryl)benzonitrile (Br-BBAA'-CN). According to the general HWE procedure, **Br-BBA'-CHO** (300 mg, 0.380 mmol), **P-A'-CN** (**3**) (130 mg, 0.577 mmol), and LiCl (37.0 mg, 0.873 mmol) were dissolved in THF (5 mL) and cooled to 0 °C under N_2. KO^{t}Bu (98.0 mg, 0.873 mmol) was added portionwise over 5 minutes, and the reaction was allowed to come to rt overnight with stirring. After workup, column chromatography (silica gel, 1:1 hexanes:DCM) gave the title compound as an orange solid (338 mg, 100%). ^{1}H NMR (CD_2Cl_2, 400 MHz) δ 0.85-1.00 (12H, mult), 1.30-1.45 (16H, mult), 1.45-1.60 (8H, mult), 1.80-1.95 (8H, mult), 3.97 (2H, t, J = 6.4 Hz, OCH_2), 4.04 (2H, t, J = 6.4

Hz, OCH_2), 4.07 (4H, t, *J* = 6.4 Hz, OCH_2), 7.11 (1H, s), 7.14 (1H, d, *J* = 16.0 Hz, *trans* CH=CH), 7.16 (2H, br s), 7.18 (1H, d, *J* = 16.4 Hz, *trans* CH=CH), 7.18 (1H, s), 7.25 (1H, d, *J* = 16.0 Hz, *trans* CH=CH), 7.44 (1H, d, *J* = 16.8 Hz, *trans* CH=CH), 7.50 (1H, d, *J* = 16.8 Hz, *trans* CH=CH), 7.54 (1H, d, *J* = 16.4 Hz, *trans* CH=CH), 7.56 (4H, br s, *p*-C_6H_4), 7.61 (2H, s, *J* = 8.4 Hz, *p*-C_6H_4), 7.65 (2H, s, *J* = 8.4 Hz, *p*-C_6H_4) ppm. ^{13}C NMR (CD_2Cl_2, 100 MHz) δ 14.40 (CH_3), 14.42 (CH_3), 14.43 (CH_3), 23.20 (CH_2), 23.23 (CH_2), 23.25 (CH_2), 23.26 (CH_2), 26.28 (CH_2), 26.41 (CH_2), 26.50 (CH_2), 26.55 (CH_2), 29.86 (CH_2), 30.04 (CH_2), 32.14 (CH_2), 32.18 (CH_2), 32.24 (CH_2), 70.00 (OCH_2), 69.96 (OCH_2), 69.97 (OCH_2), 70.13 (OCH_2), 70.65 (OCH_2), 110.83 (Ar CH), 110.96 (Ar CH), 111.03 (ArCN quat), 111.85 (Ar CH), 111.93 (ArBr quat), 118.25 (Ar CH), 119.53 (CN), 123.61 (vinylene CH), 124.42 (vinylene CH), 124.52 (vinylene CH), 126.91 (vinylene CH), 127.07 (Ar quat), 127.36 (Ar CH), 127.41 (Ar CH), 127.66 (Ar quat), 127.85 (Ar CH), 127.89 (Ar quat), 128.51 (vinylene CH), 132.38 (vinylene CH), 136.06 (Ar quat), 138.92 (Ar quat), 142.43 (Ar quat), 150.33 (ArO quat), 151.62 (ArO quat), 151.73 (ArO quat) ppm. HRMS calc. for $C_{55}H_{71}NO_4Br$: 888.4566 g/mol. Found: 888.4573 g/mol.

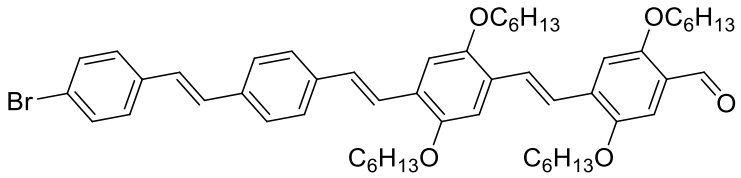

4-(4-(4-(4-bromostyryl)styryl)-2,5-bis(hexyloxy)styryl)-2,5-bis(hexyloxy)benzaldehyde (Br-AABB'-CHO). According to the general DIBAL-H procedure, **Br-AABB'-CN** (1.1347 g, 1.20 mmol) was dissolved in DCM (10 mL) and cooled to 0 ^{O}C. DIBAL-H (1.0M in hexanes, 1.60 mL, 1.60 mmol) was added dropwise. After workup, column

chromatography (silica gel, 7:3 hexanes:DCM) gave the title compound as an orange solid (675.3 mg, 63%).[1]H NMR (400 MHz, CDCl3) δ 10.38 (s, 1H), 7.57 – 7.37 (m, 9H), 7.32 (d, *J* = 8.5 Hz, 3H), 7.16 – 6.92 (m, 6H), 4.12 – 3.90 (m, 8H), 1.91 – 1.70 (m, 8H), 1.57 – 1.39 (m, 8H), 1.39 – 1.22 (m, 16H), 1.00 – 0.71 (m, 12H). [13]C NMR (100 MHz, CD_2Cl_2) δ 189.06, 156.60, 151.77, 151.47, 151.08, 151.08, 137.95, 137.95, 136.80, 136.62, 135.17, 135.17, 132.14, 129.34, 128.88, 128.36, 127.76, 127.43, 127.28, 127.24, 127.05, 124.50, 123.69, 123.15, 121.53, 111.04, 110.77, 110.59, 110.21, 69.82, 69.77, 69.59, 69.51, 32.03, 31.99, 31.94, 29.83, 29.62, 26.35, 26.31, 26.24, 26.16, 23.07, 23.05, 22.98, 14.21, 14.21, 14.18, 14.18. HRMS calc. for $C_{55}H_{72}O_5Br$: 891.4563 g/mol. Found: 888.4579 g/mol.

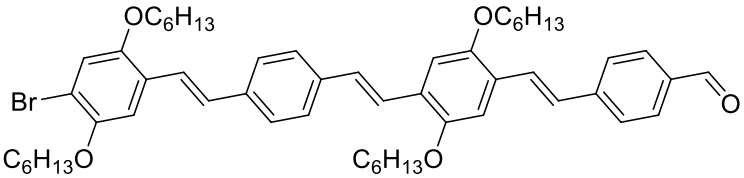

4-(4-(4-(4-bromo-2,5-bis(hexyloxy)styryl)styryl)-2,5-bis(hexyloxy)styryl)benzaldehyde (Br-BABA'-CHO). According to the general DIBAL-H procedure, **Br-BABA'-CN** (1.3587 g, 1.50 mmol) was dissolved in DCM (15 mL) and cooled to 0 [O]C. DIBAL-H (1.0M in hexanes, 1.90 mL, 1.90 mmol) was added dropwise. After workup, column chromatography (silica gel, 7:3 hexanes:DCM) gave the title compound as an orange solid (1.2502 g, 93%).[1]H NMR (400 MHz, $CDCl_3$) δ 10.00 (s, 1H), 7.87 (d, *J* = 8.2 Hz, 2H), 7.66 (m, 3H), 7.57 – 7.46 (m, 5H), 7.42 (d, *J* = 16.4 Hz, 1H), 7.15 (m 7H), 4.04 (m, 8H), 1.98 – 1.78 (m, 8H), 1.64 – 1.47 (m, 8H), 1.47 – 1.31 (m, 16H), 1.00 – 0.83 (m, 12H). [13]C NMR (100 MHz, CD_2Cl_2) δ 191.76, 151.86, 151.47, 151.43, 150.17, 144.42, 137.61, 137.40, 135.61, 130.43, 129.19, 129.11, 128.10, 127.62, 127.21, 127.15, 126.85, 126.25, 123.42, 123.07, 118.15, 111.95, 111.63, 111.00, 110.58, 70.53, 70.03, 69.89, 69.83, 32.03, 32.02, 31.96, 31.94, 29.83, 29.80, 29.66,

26.34, 26.23, 26.06, 23.05, 23.01, 23.00, 14.20. HRMS calc. for $C_{55}H_{72}O_5BrNa$: 913.4383 g/mol. Found: 913.4297 g/mol.

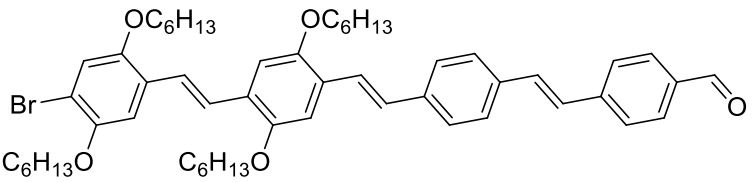

4-(4-(4-(4-bromo-2,5-bis(hexyloxy)styryl)-2,5-bis(hexyloxy)styryl)styryl)benzaldehyde (Br-BBAA'-CHO). According to the general DIBAL-H procedure, **Br-BBAA'-CN** (1.3952 g, 1.60 mmol) was dissolved in DCM (15 mL) and cooled to 0 ^{O}C. DIBAL-H (1.0M in hexanes, 2.00 mL, 2.00 mmol) was added dropwise. After workup, column chromatography (silica gel, 7:3 hexanes:DCM) gave the title compound as an orange solid (1.2957 g, 91%).^{1}HNMR(300MHz, $CDCl_3$) 10.00 (s, 1H), 7.89-7.86 (d, *J*= 9 Hz, 2H), 7.68-7.65 (d, *J*=9 Hz, 2H), 7.56-7.50 (m, 5H), 7.44-7.42 (d, *J*= 6 Hz, 2H), 7,25-7.08 (m, 7H), 4.08-3.94 (m, 8H), 1.91-1.82 (m, 8H), 1.56-1.51 (m, 8H), 1.43-1.36 (m, 16H), 0.94-0.87 (m, 12H). ^{13}C NMR (100 MHz, CD_2Cl_2) δ 191.75, 151.53, 151.43, 150.14, 143.76, 138.61, 136.12, 135.77, 131.99, 130.44, 128.37, 127.63, 127.48, 127.32, 127.20, 126.92, 124.34, 124.14, 123.41, 118.06, 111.67, 110.79, 110.63, 70.47, 69.95, 69.77, 32.03, 31.97, 31.93, 29.83, 29.66, 26.35, 26.30, 26.20, 26.07, 23.04, 23.03, 22.99, 14.20, 14.18. HRMS calc. for $C_{55}H_{72}O_5BrNa$: 913.4383 g/mol. Found: 913.4302 g/mol.

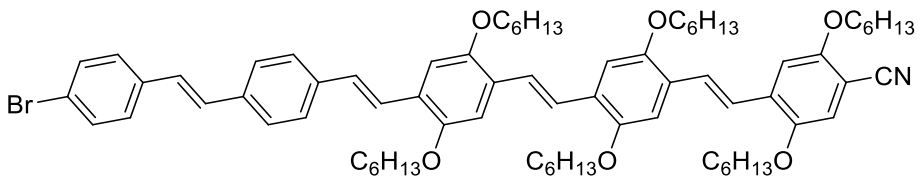

4-(4-(4-(4-(4-bromostyryl)styryl)-2,5-bis(hexyloxy)styryl)-2,5-bis(hexyloxy)styryl)-2,5-bis(hexyloxy)benzonitrile (Br-AABBB'-CN). According to the general HWE procedure, **Br-AABB' -CHO** (546.7 mg, 0.61 mmol), **P-B'-CN** (4) (387.2 mg, 0.91 mmol), and LiCl (59.6 mg, 1.41 mmol) were dissolved in THF (10 mL) and cooled to 0 ^{o}C under N_2. KO^{t}Bu (157.4 mg, 1.41 mmol) was added portionwise over 5 minutes, and the reaction was allowed to come to rt overnight with stirring. After workup, column chromatography (silica gel, 7:3 hexanes: DCM) gave the title compound as an orange solid (669.3 mg, 93%). ^{1}H NMR (400 MHz, CDCl3) δ 7.60 – 7.44 (m, 10H), 7.40 (t, *J* = 7.5 Hz, 3H), 7.17 (d, *J* = 1.6 Hz, 4H), 7.13 (d, *J* = 4.1 Hz, 2H), 7.08 (d, *J* = 8.0 Hz, 2H), 7.00 (q, *J* = 6.7 Hz, 2H), 4.13 – 3.93 (m, 12H), 1.92 – 1.79 (m, 12H), 1.61 – 1.46 (m, 12H), 1.43 – 1.29 (m, 24H), 0.99 – 0.83 (m, 18H).^{13}C NMR (100 MHz, CD_2Cl_2) δ 155.52, 151.77, 151.50, 150.49, 136.79, 133.83, 132.12, 129.34, 128.58, 128.34, 127.72, 127.35, 127.26, 127.17, 124.13, 124.11, 121.50, 117.15, 116.75, 111.02, 110.63, 110.46, 110.32, 110.26, 100.27, 78.08, 69.93, 69.77, 69.66,32.04, 31.95, 31.88, 29.84, 29.53, 29.43, 26.35, 26.32, 26.18, 25.93, 23.05, 23.01, 22.95, 14.20, 14.16. HRMS calc. for $C_{75}H_{101}NO_6Br$: 1190.6812 g/mol. Found: 1190.6786 g/mol.

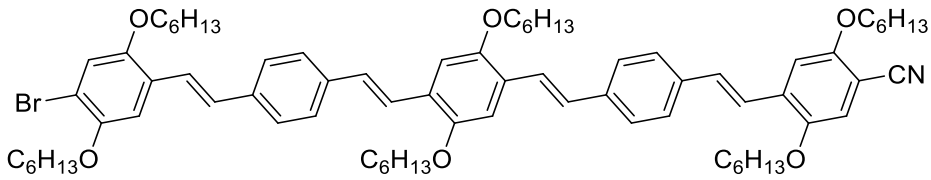

4-(4-(4-(4-(4-bromo-2,5-bis(hexyloxy)styryl)styryl)-2,5-bis(hexyloxy)styryl)styryl)-2,5-bis(hexyloxy)benzonitrile (Br-BABA'-CN). According to the general HWE procedure, **Br-**

BABA'-CHO (300 mg, 0.380 mmol), **P-B'-CN** (4) (1.1465 g, 1.3 mmol), and LiCl (127.5 mg, 3.0 mmol) were dissolved in THF (17 mL) and cooled to 0 °C under N_2. KO^{t}Bu (336.6 mg, 3.0 mmol) was added portionwise over 5 minutes, and the reaction was allowed to come to rt overnight with stirring. After workup, column chromatography (silica gel, 7:3 hexanes: DCM) gave the title compound as an orange solid (1.5040 g, 97%). ^{1}H NMR (400 MHz, $CDCl_3$) δ 7.58 – 7.37 (m, 12H), 7.13 (m, 10H), 4.15 – 3.92 (m, 12H), 1.95 – 1.77 (m, 12H), 1.64 – 1.47 (m, 12H), 1.46 – 1.29 (m, 24H), 1.01 – 0.80 (m, 18H). ^{13}C NMR (100 MHz, $CDCl_3$) δ 155.24, 151.19, 151.13, 151.10, 150.14, 149.81, 138.12, 137.30, 136.88, 136.10, 132.87, 131.85, 128.95, 128.46, 128.12, 127.23, 127.12, 126.85, 126.73, 126.58, 123.85, 123.28, 122.77, 121.95, 117.83, 116.82, 116.46, 111.86, 111.56, 110.55, 110.48, 110.09, 100.38, 70.30, 69.67, 69.60, 31.64, 31.56, 31.51, 29.47, 29.28, 29.15, 29.07, 25.97, 25.85, 25.82, 25.70, 25.58, 22.66, 22.61, 22.57, 14.05, 14.03. HRMS calc. for $C_{75}H_{100}NO_6Br$+Na: 1212.6632 g/mol. Found: 1212.6569 g/mol.

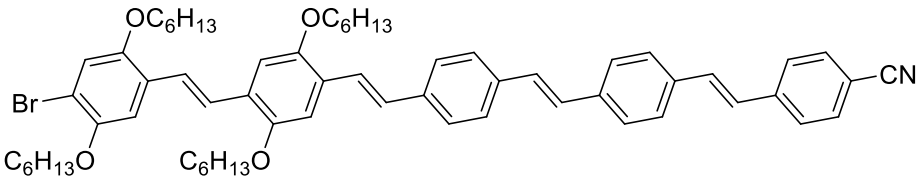

4-(4-(4-(4-(4-bromo-2,5-bis(hexyloxy)styryl)-2,5-bis(hexyloxy)styryl)styryl)styryl) benzonitrile (Br-BBAAA'-CN). According to the general HWE procedure, **Br-BBAA'-CHO** (1.1539 mg, 1.3 mmol), **P-A'-CN** (3) (450.4 mg, 2.0 mmol), and LiCl (127.5 mg, 3.0 mmol) were dissolved in THF (16 mL) and cooled to 0 °C under N_2. KO^{t}Bu (336.6 mg, 3.0 mmol) was added portionwise over 5 minutes, and the reaction was allowed to come to rt overnight with stirring. After workup, column chromatography (silica gel, 7:3 hexanes: DCM) gave the title compound as an orange solid (1.2552 g, 97%). ^{1}H NMR (400 MHz, $CDCl_3$) δ 7.64 (d, *J* = 8.4 Hz, 2H), 7.58 (d, *J* = 8.4 Hz, 2H), 7.56 – 7.48 (m, 9H), 7.42 (t, *J* = 13.5 Hz, 2H), 7.25 – 7.04 (m, 9H), 4.11 – 3.93

(m, 8H), 1.96 – 1.78 (m, 8H), 1.64 – 1.47 (m, 8H), 1.44 – 1.29 (m, 16H), 1.02 – 0.84 (m, 12H). ^{13}C NMR (100 MHz, $CDCl_3$) δ 151.15, 151.06, 151.03, 149.81, 141.83, 137.79, 137.63, 136.22, 135.50, 132.48, 131.94, 128.92, 128.22, 127.65, 127.37, 127.31, 127.23, 126.91, 126.86, 126.81, 126.43, 123.99, 123.57, 123.03, 119.04, 117.78, 111.62, 111.55, 110.61, 110.48, 70.21, 69.54, 69.48, 31.64, 31.58, 29.45, 29.29, 25.97, 25.92, 25.82, 25.71, 22.65, 22.63, 22.60, 14.05. HRMS calc. for $C_{63}H_{76}NO_4Br$+Na: 1012.4855 g/mol. Found: 1012.4783 g/mol.

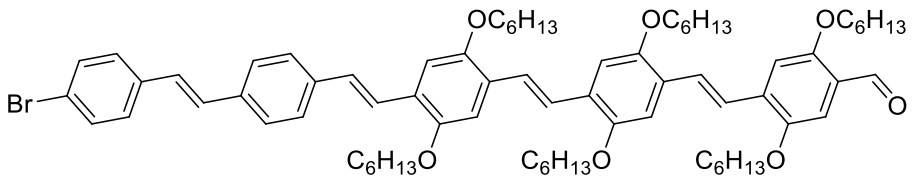

4-(4-(4-(4-(4-bromostyryl)styryl)-2,5-bis(hexyloxy)styryl)-2,5-bis(hexyloxy)styryl)-2,5-bis(hexyloxy)benzaldehyde (Br-AABBB'-CHO). According to the general DIBAL-H procedure, **Br-AABBB'-CN** (150.0 Mg, 0.13 mmol) was dissolved in DCM (7 mL) and cooled to 0 ^{O}C. DIBAL-H (1.0M in hexanes, 0.17 mL, 0.17 mmol) was added dropwise. After workup, column chromatography (silica gel, 7:3 hexanes: DCM) gave the title compound as an orange solid (108.0 mg, 72%).1H NMR (400 MHz, CDCl3) δ 10.45 (s, 1H), 7.69 – 7.42 (m, 10H), 7.42 – 7.29 (m, 3H), 7.23 – 7.01 (m, 9H), 4.08 (m, 12H), 1.85 (m, 12H), 1.53 (m, 12H), 1.39 (m, 24H), 1.06 – 0.76 (m, 18H). ^{13}C NMR (100 MHz, CD_2Cl_2) δ 188.86, 156.65, 151.84, 151.58 151.53, 151.44, 151.11, 131.96, 129.22, 128.91, 128.30, 128.18, 127.20, 127.17, 127.10, 127.01, 123.94, 123.68, 123.51, 122.82, 110.87, 110.62, 110.58, 110.55, 110.43, 110.10, 69.69, 69.64, 69.57, 69.46, 69.38, 54.08, 53.81, 53.53, 31.88, 31.86, 31.82, 31.76, 29.88, 29.69, 29.45, 26.19, 26.15, 26.07, 25.98, 22.88, 22.79, 14.02, 13.98. HRMS calc. for $C_{75}H_{102}O_7Br$: 1193.6809 g/mol. Found: 1193.6865 g/mol.

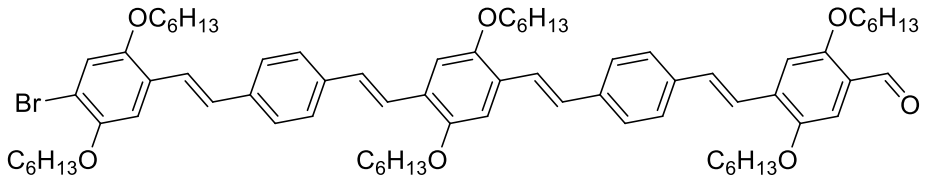

4-(4-(4-(4-(4-bromo-2,5-bis(hexyloxy)styryl)styryl)-2,5-bis(hexyloxy)styryl)styryl)-2,5-bis(hexyloxy)benzaldehyde (Br-BABAB'-CHO). According to the general DIBAL-H procedure, **Br-BABAB'-CN** (600.0 mg, .050 mmol) was dissolved in DCM (5 mL) and cooled to 0 ^{O}C. DIBAL-H (1.0M in hexanes, 0.65 mL, 0.65 mmol) was added dropwise. After workup, column chromatography (silica gel, 7:3 hexanes:DCM) gave the title compound as an orange solid (517.1 mg, 87%).^{1}H NMR (400 MHz, $CDCl_3$) δ 10.62 – 10.33 (m, 1H), 7.57 – 7.46 (m, 11H), 7.42 (d, *J* = 16.4 Hz, 1H), 7.31 (d, *J* = 24.7 Hz, 2H), 7.24 – 7.07 (m, 8H), 4.26 – 3.85 (m, 12H), 2.06 – 1.75 (m, 12H), 1.56 (m, 12H), 1.46 – 1.31 (m, 24H), 1.00 – 0.86 (m, 18H). ^{13}C NMR (100 MHz, CD_2Cl_2) δ 189.06, 156.58, 151.56, 151.51, 151.47, 151.12, 150.17, 138.37, 137.74, 137.29, 136.82, 134.48, 132.07, 129.22, 128.66, 128.46, 127.59, 127.28, 127.21, 127.18, 127.04, 126.88, 124.65, 123.97, 123.55, 122.99, 122.81, 118.14, 111.93, 111.62, 110.82, 110.68, 110.63, 110.29, 70.53, 70.04, 69.88, 69.66, 69.59, 32.06, 31.98, 31.96, 29.87, 29.67, 29.62, 26.37, 26.27, 26.25, 26.15, 26.08, 23.07, 23.03, 23.02, 23.00, 14.24, 14.21. HRMS calc. for $C_{75}H_{101}O_7Br$+Na: 1215.6628 g/mol. Found: 1215.6561 g/mol.

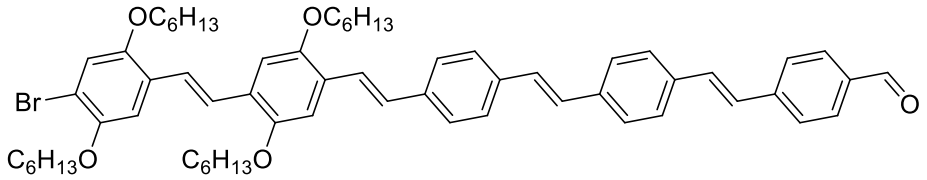

4-(4-(4-(4-(4-bromo-2,5-bis(hexyloxy)styryl)-2,5-bis(hexyloxy)styryl)styryl)styryl) benzaldehyde (Br-BBAAA'-CHO). According to the general DIBAL-H procedure, **Br-BBAAA'-CN** (601.8 mg, 0.60 mmol) was dissolved in DCM (7 mL) and cooled to 0 ^{O}C. DIBAL-

H (1.0M in hexanes, 0.80 mL, 0.80 mmol) was added dropwise. After workup, column chromatography (silica gel, 7:3 hexanes:DCM) gave the title compound as an orange solid (500.1 mg, 84%).[1]H NMR (400 MHz, $CDCl_3$) δ 10.00 (s, 1H), 7.88 (d, *J* = 8.2 Hz, 2H), 7.66 (d, *J* = 8.2 Hz, 2H), 7.59 – 7.47 (m, 9H), 7.42 (t, *J* = 13.6 Hz, 2H), 7.27 (d, *J* = 16.3 Hz, 1H), 7.20 – 7.04 (m, 8H), 4.14 – 3.89 (m, 8H), 2.01 – 1.78 (m, 8H), 1.64 – 1.45 (m, 8H), 1.45 – 1.28 (m, 16H), 1.02 – 0.77 (m, 12H). [13]C NMR (100 MHz, $CDCl_3$) δ 191.57, 151.15, 151.06, 151.04, 149.81, 143.43, 137.66, 137.60, 136.27, 135.79, 135.27, 131.75, 130.25, 128.83, 128.24, 127.73, 127.37, 127.30, 127.25, 127.08, 126.91, 126.87, 126.81, 123.55, 123.03, 117.79, 111.62, 110.62, 70.22, 69.49, 31.64, 31.56, 29.46, 29.29, 25.98, 25.92, 25.83, 25.71, 22.66, 22.64, 22.60, 14.04. HRMS calc. for $C_{63}H_{77}O_5Br$+Na: 1015.4852 g/mol. Found: 1015.4802 g/mol.

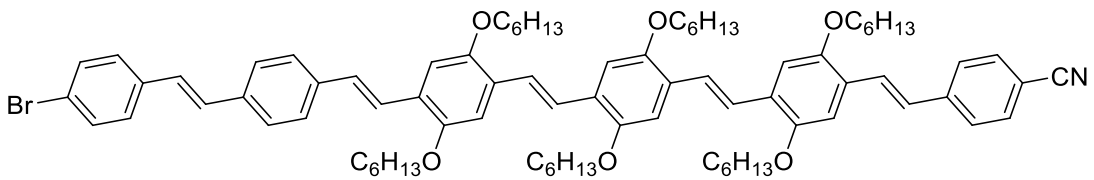

4-(4-(4-(4-(4-(4-bromostyryl)styryl)-2,5-bis(hexyloxy)styryl)-2,5-bis(hexyloxy)styryl)-2,5-bis(hexyloxy)styryl)benzonitrile(Br-AABBBA'-CN). According to the general HWE procedure, **Br-AABBB'-CHO** (141.7 mg, 0.12 mmol), **P-A'-CN** (3) (81.1 mg, 0.36 mmol), and LiCl (11.4 mg, 0.27 mmol) were dissolved in THF (10 mL) and cooled to 0 ºC under N_2. KO^{t}Bu (30.3 mg, 0.27 mmol) was added portionwise over 5 minutes, and the reaction was allowed to come to rt overnight with stirring. After workup, column chromatography (silica gel, 7:3 hexanes: DCM) gave the title compound as an orange solid (147.0 mg, 92%). [1]H NMR (400 MHz, CD2Cl2) δ 7.66 – 7.30 (m, 18H), 7.19 – 6.96 (m, 10H), 3.99 (d, *J* = 6.1 Hz, 12H), 1.87 – 1.72 (m, 12H), 1.47 (d, *J* = 17.0 Hz, 12H), 1.39 – 1.22 (m, 24H), 0.97 – 0.69 (m, 18H).[13]C NMR (100 MHz, CD_2Cl_2) δ 151.86, 151.86, 151.50, 151.50, 142.92, 138.11, 138.08, 138.07, 136.80,

136.48, 132.83, 132.12, 129.35, 128.34, 127.88, 127.44, 127.43, 127.32, 127.26, 127.17, 127.08, 126.86, 125.76, 123.72, 121.49, 119.45, 110.94, 110.58, 110.50, 69.79, 69.72, 32.06, 32.00, 30.42, 30.05, 29.86, 29.79, 26.34, 23.07, 23.03, 14.24, 14.22, 14.19. HRMS calc. for $C_{83}H_{107}NO_6$+Br: 1292.7282 g/mol. Found: 1292.7290 g/mol.

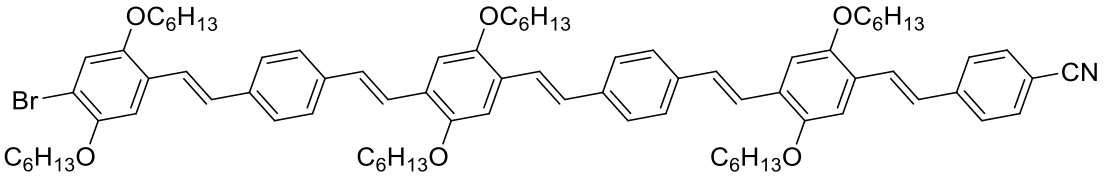

4-(4-(4-(4-(4-(4-bromo-2,5-bis(hexyloxy)styryl)styryl)-2,5-bis(hexyloxy)styryl)styryl)-2,5-bis(hexyloxy)styryl)benzonitrile (Br-BABABA'-CN).

According to the general HWE procedure, **Br-BABAB'-CHO** (300.0 mg, 0.25 mmol), **P-A'-CN** (3) (85.6 mg, 0.38 mmol), and LiCl (24.7 mg, 0.58 mmol) were dissolved in THF (5 mL) and cooled to 0 ^{o}C under N_2. KO^{t}Bu (65.1 mg, 0.58 mmol) was added portionwise over 5 minutes, and the reaction was allowed to come to rt overnight with stirring. After workup, column chromatography (silica gel, 7:3 hexanes: DCM) gave the title compound as an orange solid (273.2 mg, 84.5%). ^{1}H NMR (400 MHz, $CDCl_3$) δ 7.68 – 7.56 (m, 5H), 7.51 (m, 11H), 7.41 (d, *J* = 16.4 Hz,1H), 7.22 – 7.02 (m, 11H), 4.16 – 3.92 (m, 12H), 1.99 – 1.78 (m, 12H), 1.70 – 1.46 (m, 12H), 1.39 (dd, *J* = 6.1, 2.8 Hz, 24H), 1.10 – 0.83 (m, 18H).^{13}C NMR (100 MHz, CD_2Cl_2) δ 151.86, 151.50, 150.16, 150.16, 142.88, 137.72, 132.82, 129.25, 127.15, 127.15, 127.10, 127.10, 123.54, 123.53, 118.14, 111.90, 111.61, 111.03, 110.55, 110.55, 109.67, 70.52, 70.52, 70.03, 69.88, 69.88, 69.81, 54.33, 54.06, 53.79, 53.52, 53.25, 32.03, 31.99, 31.95, 29.85, 29.64, 26.34, 26.22, 26.05, 23.05, 23.00, 14.21, 14.18. HRMS calc. for $C_{83}H_{106}NO_6Br$+Na: 1314.7101 g/mol. Found: 1314.7034 g/mol.

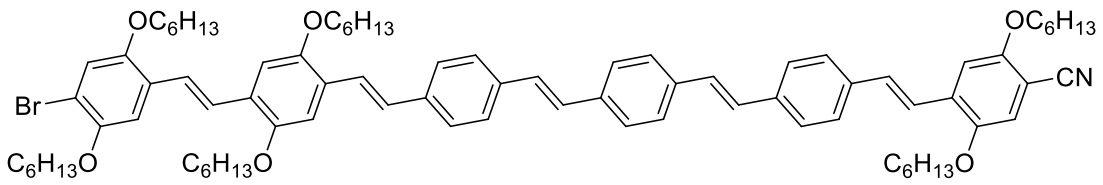

4-(4-(4-(4-(4-(4-bromo-2,5-bis(hexyloxy)styryl)-2,5-bis(hexyloxy)styryl)styryl)styryl)styryl)-2,5-bis(hexyloxy)benzonitrile (Br-BBAAAB'-CN). According to the general HWE procedure, **Br-BBAAA'-CHO** (300 mg, 0.30 mmol), **P-B'-CN** (4) (191.3 mg, 0.45 mmol), and LiCl (29.3 mg, 0.69 mmol) were dissolved in THF (10 mL) and cooled to 0 oC under N_2. KO^{t}Bu (77.4 mg, 0.69 mmol) was added portionwise over 5 minutes, and the reaction was allowed to come to rt overnight with stirring. After workup, column chromatography (silica gel, 7:3 hexanes: DCM) gave the title compound as an orange solid (280.3 mg, 72.2%). ^{1}H NMR (400 MHz, $CDCl_3$) δ 7.62 – 7.35 (m, 16H), 7.26 – 7.00 (m, 12H), 4.03 (m, 12H), 1.96 – 1.76 (m, 12H), 1.53 (d, J = 5.8 Hz, 12H), 1.37 (s, 24H), 1.06 – 0.81 (m, 18H).^{13}C NMR (100 MHz, $CDCl_3$) δ 155.24, 151.14, 151.06, 151.03, 150.15, 149.81, 137.47, 137.41, 136.93, 136.51, 136.40, 136.35, 132.81, 131.77, 128.61, 128.37, 128.27, 127.90, 127.34, 127.26, 126.90, 126.85, 124.00, 123.46, 123.01, 122.16, 117.79, 116.80, 116.46, 111.60, 110.62, 110.48, 110.13, 100.44, 70.21, 69.67, 69.49, 31.65, 31.56, 31.54, 31.51, 29.48, 29.29, 29.14, 29.06, 25.98, 25.92, 25.81, 25.71, 25.58, 22.66, 22.64, 22.60, 22.57, 14.04. HRMS calc. for $C_{83}H_{107}NO_6Br$: 1292.7282 g/mol. Found: 1292.7288 g/mol.

2.7 REFERENCE

1. Norris, B. N.; Zhang, S.; Campbell, C. M.; Auletta, J. T.; Calvo-Marzal, P.; Hutchison, G. R.; Meyer, T. Y., Sequence Matters: Modulating Electronic and Optical Properties of Conjugated Oligomers via Tailored Sequence. *Macromolecules* **2013,** *46* (4), 1384-1392.

2. Blankenship, R. E.; Tiede, D. M.; Barber, J.; Brudvig, G. W.; Fleming, G.; Ghirardi, M.; Gunner, M. R.; Junge, W.; Kramer, D. M.; Melis, A.; Moore, T. A.; Moser, C. C.; Nocera, D. G.; Nozik, A. J.; Ort, D. R.; Parson, W. W.; Prince, R. C.; Sayre, R. T., Comparing Photosynthetic and Photovoltaic Efficiencies and Recognizing the Potential for Improvement. *Science* **2011,** *332* (6031), 805-809.

3. Facchetti, A., π-Conjugated Polymers for Organic Electronics and Photovoltaic Cell Applications. *Chemistry of Materials* **2011,** *23*, 733-758.

4. Szarko, J. M.; Guo, J.; Rolczynski, B. S.; Chen, L. X., Current trends in the optimization of low band gap polymers in bulk heterojunction photovoltaic devices. *Journal of Materials Chemistry* **2011,** *21* (22), 7849-7857.

5. Zhao, X.; Zhan, X., Electron transporting semiconducting polymers in organic electronics. *Chemical Society Reviews* **2011,** *40*, 3728-3743.

6. Heeger, A. J., Semiconducting polymers: the Third Generation. *Chemical Society Reviews* **2010,** *39* (7), 2354-2371.

7. Kroon, R.; Lenes, M.; Hummelen, J. C.; Blom, P. W. M.; de Boer, B., Small bandgap polymers for organic solar cells (polymer material development in the last 5 years). *Polymer Reviews* **2008,** *48* (3), 531-582.

8. Rasmussen, S. C.; Pomerantz, M., Low bandgap conducting polymers. In *Handbook of Conducting Polymers*, 3rd ed.; Skotheim, T. A.; Reynolds, J. R., Eds. CRC Press: 2007; Vol. 1, pp 12/1-12/42.

9. Roncali, J., Synthetic principles for bandgap control in linear pi-conjugated systems. *Chemical Reviews* **1997,** *97* (1), 173-205.

10. Grimsdale, A. C.; Chan, K. L.; Martin, R. E.; Jokisz, P. G.; Holmes, A. B., Synthesis of Light-Emitting Conjugated Polymers for Applications in Electroluminescent Devices. *Chemical Reviews* **2009,** *109* (3), 897-1091.

11. Guo, X. G.; Ortiz, R. P.; Zheng, Y.; Hu, Y.; Noh, Y. Y.; Baeg, K. J.; Facchetti, A.; Marks, T. J., Bithiophene-Imide-Based Polymeric Semiconductors for Field-Effect Transistors: Synthesis, Structure-Property Correlations, Charge Carrier Polarity, and Device Stability. *Journal of the American Chemical Society* **2011,** *133* (5), 1405-1418.

12. Izuhara, D.; Swager, T. M., Bispyridinium-phenylene-based copolymers: low band gap n-type alternating copolymers. *Journal of Materials Chemistry* **2011,** *21* (11), 3579-3584.

13. Choi, S. H.; Frisbie, C. D., Enhanced Hopping Conductivity in Low Band Gap Donor-Acceptor Molecular Wires Up to 20 nm in Length. *Journal of the American Chemical Society* **2010,** *132* (45), 16191-16201.

14. Kim, D. H.; Lee, B. L.; Moon, H.; Kang, H. M.; Jeong, E. J.; Park, J. I.; Han, K. M.; Lee, S.; Yoo, B. W.; Koo, B. W.; Kim, J. Y.; Lee, W. H.; Cho, K.; Becerril, H. A.; Bao, Z., Liquid-Crystalline Semiconducting Copolymers with Intramolecular Donor-Acceptor Building Blocks for High-Stability Polymer Transistors. *Journal of the American Chemical Society* **2009,** *131* (17), 6124-6132.

15. Chen, A. C. A.; Culligan, S. W.; Geng, Y.; Chen, S. H.; Klubek, K. P.; Vaeth, K. M.; Tang, C. W., Organic polarized light-emitting diodes via Foerster energy transfer using monodisperse conjugated oligomers. *Advanced Materials* **2004**, 16, 783-788.

16. Ellinger, S.; Graham, K. R.; Shi, P.; Farley, R. T.; Steckler, T. T.; Brookins, R. N.; Taranekar, P.; Mei, J.; Padilha, L. A.; Ensley, T. R.; Hu, H.; Webster, S.; Hagan, D. J.; Van, S. E. W.; Schanze, K. S.; Reynolds, J. R., Donor-Acceptor-Donor-based π-Conjugated Oligomers for Nonlinear Optics and Near-IR Emission. *Chemistry of Materials* **2011,** *23* (17), 3805-3817.

17. Geng, Y.; Chen, A. C. A.; Ou, J. J.; Chen, S. H.; Klubek, K.; Vaeth, K. M.; Tang, C. W., Monodisperse Glassy-Nematic Conjugated Oligomers with Chemically Tunable Polarized Light Emission. *Chemistry of Materials* **2003,** *15*, 4352-4360.

18. Henson, Z. B.; Welch, G. C.; van der Poll, T.; Bazan, G. C., Pyridalthiadiazole-Based Narrow Band Gap Chromophores. *Journal of the American Chemical Society* **2012,** *134* (8), 3766-3779.

19. Mallet, C.; Savitha, G.; Allain, M.; Kozmik, V.; Svoboda, J.; Frere, P.; Roncali, J., Synthesis and Electronic Properties of D-A-D Triads Based on 3-Alkoxy-4-cyanothiophene and Benzothienothiophene Blocks. *Journal of Organic Chemistry* **2012,** *77* (4), 2041-2046.

20. Poander, L. E.; Pandey, L.; Barlow, S.; Tiwari, P.; Risko, C.; Kippelen, B.; Bredas, J. L.; Marder, S. R., Benzothiadiazole-Dithienopyrrole Donor-Acceptor-Donor and Acceptor-Donor-Acceptor Triads: Synthesis and Optical, Electrochemical, and Charge-Transport Properties. *Journal of Physical Chemistry C* **2011,** *115* (46), 23149-23163.

21. Beaujuge, P. M.; Amb, C. M.; Reynolds, J. R., Spectral engineering in pi-conjugated polymers with intramolecular donor-acceptor interactions. *Accounts of Chemical Research* **2010,** *43* (11), 1396-1407.

22. Jorgensen, M.; Krebs, F. C., Stepwise Unidirectional Synthesis of Oligo Phenylene Vinylenes with a Series of Monomers. Use in Plastic Solar Cells. *Journal of Organic Chemistry* **2005,** *70*, 6004-6017.

23. Horhold, H. H.; Tillmann, H.; Bader, C.; Stockmann, R.; Nowotny, J.; Klemm, E.; Holzer, W.; Penzkofer, A., MEH-PPV and dialkoxy phenylene vinylene copolymers. Synthesis and lasing characterization. *Synthetic Metals* **2001,** *119* (1-3), 199-200.

24. Jian, H. H.; Tour, J. M., Preparative fluorous mixture synthesis of diazonium-functionalized oligo(phenylene vinylene)s. *Journal of Organic Chemistry* **2005,** *70* (9), 3396-3424.

25. O'Boyle, N. M.; Campbell, C. M.; Hutchison, G. R., Computational Design and Selection of Optimal Organic Photovoltaic Materials. *Journal of Physical Chemistry C* **2011,** *115* (32), 16200-16210.

26. Badi, N.; Lutz, J.-F., Sequence control in polymer synthesis. *Chemical Society Reviews* **2009,** *38* (12), 3383-3390.

27. Jones, R., Why nanotechnology needs better polymer chemistry. *Nature Nanotechnology* **2008,** *3* (12), 699-700.

28. Lutz, J.-F., Sequence-controlled polymerizations: the next Holy Grail in polymer science? *Polymer Chemistry* **2010,** *1* (1), 55-62.

29. Copenhafer, J. E.; Walters, R. W.; Meyer, T. Y., Synthesis and Characterization of Repeating Sequence Copolymers of Fluorene and Methylene Monomers. *Macromolecules* **2008,** *41* (1), 31-35.

30. Li, J.; Stayshich, R. M.; Meyer, T. Y., Exploiting Sequence To Control the Hydrolysis Behavior of Biodegradable PLGA Copolymers. *Journal of the American Chemical Society* **2011,** *133* (18), 6910-6913.

31. Stayshich, R. M.; Meyer, T. Y., Preparation and microstructural analysis of poly(lactic-alt-glycolic acid). *Journal of Polymer Science, Part A: Polymer Chemistry* **2008,** *46* (14), 4704-4711.

32. Stayshich, R. M.; Meyer, T. Y., New Insights into Poly(lactic-co-glycolic acid) Microstructure: Using Repeating Sequence Copolymers To Decipher Complex NMR and Thermal Behavior. *Journal of the American Chemical Society* **2010,** *132* (31), 10920-10934.

33. Stayshich, R. M.; Weiss, R. M.; Li, J.; Meyer, T. Y., Periodic Incorporation of Pendant Hydroxyl Groups in Repeating Sequence PLGA Copolymers. *Macromolar Rapid Communications* **2011,** *32* (2), 220-225.

34. Weiss, R. M.; Jones, E. M.; Shafer, D. E.; Stayshich, R. M.; Meyer, T. Y., Synthesis of repeating sequence copolymers of lactic, glycolic, and caprolactic acids. *Journal of Polymer Science, Part A: Polymer Chemistry* **2011,** *49* (8), 1847-1855.

35. Coates, G. W., Precise Control of Polyolefin Stereochemistry Using Single-Site Metal Catalysts. *Chemical Reviews* **2000,** *100* (4), 1223-1252.

36. Kramer, J. W.; Treitler, D. S.; Dunn, E. W.; Castro, P. M.; Roisnel, T.; Thomas, C. M.; Coates, G. W., Polymerization of Enantiopure Monomers Using Syndiospecific Catalysts: A New Approach To Sequence Control in Polymer Synthesis. *Journal of the American Chemical Society* **2009,** *131* (44), 16042-16044.

37. Binauld, S.; Damiron, D.; Connal, L. A.; Hawker, C. J.; Drockenmuller, E., Precise Synthesis of Molecularly Defined Oligomers and Polymers by Orthogonal Iterative Divergent/Convergent Approaches. *Macromolar Rapid Communications* **2011,** *32* (2), 147-168.

38. Ueda, M., Sequence control in one-step condensation polymerization. *Progress in Polymer Science* **1999,** *24* (5), 699-730.

39. Opper, K. L.; Wagener, K. B., ADMET: Metathesis polycondensation. *Journal of Polymer Science, Part A: Polymer Chemistry* **2011,** *49* (4), 821-831.

40. Pfeifer, S.; Lutz, J.-F., A Facile Procedure for Controlling Monomer Sequence Distribution in Radical Chain Polymerizations. *Journal of the American Chemical Society* **2007,** *129* (31), 9542-9543.

41. Satoh, K.; Matsuda, M.; Nagai, K.; Kamigaito, M., AAB-Sequence Living Radical Chain Copolymerization of Naturally Occurring Limonene with Maleimide: An End-to-End Sequence-Regulated Copolymer. *Journal of the American Chemical Society* **2010,** *132* (29), 10003-10005.

42. Soeriyadi, A. H.; Boyer, C.; Nystrom, F.; Zetterlund, P. B.; Whittaker, M. R., High-Order Multiblock Copolymers via Iterative Cu(0)-Mediated Radical Polymerizations (SET-LRP): Toward Biological Precision. *Journal of the American Chemical Society* **2011,** *133* (29), 11128-11131.

43. Tong, X.; Guo, B.-h.; Huang, Y., Toward the synthesis of sequence-controlled vinyl copolymers. *Chemical Communications* **2011,** *47* (5), 1455-1457.

44. Ida, S.; Ouchi, M.; Sawamoto, M., Template-Assisted Selective Radical Addition toward Sequence-Regulated Polymerization: Lariat Capture of Target Monomer by Template Initiator. *Journal of the American Chemical Society* **2010,** *132* (42), 14748-14750.

45. Maddux, T.; Li, W. J.; Yu, L. P., Stepwise synthesis of substituted oligo(phenylenevinylene) via an orthogonal approach. *Journal of the American Chemical Society* **1997,** *119* (4), 844-845.

46. Iwadate, N.; Suginome, M., Synthesis of B-Protected beta -Styrylboronic Acids via Iridium-Catalyzed Hydroboration of Alkynes with 1,8-Naphthalenediaminatoborane Leading to Iterative Synthesis of Oligo(phenylenevinylene)s. *Organic Letters* **2009,** *11* (9), 1899-1902.

47. Norris, B. N.; Pan, T.; Meyer, T. Y., Iterative synthesis of heterotelechelic oligo(phenylene-vinylene)s by olefin cross-metathesis. *Organic Letters* **2010,** *12* (23), 5514-5517.

48. Krebs, F. C.; Nyberg, R. B.; Jorgensen, M., Influence of Residual Catalyst on the Properties of Conjugated Polyphenylenevinylene Materials: Palladium Nanoparticles and Poor Electrical Performance. *Chemistry of Materials* **2004,** *16* (7), 1313-1318.

49. Norris, B. N., Sequenced Phenylene-Vinylene Oligomers and Copolymers. 2011.

50. Hutchison, G. R., Accurate Prediction of Band Gaps in Neutral Heterocyclic Conjugated Polymers. *Journal Of Physical Chemistry A* **2002,** *106* (44), 10596-10605.

51. Hutchison, G. R.; Zhao, Y.; Delley, B.; Freeman, A.; Ratner, M.; Marks, T., Electronic structure of conducting polymers: Limitations of oligomer extrapolation approximations and effects of heteroatoms. *Physical Review B: Condensed Matter and Materials Physics* **2003,** *68* (3), 035204.

52. Patra, A.; Wijsboom, Y. H.; Leitus, G.; Bendikov, M., Tuning the Band Gap of Low-Band-Gap Polyselenophenes and Polythiophenes: The Effect of the Heteroatom. *Chemistry of Materials* **2011,** *23* (3), 896-906.

53. Bredas, J.-L.; Norton, J. E.; Cornil, J.; Coropceanu, V., Molecular Understanding of Organic Solar Cells: The Challenges. *Accounts of Chemical Research* **2009,** *42* (11), 1691-1699.

54. Mondal, R.; Ko, S.; Norton, J. E.; Miyaki, N.; Becerril, H. A.; Verploegen, E.; Toney, M. F.; Bredas, J.-L.; McGehee, M. D.; Bao, Z., Molecular design for improved photovoltaic efficiency: band gap and absorption coefficient engineering. *Journal of Materials Chemistry* **2009,** *19* (39), 7195-7197.

55. Hachmann, J.; Olivares-Amaya, R.; Atahan-Evrenk, S.; Amador-Bedolla, C.; Sanchez-Carrera, R. S.; Gold-Parker, A.; Vogt, L.; Brockway, A. M.; Aspuru-Guzik, A., The Harvard Clean Energy Project: Large-Scale Computational Screening and Design of Organic Photovoltaics on the World Community Grid. *The Journal Of Physical Chemistry Letters* **2011,** *2* (17), 2241-2251.

56. Perdew, J.; Levy, M., Comment on "Significance of the highest occupied Kohn-Sham eigenvalue". *Physical Review B: Condensed Matter and Materials Physics* **1997,** *56* (24), 16021-16028.

57. Levy, M., Excitation-Energies from Density-Functional Orbital Energies. *Physical Review A: Atomic, Molecular, and Optical Physics* **1995,** *52* (6), R4313-R4315.

58. Zhan, C.; Nichols, J.; Dixon, D., Ionization potential, electron affinity, electronegativity, hardness, and electron excitation energy: Molecular properties from density functional theory orbital energies. *Journal Of Physical Chemistry A* **2003,** *107* (20), 4184-4195.

59. Rienstra-Kiracofe, J.; Tschumper, G.; Schaefer, H.; Nandi, S.; Ellison, G., Atomic and molecular electron affinities: Photoelectron experiments and theoretical computations. *Chemical Reviews* **2002,** *102* (1), 231-282.

60. Winget, P.; Weber, E.; Cramer, C.; Truhlar, D. G., Computational electrochemistry: aqueous one-electron oxidation potentials for substituted anilines. *Physical Chemistry Chemical Physics* **2000,** *2* (6), 1231-1239.

61. Jaque, P.; Marenich, A. V.; Cramer, C. J.; Truhlar, D. G., Computational electrochemistry: The aqueous Ru3+| Ru2+ reduction potential. *Journal of Physical Chemistry. C* **2007,** *111* (15), 5783-5799.

62. Kamlet, M.; Abboud, J.; Abraham, M.; Taft, R., Linear Solvation Energy Relationships .23. A Comprehensive Collection of the Solvatochromic Parameters, Pi-Star, Alpha and Beta, and Some Methods for Simplifying the Generalized Solvatochromic Equation. *Journal of Organic Chemistry* **1983,** *48* (17), 2877-2887.

63. Sherwood, G. A.; Cheng, R.; Smith, T. M.; Werner, J. H.; Shreve, A. P.; Peteanu, L. A.; Wildeman, J., Aggregation Effects on the Emission Spectra and Dynamics of Model Oligomers of MEH-PPV. *The Journal of Physical Chemistry C* **2009,** *113* (43), 18851-18862.

64. So, W. Y.; Hong, J.; Kim, J. J.; Sherwood, G. A.; Chacon-Madrid, K.; Werner, J. H.; Shreve, A. P.; Peteanu, L. A.; Wildeman, J., Effects of Solvent Properties on the Spectroscopy and Dynamics of Alkoxy-Substituted PPV Oligomer Aggregates. *The Journal of Physical Chemistry B* **2012,** *116* (35), 10504-10513.

65. Thulstrup, P. W.; Hoffmann, S. V.; Hansen, B. K. V.; Spanget-Larsen, J., Unique interplay between electronic states and dihedral angle for the molecular rotor diphenyldiacetylene. *Physical Chemistry Chemical Physics* **2011,** *13* (36), 16168-16174.

66. Tilley, A. J.; Danczak, S. M.; Browne, C.; Young, T.; Tan, T.; Ghiggino, K. P.; Smith, T. A.; White, J., Synthesis and Fluorescence Characterization of MEHPPV Oligomers. *Journal of Organic Chemistry* **2011,** *76* (9), 3372-3380.

67. Miyakoshi, R.; Shimono, K.; Yokoyama, A.; Yokozawa, T., Catalyst-Transfer Polycondensation for the Synthesis of Poly(p-phenylene) with Controlled Molecular Weight and Low Polydispersity. *Journal of the American Chemical Society* **2006,** *128* (50), 16012-16013.

68. Li, Y.; Li, H.; Xu, B.; Li, Z.; Chen, F.; Feng, D.; Zhang, J.; Tian, W., Molecular structure-property engineering for photovoltaic applications: Fluorene-acceptor alternating conjugated copolymers with varied bridged moieties. *Polymer* **2010,** *51* (8), 1786-1795.

69. Peng, Z.; Gharavi, A. R.; Yu, L., Synthesis and characterization of photorefractive polymers containing transition metal complexes as photosensitizer. *Journal of the American Chemical Society* **1997,** *119* (20), 4622-4632.

70. Olah, G. A.; Keumi, T., Synthetic methods and reactions. 60. Improved one-step conversion of aldehydes into nitriles with hydroxylamine in formic acid solution. *Synthesis* **1979,** (2), 112-13.

71. Yang, J.-S.; Hwang, C.-Y.; Hsieh, C.-C.; Chiou, S.-Y., Spectroscopic correlations between supermolecules and molecules. Anatomy of the ion-modulated electronic properties of the nitrogen donor in monoazacrown-derived intrinsic fluoroionophores. *Journal of Organic Chemistry* **2004,** *69* (3), 719-726.

72. Li, Z.; Badaeva, E.; Zhou, D.; Bjorgaard, J.; Glusac, K. D.; Killina, S.; Sun, W., Tuning Photophysics and Nonlinear Absorption of Bipyridyl Platinum(II) Bisstilbenylacetylide Complexes by Auxiliary Substituents. *The Journal of Physical Chemistry A* **2012,** *116* (20), 4878-4889.

73. Albers, H. M. H. G.; Hendrickx, L. J. D.; van Tol, R. J. P.; Hausmann, J.; Perrakis, A.; Ovaa, H., Structure-Based Design of Novel Boronic Acid-Based Inhibitors of Autotaxin. *Journal of Medicinal Chemistry* **2011,** *54* (13), 4619-4626.

3.0 SEQUENCE EFFECTS IN DONOR-ACCEPTOR OLIGOMERIC SEMICONDUCTORS COMPRISING BENZOTHIADIAZOLE AND PHENYLENE VINYLENE MONOMERS

3.1 OVERVIEW

To understand the influence of monomer sequence on the properties and performance of donor-acceptor type conjugated oligomers, a series of dimers, trimers, and tetramers were prepared from phenylene (**P**) and benzothiadiazole (**B**) monomers linked by vinylene groups. Optical and electrochemical studies established the influence of sequence on both the λ_{max} and redox potentials of this series of structurally related oligomers. The effect of end groups (cyano, bromo, and alkyl) was also demonstrated to be important for the properties of these oligomers. DFT calculations of the tetramers were performed and the energy levels were correlated well with the experimentally determined spectroscopic data. Bulk heterojunction (BHJ) solar cells fabricated with selected tetramers as the donor and $PC_{61}BM$ as the acceptor exhibited power conversion efficiencies that varied by a factor of three as a function of sequence. These results suggest that sequence control is important for tuning optoelectronic properties and photovoltaic performance of these structurally related conjugated oligomers.

In order to provide the full picture of our discoveries, the work of several coworkers will be included in this chapter. These contributions will be highlighted as they are discussed. Nicole Bauer and Wei You are acknowledged for their contribution to the device fabrication and testing and Ilana Kanal and Prof. Hutchison for their computational work. The majority of the work presented in this chapter was previously published in Zhang, S.; Bauer, N. E.; Kanal, I. Y.; You,

W.; Hutchison, G. R.; Meyer, T. Y., Sequence Effects in Donor–Acceptor Oligomeric Semiconductors Comprising Benzothiadiazole and Phenylenevinylene Monomers. *Macromolecules* **2017**, 50 (1), 151-161.[1]

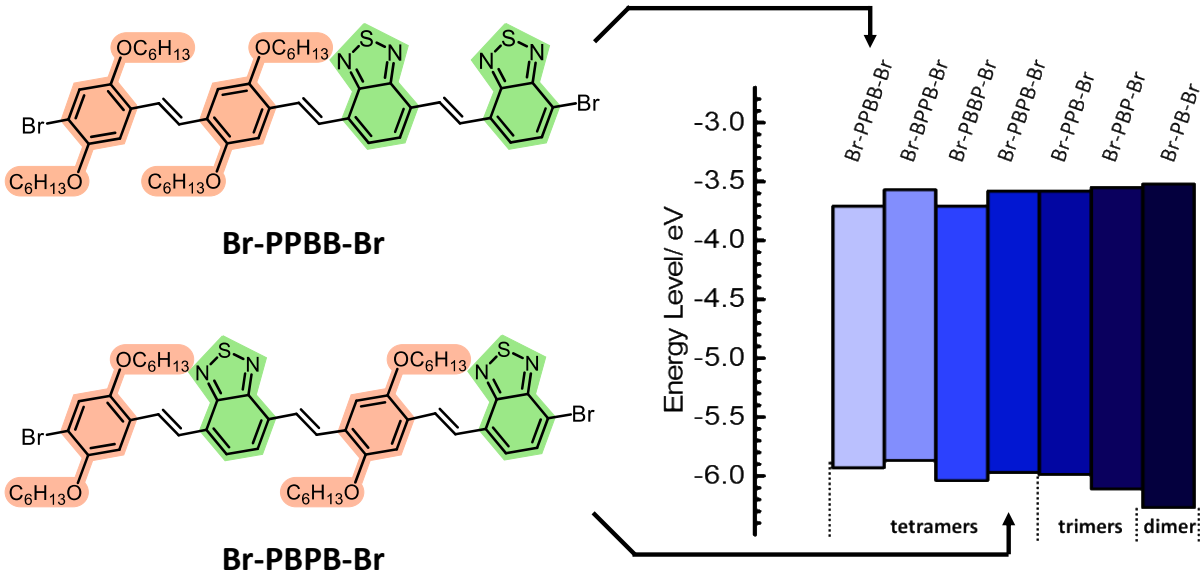

3.2 INTRODUCTION

The power and potential of conjugated organic materials stems from their rich diversity and ease of tailoring key properties including optical band gap, absorption and emission intensities, packing, and charge transport properties.[2-5] Applications include photovoltaics, efficient organic light-emitting displays, photocatalytic systems, polymer batteries and supercapacitors, and more.[4,6-12] While the majority of the conjugated materials have been polymeric systems, more

recent scientific efforts have demonstrated that oligomers, with complete control over chain length, chain ends, and chemical purity, offer unique advantages.[6-7, 10-11, 13]

Controlling monomer sequence is increasingly used to engineer properties in (non-conjugated) copolymers, but has not been widely exploited in conjugated systems.[14-16] In order to achieve desirable properties for these applications-oriented conjugated polymers, researchers have largely focused on designing increasingly sophisticated repeat units,[3, 17] tailoring side-chains,[18-19] and combining electron-rich and electron-poor monomers (donor-acceptor strategy).[4, 20-24] Some efforts have also focused on the use of end group modification to control *p*- and *n*-type carrier transport, oxidation and reduction potentials, and optical properties.[7, 25] Nevertheless, sequence remains largely unexplored in these conjugated materials; in contrast, results from non-conjugated materials have demonstrated that sequence control is important and has significant impact on properties of materials.[26-36]

We are interested in applying the sequence control strategy to conjugated oligomers and polymers; more importantly, we intend to study these structurally related materials to understand the effects of sequence on properties related to the use of these materials in photovoltaic devices. Though scarcely reported, there have been some promising examples of sequence effects.[27, 37-40] For example, Liang and coworkers reported that two sequence-isomeric conjugated oligomers exhibited power conversion efficiencies that were significantly different, 4.53% vs. 1.58%.[40] Sequence-based differences in morphology were also observed by Palermo *et al.* in their investigation of thiophene- and selenophene-based conjugated polymers with gradient sequence, block, and random structures.[37] The influence of sequence on properties, particularly photophysical properties, was also established by Noonan and coworkers for a series of copolymers comprising sequences of furan, thiophene, and selenophene.[41]

These intriguing reports have inspired us to further understand the influence of sequence on copolymer properties through the systematic preparation, characterization, and modelling of sequenced conjugated oligomers and polymers. In a prior study, we synthesized a series of oligomers using two monomers – an un-substituted and a dialkoxy-substituted phenylene vinylene, and discovered that the sequence strongly affected oxidation potentials, HOMO energies, and band gaps of these otherwise largely identical oligomers.[15] In tetramers, we found that the optical band gaps could be tuned over a range of 0.2 eV, based only on sequence and the end groups, despite that both monomers are electronically similar.

In the present investigation, we further explore the effect of sequence with two electronically different monomers: dialkoxy-substituted phenylene vinylene (electron-rich, **P**) and benzothiadiazole vinylene (electron-poor, **B**). While these monomers have been widely investigated for applications in OLED and solar cells,[42-47] the effect of sequencing these monomers have not been probed.[48] Herein, we extend our earlier study to tetrameric oligomers, and comprehensively investigate the effect of sequence and end groups on optoelectronic properties of these materials and their performance in bulk heterojunction solar cells.

3.3 RESULTS

3.3.1 Monomer Synthesis.

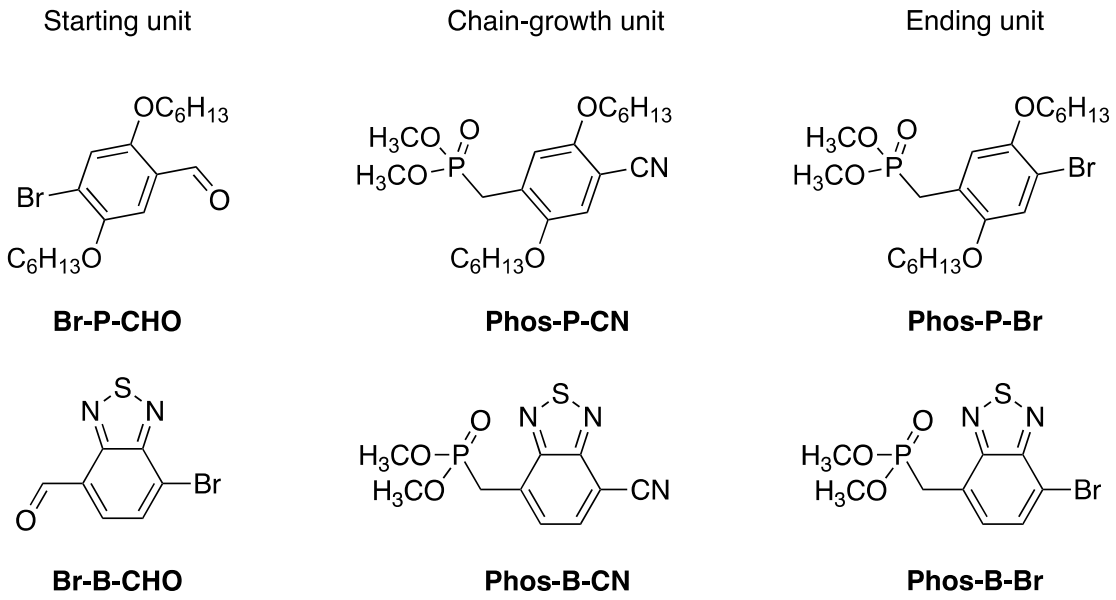

Figure 17. Structures of six monomers used in oligomer synthesis.

A series of conjugated oligomers with varying sequences were prepared by connecting two units, benzothiadiazole (**B**) and 2,5-dihexylalkoxy-substituted phenylene (**P**), with vinylene linkers. The oligomers comprised dimers, trimers and tetramers, based on the total number of **P**/**B** units, and bore either two bromo (**Br**) end groups, one **Br** and one cyano (**CN**) end group, or two α-olefinic alkyl groups (**C8**). Species with reactive end groups including aldehyde (**CHO**) and dimethyl phosphonate (**Phos**) were also prepared as synthetic intermediates. Oligomers are named throughout by listing their **P**/**B** sequence and end groups, e.g., **Br-PB-CN**.

In this study, we targeted oligomers with dibromo endgroups to minimize the endgroup effects seen in our previous work. It allows us to isolate more clearly property differences due

primarily to sequence. These dibromo-terminated oligomers were, however, also compared to oligomers bearing one bromo and one cyano endgroups or two **C8** endgroups. Six monomers were selected as building blocks for the sequenced oligomers (**Figure 17**). **Br-P-CHO** and **Br-B-CHO** are used as the starting units for all oligomers. **Phos-P-Br** and **Phos-B-Br** are used as the end units for dibromo oligomers. The remaining units, **Phos-P-CN** and **Phos-B-CN**, are used for both chain-growth or ending for oligomer with nitrile termination. The synthesis of **Br-P-CHO** and **Phos-P-CN** are described at chapter 2. We prepared **Br-B-CHO**, **Phos-P-Br**, and **Phos-B-Br** according to previously published methods, with some small optimizations.[15, 49] Their synthesis schemes are shown below.

The synthesis of 4-cyanobenzothiadiazolphosphonate (**Phos-B-CN**) was developed and optimized for the current study **(Figure 18)** although some portions of the synthesis were either based the synthesis of a similar substrate (**1, 4**) or involved the optimization of reactions from previously published protocols (**2**) [49-52] First, commercially available 2,3-diaminotoluene was treated with thionyl chloride in the presence of triethylamine to form methylbenzothiadiazole (**1**) in 85% yield after purification.[50] Bromination gave the bromine substituted benzothiadiazole (**2**) in a 65% yield.[49-50] The cyanation reaction was performed using a procedure that was previous reported to give cyano-BTD in 83% yield (**3**).[51] Characterization by ^{13}C NMR and mass spectroscopy confirmed the full conversion of **2** to **3**. To convert cyano-BTD to the HWE-substrate required two reactions. Bromination of the methyl group with NBS gave BTD-derivative (**4**). After isolation but without further purification, the product was treated with trimethylphosphite liquid to give **Phos-B-CN** in a yield over both reactions of 82%.[49]

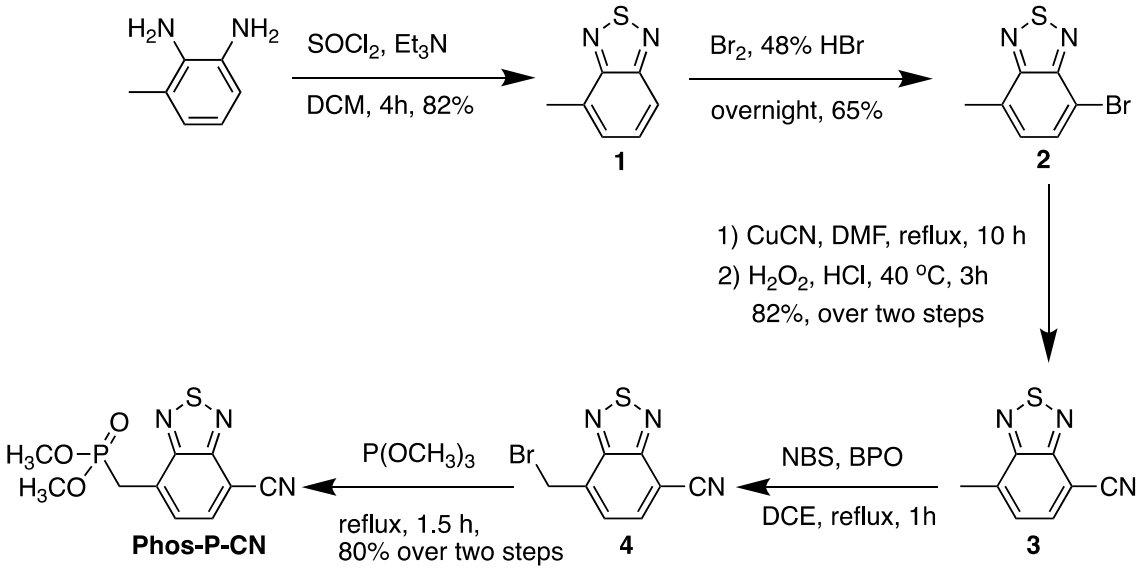

Figure 18. Synthesis of **Phos-B-CN**.

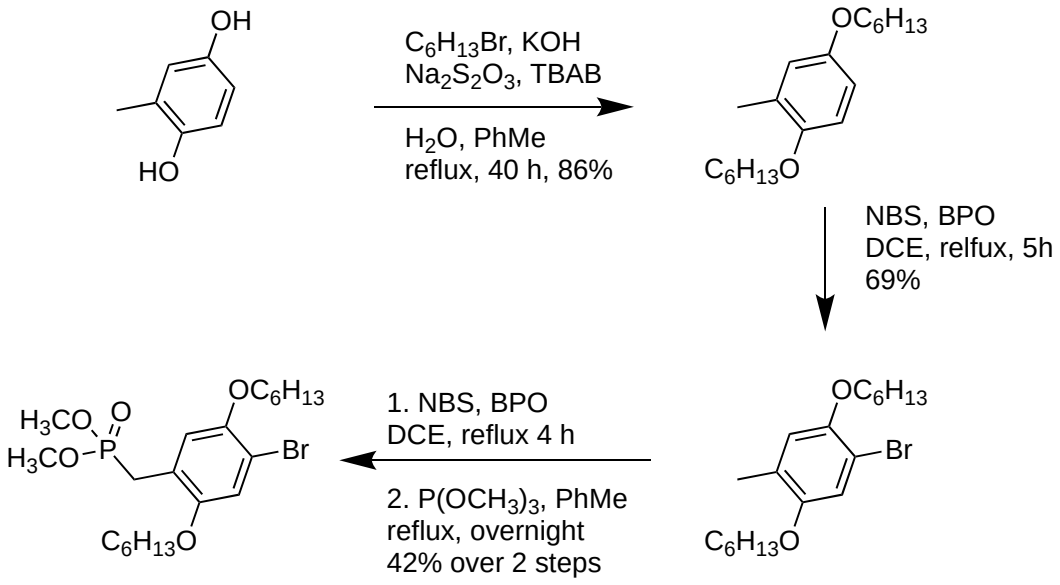

Figure 19. Synthesis of **Phos-P-Br**.

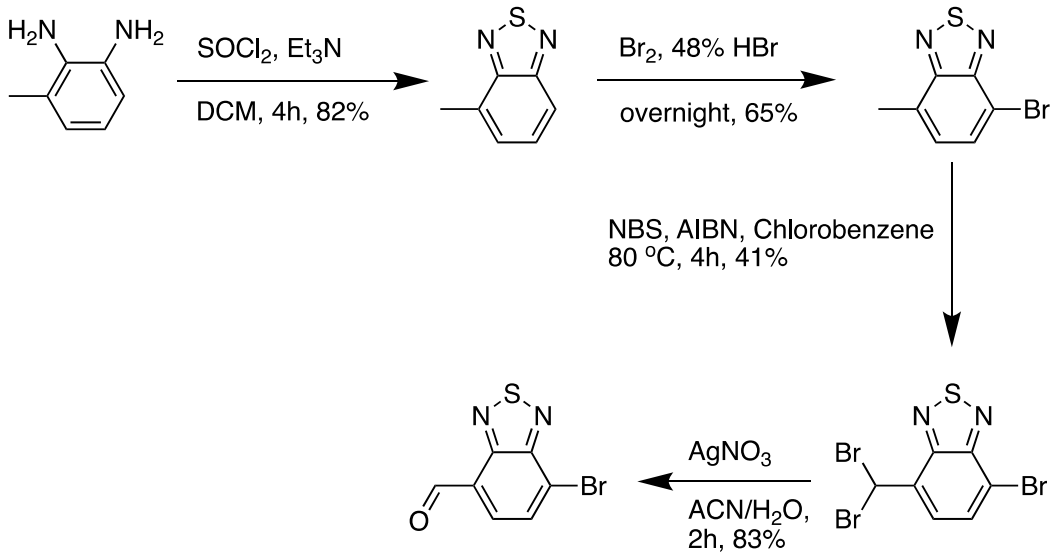

Figure 20. Synthesis of **Br-B-CHO**.

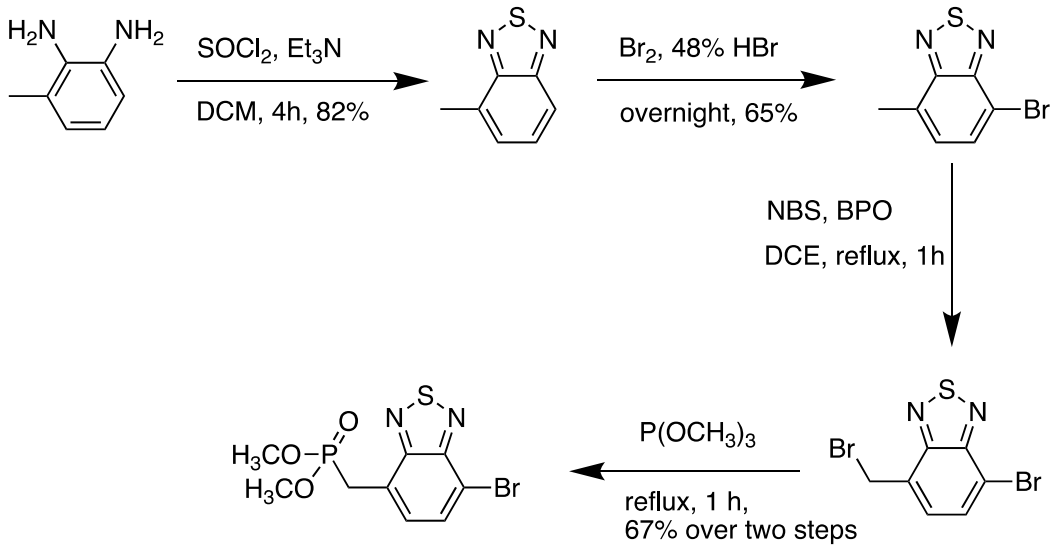

Figure 21. Synthesis of **Phos-B-Br**.

3.3.2 Oligomer Synthesis

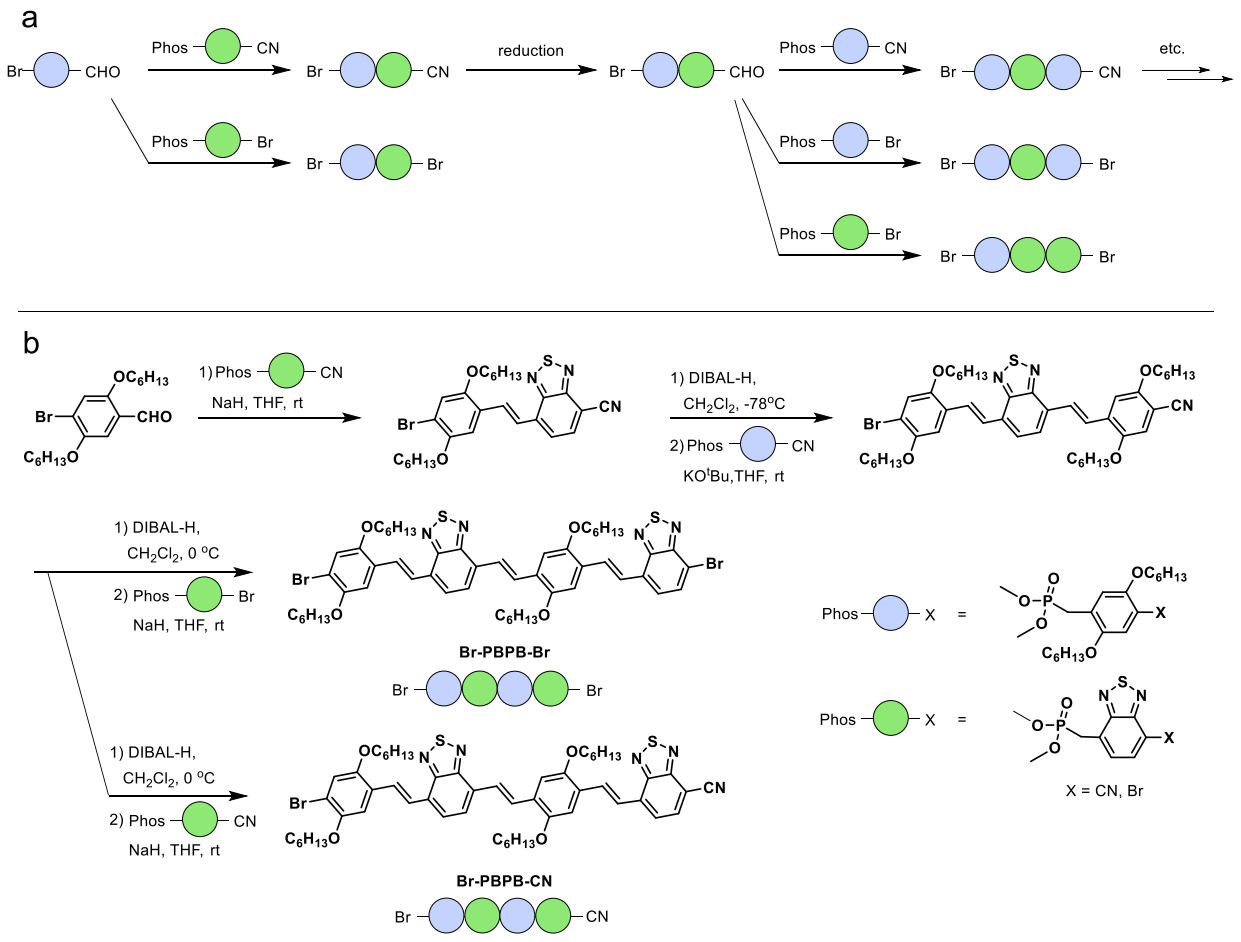

Figure 22. (a) Schematic depicting synthetic strategy, (b) Example synthesis of two sequenced oligomers.

Sequenced oligomers were synthesized from six small-molecule building units mentioned above, **Br-B-CHO**, **Phos-P-Br**, **Phos-P-CN**, **Phos-B-CN, Phos-B-Br** and **Br-B-CHO**. Coupling these units together sequentially with Horner-Wadsworth-Emmons (HWE) reactions facilitated the creation of oligomeric structures with defined sequences and end groups (**Figure 22**). Initial coupling between the aldehyde and phosphonate groups of the appropriate **P** and **B** building units produced nitrile-terminated dimers. These dimers were then prepared for subsequent additions by reductive conversion of the terminal nitrile to an aldehyde. We and others have previously accessed sequenced arylene vinylene oligomers using this general approach.[15, 49, 53]

The inclusion of the less reactive **B** unit required modifications to the chemical procedures used for the more electron-rich **P** units. In particular, a stronger base (NaH) was required to couple the benzothiadiazole phosphonate (**Phos-B-CN**) to aldehyde-bearing subunits.[52] The conversion of the terminal cyano-group to an aldehyde for the **B** unit was also challenging as the conditions used for DIBAL-H reduction of aldehydes on phenylene vinylene units resulted in significant decomposition. For reduction of oligomers with **B** linked with nitrile (for example **Br-PB-CN)**, therefore, the reaction was carried out at -78 ^{o}C and it was necessary to add the DIBAL-H in portions to prevent exposure of the oligomers to a large excess of the unreacted reductant. Reduction of the **P**-unit nitrile (for example **Br-BP-CN)** could, however, be performed as reported previously. Using this approach, two dimers, six trimers and six tetramers were prepared.

3.3.3 Optical and Electronic Properties.

The optical and electrochemical properties of the sequenced oligomers were determined and are presented in **Table 6** and **Table 7**. As expected, the absorption maxima show a red-shift with increasing oligomer length: dimers (429-450 nm), trimers (458-479 nm), and tetramers (490-530 nm). Emissions likewise shift towards longer wavelengths; and band gaps, both optical and electrochemical, narrow as expected with increasing conjugation length.

Although it is challenging to deconvolute the end group effects from the sequence effects in these oligomeric structures, we were able, with such a rich library of oligomers, to understand the trends and focus our attention on bromo end groups, which have only a minor impact on the electronic properties. In considering end group effects, it is important to understand that terminal units are distinct from internal ones due to the neighboring free space, independent of the identity of the functional end group. As tetramers comprise 50% terminal monomers and 50% internal

monomers, many changes in sequence will necessarily involve changes in the terminal monomers as well.

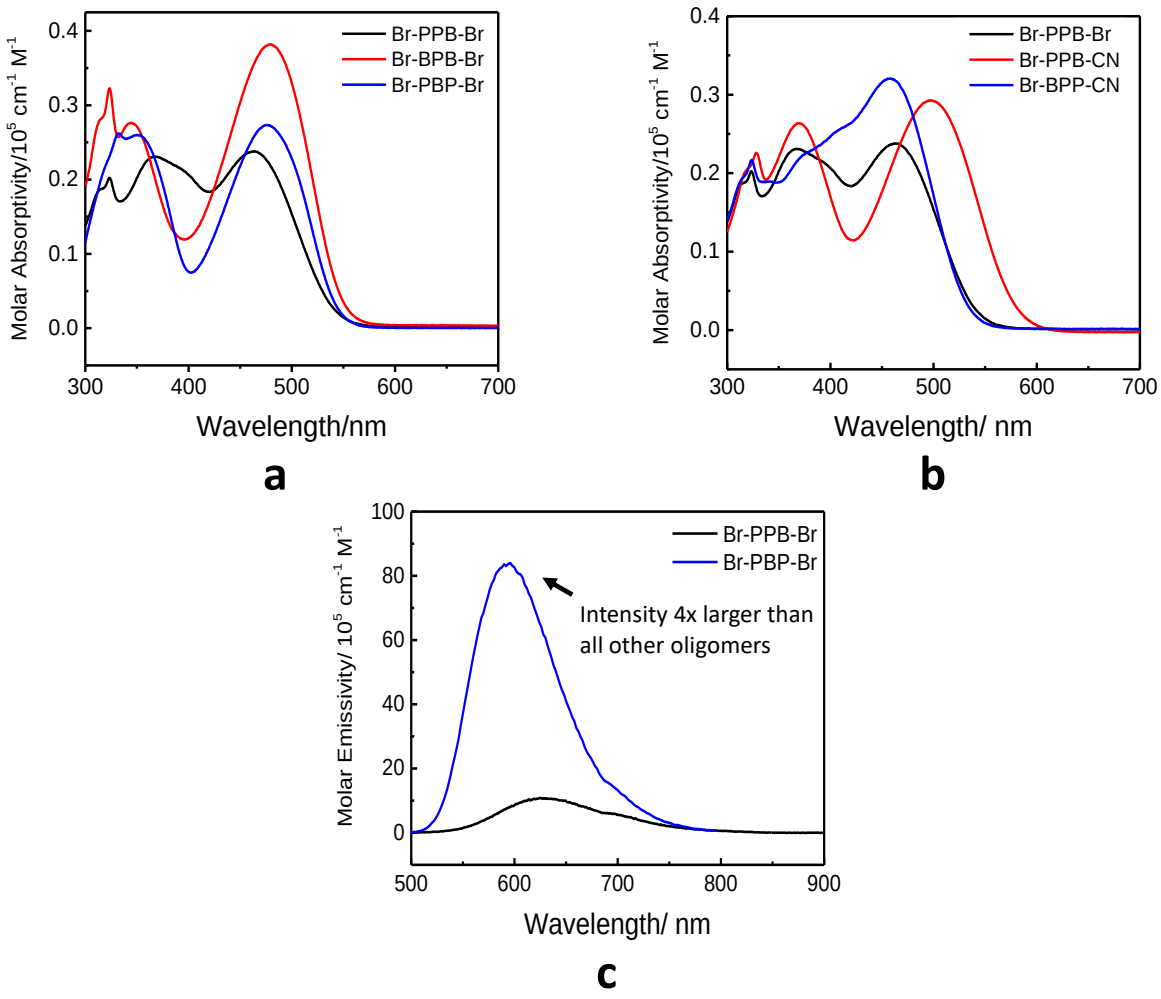

Figure 23. Absorption and emission spectra: (a) absorption spectra for all dibromo trimers in chloroform (1.0×10^{-5} M); (b) absorption spectra for **PPB** trimers bearing cyano and bromo end groups in chloroform (1.0×10^{-5} M); (c) emission spectra for selected trimers in chloroform (1.0×10^{-5} M).

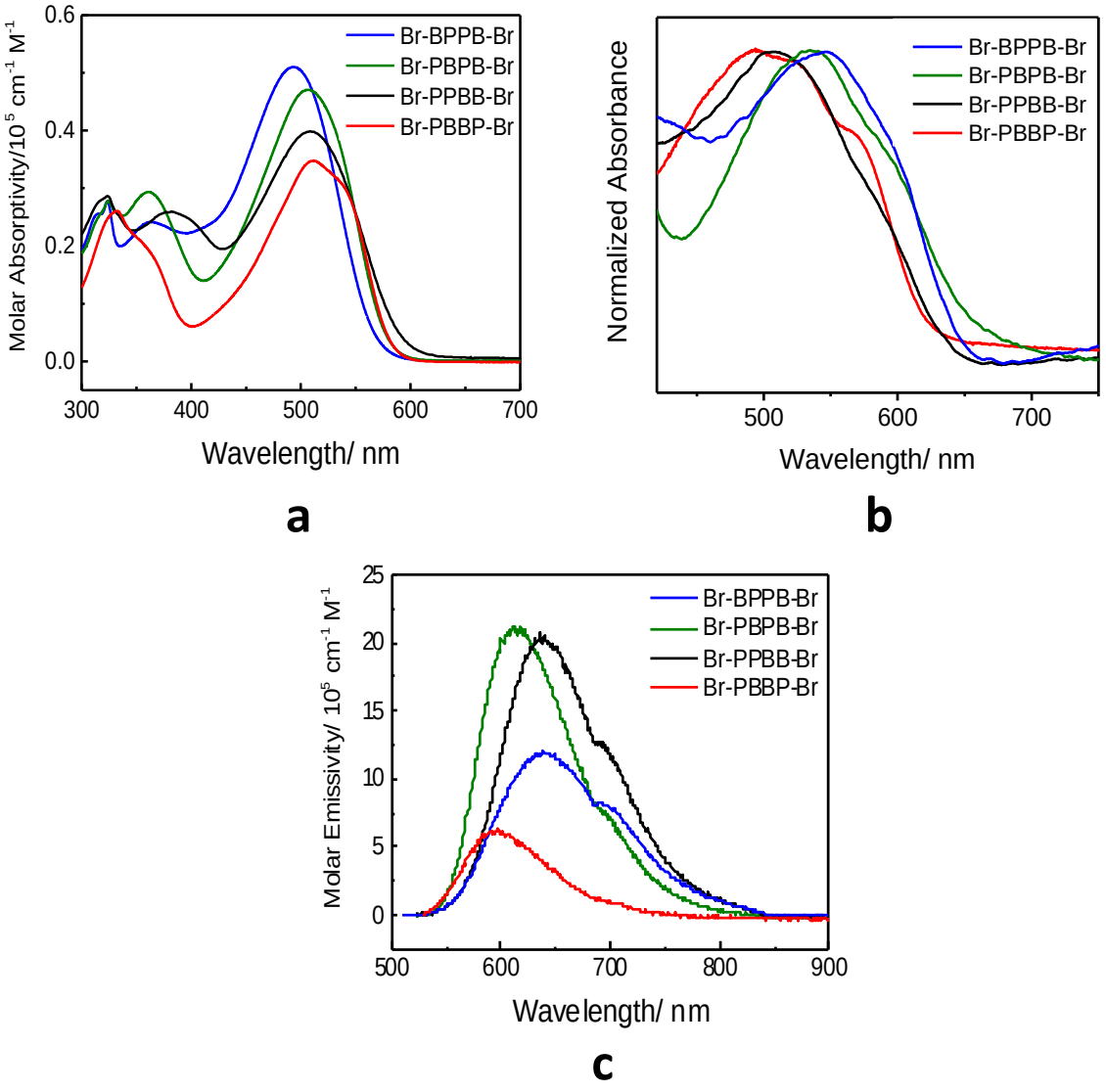

Figure 24. Absorption and emission spectra: (a) absorption spectra for all dibromo tetramers in chloroform (1.0×10^{-5} M); (b) film absorption spectra of PB tetramers, cast from chloroform solution; (c) emission spectra for dibromo tetramers in chloroform (1.0×10^{-5} M).

Table 6. Optical data for sequenced oligomers

Oligomer [c]	λ_{max}^{abs} [a] / nm	λ_{max}^{em} [a] / nm	E_{gap}^{opt} [b] / V
Br-PB-Br	432	576	2.97
Br-PB-CN	450	593	
C8-PB-C8	429	585	2.98
Br-BPB-Br	479	-	-
Br-PPB-Br	464	628	2.29
Br-PBP-Br	476	594	2.28
Br-PBP-CN	467	583	2.29
Br-PPB-CN	498	658	2.14
Br-BPP-CN	458	609	2.33
C8-BPP-C8	448	613	-
C8-PBP-C8	489	618	-
Br-BPPB-Br	493	639	2.19
Br-PBPB-Br	507	613	2.15
Br-PBPB-CN	523	702	2.07
Br-PPBB-Br	508	637	2.10
Br-PPBB-CN	530	707	1.99
Br-PBBP-Br	512	595	2.13

[a] Measured in chloroform (1.0×10^{-5} M); [b] Determined at the onset of absorption spectra; [c] **B**: benzothiadiazole unit, **P**: 2,5-dihexylalkoxy substituted phenylene units, **Br**: bromo end group, **CN**: cyano end group; **C8**: -$CH_2(CH_2)_5CH=CH_2$

Consistent with our earlier studies on sequenced phenylene vinylene oligomers, the effect of the unsaturated, electron-withdrawing cyano substituent was profound and depended significantly on the identity of the terminal monomer to which it was attached. Comparing two oligomers that have the same inherent sequence, **PPB**, but reversed end groups, **Br-BPP-CN** vs. **Br-PPB-CN** (= **CN-BPP-Br**), it was observed that the λ_{max} red-shifted nearly 40 nm (**Figure 23b**). Adding the cyano end group to a **B** monomer created a much stronger electron-withdrawing unit.

Oligomers with **–CN** attached to a **P** monomer absorbed at a slightly higher energy than the other **PPB** analogues studied. Oligomers with the **–CN** located on a **B**-monomer absorbed at lower energies than the dibromo-terminated sequences (e.g., **Br-PPB-CN** and **Br-PBPB-CN**)

Table 7. Electrochemical data for sequenced oligomers

Oligomer	$\boldsymbol{E^{ox}_{peak}}$ [a]**/ V**	$\boldsymbol{E^{red}_{peak}}$ [a]**/ V**	$\boldsymbol{\Delta E^{ec}_{gap}}$ [b]**/ eV**
Br-PB-Br	1.05	-1.50	2.55
Br-PPB-Br	0.77	-1.44	2.21
Br-PBP-Br	0.89	-1.47	2.36
Br-BPPB-Br	0.65	-1.45	2.10
Br-PBPB-Br	0.75	-1.44	2.19
Br-PPBB-Br	0.71	-1.31	2.02
Br-PBBP-Br	0.82	-1.31	2.13

[a] Potential vs. Ag/Ag+, 240 μM in 0.1 M Bu_4NPF_6 in THF; [b] Determined as $\boldsymbol{\Delta E^{ec}_{gap} = e(E^{ox}_{peak} - E^{red}_{peak})}$

Bromo and **C8** end groups appeared to exert only a modest influence on the optical properties, especially when compared to the highly perturbing –**CN.** That being said, the same pattern of dependence on the identity of the terminal monomer which was noted for **–CN** was also observed for these two end groups. The **C8** (C8 = $–(CH_2)_6CH=CH_2$) group would be expected to be only a mild σ-donor while the bromo group should be modestly σ-withdrawing and π-donating. In solution, a red shift of 13 nm was observed when changing the electron-withdrawing **Br** to an electron-donating **C8** on **P** units in the **PBP** analogues, **Br-PBP-Br** (λ_{max} = 476 nm) and **C8-PBP-C8** (λ_{max} = 489 nm). The effect of the interaction of the end group with the attached monomer can also be seen in the comparison of **Br-PB-Br** (λ_{max} = 429 nm) vs **C8-PB-C8** (λ_{max} = 432 nm) and

Br-PPB-Br (λ_{max} = 464 nm) vs **C8-PPB-C8** (λ_{max} = 448 nm). Based on these data, we hypothesize that when a **Br** attached to a **B** unit is replaced with a **C8,** eg, **Br-PB-Br** to **Br-PB-C8**, the blue shift of the λ_{max} is partly canceled by the red shift due to the **C8** substitution of the **Br** on the **P** unit, eg, **Br-PB-Br** to **C8-PB-Br**. As these effects were relatively modest relative to those observed with the **-CN** group, we elected to focus our sequence comparison studies on the dibromo-substituted oligomers.

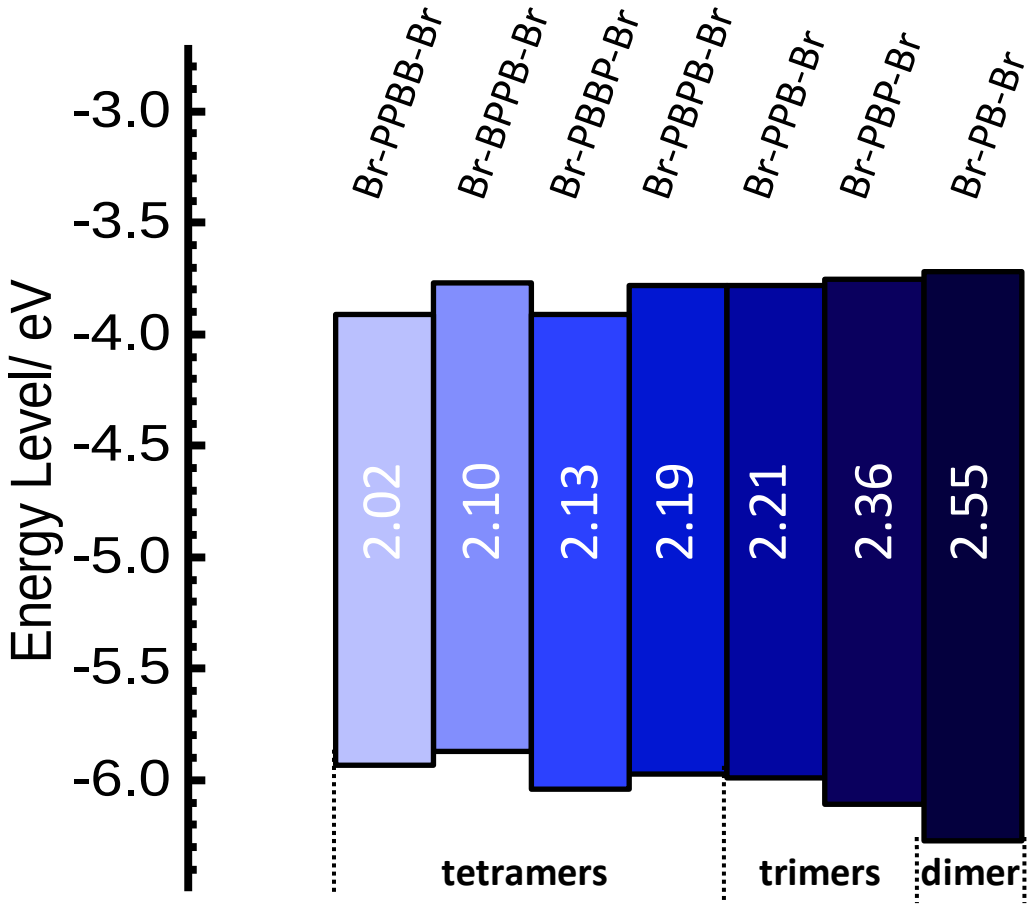

Figure 25. Electrochemical redox potentials and band gaps of sequenced oligomers, expressed relative to vacuum. Electrochemical band-gaps are indicated in eV. The color gradient is for illustration purposes only.

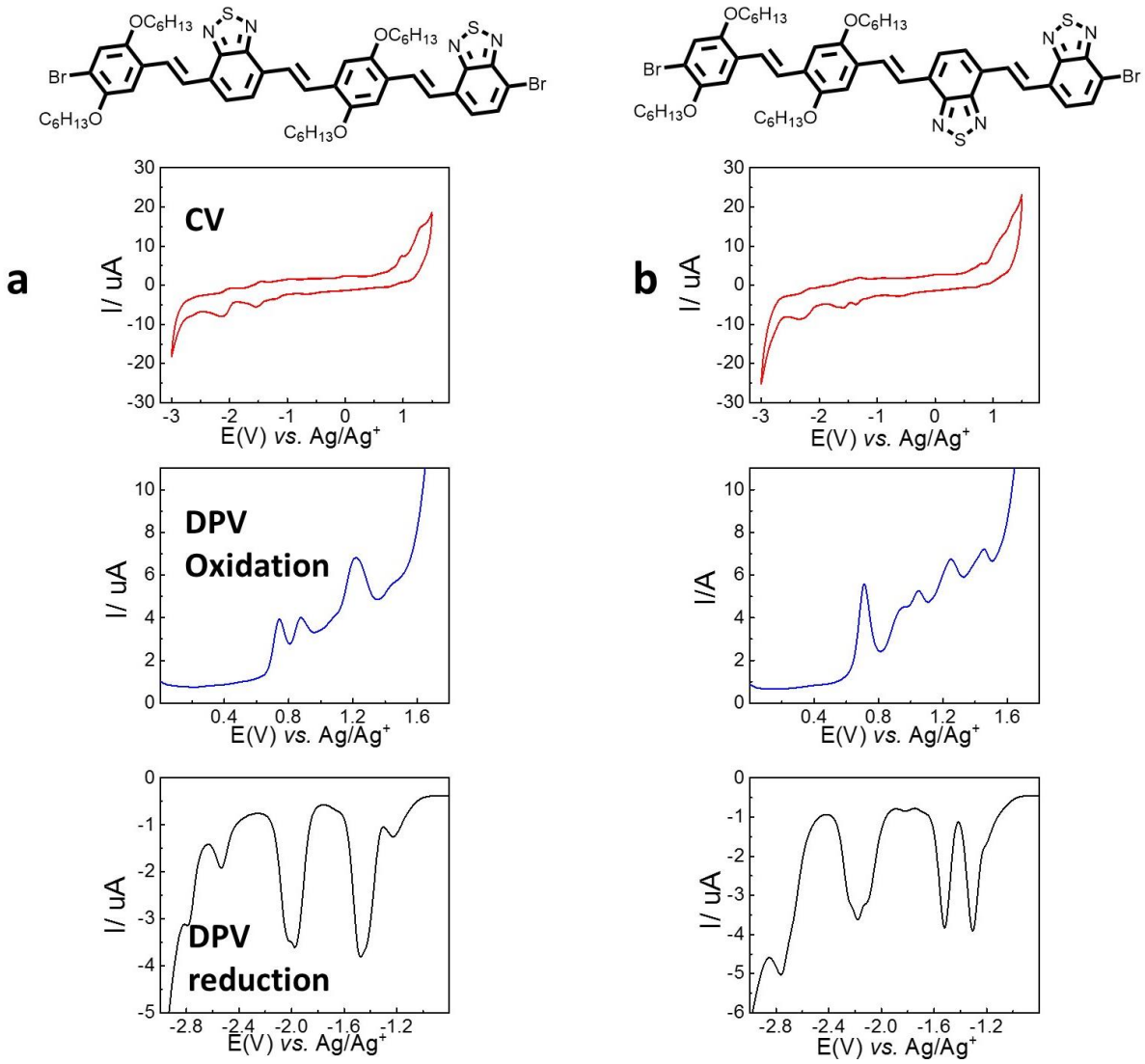

Figure 26. Example cyclic voltammograms and differential pulse voltammograms of (a) **Br-PBPB-Br** and (b) **Br-PPBB-Br**

In examining the Br-terminated oligomers, we did indeed find evidence for sequence effects in both the trimer and tetramer series (**Figure 23** and **Figure 24**). Focusing only on the two trimers with the same 2:1 ratio of **P:B** and bromo end groups, **Br-PBP-Br** and **Br-PPB-Br**, differences in absorption maxima (Δ = 10 nm), oxidation potential (Δ = 0.12 V), and electrochemical gap (Δ = 0.15 V) were observed. The reduction potentials were, however, similar (Δ= 0.03 V), suggesting that they are determined primarily by the single **B**-unit. It should be noted

that **Br-PPB-Br**, which is the name used throughout this chapter, could also be written as **Br-BPP-Br**.

Unambiguous sequence effects are also clearly seen in the dibromo-terminated tetramer series all of which have the same 1:1 **P:B** ratio. Most persuasively, the two bromo-terminated tetramers **Br-PPBB-Br** and **Br-PBPB-Br,** exhibited the largest difference in the magnitude of their electrochemical gaps (0.17 V). Since both of these oligomers have exactly one **P**-Br and one **B**-Br interaction, the difference must be attributed to sequence alone. **Br-PPBB-Br** exhibited both a less positive reduction and less negative oxidation potential than the alternating sequence isomer (**Br-PBPB-Br**). In examining the other two oligomers in the series, it became clear the presence of a **BB**-pairing defines the reduction potential: both **Br-PPBB-Br** and **Br-PBBP-Br** were reduced at – 1.31 V. The oligomers **Br-BPPB-Br** and **Br-PBPB-Br** exhibited more negative reduction potentials of -1.45 and -1.46 V, respectively. The trend in oxidation potentials appears to depend more on the distance between **P** units. Those oligomers with **PP**-pairing, **Br-BPPB-Br** and **Br-PPBB-Br**, exhibited lower oxidation potentials than those with separated **P** units. The trend is gradual, however, not binary as was the case for the reduction potentials vs. **BB**-pairings.

We also observe some intriguing sequence effects in the solution phase absorption and emission spectra, especially in absorption/emission intensities. For the trimers with a 2:1 **P:B** ratio, the absorption intensities at 10^{-5} M in chloroform are similar (ca. 0.3×10^5 cm^{-1} M^{-1}) but the emission intensities are dramatically different (**Figure 23c**). In particular, the intensity of the emission for **Br-PBP-Br** of 80×10^5 cm^{-1} M^{-1} is at least 4× larger than that for all other oligomers characterized. Within the 1:1 **P:B** tetramer series, the absorption intensities are modestly different (range $0.35\text{-}0.5 \times 10^5$ cm^{-1} M^{-1}) with **Br-BPPB-Br** > **Br-PBPB-Br** > **Br-PPBB-Br** > **Br-PBBP-Br** which is inversely related to the increase in absorption wavelength (**Figure 24a**). The emission

intensities for these tetramers exhibited larger differences (range 5-20 × 10^5 cm^{-1} M^{-1}) but follow the order **Br-PBPB-Br** ≈ **Br-PPBB-Br** > **Br-BPPB-Br** > **Br-PBBP-Br** which does not appear to correlate with the changes in emission wavelength (**Figure 24c**). These differences in intensity cannot be simply explained as the trends differ between the trimeric and tetrameric oligomers. For example, the two oligomers with the highest degree of quenching, **Br-PPB-Br** and **Br-PBBP-Br**, are dissimilar in both symmetry and end group attachment. The lack of correlation between the trimer and tetramer systems suggests that these differences could only be explained by a full photophysical study which lies beyond the scope of the current work.

Absorption data for thin films were also collected for those tetramers that were selected for incorporation in devices (**Figure 24b**). The λ_{max} of films cast from chloroform solutions followed the trend **Br-BPPB-Br** (λ_{max} = 546 nm) > **Br-PBPB-Br** (λ_{max} = 536 nm) > **Br-PPBB-Br** (λ_{max} = 510 nm) > **Br-PBBP-Br** (λ_{max} = 494 nm). Notably this trend is opposite to their absorption maxima in solution **Br-BPPB-Br** (λ_{max} = 493 nm) < **Br-PBPB-Br** (λ_{max} = 507 nm) < **Br-PPBB-Br** (λ_{max} = 508 nm) < **Br-PBBP-Br** (λ_{max} = 512 nm) (**Figure 24a**). The fact that these sequences exhibit a different pattern of absorption in the solid state suggests that the interchain interactions and short-range order are also sequence-dependent, with **Br-BPPB-Br** exhibiting the largest red-shift and potentially the highest degree of aggregation. Also consistent is the fact that we observe larger sequence-based differences in the λ_{max} absorptions in the solid state (52 nm) than in solution (19 nm).

3.3.4 Solar cell properties of sequenced oligomers

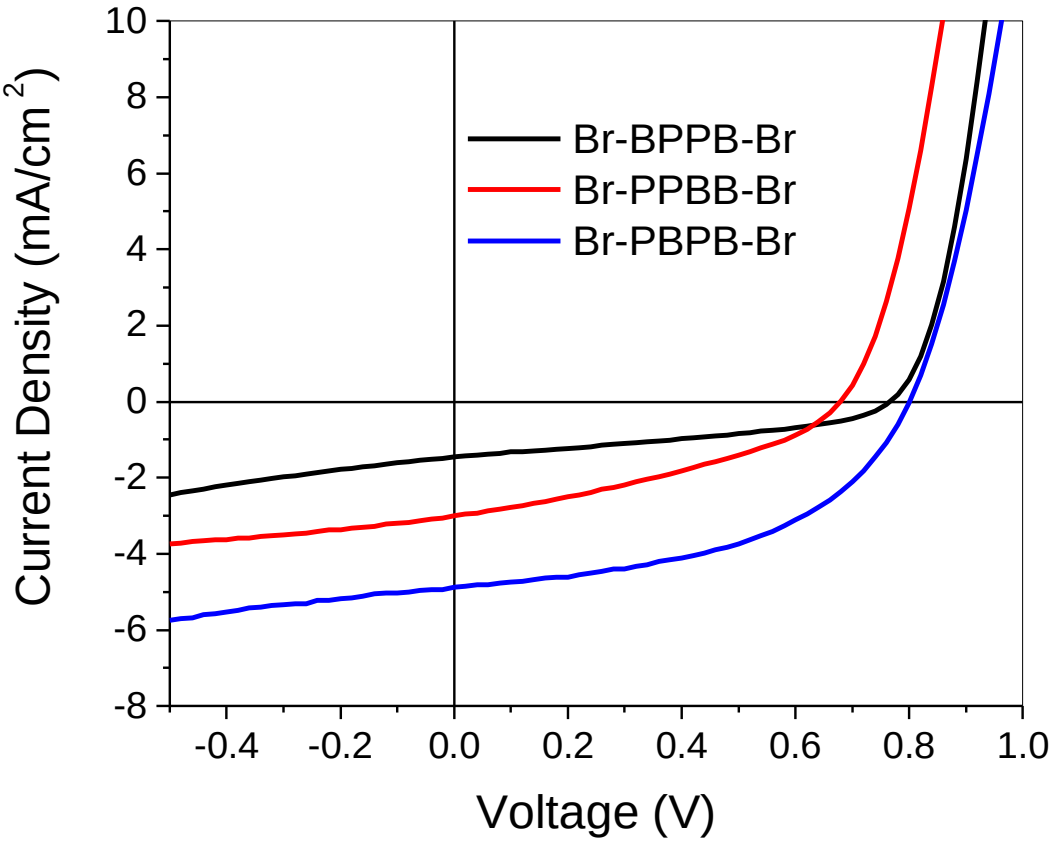

Figure 27. Representative J-V output of photovoltaic devices based on oligomers.

A selection of these oligomers were incorporated into solar cells to further understand the impact of sequence on the device performance (**Figure 27 and Table 8**). The device fabrication and testing in this section were performed by Nicole Bauer and Prof. Wei You. Based on literature reports of related molecules and the relatively short conjugation lengths, we would only expect modest power conversion efficiencies for these materials;[6] however, we hypothesized that any observed differences in the device-related characteristics would offer insight into the effect of sequence on the multiplicity of properties that contribute to device performance. To investigate

these properties, bulk heterojunction (BHJ) solar cells were fabricated with the configuration of ITO/PEDOT:PSS/oligomer:$PC_{61}BM$ (1:1)/Ca/Al for selected oligomers: **Br-PBP-Br**, **Br-PPB-Br**, **Br-PBPB-Br**, **Br-BPPB-Br**, and **Br-PPBB-Br**. The tetramer, **Br-PBBP-Br** was not included due to synthetic challenges (extremely poor solubility of intermediates) that precluded the preparation of the quantities necessary for these studies.

Table 8. Device characteristics of BHJ solar cell with oligomers: PCBM (1:1)

Oligomers	**Thickness /nm**	J_{sc}[a] **/mA·cm^{-2}**	V_{oc}[b] **/V**	*FF*[c] **/%**	**PCE**[d] **/%**
Br-PBP-Br	131	0.02±0.01	0.455±.109	27.3±1.4	0.00±0.00
Br-PPB-Br	152	0.96±0.04	0.824±.009	35.1±0.4	0.28±0.01
Br-PPB-CN	219	0.94±0.14	0.844±.067	31.3±3.6	0.25±0.07
Br-BPP-CN	146	1.46±0.21	0.666±.041	33.7±5.6	0.34±0.10
Br-BPPB-Br	85	1.45±0.11	0.770±.016	41.2±5.8	0.47±0.10
Br-PPBB-Br	84	3.16±0.16	0.717±.075	34.5±1.7	0.79±0.15
Br-PBPB-Br	89	4.85±0.42	0.768±.036	49.4±2.9	1.85±0.26

[a] Jsc: short circuit current; [b] Voc: open circuit voltage; [c] FF: fill factor; [d] PCE: power conversion efficiency.

The first sequence-based difference was observed in the trimer series with the same 2:1 **P**:**B** ratio (**Table 8**). **Br-PBP-Br** did not give any measurable performance in the solar cell, while **Br-PPB-Br** exhibited a small but reproducible power conversion efficiency (PCE) of 0.28%. **PPB** analogs with different end groups (**Br-BPP-CN** and **Br-PPB-CN**) were also studied. The differences in PCE (0.28% - 0.37%) between all three **PPB** analogs were negligible, therefore no reliable conclusion about end group effects on solar cell performance can be drawn from these data. Increasing the conjugation length from trimer to tetramer increased the overall performance of the materials as would be expected.[54]

Table 9. Hole mobilities of tetramers measured by space charge limited current method.

Oligomers	Thickness /nm	Hole Mobility / $\times 10^{-5}$ $cm^2 \cdot V^{-1} \cdot s^{-1}$
Br-BPPB-Br	118	5.94 ± 1.73
Br-PPBB-Br	137	1.58 ± 0.43
Br-PBPB-Br	118	2.87 ± 1.01

For the 1:1 P:B ratio tetramers, the measured efficiencies ranged from 0.47% for **Br-BPPB-Br** to 1.86% for **Br-PBPB-Br**, a difference of ~3×. Devices prepared with **Br-PPBB-Br** exhibited an intermediate PCE of 0.79%. Please note that all three devices had similarly thin active layers (~85 nm) such that the observed device performance can be directly correlated with the optoelectronic properties of these oligomers. To provide more insight into the reasons for these differences, the hole mobilities of the BHJ blends were measured via the space charge limited current (SCLC) method by fabricating hole-only devices with the structure ITO/PEDOT:PSS/Oligomer:$PC_{61}BM$ (1:1)/MoO_3/Al (**Table 9**). The hole mobilities follow the trend **Br-BPPB-Br** (5.94×10^{-5} $cm^2V^{-1}s^{-1}$) > **Br-PBPB-Br** (2.87×10^{-5} $cm^2V^{-1}s^{-1}$) > **Br-PPBB-Br** (1.58×10^{-5} $cm^2V^{-1}s^{-1}$). The relatively low hole mobilities are consistent with the modest PCEs exhibited by these oligomers; high fill factors are normally associated with mobility values of ~10^{-3} $cm^2V^{-1}s^{-1}$.[55-58]

Film topologies of neat tetramer films and photoactive layers (tetramers/$PC_{61}BM$) in solar cells were further characterized by tapping mode atomic force microscopy (AFM). As shown in **Figure 28,** distinct topologies in spin-cast neat films of three tetramers were observed. Particularly, the root mean squared (RMS) height of the neat **Br-PBPB-Br** film is much smaller than that of the other two sequences (0.843 nm vs 14.2 nm and 17.2 nm). However, no obvious topology differences in photoactive layers were observed between sequences (**Figure 29**).

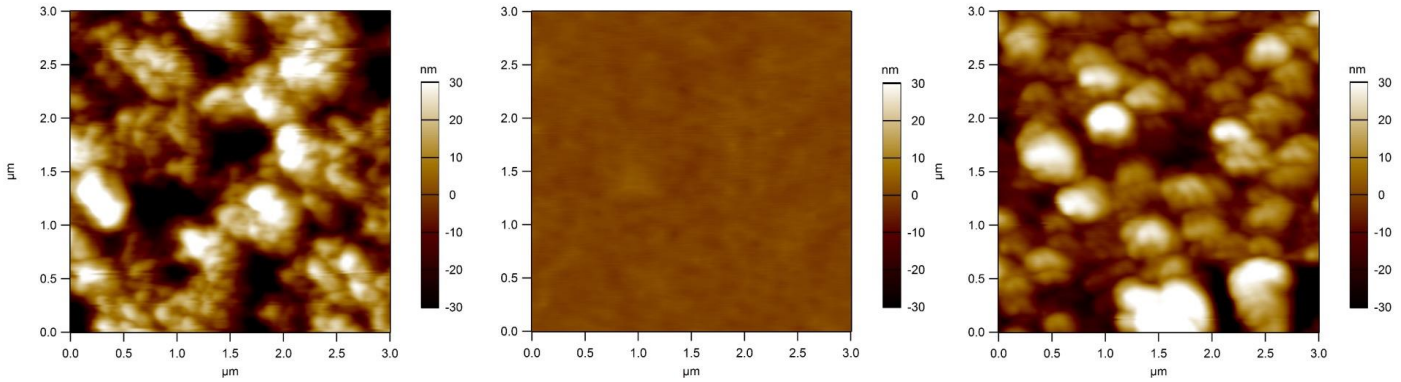

Figure 28. Height scans for tetramer films cast from chloroform solution.

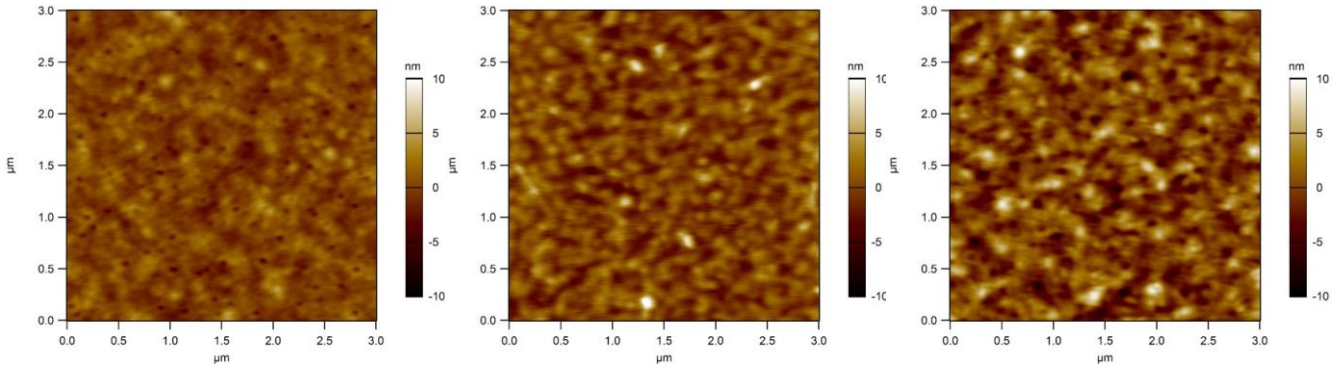

Figure 29. Height scans for tetramer:PCBM (1:1) blend films cast from chloroform solution**.**

3.3.5 Computational approach.

Table 10. Consensus model predicted oxidation, reduction and gap energies for dimers, trimers and tetramers.

Oligomer	Predicted E_{peak}^{ox}/ V	Predicted E_{peak}^{red}/ V	ΔE_{gap}^{comp}/eV
Br-PB-Br[a]	1.06	-1.47	2.55
Br-PB-CN	1.20	-1.53	-
Br-BP-CN	1.27	-1.43	-
Br-BPB-Br	0.84	-.143	3.23
Br-PBP-Br	0.82	-1.44	3.36
Br-PBP-CN	0.96	-1.41	3.31
Br-PPB-Br[a]	0.81	-1.46	3.34
Br-PPB-CN	0.83	-1.45	3.12
Br-BPP-CN	0.99	-1.44	3.41
Br-PBB-CN	0.96	-1.40	3.09
Br-BPB-CN	0.94	-1.42	3.13
Br-BPPB-Br	0.66	-.144	3.09
Br-PBPB-Br[a]	0.76	-1.41	3.07
Br-PBPB-CN	0.63	-1.41	3.11
Br-PPBB-Br[a]	0.71	-1.36	3.05
Br-PPBB-CN	0.80	-1.40	3.11
Br-PBBP-Br	0.76	-1.37	3.10
Br-PBBP-CN	0.70	-1.38	3.11
Br-BPPB-CN	0.65	-1.44	3.19
Br-BPBP-CN	0.63	-1.41	3.11
Br-BBPP-CN	0.64	-1.41	3.04

[a] average of values for two conformations

Computational experiments in this chapter were performed by Ilana Kanal and Prof. Hutchison. Computational methods provide a fast and relatively inexpensive mechanism to screen optoelectronic properties of π-conjugated materials. Several studies have found a high degree of correlation between density functional theory (DFT) computed orbital eigenvalues, vertical

ionization potentials and electron affinities,[59-60] though these calculations yield nonphysical results.[61-62] In addition, DFT calculations provide accurate predictions of optical band gaps.[63] In solution electrochemistry, redox potentials can be predicted based on the free energy change.[64-65] The adiabatic difference in total energy between the neutral and positively or negatively charged systems (ΔSCF) provides oxidation or reduction potentials, respectively.

Table 11. Computed HOMO, LUMO and gap eigenvalues for hexamers.

Oligomer	Computed HOMO[a] /eV	Computed LUMO[a] /eV	$\Delta E_{\mathrm{gap}}^{\mathrm{comp}}$[a]/ eV
Br-PPPBBB-Br	-4.79	-2.99	1.80
Br-PPBPBB-Br	-4.80	-2.91	1.89
Br-PBPPBB-Br	-4.81	-2.87	1.94
Br-BPPPBB-Br	-4.77	-2.82	1.95
Br-BPBBPP-Br	-4.81	-2.88	1.93
Br-BPPBPB-Br	-4.83	-2.74	2.09
Br-BPPBBP-Br	-4.70	-2.78	1.91
Br-PBBBPP-Br	-4.86	-3.01	1.85
Br-PBPBBP-Br	-4.87	-2.92	1.96
Br-PBPBPB-Br	-4.66	-2.70	1.96

[a]average of values for two conformations

Since our objective was to reliably and accurately screen for targeted properties of sequenced oligomers, a "consensus model" was chosen to extend these regression techniques to minimize both systematic and random errors, i.e., to improve accuracy and correlation. The consensus model used here combines two different computational predictions of an experimental property using multivariate regression, e.g., oxidation potential. For redox potentials, calculated HOMO or LUMO eigenvalues and adiabatic total energy differences (ΔSCF) were both used, and to predict optical absorption energies, ZINDO and time-dependent DFT (TDDFT) methods were combined with the HOMO-LUMO difference.

The computational method was parameterized on the trimer and tetramer compounds that were synthesized. The electronic properties of all possible dimer, trimer and tetramer sequences were then predicted based on the derived models. (**Table 10**) When palindromic sequences were examined (i.e. **Br-PPB-Br** and **Br-BPP-Br**), energy differences in predicted oxidation potentials (~0.04 V), reduction potentials (~0.01 V) and optical absorption energies (~0.03 eV) were observed due to conformational differences.[47]

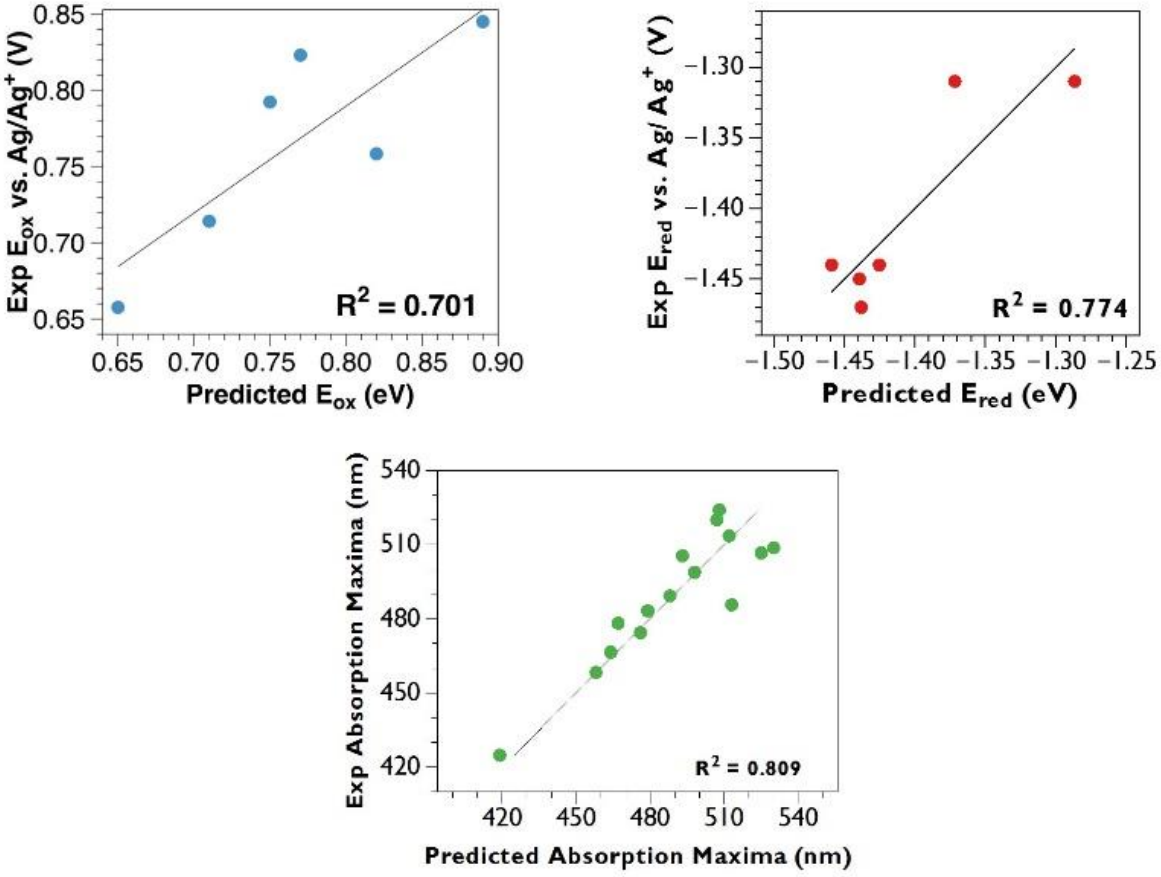

Figure 30. Correlations between computed first oxidation potential, first reduction potential, and optical excitation energies with their experimental counterparts. Note that for all predicted properties, a consensus model of two predictors yields small residual errors compared to their experimental counterparts.

In general, computed and experimental parameters show only small residual errors compared to their experimental counterparts (**Figure 30**). The mean unsigned errors (MUE) between computed and experimental parameters after the linear regression analysis was found to

be very low, with 0.03 V MUE for oxidation potentials (R^2 = 0.70), 0.04 V MUE for reduction potentials (R^2 = 0.77), and 9 nm MUE for optical absorption maxima (R^2 = 0.89). The high degree of agreement is not surprising because the sequenced oligomers define a closely analogous series, and the consensus technique minimizes systematic and random errors. With the limited number of experimental electrochemical measurements, the correlation coefficient R^2 is deceivingly poor. Orbital shapes for each of the oligomers prepared were computed and are plotted in **Figure 31.**

As the MUEs between experiment and computed properties were low, we extended the calculations to longer oligomers to explore the role of sequence and **PP**/**BB** pairings. The electronic structure of all hexamers with 50:50 **B:P** ratios were computed (**Table 11**). Since conformational effects can be significant, we again computed low energy conformers for both " palindromic" orders (e.g., **Br-PBPBPB-Br** and **Br-BPBPBP-Br**) to estimate the variations due to conformational local minima. We find the variation to be ~0.1 eV, on par with other estimates.[47]

3.4 DISCUSSION

There are notable but not surprising trends in the coupling of the end groups to **P** vs. **B** terminal units. When an electron-withdrawing end group is attached to the acceptor **B** units, the absorption maximum shifts to the red. In contrast, a blue shift is observed when the electron-withdrawing group is attached to the donor **P** unit, although the effect is smaller in magnitude. Not surprisingly, the **–CN** group exhibited a larger effect than the more mildly withdrawing **Br** end group. The electron-donating **C8** groups modestly increase the absorption maxima when attached to **P** units and decrease it when attached to **B** units. Overall, the **Br** group's effects were found to

be sufficiently modest that sequence-based differences could be differentiated without being masked/dominated by these **Br** groups.

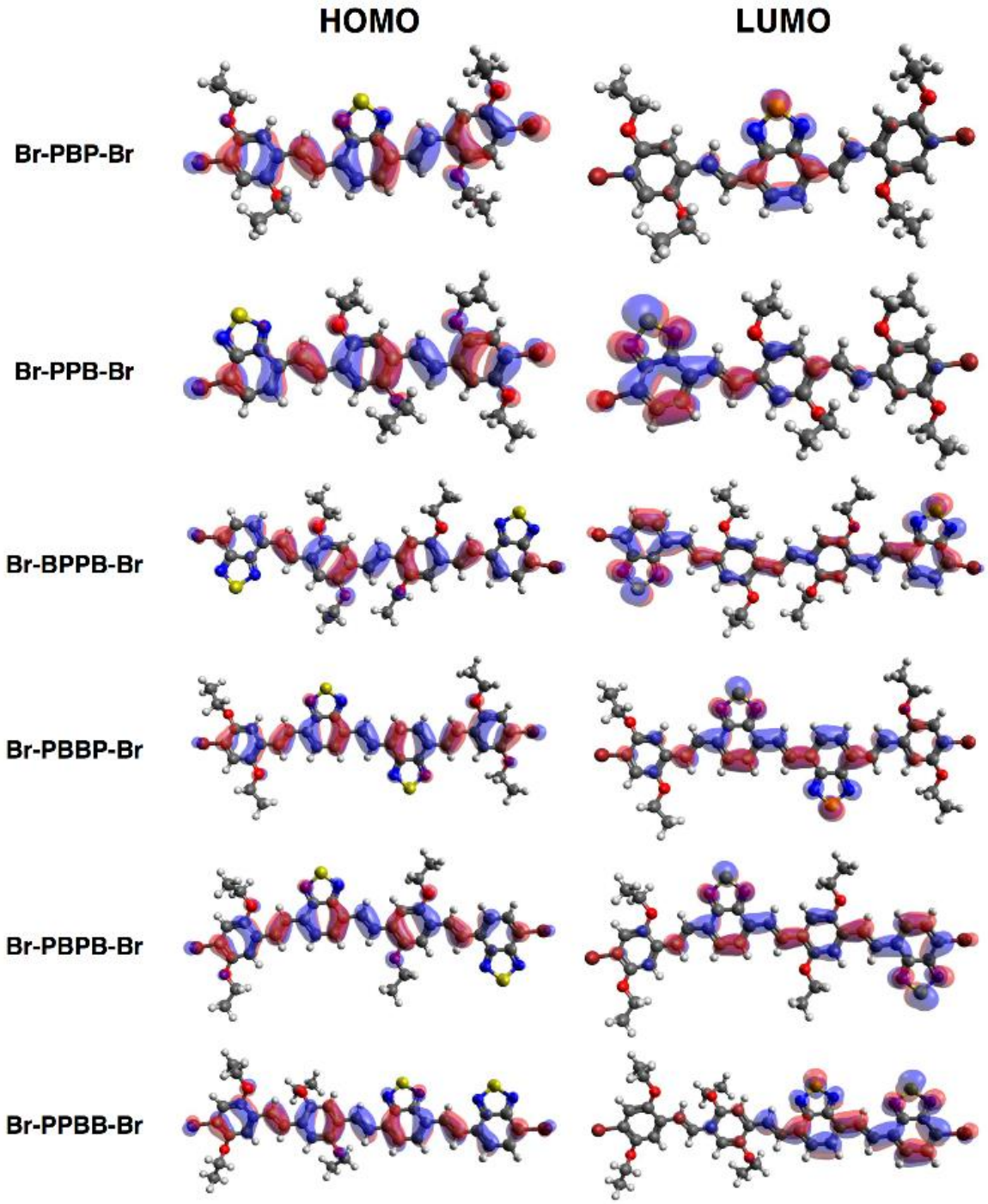

Figure 31. Computed orbital shapes for trimers and tetramers studied.

In examining the data, we observe that adjacent P units result in higher HOMO levels and adjacent B units result lower LUMO levels. For example the two dibromo tetramers with higher HOMO levels (lower E^{ox}) are **Br-PPBB-Br** and **Br-BPPB-Br**, respectively. An even more dramatic difference is seen for the LUMO levels, with **Br-PPBB-Br** and **Br-PBBP-Br** exhibiting similar and much lower E^{red} levels. The smallest band gap is necessarily exhibited by the tetramer with both, i.e., **Br-PPBB-Br**.

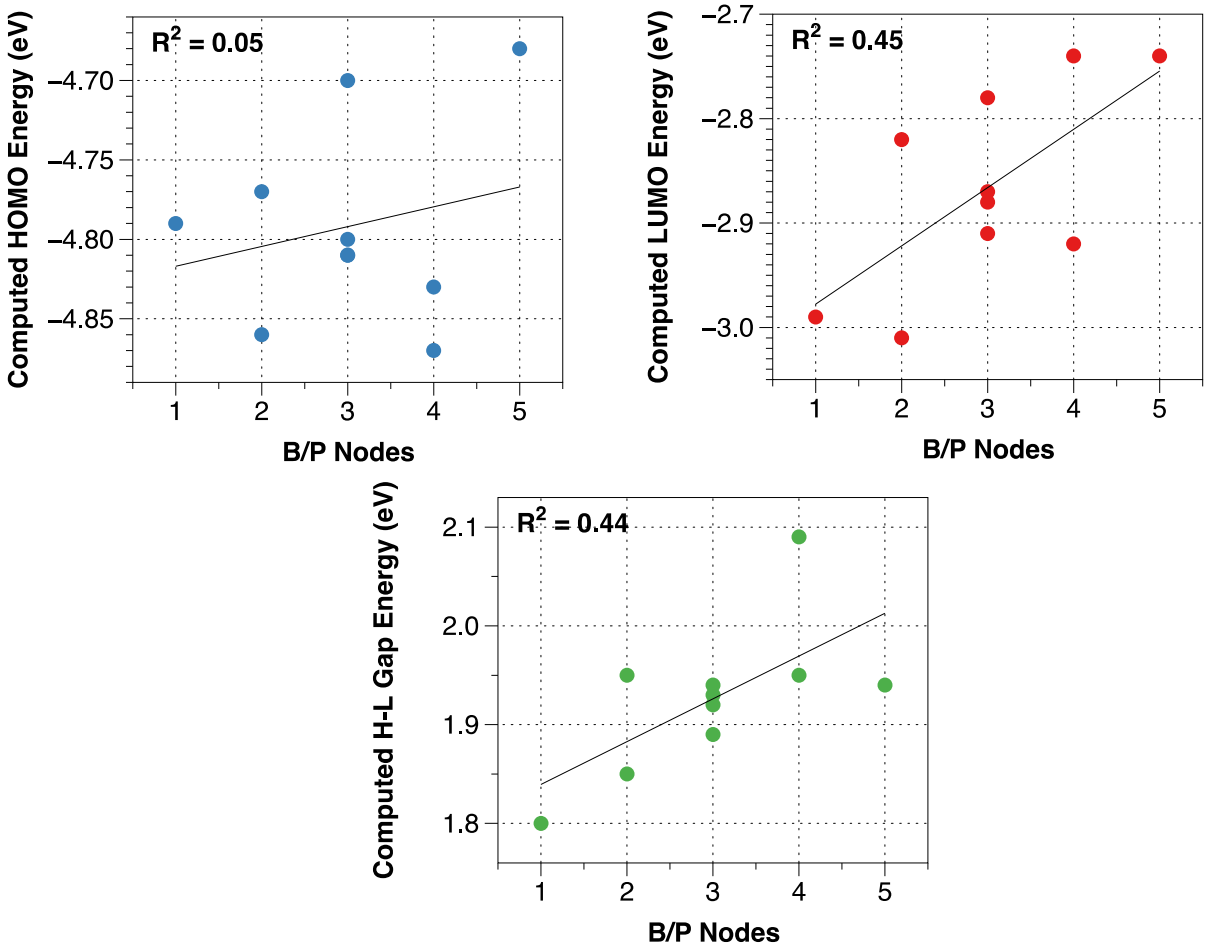

Figure 32. Computed HOMO (top), LUMO (middle), and HOMO-LUMO Gap (bottom) values for hexamers as a function of the number of nodes.

In examining the calculations there are interesting finding relevant both to end group effects and to sequence effects. We observed that in longer sequenced oligomers, synthesized *in*

silico rather than more laboriously in the lab, the role of the terminal groups is inherently lessened, and the effect of internal sequence is therefore magnified. With regard to the effects of alternation vs. localized structures, we observe in these calculated structures a noticeable correlation between the number of "nodes" between **P** and **B** monomers and the computed LUMO energies of the hexamers (**Figure 32**), but little correlation with the HOMO energies. Since the benzothiadiazole **B** repeat is known as a strong acceptor, this suggests in longer oligomers, **BB, BBB** and similar short blocks play a significant role in influencing the optoelectronic properties. Indeed, fewer nodes (i.e., longer $\mathbf{B_n}$ block length) result in more negative LUMO energies and consequently narrower band gaps. Consistently, our previous computational data mining to estimate a general sequence effect in hexamers suggested that acceptor block length, and not necessarily donor effects, should be the most significant factor in controlling optoelectronic properties,[16] in good agreement with this work.

We note that our previous combined experimental-computational investigation of the sequence effect in phenylene-vinylene based oligomers also showed a similar range of electrical and optical properties for the tetramers.[15] The electrochemical gaps varied by ~0.2 eV for both the series discussed herein and the previous PPV-based oligomers. Thus, despite the large difference in redox properties between the **B** and **P** monomers (i.e., a strong donor-acceptor variation), this does not translate into a larger sequence effect. These results combined with previous computational investigations suggest that sequence based effects may be easily investigated and exploited in the more synthetically accessible donor-donor polymers.[14]

Complex but distinct sequence effects were also manifested in the solar cell studies of these materials. Due to the relatively short conjugation lengths of these tetramers, the PCEs of solar cells incorporating these oligomers in the photoactive layer were modest (< 2%). Nonetheless, these

measurements, combined with the related hole mobility and spectroscopic studies, provide some interesting insights into how sequence can potentially be used in the design of higher performing materials. The symmetric tetramer **Br-BPPB-Br** showed a thin film λ_{max} that was 36 nm higher (i.e., red-shifted) than that of **Br-PPBB-Br**. Interestingly, the absorption maximum for all of these tetramers is red-shifted relative to that observed for a 50:50 random copolymer of the **P** and **B** monomers reported by Li, *et al.*[47] This observation suggests that either the effective conjugation length in these random copolymers is shorter than that of the tetramers or the tetramers are packed more effectively in the solid state. The latter explanation is supported to some degree by the fact that the absorption maxima for the three tetramers follow the reverse order in solution as they do in the solid state. The mobilities also follow the same sequence-based trend as that observed for the film absorption—the oligomer **Br-BPPB-Br** exhibited both the largest hole mobility and the longest solid-state λ_{max}.

A close inspection of photovoltaic device characteristics of these three bromo-terminated oligomers (**BPPB**, **PPBB** and **PBPB**) show that the open circuit voltage (V_{oc}) only varies slightly between 0.72 V and 0.77 V. Given that V_{oc} is largely determined by the energy level difference between the HOMO of the donor material (oligomers in this case) and the LUMO of the acceptor material ($PC_{61}BM$), the observed small difference (~ 0.05 V) is consistent with the observed HOMO energy level difference among these three oligomers (~ 0.10 eV). The small difference is not surprising, since one is comparing a solution measurement (CV) to a film measurement (V_{oc}).

The short circuit current (J_{sc}), on the other hand, did show a significant dependence on sequence. If we consider **P** as the "donor", and **B** as the "acceptor", then we have three cases that can be analyzed: **BPPB** (D-A-A-D), **PPBB** (D-D-A-A), vs. **PBPB** (D-A-D-A). As the D-A alternating structure is the dominant motif in conjugated copolymers,[13, 19, 66-68] it might not be

surprising to find that the **PBPB** (D-A-D-A)-based device gives the highest J_{sc} (and highest efficiency) in the studied series. The D-D-A-A motif is the second best performing sequence. The poorest performing sequence is the symmetric, **BPPB** (D-A-A-D) motif. This behavior is consistent with the hypothesis that a D-A structure (i.e., typically having a strong dipole) weakens the exciton binding energy and the geminate recombination, thereby benefitting the exciton separation and charge generation.[48, 69-71] Also consistent with this pattern we found that the asymmetric trimer **PPB** gave a modest overall solar cell performance while the symmetric PBP gave no measurable response.

3.5 CONCLUSIONS

We find that sequence is important in both solar cell performance and related properties. In addition to PCE, we find that absorption, emission, solid-state packing, hole mobilities, and HOMO-LUMO energy levels are all sequence dependent. We also demonstrate that using calculations we can explore sequence-space to facilitate our understanding of sequence-dependent behavior.

Although we see sequence dependence, it is clear that it remains challenging to fully correlate structure with properties in these oligomers. For example, while the optical and electrochemical properties of oligomers can be readily correlated with the sequence both experimentally and computationally, the impact of sequence on the oligomer-based device characteristics is much more difficult to understand. This is not a surprise, given that it is still a grand challenge to draw such correlations even with conjugated polymers having multiple constructing units.[72]

Although not measured for these materials, it seems likely that other characteristics that are important to device performance, including domain size in BHJ blends, thermal stability, etc. will likewise exhibit sequence dependence. Particularly exciting is the potential for using sequence to engineer multiple properties simultaneously. Amongst sequences that exhibit a targeted intrinsic property, such as HOMO-LUMO gap, a range of bulk properties could be exhibited—some sequences might pack well while others do not. The inverse is also possible—a range of sequences could be identified that exhibit a particular morphological trait and then refined on a desired intrinsic property, such as HOMO level. Future efforts will aim to correlate intermolecular interactions, packing, film morphology, and interfacial organization with sequence effects. The results should allow for combined computational and synthetic rational design of materials that can fulfill the complex set of requirements necessary for highly efficient organic solar cells and other applications.

3.6 EXPERIMENTAL

3.6.1 General materials

Br-P-CHO, **Phos-P-CN**, **Br-P-Br**, and **Br-PP-CHO,** were synthesized as described previously.[15, 48] **Phos-B-Br** and **Br-B-CHO** were prepared according to the method of Jorgenson, *et al*[49] and Lin, *et al*,[73] respectively. Synthesis and characterization of sequenced oligomers with **C8** endgroups will be discussed in detail at next chapter. DIBAL-H (1.0 M in hexanes) was purchased from Aldrich and dispensed using air-sensitive techniques. LiCl was stored in a 120 ^{o}C

oven for at least 24 h before use. Dry THF from Sigma Aldrich was used for all reactions. CH_2Cl_2 was dried by passage through an alumina-packed column. All other reagents and solvents were used as received. Column chromatography was carried out on standard grade silica gel (60 Å pore size, 40-63 μm particle size), which was purchased and used as received.

3.6.2 Spectroscopy

NMR Spectroscopy. ^{1}H (400 and 500 MHz) and ^{13}C (100, 125 and 150 MHz) NMR spectra were recorded on Bruker spectrometers. Chemical shifts were referenced to residual ^{1}H or ^{13}C signals in deuterated solvents (7.26 and 77.0 ppm, respectively, for $CDCl_3$ and 5.32 and 54.0 ppm, respectively, for CD_2Cl_2).

Mass Spectrometry. High resolution mass spectra were recorded on EI-quadrupole or ESI-TOF instruments in the Mass Spectrometry Facility of the University of Pittsburgh. MALDI spectra were recorded on Voyager-DE PRO instrument.

Optical Spectroscopy. Solution ($CHCl_3$) UV/VIS absorption spectra were recorded on a Perkin Elmer Lambda 9 UV/VIS/NIR spectrometer. UV/VIS absorption spectra of films on glass substrates were recorded on an Ocean Optics HR2000+CG-UV-NIR high-resolution spectrometer. Solution ($CHCl_3$) emission spectra were recorded on a Varian Cary Eclipse Fluorimeter.

Electrochemistry. Cyclic voltammetry (CV) and differential pulse voltammetry (DPV) were performed on a CHI Electrochemical Workstation Model 430a (Austin, TX) collected using a three electrode system consisting of a glassy carbon disk (3 mm dia.) as working electrode, a non-aqueous Ag/Ag+ reference electrode (1 mM $AgNO_3$ in acetonitrile), and a Pt-wire as auxiliary electrode in 0.1 M Bu_4NPF_6 in dry THF. CV were recorded at 100 mV/s. DPV parameters were as follows: scan rate of 25 mV/s, pulse amplitude 0.05 V and pulse period 0.16s.

3.6.3 Computational Methods

Each possible trimer and tetramer sequence permutation was generated with a python script from the monomer SMILES.[74] An initial 3D structure was generated using Open Babel 2.3.0[75] (accessed through Pybel[76]) and was minimized using the MMFF94 force field[77-81] to find a low energy minima conformation. Final geometries were optimized using Gaussian 09[82] with density functional theory (DFT) B3LYP/6-31G*.[83-84] To compare computational results with electrochemical experiments, redox potentials were determined using a combination of orbital energies (i.e., vertical ionization potential and electron affinity) and the ΔSCF procedure, taking the adiabatic energy difference between the optimized geometries of neutral and charged species using the conductor polarizable continuum model (C-PCM) model for tetrahydrofuran (THF).[85] To compare with optical absorptions, excitation energies and oscillator strengths were computed using ZINDO[86] and TDDFT using the optimized solution geometry of the neutral species using the C-PCM solvation model[87] for $CHCl_3$. Images of molecules and orbitals in the Supporting Information were prepared using Avogadro.[88]

3.6.4 Device Fabrication and Testing

Photovoltaic devices were fabricated on glass substrates coated with patterned indium doped tin oxide (ITO). Prior to use, the substrates were sonicated in deionized water, acetone, and isopropyl alcohol for fifteen minutes each, followed by UV-ozone treatment for 15 minutes. PEDOT:PSS (Clevios PH500 from Heraeus) was then spun cast onto the cleaned ITO substrates at 4000 rpm for 60 s and baked at 130°C for fifteen minutes. Blends of tetramer:PCBM (1:1 w/w, 9 mg/mL tetramer) were dissolved in chloroform and heated at 40°C for 1 hour, then stirred at

room temperature for an additional 4 hours. The solutions were then spun cast on the PEDOT:PSS films for 60 s to yield ~85 nm films. The devices were finished for measurement by evaporation of 30 nm of calcium and 70 nm of aluminum as the cathode at a pressure of $3x10^{-6}$ mbar. Device testing was carried out under AM 1.5G irradiation calibrated with an NREL certified standard silicon solar cell. Current density-voltage curves were measured via a Keithley 2400 digital source meter. All steps after PEDOT:PSS deposition were carried out in N_2-filled gloveboxes.

Hole mobility was measured via the space-charge limited current (SCLC) method through hole-only devices with a configuration of ITO/PEDOT:PSS/tetramer:PCBM/MoO_3/Al. The dark current densities of the devices were measured with a Keithley 2400 digital source meter with an applied voltage from 0 V to 6 V. The applied voltage was corrected from the voltage drop due to series and contact resistance from ITO/PEDOT:PSS. Mobility values were extracted from the Mott-Gurneys law:

$$J = \frac{9}{8}\varepsilon_r\varepsilon_0\mu_h\frac{V^2}{L^3}$$

where ε_r is the dielectric constant of the tetramer, ε_0 is the permittivity of free space, μ_h is the hole mobility, V is the voltage drop across the device, and L is the thickness of the active layer.

3.6.5 Synthesis of Phos-B-CN

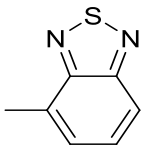

4-Methylbenzo[c][1,2,5]thiadiazole (1)

Synthesis of **1** was adapted from the procedure reported by Dasilveiraneto, *et. al*.[5] $SOCl_2$ (0.829 g, 6.90 mmol) was added slowly to a solution of Et_3N (1.78 g, 17.6 mmol) and 2,3-diaminotoluene (0.5 g, 4.10 mmol) in CH_2Cl_2 (16 mL). The mixture was allowed to reflux for 4 h. After refluxing, solvent was removed *in vacuo*. H_2O (150 mL) was added and the pH was adjusted to 2 by addition of concentrated HCl. Steam distillation of the mixture followed by extraction with CH_2Cl_2 (3 x 100 ml). The organic layer was dried over $MgSO_4$ and solvent was removed *in vacuo* to give the title compound (0.52 g, 82%). ^{1}H NMR (400 MHz, $CDCl_3$) δ 7.80 (d, J = 8.8 Hz, 1H), 7.45 (t, J = 7.8 Hz, 1H), 7.30 (d, J = 6.7 Hz, 1H), 2.73 (s, 3H). The spectrum corresponds to previously reported NMR data for this compound.[49]

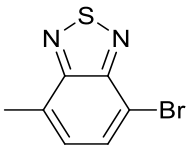

4-Bromo-7-methylbenzo[c][1,2,5]thiadiazole (2)

Synthesis of **2** was modified from a published procedure.[5] 4-methylbenzo[c][1,2,5]thiadiazole (3.97 g, 28.4 mmol) was dissolved in 48% HBr (15 mL), and Br_2 (2.11 g, 28.4 mmol) with 48% HBr (15 mL) was added very slowly. After the addition, the

mixture was allowed to reflux for 16 h. The reaction was quenched by saturated Na_2SO_3 solution. Purification by column chromatography produced a white solid (4.2 g, 65%). ^{1}H NMR (400 MHz, $CDCl_3$) δ 7.73 (d, *J* = 7.3 Hz, 1H), 7.24 (d, *J* = 1.1 Hz, 2H), 2.70 (d, *J* = 0.9 Hz, 3H). The spectrum corresponds to previously reported NMR data for this compound.[49]

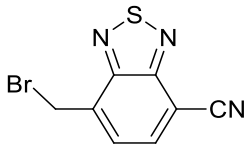

7-(Bromomethyl)benzo[c][1,2,5]thiadiazole-4-carbonitrile (4)

Synthesis of **4** was modified from a published procedure.[49] 7-methylbenzo[c][1,2,5]thiadiazole-4-carbonitrile (0.14 g, 0.800 mmol), NBS (0.142 g, 0.80 mmol) and benzoylperoxide (0.5 mg) were dissolved in DCE (7 mL) and heated to reflux. A solution of 33% HBr in AcOH (1 mL) was added. The reaction was cooled to RT after 1 h and solvent was removed *in vacuo*. The product, a white solid (0.21 g) was used for subsequent reactions without further purification. ^{1}H NMR (300 MHz, $CDCl_3$) δ 8.03 (d, *J* = 7.2 Hz, 1H), 7.75 (d, *J* = 7.2 Hz, 1H), 4.99 (s, 2H).

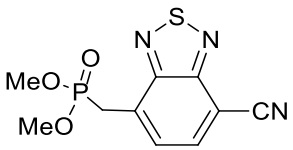

Dimethyl ((7-cyanobenzo[c][1,2,5]thiadiazol-4-yl)methyl)phosphonate (Phos-B-CN)

Phos-B-CN was synthesized by modification of a published procedure.[49] Unpurified 7-(bromomethyl)benzo[c][1,2,5]thiadiazole-4-carbonitrile (0.140 g) was dissolved in $P(OCH_3)_3$ (5 mL) and heated to reflux. The mixture was allowed to stand for 1.5 h to reach RT. $P(OCH_3)_3$ was

removed *in vacuo*. The mixture was purified by column chromatography (silica gel, hexanes and ethyl acetate) to give the title compound (0.12 g, 80% over two steps). ^{1}H NMR (500 MHz, $CDCl_3$) δ 8.03 (dd, *J* = 7.2, 1.1 Hz, 1H), 7.70 (ddt, *J* = 7.3, 3.9, 0.8 Hz, 1H), 3.85 (d, *J* = 0.8 Hz, 1H), 3.80 (d, *J* = 0.8 Hz, 1H), 3.75 (s, 3H), 3.73 (s, 3H). ^{13}C NMR (101 MHz, $CDCl_3$) δ 154.36, 152.97, 136.06, 136.01, 132.05, 131.94, 129.02, 128.94, 115.40, 115.38, 104.87, 104.83, 53.34, 53.27, 29.75, 28.38. HRMS calcd for $C_{10}H_{11}O_3N_3PS$: 284.02588 g/mol. Found: 284.02458 g/mol.

3.6.6 Synthesis of Sequenced Oligomers

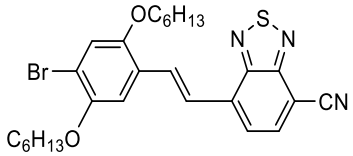

(E)-7-(4-Bromo-2,5-bis(hexyloxy)styryl)benzo[c][1,2,5]thiadiazole-4-carbonitrile (Br-PB-CN)

Phos-B-CN (0.882 g, 3.11 mmol) was dissolved in dry THF (40 mL) under N_2. NaH (0.622 g, 60% dispersion in mineral oil) was added and the resulting mixture was stirred for 1 h at room temperature. RT. **Br-P-CHO** (0.600 g, 1.55 mmol) was added to the reaction mixture and the reaction was stirred at RT for 5 h. The solvent was evaporated *in vacuo*. Saturated aqueous NH_4Cl was added to the residue. The aqueous layers were extracted 3x with CH_2Cl_2 (equal volume). The combined organic layers were dried over $MgSO_4$, and the solvent was removed *in vacuo*. The residues were purified by column chromatography (silica gel, hexanes and methylene chloride) to give the title compound as a red solid (0.73 g, 87%). ^{1}H NMR (400 MHz, $CDCl_3$) δ 8.35 (d, *J* =

16.6 Hz, 1H), 8.02 (d, *J* = 7.4 Hz, 1H), 7.83 – 7.63 (m, 2H), 7.18 (d, *J* = 25.1 Hz, 2H), 4.05 (dt, *J* = 16.3, 6.3 Hz, 4H), 2.01 – 1.74 (m,4H), 1.53 (s, 4H), 1.38 (s, 8H), 0.92 (d, *J* = 5.2 Hz, 6H). ^{13}C NMR (101 MHz, $CDCl_3$) δ 152.68, 151.98, 149.92, 136.49, 136.04, 132.63， 132.26, 125.38, 123.58, 117.92, 114.39, 112.16, 103.07, 77.22, 70.41, 69.58, 31.63, 31.57, 29.29, 25.88, 25.72, 22.69, 22.62, 14.07. HRMS calcd for $C_{27}H_{33}O_2N_3BrS$: 542.14769 g/mol. Found: 542.14638 g/mol.

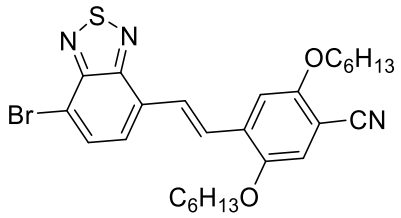

(E)-4-(2-(7-Bromobenzo[c][1,2,5]thiadiazol-4-yl)vinyl)-2,5-bis(hexyloxy)benzonitrile (Br-BP-CN)

Phos-P-CN (1.075 g, 2.53 mmol) and **Br-B-CHO** (0.3 g, 1.23 mmol) were dissolved in dry THF (40 mL) under N_2. KO^{t}Bu in hexanes (3.87 mL x 1.0 M, 3.87 mmol) was added via syringe and the resulting mixture was allowed to stand overnight with stirring. The solvent was evaporated *in vacuo*. Saturated aqueous NH_4Cl was added to the residue. The aqueous layers were extracted 3x with CH_2Cl_2 (equal volume). The combined organic layers were dried over $MgSO_4$, and the solvent was removed *in vacuo*. The residues were purified by column chromatography (silica gel, hexanes and methylene chloride) to give the title compound as red solid (0.51 g, 77%). ^{1}H NMR (400 MHz, $CDCl_3$) δ 8.21 (d, *J* = 16.5 Hz, 1H), 7.79 (d, *J* = 7.6 Hz, 1H), 7.69 – 7.44 (m, 2H), 7.16 (s, 1H), 6.99 (s, 1H), 4.05 (t, *J* = 6.5 Hz, 2H), 3.95 (t, *J* = 6.4 Hz, 2H), 1.99 – 1.68 (m, 4H), 1.59 – 1.38 (m, 4H), 1.38 – 1.09 (m, 8H), 0.85 (td, *J* = 6.9, 4.1 Hz, 6H). ^{13}C NMR (101 MHz, $CDCl_3$) δ 155.21, 153.87, 152.91, 150.63, 132.35, 132.29, 130.04, 128.13, 127.50, 127.07, 116.62,

116.57, 113.39, 110.67, 101.44, 69.80, 69.55, 31.61, 31.52, 29.20, 29.08, 25.85, 25.60, 22.67, 22.57, 14.06, 14.04. HRMS calcd for $C_{27}H_{32}O_2N_3BrS$: 541.13986 g/mol. Found: 541.13708 g/mol.

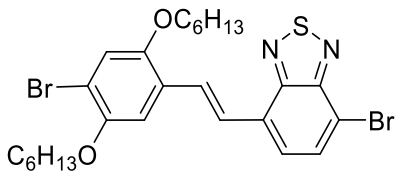

(E)-4-bromo-7-(4-bromo-2,5-bis(hexyloxy)styryl)benzo[c][1,2,5]thiadiazole (Br-PB-Br) According to the general procedure, **Phos-B-Br** (0.685 g, 2.032 mmol) was dissolved in dry THF (40 mL) under N_2. NaH (0.406 g, 60% dispersion in mineral oil) was added and the resulting mixture was stirred for 1 h at room temperature. **Br-P-CHO** (0.6023 g, 1.56 mmol) was added to the reaction mixture. The reaction was kept at room temperature for 5 h. After workup, column chromatography (silica gel, hexanes and methylene chloride) was performed to give the title compound as red solid (0.836 g, 90%). ^{1}H NMR (400 MHz, $CDCl_3$) δ 8.20 (d, *J* = 16.5 Hz, 1H), 7.84 (d, *J* = 7.6 Hz, 1H), 7.71 – 7.50 (m, 2H), 7.21 (s, 1H), 7.12 (s, 1H), 4.04 (dt, *J* = 23.0, 6.4 Hz, 4H), 1.86 (p, *J* = 7.0 Hz, 4H), 1.54 (ddd, *J* = 15.3, 12.0, 7.1 Hz, 4H), 1.38 (tt, *J* = 7.2, 2.9 Hz, 8H), 0.97 – 0.70 (m, 6H).^{13}C NMR (101 MHz, $CDCl_3$) δ 154.03 , 151.77 , 150.08 , 132.54 , 130.95 , 128.94 , 126.66 , 126.34 , 124.34 , 118.08 , 113.29 , 112.49 , 112.13 , 77.40 , 70.58 , 69.78 , 31.82 , 31.76 , 29.51 , 29.49 , 26.07 , 25.91 , 22.87 , 22.81 , 14.26 , 14.24 . HRMS calcd for $C_{26}H_{33}O_2N_2Br_2S$: 595.06295 g/mol. Found: 595.06118 g/mol.

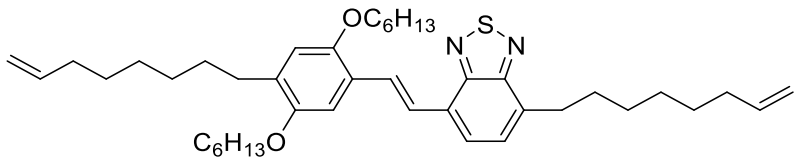

(E)-4-(2,5-bis(hexyloxy)-4-(oct-7-en-1-yl)styryl)-7-(oct-7-en-1-yl)benzo[c][1,2,5]thiadiazole (C_8-PB-C_8) Synthesis of **C8-PB-C8** was modified from our previous publication.[27] 1-(hept-6-en-1-yl)-7-boratricyclo[4.1.1.03,7]octane (**C_8-9-BBN**) was synthesized according to literature[89] and stored in the glove box. In a Schlenk flask, **Br-PB-Br** (0.0831 g, 0.139 mmol) and $Pd(PPh_3)_2Cl_2$ (0.0049 g, 5% mol) were added and transferred into the glove box. DMF (7.5 mL) and toluene (7.5 mL) were added as solvent for the reaction, followed by the addition of **C_8-9-BBN** (0.150 g, 0.742 mmol). The Schlenk flask was sealed by septa and carried out of the glove box. The reaction mixture was protected under N_2 and heated to 60 °C overnight. The reaction was stopped by pouring into large amount of water. The organic phase was separated and the aqueous phase was extracted with CH_2Cl_2 twice. The combined organic layer was washed by brine and dried over $MgSO_4$. Solvent was removed *in vacuo*. Column chromatography (silica gel, hexanes and methylene chloride) gave the product as orange solid (0.0697 g, 76%). ^{1}H NMR (400 MHz, $CDCl_3$) δ 8.20 (d, *J* = 16.5 Hz, 1H), 7.62 (dd, *J* = 11.9, 4.6 Hz, 2H), 7.34 (d, *J* = 7.2 Hz, 1H), 7.16 (s, 1H), 6.73 (s, 1H), 5.81 (dddd, *J* = 17.0, 10.8, 7.0, 4.2 Hz, 2H), 5.09 – 4.81 (m, 4H), 4.01 (td, *J* = 6.4, 2.0 Hz, 4H), 3.12 (t, *J* = 7.7 Hz, 2H), 2.61 (t, *J* = 7.7 Hz, 2H), 2.05 (d, *J* = 6.8 Hz, 4H), 1.84 (dt, *J* = 20.0, 7.2 Hz, 4H), 1.69 – 1.48 (m, 6H), 1.48 – 1.05 (m, 22H), 0.91 (t, *J* = 6.9 Hz, 6H). ^{13}C NMR (101 MHz, $CDCl_3$) δ 155.72 , 153.92 , 151.52 , 151.18 , 139.39 , 139.31 , 134.58 , 133.28 , 129.46 , 127.82 , 126.04 , 124.89 , 123.61 , 115.57 , 114.37 , 114.31 , 109.60 , 77.40 , 69.96 , 68.95 , 34.02 , 33.96 , 32.47 , 31.92 , 31.81 , 30.78 , 30.26 , 29.87 , 29.80 , 29.75 , 29.65 , 29.59 , 29.22 , 29.15 , 29.11 , 29.06 , 26.16 , 26.13 , 22.89 , 22.86 , 14.28 , 14.25 . HRMS calcd for $C_{42}H_{63}O_2N_2S$: 659.46103 g/mol. Found: 659.45803 g/mol.

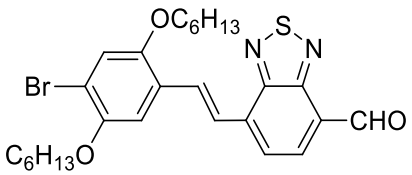

(E)-7-(4-Bromo-2,5-bis(hexyloxy)styryl)benzo[c][1,2,5]thiadiazole-4-carbaldehyde (Br-PB-CHO)

Br-PB-CN (0.0471 g, 0.0868 mmol) was dissolved in dry CH_2Cl_2 and cooled to -40 °C. DIBAL-H (1, equiv, 1.0 M in hexanes) was added every 45 min until all the starting material was consumed as observed by TLC. Wet silica (0.4 mL H_2O and 1.3 g SiO_2 per mmol DIBAL-H) was added and the mixture was stirred at 0 °C for 1 h. K_2CO_3 (0.5 g per mmol DIBAL-H) and $MgSO_4$ (0.5 g per mmol DIBAL-H) were added. The reaction mixture was filtered and the solids washed with CH_2Cl_2. The combined filtrate and washes were reduced in volume *in vacuo*, and the residues were purified by column chromatography (silica gel, hexanes and methylene chloride) to give the title compound as red solid (0.0335 g, 71%). ^{1}H NMR (400 MHz, CD_2Cl_2) δ 10.65 (s, 1H), 8.38 (d, *J* = 16.4 Hz, 1H), 8.13 (d, *J* = 7.4 Hz, 1H), 7.76 (dd, *J* = 24.2, 11.9 Hz, 2H), 7.14 (d, *J* = 36.7 Hz, 2H), 4.12 – 3.89 (m, 4H), 1.90 – 1.68 (m, 4H), 1.60 – 1.39 (m, 4H), 1.31 (s, 8H), 1.03 – 0.65 (m, 6H). ^{13}C NMR (101 MHz, CD_2Cl_2) δ 188.83, 152.34, 150.28, 137.31, 132.60, 132.09, 126.24, 126.15, 125.80, 124.77, 118.33, 114.13, 112.26, 70.67, 70.11, 54.27, 32.03, 31.95, 30.07, 29.70, 29.67, 26.28, 26.08, 23.08, 23.01, 14.23, 14.20. HRMS calcd for $C_{27}H_{34}O_3N_2BrS$: 545.14735 g/mol. Found: 545.14587 g/mol.

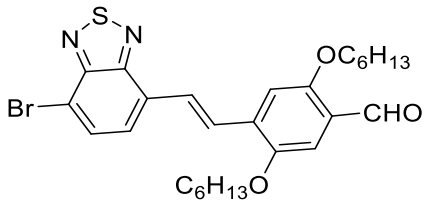

(E)-4-(2-(7-Bromobenzo[c][1,2,5]thiadiazol-4-yl)vinyl)-2,5-bis(hexyloxy)benzaldehyde (Br-BP-CHO)

Br-BP-CN (0.103 g, 0.190 mmol) was dissolved in dry CH_2Cl_2 and cooled to 0 ^{O}C. DIBAL-H (1, equiv, 1.0 M in hexanes) was added every 45 min until all the starting material was consumed as observed by TLC. Wet silica (0.4 mL H_2O and 1.3 g SiO_2 per mmol DIBAL-H) was added and the mixture was stirred at 0 $^{\circ}$C for 1 h. K_2CO_3 (0.5 g per mmol DIBAL-H) and $MgSO_4$ (0.5 g per mmol DIBAL-H) were added. The reaction mixture was filtered and the solids washed with CH_2Cl_2. The combined filtrate and washes were reduced in volume *in vacuo*, and the residues were purified by column chromatography (silica gel, hexanes and methylene chloride) to give the title compound as red solid (0.086 g, 83%).^{1}H NMR (400 MHz, CD_2Cl_2) δ 10.38 (s, 1H), 8.30 (d, *J* = 16.5 Hz, 1H), 7.80 (d, *J* = 7.6 Hz, 1H), 7.67 (d, *J* = 16.5 Hz, 1H), 7.54 (d, *J* = 7.7 Hz, 1H), 7.25 (d, *J* = 7.6 Hz, 2H), 4.04 (dt, *J* = 28.7, 6.4 Hz, 4H), 1.85 – 1.73 (m, 4H), 1.55 – 1.40 (m, 4H), 1.31 (dq, *J* = 10.3, 4.1, 3.7 Hz, 8H), 0.84 (td, *J* = 6.9, 5.5 Hz, 6H). ^{13}C NMR (101 MHz, CD_2Cl_2) δ 189.16, 156.51, 154.29, 151.61, 134.05, 132.74, 130.62, 128.99, 128.06, 127.52, 125.34, 113.45 , 111.48, 110.51, 69.80, 69.67, 54.27, 54.00, 32.04, 31.94, 29.67, 29.61, 26.29, 26.15, 23.08, 22.99, 14.22, 14.18 . HRMS calcd for $C_{27}H_{34}O_3N_2BrS$: 545.14735 g/mol. Found: 545.14455 g/mol.

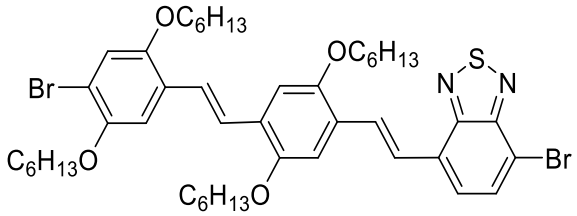

4-Bromo-7-((E)-4-((E)-4-bromo-2,5-bis(hexyloxy)styryl)-2,5-bis(hexyloxy)styryl)benzo[c][1,2,5]thiadiazole (Br-PPB-Br)

Phos-P-Br (0.4432 g, 0.924 mmol) and **Br-BP-CHO** (0.2522 g, 0.462 mmol) were dissolved in dry THF (20 mL) under N_2. KO^{t}Bu in hexanes (1.06 mL x 1.0 M, 1.06 mmol) was added via syringe and the resulting mixture was allowed to stand overnight with stirring. The reaction mixture was poured into saturated aqueous NH_4Cl (50 mL). The aqueous layers were extracted 3x with CH_2Cl_2 (equal volume). The combined organic layers were dried over $MgSO_4$, and the solvent was removed *in vacuo*. The residues were purified by column chromatography (silica gel, hexanes and methylene chloride) was performed to give the title compound as red solid (0.049 g, 85%). ^{1}H NMR (400 MHz, CD_2Cl_2) δ 8.27 (d, *J* = 16.5 Hz, 1H), 7.78 (d, *J* = 7.9 Hz, 1H), 7.59 (d, *J* = 16.5 Hz, 1H), 7.51 (d, *J* = 7.7 Hz, 1H), 7.48 – 7.31 (m, 2H), 7.16 (s, 1H), 7.10 (s, 2H), 7.03 (s, 1H), 4.14 – 3.82 (m, 8H), 1.78 (dp, *J* = 22.3, 8.4, 7.4 Hz, 8H), 1.60 – 1.39 (m, 8H), 1.30 (d, *J* = 10.6 Hz, 13H), 1.18 (s, 3H), 0.83 (d, *J* = 5.7 Hz, 12H). ^{13}C NMR (101 MHz, $CDCl_3$) δ 151.86, 151.28, 151.25, 150.02, 132.59, 131.29, 129.31, 128.53, 127.34, 126.61, 126.31, 124.11, 123.72 , 123.65, 118.01, 112.11, 112.00, 111.82, 111.07, 110.74, 77.40, 70.44, 69.76, 69.64, 31.90, 31.85, 31.78, 31.76, 29.72, 29.66, 29.49, 26.19, 26.13, 26.04, 25.91, 22.90, 22.86, 22.84, 22.80, 14.28, 14.25, 14.24 . HRMS calcd for $C_{46}H_{62}O_4N_2Br_2S$: 896.27970 g/mol. Found: 896.27471 g/mol.

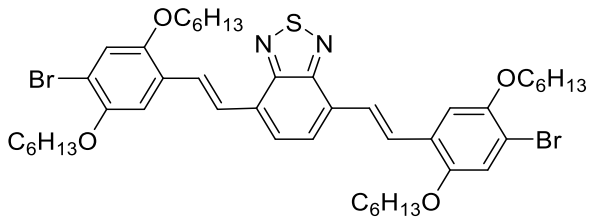

4,7-Bis((E)-4-bromo-2,5-bis(hexyloxy)styryl)benzo[c][1,2,5]thiadiazole (Br-PBP-Br)

Phos-P-Br (0.0302 g, 0.063 mmol) and **Br-PB-CHO** (0.0229 g, 0.0420 mmol) were dissolved in dry THF (10 mL) under N_2. KO^{t}Bu in hexanes (0.10 mL x 1.0 M, 0.10 mmol) was added via syringe and the resulting mixture was allowed to stand overnight with stirring. The reaction mixture was poured into saturated aqueous NH_4Cl (25 mL). The aqueous layers were extracted 3x with CH_2Cl_2 (equal volume). The combined organic layers were dried over $MgSO_4$, and the solvent was removed *in vacuo*. The residues were purified by column chromatography (silica gel, hexanes and methylene chloride) was performed to give the title compound as red solid (0.038 g, 99%).^{1}H NMR (300 MHz, $CDCl_3$) δ 8.17 (d, *J* = 16.4 Hz, 2H), 7.81 – 7.47 (m, 4H), 7.18 (d, *J* = 3.3 Hz, 2H), 7.06 (s, 2H), 3.98 (dt, *J* = 18.2, 6.4 Hz, 8H), 1.81 (q, *J* = 7.4 Hz, 8H), 1.49 (s, 4H), 1.38 – 0.97 (m, 16H), 0.85 (q, *J* = 6.1, 5.5 Hz, 12H).^{13}C NMR (101 MHz, $CDCl_3$) δ 154.17, 151.72, 150.09, 129.90, 127.72, 126.88, 126.83, 125.17, 118.09, 112.00, 77.40, 70.58, 69.84, 31.86, 31.77, 29.90, 29.55, 29.51, 26.10, 25.92, 22.88, 22.82, 14.27, 14.25. HRMS calcd for $C_{46}H_{63}O_4N_2Br_2S$: 897.28753 g/mol. Found: 897.28369 g/mol.

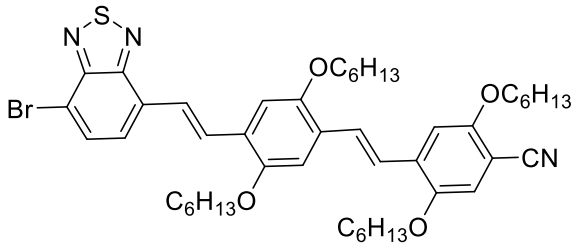

4-((E)-4-((E)-2-(7-bromobenzo[c][1,2,5]thiadiazol-4-yl)vinyl)-2,5-bis(hexyloxy)styryl)-2,5-bis(hexyloxy)benzonitrile (Br-BPP-CN) According to the general

procedure, **Phos-P-CN** (0.242 g, 0.568 mmol) and **Br-BP-CHO** (0.206 g, 0.378 mmol) were dissolved in dry THF (10 mL) under N_2. 1.0 M KO^{t}Bu in hexanes (0.11 mL, 0.11 mmol) was added via syringe and the resulting mixture was allowed to stand overnight with stirring. After workup, column chromatography (silica gel, hexanes and methylene chloride) was performed to give the title compound as red solid (0.273 g, 85%).^{1}H NMR (300 MHz, CD_2Cl_2) δ 8.36 (d, *J* = 16.5 Hz, 1H), 7.87 (d, *J* = 7.6 Hz, 1H), 7.74 – 7.43 (m, 4H), 7.34 – 6.98 (m, 4H), 4.20 – 3.90 (m, 8H), 1.89 (dt, *J* = 16.2, 7.3 Hz, 8H), 1.52 (s, 8H), 1.37 (d, *J* = 9.0 Hz, 16H), 0.92 (d, *J* = 6.7 Hz, 12H). ^{13}C NMR (126 MHz, $CDCl_3$) δ 155.26 , 153.08 , 151.58 , 151.36 , 150.12 , 133.46 , 132.37 , 130.93 , 128.97 , 127.44 , 127.28 , 126.90 , 126.32 , 123.97 , 122.73 , 116.84 , 116.44 , 112.14 , 110.81 , 110.78 , 110.15 , 100.31 , 77.20 , 69.62 , 69.47 , 31.69 , 31.62 , 31.56 , 31.51 , 31.43 , 29.50 , 29.42 , 29.17 , 29.08 , 25.98 , 25.92 , 25.81 , 25.60 , 22.69 , 22.66 , 22.62 , 22.56 , 22.52 , 14.07 , 14.04 , 14.02 , 13.97 . HRMS calcd for $C_{48}H_{64}O_2N_2BrS_2$: 843.35926 g/mol. Found: 843.35991 g/mol.

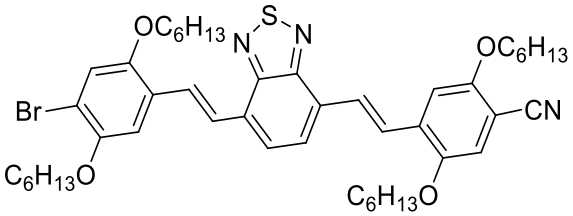

4-((E)-2-(7-((E)-4-bromo-2,5-bis(hexyloxy)styryl)benzo[c][1,2,5]thiadiazol-4-yl)vinyl)-2,5-bis(hexyloxy)benzonitrile (Br-PBP-CN) According to the general procedure, **Br-PB-CHO** (0.0260 g, 0.0480 mmol) and **Phos-P-CN** (0.0408 g, 0.150 mmol) were dissolved in THF (10 mL) under N_2. 1.0M KO^{t}Bu solution in THF (0.15 ml, 0.15 mmol) was added and the reaction was allowed to stand overnight with stirring. After workup, column chromatography

(silica gel, hexanes and methylene chloride) gave the title compound as red solid (0.0353 g, 87%).^{1}H NMR (400 MHz, CD_2Cl_2) δ 8.41 (dd, *J* = 26.0, 16.5 Hz, 2H), 7.90 – 7.65 (m, 4H), 7.33 (d, *J* = 11.6 Hz, 2H), 7.17 (d, *J* = 28.0 Hz, 2H), 4.14 (ddd, *J* = 20.6, 13.0, 4.5 Hz, 8H), 1.94 (d, *J* = 5.6 Hz, 8H), 1.74 – 1.53 (m, 8H), 1.45 (s, 16H), 0.99 (s, 12H). ^{13}C NMR (101 MHz, $CDCl_3$) δ 155.41 , 154.12 , 154.06 , 151.75 , 150.72 , 150.06 , 133.03 , 130.71 , 129.09 , 128.27 , 128.06 , 127.95 , 126.98 , 126.63 , 126.61 , 124.95 , 118.04 , 116.92 , 116.69 , 113.09 , 111.99 , 110.58 , 101.15 , 70.55 , 69.94 , 69.79 , 69.73 , 31.84 , 31.83 , 31.76 , 31.71 , 29.53 , 29.49 , 29.43 , 29.28 , 26.08 , 26.05 , 25.91 , 25.79 , 22.86 , 22.80 , 22.76 , 14.26 , 14.24 , 14.22 . HRMS calcd for $C_{47}H_{62}O_4N_3BrS$: 843.36444 g/mol. Found: 843.36072 g/mol.

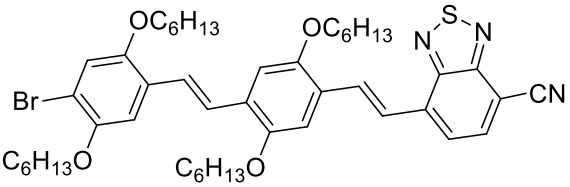

7-((E)-4-((E)-4-bromo-2,5-bis(hexyloxy)styryl)-2,5-bis(hexyloxy)styryl)benzo[c][1,2,5]thiadiazole-4-carbonitrile (Br-PPB-CN) According to the general procedure, **Phos-B-CN** (0.0643 g, 0.227 mmol) was dissolved in dry THF (20 mL) under N_2. NaH (0.0454 g, 60% dispersion in mineral oil) was added and the resulting mixture was stirred for 1 h at room temperature. **Br-PP-CHO** (0.104 g, 0.151 mmol) was added to the reaction mixture. The reaction was kept at room temperature for 5 h. After workup, column chromatography (silica gel, hexanes and methylene chloride) was performed to give the title compound as red solid (0.114 g, 89%).^{1}H NMR (400 MHz, CD_2Cl_2) δ 8.50 (d, *J* = 16.5 Hz, 1H), 8.04 (d, *J* = 7.5 Hz, 1H), 7.77 (dd, *J* = 11.5, 8.6 Hz, 2H), 7.63 – 7.42 (m, 2H), 7.19 (dd, *J* = 30.6, 22.6 Hz, 4H), 4.22 – 3.89 (m, 8H), 1.88 (ddd, *J* = 22.2, 14.1, 7.0 Hz, 8H), 1.73 – 1.48 (m, 8H),

1.38 (s, 16H), 0.92 (d, J = 5.1 Hz, 12H). ^{13}C NMR (126 MHz, $CDCl_3$) δ 152.15 , 151.14 , 151.01 , 149.84 , 136.85 , 136.05 , 132.65 , 129.47 , 126.95 , 125.59 , 124.18 , 124.14 , 123.74 , 122.83 , 117.82 , 115.93 , 111.69 , 111.15 , 110.40 , 77.20 , 70.27 , 69.56 , 69.36 , 31.70 , 31.64 , 31.58 , 31.57 , 29.48 , 29.44 , 29.30 , 29.28 , 25.99 , 25.93 , 25.84 , 25.72 , 22.70 , 22.66 , 22.64 , 22.61 , 14.08 , 14.05 , 14.04 . HRMS calcd for $C_{50}H_{58}O_4N_3Br$: 843.36107g/mol. Found: 843.35852 g/mol.

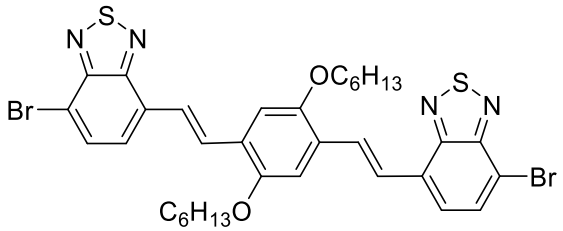

7,7'-((1E,1'E)-(2,5-bis(hexyloxy)-1,4-phenylene)bis(ethene-2,1-diyl))bis(4-bromobenzo[c][1,2,5]thiadiazole) (Br-BPB-Br) According to the general procedure, **Phos-B-Br** (0.0324 g, 0.0962 mmol) was dissolved in dry THF (5 mL) under N_2. NaH (0.0192 g, 60% dispersion in mineral oil) was added and the resulting mixture was stirred for 1 h at room temperature. **Br-BP-CHO** (0.0350 g, 0.0642 mmol) was added to the reaction mixture. The reaction mixture was kept at room temperature for 5 h. After workup, column chromatography (silica gel, hexanes and methylene chloride) was performed to give the title compound as red solid (0.0447 g, 92%).^{1}H NMR (400 MHz, CD_2Cl_2) δ 8.42 (d, J = 16.6 Hz, 2H), 7.92 (d, J = 7.6 Hz, 2H), 7.75 (dd, J = 16.5, 0.8 Hz, 2H), 7.65 (dd, J = 7.5, 0.7 Hz, 2H), 7.34 (s, 2H), 4.20 (t, J = 6.4 Hz, 4H), 2.05 – 1.92 (m, 4H), 1.66 (s, 4H), 1.51 – 1.40 (m, 8H), 1.03 – 0.81 (m, 6H). ^{13}C NMR not acquired due to poor solubility. HRMS calcd for $C_{34}H_{36}O_2N_4Br_2S_2$: 754.06464 g/mol. Found: 754.05968 g/mol. Compound has very low solubility which is reflected in the ^{1}H NMR spectrum.

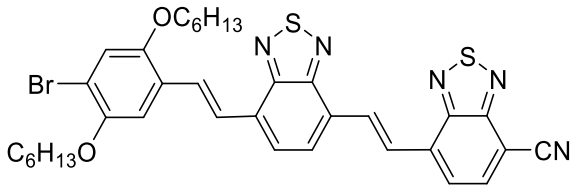

7-((E)-2-(7-((E)-4-bromo-2,5-bis(hexyloxy)styryl)benzo[c][1,2,5]thiadiazol-4-yl)vinyl)benzo[c][1,2,5]thiadiazole-4-carbonitrile (Br-PBB-CN) According to the general procedure, **Phos-B-CN** (0.0680 g, 0.240 mmol) was dissolved in dry THF (20 mL) under N_2. NaH (0.0384 g, 60% dispersion in mineral oil) was added and the resulting mixture was stirred for 1 h at room temperature. **Br-PB-CHO** (0.0655 g, 0.120 mmol) was added to the reaction mixture. The reaction was kept at room temperature for 5 h. After workup, column chromatography (silica gel, hexanes and chloroform) was performed to give the title compound as red solid (0.0702 g, 83%).^{1}H NMR (400 MHz, $CDCl_3$) δ 8.64 (t, *J* = 3.1 Hz, 2H), 8.29 (d, *J* = 16.6 Hz, 1H), 8.06 (d, *J* = 7.5 Hz, 1H), 7.86 (dd, *J* = 7.8, 1.2 Hz, 2H), 7.79 – 7.71 (m, 2H), 7.26 (s, 1H), 7.15 (s, 1H), 4.07 (dt, *J* = 19.3, 6.4 Hz, 4H), 1.89 (ddd, *J* = 12.9, 8.4, 6.5 Hz, 4H), 1.65 – 1.50 (m, 4H), 1.46 – 1.23 (m, 8H), 0.94 (tdd, *J* = 7.2, 3.8, 2.0 Hz, 6H). Compound has very low solubility which is reflected in the ^{1}H NMR spectrum. ^{13}C NMR not acquired.

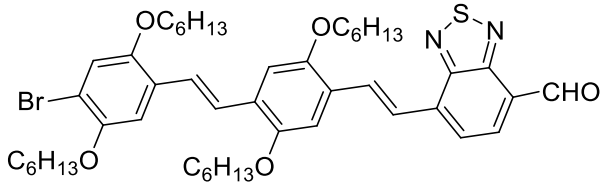

7-((E)-4-((E)-4-bromo-2,5-bis(hexyloxy)styryl)-2,5-bis(hexyloxy)styryl)benzo[c][1,2,5]thiadiazole-4-carbaldehyde (Br-PPB-CHO) According to the general procedure, **Br-PPA-CN** (0.101g, 0.120 mmol) was dissolved in dry CH_2Cl_2 and cooled

to -78 °C. 1 equivalent DIBAL-H (1.0M in hexanes) was added every 45 min until all OPV nitriles were consumed. After workup, column chromatography (silica gel, hexanes and methylene chloride) gave the title compound as red solid (0.0737 g, 72%).^{1}H NMR (400 MHz, CD_2Cl_2) δ 10.72 (s, 1H), 8.53 (d, *J* = 16.5 Hz, 1H), 8.21 (d, *J* = 7.4 Hz, 1H), 7.92 – 7.76 (m, 2H), 7.64 – 7.38 (m, 2H), 7.27 (s, 1H), 7.19 (d, *J* = 7.4 Hz, 2H), 7.12 (s, 1H), 4.20 – 3.90 (m, 8H), 2.17 – 1.69 (m, 8H), 1.69 – 1.36 (m, 24H), 0.92 (d, *J* = 5.9 Hz, 12H). ^{13}C NMR (101 MHz, CD_2Cl_2) δ 188.78 , 154.21 , 152.48 , 151.52 , 151.43 , 150.18 , 137.68 , 132.52 , 129.39 , 127.31 , 126.30 , 125.96 , 124.31 , 124.19 , 124.05 , 118.12 , 112.06 , 111.79 , 110.75 , 70.52 , 69.82 , 54.27 , 32.12 , 32.05 , 31.99 , 31.95 , 30.07 , 29.90 , 29.84 , 29.68 , 26.40 , 26.32 , 26.23 , 26.09 , 23.11 , 23.07 , 23.05 , 23.00 , 14.25 , 14.23 , 14.21 , 14.19 . HRMS calcd for $C_{47}H_{64}O_5N_2BrS$: 847.37193 g/mol. Found: 847.38022 g/mol.

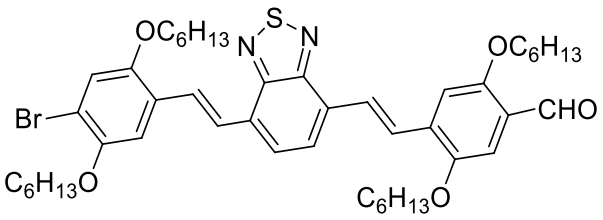

4-((E)-2-(7-((E)-4-bromo-2,5-bis(hexyloxy)styryl)benzo[c][1,2,5]thiadiazol-4-yl)vinyl)-2,5-bis(hexyloxy)benzaldehyde (Br-PBP-CHO) According to the general procedure **Br-PPB-CN** (0.0318 g, 0.376 mmol) was dissolved in dry CH_2Cl_2 and cooled to -78 °C. 1 equivalent DIBAL-H (1.0M in hexanes) was added every 45 min until all OPV nitriles were consumed. After workup, column chromatography (silica gel, hexanes and methylene chloride) gave the title compound as red solid (0.0264 g, 83%). ^{1}H NMR (400 MHz, CD_2Cl_2) δ 10.46 (s, 1H), 8.37 (dd, *J* = 36.0, 16.5 Hz, 2H), 7.76 (dt, *J* = 22.7, 17.5 Hz, 4H), 7.40 – 7.08 (m, 4H), 4.29 – 3.92 (m, 8H), 1.99 – 1.77 (m, 8H), 1.71 (t, *J* = 14.4 Hz, 4H), 1.58 (d, *J* = 30.7 Hz, 8H), 1.46 –

1.17 (m, 16H), 0.91 (tt, *J* = 17.8, 8.9 Hz, 12H). ^{13}C NMR (101 MHz, $CDCl_3$) δ 189.33 , 156.37 , 154.13 , 151.75 , 151.31 , 150.07 , 134.42 , 128.14 , 128.01 , 127.73 , 127.44 , 126.69 , 126.63 , 124.98 , 124.75 , 118.01 , 111.90 , 110.90 , 110.30 , 70.53 , 69.78 , 69.47 , 69.34 , 31.94 , 31.84 , 31.83 , 29.61 , 29.57 , 29.56 , 29.50 , 26.16 , 26.06 , 25.98 , 22.96 , 22.88 , 22.86 , 14.35 , 14.32 , 14.30 . HRMS calcd for $C_{47}H_{64}O_5N_2BrS$: 847.37193 g/mol. Found: 847.37985 g/mol.

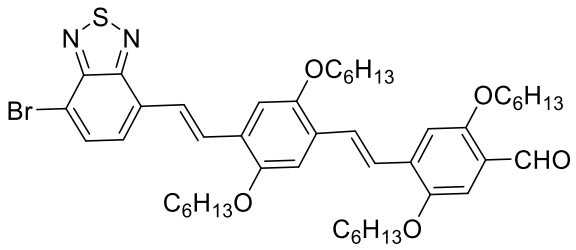

4-((E)-4-((E)-2-(7-bromobenzo[c][1,2,5]thiadiazol-4-yl)vinyl)-2,5-bis(hexyloxy)styryl)-2,5-bis(hexyloxy)benzaldehyde (Br-BPP-CHO) According to the general procedure **Br-BPP-CN** (0.151 g, 0.179 mmol) was dissolved in dry CH_2Cl_2 and cooled to -78 °C. 1 equivalent DIBAL-H (1.0M in hexanes) was added every 45 min until all OPV nitriles were consumed. After workup, column chromatography (silica gel, hexanes and methylene chloride) gave the title compound as red solid (0.121 g, 80%). ^{1}H NMR (400 MHz, $CDCl_3$) δ 10.38 (s, 1H), 8.22 (d, *J* = 16.5 Hz, 1H), 7.77 (d, *J* = 7.7 Hz, 1H), 7.71 – 7.36 (m, 4H), 7.30 – 7.06 (m, 4H), 4.13 – 3.85 (m, 8H), 1.81 (dp, *J* = 21.3, 6.5 Hz, 8H), 1.61 – 1.39 (m, 8H), 1.39 – 1.06 (m, 16H), 0.84 (qd, *J* = 6.7, 3.4 Hz, 12H). ^{13}C NMR (101 MHz, $CDCl_3$) δ 189.14 , 156.24 , 151.61 , 151.36 , 150.70 , 134.93 , 132.39 , 130.97 , 129.01 , 127.72 , 127.17 , 126.88 , 126.28 , 124.14 , 123.88 , 123.28 , 110.81 , 110.74 , 110.40 , 110.07 , 77.20 , 69.51 , 69.44 , 69.15 , 69.07 , 31.70 , 31.65 , 31.59 , 31.55 , 29.50 , 29.44 , 29.24 , 29.22 , 25.99 , 25.94 , 25.85 , 25.80 , 22.70 , 22.67 , 22.65 , 22.62 , 22.59 , 14.08 , 14.05 , 14.02 . HRMS calcd for $C_{47}H_{64}O_5N_2BrS$: 847.37193 g/mol. Found: 847.37979 g/mol.

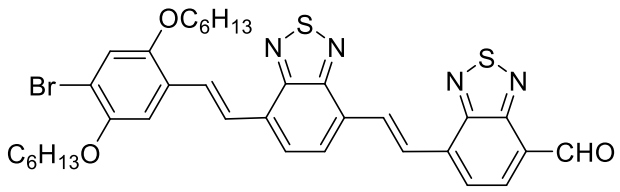

7-((E)-2-(7-((E)-4-bromo-2,5-bis(hexyloxy)styryl)benzo[c][1,2,5]thiadiazol-4-yl)vinyl)benzo[c][1,2,5]thiadiazole-4-carbaldehyde (Br-PBB-CHO) According to the general procedure **Br-PBB-CN** (0.0654 g, 0.0931 mmol) was dissolved in dry chloroform and cooled to -40 °C. 1 equivalent DIBAL-H (1.0M in hexanes) was added every 45 min until all OPV nitriles were consumed. After workup, column chromatography (silica gel, hexanes and chloroform) gave the title compound as red solid (0.0267 g, 56%). ^{1}H NMR (300 MHz, $CDCl_3$) δ 10.69 (s, 1H), 8.76 – 8.47 (m, 2H), 8.28 – 8.14 (m, 2H), 7.91 (d, *J* = 7.5 Hz, 1H), 7.80 (d, *J* = 7.6 Hz, 1H), 7.73 – 7.55 (m, 2H), 7.18 (s, 1H), 7.06 (s, 1H), 3.98 (dt, *J* = 16.1, 6.4 Hz, 4H), 1.93 – 1.68 (m, 4H), 1.50 (dt, *J* = 14.9, 7.4 Hz, 4H), 1.40 – 1.04 (m, 8H), 0.97 – 0.66 (m, 6H). ^{13}C NMR (101 MHz, $CDCl_3$) δ 188.90 , 153.98 , 151.84 , 150.08 , 137.02 , 133.45 , 132.78 , 131.71 , 129.89 , 128.95 , 128.64 , 128.40 , 126.51 , 126.49 , 126.40 , 126.26 , 124.86 , 113.35 , 112.04 , 70.57 , 69.80 , 31.87 , 31.77 , 29.89 , 29.55 , 29.50 , 26.11 , 25.92 , 22.90 , 22.82 , 14.30 , 14.25. HRMS calcd for $C_{35}H_{38}O_3N_4S_2$: 705.15632 g/mol. Found: 705.15975 g/mol.

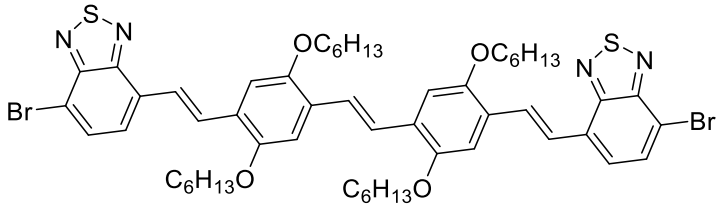

(E)-1,2-bis(4-((E)-2-(7-bromobenzo[c][1,2,5]thiadiazol-4-yl)vinyl)-2,5-bis(hexyloxy)phenyl)ethane (Br-BPPB-Br) According to the general procedure, **Phos-B-Br**

(0.0948 g, 0.281 mmol) was dissolved in dry THF (20 mL) under N_2. NaH (0.0562 g, 60% dispersion in mineral oil) was added and the resulting mixture was stirred for 1 h at room temperature. **Br-BPP-CHO (**0.0795 g, 0.0938 mmol) was added to the reaction mixture. The reaction was kept at room temperature for 5 h. After workup, column chromatography (silica gel, hexanes and methylene chloride) gave the title compound as red solid (0.0904 g, 91%).^{1}H NMR (400 MHz, $CDCl_3$) δ 8.27 (d, *J* = 16.5 Hz, 1H), 7.84 (d, *J* = 7.6 Hz, 1H), 7.68 (d, *J* = 16.5 Hz, 1H), 7.61 – 7.50 (m, 2H), 7.24 (s, 1H), 7.21 (s, 1H), 4.12 (td, *J* = 6.4, 2.8 Hz, 4H), 1.92 (ddt, *J* = 14.8, 8.4, 6.4 Hz, 4H), 1.68 – 1.53 (m, 4H), 1.47 – 1.31 (m, 8H), 0.99 – 0.85 (m, 6H).^{13}C NMR (101 MHz, $CDCl_3$) δ 153.21 , 151.86 , 151.27 , 132.36 , 131.24 , 129.29 , 128.80 , 126.63 , 125.99 , 123.96 , 123.51 , 111.95 , 111.31 , 77.13 , 69.80 , 69.63 , 31.68 , 31.65 , 29.56 , 29.53 , 25.97 , 25.93 , 22.63 , 22.61 , 13.95 . HRMS calcd for $C_{54}H_{66}O_4N_4Br_2S_2$: 1056.28922 g/mol. Found: 1056.28639 g/mol.

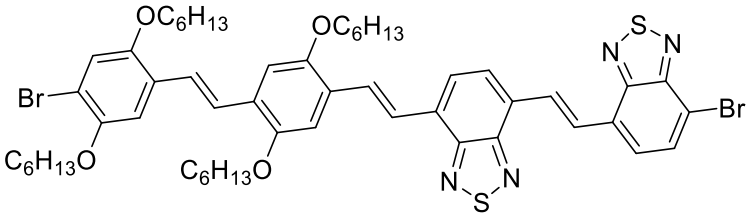

4-bromo-7-((E)-2-(7-((E)-4-((E)-4-bromo-2,5-bis(hexyloxy)styryl)-2,5-bis(hexyloxy)styryl)benzo[c][1,2,5]thiadiazol-4-yl)vinyl)benzo[c][1,2,5]thiadiazole (Br-PPBB-Br) According to the general procedure, **Phos-B-Br** (0.0343 g, 0.102 mmol) was dissolved in dry THF (10 mL) under N_2. NaH (0.0204 g, 60% dispersion in mineral oil) was added and the resulting mixture was stirred for 1 h at room temperature. **Br-PPB-CHO** (0.0431 g, 0.0508 mmol)

was added to the reaction mixture. The reaction was kept at room temperature for 5 h. After workup, column chromatography (silica gel, hexanes and methylene chloride) gave the title compound as red solid (0.0456 g, 85%).^{1}H NMR (400 MHz, CD_2Cl_2) δ 8.55 – 8.34 (m, 3H), 7.95 – 7.65 (m, 5H), 7.56 – 7.40 (m, 2H), 7.18 (t, *J* = 29.2 Hz, 4H), 4.18 – 3.90 (m, 8H), 1.89 (ddt, *J* = 33.6, 14.4, 7.2 Hz, 8H), 1.71 – 1.46 (m, 8H), 1.47 – 1.16 (m, 16H), 0.92 (h, *J* = 7.4 Hz, 12H). ^{13}C NMR (101 MHz, $CDCl_3$) δ 154.14 , 153.95 , 153.85 , 151.69 , 151.08 , 149.83 , 132.39 , 131.09 , 130.56 , 128.71 , 128.65 , 128.20 , 127.63 , 127.19 , 126.77 , 123.95 , 123.42 , 111.77 , 110.55 , 77.20 , 70.25 , 69.56 , 31.75 , 31.67 , 31.60 , 31.57 , 29.56 , 29.48 , 29.30 , 26.04 , 25.95 , 25.85 , 25.72 , 22.73 , 22.68 , 22.65 , 22.61 , 14.12 , 14.04. Calcd for $C_{54}H_{66}O_4N_4Br_2S_2$: 1056.28922 g/mol. MALDI Found: 1056.3917 g/mol.

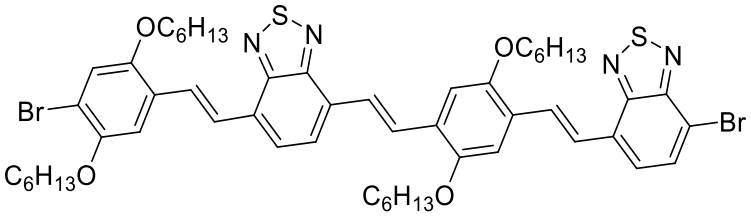

4-bromo-7-((E)-4-((E)-2-(7-((E)-4-bromo-2,5-bis(hexyloxy)styryl)benzo[c][1,2,5]thiadiazol-4-yl)vinyl)-2,5-bis(hexyloxy)styryl)benzo[c][1,2,5]thiadiazole (Br-PBPB-Br) According to the general procedure, **Phos-B-Br** (0.0229 g, 0.068 mmol) was dissolved in dry THF (10 mL) under N_2. NaH (0.0136 g, 60% dispersion in mineral oil) was added and the resulting mixture was stirred for 1 h at room temperature. **Br-PBP-CHO (**0.0314 g, 0.0370 mmol) was added to the reaction mixture. The reaction was kept at room temperature for 5 h. After workup, column chromatography (silica

gel, hexanes and methylene chloride) gave the title compound as red solid (0.0304 g, 77%).[1]H NMR (400 MHz, $CDCl_3$) δ 8.51 – 8.18 (m, 4H), 7.93 – 7.55 (m, 8H), 7.29 (s, 1H), 7.13 (s, 1H), 4.20 – 3.99 (m, 8H), 1.91 (m, *J* = 33.6, 12.5, 9.4, 5.0 Hz, 8H), 1.72 – 1.47 (m, 8H), 1.45 – 1.10 (m, 16H), 0.94 (m, *J* = 7.2, 2.8, 2.0 Hz, 12H). [13]C NMR (101 MHz, $CDCl_3$) δ 153.26 , 151.84 , 151.73 , 151.67 , 150.04 , 132.55 , 131.18 , 130.05 , 129.72 , 129.20 , 128.11 , 127.91 , 127.54 , 127.22 , 126.87 , 126.80 , 126.68 , 126.36 , 125.13 , 124.97 , 123.87 , 118.02 , 111.89 , 110.96 , 110.74 , 70.53 , 69.79 , 69.77 , 69.70 , 31.96 , 31.94 , 31.87 , 31.77 , 29.77 , 29.74 , 29.56 , 29.51 , 26.23 , 26.21 , 26.10 , 25.92 , 22.92 , 22.88 , 22.81 , 14.31 , 14.28 , 14.25. Calcd for $C_{54}H_{66}O_4N_4Br_2S_2$: 1056.28922 g/mol. MALDI found: 1056.3657 g/mol.

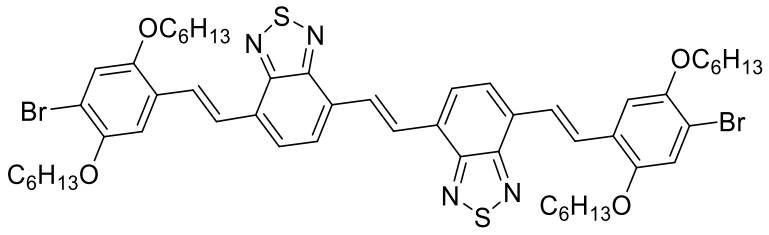

(E)-1,2-bis(7-((E)-4-bromo-2,5-bis(hexyloxy)styryl)benzo[c][1,2,5]thiadiazol-4-yl)ethane (Br-PBBP-Br) According to the general procedure, **Phos-P-Br** (0.0691 g, 0.144 mmol) and **Br-PBB-CHO** (0.267 g, 0.378 mmol) were dissolved in dry THF (30 mL) under N_2. 1.0 M KO^{t}Bu in hexanes (0.15 mL, 0.15 mmol) was added via syringe and the resulting mixture was allowed to stand overnight with stirring. After workup, column chromatography (silica gel, hexanes and methylene chloride) was performed to give the title compound as red solid (0.0239 g, 60%).[1]H NMR (400 MHz, $CDCl_3$) δ 8.53 (s, 2H), 8.25 (d, *J* = 16.5 Hz, 2H), 7.81 (d, *J* = 7.6 Hz, 3H), 7.76 – 7.70 (m, 3H), 7.24 (s, 2H), 7.12 (s, 2H), 4.05 (dt, *J* = 24.3, 6.4 Hz, 8H), 1.96 – 1.80 (m, 8H), 1.67 – 1.48 (m, 8H), 1.46 – 1.31 (m, 16H), 0.92 (q, *J* = 10.6, 8.8 Hz, 12H). [13]C NMR (101 MHz, $CDCl_3$) δ 154.34 , 154.23 , 151.86 , 150.18 , 130.56 , 129.70 , 129.33 , 128.27 , 128.17

, 126.89 , 126.85 , 125.19 , 118.17 , 113.09 , 112.09 , 77.50 , 70.67 , 69.93 , 31.98 , 31.88 , 30.00 , 29.67 , 29.62 , 26.22 , 26.03 , 23.00 , 22.92 , 14.40 , 14.36 , 1.31 . .HRMS calcd for $C_{54}H_{66}O_4N_4Br_2S_2$: 1056.28922 g/mol. Found: 1056.28471 g/mol.

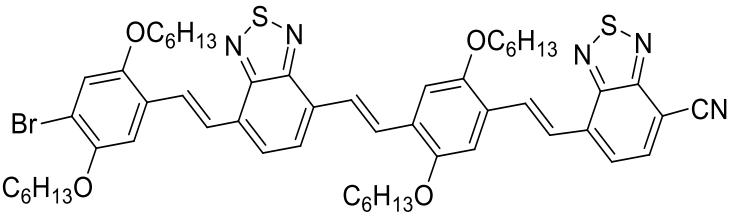

7-((E)-4-((E)-2-(7-((E)-4-bromo-2,5-bis(hexyloxy)styryl)benzo[c][1,2,5]thiadiazol-4-yl)vinyl)-2,5-bis(hexyloxy)styryl)benzo[c][1,2,5]thiadiazole-4-carbonitrile (Br-PBPB-CN)

According to the general procedure, **Phos-B-CN** (0.0175 g, 0.062 mmol) was dissolved in dry THF (15 mL) under N_2. NaH (0.0124 g, 60% dispersion in mineral oil) was added and the resulting mixture was stirred for 1 h at room temperature. **Br-PBP-CHO** (0.0264 g, 0.031 mmol) was added to the reaction mixture. The reaction was kept at room temperature for 5 h. After workup, column chromatography (silica gel, hexanes and methylene chloride) gave the title compound as red solid (0.0221 g, 70%).^{1}H NMR (400 MHz, CD_2Cl_2) δ 8.61 – 8.22 (m, 3H), 8.03 (d, *J* = 7.4 Hz, 1H), 7.85 – 7.61 (m, 6H), 7.24 (dd, *J* = 31.8, 28.4 Hz, 4H), 4.24 – 3.94 (m, 8H), 2.09 – 1.77 (m, 8H), 1.77 – 1.14 (m, 24H), 0.94 (d, *J* = 5.6 Hz, 12H). ^{13}C NMR (101 MHz, $CDCl_3$) δ 154.19 , 153.93 , 152.34 , 151.71 , 150.07 , 136.95 , 136.23 , 132.76 , 129.99 , 129.89 , 129.27 , 127.78 , 127.01 , 126.86 , 126.78 , 126.41 , 125.67 , 125.12 , 124.44 , 123.30 , 118.06 , 116.11 , 112.91 , 111.96 , 111.32 , 110.68 , 102.83 , 70.56 , 69.82 , 69.67 , 31.94 , 31.91 , 31.86 , 31.77 , 29.89 , 29.73 , 29.69

, 29.55 , 29.51 , 26.22 , 26.20 , 26.10 , 25.92 , 22.92 , 22.88 , 22.81 , 14.30 , 14.27 , 14.25. HRMS calcd for $C_{55}H_{66}O_4N_5BrS_2$: 1003.37341 g/mol. Found: 1003.37827 g/mol.

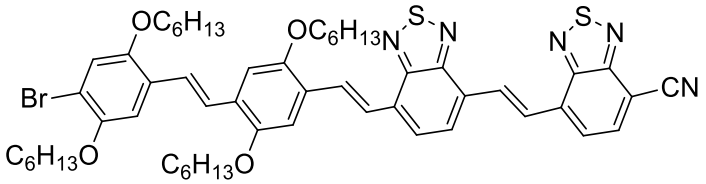

7-((E)-2-(7-((E)-4-((E)-4-bromo-2,5-bis(hexyloxy)styryl)-2,5-bis(hexyloxy)styryl)benzo[c][1,2,5]thiadiazol-4-yl)vinyl)benzo[c][1,2,5]thiadiazole-4-carbonitrile (Br-PPBB-CN) According to the general procedure, **Phos-B-CN** (0.0260 g, 0.092 mmol) was dissolved in dry THF (10 mL) under N_2. NaH (0.0221 g, 60% dispersion in mineral oil) was added and the resulting mixture was stirred for 1 h at room temperature. **Br-PP-CHO** (0.0390 g, 0.046 mmol) was added to the reaction mixture. The reaction was kept at room temperature for 5 h. After workup, column chromatography (silica gel, hexanes and methylene chloride) gave the title compound as red solid (0.0412 g, 89%).^{1}H NMR (400 MHz, CD_2Cl_2) δ 8.78 – 8.57 (m, 2H), 8.45 (d, *J* = 16.4 Hz, 1H), 8.09 (d, *J* = 7.4 Hz, 1H), 7.90 (d, *J* = 7.4 Hz, 2H), 7.86 – 7.71 (m, 2H), 7.61 – 7.39 (m, 2H), 7.35 – 7.03 (m, 4H), 4.22 – 3.90 (m, 8H), 2.03 – 1.76 (m, 8H), 1.53 (s, 8H), 1.47 – 1.00 (m, 16H), 1.00 – 0.76 (m, 12H). Calcd for $C_{55}H_{66}O_4N_5BrS_2$: 1003.37341 g/mol. MALDI found: 1003.3201 g/mol. Compound has very low solubility. ^{13}C NMR not acquired.

3.7 REFERENCE

1. Zhang, S.; Bauer, N. E.; Kanal, I. Y.; You, W.; Hutchison, G. R.; Meyer, T. Y., Sequence Effects in Donor–Acceptor Oligomeric Semiconductors Comprising Benzothiadiazole and Phenylenevinylene Monomers. *Macromolecules* **2017,** *50* (1), 151-161.

2. Henson, Z. B.; Mullen, K.; Bazan, G. C., Design strategies for organic semiconductors beyond the molecular formula. *Nat Chem* **2012,** *4* (9), 699-704.

3. Grimsdale, A. C.; Chan, K. L.; Martin, R. E.; Jokisz, P. G.; Holmes, A. B., Synthesis of Light-Emitting Conjugated Polymers for Applications in Electroluminescent Devices. *Chemical Reviews* **2009,** *109* (3), 897-1091.

4. Facchetti, A., π-Conjugated Polymers for Organic Electronics and Photovoltaic Cell Applications. *Chem. Mater.* **2011,** *23*, 733-758.

5. Yassar, A.; Miozzo, L.; Gironda, R.; Horowitz, G., Rod–coil and all-conjugated block copolymers for photovoltaic applications. *Progress in Polymer Science* **2013,** *38* (5), 791-844.

6. Mishra, A.; Bäuerle, P., Small Molecule Organic Semiconductors on the Move: Promises for Future Solar Energy Technology. *Angewandte Chemie International Edition* **2012,** *51* (9), 2020-2067.

7. Chen, Y.; Wan, X.; Long, G., High Performance Photovoltaic Applications Using Solution-Processed Small Molecules. *Accounts of Chemical Research* **2013,** *46* (11), 2645-2655.

8. Wang, C.; Dong, H.; Hu, W.; Liu, Y.; Zhu, D., Semiconducting π-Conjugated Systems in Field-Effect Transistors: A Material Odyssey of Organic Electronics. *Chemical Reviews* **2011**.

9. Rochat, S.; Swager, T. M., Conjugated Amplifying Polymers for Optical Sensing Applications. *ACS Applied Materials & Interfaces* **2013,** *5* (11), 4488-4502.

10. Duan, L.; Hou, L.; Lee, T.-W.; Qiao, J.; Zhang, D.; Dong, G.; Wang, L.; Qiu, Y., Solution processable small molecules for organic light-emitting diodes. *Journal of Materials Chemistry* **2010,** *20* (31), 6392-6407.

11. Zhang, L.; Colella, N. S.; Cherniawski, B. P.; Mannsfeld, S. C. B.; Briseno, A. L., Oligothiophene Semiconductors: Synthesis, Characterization, and Applications for Organic Devices. *ACS Applied Materials & Interfaces* **2014,** *6* (8), 5327-5343.

12. Ellinger, S.; Graham, K. R.; Shi, P.; Farley, R. T.; Steckler, T. T.; Brookins, R. N.; Taranekar, P.; Mei, J.; Padilha, L. A.; Ensley, T. R.; Hu, H.; Webster, S.; Hagan, D. J.; Van Stryland, E. W.; Schanze, K. S.; Reynolds, J. R., Donor–Acceptor–Donor-based π-

Conjugated Oligomers for Nonlinear Optics and Near-IR Emission. *Chemistry of Materials* **2011,** *23* (17), 3805-3817.

13. Roncali, J.; Leriche, P.; Blanchard, P., Molecular Materials for Organic Photovoltaics: Small is Beautiful. *Advanced Materials* **2014,** *26* (23), 3821-3838.

14. O'Boyle, N. M.; Campbell, C. M.; Hutchison, G. R., Computational Design and Selection of Optimal Organic Photovoltaic Materials. *The Journal of Physical Chemistry C* **2011,** *115* (32), 16200-16210.

15. Norris, B. N.; Zhang, S.; Campbell, C. M.; Auletta, J. T.; Calvo-Marzal, P.; Hutchison, G. R.; Meyer, T. Y., Sequence Matters: Modulating Electronic and Optical Properties of Conjugated Oligomers via Tailored Sequence. *Macromolecules* **2013,** *46* (4), 1384-1392.

16. Ilana, Y. K.; Jonathon, S. B.; Geoffrey, R. H., Sequence Matters: Determining the Sequence Effect of Electronic Structure Properties in π-Conjugated Polymers. In *Sequence-Controlled Polymers: Synthesis, Self-Assembly, and Properties*, American Chemical Society: 2014; Vol. 1170, pp 379-393.

17. Liang, Y.; Yu, L., A New Class of Semiconducting Polymers for Bulk Heterojunction Solar Cells with Exceptionally High Performance. *Accounts of Chemical Research* **2010,** *43* (9), 1227-1236.

18. Mei, J.; Bao, Z., Side Chain Engineering in Solution-Processable Conjugated Polymers. *Chemistry of Materials* **2013,** *26* (1), 604-615.

19. Lu, L.; Zheng, T.; Wu, Q.; Schneider, A. M.; Zhao, D.; Yu, L., Recent Advances in Bulk Heterojunction Polymer Solar Cells. *Chemical Reviews* **2015,** *115* (23), 12666-12731.

20. Szarko, J. M.; Guo, J.; Rolczynski, B. S.; Chen, L. X., Current trends in the optimization of low band gap polymers in bulk heterojunction photovoltaic devices. *Journal of Materials Chemistry* **2011**.

21. Zhao, X.; Zhan, X., Electron transporting semiconducting polymers in organic electronics. *Chemical Society Reviews* **2011,** *40* (7), 3728-3743.

22. Risko, C.; McGehee, M. D.; Bredas, J.-L., A quantum-chemical perspective into low optical-gap polymers for highly-efficient organic solar cells. *Chemical Science* **2011,** *2* (7), 1200-1218.

23. Beaujuge, P. M.; Amb, C. M.; Reynolds, J. R., Spectral Engineering in π-Conjugated Polymers with Intramolecular Donor−Acceptor Interactions. *Accounts of Chemical Research* **2010,** *43* (11), 1396-1407.

24. Park, Y. S.; Kale, T. S.; Nam, C. Y.; Choi, D.; Grubbs, R. B., Effects of heteroatom substitution in conjugated heterocyclic compounds on photovoltaic performance: from sulfur to tellurium. *Chemical Communications* **2014,** *50* (59), 7964-7967.

25. Lin, L.-Y.; Lu, C.-W.; Huang, W.-C.; Chen, Y.-H.; Lin, H.-W.; Wong, K.-T., New A-A-D-A-A-Type Electron Donors for Small Molecule Organic Solar Cells. *Organic Letters* **2011,** *13* (18), 4962-4965.

26. Schulz, M. D.; Wagener, K. B., Precision Polymers through ADMET Polymerization. *Macromolecular Chemistry and Physics* **2014,** *215* (20), 1936-1945.

27. Copenhafer, J. E.; Walters, R. W.; Meyer, T. Y., Synthesis and Characterization of Repeating Sequence Copolymers of Fluorene and Methylene Monomers. *Macromolecules* **2008,** *41* (1), 31-35.

28. Edwardson, T. G. W.; Carneiro, K. M. M.; Serpell, C. J.; Sleiman, H. F., An Efficient and Modular Route to Sequence-Defined Polymers Appended to DNA. *Angewandte Chemie, International Edition* **2014,** *53* (18), 4567-4571.

29. Stayshich, R. M.; Meyer, T. Y., New Insights into Poly(lactic-co-glycolic acid) Microstructure: Using Repeating Sequence Copolymers To Decipher Complex NMR and Thermal Behavior. *Journal of the American Chemical Society* **2010,** *132* (31), 10920-10934.

30. Lutz, J.-F.; Ouchi, M.; Liu, D. R.; Sawamoto, M., Sequence-Controlled Polymers. *Science* **2013,** *341* (6146).

31. De Bo, G.; Kuschel, S.; Leigh, D. A.; Lewandowski, B.; Papmeyer, M.; Ward, J. W., Efficient assembly of threaded molecular machines for sequence-specific synthesis. *Journal of the American Chemical Society* **2014,** *136* (15), 5811-5814.

32. Li, J.; Stayshich, R. M.; Meyer, T. Y., Exploiting Sequence To Control the Hydrolysis Behavior of Biodegradable PLGA Copolymers. *Journal of the American Chemical Society* **2011,** *133* (18), 6910-6913.

33. Li, J.; Rothstein, S. N.; Little, S. R.; Edenborn, H. M.; Meyer, T. Y., The Effect of Monomer Order on the Hydrolysis of Biodegradable Poly(lactic-co-glycolic acid) Repeating Sequence Copolymers. *Journal of the American Chemical Society* **2012,** *134* (39), 16352-16359.

34. Rosales, A. M.; Segalman, R. A.; Zuckermann, R. N., Polypeptoids: a model system to study the effect of monomer sequence on polymer properties and self-assembly. *Soft Matter* **2013,** *9* (35), 8400-8414.

35. Ward, R. E.; Meyer, T. Y., o,p-Polyaniline: A New Form of a Classic Conducting Polymer. *Macromolecules* **2003,** *36* (12), 4368-4373.

36. Rowan, S. J.; Barner-Kowollik, C.; Klumperman, B.; Gaspard, P.; Grubbs, R. B.; Hillmyer, M. A.; Hutchings, L. R.; Mahanthappa, M. K.; Moatsou, D.; O'Reilly, R. K.; Ouchi, M.; Sawamoto, M.; Lodge, T. P., Discussion on "Aperiodic Copolymers". *ACS Macro Letters* **2016,** *5* (1), 1-3.

37. Palermo, E. F.; McNeil, A. J., Impact of Copolymer Sequence on Solid-State Properties for Random, Gradient and Block Copolymers containing Thiophene and Selenophene. *Macromolecules* **2012,** *45* (15), 5948-5955.

38. Fitzner, R.; Mena-Osteritz, E.; Mishra, A.; Schulz, G.; Reinold, E.; Weil, M.; Körner, C.; Ziehlke, H.; Elschner, C.; Leo, K.; Riede, M.; Pfeiffer, M.; Uhrich, C.; Bäuerle, P., Correlation of π-Conjugated Oligomer Structure with Film Morphology and Organic Solar Cell Performance. *Journal of the American Chemical Society* **2012,** *134* (27), 11064-11067.

39. Doval, D. A.; Molin, M. D.; Ward, S.; Fin, A.; Sakai, N.; Matile, S., Planarizable push-pull oligothiophenes: in search of the perfect twist. *Chemical Science* **2014,** *5* (7), 2819-2825.

40. Liang, L.; Wang, J.-T.; Xiang, X.; Ling, J.; Zhao, F.-G.; Li, W.-S., Influence of moiety sequence on the performance of small molecular photovoltaic materials. *Journal of Materials Chemistry A* **2014,** *2* (37), 15396-15405.

41. Tsai, C.-H.; Fortney, A.; Qiu, Y.; Gil, R. R.; Yaron, D.; Kowalewski, T.; Noonan, K. J. T., Conjugated Polymers with Repeated Sequences of Group 16 Heterocycles Synthesized through Catalyst-Transfer Polycondensation. *Journal of the American Chemical Society* **2016,** *138* (21), 6798-6804.

42. Yamamoto, T.; Fang, Q.; Morikita, T., New Soluble Poly(aryleneethynylene)s Consisting of Electron-Accepting Benzothiadiazole Units and Electron-Donating Dialkoxybenzene Units. Synthesis, Molecular Assembly, Orientation on Substrates, and Electrochemical and Optical Properties. *Macromolecules* **2003,** *36* (12), 4262-4267.

43. Lu, S.; Yang, M.; Luo, J.; Cao, Y., Photovoltaic devices based on a novel poly(phenylene ethynylene) derivative. *Synthetic Metals* **2004,** *140* (2–3), 199-202.

44. Liu, L.; Pei, J.; Wen, S.; Li, J.; Yao, B.; Tian, W., Optimization of Polymer Solar Cells Based on the Conjugated Copolymer of Poly(phenylenevinylene-alt-4,7-diphenyl-2,1,3-benzothiadiazole) (PP-DBT). *Macromolecular Chemistry and Physics* **2013,** *214* (16), 1836-1844.

45. Nguyen, T. L.; Choi, H.; Ko, S. J.; Uddin, M. A.; Walker, B.; Yum, S.; Jeong, J. E.; Yun, M. H.; Shin, T. J.; Hwang, S.; Kim, J. Y.; Woo, H. Y., Semi-crystalline photovoltaic polymers with efficiency exceeding 9% in a [similar]300 nm thick conventional single-cell device. *Energy & Environmental Science* **2014,** *7* (9), 3040-3051.

46. Kim, J.; Han, A. R.; Hong, J.; Kim, G.; Lee, J.; Shin, T. J.; Oh, J. H.; Yang, C., Ambipolar Semiconducting Polymers with π-Spacer Linked Bis-Benzothiadiazole Blocks as Strong Accepting Units. *Chemistry of Materials* **2014,** *26* (17), 4933-4942.

47. Li, X.; Zhang, Y.; Yang, R.; Huang, J.; Yang, W.; Cao, Y., Novel saturated red-emitting poly(p-phenylenevinylene) copolymers with narrow-band-gap units of 2,1,3-benzothiadiazole synthesized by a palladium-catalyzed Stille coupling reaction. *Journal of Polymer Science Part A: Polymer Chemistry* **2005,** *43* (11), 2325-2336.

48. Zhou, C.; Zhang, G.; Zhong, C.; Jia, X.; Luo, P.; Xu, R.; Gao, K.; Jiang, X.; Liu, F.; Russell, T. P.; Huang, F.; Cao, Y., Toward High Efficiency Polymer Solar Cells: Influence of Local Chemical Environment and Morphology. *Advanced Energy Materials* **2016**.

49. Jorgensen, M.; Krebs, F. C., Stepwise Unidirectional Synthesis of Oligo Phenylene Vinylenes with a Series of Monomers. Use in Plastic Solar Cells. *Journal of organic chemistry* **2005,** *70*, 6004-6017.

50. Dasilveiraneto, B.; Lopes, A.; Ebeling, G.; Goncalves, R.; Costa, V.; Quina, F.; Dupont, J., Photophysical and electrochemical properties of π-extended molecular 2,1,3-benzothiadiazoles. *Tetrahedron* **2005,** *61* (46), 10975-10982.

51. K.Pilgram; Skiles, R. D., Synthesis of 2,1,3-Benzothiadiazolecarbonitriles. *Journal of heterocyclic chemistry* **1974,** *11*.

52. Liu, Y.; Lai, H.; Zhong, H.; Xu, E.; Du, J.; Li, Y.; Fang, Q., New low bandgap molecules based on ethylene-separated benzothiadiazoles: synthesis and bandgap comparison. *Tetrahedron Letters* **2010,** *51* (33), 4462-4465.

53. McNulty, J.; McLeod, D., An iterative approach toward the synthesis of discrete oligomeric p-phenylene vinylene organic dyes employing aqueous Wittig chemistry. *Tetrahedron Letters* **2011,** *52* (42), 5467-5470.

54. Zhou, C.; Liang, Y.; Liu, F.; Sun, C.; Huang, X.; Xie, Z.; Huang, F.; Roncali, J.; Russell, T. P.; Cao, Y., Chain Length Dependence of the Photovoltaic Properties of Monodisperse Donor–Acceptor Oligomers as Model Compounds of Polydisperse Low Band Gap Polymers. *Advanced Functional Materials* **2014,** *24* (47), 7538-7547.

55. Li, W.; Albrecht, S.; Yang, L.; Roland, S.; Tumbleston, J. R.; McAfee, T.; Yan, L.; Kelly, M. A.; Ade, H.; Neher, D.; You, W., Mobility-Controlled Performance of Thick Solar Cells Based on Fluorinated Copolymers. *Journal of the American Chemical Society* **2014,** *136* (44), 15566-15576.

56. Bartelt, J. A.; Lam, D.; Burke, T. M.; Sweetnam, S. M.; McGehee, M. D., Charge-Carrier Mobility Requirements for Bulk Heterojunction Solar Cells with High Fill Factor and External Quantum Efficiency >90%. *Advanced Energy Materials* **2015,** *5* (15), 1500577-n/a.

57. Proctor, C. M.; Love, J. A.; Nguyen, T.-Q., Mobility Guidelines for High Fill Factor Solution-Processed Small Molecule Solar Cells. *Advanced Materials* **2014,** *26* (34), 5957-5961.

58. Bartesaghi, D.; Perez, I. d. C.; Kniepert, J.; Roland, S.; Turbiez, M.; Neher, D.; Koster, L. J. A., Competition between recombination and extraction of free charges determines the fill factor of organic solar cells. *Nature Communications* **2015,** *6*. 7083

59. Zhan, C.-G.; Nichols, J. A.; Dixon, D. A., Ionization Potential, Electron Affinity, Electronegativity, Hardness, and Electron Excitation Energy: Molecular Properties from

Density Functional Theory Orbital Energies. *The Journal of Physical Chemistry A* **2003,** *107* (20), 4184-4195.

60. Rienstra-Kiracofe, J. C.; Tschumper, G. S.; Schaefer, H. F.; Nandi, S.; Ellison, G. B., Atomic and Molecular Electron Affinities: Photoelectron Experiments and Theoretical Computations. *Chemical Reviews* **2002,** *102* (1), 231-282.

61. Perdew, J. P.; Levy, M., Comment on "Significance of the highest occupied Kohn-Sham eigenvalue". *Physical Review B* **1997,** *56* (24), 16021.

62. Levy, M., Excitation energies from density-functional orbital energies. *Physical Review A* **1995,** *52* (6), R4313.

63. Hutchison, G. R.; Ratner, M. A.; Marks, T. J., Accurate Prediction of Band Gaps in Neutral Heterocyclic Conjugated Polymers. *J. Phys. Chem. A* **2002,** *106* (44), 10596-10605.

64. Winget, P.; Weber, E. J.; Cramer, C. J.; Truhlar, D. G., Computational electrochemistry: aqueous one-electron oxidation potentials for substituted anilines. *Physical Chemistry Chemical Physics* **2000,** *2* (6), 1231-1239.

65. Jaque, P.; Marenich, A. V.; Cramer, C. J.; Truhlar, D. G., Computational Electrochemistry: The Aqueous Ru3+|Ru2+ Reduction Potential. *The Journal of Physical Chemistry* **2007,** *111* (15), 5783-5799.

66. Zhou, H.; Yang, L.; You, W., Rational Design of High Performance Conjugated Polymers for Organic Solar Cells. *Macromolecules* **2012,** *45* (2), 607-632.

67. Sun, Y.; Welch, G. C.; Leong, W. L.; Takacs, C. J.; Bazan, G. C.; Heeger, A. J., Solution-processed small-molecule solar cells with 6.7% efficiency. *Nature Materials* **2012,** *11* (1), 44-48.

68. Zhang, Q.; Kan, B.; Liu, F.; Long, G.; Wan, X.; Chen, X.; Zuo, Y.; Ni, W.; Zhang, H.; Li, M.; Hu, Z.; Huang, F.; Cao, Y.; Liang, Z.; Zhang, M.; Russell, T. P.; Chen, Y., Small-molecule solar cells with efficiency over 9%. *Nature Photonics* **2015,** *9* (1), 35-41

69. Stuart, A. C.; Tumbleston, J. R.; Zhou, H.; Li, W.; Liu, S.; Ade, H.; You, W., Fluorine Substituents Reduce Charge Recombination and Drive Structure and Morphology Development in Polymer Solar Cells. *Journal of the American Chemical Society* **2013,** *135* (5), 1806-1815.

70. Carsten, B.; Szarko, J. M.; Lu, L.; Son, H. J.; He, F.; Botros, Y. Y.; Chen, L. X.; Yu, L., Mediating Solar Cell Performance by Controlling the Internal Dipole Change in Organic Photovoltaic Polymers. *Macromolecules* **2012,** *45* (16), 6390-6395.

71. Carsten, B.; Szarko, J. M.; Son, H. J.; Wang, W.; Lu, L.; He, F.; Rolczynski, B. S.; Lou, S. J.; Chen, L. X.; Yu, L., Examining the Effect of the Dipole Moment on Charge Separation in Donor–Acceptor Polymers for Organic Photovoltaic Applications. *Journal of the American Chemical Society* **2011,** *133* (50), 20468-20475.

72. Zhang, Q.; Kelly, M. A.; Hunt, A.; Ade, H.; You, W., Comparative Photovoltaic Study of Physical Blending of Two Donor–Acceptor Polymers with the Chemical Blending of the Respective Moieties. *Macromolecules* **2016,** *49* (7), 2533-2540.

73. Lin, L.-Y.; Chen, Y.-H.; Huang, Z.-Y.; Lin, H.-W.; Chou, S.-H.; Lin, F.; Chen, C.-W.; Liu, Y.-H.; Wong, K.-T., A Low-Energy-Gap Organic Dye for High-Performance Small-Molecule Organic Solar Cells. *Journal of the American Chemical Society* **2011,** *133* (40), 15822-15825.

74. Weininger, D., SMILES, A CHEMICAL LANGUAGE AND INFORMATION-SYSTEM .1. INTRODUCTION TO METHODOLOGY AND ENCODING RULES. *Journal of Chemical Information and Computer Sciences* **1988,** *28* (1), 31-36.

75. O'Boyle, N. M.; Banck, M.; James, C. A.; Morley, C.; Vandermeersch, T.; Hutchison, G. R., Open Babel: An open chemical toolbox. *Journal of Cheminformatics* **2011,** *3*(1), 33.

76. O'Boyle, N. M.; Morley, C.; Hutchison, G. R., Pybel: a Python wrapper for the OpenBabel cheminformatics toolkit. *Chemistry Central Journal* **2008,** *2*, Article #5.

77. Halgren, T. A., Merck molecular force field .1. Basis, form, scope, parameterization, and performance of MMFF94. *Journal of Computational Chemistry* **1996,** *17* (5-6), 490-519.

78. Halgren, T. A., Merck molecular force field .2. MMFF94 van der Waals and electrostatic parameters for intermolecular interactions. *Journal of Computational Chemistry* **1996,** *17* (5-6), 520-552.

79. Halgren, T. A., Merck molecular force field .3. Molecular geometries and vibrational frequencies for MMFF94. *Journal of Computational Chemistry* **1996,** *17* (5-6), 553-586.

80. Halgren, T. A., Merck molecular force field .5. Extension of MMFF94 using experimental data, additional computational data, and empirical rules. *Journal of Computational Chemistry* **1996,** *17* (5-6), 616-641.

81. Halgren, T. A.; Nachbar, R. B., Merck molecular force field .4. Conformational energies and geometries for MMFF94. *Journal of Computational Chemistry* **1996,** *17* (5-6), 587-615.

82. Frisch, M. J. T., G. W.; Schlegel, H. B.; Scuseria, G. E.; Robb, M. A.; Cheeseman, J. R.; Scalmani, G.; Barone, V.; Mennucci, B.; Petersson, G. A.; Nakatsuji, H.; Caricato, M.; Li, X.; Hratchian, H. P.; Izmaylov, A. F.; Bloino, J.; Zheng, G.; Sonnenberg, J. L.; Hada, M.; Ehara, M.; Toyota, K.; Fukuda, R.; Hasegawa, J.; Ishida, M.; Nakajima, T.; Honda, Y.; Kitao, O.; Nakai, H.; Vreven, T.; Montgomery, Jr., J. A.; Peralta, J. E.; Ogliaro, F.; Bearpark, M.; Heyd, J. J.; Brothers, E.; Kudin, K. N.; Staroverov, V. N.; Kobayashi, R.; Normand, J.; Raghavachari, K.; Rendell, A.; Burant, J. C.; Iyengar, S. S.; Tomasi, J.; Cossi, M.; Rega, N.; Millam, N. J.; Klene, M.; Knox, J. E.; Cross, J. B.; Bakken, V.; Adamo, C.; Jaramillo, J.; Gomperts, R.; Stratmann, R. E.; Yazyev, O.; Austin, A. J.; Cammi, R.; Pomelli, C.; Ochterski, J. W.; Martin, R. L.; Morokuma, K.; Zakrzewski, V. G.; Voth, G. A.; Salvador, P.; Dannenberg, J. J.; Dapprich, S.; Daniels, A. D.; Farkas, Ö.; Foresman, J.

B.; Ortiz, J. V.; Cioslowski, J.; Fox, D. J. *Gaussian 09, Revision A.2*, Gaussian, Inc., : Wallingford CT, 2009.

83. Becke, A., Density-functional thermochemistry. III. The role of exact exchange. *The Journal of Chemical Physics* **1993,** *98* (7), 5648-5652.

84. Lee, C.; Yang, W.; Parr, R., Development of the Colle-Salvetti correlation-energy formula into a functional of the electron density. *Physical Review B: Condensed Matter and Materials Physics* **1988,** *37* (2), 785-789.

85. Tomasi, J.; Mennucci, B., Quantum mechanical continuum solvation models. *Chemical Reviews* **2005**.

86. Ridley, J.; Zerner, M., An Intermediate Neglect of Differential Overlap Technique for Spectroscopy: Pyrrole and the Azines. *Theoretica Chimica Acta* **1973,** *32*, 111-134.

87. Cossi, M.; Barone, V., Time-dependent density functional theory for molecules in liquid solutions. *The Journal of Chemical Physics* **2001,** *115* (10), 4708-4717.

88. Hanwell, M. D.; Curtis, D. E.; Lonie, D. C.; Vandermeersch, T.; Zurek, E.; Hutchison, G. R., Avogadro: an advanced semantic chemical editor, visualization, and analysis platform. *Journal of Cheminformatics* **2012,** *4*.

89. Chung, T. C., Synthesis of polyalcohols via Ziegler-Natta polymerization. *Macromolecules* **1988,** *21* (4), 865-869.

4.0 SEQUENCE EFFECTS IN CONJUGATED DONOR-ACCEPTOR POLYMERS

4.1 OVERVIEW

To investigate the sequence effect on donor-acceptor conjugated oligomers and polymers the trimeric isomers **PBP** and **BPP**, comprising dialkoxy phenylene vinylene (**P**), benzothiadiazole vinylene (**B**), and alkyl endgroups with terminal olefins, were synthesized. Sequence effects were evident in the optical/electrochemical properties and thermal properties. The **PBP** and **BPP** trimers were used as macromonomers in an ADMET polymerization to give **PolyPBP** and **PolyBPP**. The optical and electrochemical properties were similar to those of their trimer precursors—sequence effects were still evident. These results suggest that sequence is a tunable variable for electronic materials and that the polymerization of oligomeric sequences is a useful approach to introducing sequence into polymers. The majority of the work presented in this chapter was previously published in Zhang, S.; Hutchison, G. R.; Meyer, T. Y., Sequence Effects in Conjugated Donor–Acceptor Trimers and Polymers. *Macromolecular Rapid Communications* **2016,** *37* (11), 882-887.[1]

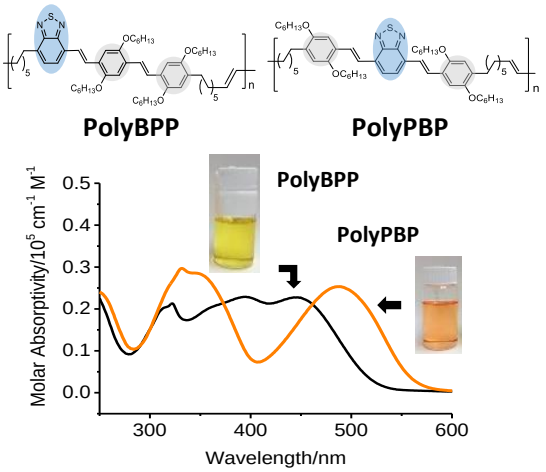

4.2 INTRODUCTION

Semiconducting organic molecules have a significant potential for a wide variety of applications due to their inherent flexibility, low density, potential cost efficiency, and roll-to-roll processibility.[2-9] These materials have been used to make electronic devices including organic field effect transistors, organic light emitting diodes and organic solar cells. In all cases, the physical and chemical properties of the conjugated materials including HOMO-LUMO band gaps, optical and electrochemical properties, film morphologies and thermal properties have a profound influence on the performance of fabricated devices.[2, 10-12]

Both semiconducting small molecules and polymers have been exploited by researchers for the creation organic electronic devices as each of them offer specific advantages. Semiconducting small molecules exhibit well-defined structure, crystallinity, chain-end control, and high chemical purity.[3-4, 7-8, 13] Conjugated polymers, which are generally less structurally controlled, are facile film-makers with better mechanical qualities.[10] To further engineer properties in both systems, there have been major efforts directed at developing structure-function relationships at the molecular level. Widely utilized approaches for designing conjugated molecules include incorporating electron-rich and electron-poor monomers (donor-acceptor strategy), tailoring side-chains, developing new repeating units and increasing the coplanarity of the polymer backbone.[2, 11, 14-19]

Recently, the control of sequence has been recognized as a powerful but underutilized structural tool for controlling the properties of oligomers and polymers.[20-22] In non-conjugated systems sequence has been observed to affect degradation, crystallinity and self-assembly behaviors.[23-29] Although it can be argued, especially in the case of conjugated oligomers, that sequence isomers are simply different molecules and that, as such, they possess different

properties, we submit that the use of the sequence descriptor is powerful. First, the semi-conducting community has long referenced and exploited the idea of individual monomer units. Copolymers/oligomers of thiophenes, phenylenes, and other molecules capable of conjugation have been prepared and their properties reported as distinctive based on unit composition. Second, the idea that properties can be controlled by rearrangement of preformed molecular units has long been recognized and utilized in biological systems—this idea has been less explored in synthetic materials. Finally, sequence provides an opportunity for both rationale design, when structure/function correlations are understood, and for the creation of libraries which can be queried proteomics-style for desirable combinations of properties, e.g., HOMO-LUMO gap, efficient π-stacking, and solubility.

Although there have been fewer reports of the effects of sequence in conjugated materials there are some intriguing results.[30-34] Liang and coworkers, for example, reported two isomeric compounds with different sequences which can be generically written as ABACABA vs. AABCBAA. Despite nominal difference in their optical properties and HOMO-LUMO band gaps, their power conversion efficiencies were significantly different, 4.53% vs. 1.58%.[34] Palermo, et al. investigated copolymers composed of thiophene and selenophene derivatives with gradient sequence, block, and random structures. The gradient sequence displayed unique thin-film morphology, optical and thermal properties.[31]

We have reported previously on the effects of sequence on oligomers comprising dialkoxy-substituted phenylene vinylene and unsubstituted phenylene monomers.[21] We found differences of ca. 0.24 V in the electrochemical band gap in tetramers and hexamers in this series, attributable to sequence effects and the coupling of sequence with end group effects.

In this study we expand our scope to include acceptor-type units, employ mildly perturbing alkyl end groups, and examine in parallel oligomers and polymers prepared from the oligomers. As the performance of semiconducting materials depends both on the intrinsic photophysical properties and on how the materials pack in the solid state, both are examined. We focus here on the conventional pair of donor-acceptor monomers, dialkoxy-substituted phenylene vinylene (**P**, donor) and benzothiadiazole vinylene (**B**, acceptor), and we examine the effect of sequence in two isomeric trimeric oligomers, **PBP** and **BPP**, which also bear polymerizable end groups. As these polymerizable end groups are mildly donating alkyl substituents, rather than the more electronically interactive cyano groups used in our previous study, the sequence effects are expected to be the primary contributor to differences in photophysical properties. Trimers, defined by the number of aryl units present in the oligomer, were chosen as they represent the smallest unit in which moiety-sequence-isomers can exist and are also the smallest unit used in semiconducting materials.

In addition to examining trimeric oligomers, we prepare and characterize polymers which bear these oligomers as isolated units separated by flexible spacers. We chose this approach over preparing a fully conjugated species for several reasons: 1) Practicality of synthesis—these materials are more easily prepared than most sequence-controlled fully conjugated polymers; 2) Control of variables—by including the pre-formed oligomers as isolated units in a polymer, they retain their chemical identity; and 3) Potential for application—structures of this type have been reported to offer, in some cases, advantages in increased solubility, improved processibility, higher charge carrier mobilities and access to novel morphologies relative to the fully conjugated analogs.[35-36]

4.3 RESULTS

4.3.1 Synthesis

As described in Chapter 3, two macromonomers, **PBP** and **BPP**, were synthesized from five small molecule building units **Br-B-CHO**, **Phos-P-Br**, **Phos-P-CN**, **Phos-B-CN** and **Br-B-CHO** (Phos = dimethyl phosphonate). For example, coupling **Br-P-CHO** and **Phos-B-CN** together with Horner-Wadsworth-Emmons (HWE) produced nitrile-terminated dimer **Br-PB-CN**. This dimer was then prepared for the subsequent additions by reductive conversion of the nitrile to an aldehyde. HWE coupling of the resultant aldehydes **Br-PB-CHO** with **Phos-P-Br** led to dibromo-terminated trimers which were subsequently functionalized with two olefin-terminated alkyl units via Suzuki coupling with a borane reagent. These final oligomers, which bear the olefin-terminated side-chains, are named **PBP** and **BPP** for simplicity. Moreover, the term "trimer" is used throughout, based on the number of aryl units present.

PolyPBP and **PolyBPP** were obtained from the diolefin-terminated macromonomers by ADMET polymerization with the Grubbs II catalyst. We found that both catalyst loading ratio and temperature control are critical for the polymerization. This reaction only yields very short oligomers with 2 mol% catalyst and 30-40 ^{o}C reaction temperature. However using a relatively high reaction temperature (70 ^{o}C) and a higher than normal catalyst loading (5 mol%) we were able to obtain polymers of higher molecular weight than those previously reported for a similar material (19-24 KDa vs 7 KDa).[37] We hypothesize that these conditions minimize the effect of reaction-inhibiting coordination of the benzothiadiazole groups to the ruthenium catalyst. The resultant polymers consisted of conjugated trimeric units separated by a flexible linker. For

PolyBPP, two regiochemical isomers could form in the polymer chain, ~**BPP**~ and ~**PPB**~, which should not change its properties in solution phase but might impact its solid state properties.

Table 12. Polymer molecular weights.

Compounds	Mn[a]/KDa	Mw[a]/KDa	PDI
PolyPBP	19	30	1.6
PolyBPP	24	41	1.7

[a] Molecular weight determined by SEC in THF vs polystyrene standards

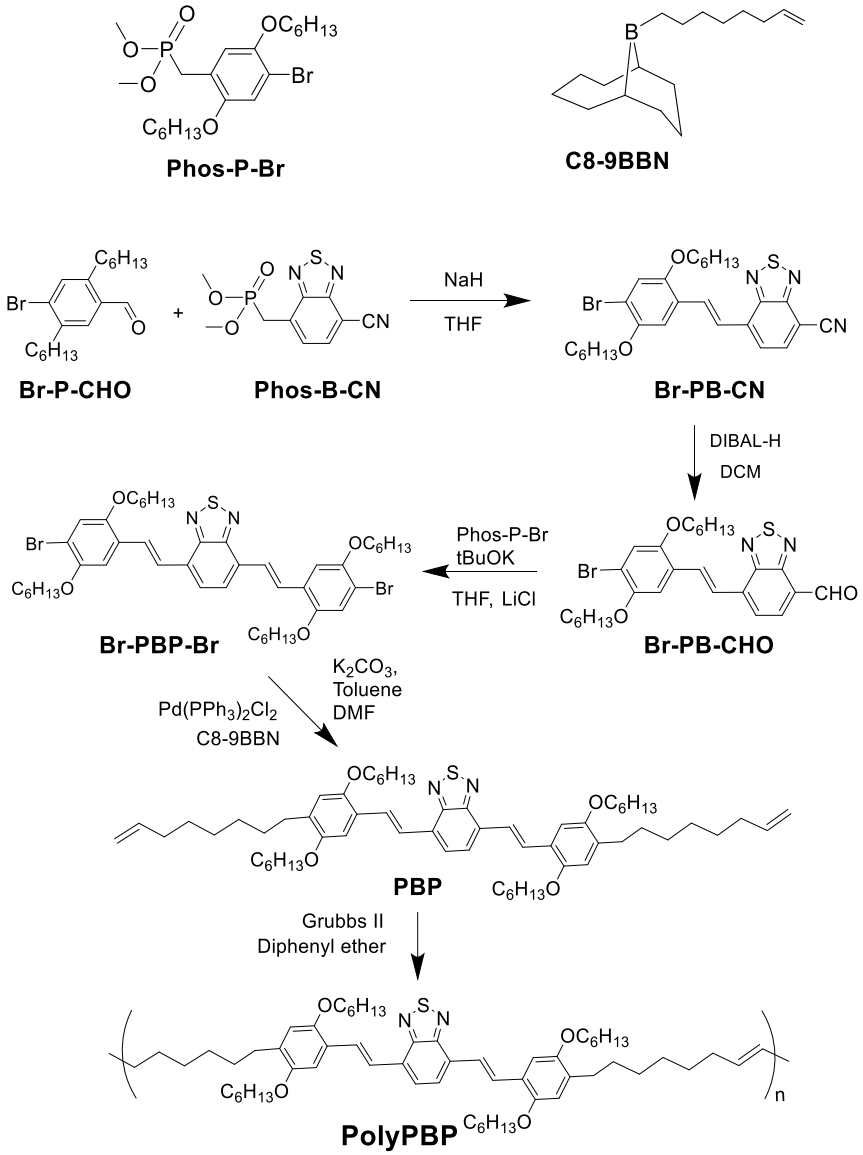

Figure 33. Synthesis of macromonomer **PBP** and **PolyPBP**.

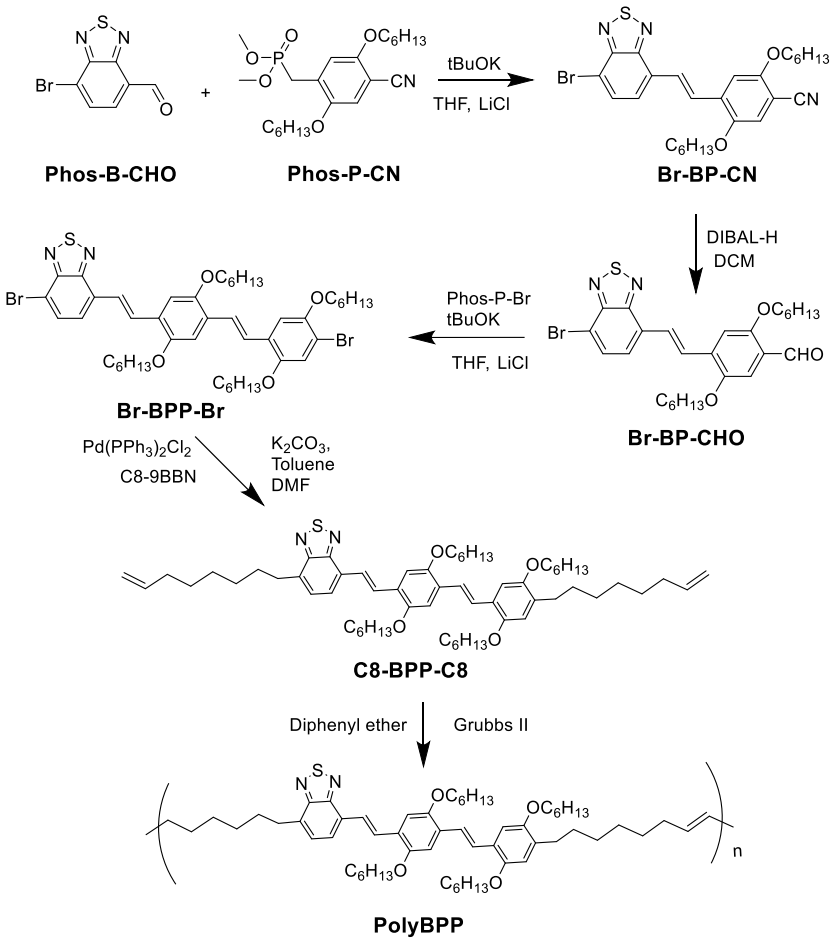

Figure 34. Synthesis of macromonomer **BPP** and Poly**BPP**.

4.3.2 Optical properties

Significant sequence-dependent optical properties of both of the macromonomers and their polymers were observed (**Table 13**, **Figure 35**). The absorption maxima of **PBP** and **BPP** are 489 and 448 nm, respectively, giving a sequence-based difference of 41 nm. Unsurprisingly, given the non-conducting nature of the spacer, the polymer λmax are nearly identical with those of their precursors. The sequence-based difference is immediately apparent in the colors of the polymers, with **PolyPBP** appearing orange in solution, while **PolyBPP** is yellow.

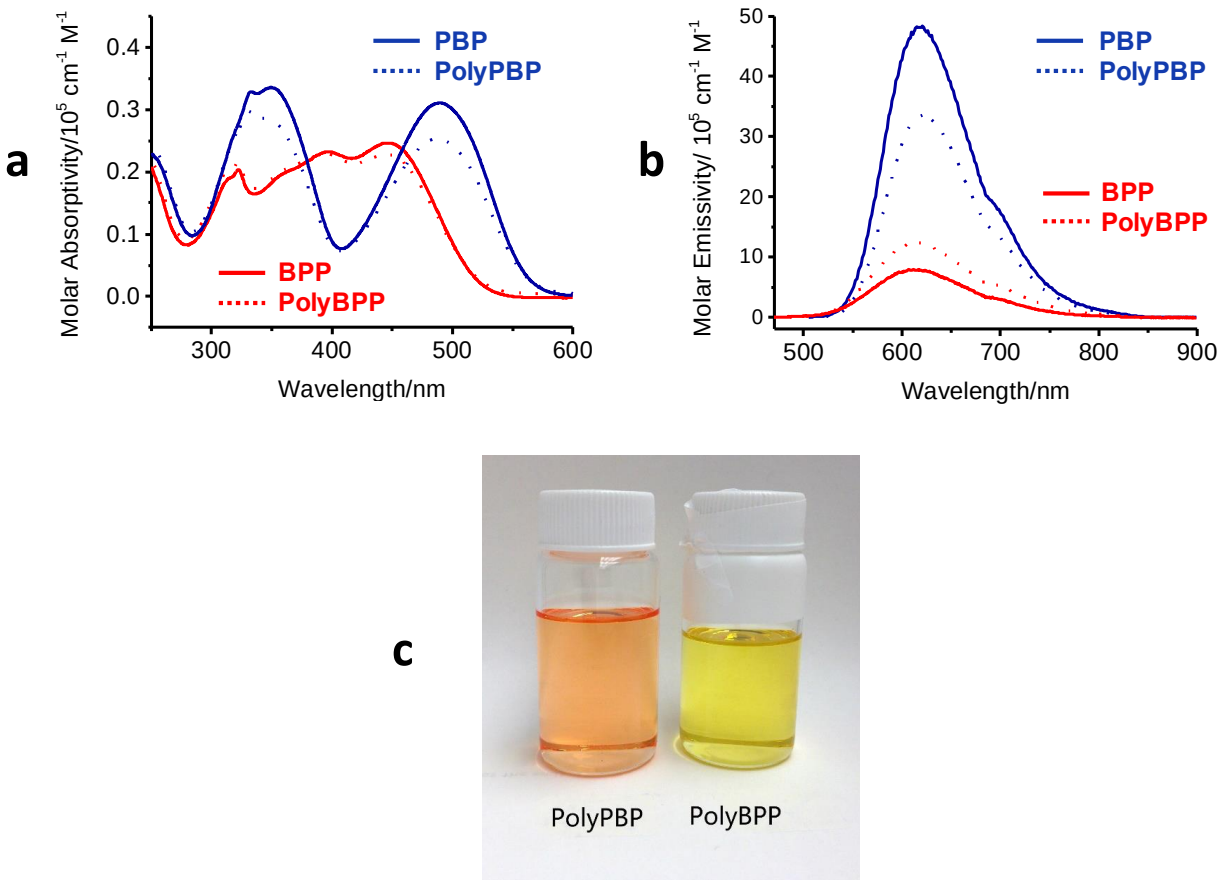

Figure 35. a) Absorption spectra of macromonomers and polymers in chloroform (1.0×10^{-5} M). b) Emission spectra of macromonomers and polymers in chloroform solution (1.0×10^{-5} M). c) **PolyPBP** and **PolyBPP** solution in chloroform (1.0×10^{-5} M). Concentrations of polymers are defined as molarity of trimeric units.

Sequence effects are also present in the solution fluorescence spectra. In this case, however, the differences are primarily in intensity of the emission. **PBP** shows an emission maximum of 618 nm which is nearly the same as that of **BPP** (615 nm). Moreover, the polymer emission spectra are only slightly different from those of their precursor monomers. The effect of sequence on emission intensity is dramatic, however. The molar emission intensity of **PBP** is approximately five times higher than that of **BPP**. The polymers follow the same trend although the ratio of intensities is only three times higher. Interestingly, in our previous studies on sequenced oligomers bearing only PPV-type units,[21] we did not observe differences of this magnitude, nor have we

found citations of similar sequence-driven differences in the literature. As emission intensity is related to the performance of organic materials in OLED-type devices, this sequence-based difference is notable.

The film emission spectra (**Figures 36**) exhibit intriguing differences in behavior both between sequences and as a function of polymerization. The 645 nm maximum of **PBP** is red-shifted significantly relative to the 618 nm maximum observed in solution. All of the other materials, including **PolyPBP** have film emissions that are blue-shifted relative to their solution-phase emission maxima.

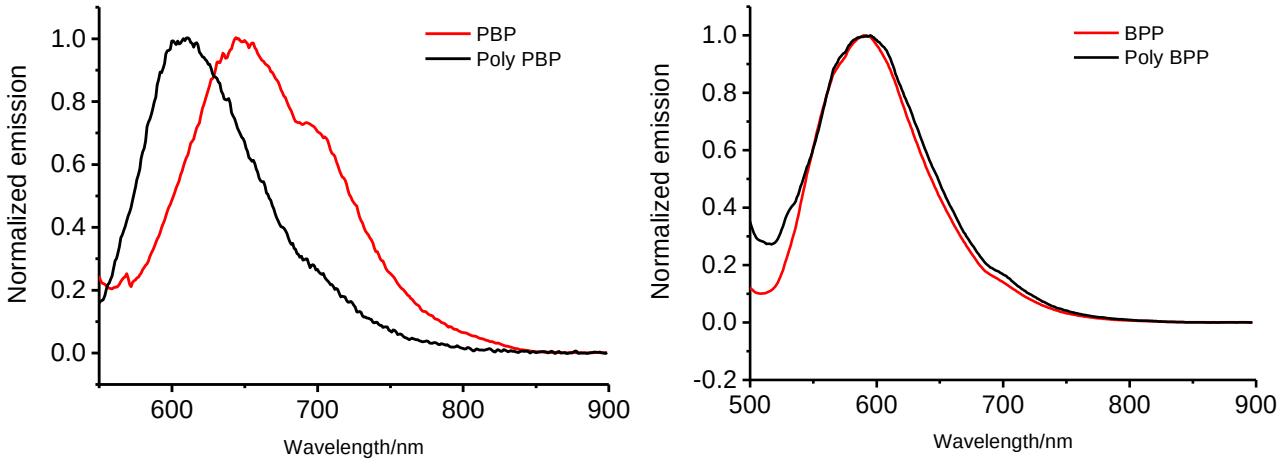

Figure 36. Film emission spectra for macromonomers and polymers. Samples were fabricated by drop casting from chloroform solution.

Table 13. Physical properties of monomers and polymers

Compounds	$\lambda_{max}^{abs\ a}$ **/ nm**	$\lambda_{max}^{em\ a}$ **/ nm**	$\lambda_{max}^{em\ film\ b}$ **/nm**	**Melting point /ºC**
PBP	489	618	645	56.2
BPP	448	613	591	73.7
PolyPBP	488	622	607	-
PolyBPP	448	613	591	-

[a] Measured in chloroform (1.0×10^{-5} M); [b] Films were fabricated by drop casting from chloroform solution on glass plate.

4.3.3 Electrochemical Properties

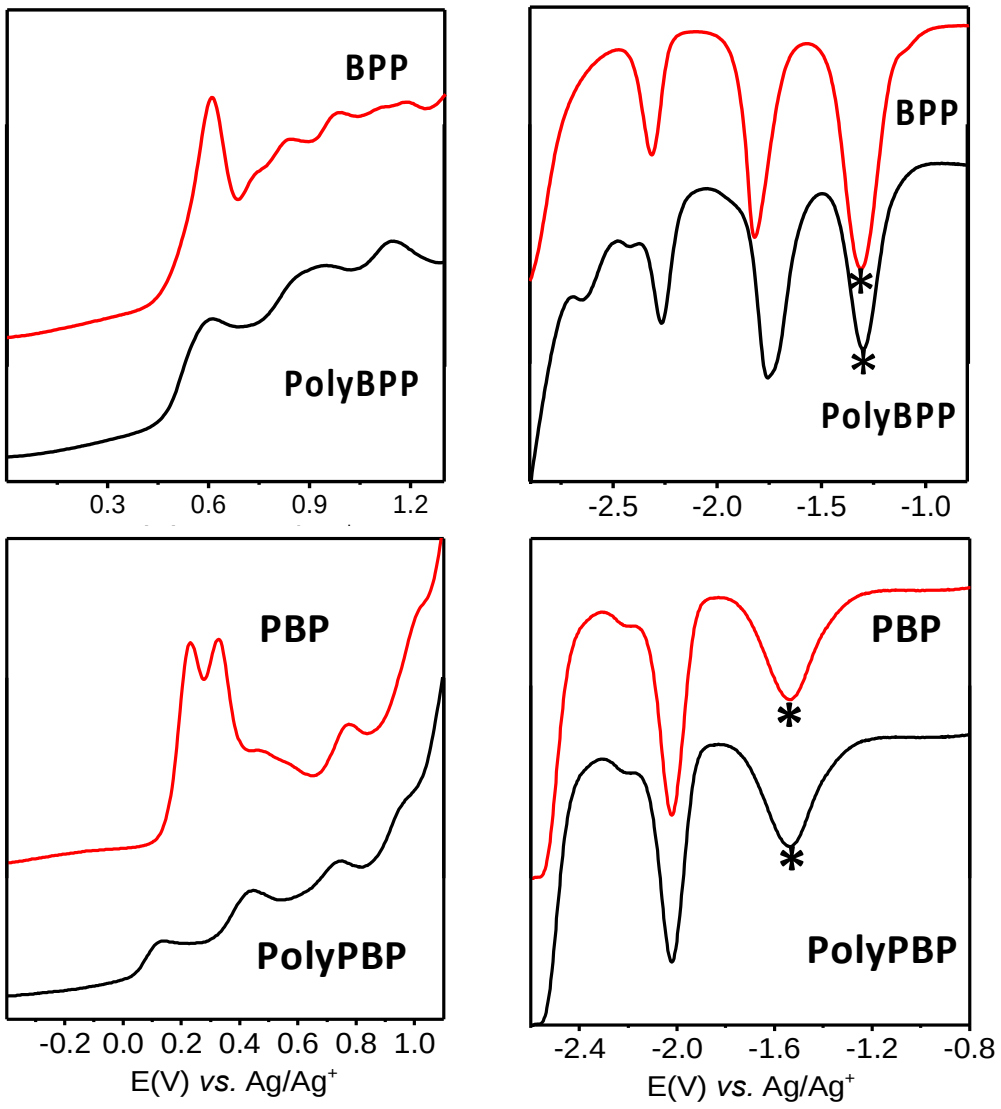

Figure 37. Differential pulse voltammetry measurements of macromonomer and polymer in THF solution. Left: Oxidation. Right: Reduction (* marks the O_2 background peak).

The electrochemical properties of these molecules were analyzed by cyclic voltammetry (CV) and differential pulse voltammetry (DPV) (**Table 14**, **Figure 37**). In the case of the macromonomers, the most significant difference is found in the first reduction peak which corresponds to some degree with the LUMO level. **PBP** has a first reduction value in THF of -

1.68 V vs. Ag/Ag^+ while the first reduction of **BPP** is found 0.15 V more negative at -1.83 V. The oxidation values are similar to each other at 0.66 and 0.61 V, respectively. The electrochemical band gaps for these two molecules, 2.34 and 2.44 V, differ by 0.1 V.

Table 14. Electrochemical properties of monomers and polymers

Compounds	$\mathbf{E_{peak}^{ox}}$ [a] **/ V**	$\mathbf{E_{peak}^{red}}$ [a] **/ V**	$\mathbf{\Delta E_{gap}^{ec}}$ [c] **/ eV**
PBP	0.66 (0.23[b])	-1.68 (-2.02[b])	2.34 (2.25[b])
BPP	0.61	-1.83	2.44
PolyPBP	1.00 (0.13[b])	-1.52 (-2.03[b])	2.52 (2.16[b])
PolyBPP	0.61	-1.76	2.37

[a] Potential vs. Ag/Ag^+, 240 µM in 0.1 M Bu_4NPF_6 in THF; [b] redox potentials measured in methylene chloride; [c] Determined as $\mathbf{\Delta}\boldsymbol{E}_{\mathbf{gap}}^{\mathbf{ec}} = \mathbf{e}(\boldsymbol{E}_{\mathbf{peak}}^{\mathbf{ox}} - \boldsymbol{E}_{\mathbf{peak}}^{\mathbf{red}})$.

The electrochemical behavior of the polymers is more complex due to aggregation effects. We initially expected the electrochemical behavior of the polymers to be quite similar to that observed for the macromonomers due to the isolation of the conjugated trimers by the non-conducting spacers. This assumption held true for the reduction DPVs, which are only slightly shifted from those of their macromonomers and exhibit a similar overall pattern (**Figure 37**). Likewise, in the oxidation portion of the DPV, the **BPP** macromonomer and the corresponding polymer are very similar. For **PolyPBP**, however, the oxidation DPV trace of the polymer was dramatically different from that of the macromonomer (Appendix C). The region in which the first oxidation peak would be expected was an ill-defined shoulder of the first clear peak at ca. 1 V vs. Ag/Ag^+. The electrochemistry for both **PBP**-derived materials was therefore repeated in methylene chloride, which we knew to be a better solvent for these molecules. Consistent with our theory of aggregation the two oxidation DPV traces became similar in methylene chloride and

exhibited identifiable first oxidation peaks in the same region (ca 0.1-0.2 V vs. Ag/Ag^{+}, **Figure 37**).

4.3.4 Thermal properties and morphology

Sequence effects were found in the thermal properties as well. The differential scanning calorimetry (DSC) trace of **PBP** exhibits an endothermal melting transition at 56.2 ^{o}C during the first heating cycle. No crystallization was noted during the cooling cycle nor a melting peak in the second heating cycle (10 deg/min). **BPP**, in contrast, exhibits both a melting transition at 73.7 ^{o}C and a crystallization at 35.5 ^{o}C during the cooling cycle. Neither polymer exhibited crystallinity even when subjected to annealing periods prior to measurement. We have observed previously that sequence copolymers are difficult to crystallize even when consisting of units that are known to crystallize at shorter chain lengths.[38]

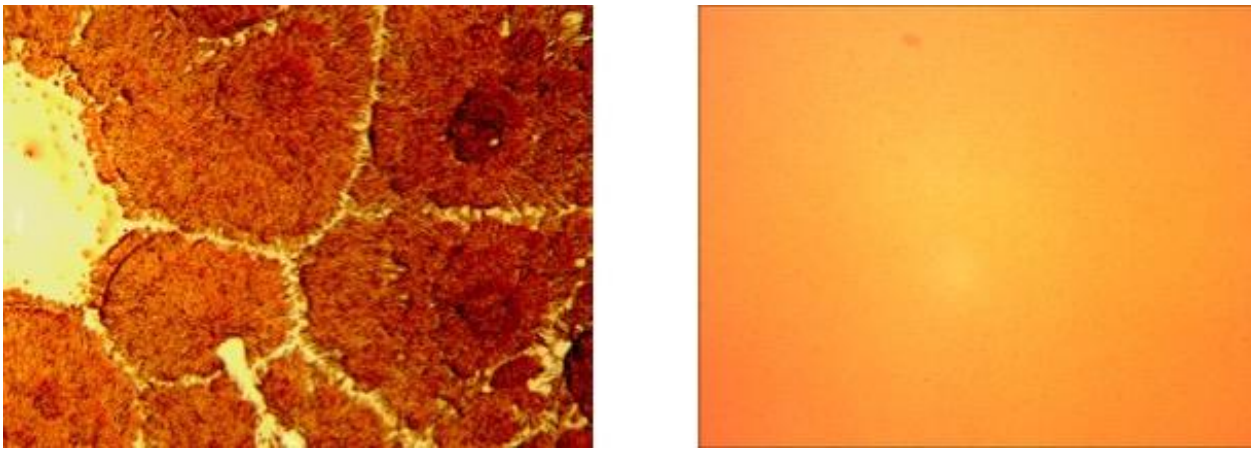

Figure 38. Microscopic image (×50) of **PBP** macromonomer (left) and **PBP** polymer (right).

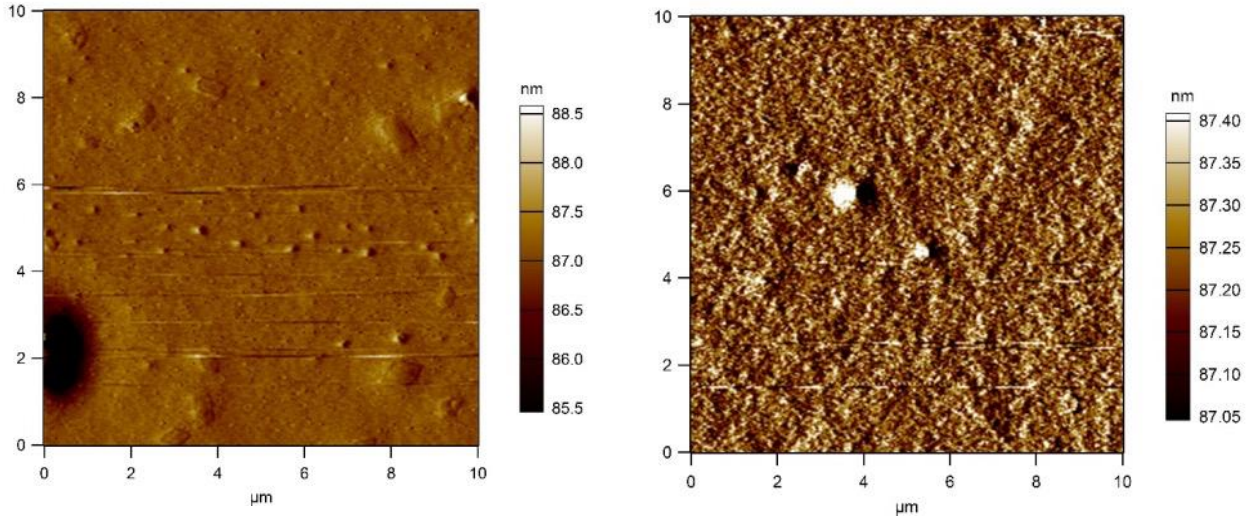

Figure 39. AFM amplitude scans for **PolyPBP** films (left) and **PolyBPP** films (right) fabricated by spin-coated from chloroform solution.

General differences in the films prepared from these four materials were also observed, although the differences were not sequence-based. Consistent with expectations, the macromonomers did not give good films by drop casting onto a glass substrate. The films were brittle and cracked when dry. The polymers, in contrast, produced homogeneous films that did not crack (**Figure 38**). AFM examination of the spin-coated polymer films, however, showed them to be featureless with no sequence-related differences or obvious signs of long-range order (**Figure 39**).

4.4 DISCUSSION

Overall we can see that the simplest of sequence differences, **PBP** vs. **BPP**, has intriguing effects both in the macromonomers and the polymers derived from them. Both the optical spectroscopy and the electrochemistry confirm that altering the sequence, which necessarily

includes changing which monomers bear the mildly donating alkyl substituents, affects the HOMO-LUMO gap, primarily due to the change in the reduction potential of the conjugated unit. These electronic properties are retained in the polymeric form. Also, interesting is the effect of sequence on the intensities of the emissions. Both **PBP**-derived materials exhibited substantially larger emission intensities. While the origin of these differences is not currently understood it seems likely that they are related to the symmetry of the oligomers (with the more symmetric trimer exhibiting stronger intensity, possibly due to the "double well" donor-acceptor-donor motif). Future studies should provide a more complete understanding.

The effect of sequence on morphology-controlling inter-/intramolecular interactions is complex. Although the more polar **BPP** macromonomer has a higher melting point and a greater tendency to crystallize, it is the **PBP** oligomer that exhibits the significant red-shift in the solid phase that is usually associated with the presence of π-stacking interactions. Likewise, it was the **PBP** based polymer that exhibited lower solubilities, consistent with facile aggregation. The fact that the **PBP** polymer did not achieve, using drop casting, the same red-shifted organization in the film state as that observed for the macromonomer may be due either to unoptimized film deposition or to an intrinsic inability of the polymer to attain the same level of organization. In any case, sequence plays a key role in determining the molecular packing that can be accessed and/or predominates.

4.5 CONCLUSIONS

In summary, we synthesized and investigated the influence of sequence on the properties of a set of oligomers and on polymers containing these oligomeric units. We found significant

differences in the optical and electrochemical properties of two trimeric macromonomers and discovered, moreover, that these differences were maintained in the polymers made from these macromonomers. The sequence effects on optical properties are among the largest reported. Differences in inter-/intrachain interactions, based on sequence, were also found in both the macromonomer trimers and in the polymers. These findings suggest that sequence could be exploited more generally in the preparation of materials for electronic applications. Future work will involve the investigation of how sequence affects device performance.

4.6 EXPERIMENTAL

4.6.1 General methods

Materials. Synthesis of **Br-PBP-Br** and **Br-PPB-Br** are described in the chapter 3. All reagents and solvents were purchased from Sigma Aldrich and used as received. Column chromatography was carried out on standard grade silica gel (60 Å pore size, 40-63 μm particle size), which was used as received.

NMR Spectroscopy. ^{1}H (300, 400, and 500 MHz) and ^{13}C (75, 100, and 125 MHz) NMR spectra were recorded on Bruker spectrometers. Chemical shifts were referenced to residual ^{1}H or ^{13}C signals in deuterated solvents (7.26 and 77.0 ppm, respectively, for $CDCl_3$).

Mass Spectrometry. High resolution mass spectra were recorded on EI-quadrupole or ESI-TOF instruments in the Mass Spectrometry Facility of the University of Pittsburgh.

Optical Spectroscopy. Solution ($CHCl_3$) UV/VIS absorption spectra were recorded on a Perkin Elmer Lambda 9 UV/VIS/NIR spectrometer. Emission spectra were recorded on a Varian Cary Eclipse Fluorimeter.

Electrochemistry. Cyclic voltammetry (CV) and differential pulse voltammetry (DPV) were performed on a CHI Electrochemical Workstation Model 430a (Austin, TX) using a three electrode system consisting of a glassy carbon disk (3 mm dia.) as working electrode, a non-aqueous Ag/Ag^+ reference electrode (1 mM $AgNO_3$ in acetonitrile), and a Pt-wire as auxiliary electrode in 0.1 M Bu_4NPF_6 in dry THF or CH_2Cl_2. CV spectra were recorded at 100 mV/s. DPV parameters were as follows: scan rate of 25 mV/s, pulse amplitude 0.05 V and pulse period 0.16 s.

Thermal Analysis. Differential scanning calorimetry (DSC) was performed on a Perkin Elmer Pyris 6 with a heating and cooling rate of 10 °C/min.

Size Exclusion Chromatography. Molecular weights and dispersities were obtained on a Waters gel permeation chromatography (THF) with Jordi 500, 1000, and 10000 Å divinyl benzene columns, and refractive index detector (Waters). The elution volumes were calibrated to polystyrene standards

Atomic force microscope. Surface topography was characterized with an Asylum Research MFP-3D atomic force microscope using tapping mode. No modifications were made to the existing instrument hood; all samples were recorded in ambient conditions. Electrilever AC240TM silicon tips with an aluminum coating (k=2 N/m and f= 70 KHz) purchased from Asylum Research were utilized. Sample data was analyzed using the Asylum Research software (version 100729B) built into IgorPro (version 6.22 A).

4.6.2 Synthesis

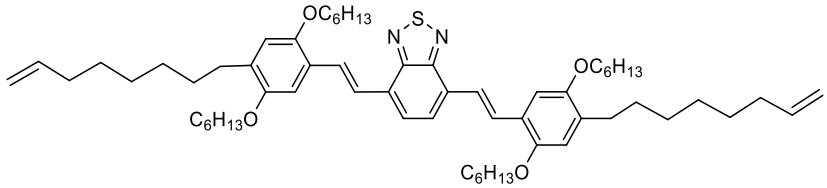

4,7-Bis((E)-2,5-bis(hexyloxy)-4-(oct-7-en-1-yl)styryl)benzo[c][1,2,5]thiadiazole (PBP)

The synthesis of **PBP** macromonomer prepared by a modification of a previously reported procedure for a similar substrate.[30] The borane reagent, 1-(hept-6-en-1-yl)-7-boratricyclo[4.1.1.03,7]octane (**C_8-9-BBN**), was synthesized according to literature[6] and stored in the glove box. In a Schlenk flask, **Br-PBP-Br** (0.212 g, 0.23 mmol), $Pd(PPh_3)_2Cl_2$ (0.0248 g, 15% mol) and K_2CO_3 (0.147 g, 1.06 mmol) were combined and transferred into the a N_2-filled glove box. Dry DMF (1.35 mL) and toluene (1.35 mL) were added and upon dissolution, **C_8-9-BBN** (0.232 g, 0.943 mmol) was added. The Schlenk flask was sealed removed from the glove box. The reaction mixture was heated to 60 ^oC overnight under N_2. After cooling to RT, the reaction was quenched by rapid addition to water. The organic phase was separated and aqueous phase was extracted with CH_2Cl_2 2x. The combined organic layers were washed with brine and dried over $MgSO_4$. Solvents were removed *in vacuo*. Column chromatography (silica gel, hexanes and methylene chloride) gave the product as an orange solid (0.16 g, 76%). ^{1}H NMR (400 MHz, Chloroform-*d*) δ 8.29 (d, *J* = 16.5 Hz, 2H), 7.71 (d, *J* = 15.6 Hz, 4H), 7.20 (s, 2H), 6.77 (s, 2H), 5.85 (ddt, *J* = 16.9, 10.2, 6.6 Hz, 2H), 5.18 – 4.80 (m, 4H), 4.04 (t, *J* = 6.4 Hz, 8H), 2.65 (dd, *J* = 8.9, 6.5 Hz, 4H), 2.08 (q, *J* = 6.8 Hz, 4H), 2.01 – 1.74 (m, 8H), 1.74 – 1.15 (m, 40H), 0.95 (m, 12H). ^{13}C NMR (126 MHz, $CDCl_3$) δ 154.11, 151.36, 151.11, 139.19, 133.30, 129.76, 127.93,

126.03, 124.71, 123.40, 115.36, 114.11, 109.41, 69.78, 68.77, 33.82, 31.74, 31.63, 30.62, 30.05, 29.62, 29.57, 29.46, 29.03, 28.92, 25.99, 25.94, 22.71, 22.67, 14.08, 14.05. HRMS calcd for $C_{62}H_{92}N_2O_4S$: 961.6856 g/mol. Found: 961.6872 g/mol.

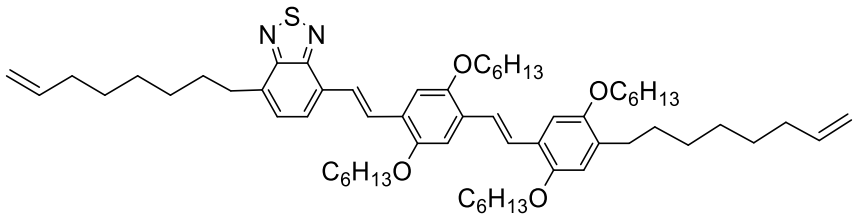

4-((E)-4-((E)-2,5-Bis(hexyloxy)-4-(oct-7-en-1-yl)styryl)-2,5-bis(hexyloxy)styryl)-7-(oct-7-en-1-yl)benzo[c][1,2,5]thiadiazole (BPP)

The synthesis of the **BPP** macromonomer was similar to that of **PBP**. The borane reagent, 1-(hept-6-en-1-yl)-7-boratricyclo[4.1.1.03,7]octane (**C_8-9-BBN**), was synthesized according to literature[6] and stored in the glove box. In a Schlenk flask, **Br-PBP-Br** (0.212 g, 0.230 mmol), $Pd(PPh_3)_2Cl_2$ (0.0248 g, 15% mol) and K_2CO_3 (0.147 g, 1.06 mmol) were combined and transferred into the a N_2-filled glove box. Dry DMF (1.35 mL) and toluene (1.35 mL) were added and upon dissolution, **C_8-9-BBN** (0.232 g, 0.943 mmol) was added. The Schlenk flask was sealed removed from the glove box. The reaction mixture was heated to 60 ^oC overnight under N_2. After cooling to RT, the reaction was quenched by rapid addition to water. The organic phase was separated and aqueous phase was extracted with CH_2Cl_2 2x. The combined organic layers were washed with brine and dried over $MgSO_4$. Solvents were removed *in vacuo*. Column chromatography (silica gel, hexanes and methylene chloride) gave the product as an orange solid (0.227 g, 75%). A small amount (< 5%) of isomerization of the terminal double bonds to an internal position was noted by NMR. ^{1}H NMR (400 MHz, Chloroform-*d*) δ 8.25 (d, *J* = 16.5 Hz, 1H), 7.79 – 7.57 (m, 2H), 7.53 – 7.38 (m, 2H), 7.36 (d, *J* = 7.2 Hz, 1H), 7.26 (s, 1H), 7.24 (s, 1H),

7.18 (s, 1H), 7.09 (s, 1H), 6.71 (s, 1H), 5.82 (m, 2H), 4.97 (dd, *J* = 24.9, 13.7 Hz, 4H), 4.20 – 3.82 (m, 8H), 3.13 (t, *J* = 7.7 Hz, 2H), 2.60 (t, *J* = 7.7 Hz, 2H), 2.15 – 1.05 (m, 52H), 0.99 – 0.75 (m, 12H). ^{13}C NMR (101 MHz, $CDCl_3$) δ 155.54, 153.69, 151.53, 151.28, 150.96, 150.55, 139.19, 139.10, 134.61, 134.60, 132.43, 132.41, 131.61, 131.44, 129.12, 128.41, 127.63, 127.33, 126.54, 126.13, 125.19, 124.72, 124.56, 124.11, 123.95, 122.33, 115.38, 114.18, 114.10, 110.83, 110.42, 109.22, 69.74, 69.66, 69.50, 68.59, 33.82, 33.76, 32.57, 32.50, 32.29, 31.74, 31.69, 31.67, 31.61, 30.53, 30.08, 29.67, 29.58, 29.55, 29.50, 29.45, 29.40, 29.05, 29.03, 28.95, 28.91, 28.85, 26.01, 25.96, 25.93, 22.71, 22.67, 22.65, 17.92, 14.09, 14.07, 14.04. HRMS calcd for $C_{62}H_{92}N_2O_4S$: 961.6856 g/mol. Found: 961.6899 g/mol.

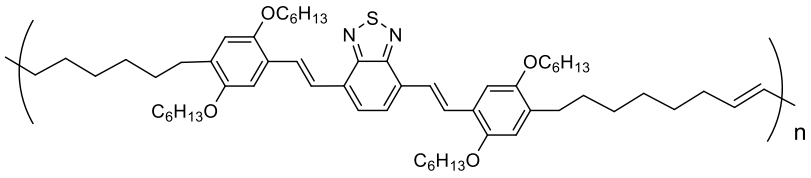

PolyPBP. PBP macromonomer (0.0670 g, 0.0697 mmol) and Grubbs II catalyst (3.5 mg) were combined and transferred into a N_2-filled glove box in a 20 mL vial. Diphenyl ether (90 mg) and toluene (0.25 mL) were added. The vial was sealed and removed from the glove box. After sonicating for 1 min, the reaction mixture was stirred under high vacuum for about 20 min, then heated to 70 ^{o}C for 21 hr. CH_2Cl_2 was added to dissolve the product, followed by ethyl vinyl ether to quench the reaction. The reaction mixture added to MeOH and the precipitate collected (60 mg). ^{1}H NMR (300 MHz, Chloroform-*d*) δ 8.26 (d, *J* = 16.4 Hz, 2H), 7.68 (d, *J* = 16.0 Hz, 4H), 7.18 (s, 2H), 6.74 (s, 2H), 5.40 (m, 2H), 4.15 – 3.79 (m, 8H), 2.62 (m, 4H), 2.12 – 1.03 (m, 48H), 0.93 (m, 12H). ^{13}C NMR (101 MHz, $CDCl_3$) δ 154.09, 151.32, 151.08, 133.34, 130.34, 129.73, 127.89, 126.04, 124.64, 123.36, 115.30, 109.33, 69.74, 68.74, 32.68, 31.75, 31.63, 30.66, 30.12, 29.70,

29.62, 29.56, 29.13, 26.00, 25.94, 22.72, 22.68, 14.11, 14.08. SEC (THF vs. PS standards) M_n: 19 KDa, M_w: 30 KDa, PDI: 1.6.

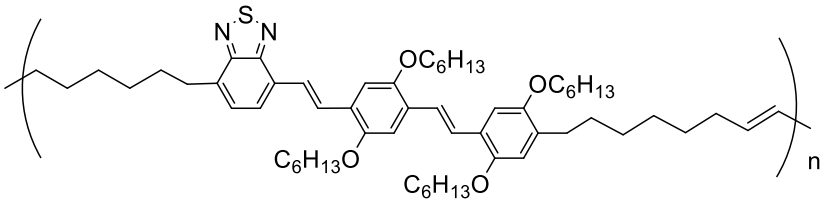

PolyBPP. BPP macromonomer (0.0800 g, 0.0832 mmol) and Grubbs II catalyst (3.5 mg) and transferred into a N_2-filled glove box in a 20 mL vial. Diphenyl ether (100 mg) and toluene (0.250 mL) were added. The vial was sealed and removed from the glove box. After sonicating for 1 min, the reaction mixture was stirred under high vacuum for about 20 min, then heated to 70 ^oC for 21 hr. CH_2Cl_2 was added to dissolve the product, followed by ethyl vinyl ether to quench the reaction. The reaction mixture added to MeOH and the precipitate collected (72 mg). ^1H NMR (400 MHz, Chloroform-*d*) δ 8.26 (m, 2H), 7.68- 6.71 (m, 9H), 5.40 (m, 2H), 4.08 – 3.98 (m, 8H), 3.12 (m, 2H), 2.60 (m, 2H) 1.99-1.27 (m, 48H), 0.91 (m, 12H). ^{13}C NMR (126 MHz, $CDCl_3$) δ 155.56, 153.71, 151.57, 151.32, 151.00, 150.60, 134.66, 130.34, 129.14, 128.45, 127.61, 127.37, 126.59, 126.15, 125.23, 124.15, 123.99, 122.36, 115.42, 110.91, 110.48, 109.28, 69.78, 69.70, 69.54, 68.64, 32.61, 32.32, 31.75, 31.69, 31.68, 31.62, 30.57, 30.15, 29.71, 29.59, 29.56, 29.16, 26.01, 25.97, 25.94, 25.86, 22.71, 22.67, 14.08, 14.07, 14.04. SEC (THF vs. PS standards) M_n: 24 KDa, M_w 39 KDa, PDI 1.7.

4.7 REFERENCE

1. Zhang, S.; Hutchison, G. R.; Meyer, T. Y., Sequence Effects in Conjugated Donor–Acceptor Trimers and Polymers. *Macromolecular Rapid Communications* **2016,** *37* (11), 882-887.

2. Facchetti, A., π-Conjugated Polymers for Organic Electronics and Photovoltaic Cell Applications. *Chemistry of Materials* **2011,** *23*, 733-758.

3. Mishra, A.; Bäuerle, P., Small Molecule Organic Semiconductors on the Move: Promises for Future Solar Energy Technology. *Angewandte Chemie International Edition* **2012,** *51* (9), 2020-2067.

4. Chen, Y.; Wan, X.; Long, G., High Performance Photovoltaic Applications Using Solution-Processed Small Molecules. *Accounts of Chemical Research* **2013,** *46* (11), 2645-2655.

5. Wang, C.; Dong, H.; Hu, W.; Liu, Y.; Zhu, D., Semiconducting π-Conjugated Systems in Field-Effect Transistors: A Material Odyssey of Organic Electronics. *Chemical Reviews* **2011**.

6. Rochat, S.; Swager, T. M., Conjugated Amplifying Polymers for Optical Sensing Applications. *ACS Applied Materials & Interfaces* **2013,** *5* (11), 4488-4502.

7. Duan, L.; Hou, L.; Lee, T.-W.; Qiao, J.; Zhang, D.; Dong, G.; Wang, L.; Qiu, Y., Solution processable small molecules for organic light-emitting diodes. *Journal of Materials Chemistry* **2010,** *20* (31), 6392-6407.

8. Zhang, H.; Tong, X.; Zhao, Y., Diverse Thermoresponsive Behaviors of Uncharged UCST Block Copolymer Micelles in Physiological Medium. *Langmuir* **2014,** *30* (38), 11433-11441.

9. Ellinger, S.; Graham, K. R.; Shi, P.; Farley, R. T.; Steckler, T. T.; Brookins, R. N.; Taranekar, P.; Mei, J.; Padilha, L. A.; Ensley, T. R.; Hu, H.; Webster, S.; Hagan, D. J.; Van Stryland, E. W.; Schanze, K. S.; Reynolds, J. R., Donor–Acceptor–Donor-based π-Conjugated Oligomers for Nonlinear Optics and Near-IR Emission. *Chemistry of Materials* **2011,** *23* (17), 3805-3817.

10. Henson, Z. B.; Mullen, K.; Bazan, G. C., Design strategies for organic semiconductors beyond the molecular formula. *Nature Chemistry* **2012,** *4* (9), 699-704.

11. Grimsdale, A. C.; Chan, K. L.; Martin, R. E.; Jokisz, P. G.; Holmes, A. B., Synthesis of Light-Emitting Conjugated Polymers for Applications in Electroluminescent Devices. *Chemical Reviews* **2009,** *109* (3), 897-1091.

12. Yassar, A.; Miozzo, L.; Gironda, R.; Horowitz, G., Rod–coil and all-conjugated block copolymers for photovoltaic applications. *Progress in Polymer Science* **2013,** *38* (5), 791-844.

13. Roncali, J.; Leriche, P.; Blanchard, P., Molecular Materials for Organic Photovoltaics: Small is Beautiful. *Advanced Materials* **2014,** *26* (23), 3821-3838.

14. Liang, Y.; Yu, L., A New Class of Semiconducting Polymers for Bulk Heterojunction Solar Cells with Exceptionally High Performance. *Accounts of Chemical Research* **2010,** *43* (9), 1227-1236.

15. Mei, J.; Bao, Z., Side Chain Engineering in Solution-Processable Conjugated Polymers. *Chemistry of Materials* **2013,** *26* (1), 604-615.

16. Szarko, J. M.; Guo, J.; Rolczynski, B. S.; Chen, L. X., Current trends in the optimization of low band gap polymers in bulk heterojunction photovoltaic devices. *Journal of Materials Chemistry* **2011**.

17. Zhao, X.; Zhan, X., Electron transporting semiconducting polymers in organic electronics. *Chemical Society Reviews* **2011,** *40* (7), 3728-3743.

18. Risko, C.; McGehee, M. D.; Bredas, J.-L., A quantum-chemical perspective into low optical-gap polymers for highly-efficient organic solar cells. *Chemical Science* **2011,** *2* (7), 1200-1218.

19. Beaujuge, P. M.; Amb, C. M.; Reynolds, J. R., Spectral Engineering in π-Conjugated Polymers with Intramolecular Donor−Acceptor Interactions. *Accounts of Chemical Research* **2010,** *43* (11), 1396-1407.

20. O'Boyle, N. M.; Campbell, C. M.; Hutchison, G. R., Computational Design and Selection of Optimal Organic Photovoltaic Materials. *The Journal of Physical Chemistry C* **2011,** *115* (32), 16200-16210.

21. Norris, B. N.; Zhang, S.; Campbell, C. M.; Auletta, J. T.; Calvo-Marzal, P.; Hutchison, G. R.; Meyer, T. Y., Sequence Matters: Modulating Electronic and Optical Properties of Conjugated Oligomers via Tailored Sequence. *Macromolecules* **2013,** *46* (4), 1384-1392.

22. Ilana, Y. K.; Jonathon, S. B.; Geoffrey, R. H., Sequence Matters: Determining the Sequence Effect of Electronic Structure Properties in π-Conjugated Polymers. In *Sequence-Controlled Polymers: Synthesis, Self-Assembly, and Properties*, American Chemical Society: 2014; Vol. 1170, pp 379-393.

23. Lutz, J.-F.; Ouchi, M.; Liu, D. R.; Sawamoto, M., Sequence-Controlled Polymers. *Science* **2013,** *341* (6146).

24. Li, J.; Stayshich, R. M.; Meyer, T. Y., Exploiting Sequence To Control the Hydrolysis Behavior of Biodegradable PLGA Copolymers. *Journal of the American Chemical Society* **2011,** *133* (18), 6910-6913.

25. Li, J.; Rothstein, S. N.; Little, S. R.; Edenborn, H. M.; Meyer, T. Y., The Effect of Monomer Order on the Hydrolysis of Biodegradable Poly(lactic-co-glycolic acid) Repeating Sequence Copolymers. *Journal of the American Chemical Society* **2012,** *134* (39), 16352-16359.

26. Rosales, A. M.; Segalman, R. A.; Zuckermann, R. N., Polypeptoids: a model system to study the effect of monomer sequence on polymer properties and self-assembly. *Soft Matter* **2013,** *9* (35), 8400-8414.

27. Ward, R. E.; Meyer, T. Y., o,p-Polyaniline: A New Form of a Classic Conducting Polymer. *Macromolecules* **2003,** *36* (12), 4368-4373.

28. Soejima, T.; Satoh, K.; Kamigaito, M., Main-Chain and Side-Chain Sequence-Regulated Vinyl Copolymers by Iterative Atom Transfer Radical Additions and 1:1 or 2:1 Alternating Radical Copolymerization. *Journal of the American Chemical Society* **2016,** *138* (3), 944-954.

29. Leibfarth, F. A.; Johnson, J. A.; Jamison, T. F., Scalable synthesis of sequence-defined, unimolecular macromolecules by Flow-IEG. *Proceedings of the National Academy of Sciences of the United States of America* **2015,** *112* (34), 10617-10622.

30. Copenhafer, J. E.; Walters, R. W.; Meyer, T. Y., Synthesis and Characterization of Repeating Sequence Copolymers of Fluorene and Methylene Monomers. *Macromolecules* **2008,** *41* (1), 31-35.

31. Palermo, E. F.; McNeil, A. J., Impact of Copolymer Sequence on Solid-State Properties for Random, Gradient and Block Copolymers containing Thiophene and Selenophene. *Macromolecules* **2012,** *45* (15), 5948-5955.

32. Fitzner, R.; Mena-Osteritz, E.; Mishra, A.; Schulz, G.; Reinold, E.; Weil, M.; Körner, C.; Ziehlke, H.; Elschner, C.; Leo, K.; Riede, M.; Pfeiffer, M.; Uhrich, C.; Bäuerle, P., Correlation of π-Conjugated Oligomer Structure with Film Morphology and Organic Solar Cell Performance. *Journal of the American Chemical Society* **2012,** *134* (27), 11064-11067.

33. Doval, D. A.; Molin, M. D.; Ward, S.; Fin, A.; Sakai, N.; Matile, S., Planarizable push-pull oligothiophenes: in search of the perfect twist. *Chemical Science* **2014,** *5* (7), 2819-2825.

34. Liang, L.; Wang, J.-T.; Xiang, X.; Ling, J.; Zhao, F.-G.; Li, W.-S., Influence of moiety sequence on the performance of small molecular photovoltaic materials. *Journal of Materials Chemistry A* **2014,** *2* (37), 15396-15405.

35. Zhao, Y.; Zhao, X.; Zang, Y.; Di, C.-a.; Diao, Y.; Mei, J., Conjugation-Break Spacers in Semiconducting Polymers: Impact on Polymer Processability and Charge Transport Properties. *Macromolecules* **2015,** *48* (7), 2048-2053.

36. Gasperini, A.; Bivaud, S.; Sivula, K., Controlling conjugated polymer morphology and charge carrier transport with a flexible-linker approach. *Chemical Science* **2014,** *5* (12), 4922-4927.

37. Speros, J. C.; Paulsen, B. D.; Slowinski, B. S.; Frisbie, C. D.; Hillmyer, M. A., Band Gap and HOMO Level Control in Poly(thienylene vinylene)s Prepared by ADMET Polymerization. *ACS Macro Letters* **2012,** *1* (8), 986-990.

38. Stayshich, R. M.; Meyer, T. Y., New Insights into Poly(lactic-co-glycolic acid) Microstructure: Using Repeating Sequence Copolymers To Decipher Complex NMR and Thermal Behavior. *Journal of the American Chemical Society* **2010,** *132* (31), 10920-10934.

5.0 CONCLUSIONS

In summary, monomer sequence effects have been investigated in two different donor-acceptor systems: phenylene vinylene and benzothiadiazole vinylene/phenylene vinylene. Optimized step-growth synthesis strategies using the Horner-Wadsworth-Emmons reaction for chain-growth were developed to precisely control the monomer sequence in oligomers. Selected sequenced oligomers were also incorporated into sequenced polymers using acyclic diene metathesis polymerization. In these polymers, the film making properties were enhanced without any loss of the electronic properties.

In all of the systems studied, key optical and electronic properties including light absorption, light emission, HOMO/LUMO energy levels, bandgaps, solubility, melting point, packing, hole mobility, and solar cell performance, were found to be strongly sequence dependent. Other important characteristics, like domain size in BHJ blends and thermal stability, although not directly studied, most probably are affected by sequence as well. These results demonstrate that monomer sequence is a powerful and versatile tool to tune conjugated molecule properties.

Our understanding of the sequence-property correlations and ability to predict the optoelectronic properties of sequenced oligomers prior to synthesis was enhanced by parallel calculations conducted by Hutchison and coworkers. For both systems, computationally predicted electronic properties were in good agreement with experimental results. For real-world applications, however, it is necessary to control more than just the fundamental optoelectronic properties. Future work must also focus on developing both an experimental and computational understanding of how sequence affects device-relevant solid state properties like intermolecular interactions, molecular packing, film morphology, and interfacial organization.

Although the systems studied in this dissertation displayed only modest device performances, they provide a strong proof-of-concept that sequence could be a powerful tool in materials engineering, especially when combined with other conventional strategies like creating novel monomers, sidechain engineering and the introduction of heteroatoms. For example, the vinylene linker in the studied oligomers could be changed to a rigid, conjugated unit like thiophene (Figure X). The coplanarity, packing, charge transport and device performance of the new sequenced molecules would be expected to improve the overall performance while still allowing for sequence-based property tuning.

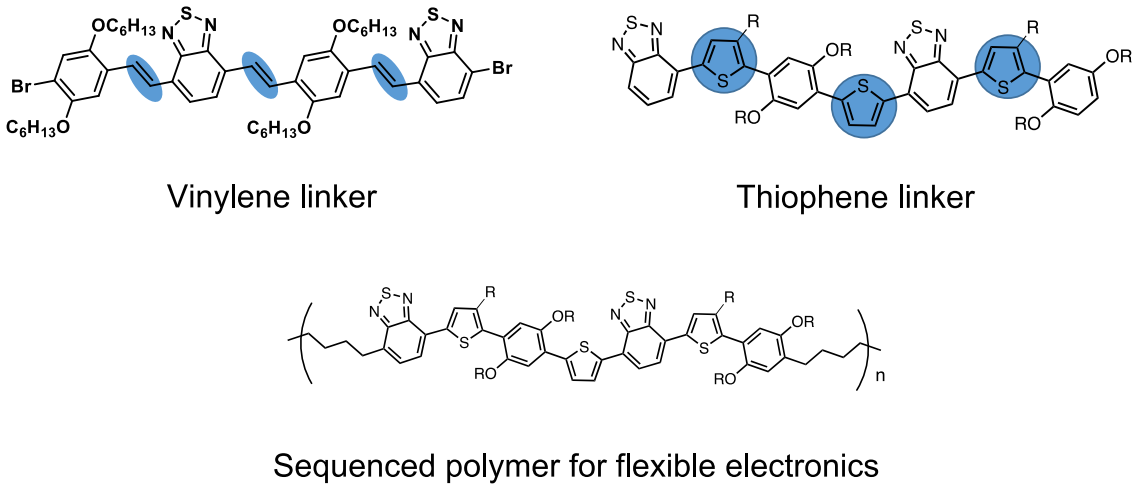

Figure 40. Proposed molecules for future work.

APPENDIX A

CHAPTER 2 SEQUENCE EFFECTS ON ELECTRONIC AND OPTICAL PROPERTIES OF CONJUGATED OLIGMERS COMPRISING PHENYLENE VINYLENES

A.1 NMR SPECTROSCOPY

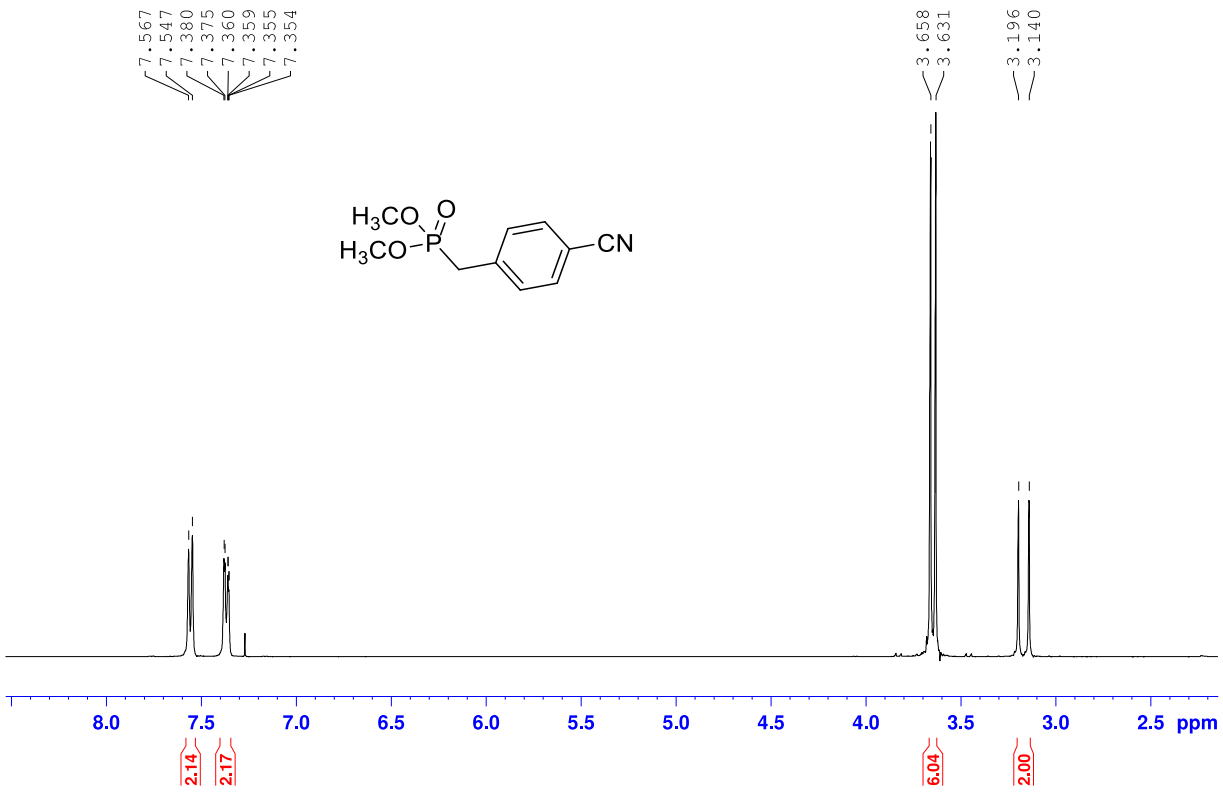

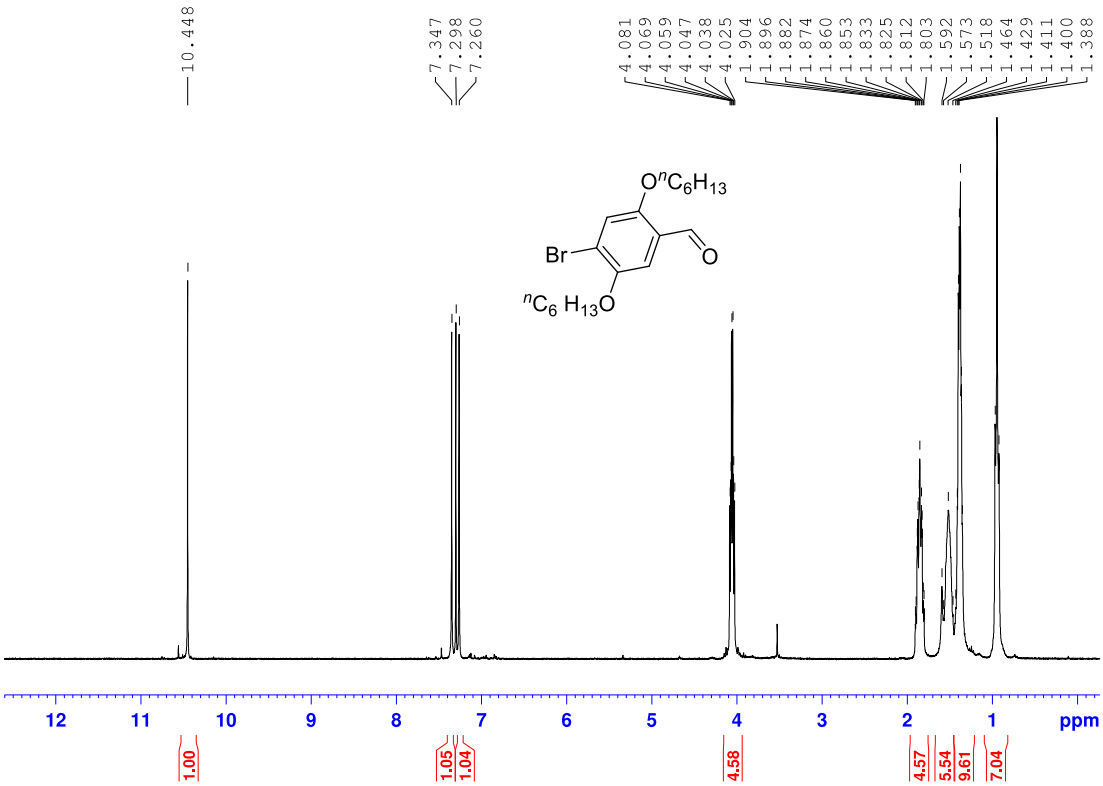
10.448
7.347
7.298
7.260
4.081
4.069
4.059
4.047
4.038
4.025
1.904
1.896
1.882
1.874
1.860
1.853
1.833
1.825
1.812
1.803
1.592
1.573
1.518
1.464
1.429
1.411
1.400
1.388
O^{n}C$_6$H$_{13}$
Br
O
^{n}C$_6$ H$_{13}$O
12
11
10
9
8
7
6
5
4
3
2
1
ppm
1.00
1.05
1.04
4.58
4.57
5.54
9.61
7.04

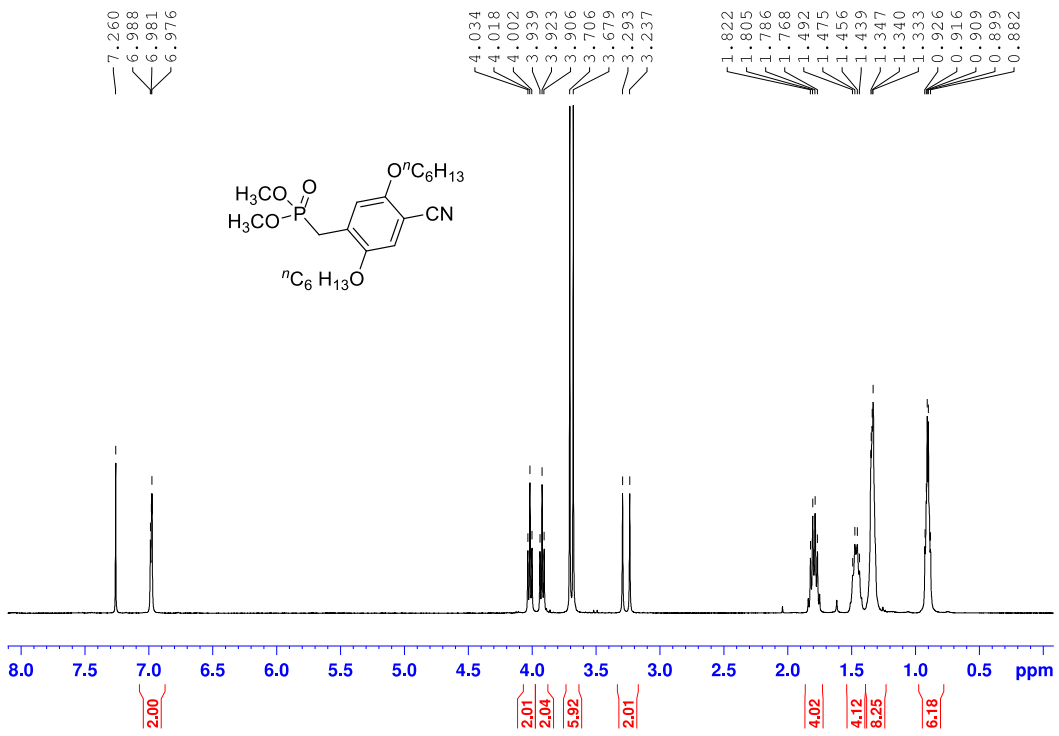
7.260
6.988
6.981
6.976
4.034
4.018
4.002
3.939
3.923
3.906
3.706
3.679
3.293
3.237
1.822
1.805
1.786
1.768
1.492
1.475
1.456
1.439
1.347
1.340
1.333
0.926
0.916
0.909
0.899
0.882
H$_3$CO
H$_3$CO
O
O^{n}C$_6$H$_{13}$
CN
^{n}C$_6$ H$_{13}$O
8.0
7.5
7.0
6.5
6.0
5.5
5.0
4.5
4.0
3.5
3.0
2.5
2.0
1.5
1.0
0.5
ppm
2.00
2.01
2.04
5.92
2.01
4.02
4.12
8.25
6.18

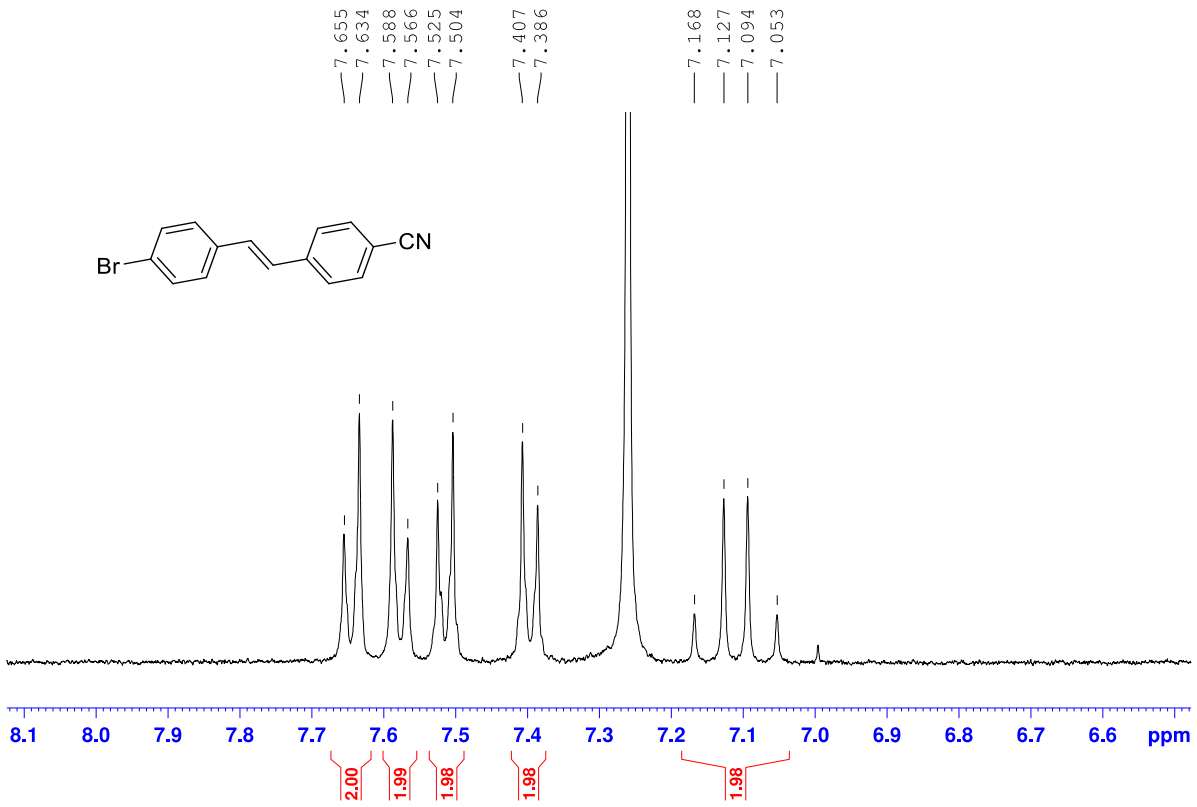
7.655
7.634
7.588
7.566
7.525
7.504
7.407
7.386
7.168
7.127
7.094
7.053
Br
CN
8.1
8.0
7.9
7.8
7.7
7.6
7.5
7.4
7.3
7.2
7.1
7.0
6.9
6.8
6.7
6.6
ppm
2.00
1.99
1.98
1.98
1.98

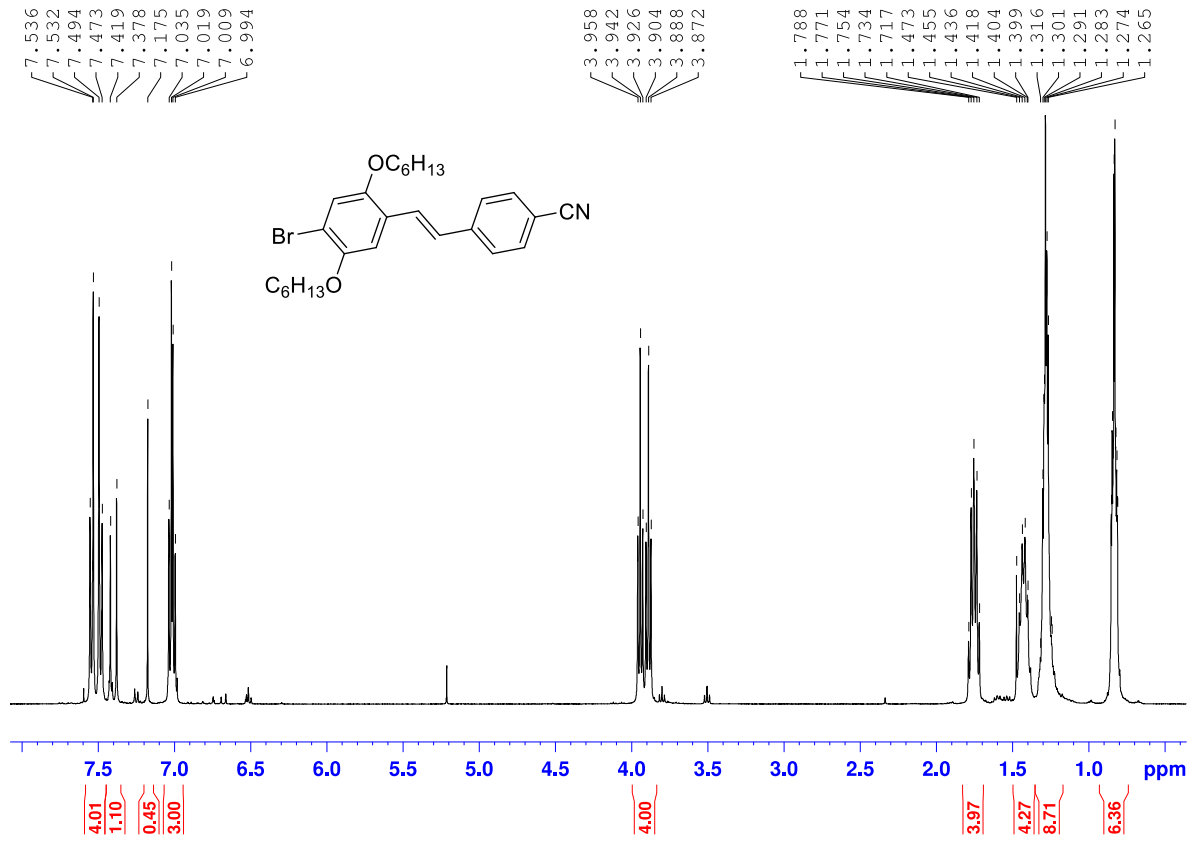
7.536
7.532
7.494
7.473
7.419
7.378
7.175
7.035
7.019
7.009
6.994
3.958
3.942
3.926
3.904
3.888
3.872
1.788
1.771
1.754
1.734
1.717
1.473
1.455
1.436
1.418
1.404
1.399
1.316
1.301
1.291
1.283
1.274
1.265
OC6H13
Br
C6H13O
CN
7.5
7.0
6.5
6.0
5.5
5.0
4.5
4.0
3.5
3.0
2.5
2.0
1.5
1.0
ppm
4.01
1.10
0.45
3.00
4.00
3.97
4.27
8.71
6.36

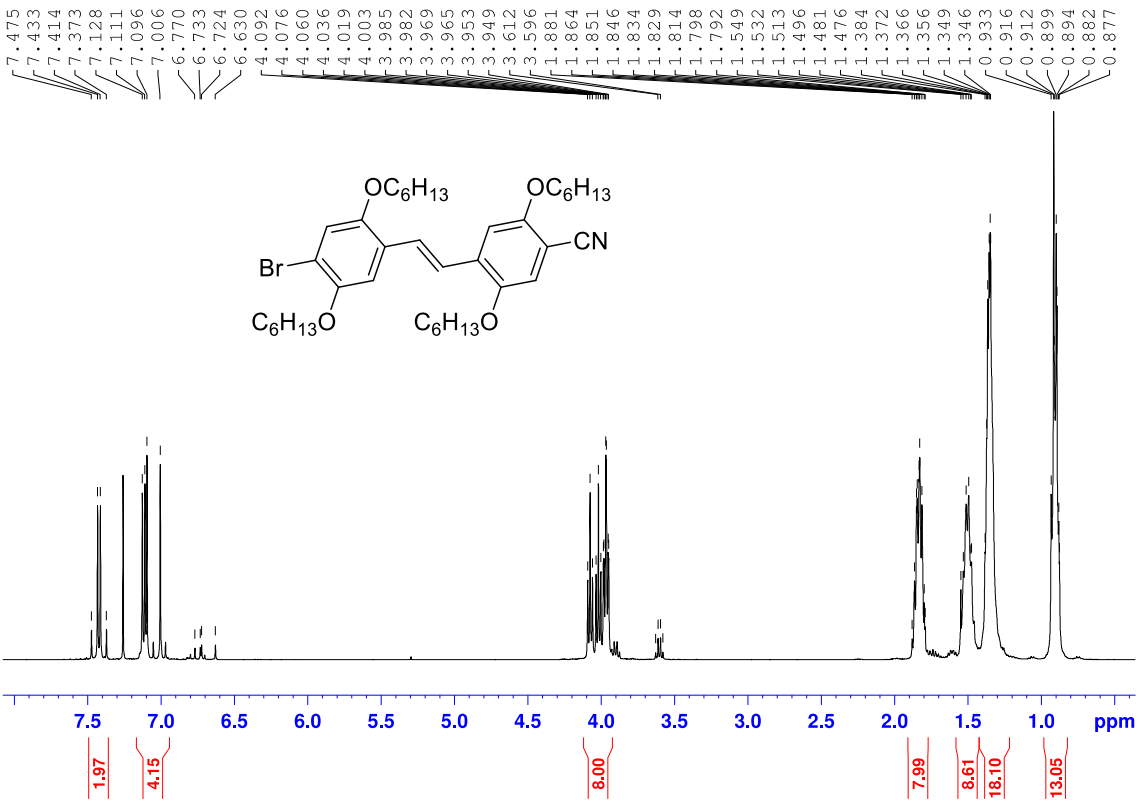
7.475
7.433
7.414
7.373
7.128
7.111
7.096
7.006
6.770
6.733
6.724
6.630
4.092
4.076
4.060
4.036
4.019
4.003
3.985
3.982
3.969
3.965
3.953
3.949
3.612
3.596
1.881
1.864
1.851
1.846
1.834
1.829
1.814
1.798
1.792
1.549
1.532
1.513
1.496
1.481
1.476
1.384
1.372
1.366
1.356
1.349
1.346
0.933
0.916
0.912
0.899
0.894
0.882
0.877
OC6H13
OC6H13
CN
Br
C6H13O
C6H13O
7.5
7.0
6.5
6.0
5.5
5.0
4.5
4.0
3.5
3.0
2.5
2.0
1.5
1.0
ppm
1.97
4.15
8.00
7.99
8.61
18.10
13.05

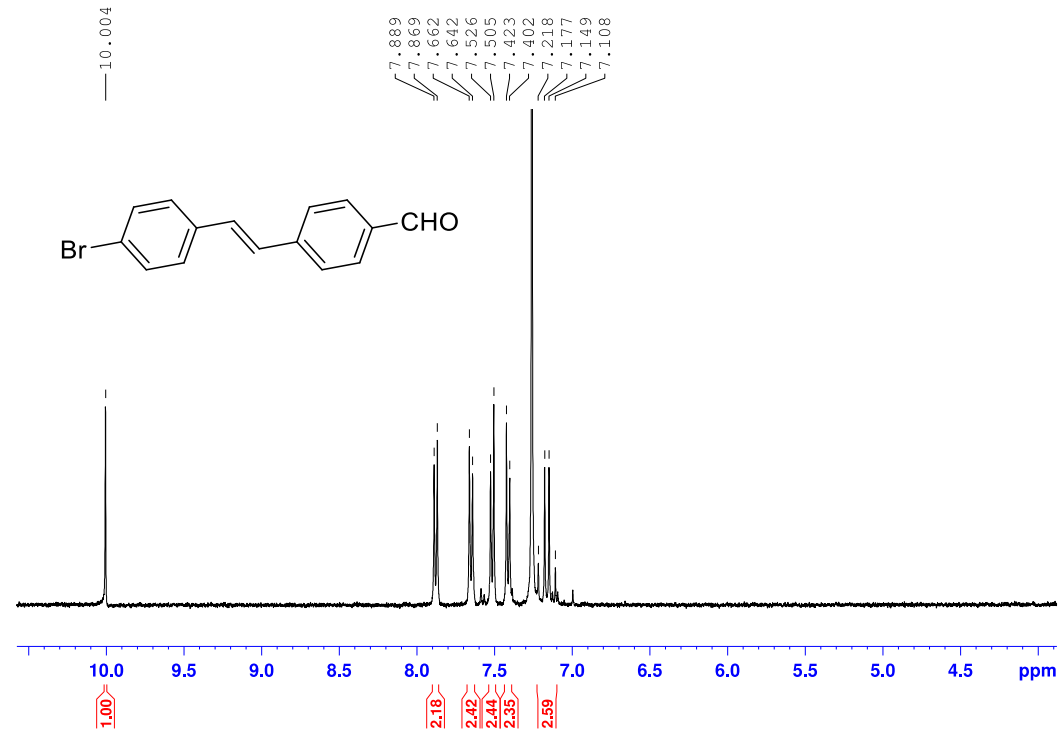
10.004
7.889
7.869
7.662
7.642
7.526
7.505
7.423
7.402
7.218
7.177
7.149
7.108
Br
CHO
10.0
9.5
9.0
8.5
8.0
7.5
7.0
6.5
6.0
5.5
5.0
4.5
ppm
1.00
2.18
2.42
2.44
2.35
2.59

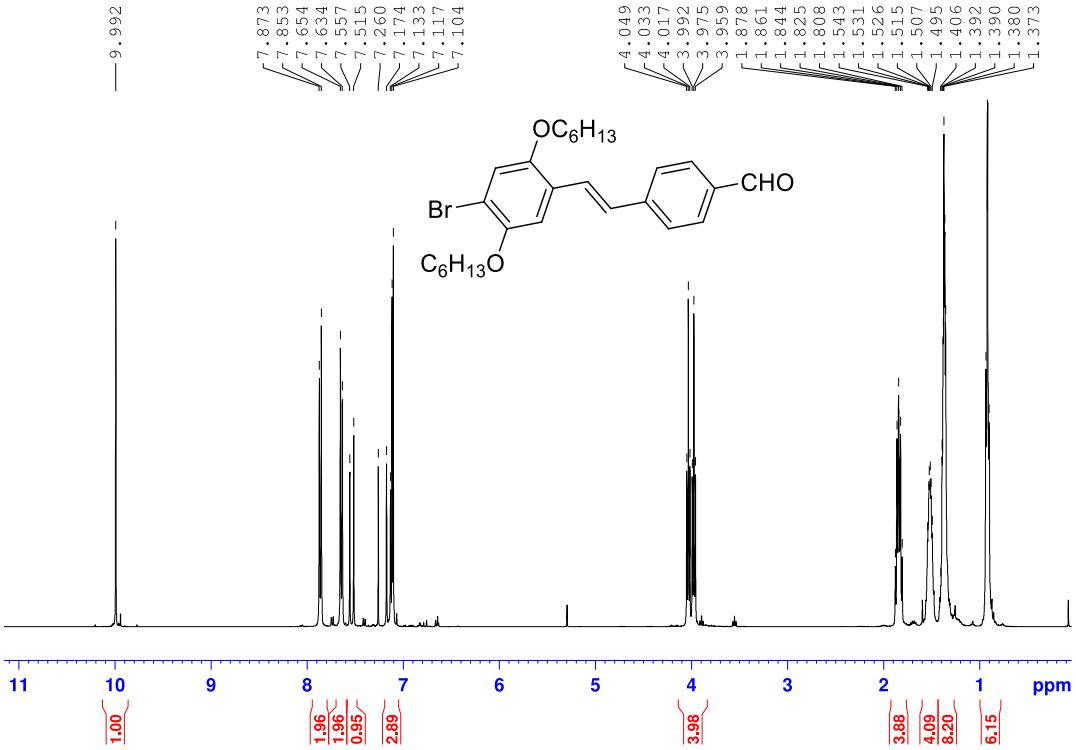
9.992
7.873
7.853
7.654
7.634
7.557
7.515
7.260
7.174
7.133
7.117
7.104
4.049
4.033
4.017
3.992
3.975
3.959
1.878
1.861
1.844
1.825
1.808
1.543
1.531
1.526
1.515
1.507
1.495
1.406
1.392
1.390
1.380
1.373
OC6H13
CHO
Br
C6H13O
11
10
9
8
7
6
5
4
3
2
1
ppm
1.00
1.96
1.96
0.95
2.89
3.98
3.88
4.09
8.20
6.15

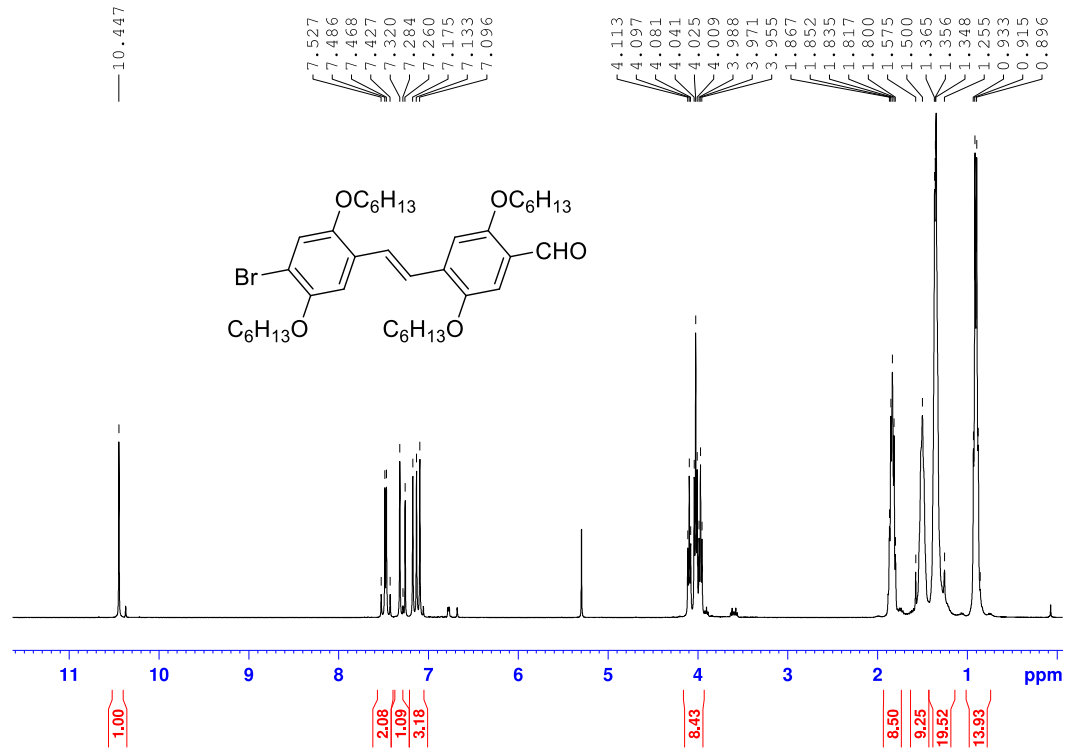
10.447
7.527
7.486
7.468
7.427
7.320
7.284
7.260
7.175
7.133
7.096
4.113
4.097
4.081
4.041
4.025
4.009
3.988
3.971
3.955
1.867
1.852
1.835
1.817
1.800
1.575
1.500
1.365
1.356
1.348
1.255
0.933
0.915
0.896
OC6H13
OC6H13
CHO
Br
C6H13O
C6H13O
11
10
9
8
7
6
5
4
3
2
1
ppm
1.00
2.08
1.09
3.18
8.43
8.50
9.25
19.52
13.93

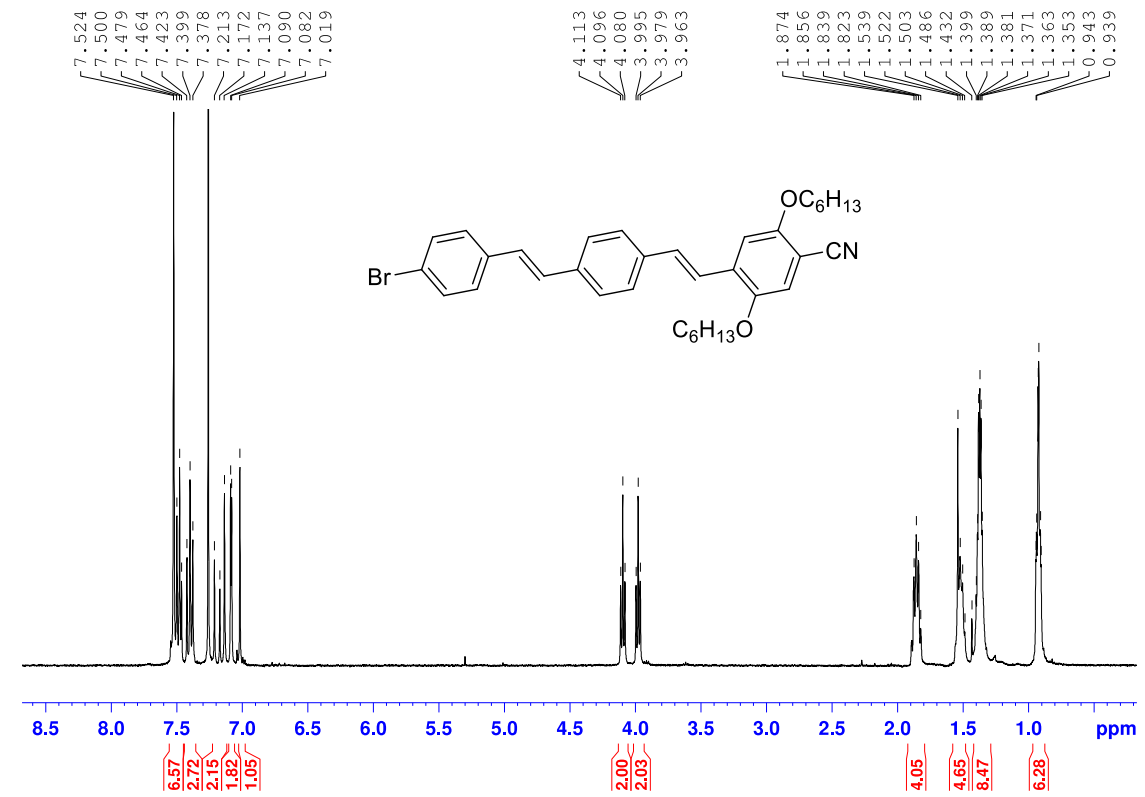
7.524
7.500
7.479
7.464
7.423
7.399
7.378
7.213
7.172
7.137
7.090
7.082
7.019
4.113
4.096
4.080
3.995
3.979
3.963
1.874
1.856
1.839
1.823
1.539
1.522
1.503
1.486
1.432
1.399
1.389
1.381
1.371
1.363
1.353
0.943
0.939
OC6H13
CN
Br
C6H13O
8.5 8.0 7.5 7.0 6.5 6.0 5.5 5.0 4.5 4.0 3.5 3.0 2.5 2.0 1.5 1.0 ppm
6.57
2.72
2.15
1.82
1.05
2.00
2.03
4.05
4.65
8.47
6.28

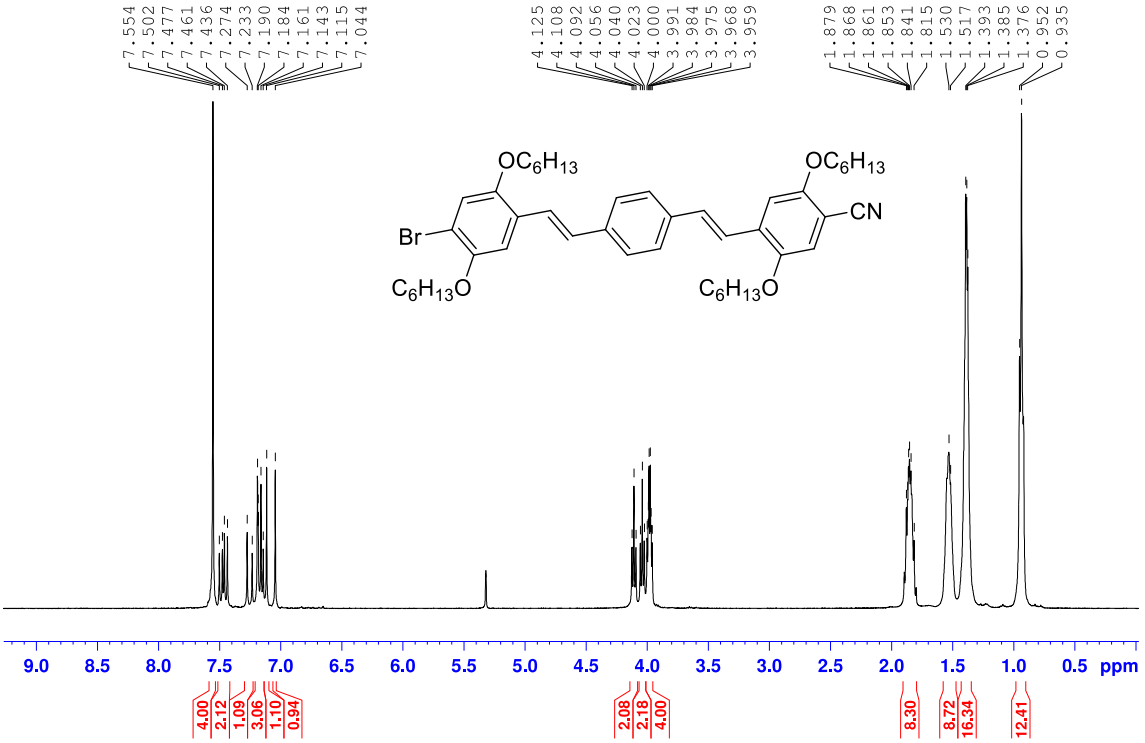
7.554
7.502
7.477
7.461
7.436
7.274
7.233
7.190
7.184
7.161
7.143
7.115
7.044
4.125
4.108
4.092
4.056
4.040
4.023
4.000
3.991
3.984
3.975
3.968
3.959
1.879
1.868
1.861
1.853
1.841
1.815
1.530
1.517
1.393
1.385
1.376
0.952
0.935
OC6H13
OC6H13
CN
Br
C6H13O
C6H13O
9.0 8.5 8.0 7.5 7.0 6.5 6.0 5.5 5.0 4.5 4.0 3.5 3.0 2.5 2.0 1.5 1.0 0.5 ppm
4.00
2.12
1.09
3.06
1.10
0.94
2.08
2.18
4.00
8.30
8.72
16.34
12.41

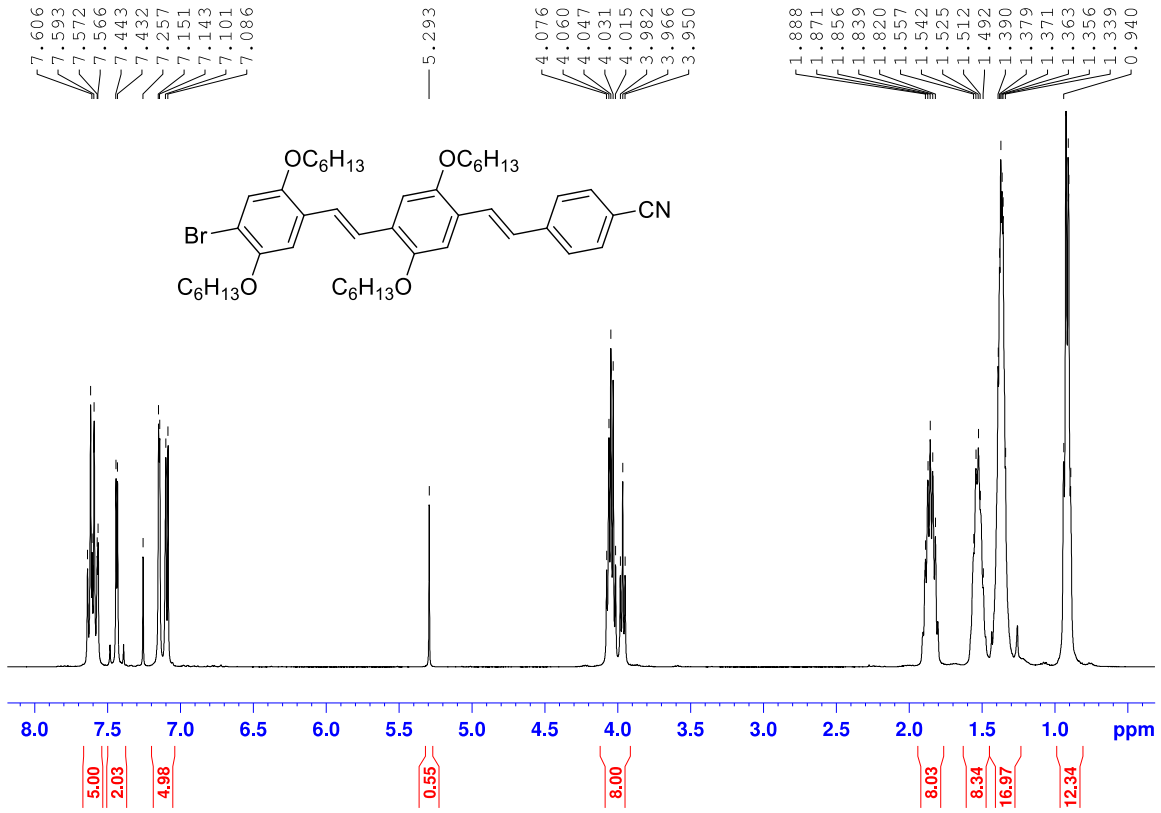
7.606
7.593
7.572
7.566
7.443
7.432
7.257
7.151
7.143
7.101
7.086
5.293
4.076
4.060
4.047
4.031
4.015
3.982
3.966
3.950
1.888
1.871
1.856
1.839
1.820
1.557
1.542
1.525
1.512
1.492
1.390
1.379
1.371
1.363
1.356
1.339
0.940
OC6H13
OC6H13
CN
Br
C6H13O
C6H13O
8.0
7.5
7.0
6.5
6.0
5.5
5.0
4.5
4.0
3.5
3.0
2.5
2.0
1.5
1.0
ppm
5.00
2.03
4.98
0.55
8.00
8.03
8.34
16.97
12.34

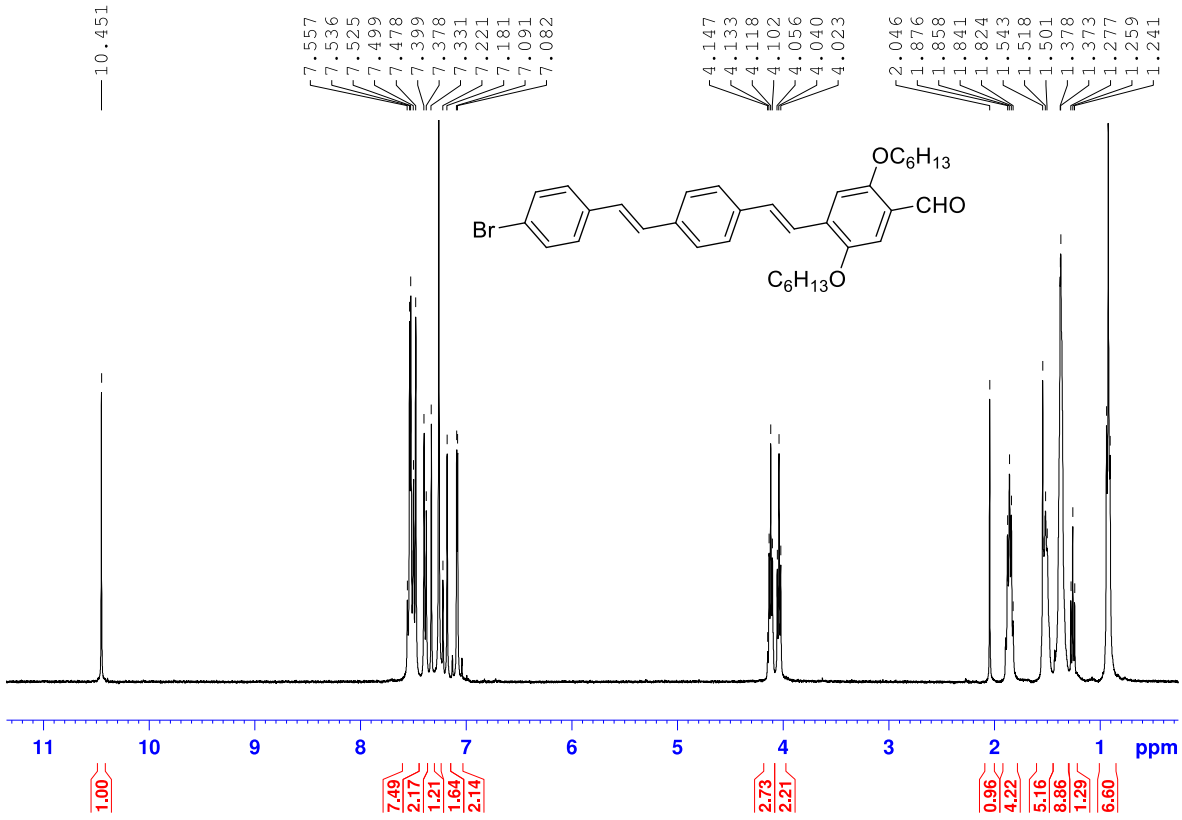
10.451
7.557
7.536
7.525
7.499
7.478
7.399
7.378
7.331
7.221
7.181
7.091
7.082
4.147
4.133
4.118
4.102
4.056
4.040
4.023
2.046
1.876
1.858
1.841
1.824
1.543
1.518
1.501
1.378
1.373
1.277
1.259
1.241
OC6H13
CHO
Br
C6H13O
11
10
9
8
7
6
5
4
3
2
1
ppm
1.00
7.49
2.17
1.21
1.64
2.14
2.73
2.21
0.96
4.22
5.16
8.86
1.29
6.60

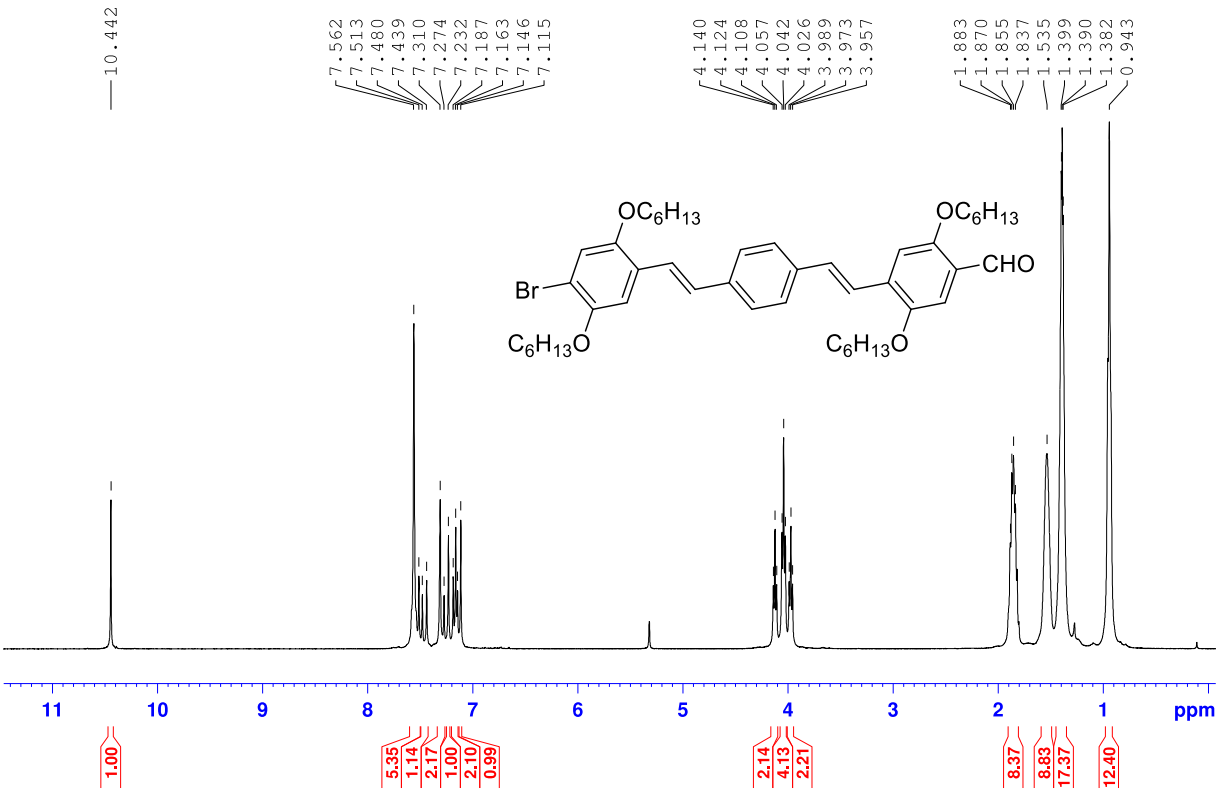
10.442
7.562
7.513
7.480
7.439
7.310
7.274
7.232
7.187
7.163
7.146
7.115
4.140
4.124
4.108
4.057
4.042
4.026
3.989
3.973
3.957
1.883
1.870
1.855
1.837
1.535
1.399
1.390
1.382
0.943
OC6H13
OC6H13
CHO
Br
C6H13O
C6H13O
11
10
9
8
7
6
5
4
3
2
1
ppm
1.00
5.35
1.14
2.17
1.00
2.10
0.99
2.14
4.13
2.21
8.37
8.83
17.37
12.40

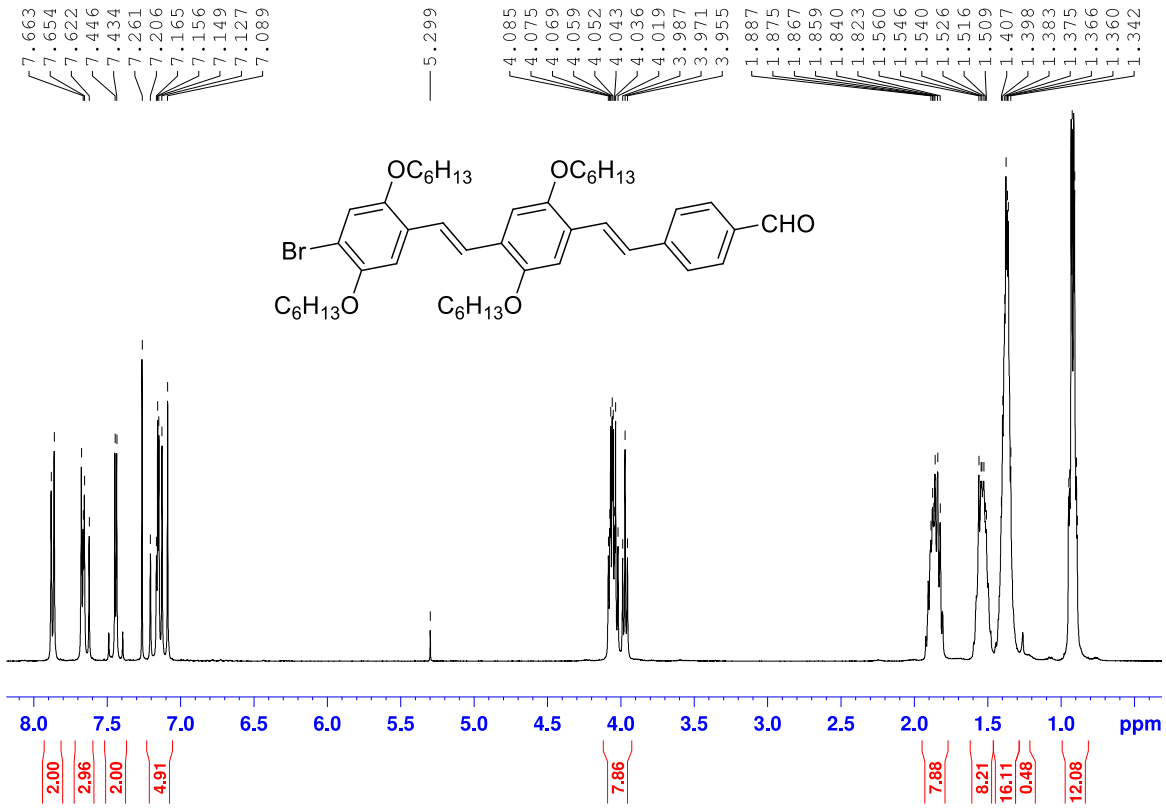
7.663
7.654
7.622
7.446
7.434
7.261
7.206
7.165
7.156
7.149
7.127
7.089
5.299
4.085
4.075
4.069
4.059
4.052
4.043
4.036
4.019
3.987
3.971
3.955
1.887
1.875
1.867
1.859
1.840
1.823
1.560
1.546
1.540
1.526
1.516
1.509
1.407
1.398
1.383
1.375
1.366
1.360
1.342
OC6H13
OC6H13
CHO
Br
C6H13O
C6H13O
8.0
7.5
7.0
6.5
6.0
5.5
5.0
4.5
4.0
3.5
3.0
2.5
2.0
1.5
1.0
ppm
2.00
2.96
2.00
4.91
7.86
7.88
8.21
16.11
0.48
12.08

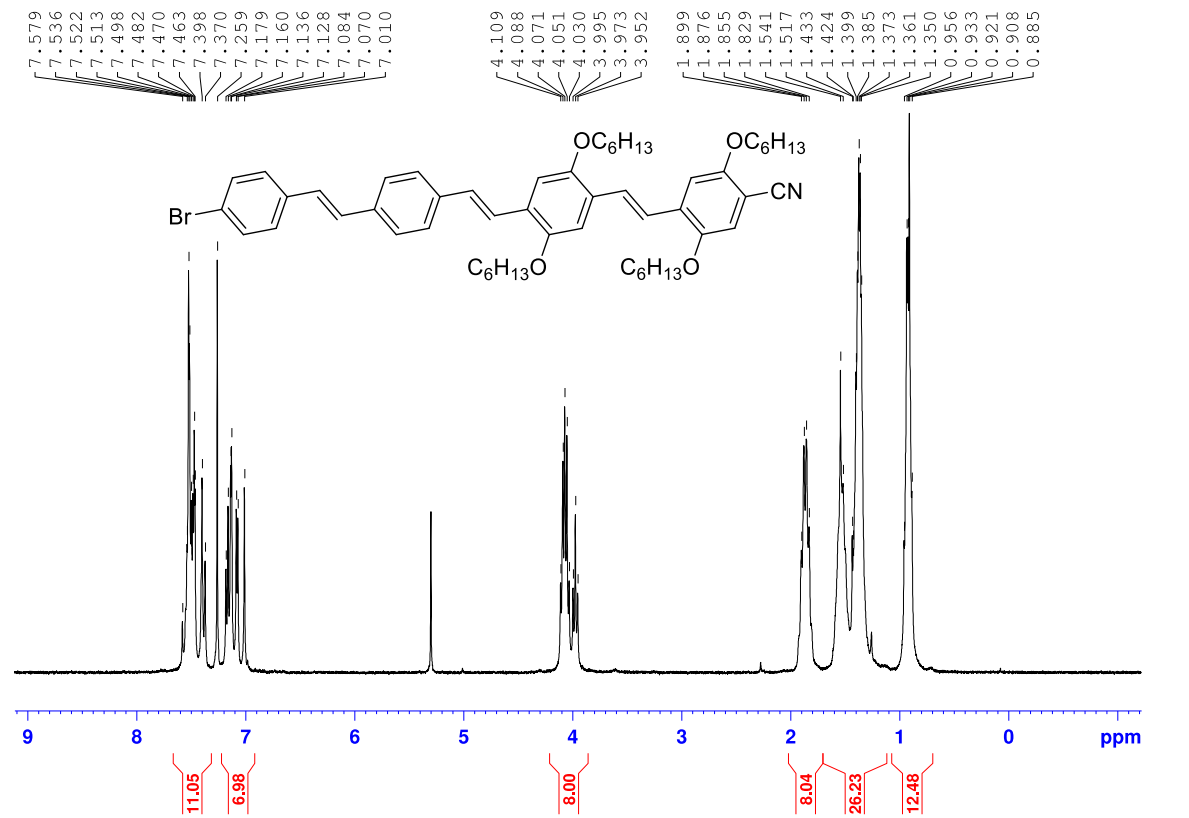
7.579
7.536
7.522
7.513
7.498
7.482
7.470
7.463
7.398
7.370
7.259
7.179
7.160
7.136
7.128
7.084
7.070
7.010
4.109
4.088
4.071
4.051
4.030
3.995
3.973
3.952
1.899
1.876
1.855
1.829
1.541
1.517
1.433
1.424
1.399
1.385
1.373
1.361
1.350
0.956
0.933
0.921
0.908
0.885
OC6H13
OC6H13
CN
Br
C6H13O
C6H13O
9
8
7
6
5
4
3
2
1
0
ppm
11.05
6.98
8.00
8.04
26.23
12.48

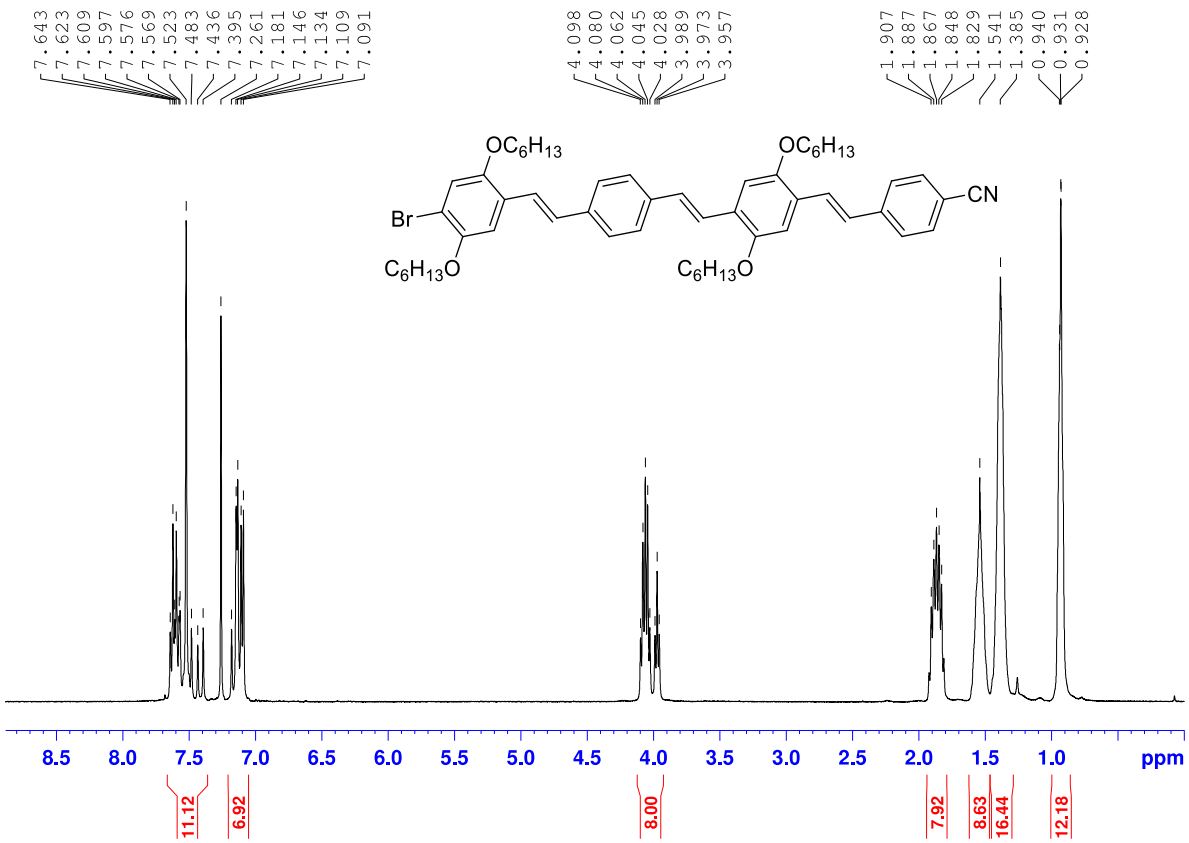
7.643
7.623
7.609
7.597
7.576
7.569
7.523
7.483
7.436
7.395
7.261
7.181
7.146
7.134
7.109
7.091
4.098
4.080
4.062
4.045
4.028
3.989
3.973
3.957
1.907
1.887
1.867
1.848
1.829
1.541
1.385
0.940
0.931
0.928
OC6H13
OC6H13
CN
Br
C6H13O
C6H13O
8.5
8.0
7.5
7.0
6.5
6.0
5.5
5.0
4.5
4.0
3.5
3.0
2.5
2.0
1.5
1.0
ppm
11.12
6.92
8.00
7.92
8.63
16.44
12.18

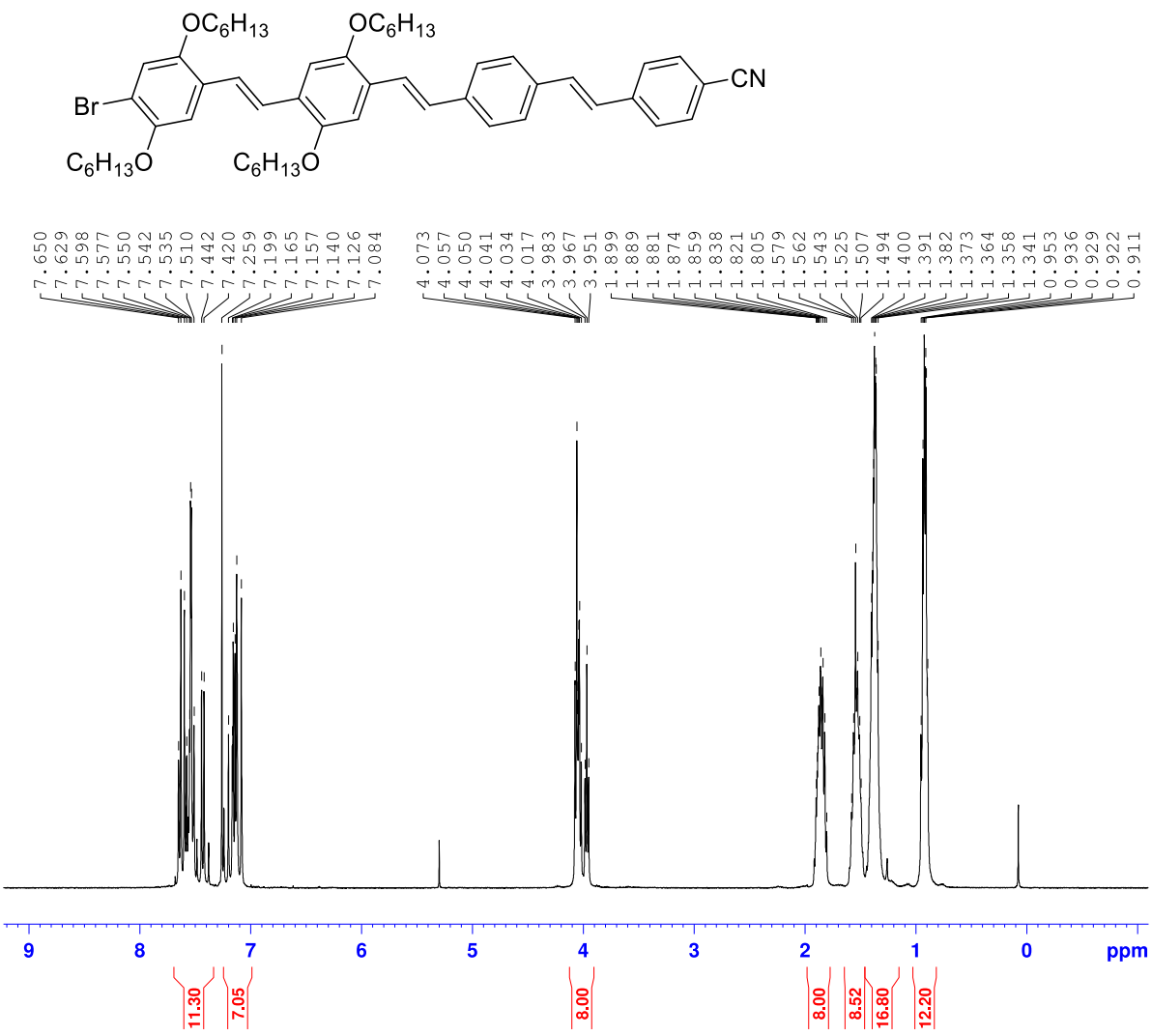
OC6H13
OC6H13
Br
CN
C6H13O
C6H13O
7.650
7.629
7.598
7.577
7.550
7.542
7.535
7.510
7.442
7.420
7.259
7.199
7.165
7.157
7.140
7.126
7.084
4.073
4.057
4.050
4.041
4.034
4.017
3.983
3.967
3.951
1.899
1.889
1.881
1.874
1.859
1.838
1.821
1.805
1.579
1.562
1.543
1.525
1.507
1.494
1.400
1.391
1.382
1.373
1.364
1.358
1.341
0.953
0.936
0.929
0.922
0.911
9
8
7
6
5
4
3
2
1
0
ppm
11.30
7.05
8.00
8.00
8.52
16.80
12.20

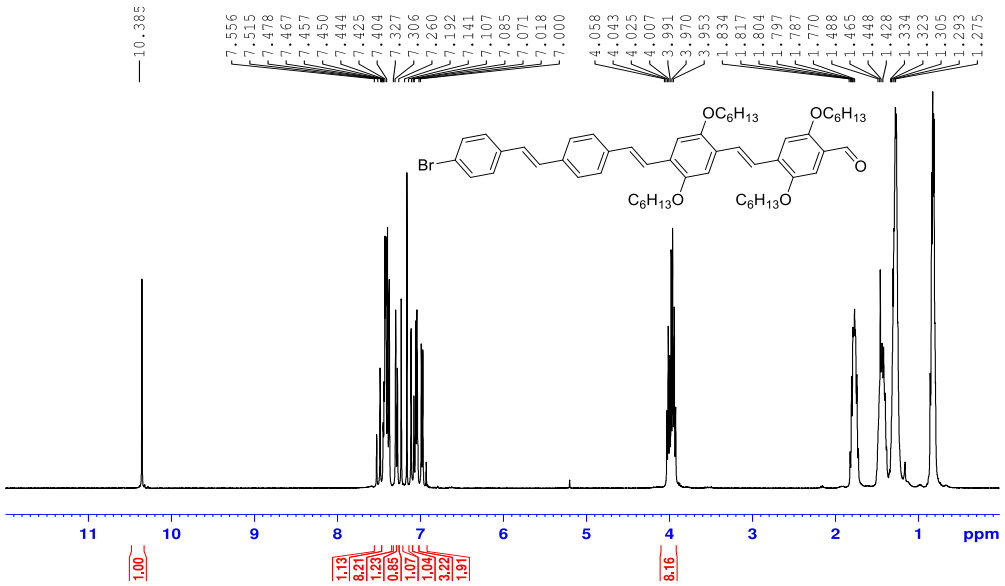
10.385
7.556
7.515
7.478
7.467
7.457
7.450
7.444
7.425
7.404
7.327
7.306
7.260
7.192
7.141
7.107
7.085
7.071
7.018
7.000
4.058
4.043
4.025
4.007
3.991
3.970
3.953
1.834
1.817
1.804
1.797
1.787
1.770
1.488
1.465
1.448
1.428
1.334
1.323
1.305
1.293
1.275
Br
OC6H13
OC6H13
C6H13O
C6H13O
O
11
10
9
8
7
6
5
4
3
2
1
ppm
1.00
1.13
8.21
1.23
0.86
1.07
1.04
3.22
1.91
8.16

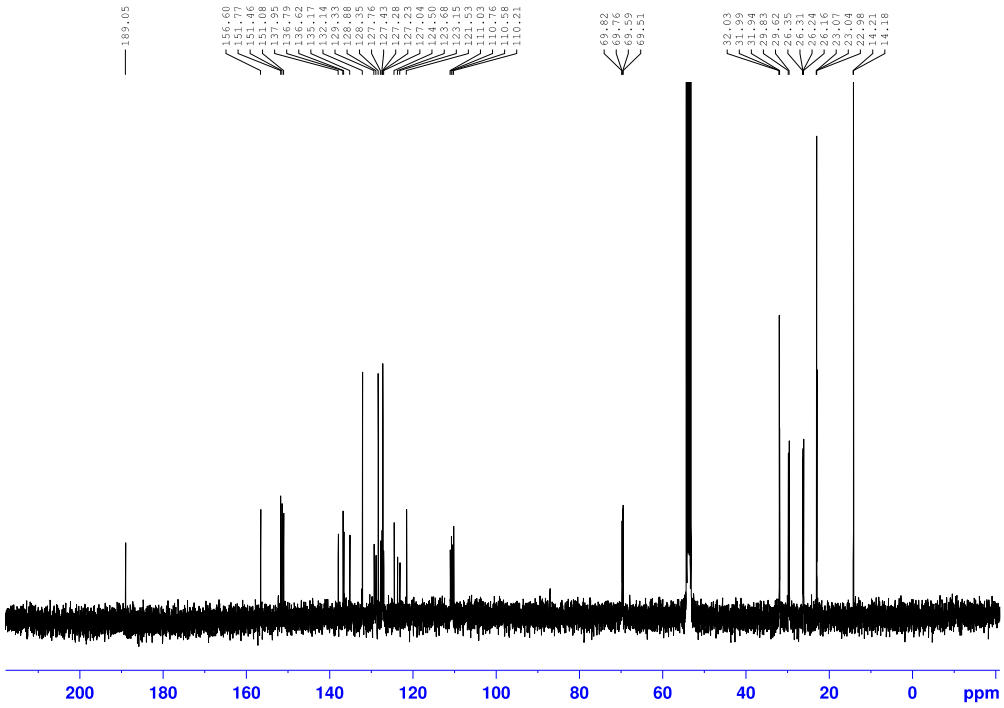
189.05
156.60
151.77
151.46
151.08
137.95
136.79
136.62
135.17
132.14
129.33
128.88
128.35
127.76
127.74
127.48
127.23
127.04
124.50
123.68
123.15
121.53
111.03
110.76
110.58
110.21
69.82
69.76
69.59
69.51
32.03
31.99
31.94
29.83
29.62
29.35
26.31
26.24
26.16
23.07
23.04
22.98
14.21
14.18
200
180
160
140
120
100
80
60
40
20
0
ppm

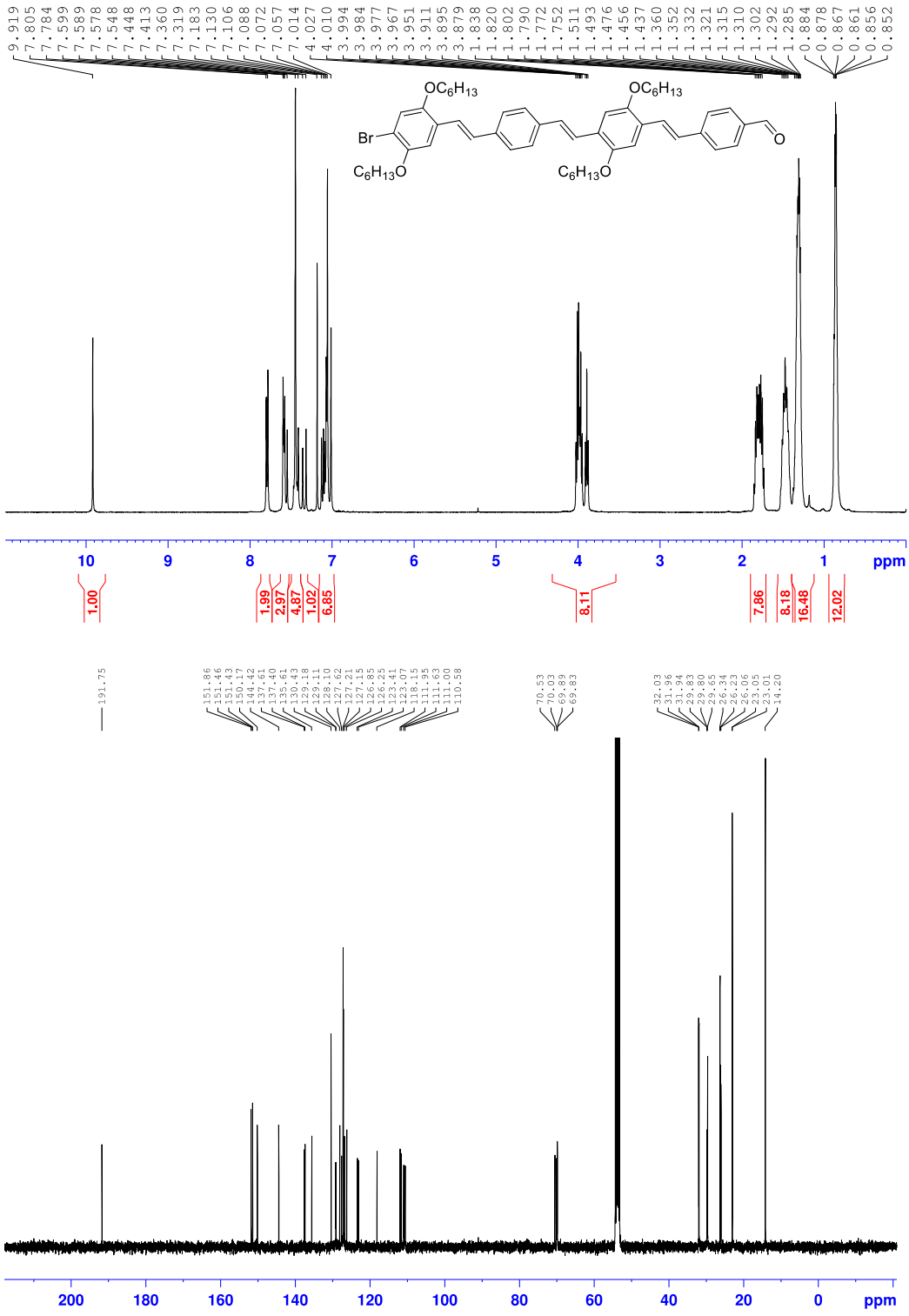
9.919
7.805
7.784
7.599
7.589
7.578
7.548
7.448
7.413
7.360
7.319
7.183
7.130
7.106
7.088
7.072
7.057
7.014
4.027
4.010
3.994
3.984
3.977
3.967
3.951
3.911
3.895
3.879
1.838
1.820
1.802
1.790
1.772
1.752
1.511
1.493
1.476
1.456
1.437
1.360
1.352
1.332
1.321
1.315
1.310
1.302
1.292
1.285
0.884
0.878
0.867
0.861
0.856
0.852
OC6H13
OC6H13
Br
C6H13O
C6H13O
O
10
9
8
7
6
5
4
3
2
1
ppm
1.00
1.99
2.97
4.87
1.02
6.85
8.11
7.86
8.18
16.48
12.02
191.75
151.86
151.46
151.43
150.17
144.42
137.61
137.40
135.61
130.43
129.18
129.11
128.10
127.62
127.21
127.15
126.85
126.25
123.41
123.07
118.15
111.95
111.63
111.00
110.58
70.53
70.03
69.89
69.83
32.03
31.96
31.94
29.83
29.80
29.65
26.34
26.23
23.06
23.05
23.01
14.20
200
180
160
140
120
100
80
60
40
20
0
ppm

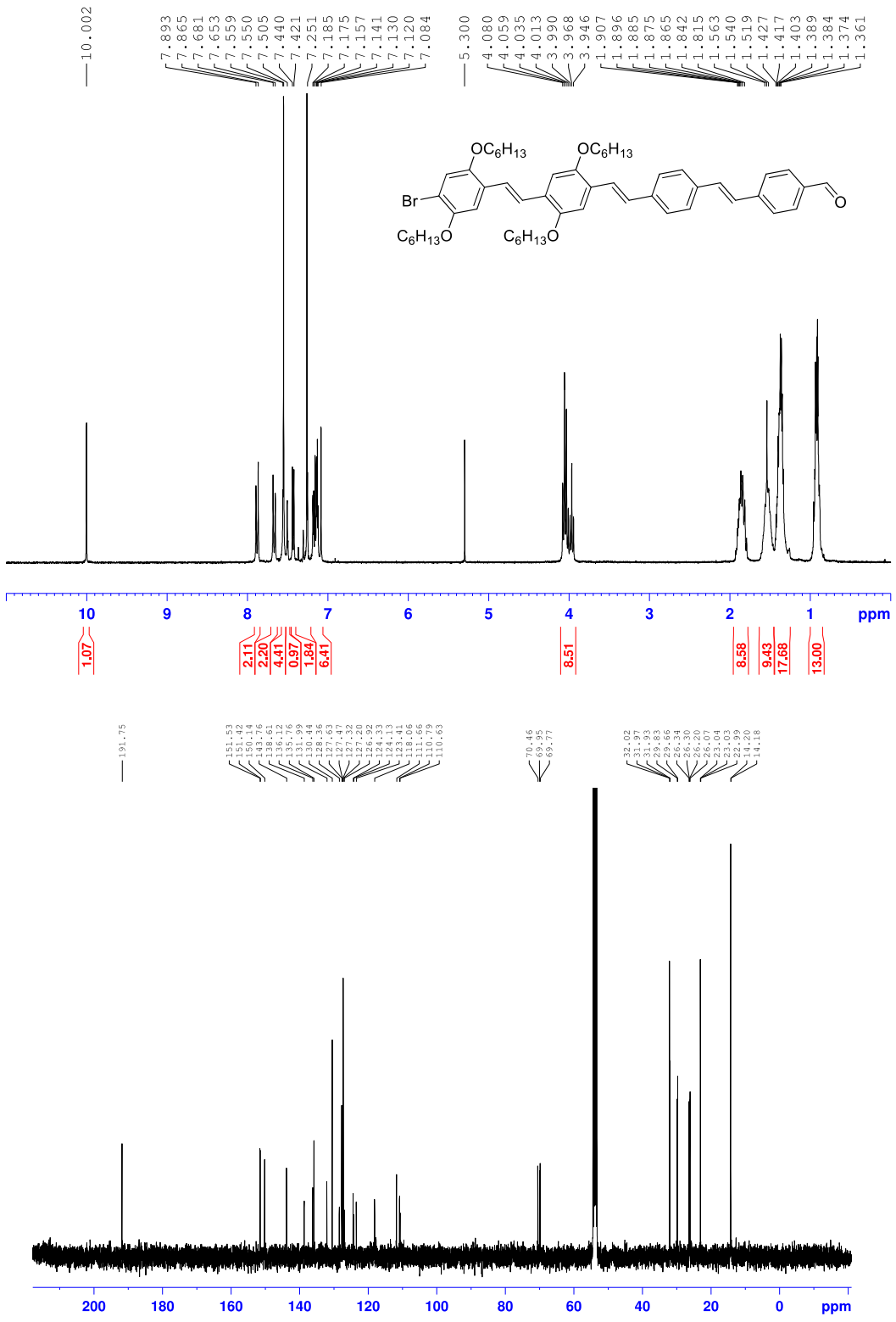
10.002
7.893
7.865
7.681
7.653
7.559
7.550
7.505
7.440
7.421
7.251
7.185
7.175
7.157
7.141
7.130
7.120
7.084
5.300
4.080
4.059
4.035
4.013
3.990
3.968
3.946
1.907
1.896
1.885
1.875
1.865
1.842
1.815
1.563
1.540
1.519
1.427
1.417
1.403
1.389
1.384
1.374
1.361
OC6H13
OC6H13
Br
C6H13O
C6H13O
O
10
9
8
7
6
5
4
3
2
1
ppm
1.07
2.11
2.20
4.41
0.97
1.84
6.41
8.51
8.58
9.43
17.68
13.00
191.75
151.53
151.42
150.14
143.76
138.61
136.12
135.76
131.99
130.44
128.36
127.63
127.47
127.32
127.20
126.92
124.33
124.13
123.41
118.06
111.66
110.79
110.63
70.46
69.95
69.77
32.02
31.97
31.93
29.83
29.66
29.34
26.30
26.20
26.07
23.03
22.99
22.20
14.18
200
180
160
140
120
100
80
60
40
20
0
ppm

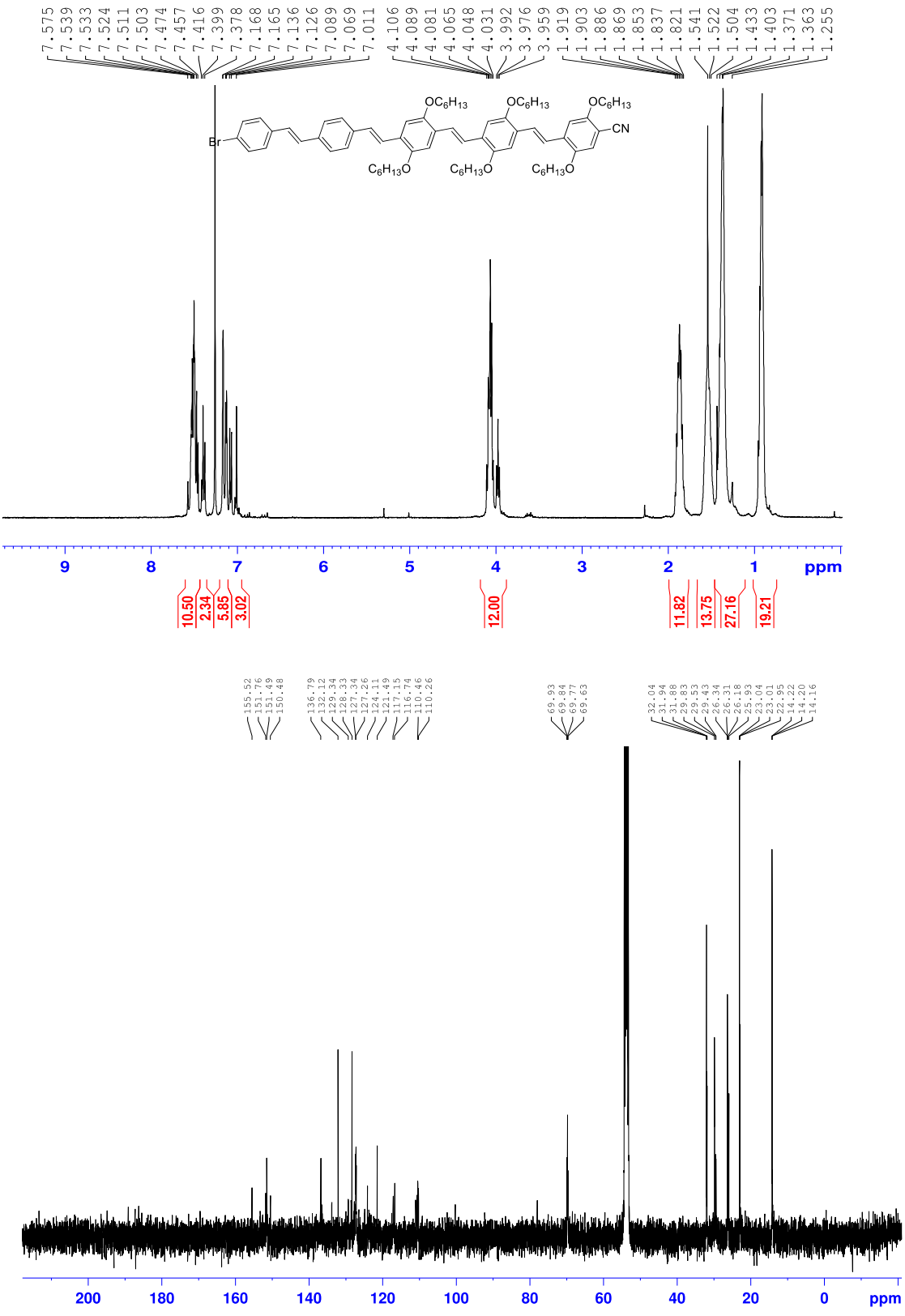
7.575
7.539
7.533
7.524
7.511
7.503
7.474
7.457
7.416
7.399
7.378
7.168
7.165
7.136
7.126
7.089
7.069
7.011
4.106
4.089
4.081
4.065
4.048
4.031
3.992
3.976
3.959
1.919
1.903
1.886
1.869
1.853
1.837
1.821
1.541
1.522
1.504
1.433
1.403
1.371
1.363
1.255
OC6H13
OC6H13
OC6H13
CN
Br
C6H13O
C6H13O
C6H13O
9
8
7
6
5
4
3
2
1
ppm
10.50
2.34
5.85
3.02
12.00
11.82
13.75
27.16
19.21
155.52
151.76
151.49
150.48
136.79
132.12
129.34
128.33
127.34
127.26
124.11
121.49
117.15
116.74
110.46
110.26
69.93
69.84
69.77
69.63
32.04
31.94
31.88
29.83
29.53
29.43
26.34
26.31
26.18
25.93
23.04
23.01
22.95
14.22
14.20
14.16
200
180
160
140
120
100
80
60
40
20
0
ppm

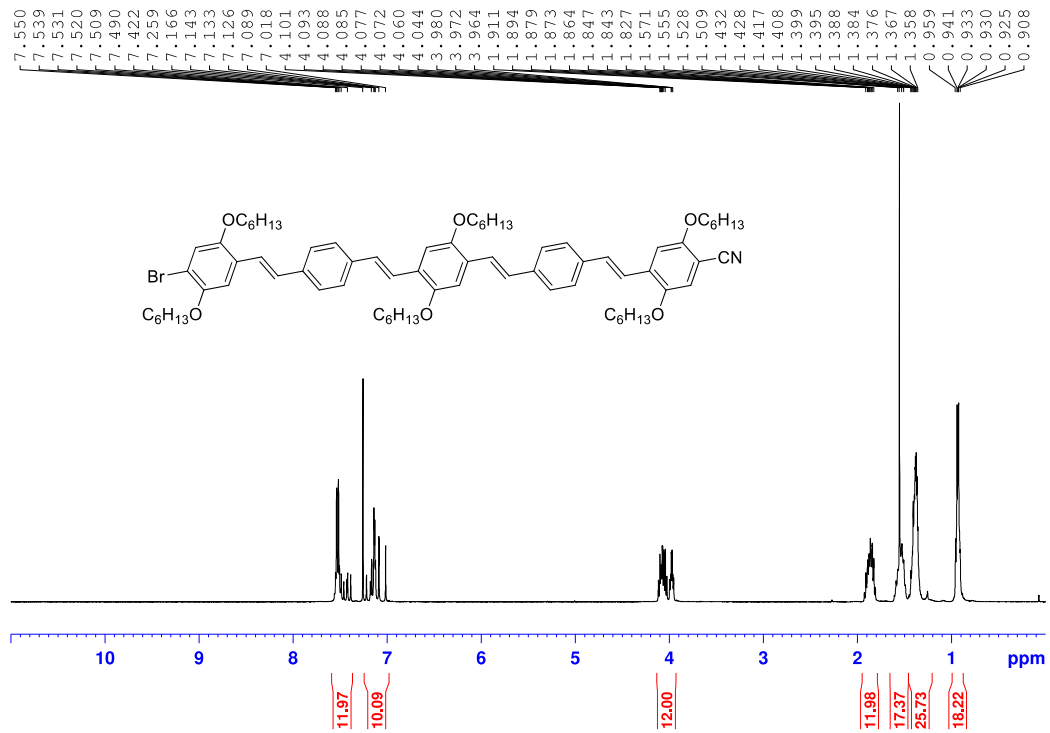
7.550
7.539
7.531
7.520
7.509
7.490
7.422
7.259
7.166
7.143
7.133
7.126
7.089
7.018
4.101
4.093
4.088
4.085
4.077
4.072
4.060
4.044
3.980
3.972
3.964
1.911
1.894
1.879
1.873
1.864
1.847
1.843
1.827
1.571
1.555
1.528
1.509
1.432
1.428
1.417
1.408
1.399
1.395
1.388
1.384
1.376
1.367
1.358
0.959
0.941
0.933
0.930
0.925
0.908
OC6H13
OC6H13
OC6H13
Br
CN
C6H13O
C6H13O
C6H13O
10
9
8
7
6
5
4
3
2
1
ppm
11.97
10.09
12.00
11.98
17.37
25.73
18.22

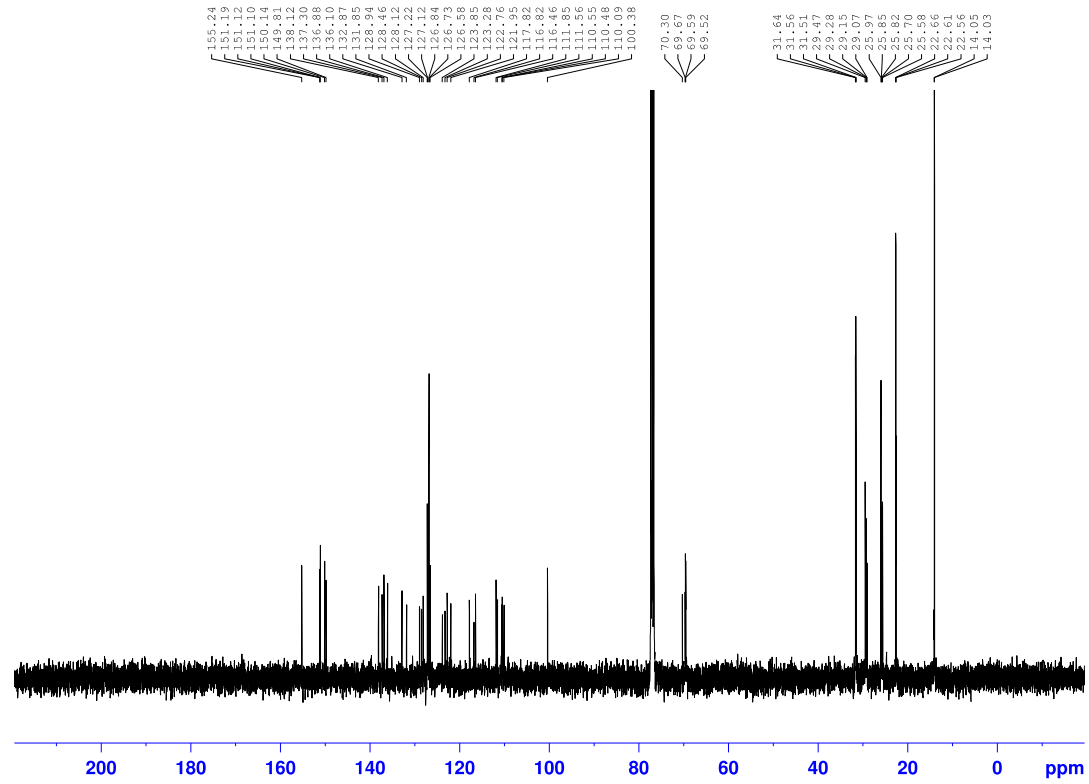
155.24
151.19
151.12
151.10
150.14
149.81
138.12
137.30
136.88
136.10
132.87
131.85
128.94
128.46
128.12
127.22
127.12
126.84
126.73
126.58
123.85
123.28
122.76
121.95
117.82
116.82
116.46
111.85
111.56
110.55
110.48
110.09
100.38
70.30
69.67
69.59
69.52
31.64
31.56
31.51
29.47
29.28
29.15
29.07
25.97
25.85
25.82
25.70
25.58
22.66
22.61
22.56
14.05
14.03
200
180
160
140
120
100
80
60
40
20
0
ppm

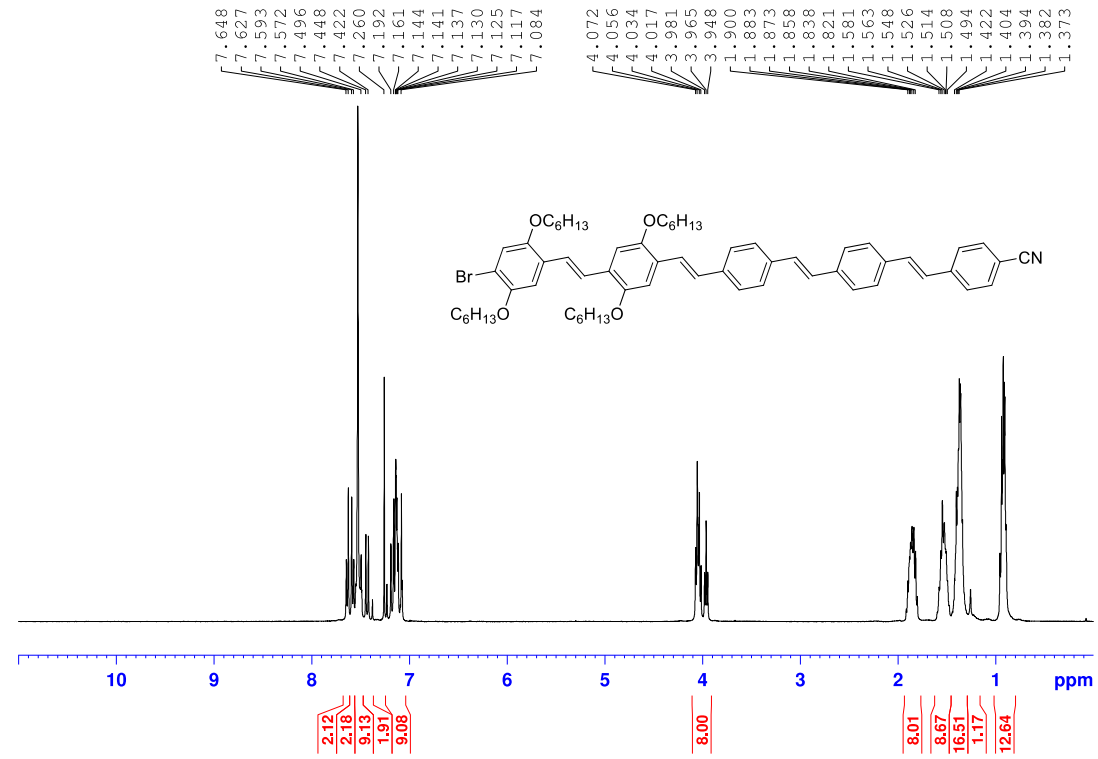
7.648
7.627
7.593
7.572
7.496
7.448
7.422
7.260
7.192
7.161
7.144
7.141
7.137
7.130
7.125
7.117
7.084
4.072
4.056
4.034
4.017
3.981
3.965
3.948
1.900
1.883
1.873
1.858
1.838
1.821
1.581
1.563
1.548
1.526
1.514
1.508
1.494
1.422
1.404
1.394
1.382
1.373
OC6H13
OC6H13
Br
C6H13O
C6H13O
CN
10
9
8
7
6
5
4
3
2
1
ppm
2.12
2.18
9.13
1.91
9.08
8.00
8.01
8.67
16.51
1.17
12.64

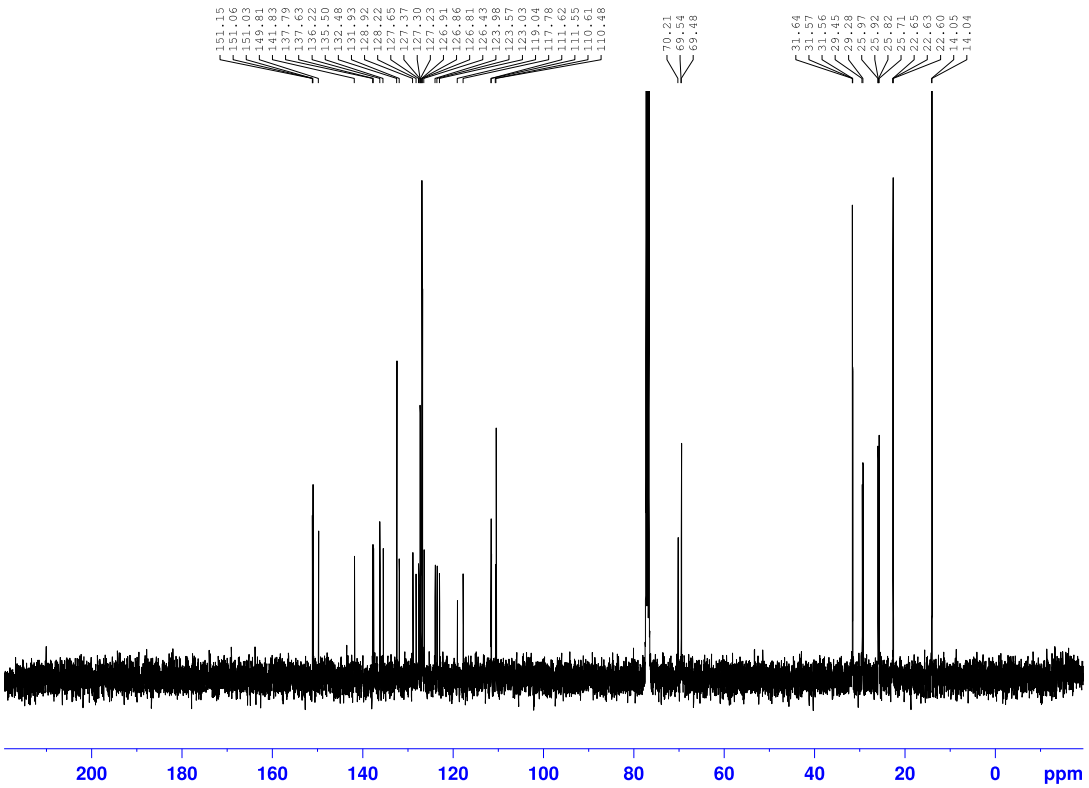
151.15
151.06
151.03
149.81
141.83
137.79
137.63
136.22
135.50
132.48
131.93
128.92
128.22
127.65
127.37
127.30
127.23
126.91
126.86
126.81
126.43
123.98
123.57
123.03
119.04
117.78
111.62
111.55
110.61
110.48
70.21
69.54
69.48
31.64
31.57
31.56
29.45
29.28
25.97
25.92
25.82
25.71
22.65
22.63
22.60
14.05
14.04
200
180
160
140
120
100
80
60
40
20
0
ppm

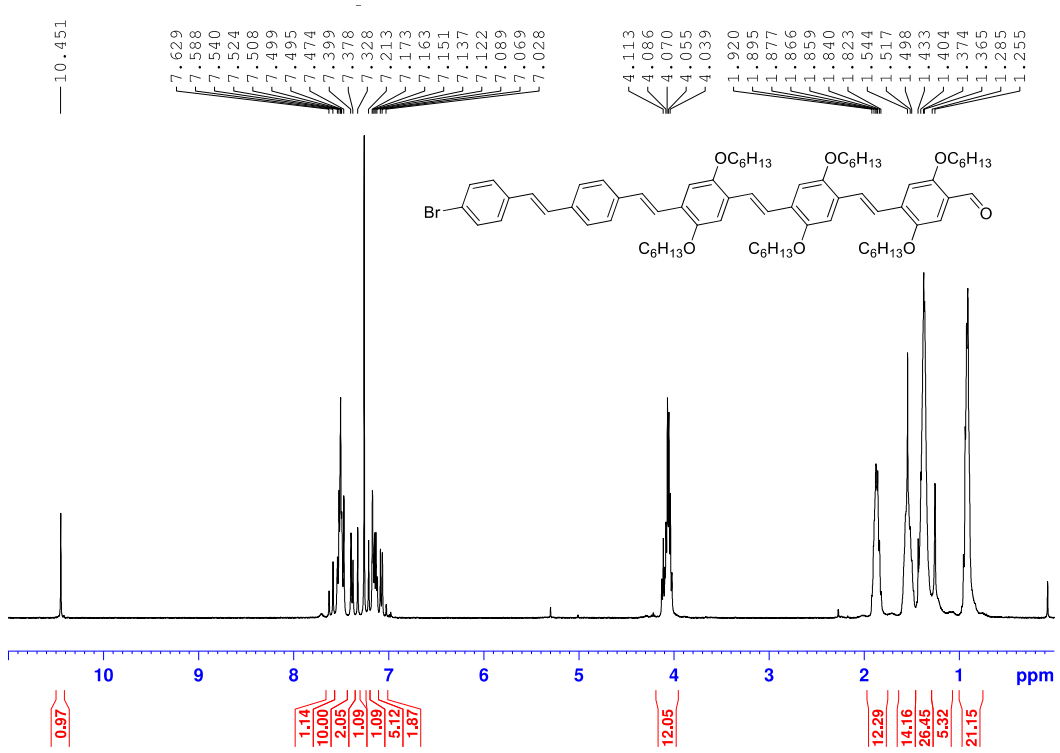
10.451
7.629
7.588
7.540
7.524
7.508
7.499
7.495
7.474
7.399
7.378
7.328
7.213
7.173
7.163
7.151
7.137
7.122
7.089
7.069
7.028
4.113
4.086
4.070
4.055
4.039
1.920
1.895
1.877
1.866
1.859
1.840
1.823
1.544
1.517
1.498
1.433
1.404
1.374
1.365
1.285
1.255
OC6H13
OC6H13
OC6H13
Br
C6H13O
C6H13O
C6H13O
O
10
9
8
7
6
5
4
3
2
1
ppm
0.97
1.14
10.00
2.05
1.09
1.09
5.12
1.87
12.05
12.29
14.16
26.45
5.32
21.15

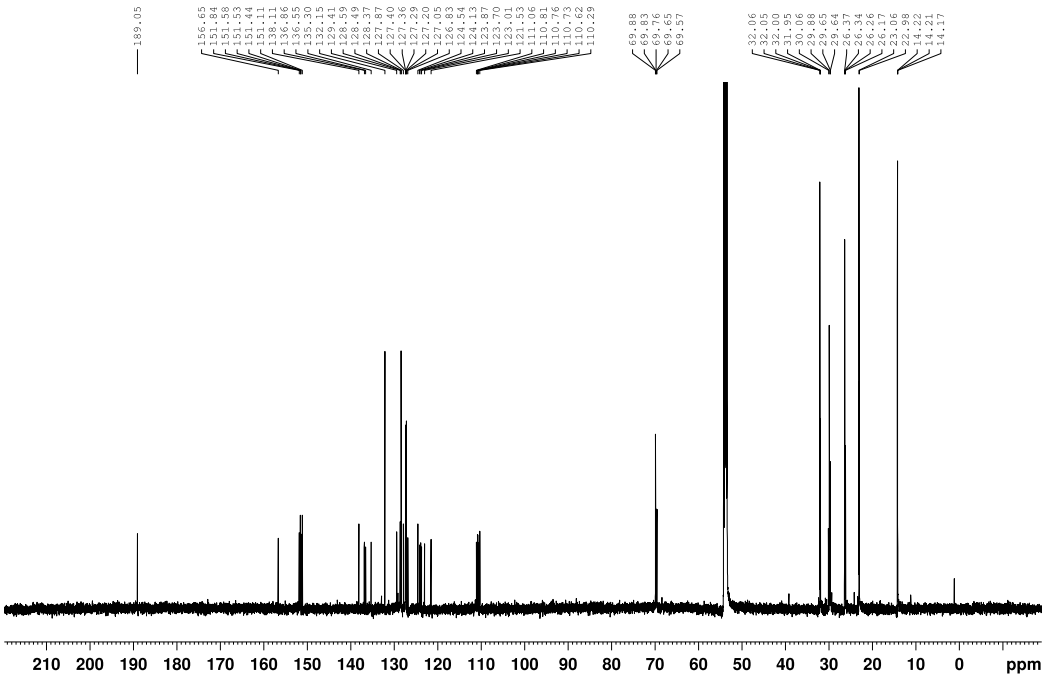
189.05
156.65
151.84
151.58
151.53
151.44
151.11
138.11
136.86
136.55
135.30
132.15
128.41
128.40
128.49
128.37
127.87
127.40
127.36
127.20
127.20
127.05
126.83
124.54
124.13
123.87
123.70
123.01
121.53
111.06
110.81
110.76
110.73
110.62
110.29
69.88
69.83
69.76
69.65
69.57
32.06
32.05
32.00
31.95
30.06
29.88
29.65
29.44
26.37
26.34
26.26
26.17
23.06
22.28
22.22
14.21
14.17
210
200
190
180
170
160
150
140
130
120
110
100
90
80
70
60
50
40
30
20
10
0
ppm

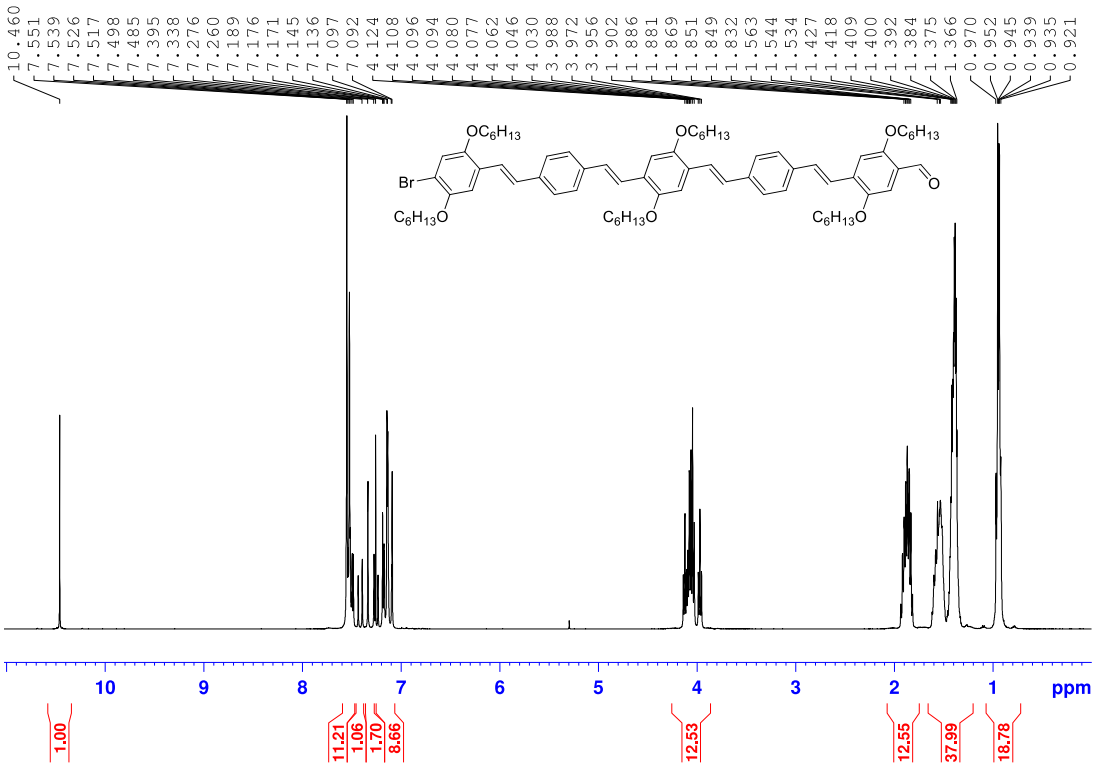
10.460
7.551
7.539
7.526
7.517
7.498
7.485
7.395
7.338
7.276
7.260
7.189
7.176
7.171
7.145
7.136
7.097
7.092
4.124
4.108
4.096
4.094
4.080
4.077
4.062
4.046
4.030
3.988
3.972
3.956
1.902
1.886
1.881
1.869
1.851
1.849
1.832
1.563
1.544
1.534
1.427
1.418
1.409
1.400
1.392
1.384
1.375
1.366
0.970
0.952
0.945
0.939
0.935
0.921
OC6H13
Br
C6H13O
O
10
9
8
7
6
5
4
3
2
1
ppm
1.00
11.21
1.06
1.70
8.66
12.53
12.55
37.99
18.78

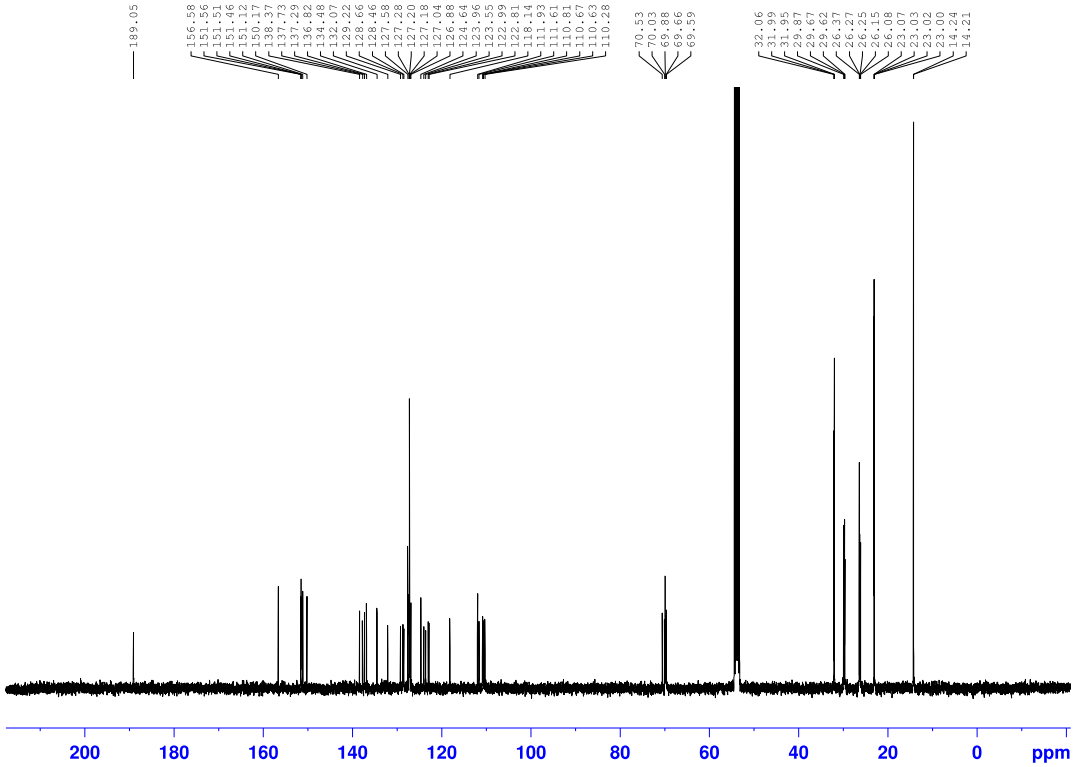
189.05
156.58
151.56
151.51
151.46
151.12
150.17
138.37
137.73
137.29
136.82
134.48
132.07
129.22
128.66
128.46
127.58
127.28
127.20
127.18
127.04
126.88
124.64
123.96
123.55
122.99
122.81
118.14
111.93
111.61
110.81
110.67
110.63
110.28
70.53
70.03
69.88
69.66
69.59
32.06
31.99
31.95
29.87
29.67
29.62
26.37
26.27
26.25
26.15
26.08
23.07
23.03
23.02
23.00
14.24
14.21
200
180
160
140
120
100
80
60
40
20
0
ppm

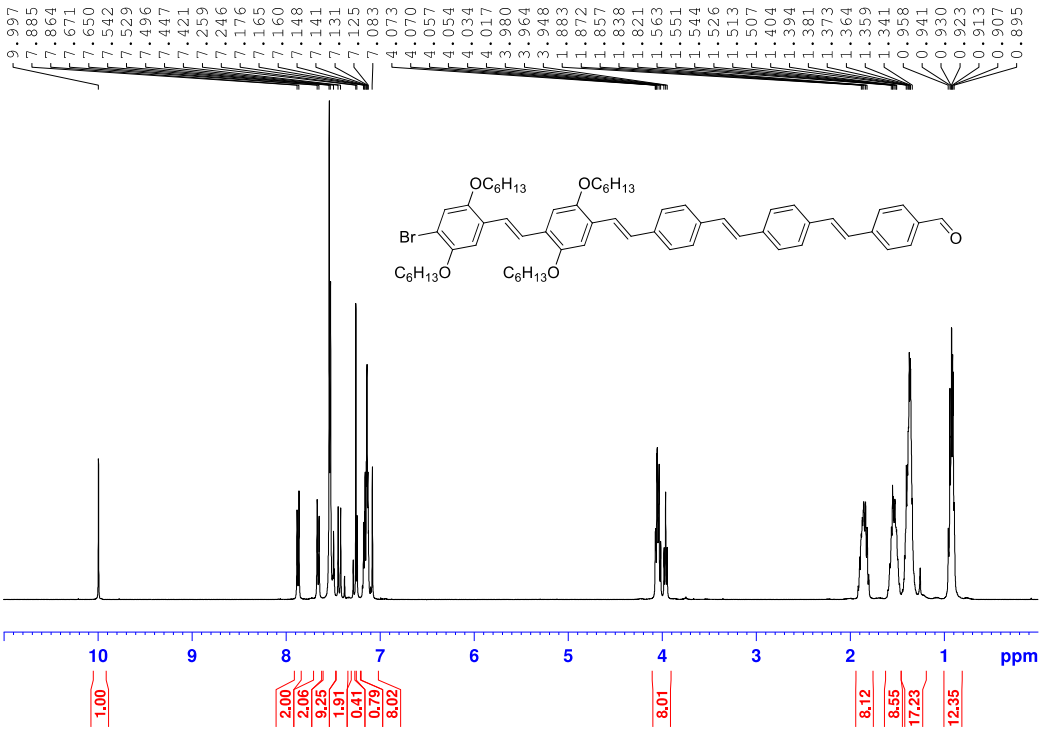
9.997
7.885
7.864
7.671
7.650
7.542
7.529
7.496
7.447
7.421
7.259
7.246
7.176
7.165
7.160
7.148
7.141
7.131
7.125
7.083
4.073
4.070
4.057
4.054
4.034
4.017
3.980
3.964
3.948
1.883
1.872
1.857
1.838
1.821
1.563
1.551
1.544
1.526
1.513
1.507
1.404
1.394
1.381
1.373
1.364
1.359
1.341
0.958
0.941
0.930
0.923
0.913
0.907
0.895
OC6H13
OC6H13
Br
C6H13O
C6H13O
O
10
9
8
7
6
5
4
3
2
1
ppm
1.00
2.00
2.06
9.25
1.91
0.41
0.79
8.02
8.01
8.12
8.55
17.23
12.35

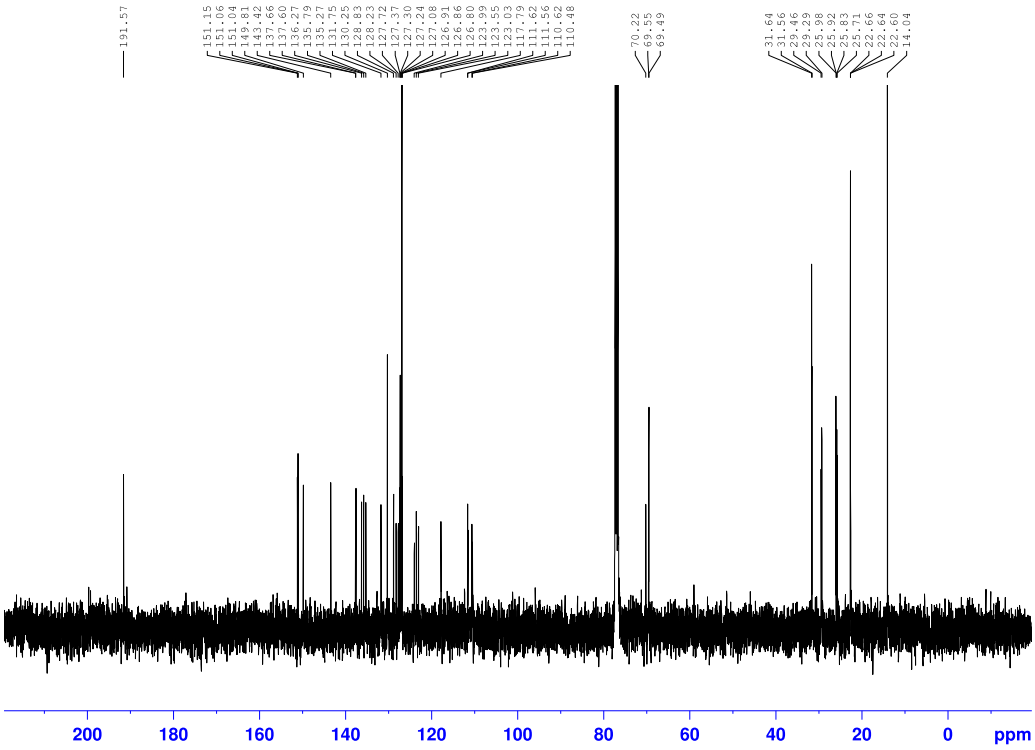
191.57
151.15
151.06
151.04
149.81
143.42
137.66
137.60
136.77
136.79
135.27
131.75
130.25
128.83
128.23
127.72
127.37
127.10
127.04
127.08
126.91
126.86
126.80
123.99
123.55
123.03
111.79
111.62
111.56
110.62
110.48
70.22
69.55
69.49
31.64
31.56
29.46
29.29
25.98
25.92
25.83
25.71
22.76
22.64
22.60
14.04
200
180
160
140
120
100
80
60
40
20
0
ppm

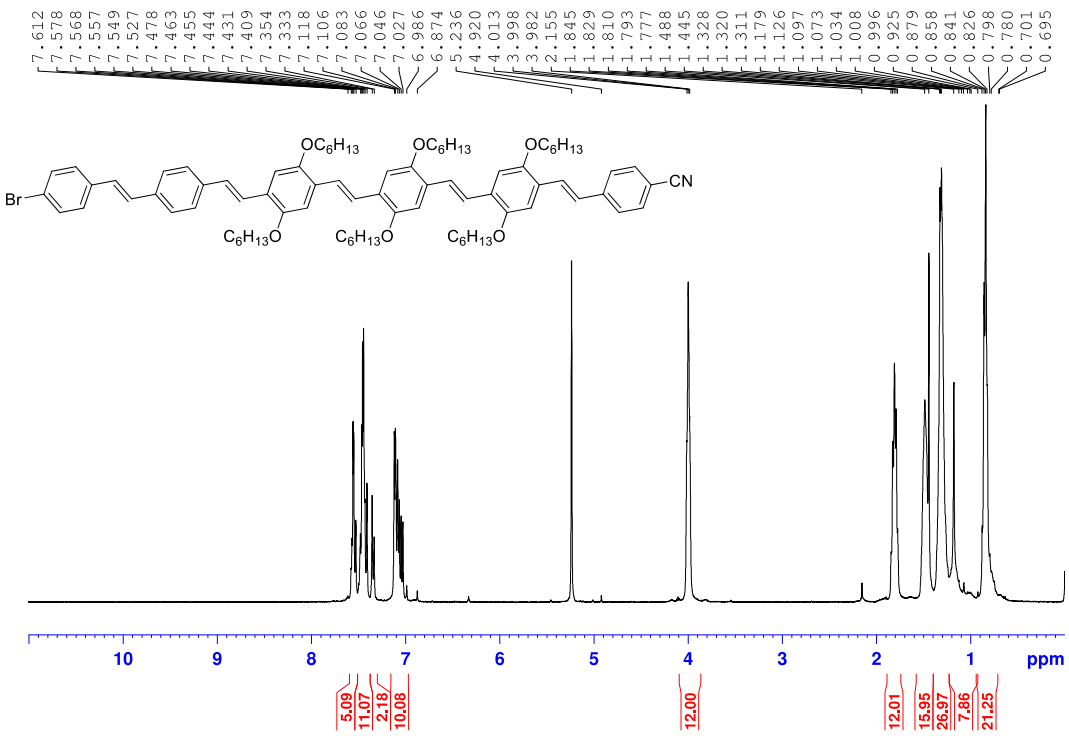
7.612
7.578
7.568
7.557
7.549
7.527
7.478
7.463
7.455
7.444
7.431
7.409
7.354
7.333
7.118
7.106
7.083
7.066
7.046
7.027
6.986
6.874
5.236
4.920
4.013
3.998
3.982
2.155
1.845
1.829
1.810
1.793
1.777
1.488
1.445
1.328
1.320
1.311
1.179
1.126
1.097
1.073
1.034
1.008
0.996
0.925
0.879
0.858
0.841
0.826
0.798
0.780
0.701
0.695
OC6H13
OC6H13
OC6H13
Br
CN
C6H13O
C6H13O
C6H13O
10
9
8
7
6
5
4
3
2
1
ppm
5.09
11.07
2.18
10.08
12.00
12.01
15.95
26.97
7.86
21.25

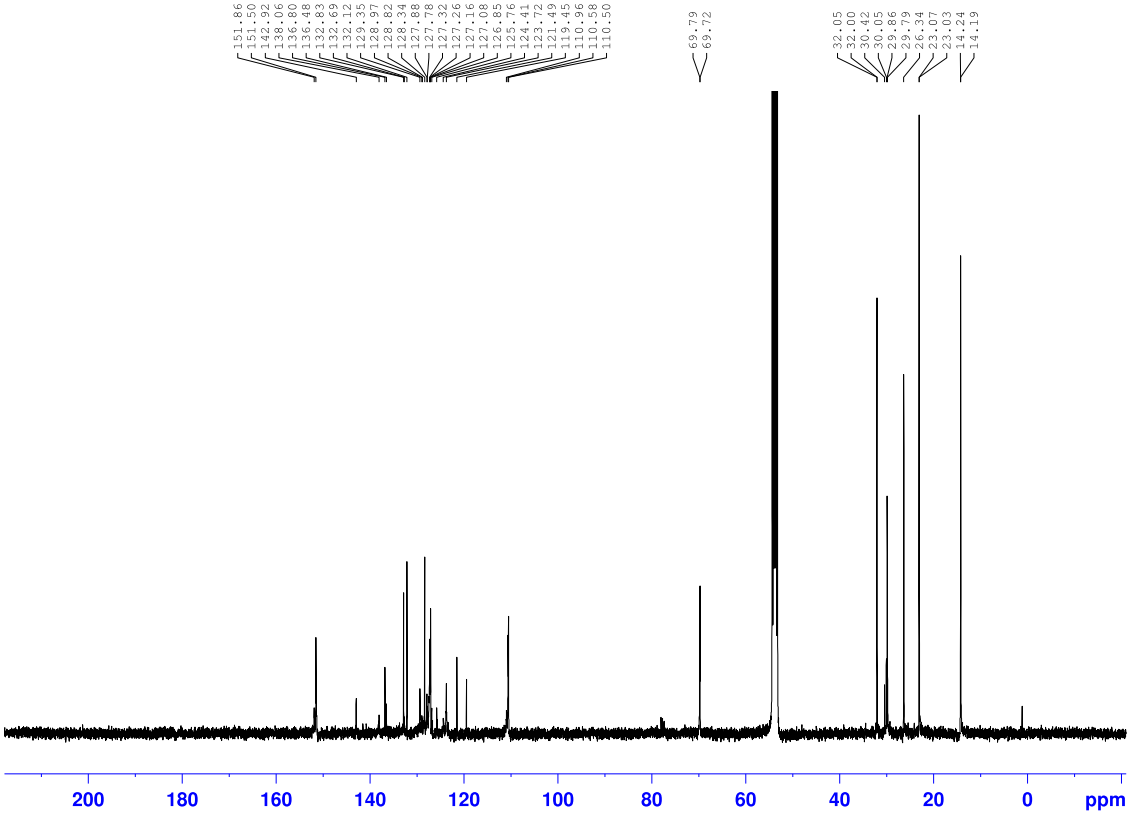
151.86
151.50
142.92
138.06
136.80
136.48
132.83
132.69
132.12
129.35
128.97
128.82
128.44
127.88
127.32
127.26
127.16
127.08
126.85
125.76
124.41
123.72
121.49
119.45
110.96
110.58
110.50
69.79
69.72
32.05
32.00
30.42
30.05
29.86
29.39
26.34
23.07
23.03
14.24
14.19
200
180
160
140
120
100
80
60
40
20
0
ppm

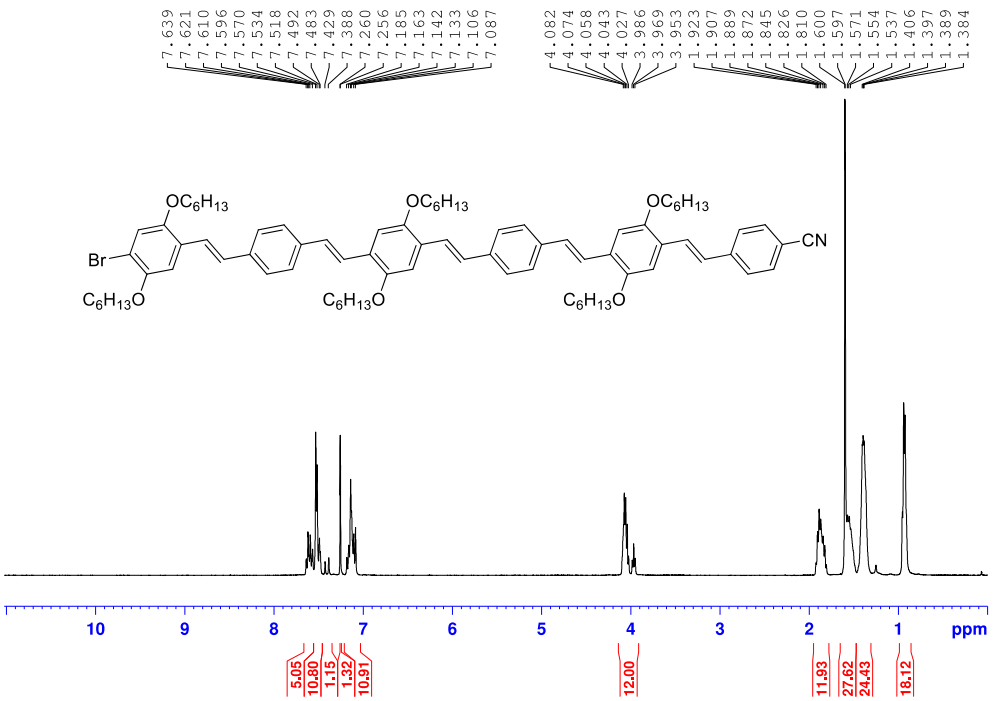
7.639
7.621
7.610
7.596
7.570
7.534
7.518
7.492
7.483
7.429
7.388
7.260
7.256
7.185
7.163
7.142
7.133
7.106
7.087
4.082
4.074
4.058
4.043
4.027
3.986
3.969
3.953
1.923
1.907
1.889
1.872
1.845
1.826
1.810
1.600
1.597
1.571
1.554
1.537
1.406
1.397
1.389
1.384
OC6H13
OC6H13
OC6H13
Br
CN
C6H13O
C6H13O
C6H13O
10
9
8
7
6
5
4
3
2
1
ppm
5.05
10.80
1.15
1.32
10.91
12.00
11.93
27.62
24.43
18.12

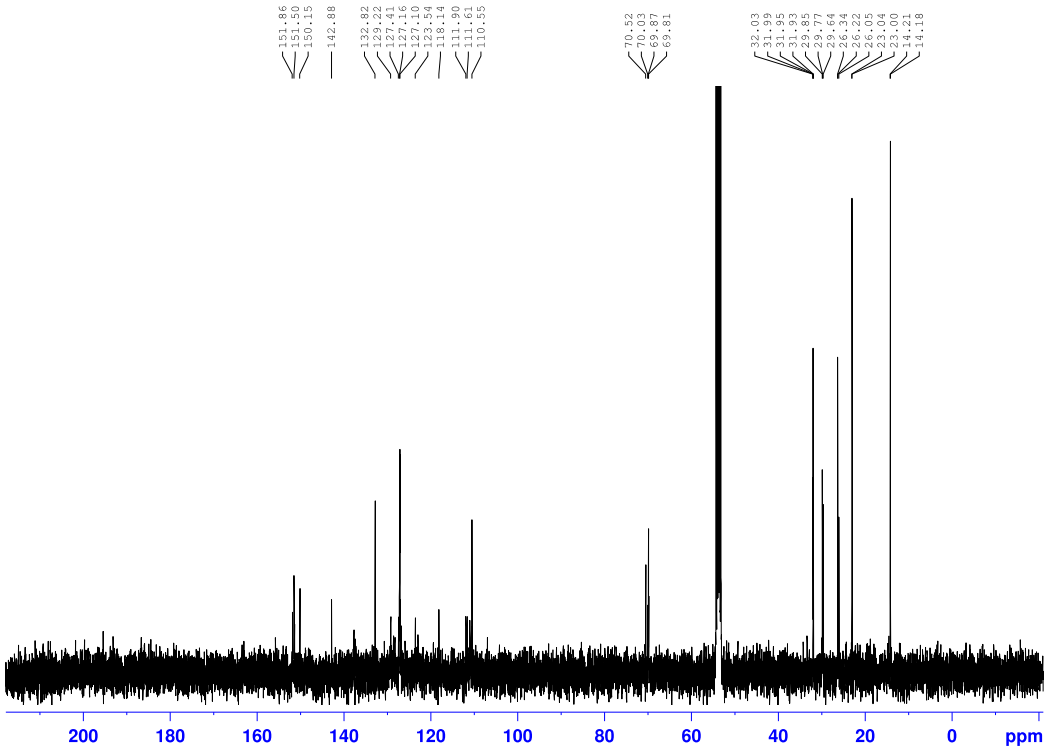
151.86
151.50
150.15
142.88
132.82
129.22
127.41
127.16
127.10
123.54
118.14
111.90
111.61
110.55
70.52
70.03
69.87
69.81
32.03
31.99
31.95
31.93
29.85
29.77
29.66
26.34
26.22
26.05
23.04
23.00
14.21
14.18
200
180
160
140
120
100
80
60
40
20
0
ppm

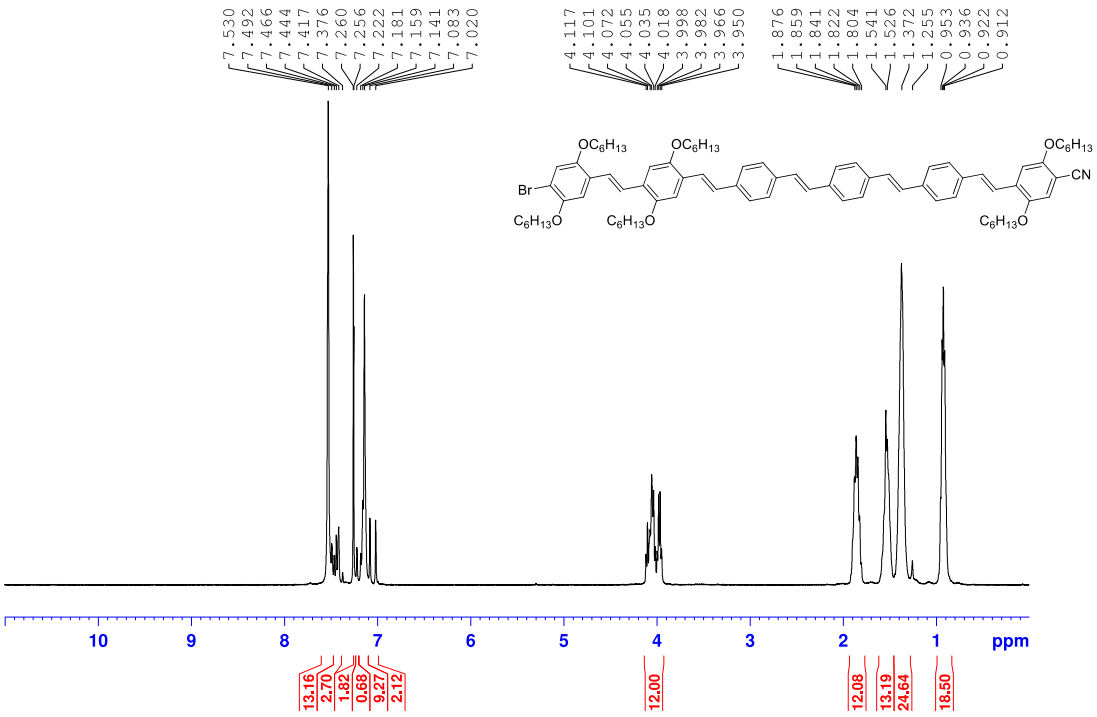
7.530
7.492
7.466
7.444
7.417
7.376
7.260
7.256
7.222
7.181
7.159
7.141
7.083
7.020
4.117
4.101
4.072
4.055
4.035
4.018
3.998
3.982
3.966
3.950
1.876
1.859
1.841
1.822
1.804
1.541
1.526
1.372
1.255
0.953
0.936
0.922
0.912
OC6H13
OC6H13
OC6H13
Br
CN
C6H13O
C6H13O
C6H13O
10
9
8
7
6
5
4
3
2
1
ppm
13.16
2.70
1.82
0.68
9.27
2.12
12.00
12.08
13.19
24.64
18.50

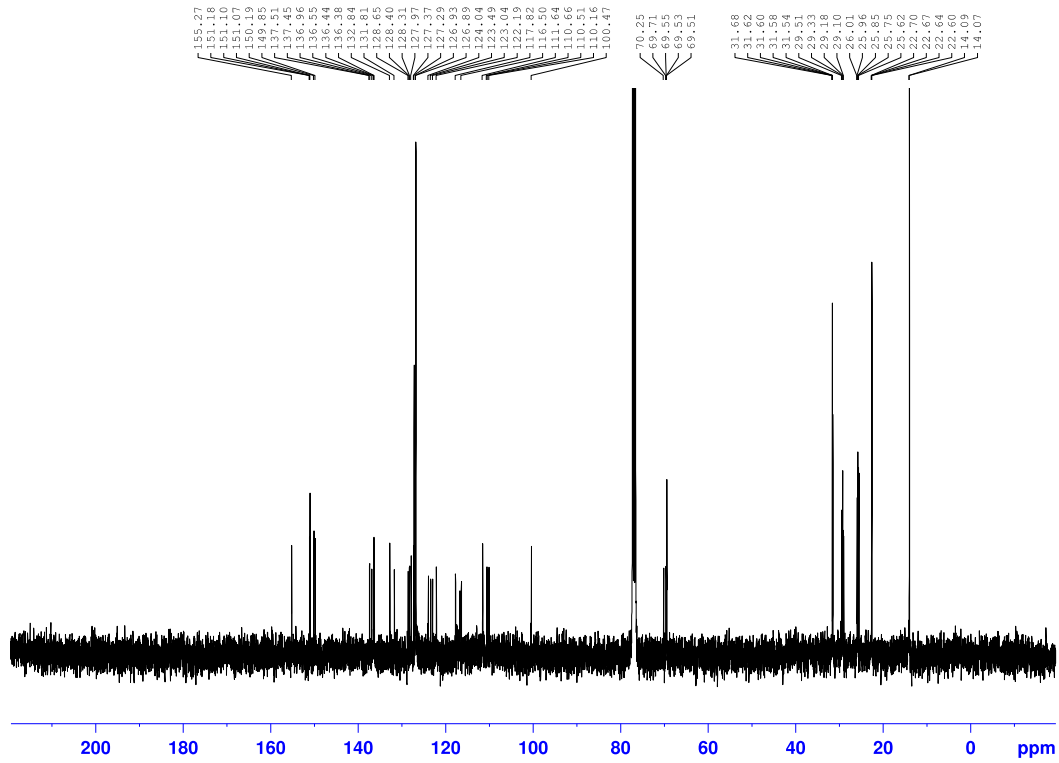
155.27
151.18
151.10
151.07
150.19
149.85
137.51
137.45
136.96
136.35
136.34
136.18
132.84
131.81
128.65
128.40
128.31
127.97
127.37
127.29
126.93
126.89
126.44
123.49
123.04
122.19
117.82
116.50
111.64
110.66
110.51
110.16
100.47
70.25
69.71
69.55
69.53
69.51
31.68
31.62
31.60
31.58
31.54
29.51
29.33
29.18
29.10
26.01
25.96
25.85
25.75
25.62
25.60
22.67
22.64
22.60
14.09
14.07
200
180
160
140
120
100
80
60
40
20
0
ppm

A.2 CYCLIC AND DIFFERENTIAL PULSE VOLTAMMOGRAMS OF OLIGOMERS

Table 15. Peak oxidation and reduction potentials of oligomers

Oligomer	E_{peak}^{Oxd} [a]/ V	E_{peak}^{Red} [a]/ V
Br-AA'-CN	1.45	-1.93, -2.07
Br-BA'-CN	1.06, 1.15	-1.96, -2.07
Br-AB'-CN	1.23, 1.34	-1.94, -2.07
Br-BB'-CN	1.06, 1.36	-2.17
Br-AAB'-CN	1.06, 1.30	-1.94,-2.18
Br-BAA'-CN	0.95, 1.15, 1.44	-1.93, -2.18
Br-BAB'-CN	0.97, 1.18, 1.32	-1.97, -2.23
Br-ABA'-CN	0.84, 1.23	-1.92, -2.16
Br-ABB'-CN	0.81, 1.02, 1.24	-1.93, -2.16
Br-BBA'-CN	0.78, 1.04, 1.24, 1.41	-1.94, -2.17
Br-BAAB'-CN	0.87, 1.02, 1.19, 1.39	-1.94, -2.04,-2.27,-2.49,-2.7, -2.83
Br-ABAB'-CN	0.69, 1.13, 1.24	–2.02, -2.31, -2.58, -2.76, -2.87
Br-BABA'-CN	0.69, 0.98, 1.18	-1.98, -2.11, -2.33, -2.53, -2.66, -2.84
Br-BBAA'-CN	0.65, 0.83, 0.97, 1.04, 1.19, 1.36	-1.99, -2.11, -2.29, -2.53, -2.80
Br-AABB'-CN	0.70, 1.01, 1.14, 1.34	-1.99, -2.31, -2.63, -2.81
Br-ABBA'-CN	0.67, 0.87, 0.97, 1.04, 1.23	-1.95, -2.14, -2.24, -2.45,-2.59, -2.75
Br-AABBB'-CN	0.63, 0.74, 0.85, 0.98,1.18, 1.39	-1.97, -2.17, -2.27, -2.44, -2.64
Br-BABAB'-CN	0.7, 0.88, 0.96, 1.08, 1.2, 1.29	-1.96, -2.17, -2.26, -2.42, -2.7, -2.8
Br-BBAAA'-CN	0.69, 0.89, 1.16, 1.22, 1.43	-1.96, -2.11, -2.25, -2.4, -2.67, -2.74, -3.04
Br-AABBBA'-CN	0.54, 0.81,1.06, 1.27,1.47	-1.92, -2.12, -2.26, -2.4, -2.65, -2.76, -3.06
Br-BABABA'-CN	0.64, 1.18, 1.26, 1.44	-1.94, -2.14, -2.26, -2.4, -2.67, -2.79, -3.08
Br-BBAAAB'-CN	0.67, 0.86,0.97, 1.05,1.3	-1.99, -2.13, -2.42, -2.49, -2.7, -2.87

[a] Potential vs. Ag/Ag^+, 240μM in 0.1 M Bu_4NPF_6 in THF

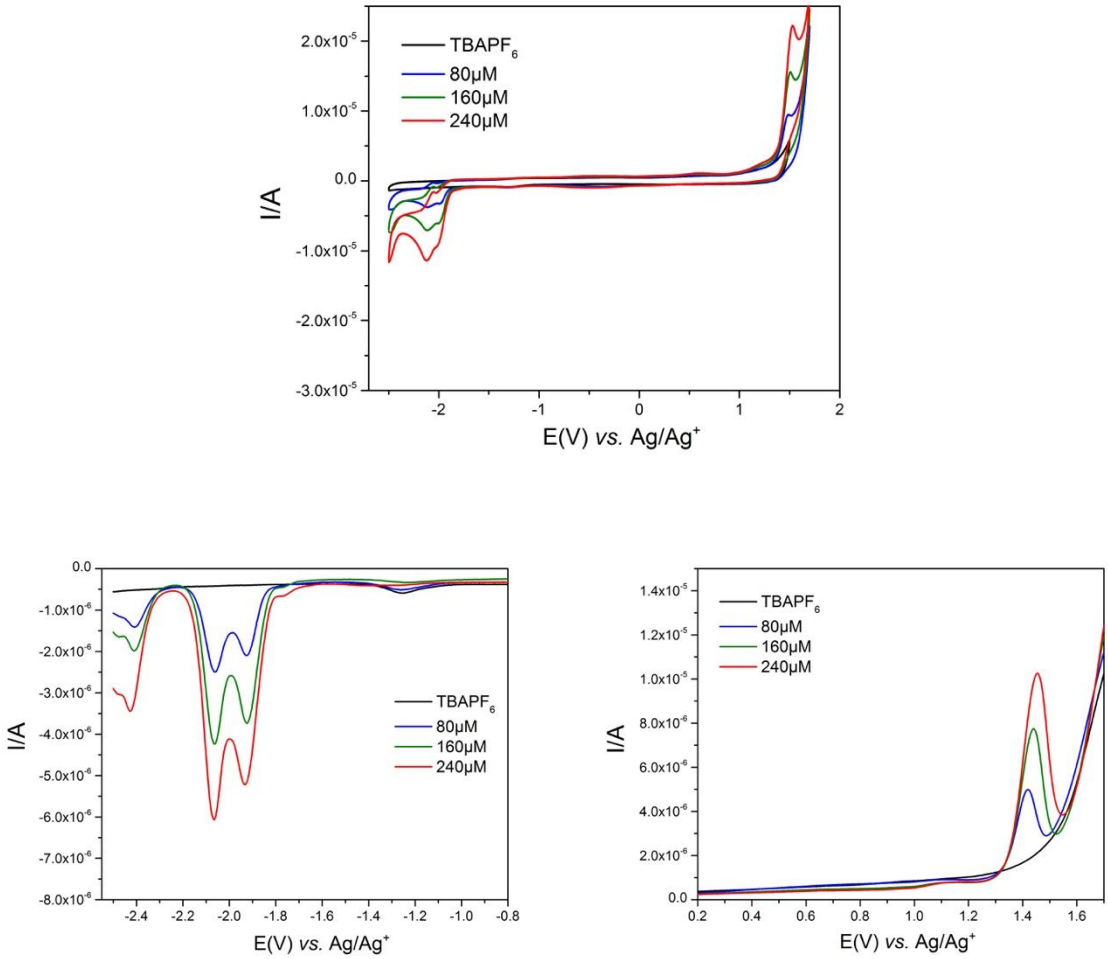

Figure 41. Top: Cyclic voltammograms of Br-AA'-CN in THF. Bottom: Differential pulse voltammograms of Br-AA'-CN in THF. Left: reduction. Right: oxidation.

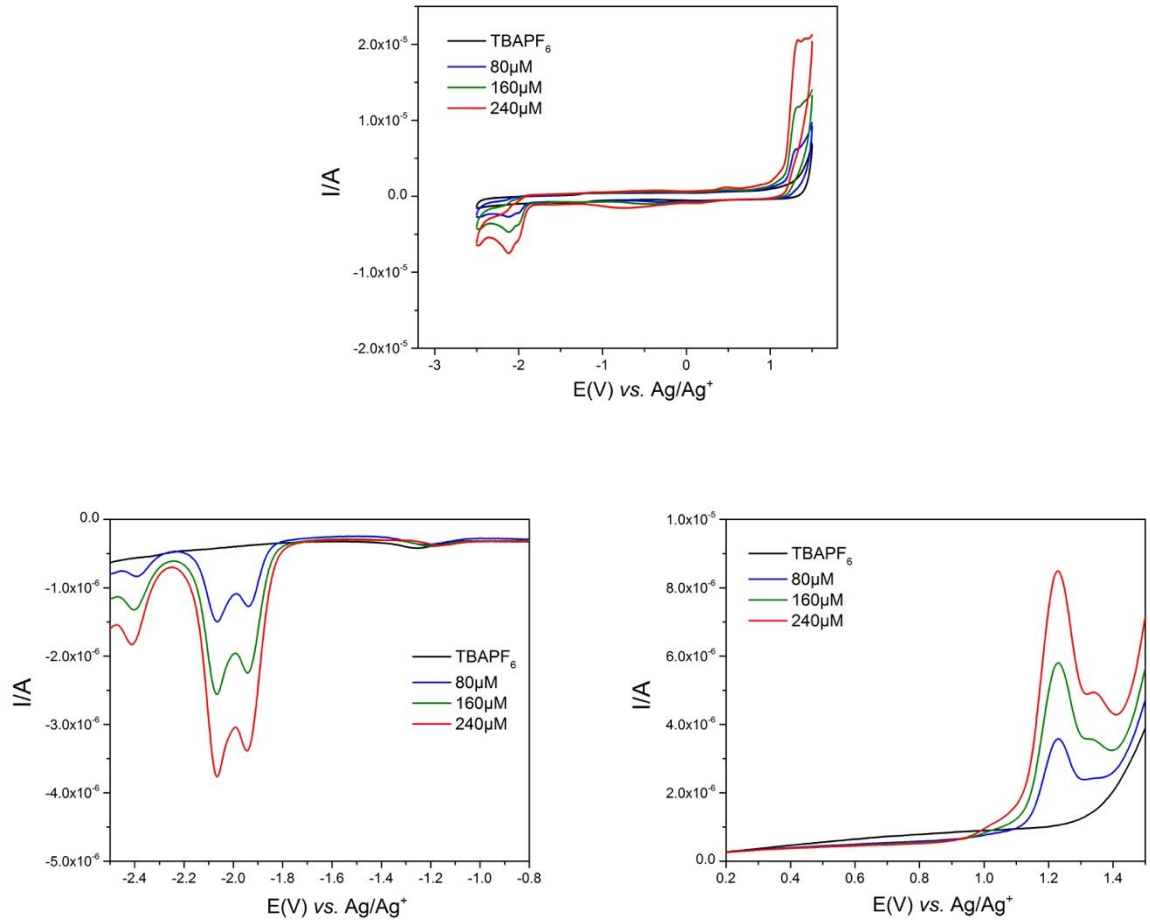

Figure 42. Top: Cyclic voltammograms of Br-AB'-CN in THF. Bottom: Differential pulse voltammograms of Br-AB'-CN in THF. Left: reduction. Right: oxidation.

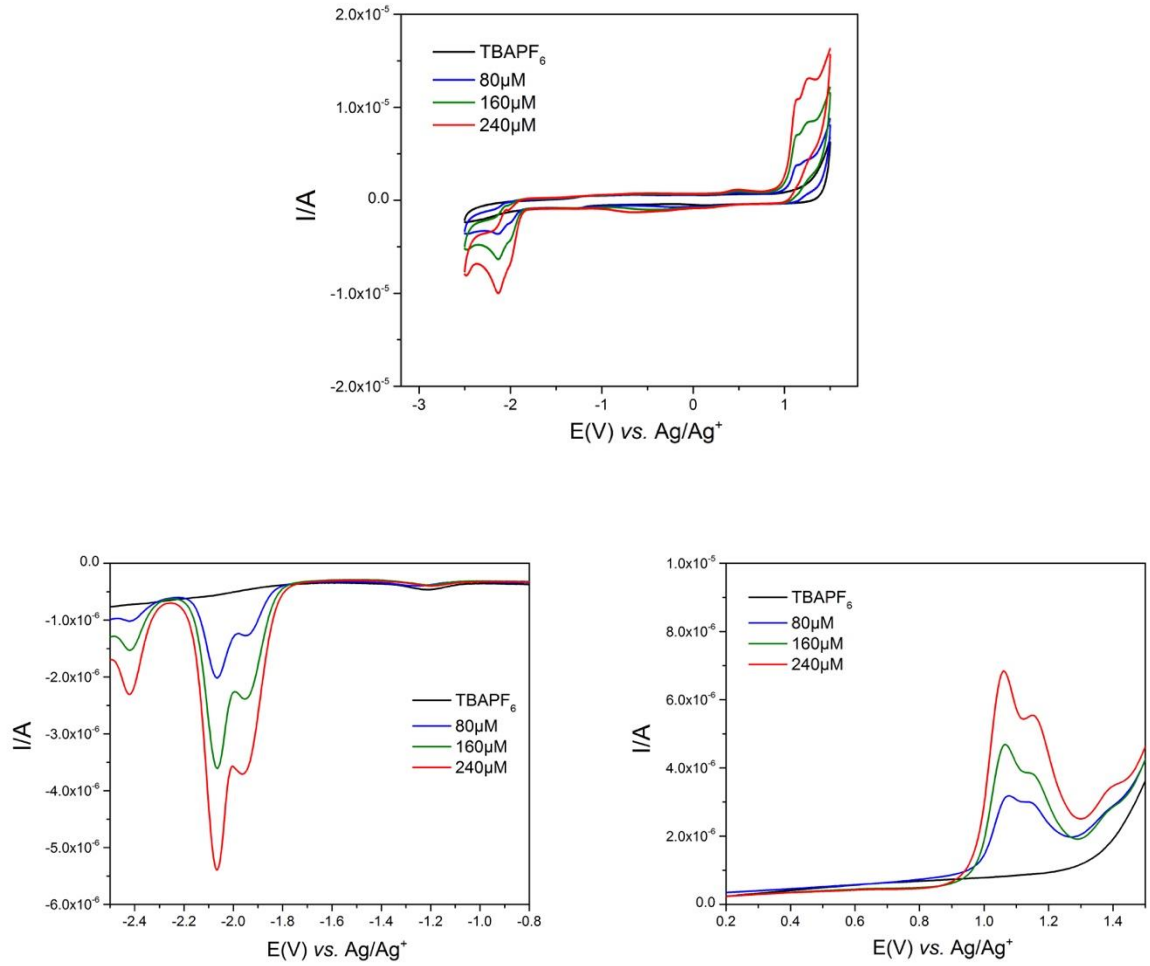

Figure 43. Top: Cyclic voltammograms of Br-BA'-CN in THF. Bottom: Differential pulse voltammograms of Br-BA'-CN in THF. Left: reduction. Right: oxidation.

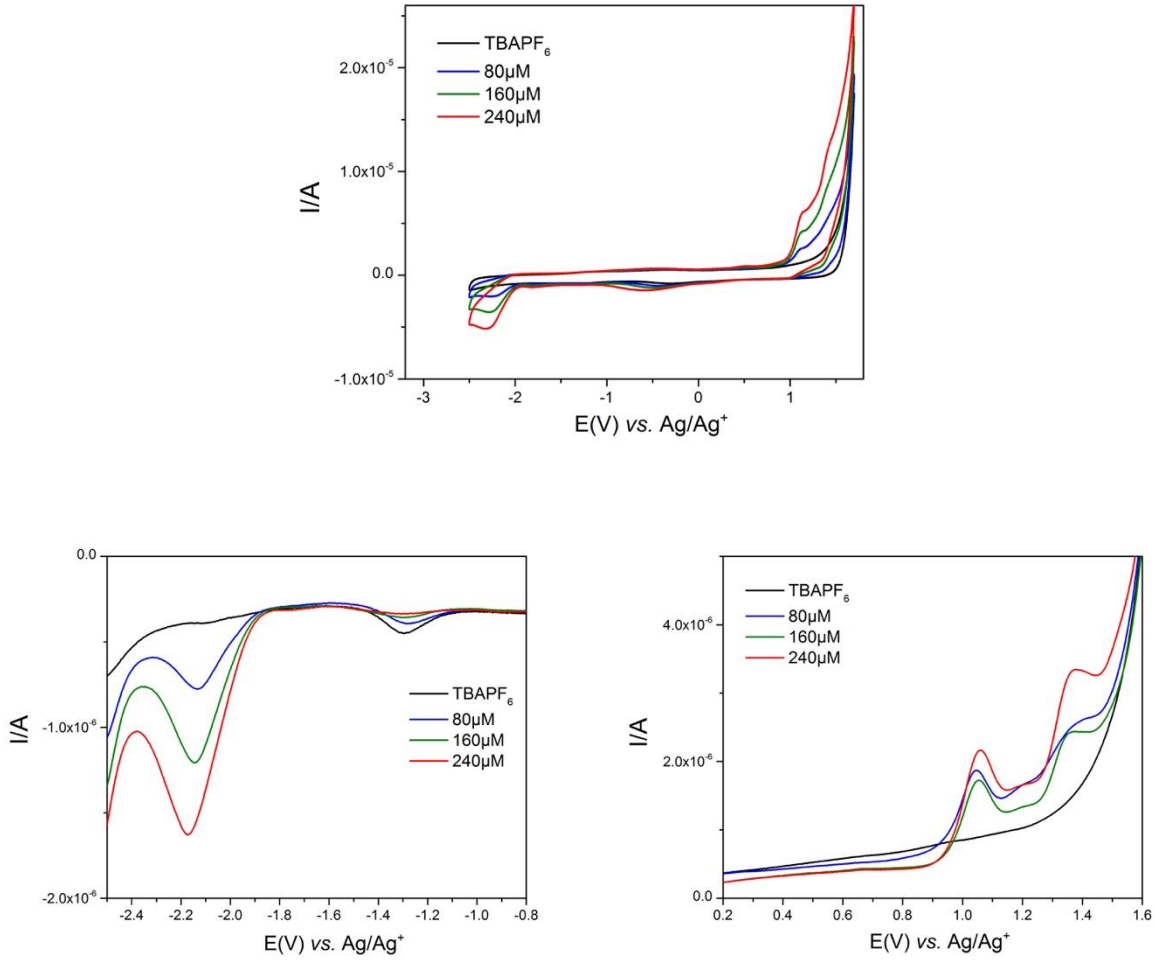

Figure 44. Top: Cyclic voltammograms of Br-BB'-CN in THF. Bottom: Differential pulse voltammograms of Br-BB'-CN in THF. Left: reduction. Right: oxidation.

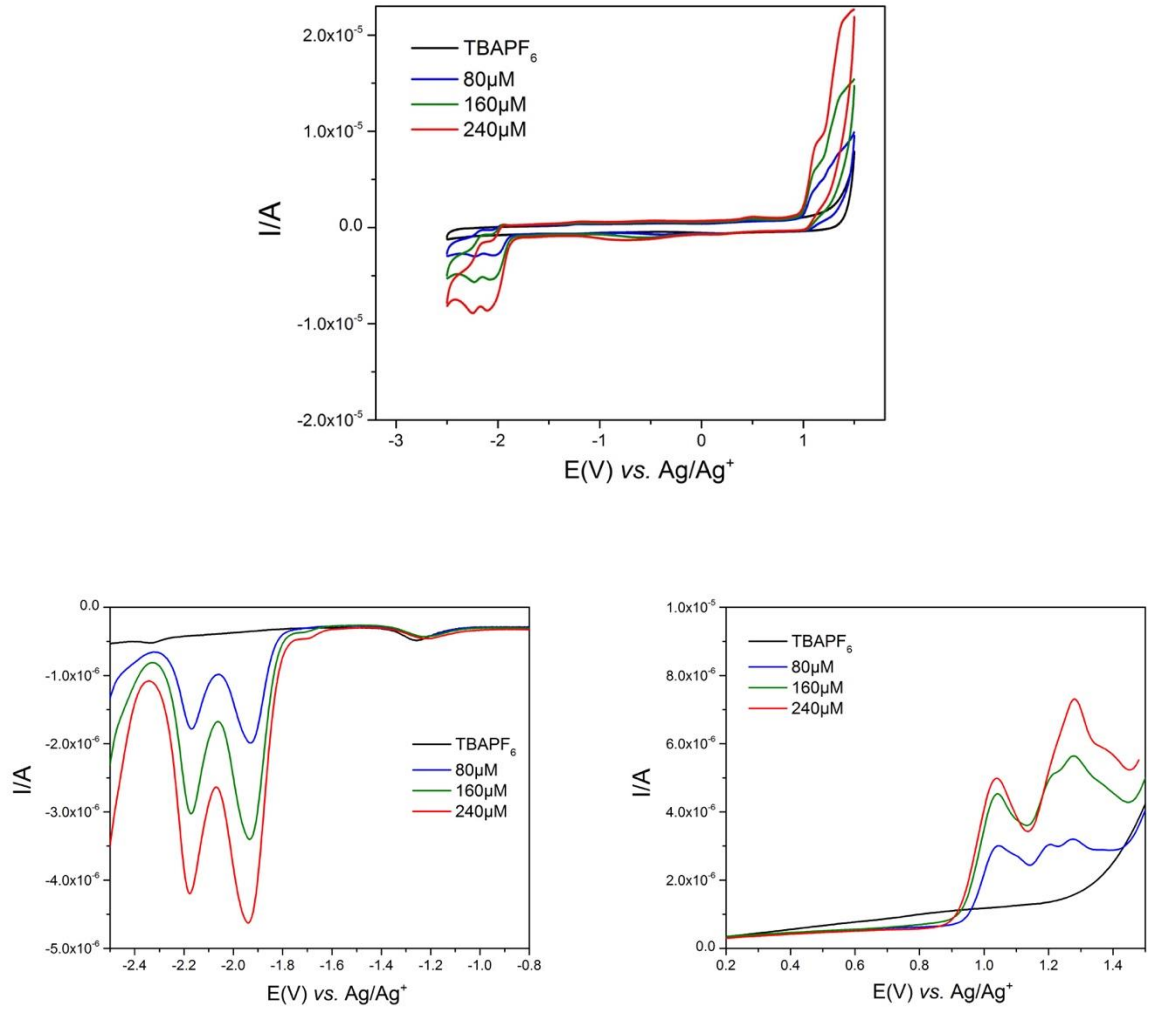

Figure 45. Top: Cyclic voltammograms of Br-AAB'-CN in THF. Bottom: Differential pulse voltammograms of Br-AAB'-CN in THF. Left: reduction. Right: oxidation.

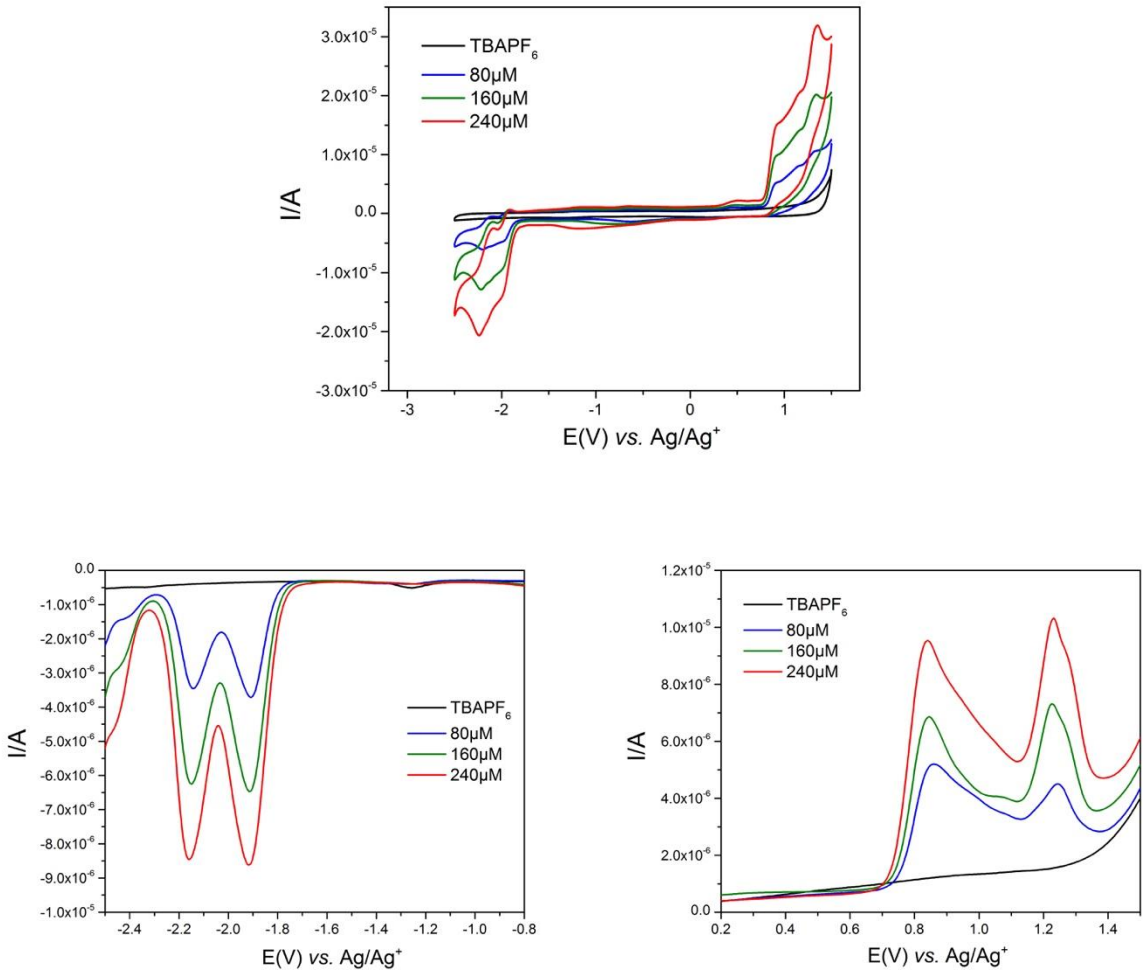

Figure 46. Top: Cyclic voltammograms of Br-ABA'-CN in THF. Bottom: Differential pulse voltammograms of Br-ABA'-CN in THF. Left: reduction. Right: oxidation.

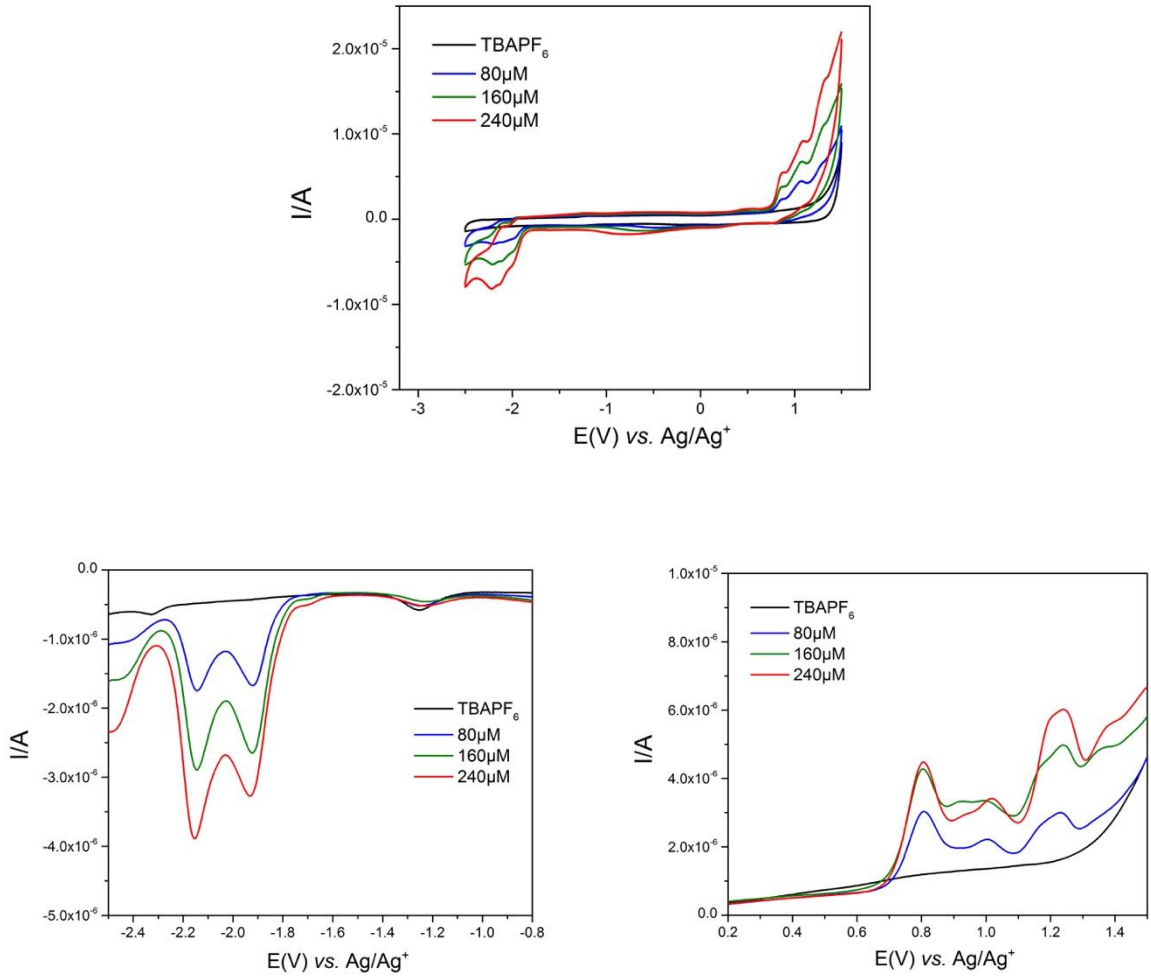

Figure 47. Top: Cyclic voltammograms of Br-ABB'-CN in THF. Bottom: Differential pulse voltammograms of Br-ABB'-CN in THF. Left: reduction. Right: oxidation.

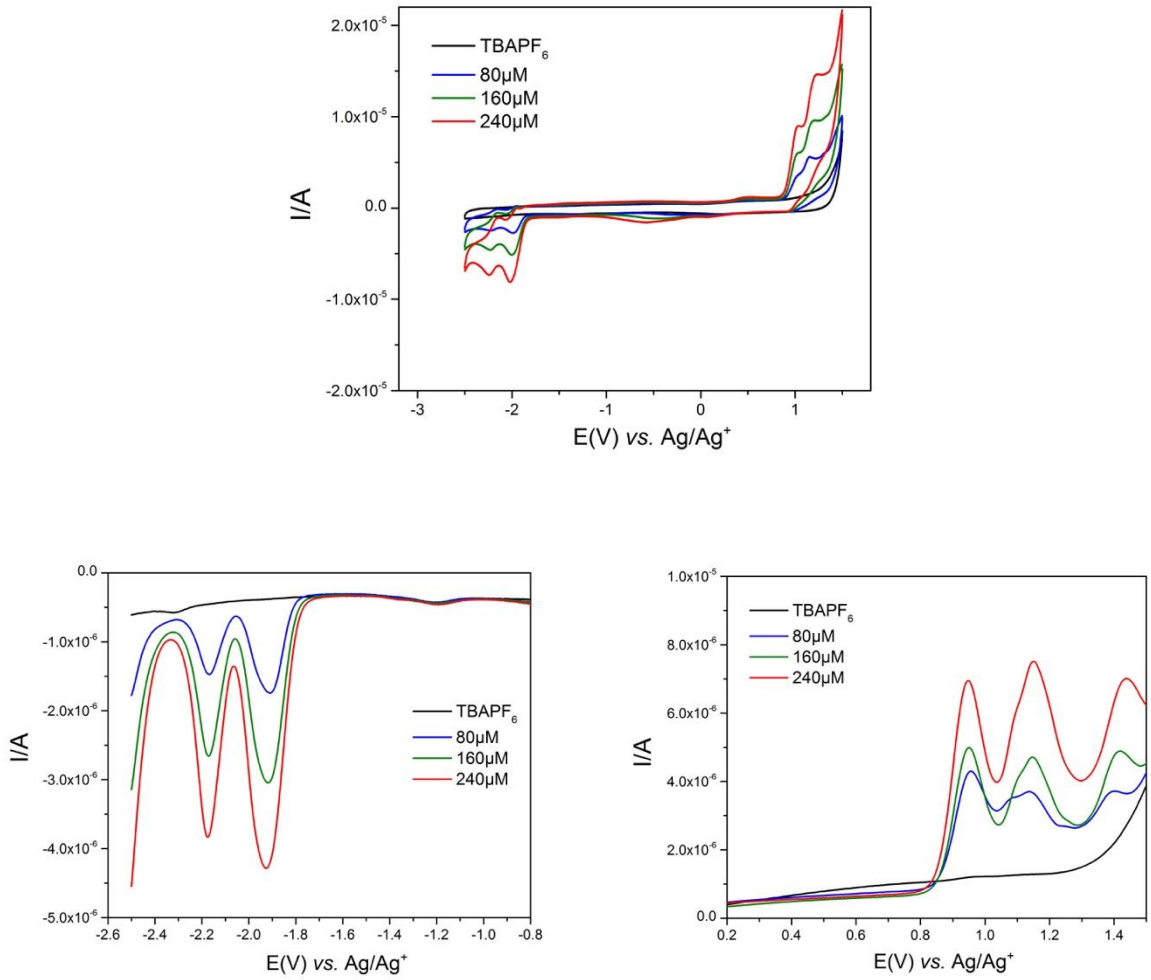

Figure 48. Top: Cyclic voltammograms of Br-BAA'-CN in THF. Bottom: Differential pulse voltammograms of Br-BAA'-CN in THF. Left: reduction. Right: oxidation**.**

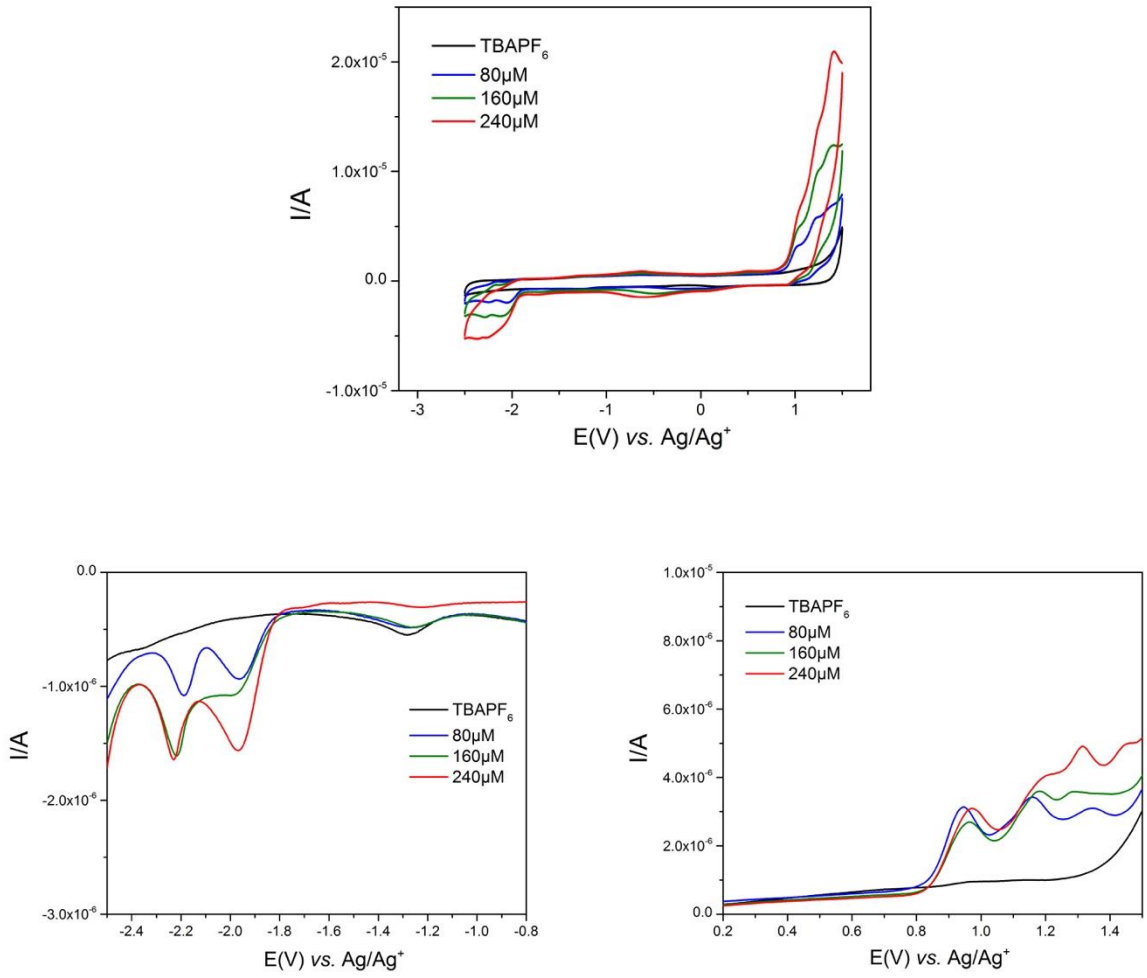

Figure 49. Top: Cyclic voltammograms of Br-BAB'-CN in THF. Bottom: Differential pulse voltammograms of Br-BAB'-CN in THF. Left: reduction. Right: oxidation.

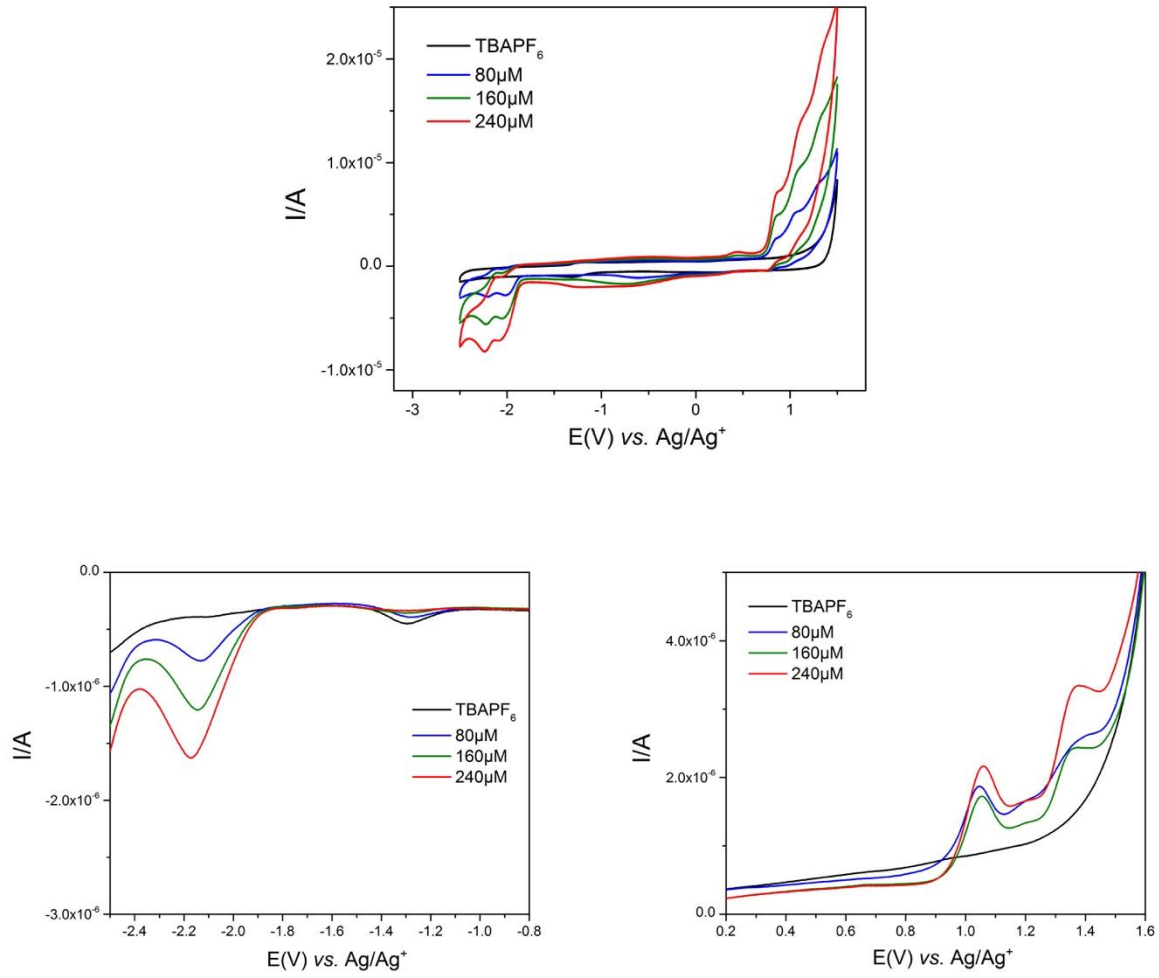

Figure 50. Top: Cyclic voltammograms of Br-BBA'-CN in THF. Bottom: Differential pulse voltammograms of Br-BBA'-CN in THF. Left: reduction. Right: oxidation.

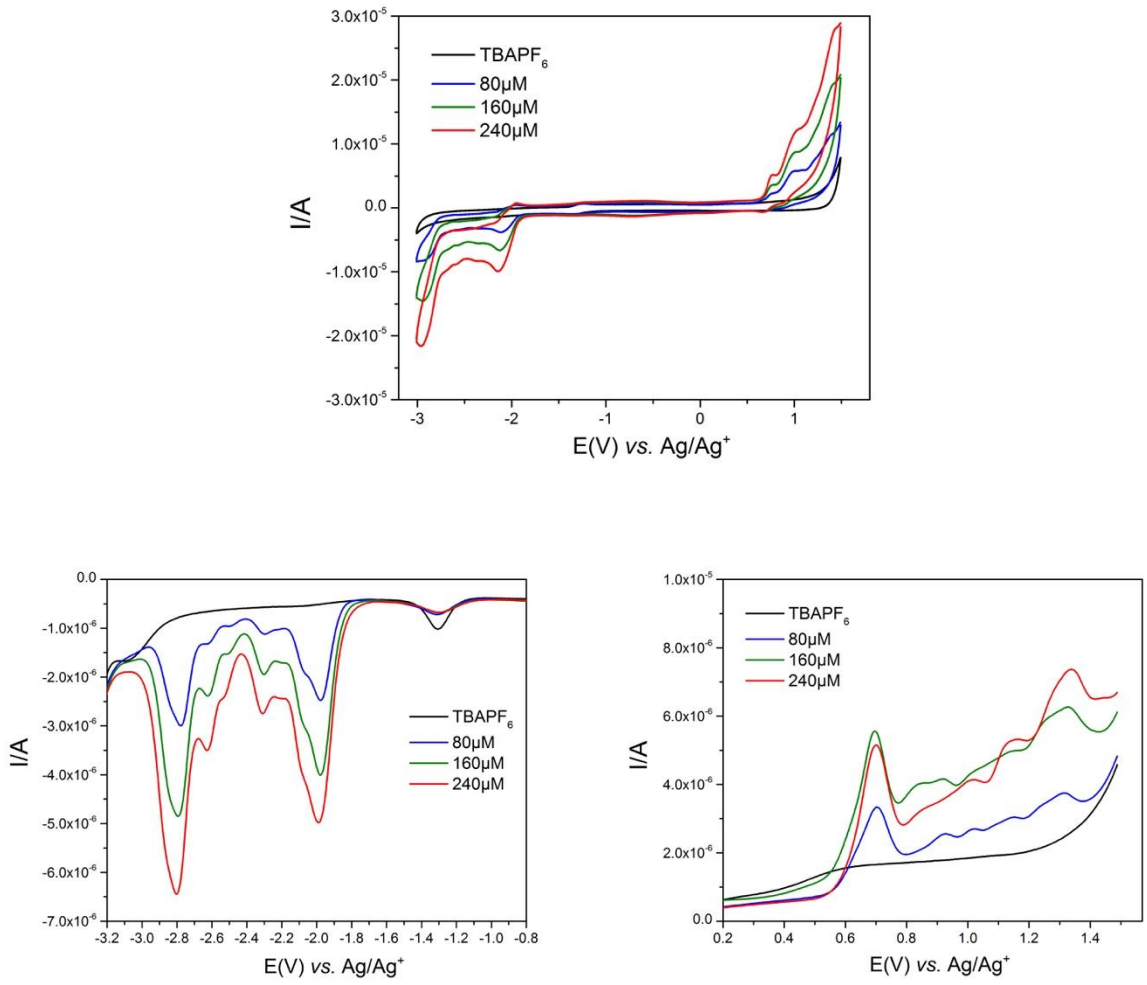

Figure 51. Top: Cyclic voltammograms of Br-AABB'-CN in THF. Bottom: Differential pulse voltammograms of Br-AABB'-CN in THF. Left: reduction. Right: oxidation.

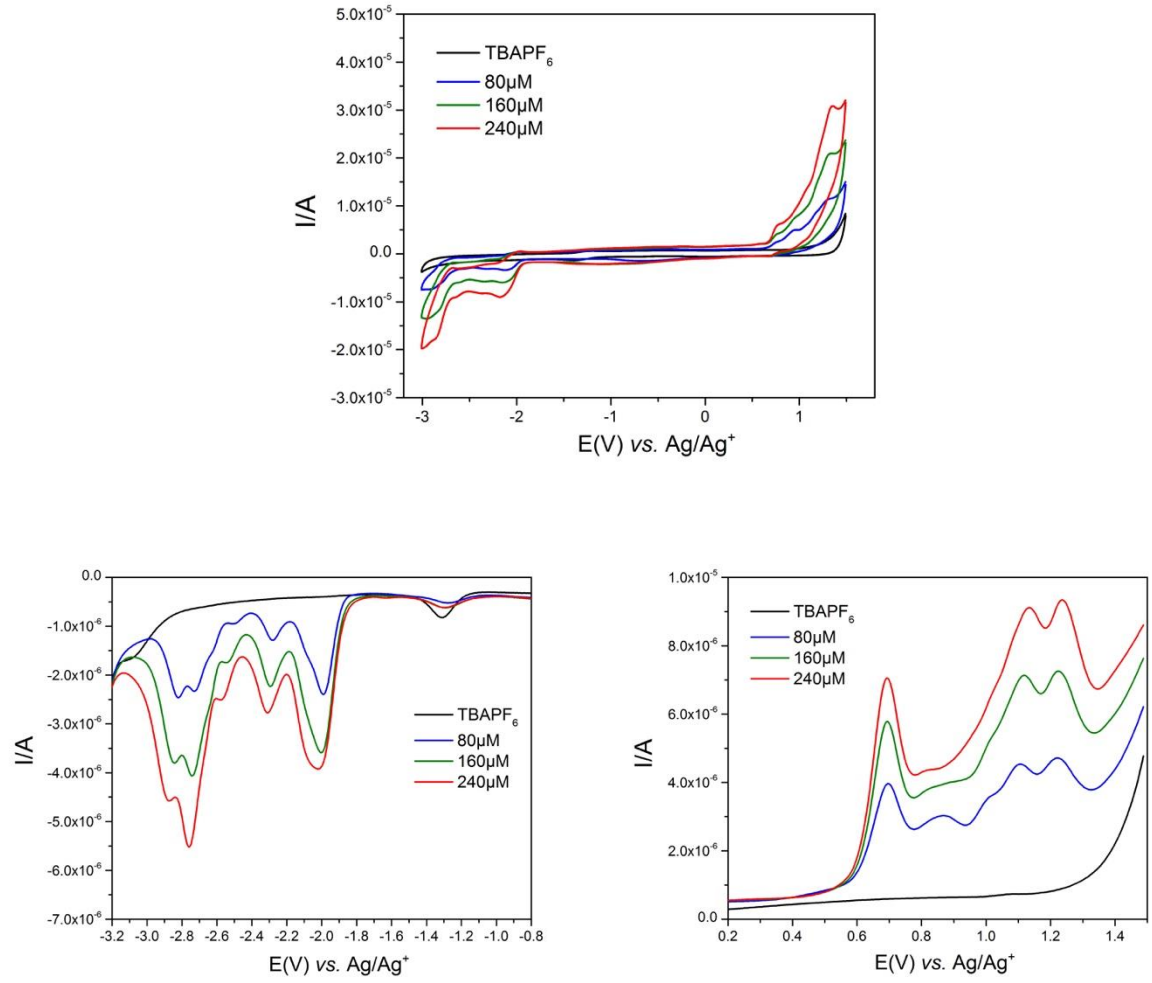

Figure 52. Top: Cyclic voltammograms of Br-ABAB'-CN in THF. Bottom: Differential pulse voltammograms of Br-AABB'-CN in THF. Left: reduction. Right: oxidation.

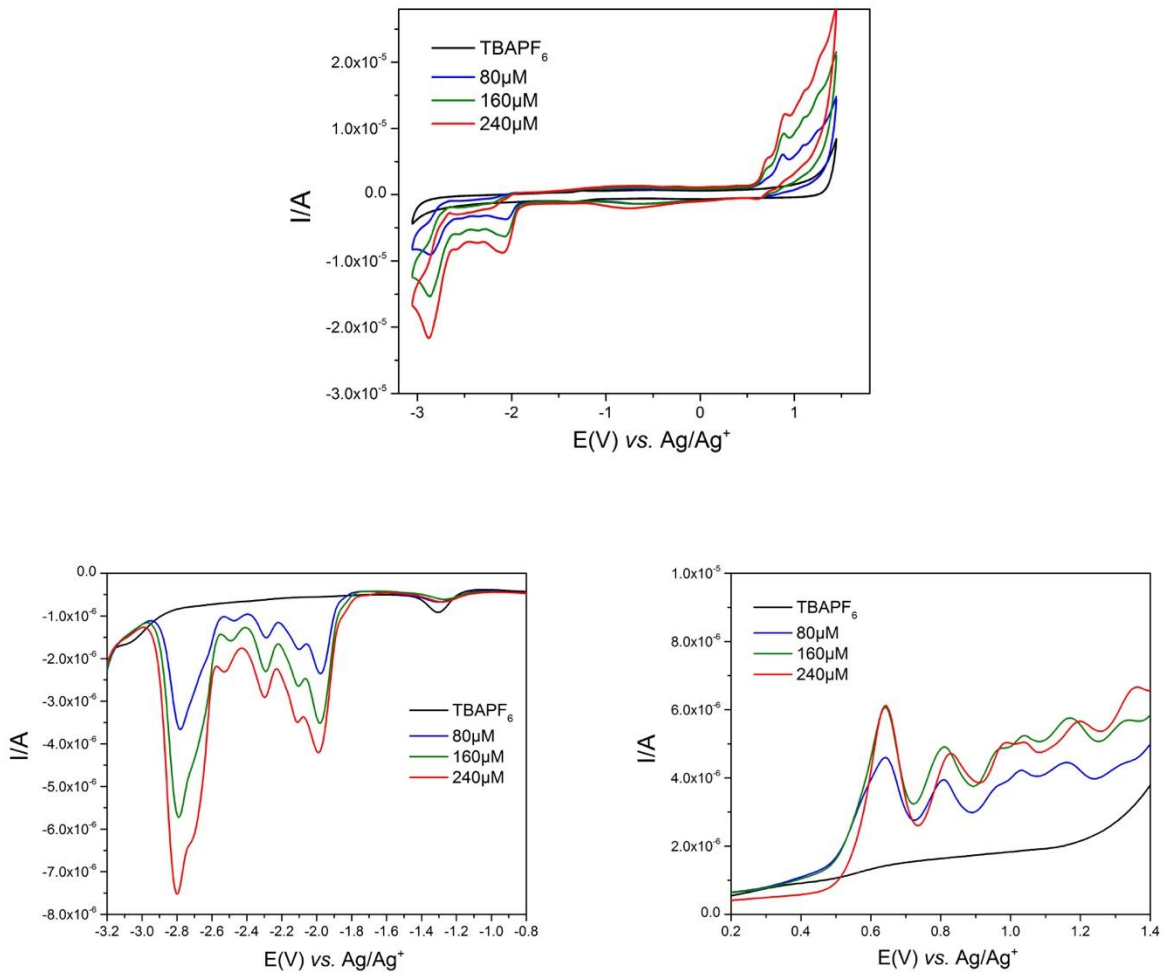

Figure 53. Top: Cyclic voltammograms of Br-BBAA'-CN in THF. Bottom: Differential pulse voltammograms of Br-BBAA'-CN in THF. Left: reduction. Right: oxidation.

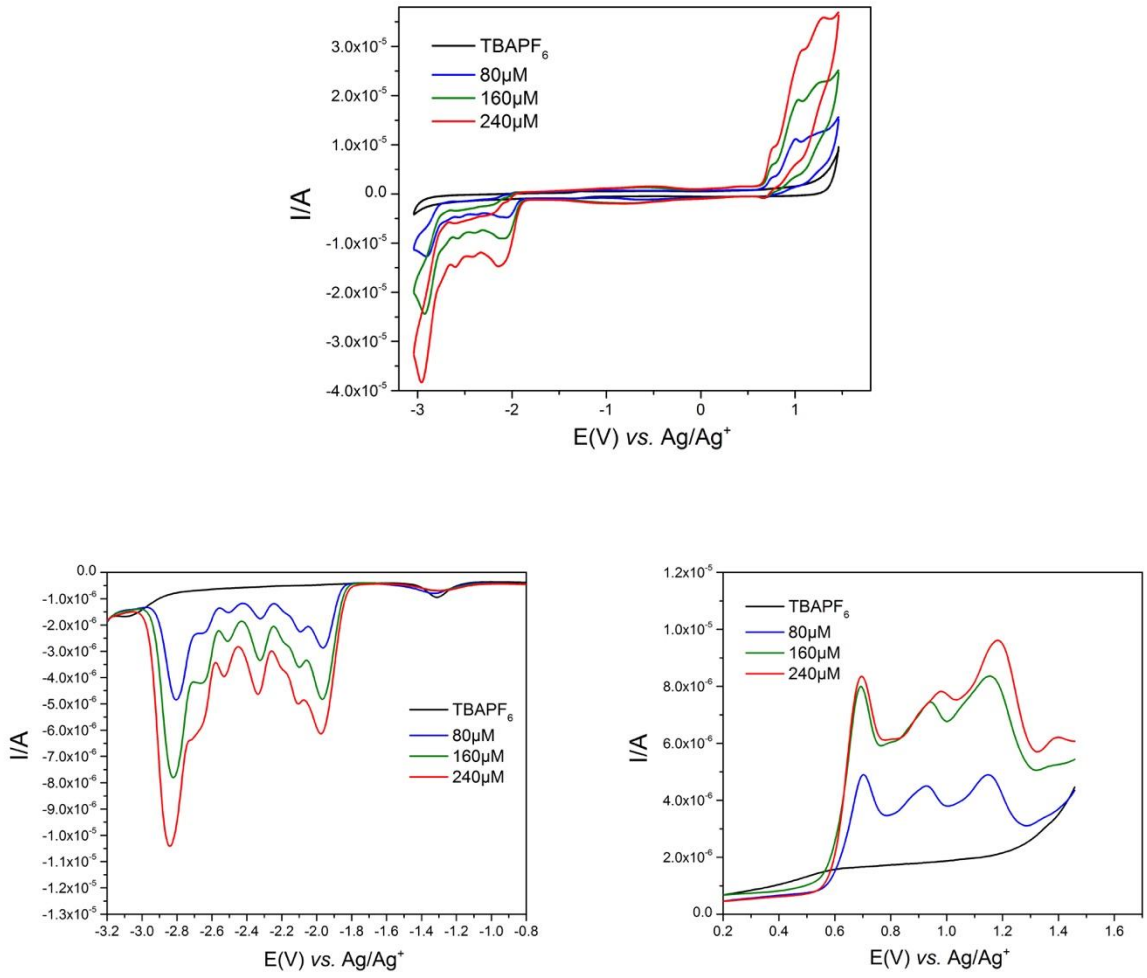

Figure 54. Top: Cyclic voltammograms of Br-BABA'-CN in THF. Bottom: Differential pulse voltammograms of Br-BABA'-CN in THF. Left: reduction. Right: oxidation.

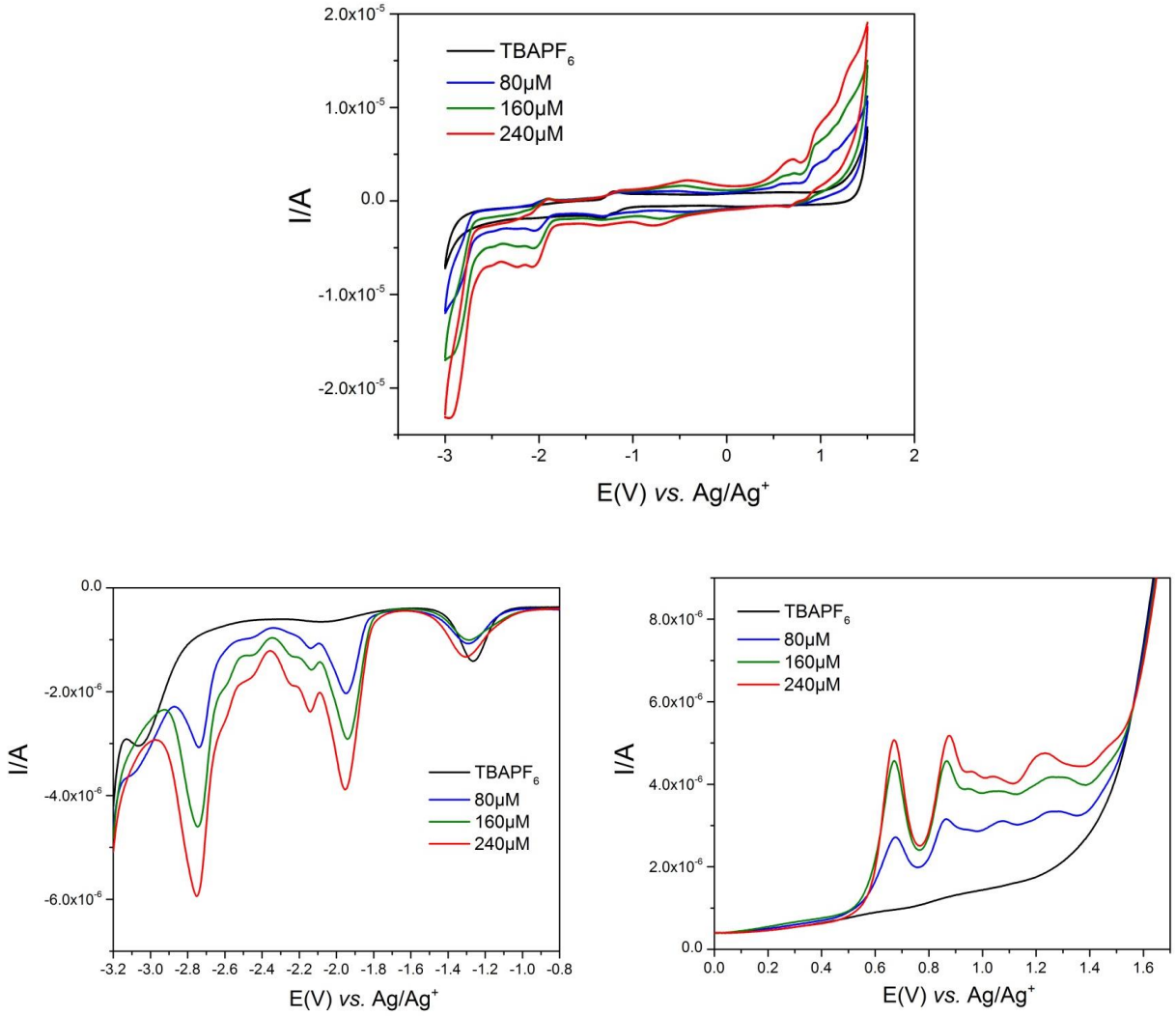

Figure 55. Top: Cyclic voltammograms of Br-ABBA'-CN in THF. Bottom: Differential pulse voltammograms of Br-ABBA'-CN in THF. Left: reduction. Right: oxidation.

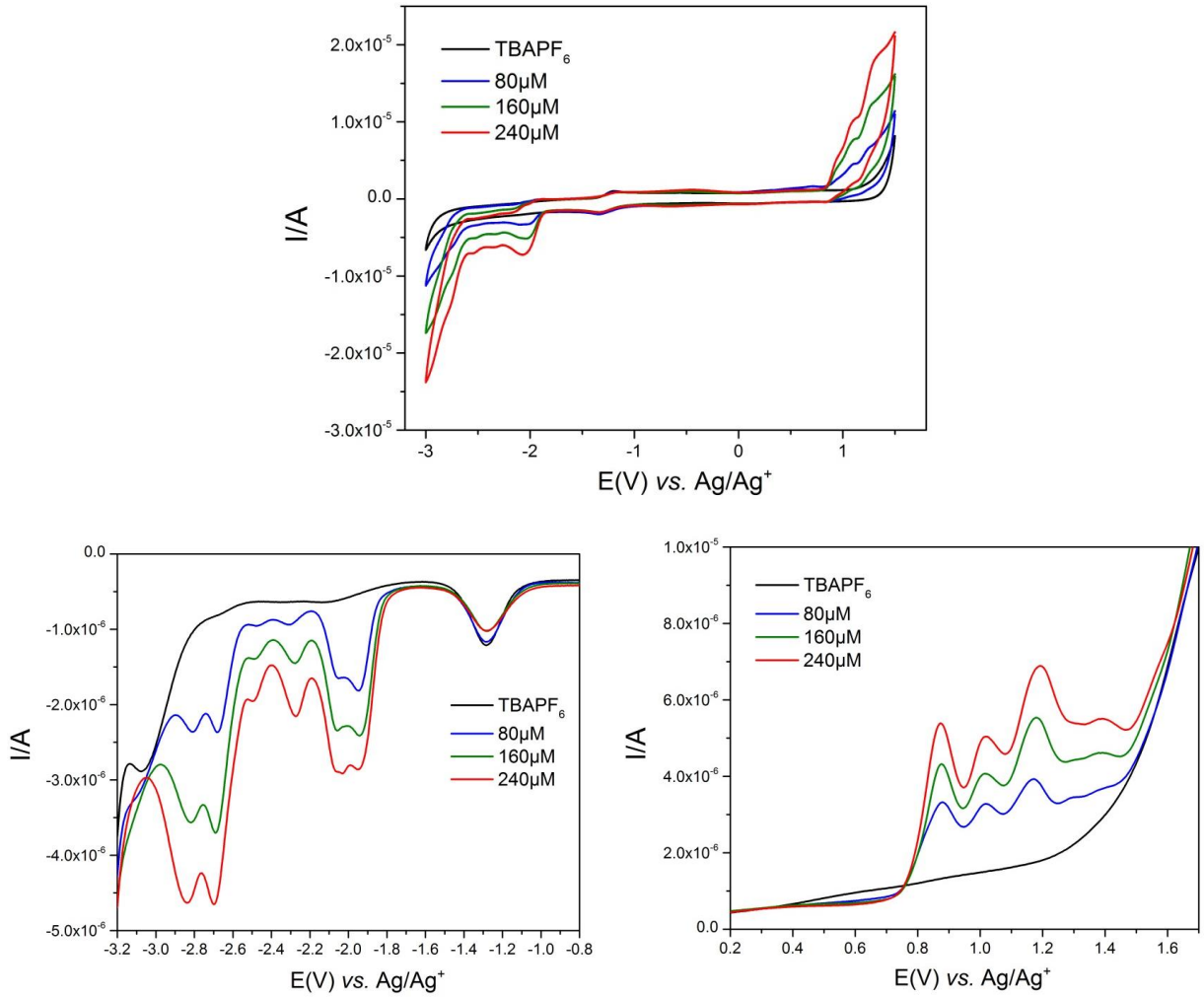

Figure 56. Top: Cyclic voltammograms of Br-BAAB'-CN in THF. Bottom: Differential pulse voltammograms of Br-BAAB'-CN in THF. Left: reduction. Right: oxidation.

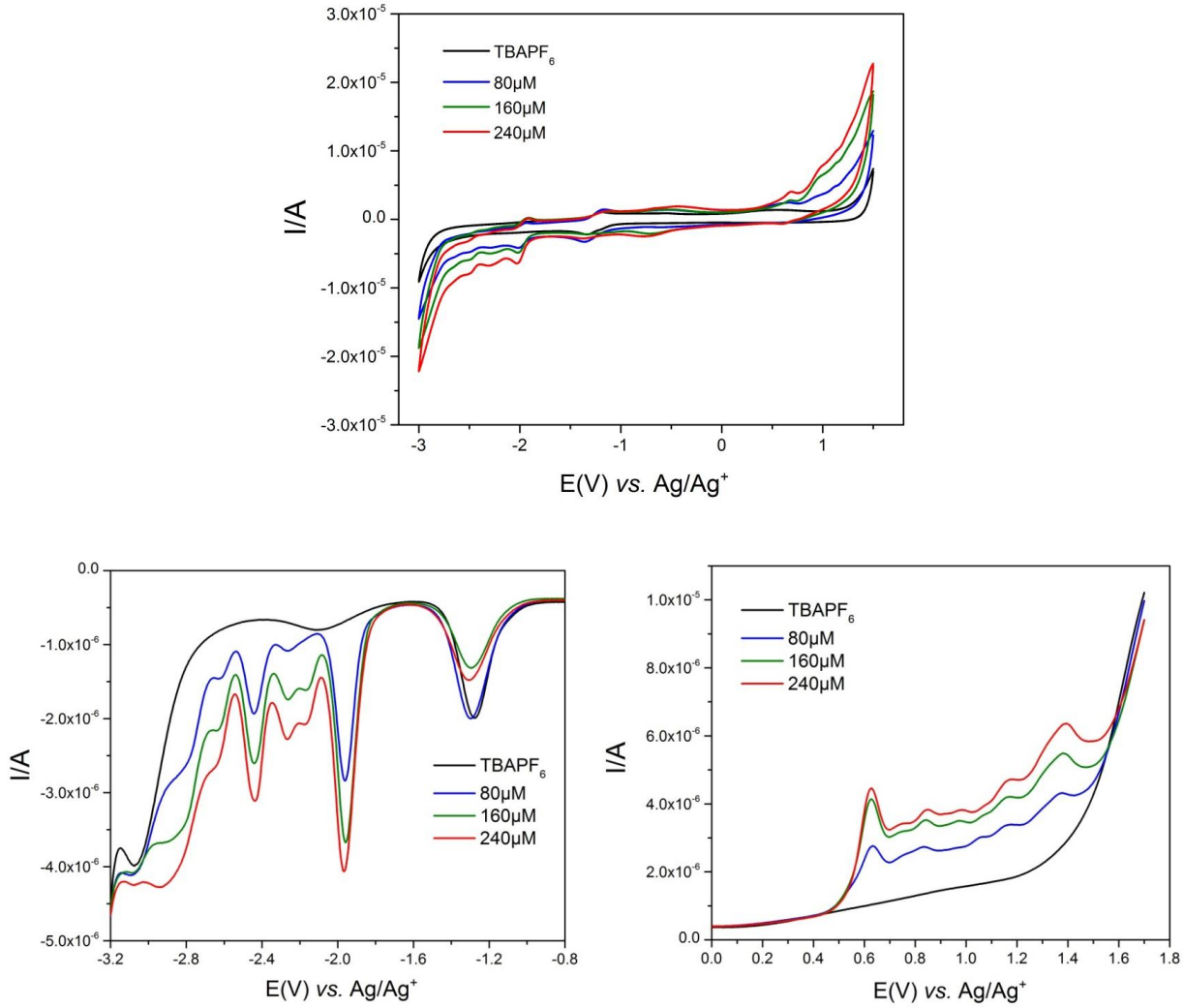

Figure 57. Top: Cyclic voltammograms of Br-AABBB'-CN in THF. Bottom: Differential pulse voltammograms of Br-AABBB'-CN in THF. Left: reduction. Right: oxidation.

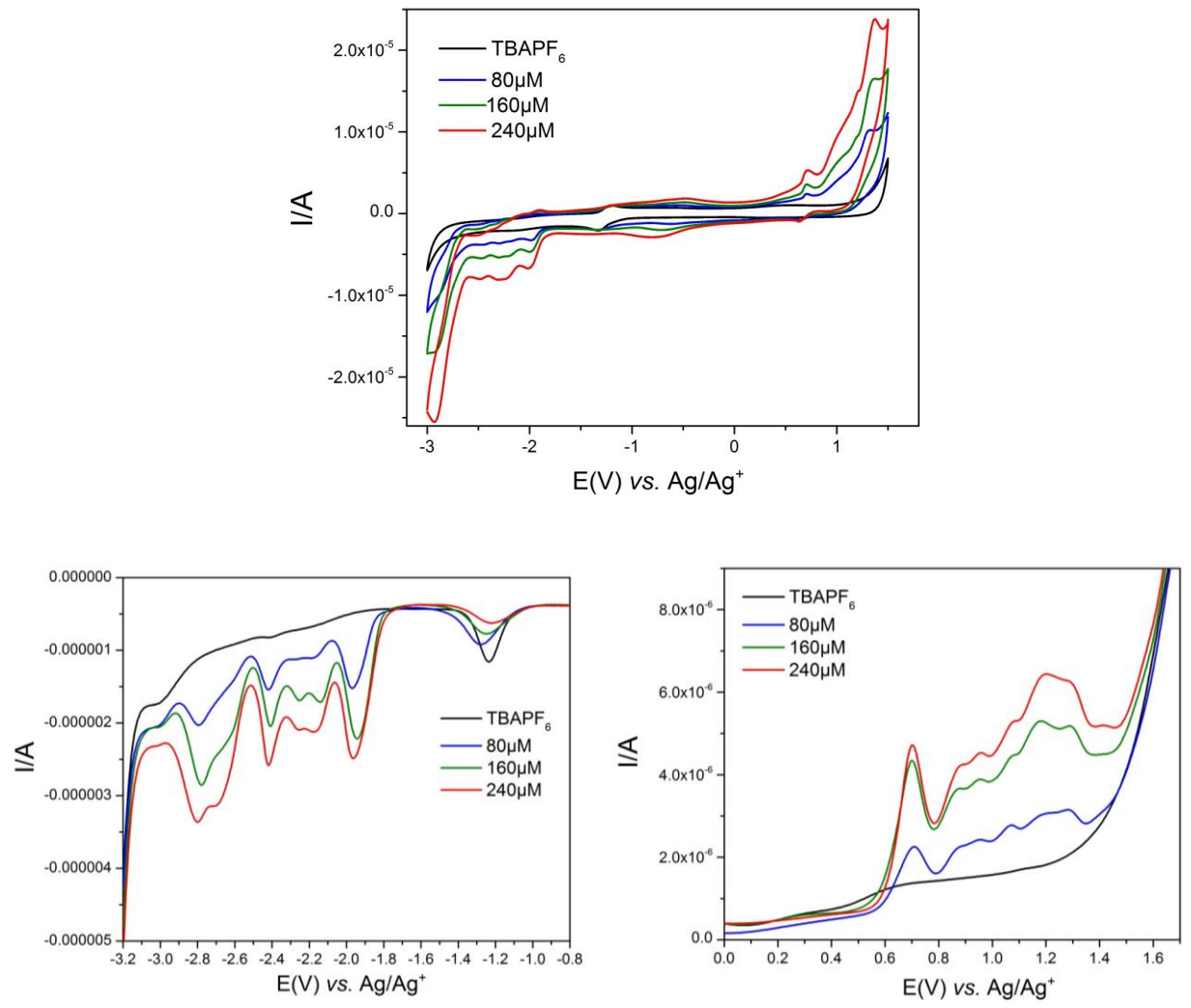

Figure 58. Top: Cyclic voltammograms of Br-BABAB'-CN in THF. Bottom: Differential pulse voltammograms of Br-BABAB'-CN in THF. Left: reduction. Right: oxidation.

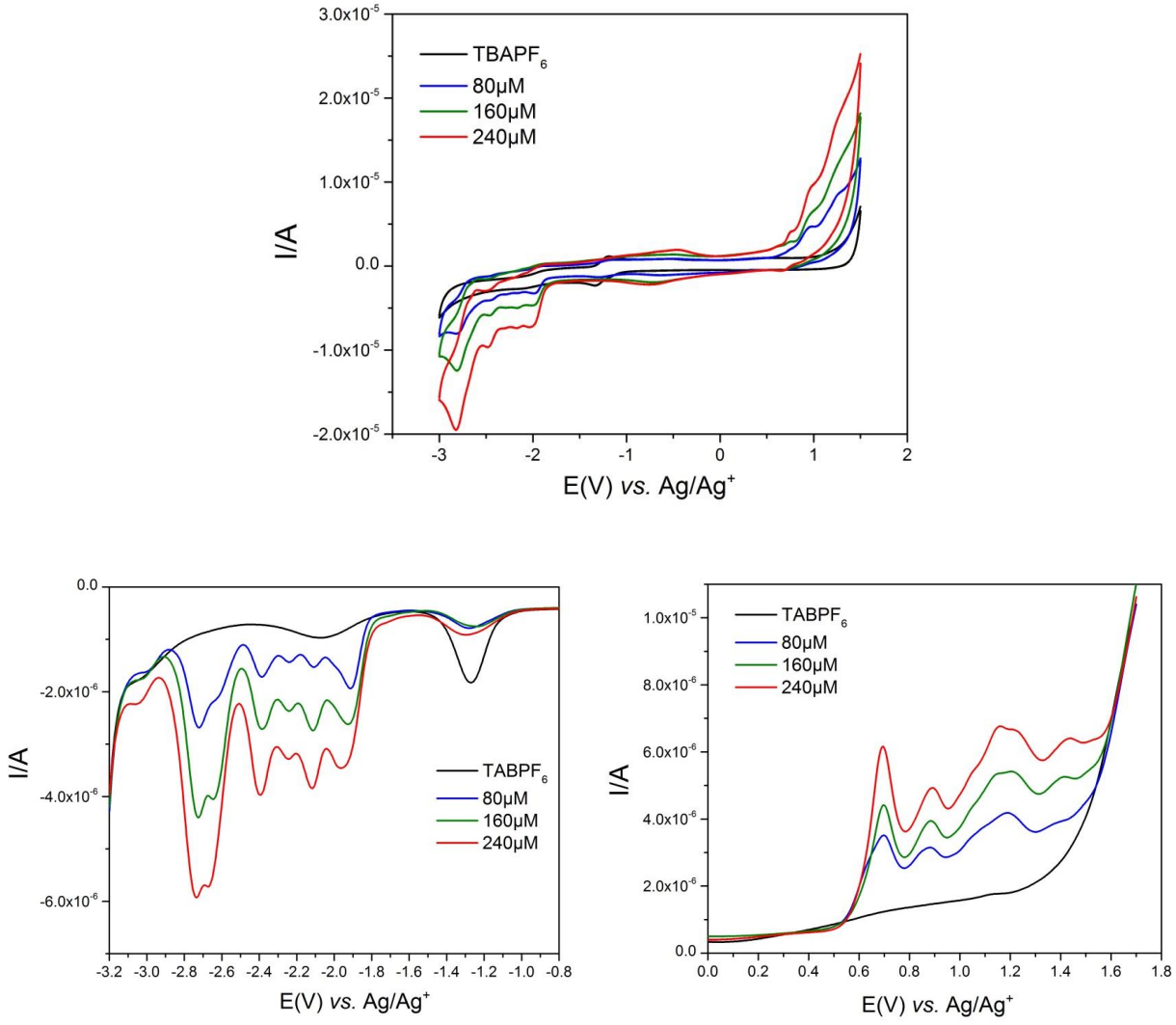

Figure 59. Top: Cyclic voltammograms of Br-BBAAA'-CN in THF. Bottom: Differential pulse voltammograms of Br-BBAAA'-CN in THF. Left: reduction. Right: oxidation.

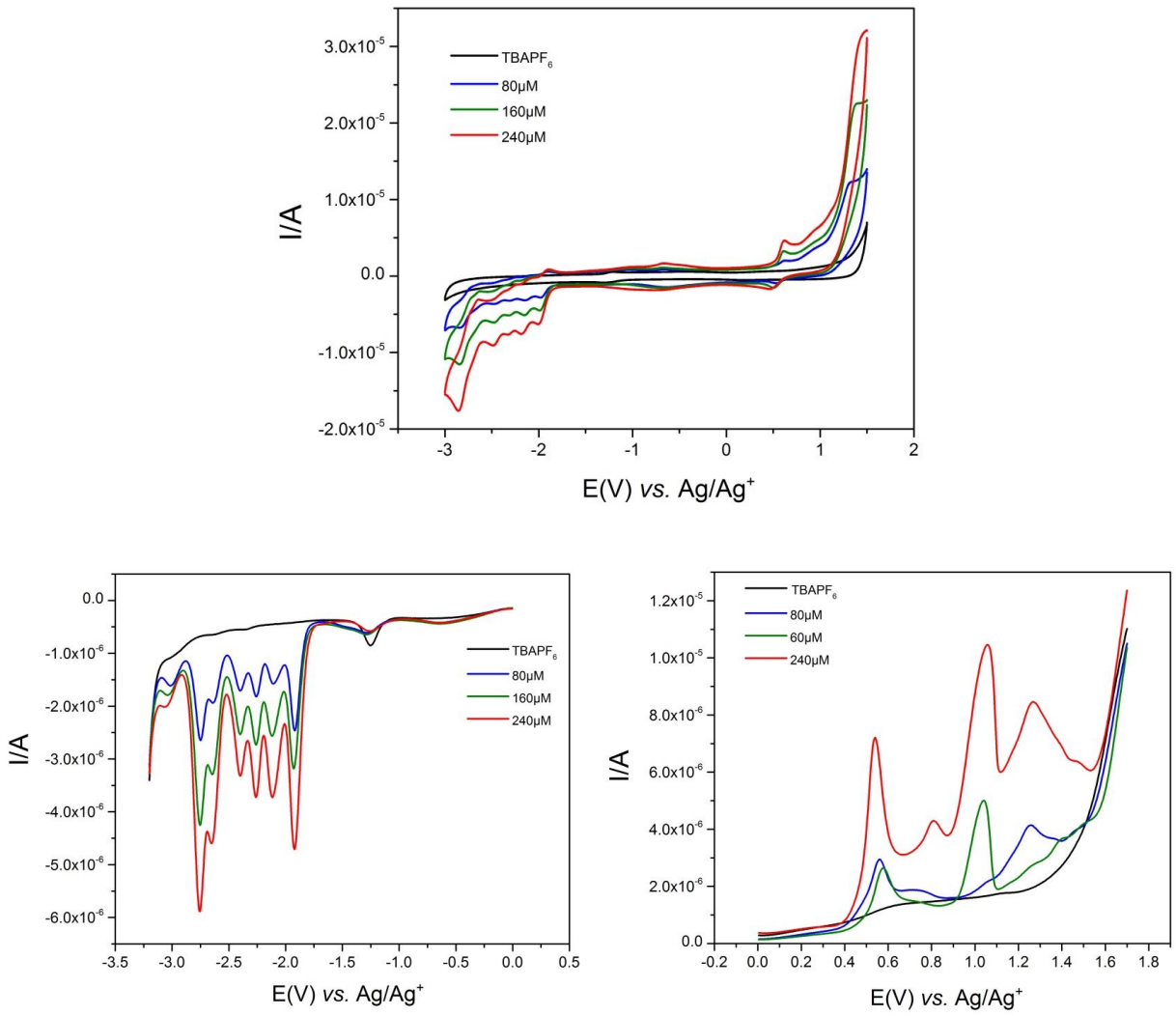

Figure 60. Top: Cyclic voltammograms of Br-AABBBA'-CN in THF. Bottom: Differential pulse voltammograms of Br-AABBBA'-CN in THF. Left: reduction. Right: oxidation.

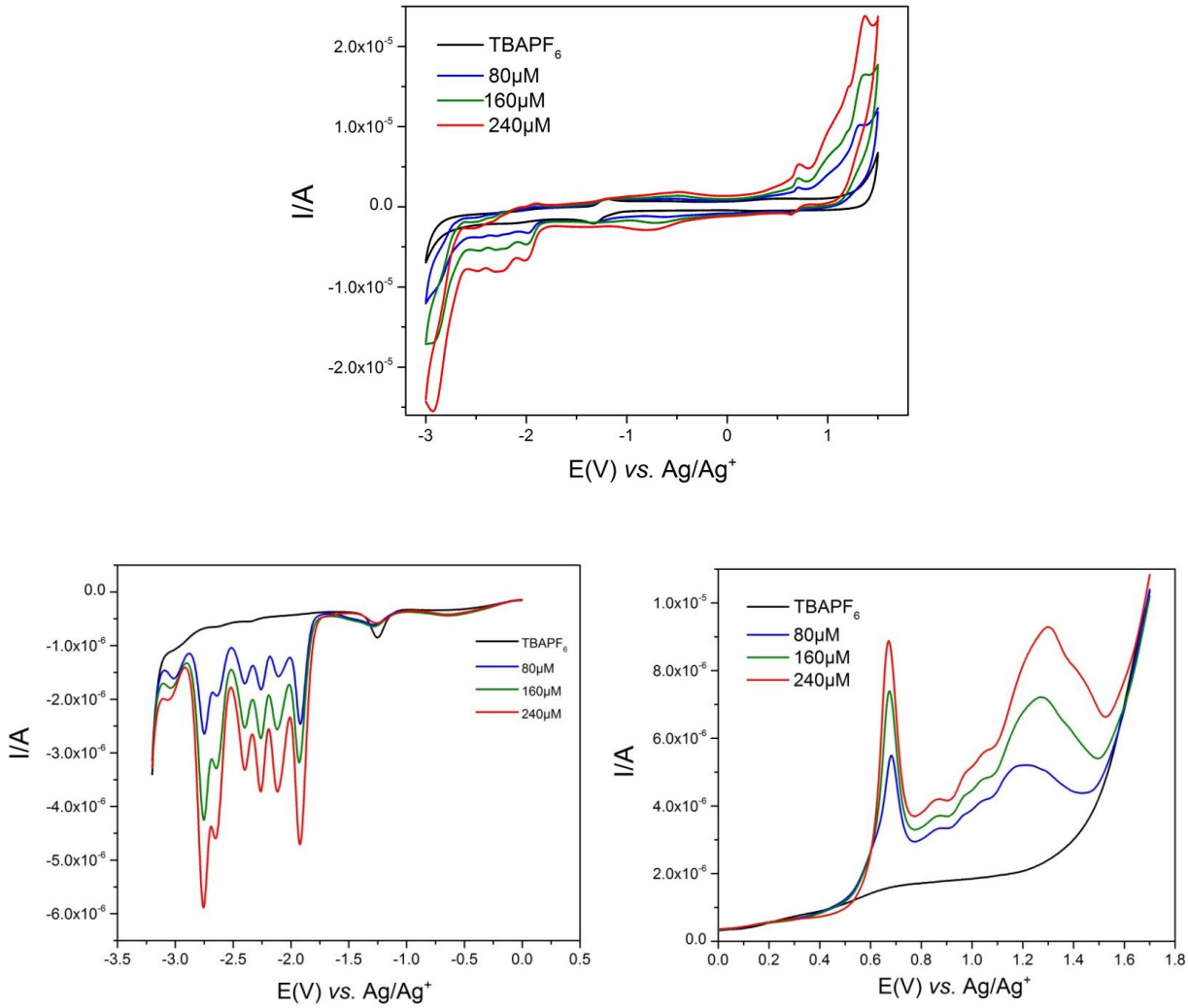

Figure 61. Top: Cyclic voltammograms of Br-BABABA'-CN in THF. Bottom: Differential pulse voltammograms of Br-BABABA'-CN in THF. Left: reduction. Right: oxidation.

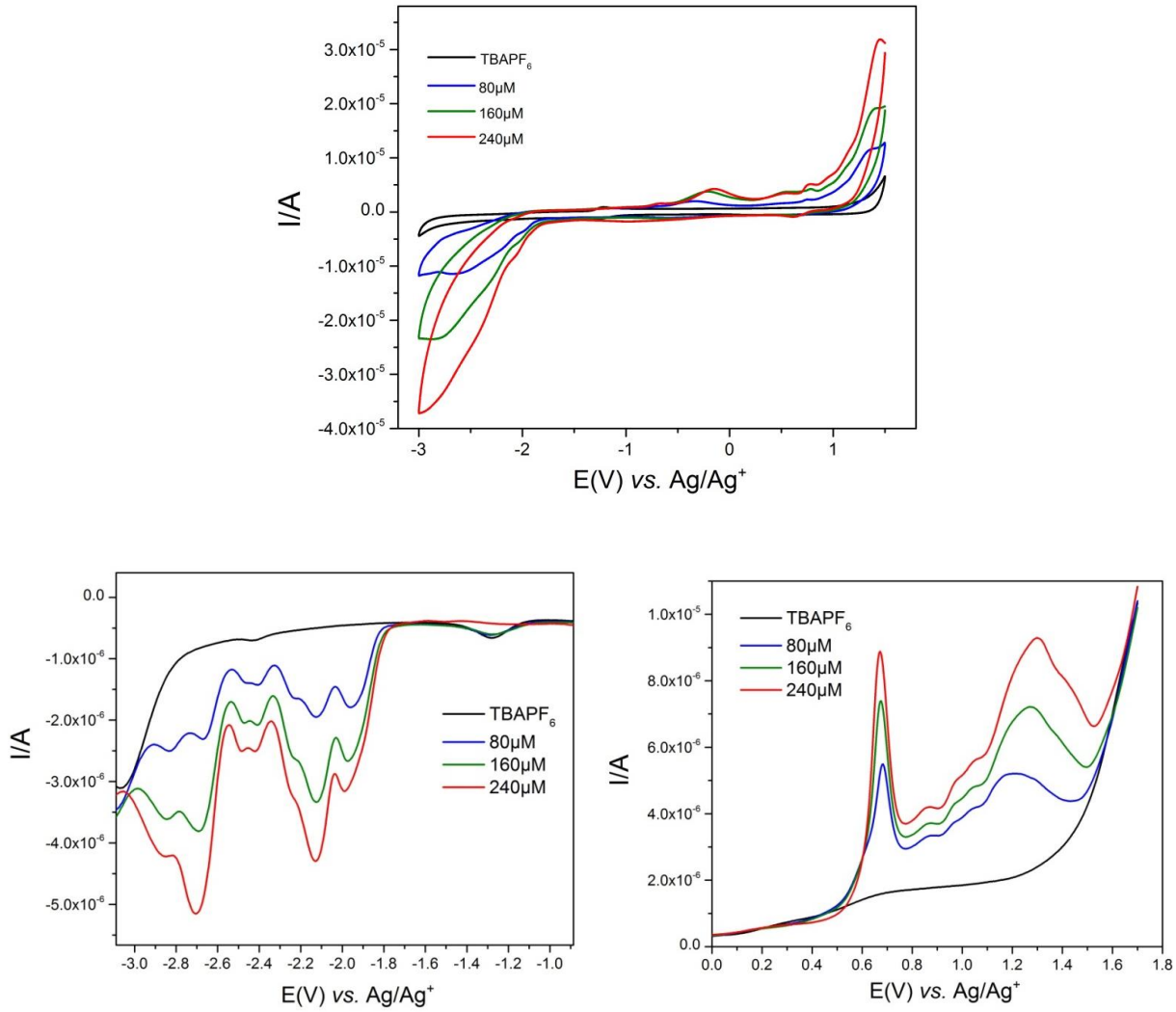

Figure 62. Top: Cyclic voltammograms of Br-BBAAAB'-CN in THF. Bottom: Differential pulse voltammograms of Br-BBAAAB'-CN in THF. Left: reduction. Right: oxidation.

A.3 ABSORBANCE AND EMISSION SPECTRA OF OPVS

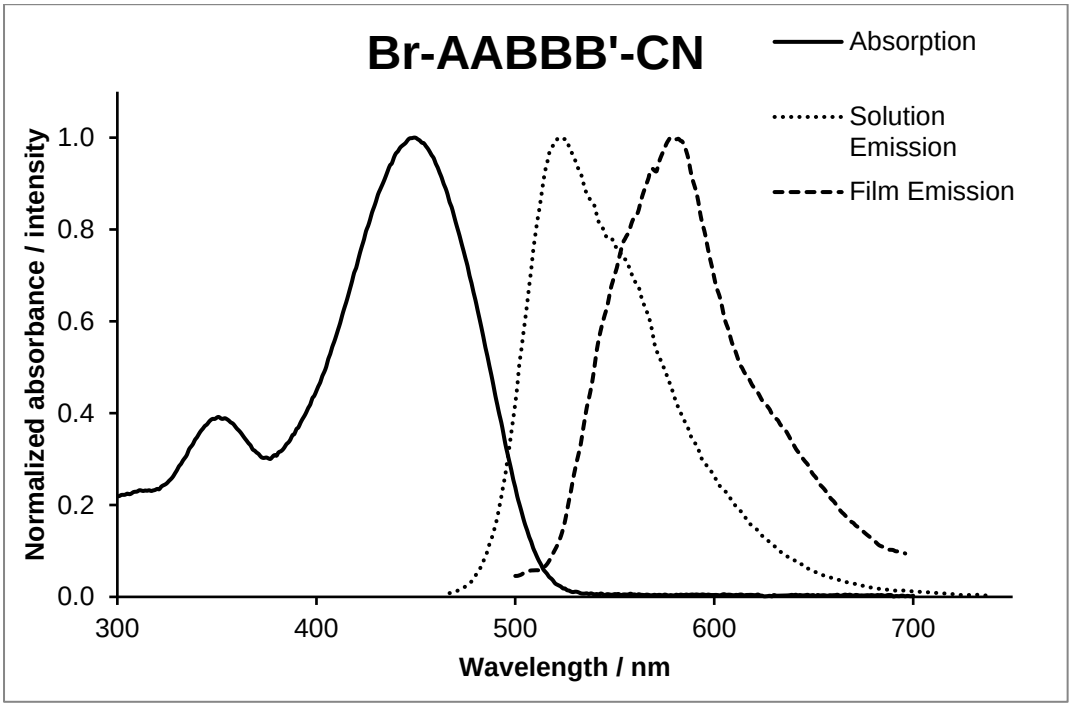

Figure 63. Absorption ($CHCl_3$) and emission ($CHCl_3$ and film) spectra of Br-AABBB'-CN.

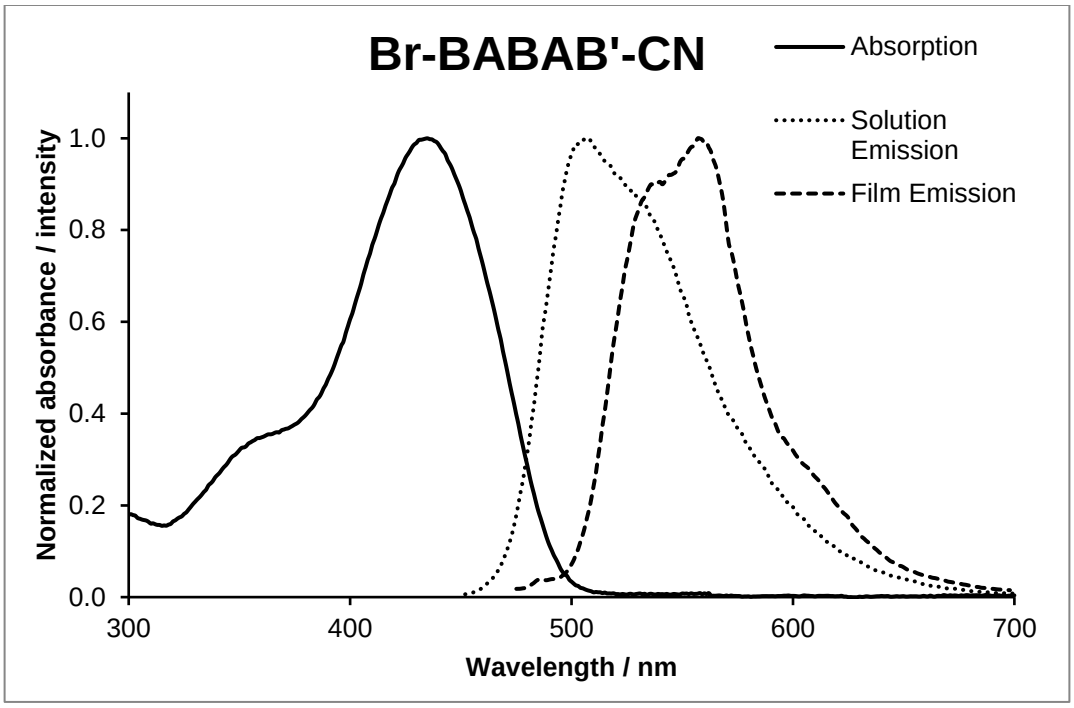

Figure 64. Absorption ($CHCl_3$) and emission ($CHCl_3$ and film) spectra of Br-BABAB'-CN.

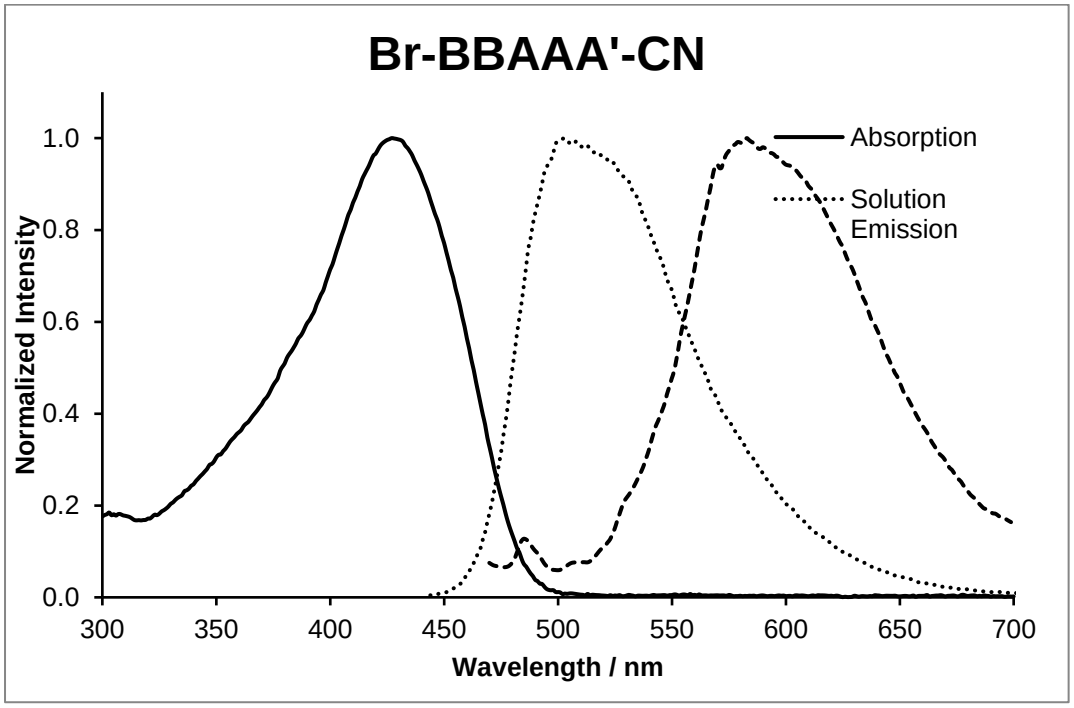

Figure 65. Absorption ($CHCl_3$) and emission ($CHCl_3$ and film) spectra of Br-BBAAA'-CN.

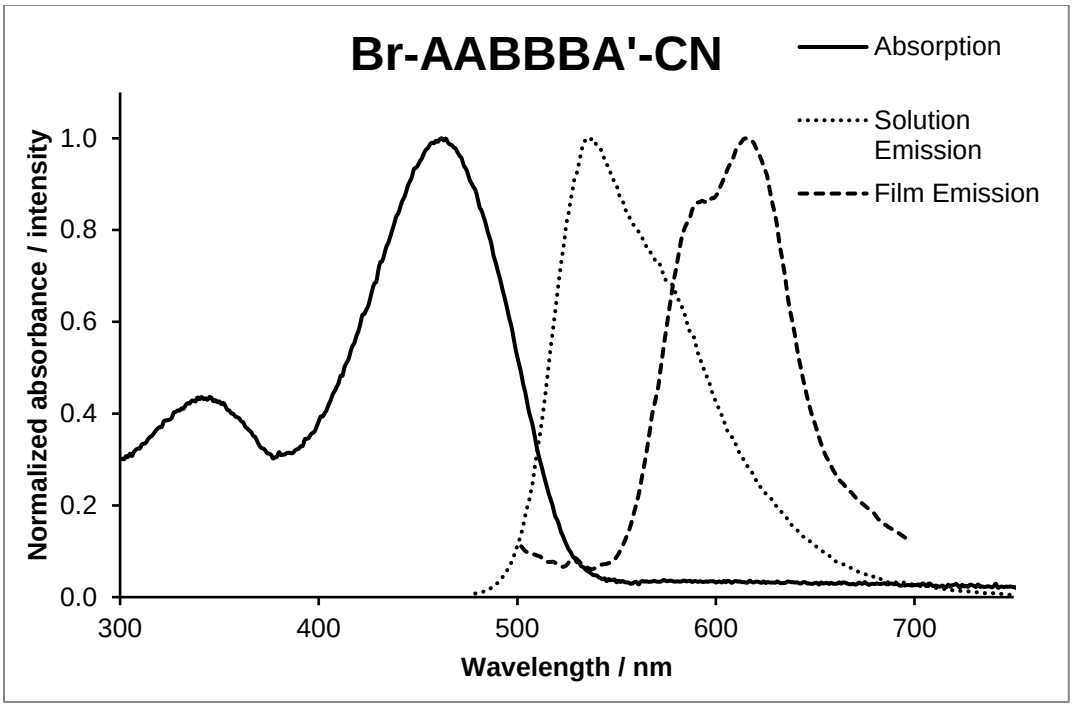

Figure 66. Absorption ($CHCl_3$) and emission ($CHCl_3$ and film) spectra of Br-AABBBA'-CN.

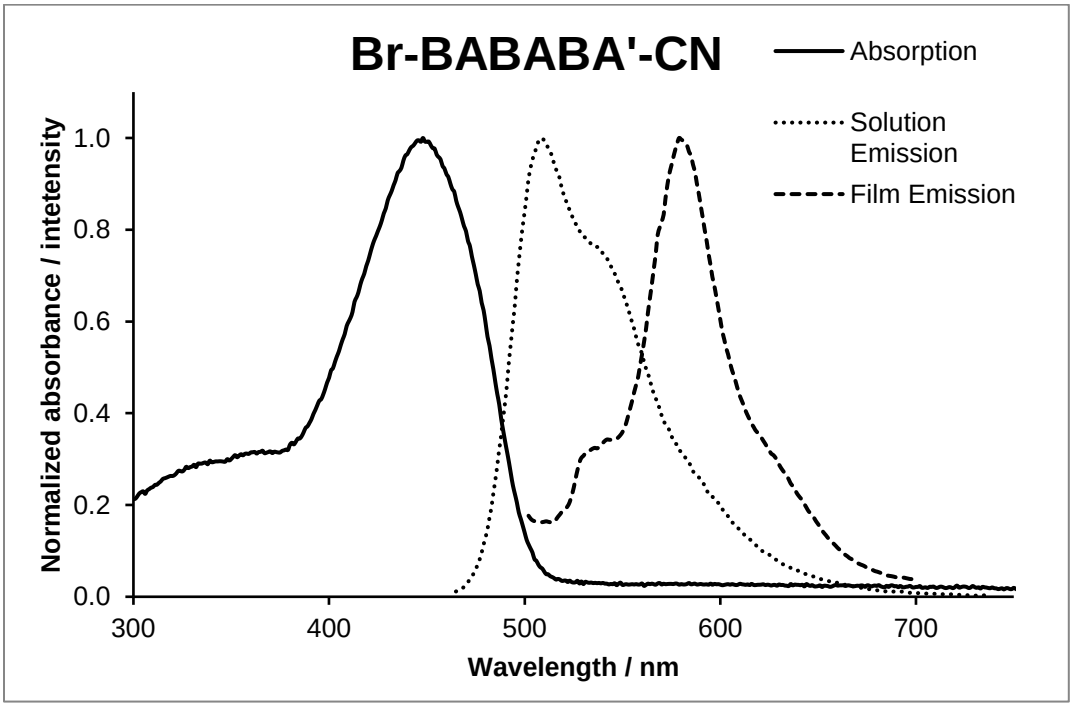

Figure 67. Absorption ($CHCl_3$) and emission ($CHCl_3$ and film) spectra of Br-BABABA'-CN.

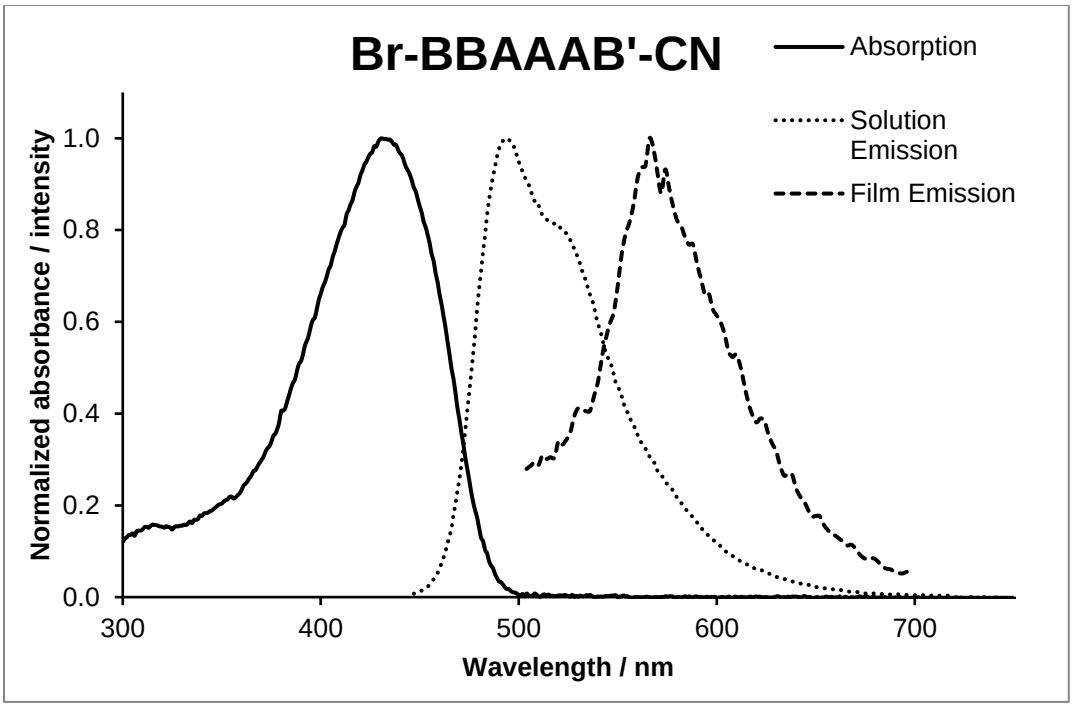

Figure 68. Absorption ($CHCl_3$) and emission ($CHCl_3$ and film) spectra of Br-BBAAAB'-CN.

A.4 DIFFERENTIAL SCANNING CALORIMOGRAMS OF OLIGOMERS

In figures 69 – 74, the heating curve is plotted in red and the cooling curve in blue.

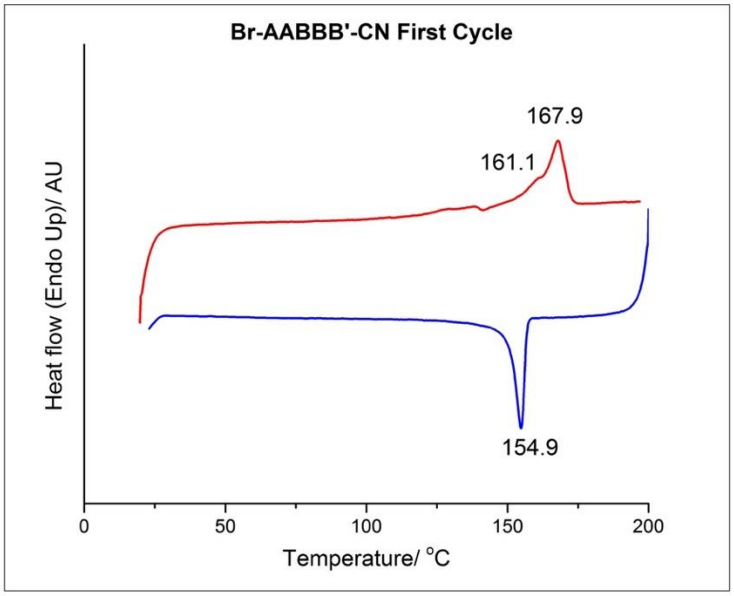

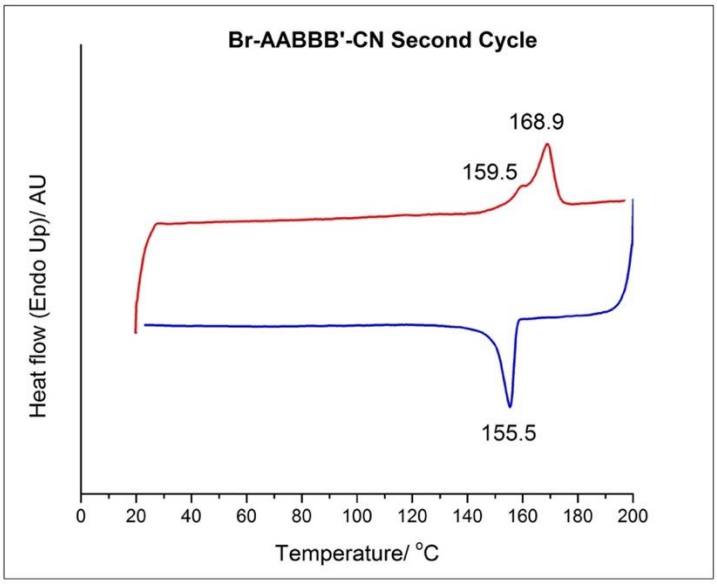

Figure 69. DSC thermograms of Br-AABBB'-CN.

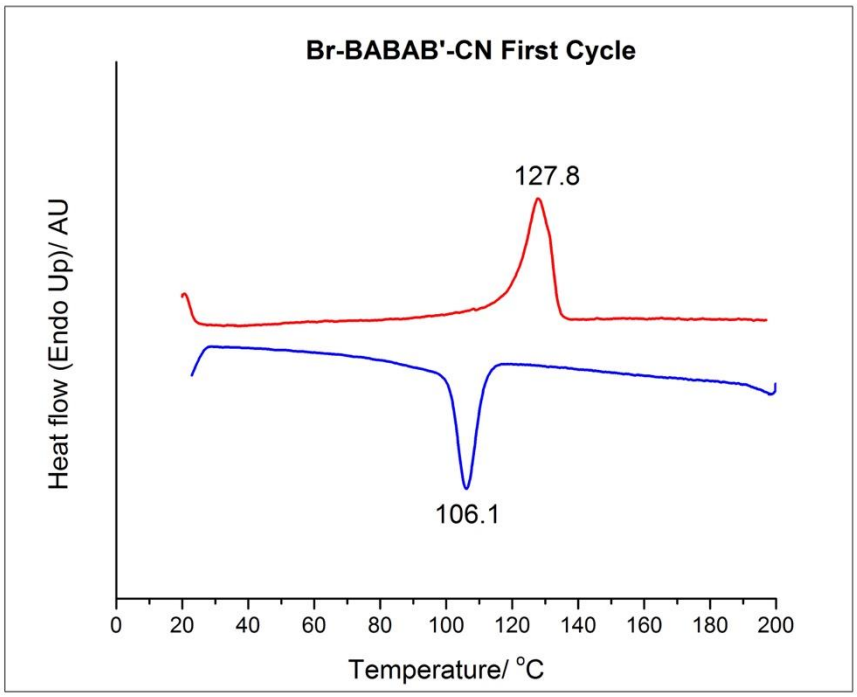

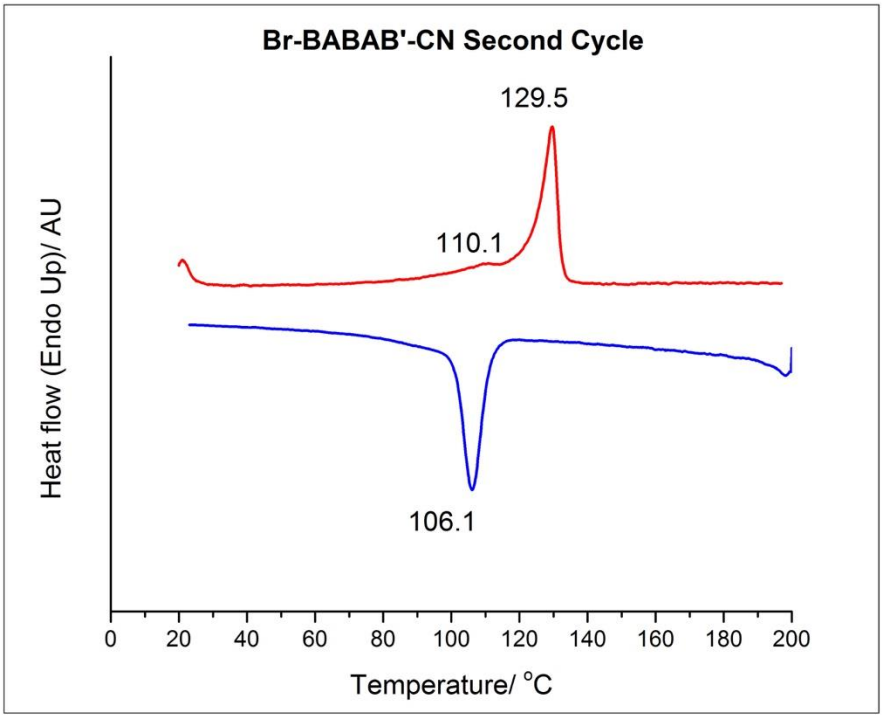

Figure 70. DSC thermograms of Br-BABAB'-CN.

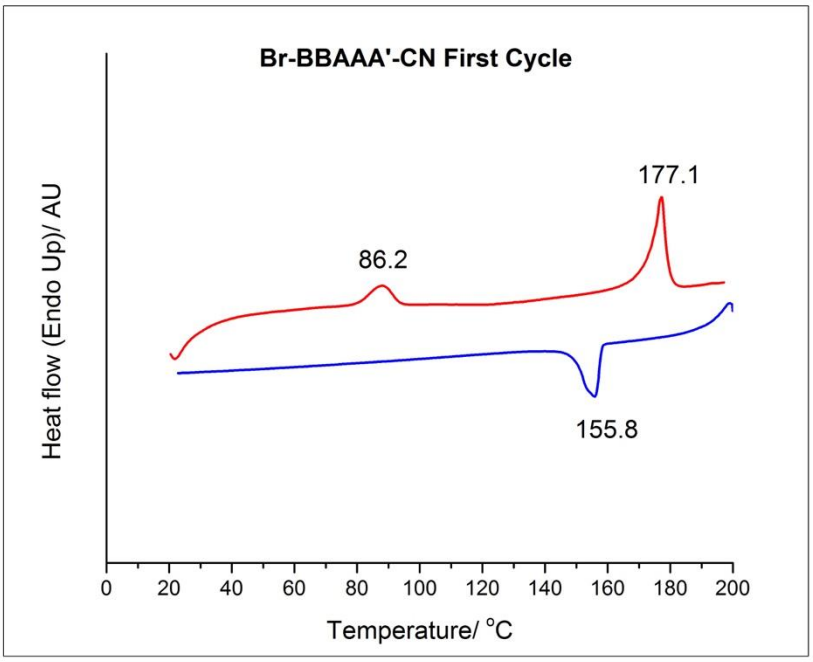

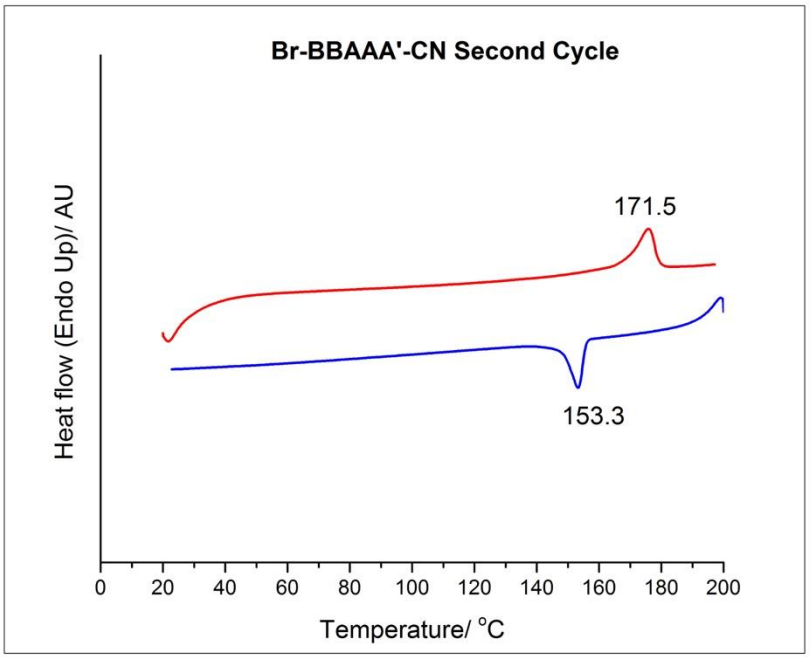

Figure 71. DSC thermograms of Br-BBAAA'-CN.

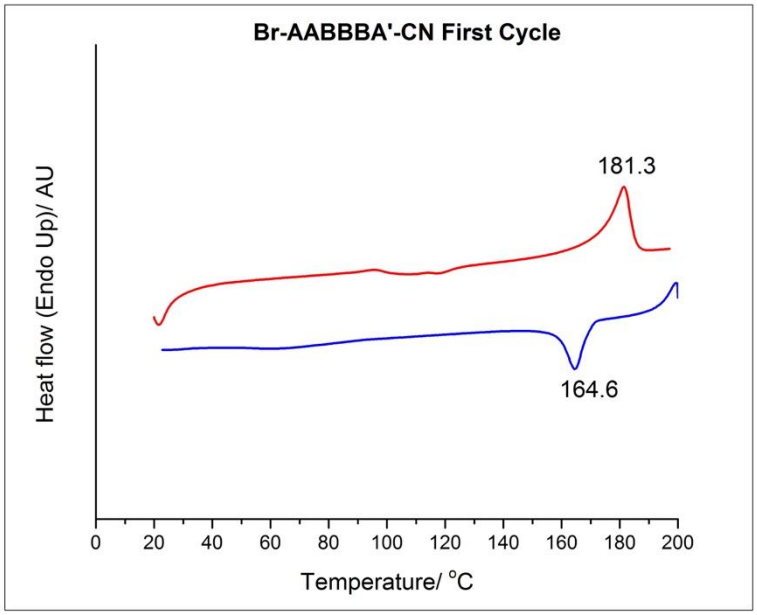

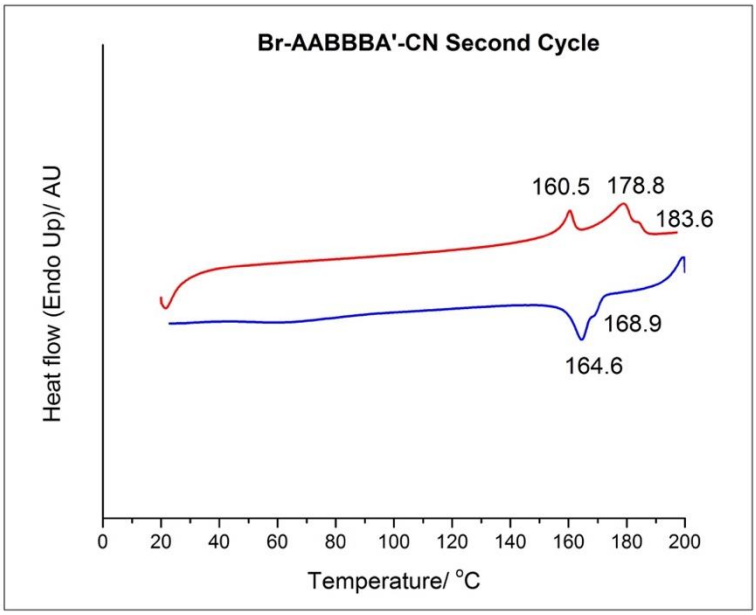

Figure 72. DSC thermograms of Br-AABBBA'-CN.

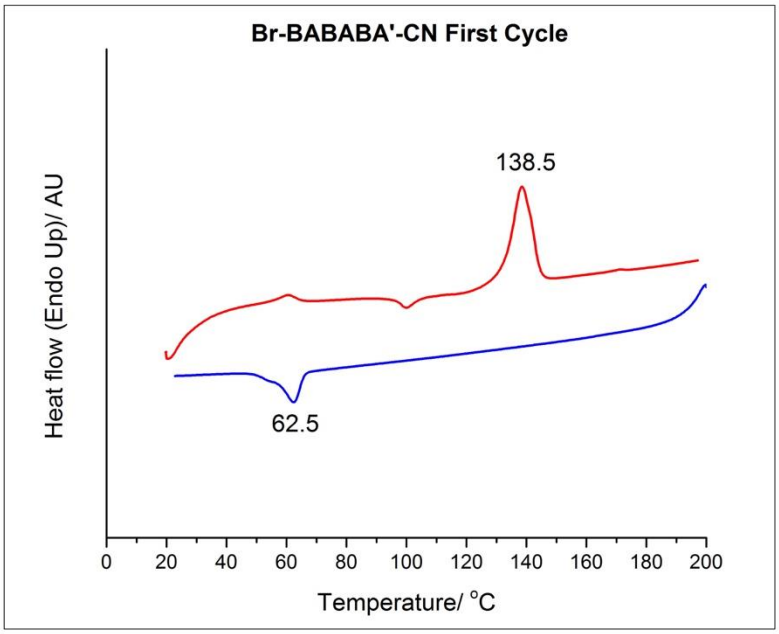

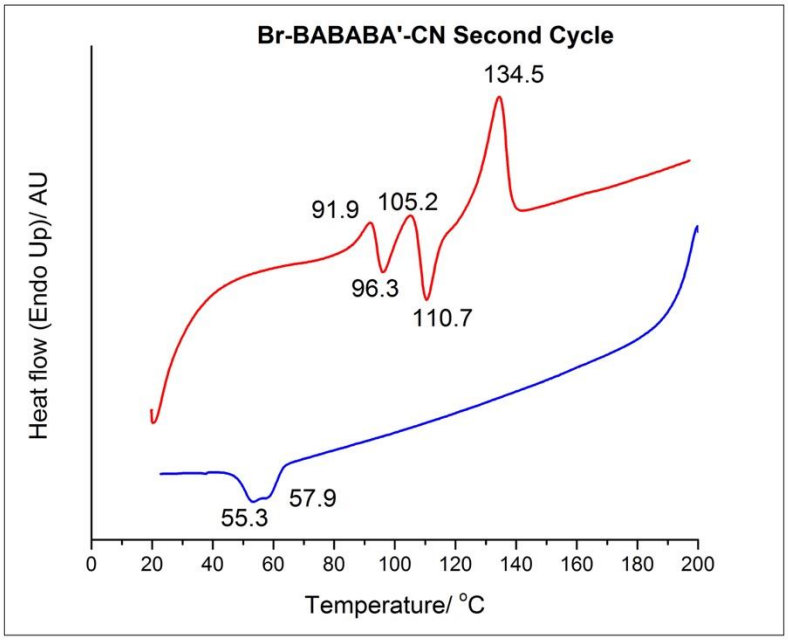

Figure 73. DSC thermograms of Br-BABABA'-CN.

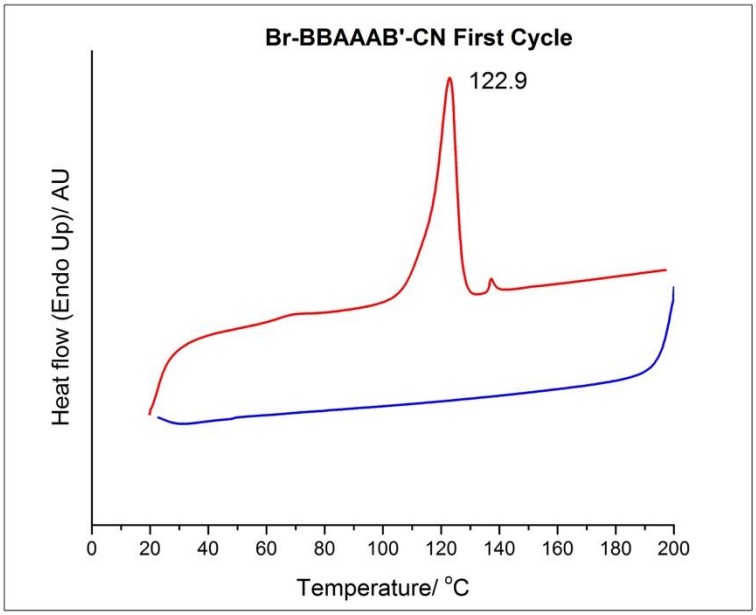

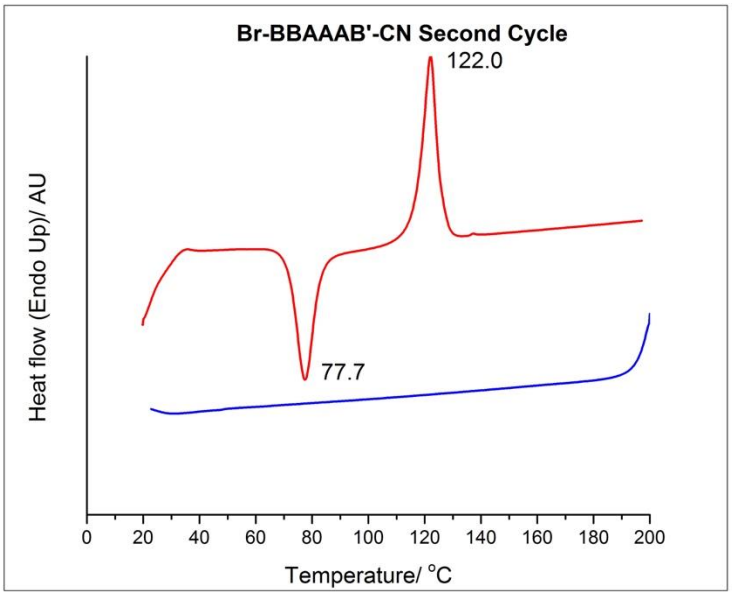

Figure 74. DSC thermograms of Br-BBAAAB'-CN

A.5 COMPUTATIONAL RESULTS

Table 16. Computed DFT HOMO and LUMO energies and ZINDO excitations for all hexamer sequences containing three A and three B units

Compound	HOMO	LUMO	Gap	ZINDO (eV)	Osc. Str.
Br-AAABBB'-CN	-4.892	-2.266	2.626	3.583	2.862
Br-AABABB'-CN	-4.836	-2.261	2.575	3.628	3.406
Br-AABBAB'-CN	-4.927	-2.290	2.637	3.600	3.070
Br-AABBBA'-CN	-4.818	-2.267	2.551	3.502	3.032
Br-ABAABB'-CN	-4.873	-2.272	2.601	3.707	3.479
Br-ABABAB'-CN	-4.834	-2.277	2.557	3.695	3.552
Br-ABABBA'-CN	-4.904	-2.287	2.616	3.562	3.291
Br-ABBAAB'-CN	-4.952	-2.312	2.641	3.652	2.715
Br-ABBABA'-CN	-4.937	-2.332	2.605	3.594	3.440
Br-ABBBAA'-CN	-4.868	-2.312	2.556	3.517	3.021
Br-BAAABB'-CN	-4.951	-2.291	2.659	3.727	2.811
Br-BAABAB'-CN	-4.876	-2.285	2.591	3.729	3.353
Br-BAABBA'-CN	-4.896	-2.288	2.608	3.603	2.875
Br-BABAAB'-CN	-4.938	-2.311	2.627	3.782	3.296
Br-BABABA'-CN	-4.903	-2.298	2.605	3.655	3.531
Br-BABBAA'-CN	-4.933	-2.330	2.604	3.593	3.111
Br-BBAAAB'-CN	-4.874	-2.309	2.565	3.778	3.063
Br-BBAABA'-CN	-4.865	-2.299	2.565	3.720	3.706
Br-BBABAA'-CN	-4.964	-2.340	2.624	3.683	3.526
Br-BBBAAA'-CN	-4.956	-2.351	2.605	3.604	2.846

APPENDIX B

CHAPTER 3 SEQUENCE EFFECTS IN DONOR-ACCEPTOR OLIGOMERIC SEMICONDUCTORS COMPRISING BENZOTHIADIAZOLE AND PHENYLENE VINYLENE MONOMERS

B.1 NMR SPECTRA

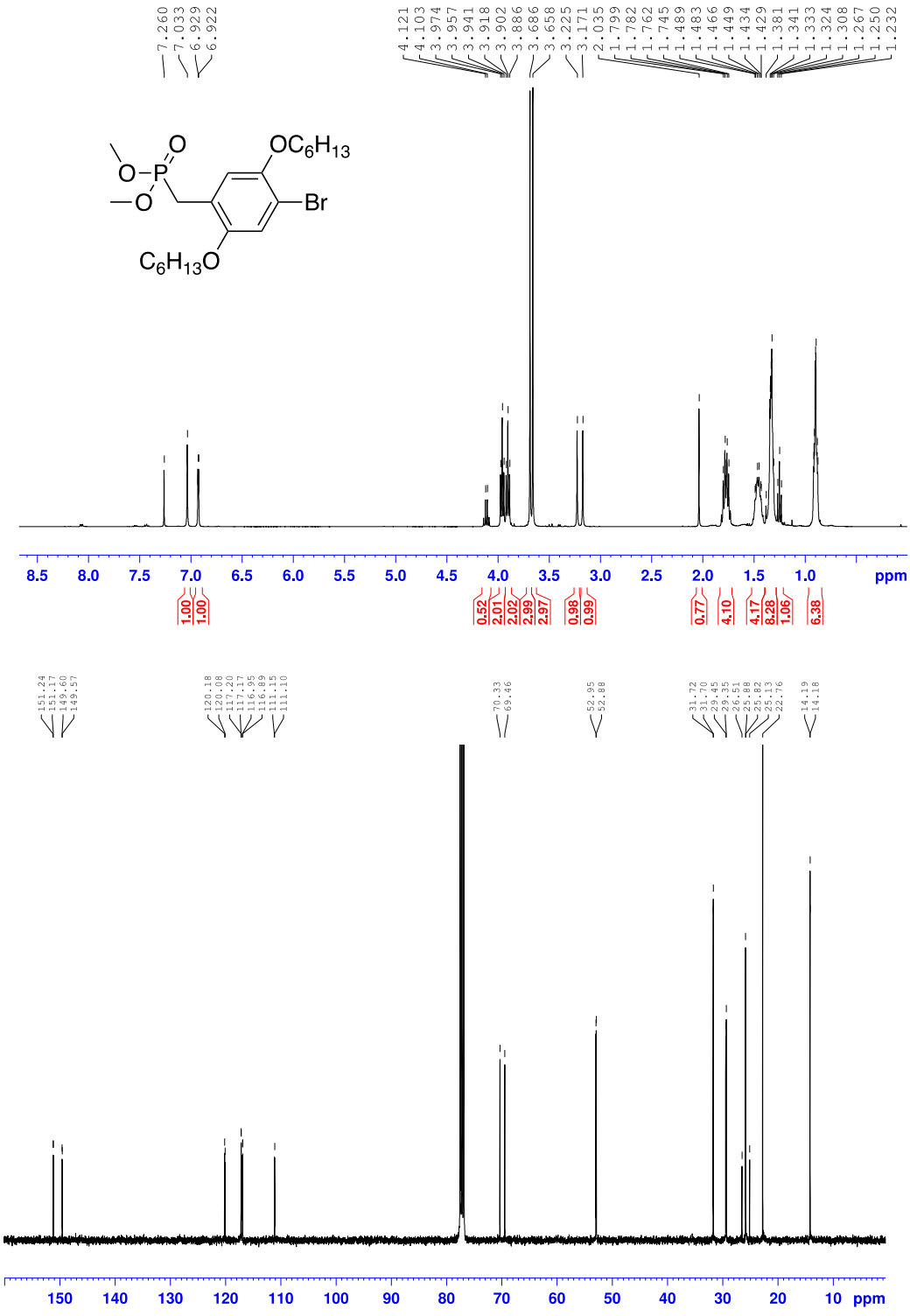

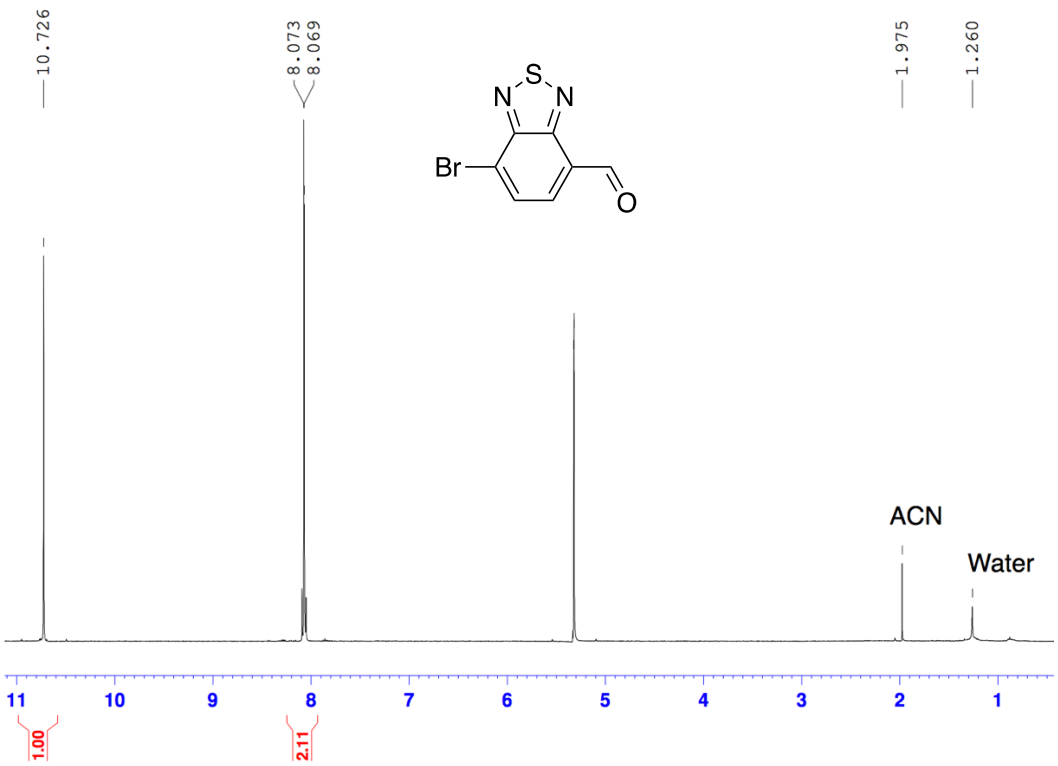
10.726
8.073
8.069
1.975
1.260
ACN
Water
11
10
9
8
7
6
5
4
3
2
1
1.00
2.11

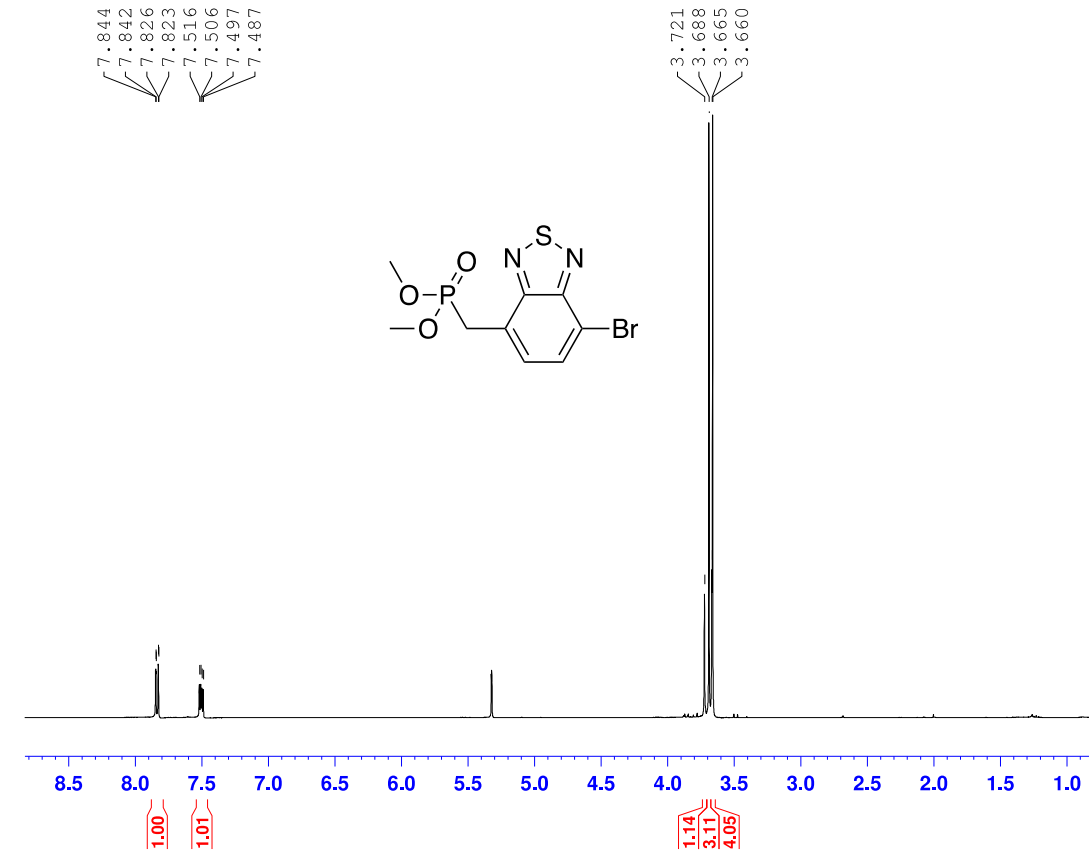
7.844
7.842
7.826
7.823
7.516
7.506
7.497
7.487
3.721
3.688
3.665
3.660
Br
8.5
8.0
7.5
7.0
6.5
6.0
5.5
5.0
4.5
4.0
3.5
3.0
2.5
2.0
1.5
1.0
1.00
1.01
1.14
3.11
4.05

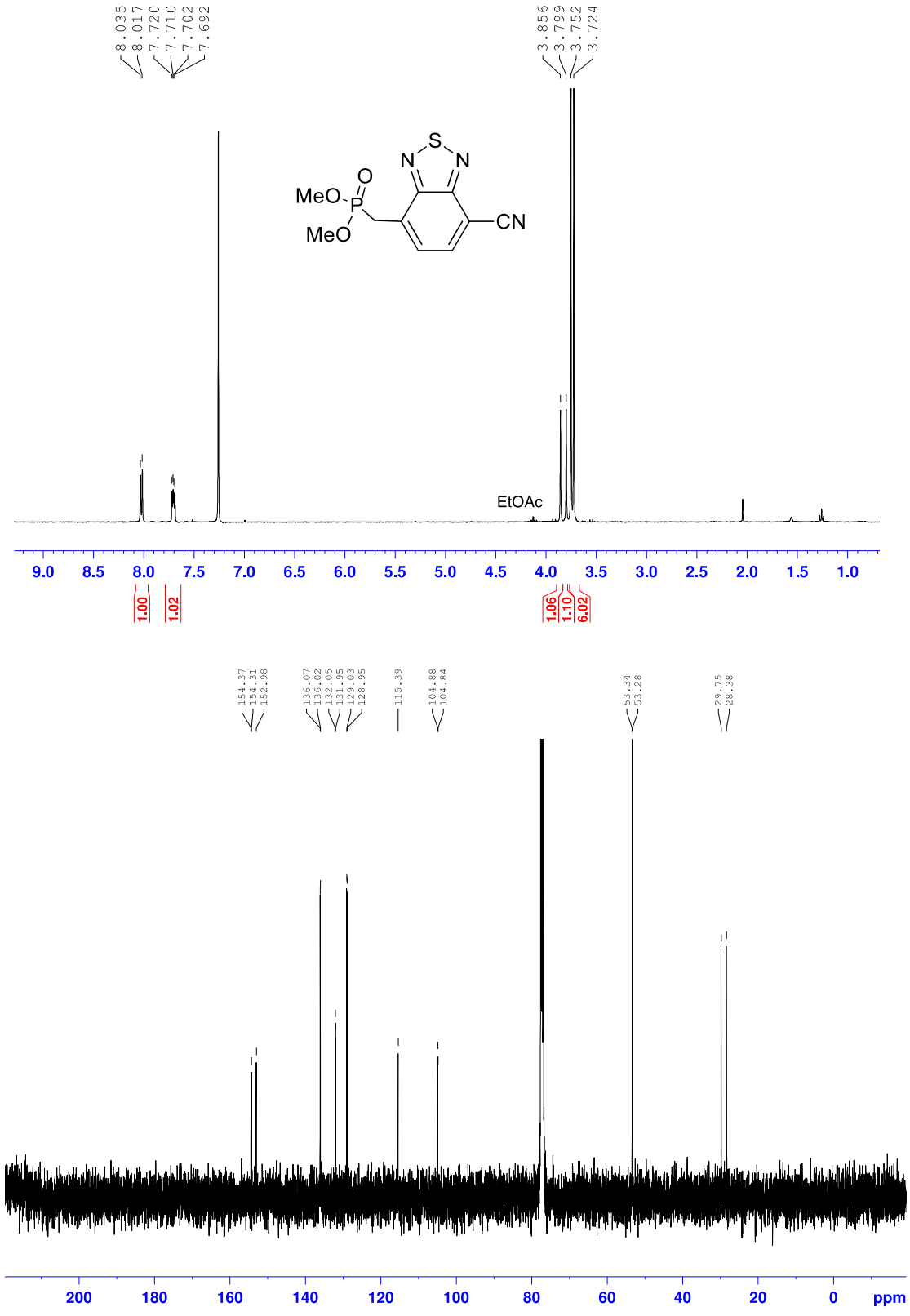
8.035
8.017
7.720
7.710
7.702
7.692
3.856
3.799
3.752
3.724
MeO
P
O
MeO
N
S
N
CN
EtOAc
9.0
8.5
8.0
7.5
7.0
6.5
6.0
5.5
5.0
4.5
4.0
3.5
3.0
2.5
2.0
1.5
1.0
1.00
1.02
1.06
1.10
6.02
154.37
154.31
152.98
136.07
136.02
132.05
131.95
129.03
128.95
115.39
104.88
104.84
53.34
53.28
29.75
28.38
200
180
160
140
120
100
80
60
40
20
0
ppm

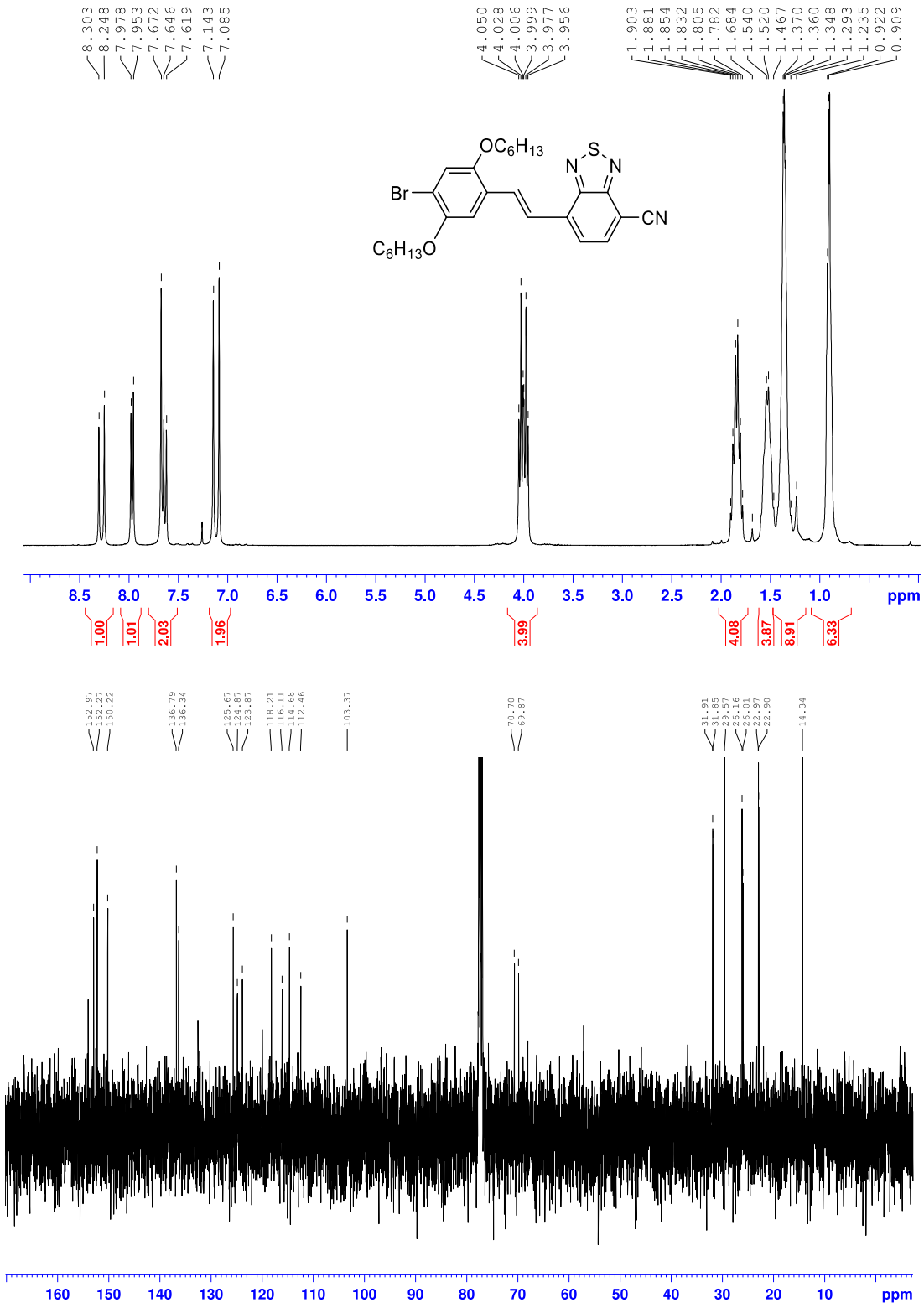
8.303
8.248
7.978
7.953
7.672
7.646
7.619
7.143
7.085
4.050
4.028
4.006
3.999
3.977
3.956
1.903
1.881
1.854
1.832
1.805
1.782
1.684
1.540
1.520
1.467
1.370
1.360
1.348
1.293
1.235
0.922
0.909
OC6H13
S
N
N
Br
CN
C6H13O
8.5
8.0
7.5
7.0
6.5
6.0
5.5
5.0
4.5
4.0
3.5
3.0
2.5
2.0
1.5
1.0
ppm
1.00
1.01
2.03
1.96
3.99
4.08
3.87
8.91
6.33
152.97
152.27
150.22
136.79
136.34
125.67
124.87
123.87
118.21
116.11
114.68
112.46
103.37
70.70
69.87
31.91
31.85
29.57
26.16
26.01
22.97
22.90
14.34
160
150
140
130
120
110
100
90
80
70
60
50
40
30
20
10
ppm

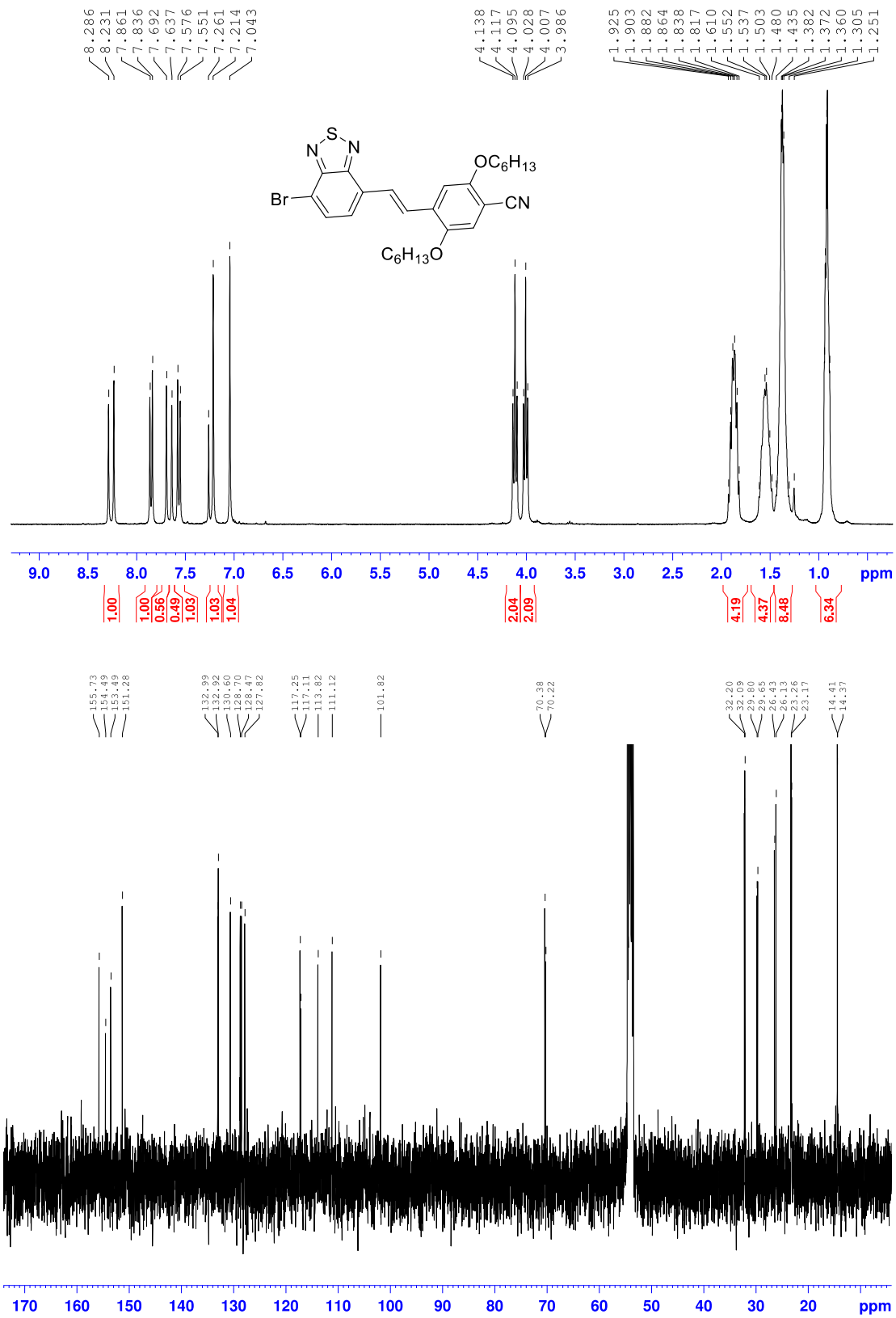
8.286
8.231
7.861
7.836
7.692
7.637
7.576
7.551
7.261
7.214
7.043
4.138
4.117
4.095
4.028
4.007
3.986
1.925
1.903
1.882
1.864
1.838
1.817
1.610
1.552
1.537
1.503
1.480
1.435
1.382
1.372
1.360
1.305
1.251
Br
OC6H13
CN
C6H13O
9.0 8.5 8.0 7.5 7.0 6.5 6.0 5.5 5.0 4.5 4.0 3.5 3.0 2.5 2.0 1.5 1.0 ppm
1.00 1.00 0.56 0.49 1.03 1.03 1.04 2.04 2.09 4.19 4.37 8.48 6.34
155.73
154.49
153.49
151.28
132.99
132.92
130.60
128.70
128.47
127.82
117.25
117.11
113.82
111.12
101.82
70.38
70.22
32.20
32.09
29.80
29.65
26.43
26.13
23.26
23.17
14.41
14.37
170 160 150 140 130 120 110 100 90 80 70 60 50 40 30 20 ppm

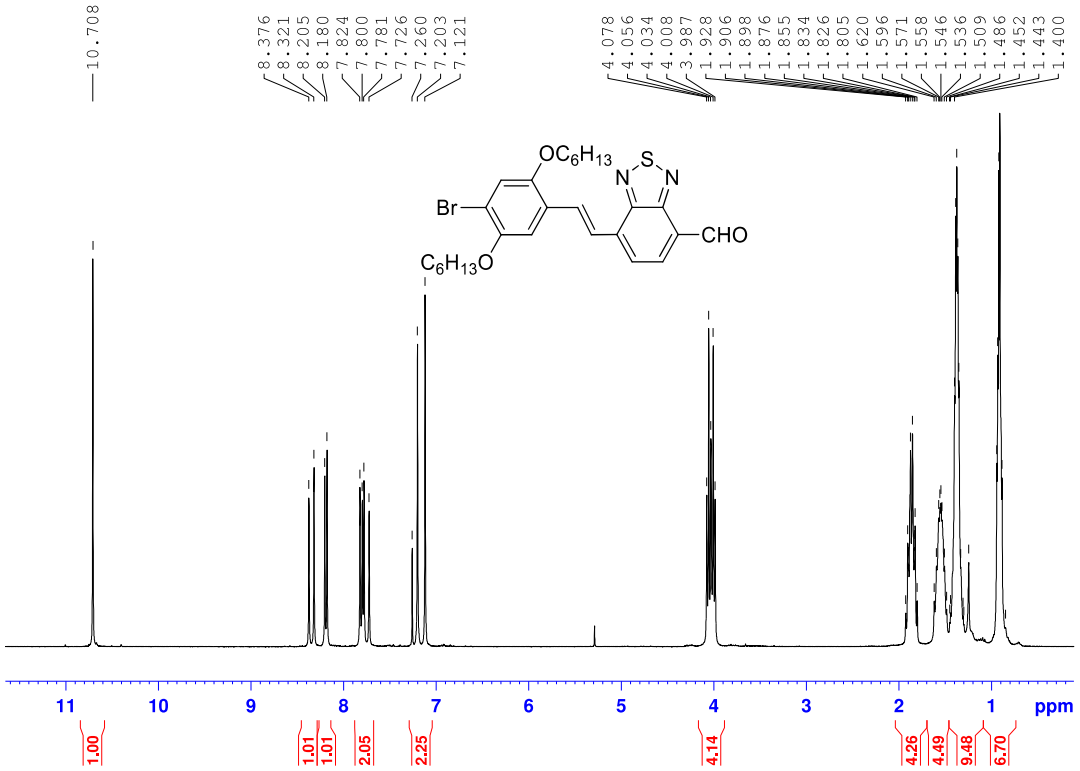
10.708
8.376
8.321
8.205
8.180
7.824
7.800
7.781
7.726
7.260
7.203
7.121
4.078
4.056
4.034
4.008
3.987
1.928
1.906
1.898
1.876
1.855
1.834
1.826
1.805
1.620
1.596
1.571
1.558
1.546
1.536
1.509
1.486
1.452
1.443
1.400
OC6H13
S
N
N
Br
CHO
C6H13O
11
10
9
8
7
6
5
4
3
2
1
ppm
1.00
1.01
1.01
2.05
2.25
4.14
4.26
4.49
9.48
6.70

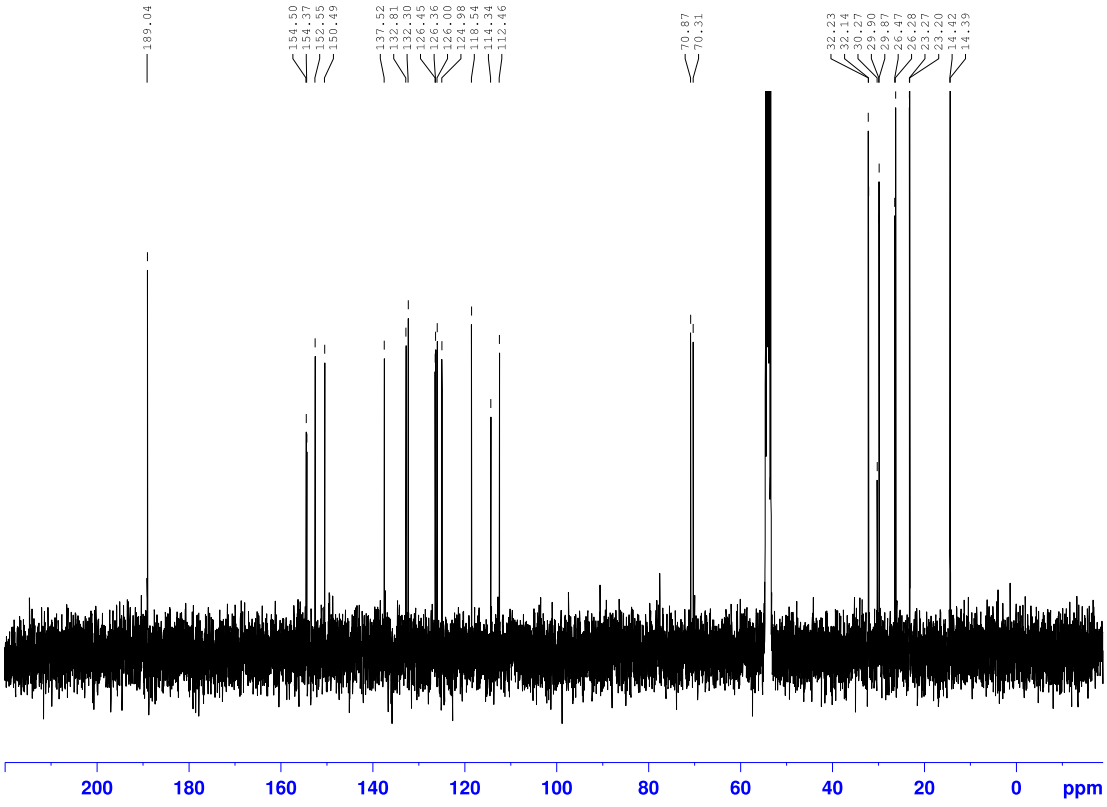
189.04
154.50
154.37
152.55
150.49
137.52
132.81
132.30
128.35
126.36
126.00
124.98
118.54
114.34
112.46
70.87
70.31
32.23
32.14
30.27
29.90
29.87
26.47
26.28
23.27
23.20
14.42
14.39
200
180
160
140
120
100
80
60
40
20
0
ppm

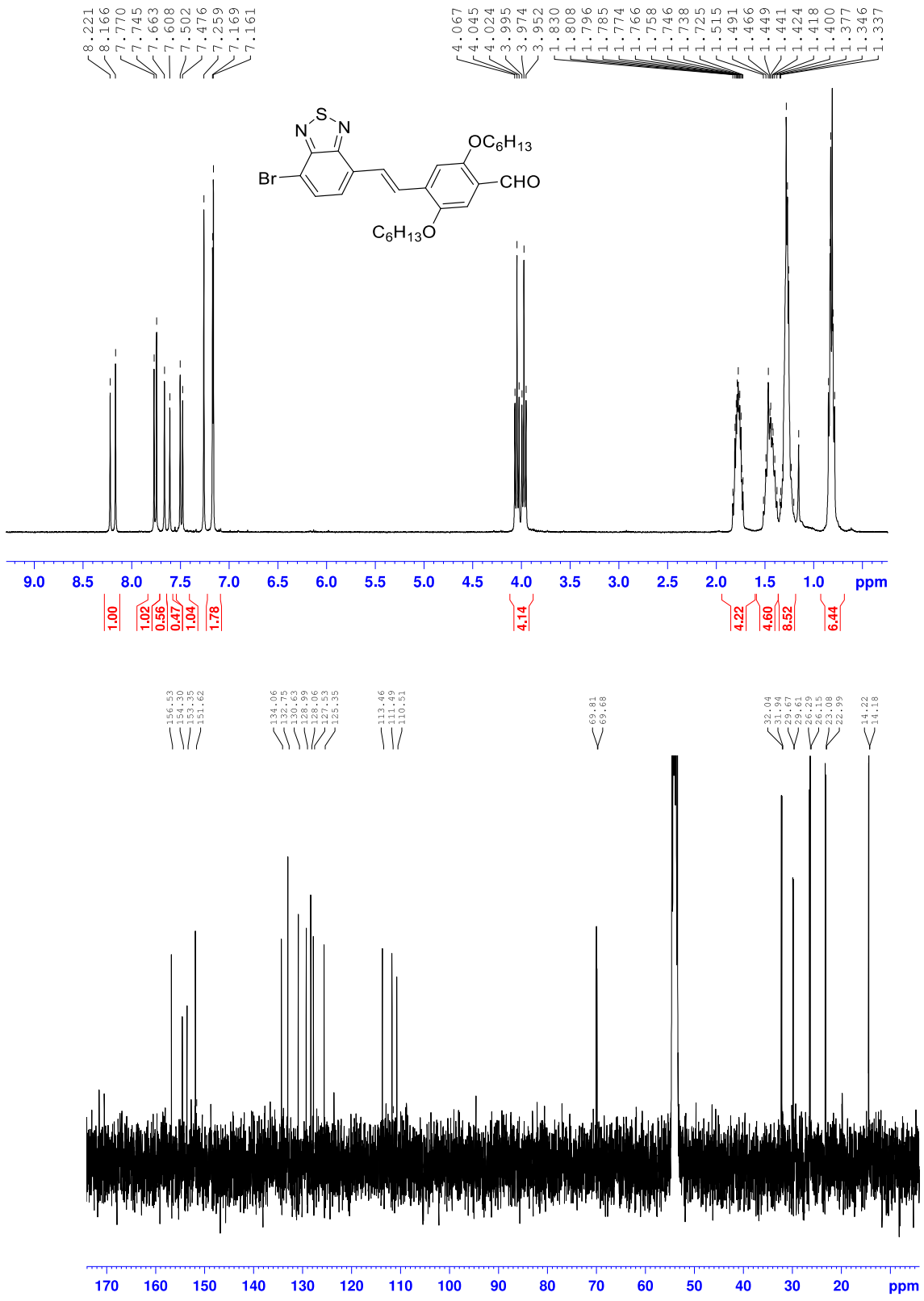
8.221
8.166
7.770
7.745
7.663
7.608
7.502
7.476
7.259
7.169
7.161
4.067
4.045
4.024
3.995
3.974
3.952
1.830
1.808
1.796
1.785
1.774
1.766
1.758
1.746
1.738
1.725
1.515
1.491
1.466
1.449
1.441
1.424
1.418
1.400
1.377
1.346
1.337
Br
OC6H13
CHO
C6H13O
9.0 8.5 8.0 7.5 7.0 6.5 6.0 5.5 5.0 4.5 4.0 3.5 3.0 2.5 2.0 1.5 1.0 ppm
1.00 1.02 0.56 0.47 1.04 1.78 4.14 4.22 4.60 8.52 6.44
156.53
154.30
153.35
151.62
134.06
132.75
130.63
128.99
128.06
127.53
125.35
113.46
111.49
110.51
69.81
69.68
32.04
31.94
29.67
29.55
26.29
26.15
23.08
22.99
14.22
14.18
170 160 150 140 130 120 110 100 90 80 70 60 50 40 30 20 ppm

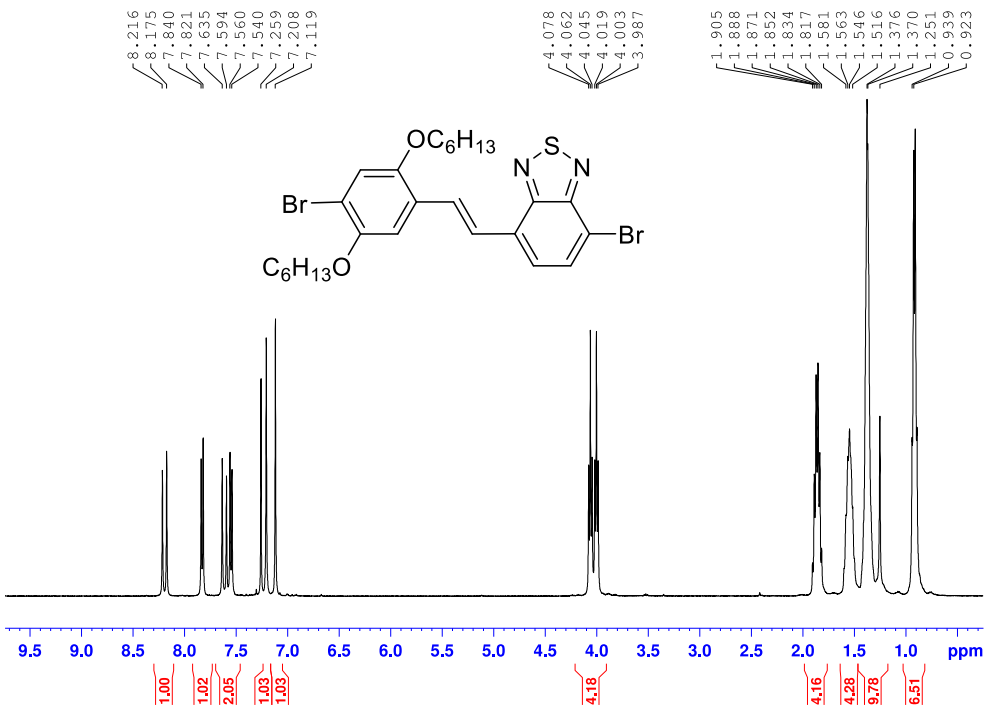
8.216
8.175
7.840
7.821
7.635
7.594
7.560
7.540
7.259
7.208
7.119
4.078
4.062
4.045
4.019
4.003
3.987
1.905
1.888
1.871
1.852
1.834
1.817
1.581
1.563
1.546
1.516
1.376
1.370
1.251
0.939
0.923
OC6H13
N
S
N
Br
Br
C6H13O
9.5 9.0 8.5 8.0 7.5 7.0 6.5 6.0 5.5 5.0 4.5 4.0 3.5 3.0 2.5 2.0 1.5 1.0 ppm
1.00
1.02
2.05
1.03
1.03
4.18
4.16
4.28
9.78
6.51

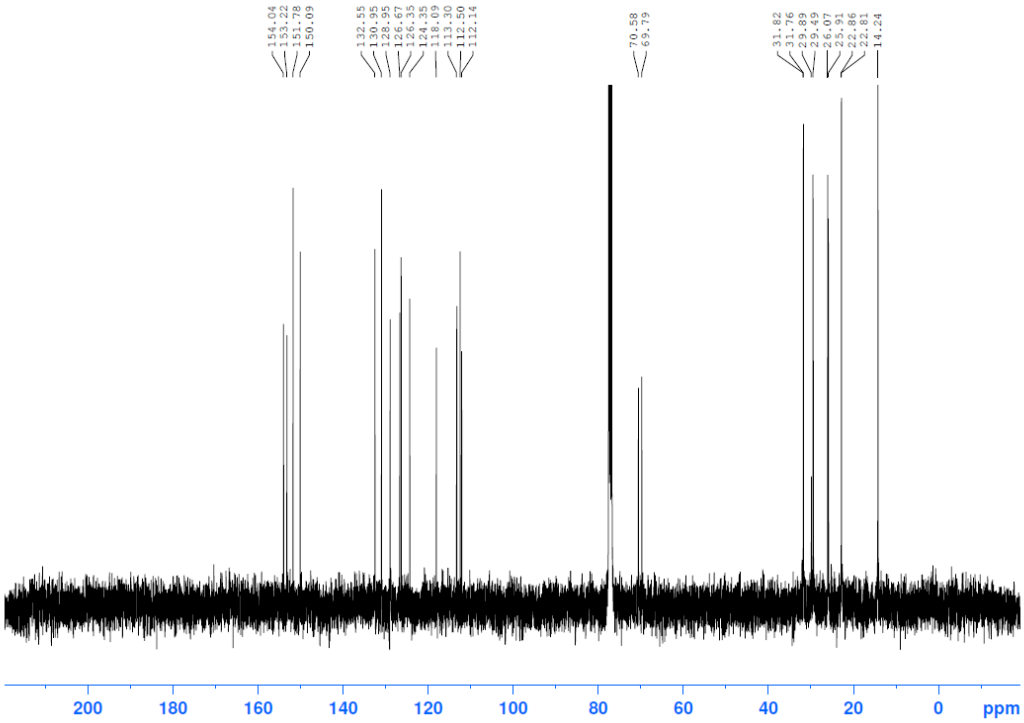
154.04
153.22
151.78
150.09
132.55
130.95
128.95
126.67
126.35
124.35
118.09
113.30
112.50
112.14
70.58
69.79
31.82
31.76
29.89
29.49
29.07
26.01
22.86
22.81
14.24
200 180 160 140 120 100 80 60 40 20 0 ppm

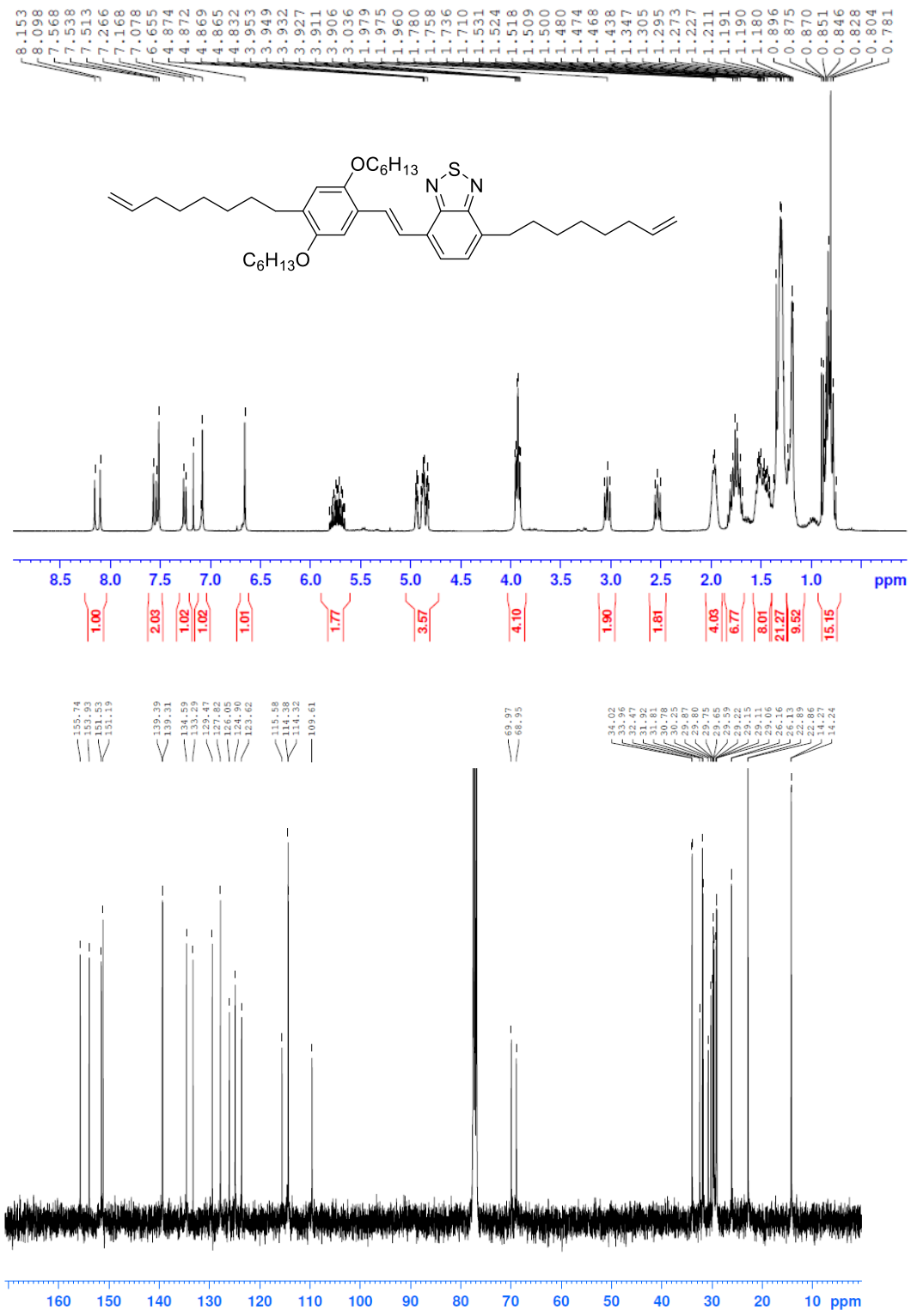
8.153
8.098
7.568
7.538
7.513
7.266
7.168
7.078
6.655
4.874
4.872
4.869
4.865
4.832
3.953
3.949
3.932
3.927
3.911
3.906
3.036
1.979
1.975
1.960
1.780
1.758
1.736
1.710
1.531
1.524
1.518
1.509
1.500
1.480
1.474
1.468
1.438
1.347
1.305
1.295
1.273
1.227
1.211
1.191
1.190
1.180
0.896
0.875
0.870
0.851
0.846
0.828
0.804
0.781
OC6H13
N
S
N
C6H13O
8.5
8.0
7.5
7.0
6.5
6.0
5.5
5.0
4.5
4.0
3.5
3.0
2.5
2.0
1.5
1.0
ppm
1.00
2.03
1.02
1.02
1.01
1.77
3.57
4.10
1.90
1.81
4.03
6.77
8.01
21.27
9.52
15.15
155.74
153.93
151.53
151.19
139.39
139.31
134.59
133.29
129.47
127.82
126.05
124.90
123.62
115.58
114.38
114.32
109.61
69.97
68.95
34.02
33.96
32.47
31.92
31.81
30.78
30.25
29.87
29.80
29.75
29.65
29.59
29.22
29.15
29.11
29.06
26.16
26.13
22.89
22.86
14.27
14.24
160
150
140
130
120
110
100
90
80
70
60
50
40
30
20
10
ppm

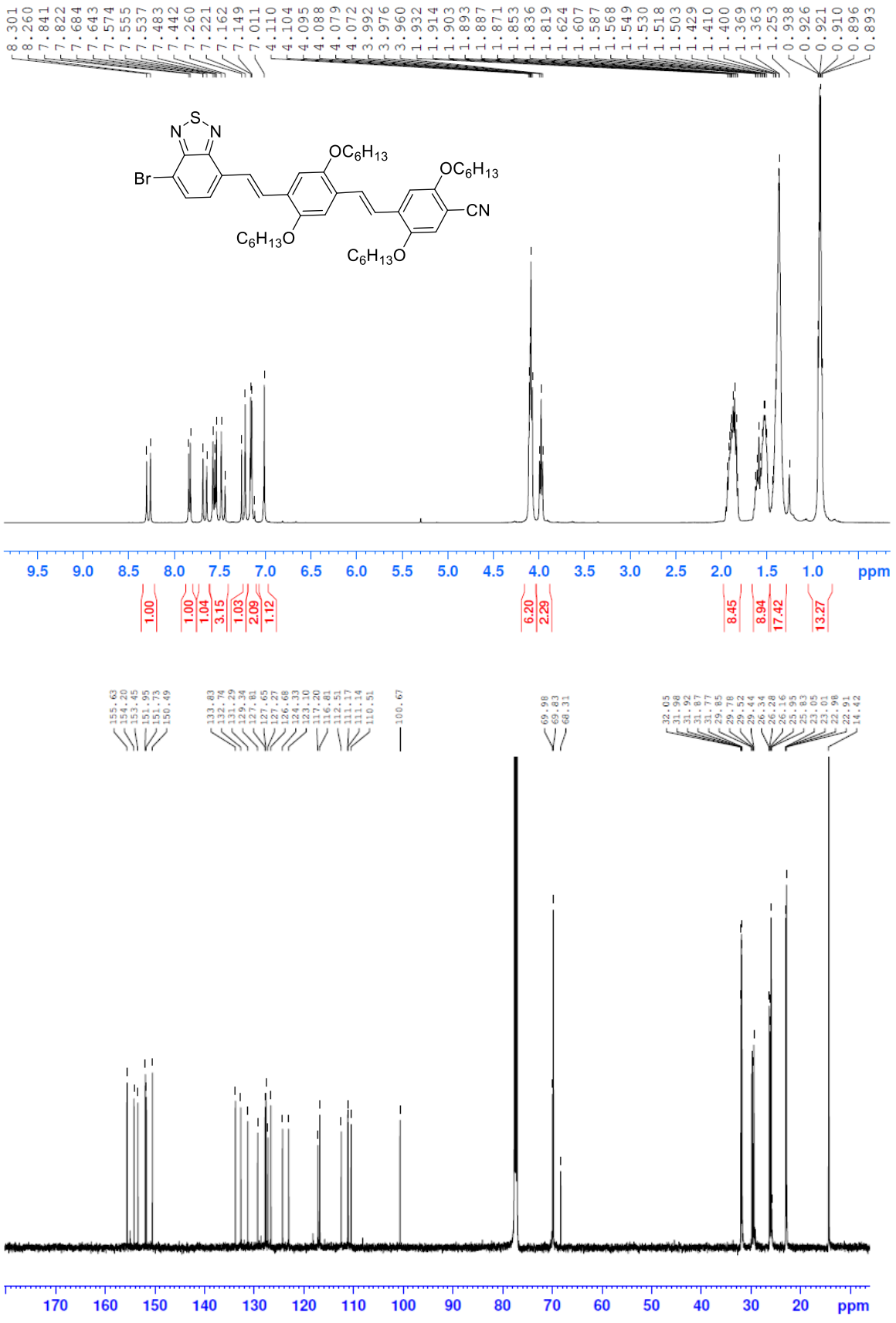
8.301
8.260
7.841
7.822
7.684
7.643
7.574
7.555
7.537
7.483
7.442
7.260
7.221
7.162
7.149
7.011
4.110
4.104
4.095
4.088
4.079
4.072
3.992
3.976
3.960
1.932
1.914
1.903
1.893
1.887
1.871
1.853
1.836
1.819
1.624
1.607
1.587
1.568
1.549
1.530
1.518
1.503
1.429
1.410
1.400
1.369
1.363
1.253
0.938
0.926
0.921
0.910
0.896
0.893
N
S
N
Br
OC6H13
OC6H13
CN
C6H13O
C6H13O
9.5
9.0
8.5
8.0
7.5
7.0
6.5
6.0
5.5
5.0
4.5
4.0
3.5
3.0
2.5
2.0
1.5
1.0
ppm
1.00
1.00
1.04
3.15
1.03
2.09
1.12
6.20
2.29
8.45
8.94
17.42
13.27
155.63
154.20
153.45
151.95
151.73
150.49
133.83
132.74
131.29
129.34
127.81
127.65
127.27
126.68
124.33
123.10
117.20
116.81
112.51
111.17
111.14
110.51
100.67
69.98
69.83
68.31
32.05
31.98
31.92
31.87
31.77
29.85
29.78
29.52
29.44
26.34
26.28
26.16
25.95
25.83
23.05
23.01
22.98
22.91
14.42
170
160
150
140
130
120
110
100
90
80
70
60
50
40
30
20
ppm

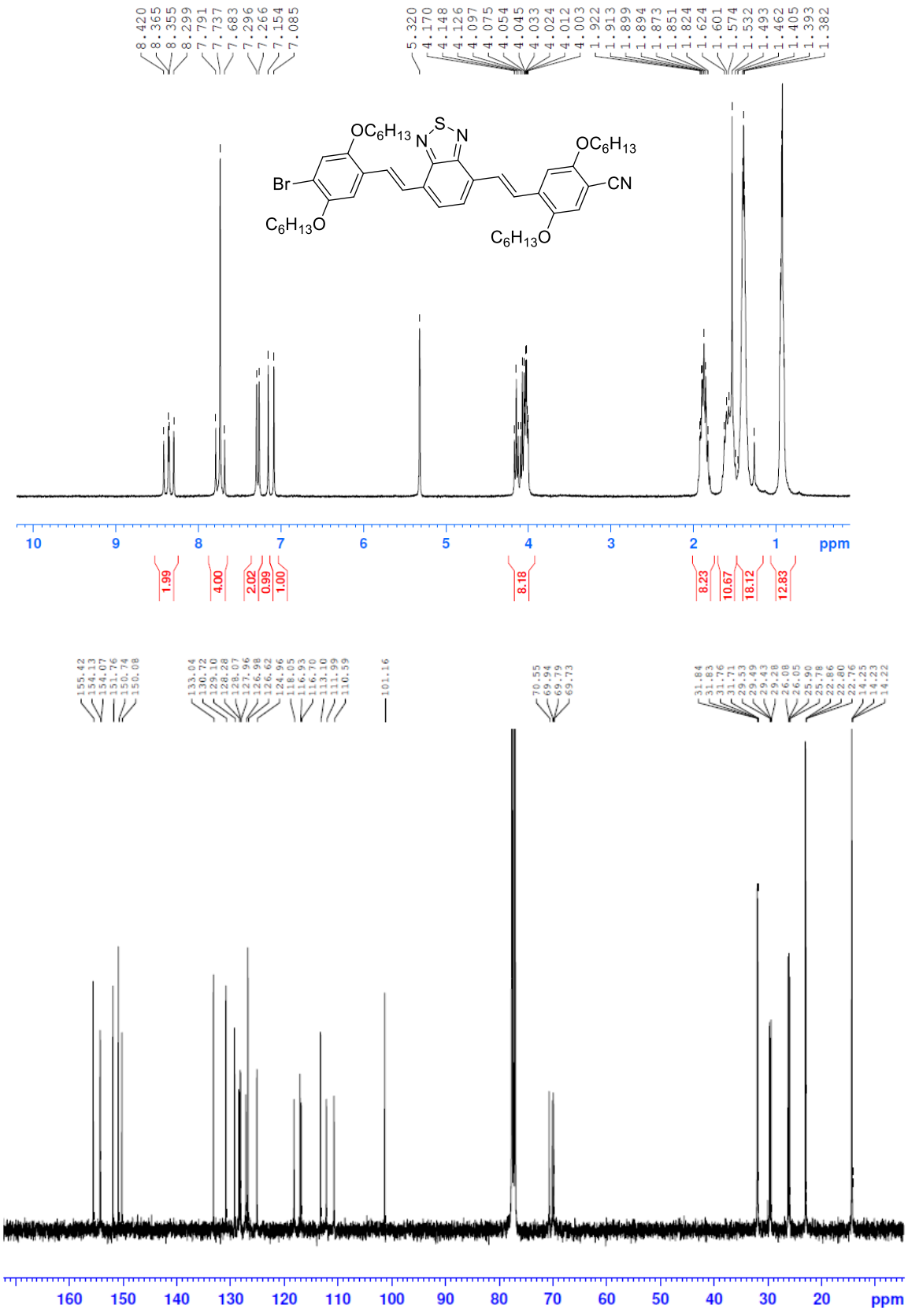
8.420
8.365
8.355
8.299
7.791
7.737
7.683
7.296
7.266
7.154
7.085
5.320
4.170
4.148
4.126
4.097
4.075
4.054
4.045
4.033
4.024
4.012
4.003
1.922
1.913
1.899
1.894
1.873
1.851
1.824
1.624
1.601
1.574
1.532
1.493
1.462
1.405
1.393
1.382
OC6H13
S
N
N
OC6H13
Br
CN
C6H13O
C6H13O
10
9
8
7
6
5
4
3
2
1
ppm
1.99
4.00
2.02
0.99
1.00
8.18
8.23
10.67
18.12
12.83
155.42
154.13
154.07
151.76
150.74
150.08
133.04
130.72
129.10
128.28
128.07
127.96
126.98
126.62
124.96
118.05
116.93
116.70
113.10
111.99
110.59
101.16
70.55
69.94
69.79
69.73
31.84
31.63
31.76
31.71
29.53
29.49
29.43
29.28
26.08
26.05
25.90
25.78
22.86
22.80
22.76
14.25
14.23
14.22
160
150
140
130
120
110
100
90
80
70
60
50
40
30
20
ppm

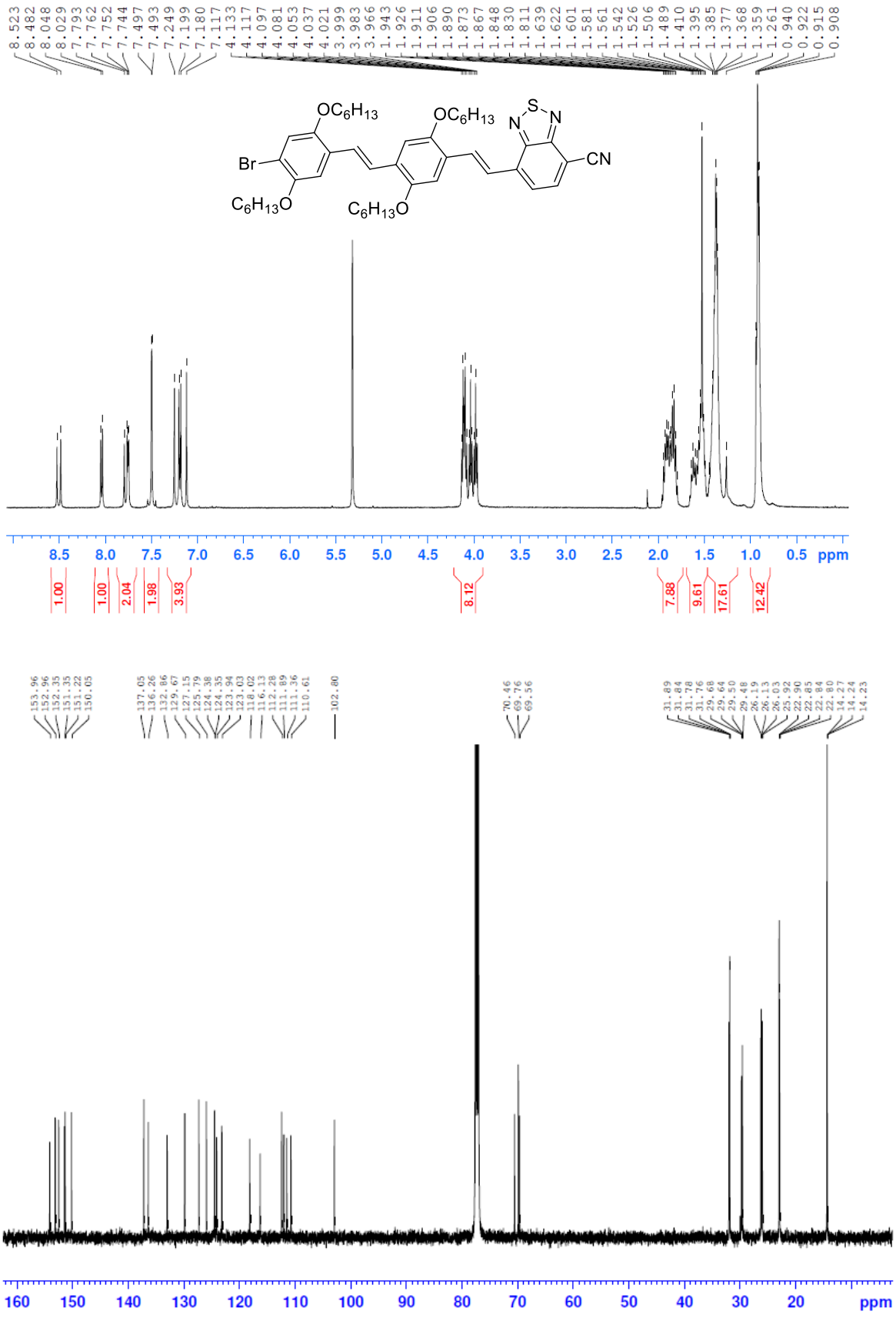
8.523
8.482
8.048
8.029
7.793
7.762
7.752
7.744
7.497
7.493
7.249
7.199
7.180
7.117
4.133
4.117
4.097
4.081
4.053
4.037
4.021
3.999
3.983
3.966
1.943
1.926
1.911
1.906
1.890
1.873
1.867
1.848
1.830
1.811
1.639
1.622
1.601
1.581
1.561
1.542
1.526
1.506
1.489
1.410
1.395
1.385
1.377
1.368
1.359
1.261
0.940
0.922
0.915
0.908
OC6H13
OC6H13
S
N
N
Br
CN
C6H13O
C6H13O
8.5
8.0
7.5
7.0
6.5
6.0
5.5
5.0
4.5
4.0
3.5
3.0
2.5
2.0
1.5
1.0
0.5
ppm
1.00
1.00
2.04
1.98
3.93
8.12
7.88
9.61
17.61
12.42
153.96
152.96
152.35
151.35
151.22
150.05
137.05
136.26
132.86
129.67
127.15
125.79
124.38
124.35
123.94
123.03
118.02
116.13
112.28
111.69
111.36
110.61
102.80
70.46
69.76
69.56
31.89
31.84
31.78
31.76
29.68
29.64
29.50
29.48
26.19
26.13
26.03
25.92
22.90
22.85
22.84
22.80
14.27
14.24
14.23
160
150
140
130
120
110
100
90
80
70
60
50
40
30
20
ppm

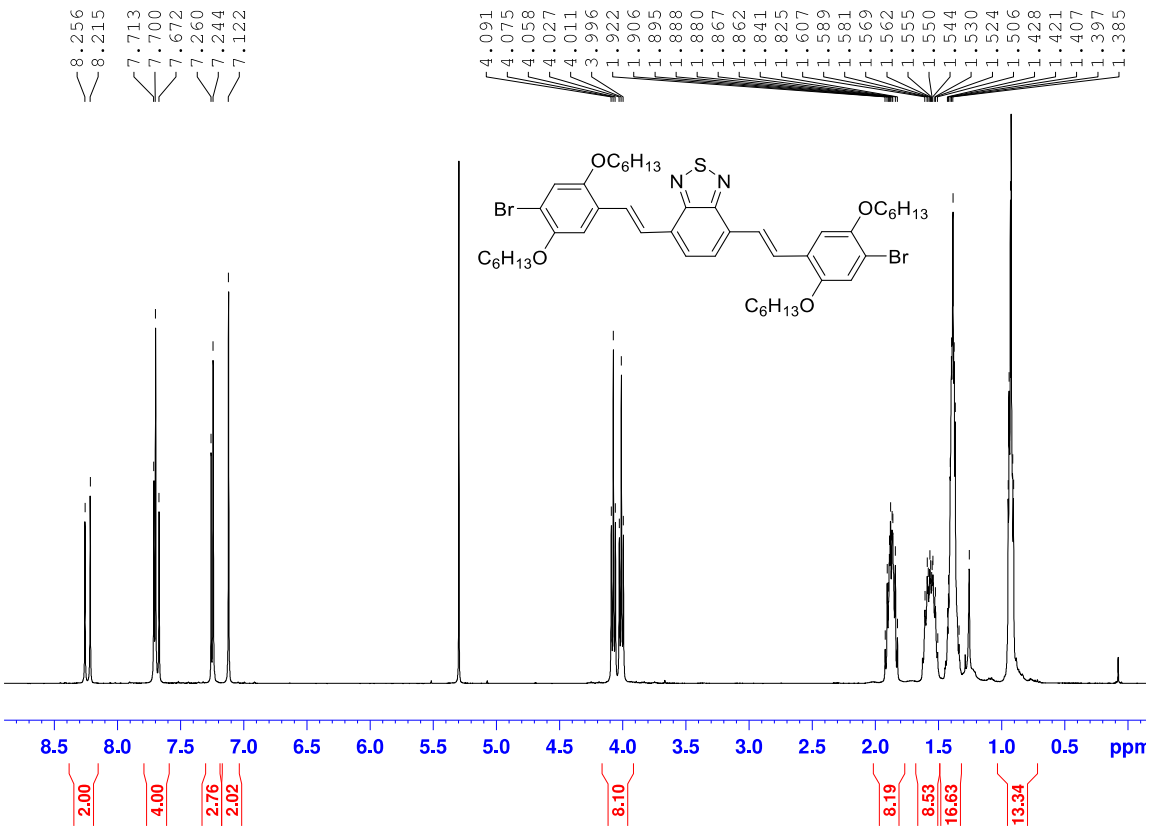
8.256
8.215
7.713
7.700
7.672
7.260
7.244
7.122
4.091
4.075
4.058
4.027
4.011
3.996
1.922
1.906
1.895
1.888
1.880
1.867
1.862
1.841
1.825
1.607
1.589
1.581
1.569
1.562
1.555
1.550
1.544
1.530
1.524
1.506
1.428
1.421
1.407
1.397
1.385
OC6H13
N
S
N
Br
C6H13O
OC6H13
Br
C6H13O
8.5
8.0
7.5
7.0
6.5
6.0
5.5
5.0
4.5
4.0
3.5
3.0
2.5
2.0
1.5
1.0
0.5
ppm
2.00
4.00
2.76
2.02
8.10
8.19
8.53
16.63
13.34

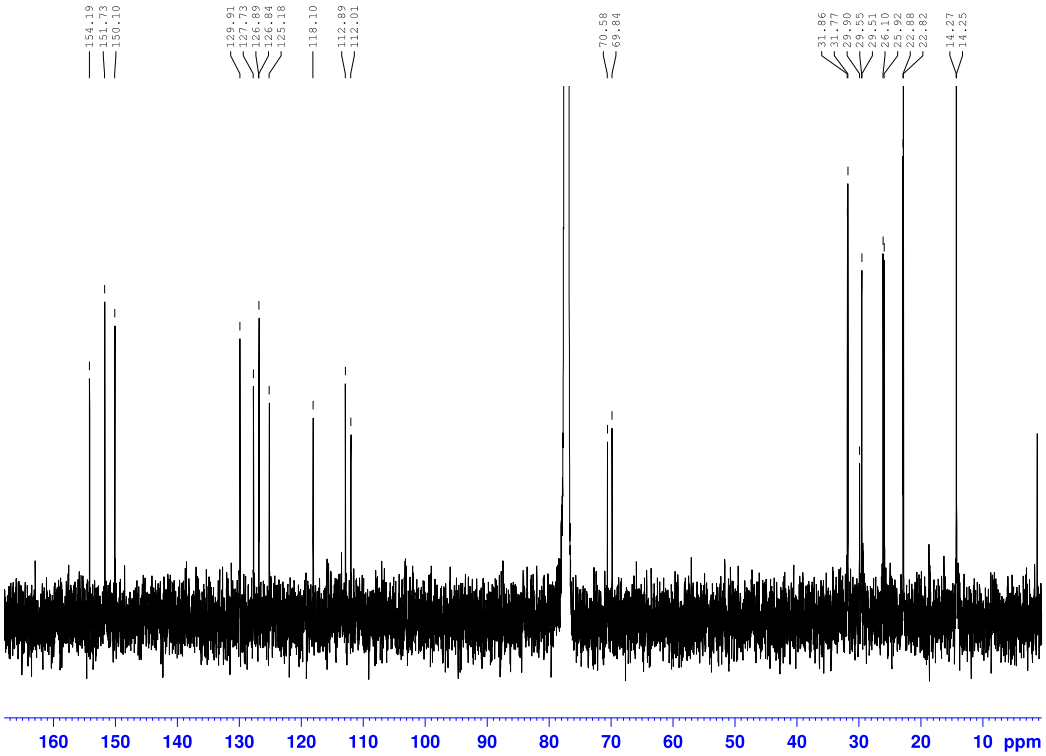
154.19
151.73
130.10
129.91
127.73
126.89
126.84
125.18
118.10
112.89
112.01
70.58
69.84
31.86
31.77
29.90
29.55
29.51
26.10
25.98
22.88
22.82
14.27
14.25
160
150
140
130
120
110
100
90
80
70
60
50
40
30
20
10
ppm

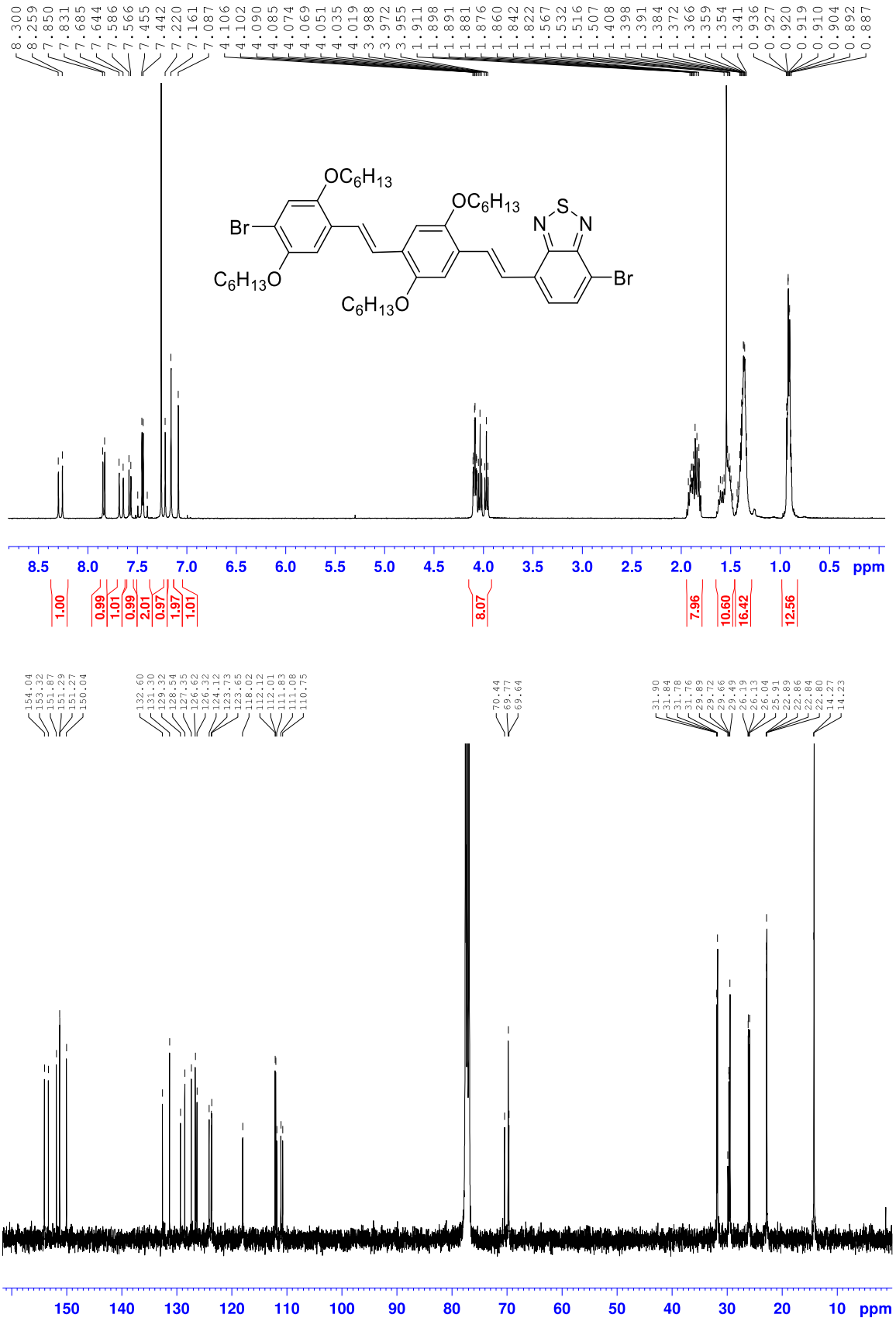
8.300
8.259
7.850
7.831
7.685
7.644
7.586
7.566
7.455
7.442
7.220
7.161
7.087
4.106
4.102
4.090
4.085
4.074
4.069
4.051
4.035
4.019
3.988
3.972
3.955
1.911
1.898
1.891
1.881
1.876
1.860
1.842
1.822
1.567
1.532
1.516
1.507
1.408
1.398
1.391
1.384
1.372
1.366
1.359
1.354
1.341
0.936
0.927
0.920
0.919
0.910
0.904
0.892
0.887
OC6H13
OC6H13
Br
N
S
N
C6H13O
C6H13O
Br
8.5
8.0
7.5
7.0
6.5
6.0
5.5
5.0
4.5
4.0
3.5
3.0
2.5
2.0
1.5
1.0
0.5
ppm
1.00
0.99
1.01
0.99
2.01
0.97
1.97
1.01
8.07
7.96
10.60
16.42
12.56
154.04
153.32
151.87
151.29
151.27
150.04
132.60
131.30
129.32
128.54
127.35
126.62
126.32
124.12
123.73
123.65
118.02
112.12
112.01
111.83
111.08
110.75
70.44
69.77
69.64
31.90
31.84
31.78
31.76
29.89
29.72
29.66
29.49
26.19
26.13
26.04
25.91
22.89
22.86
22.84
22.80
14.27
14.23
150
140
130
120
110
100
90
80
70
60
50
40
30
20
10
ppm

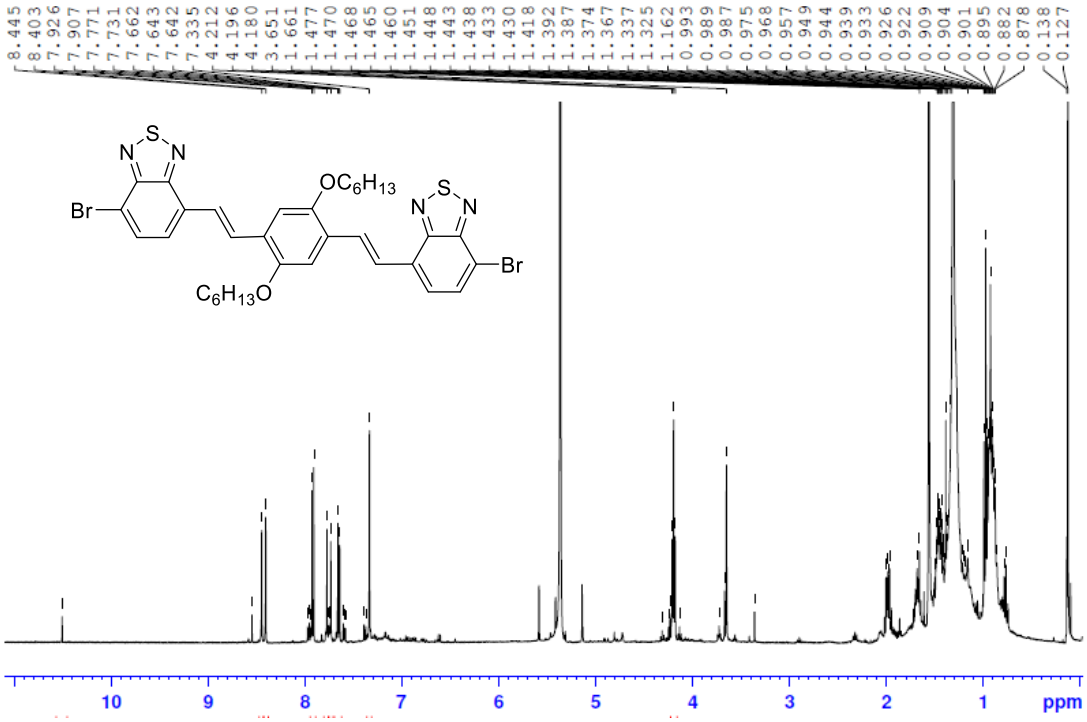
8.445
8.403
7.926
7.907
7.771
7.731
7.662
7.643
7.642
7.335
4.212
4.196
4.180
3.651
1.661
1.477
1.470
1.468
1.465
1.460
1.451
1.448
1.443
1.438
1.433
1.430
1.418
1.392
1.387
1.374
1.367
1.337
1.325
1.162
0.993
0.989
0.987
0.975
0.968
0.957
0.949
0.944
0.939
0.933
0.926
0.922
0.909
0.904
0.901
0.895
0.882
0.878
0.138
0.127
Br
OC6H13
C6H13O
Br
10
9
8
7
6
5
4
3
2
1
ppm

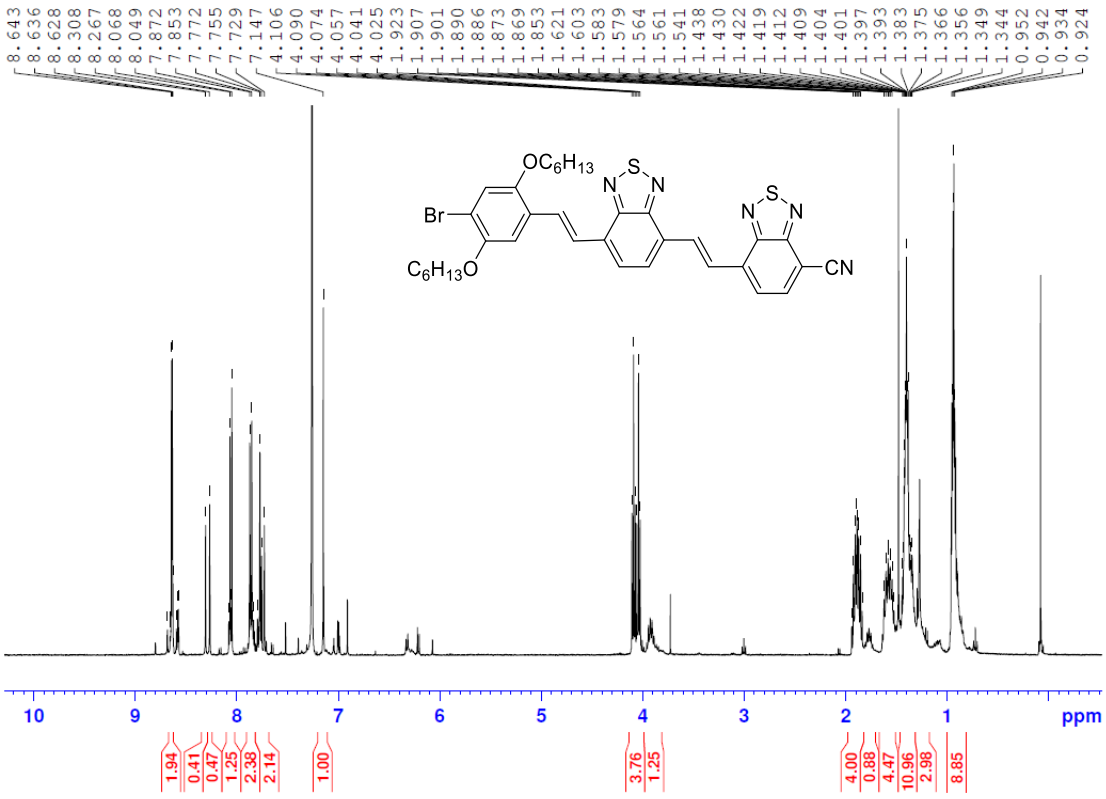
8.643
8.636
8.628
8.308
8.267
8.068
8.049
7.872
7.853
7.772
7.755
7.729
7.147
4.106
4.090
4.074
4.057
4.041
4.025
1.923
1.907
1.901
1.890
1.886
1.873
1.869
1.853
1.621
1.603
1.583
1.579
1.564
1.561
1.541
1.438
1.430
1.422
1.419
1.412
1.409
1.404
1.401
1.397
1.393
1.383
1.375
1.366
1.356
1.349
1.344
0.952
0.942
0.934
0.924
OC6H13
Br
C6H13O
CN
10
9
8
7
6
5
4
3
2
1
ppm
1.94
0.41
0.47
1.25
2.38
2.14
1.00
3.76
1.25
4.00
0.88
4.47
10.96
2.98
8.85

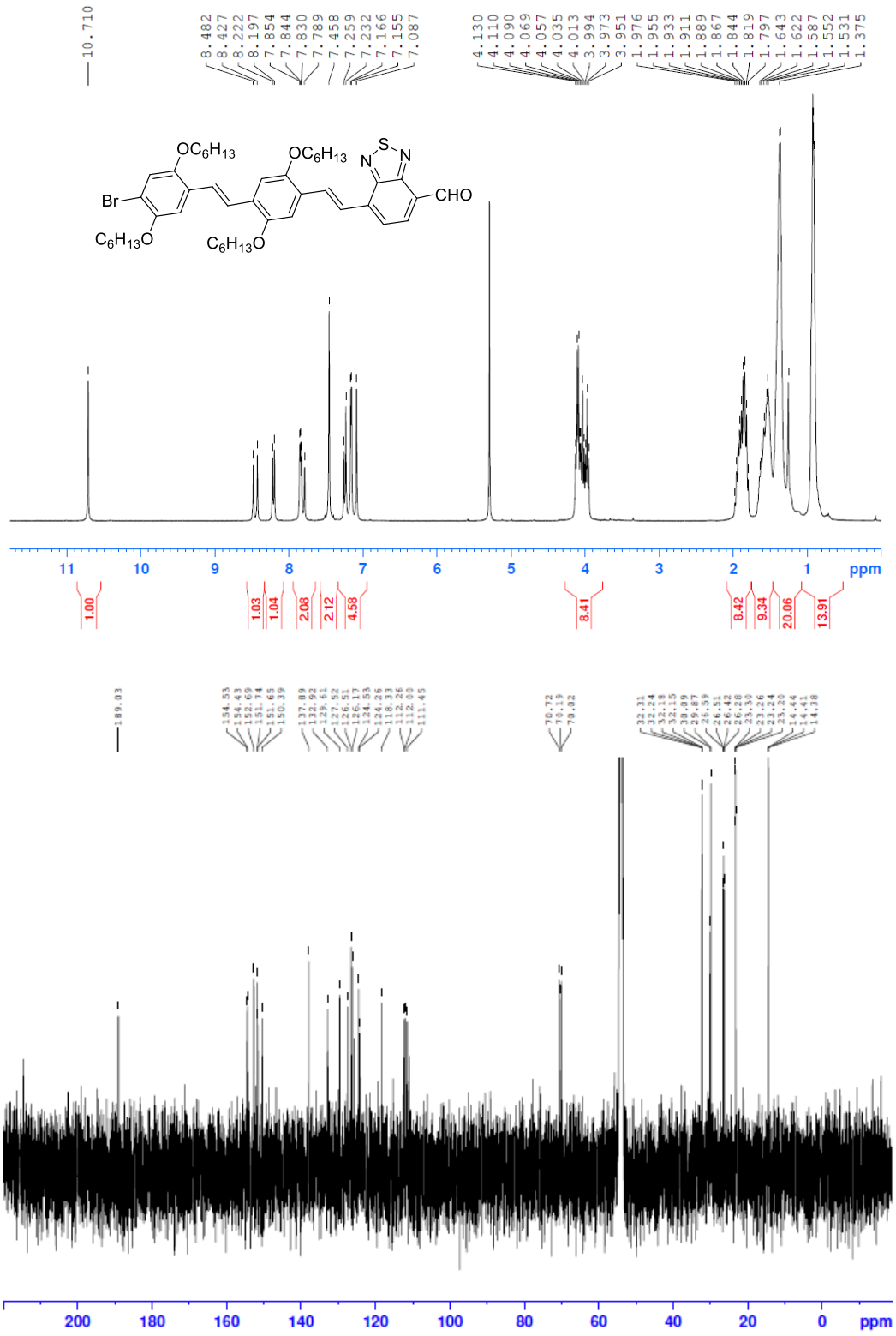
10.710
8.482
8.427
8.222
8.197
7.854
7.844
7.830
7.789
7.458
7.259
7.232
7.166
7.155
7.087
4.130
4.110
4.090
4.069
4.057
4.035
4.013
3.994
3.973
3.951
1.976
1.955
1.933
1.911
1.889
1.867
1.844
1.819
1.797
1.643
1.622
1.587
1.552
1.531
1.375
OC6H13
OC6H13
Br
C6H13O
C6H13O
N
S
N
CHO
11
10
9
8
7
6
5
4
3
2
1
ppm
1.00
1.03
1.04
2.08
2.12
4.58
8.41
8.42
9.34
20.06
13.91
189.03
154.53
154.43
152.69
151.94
151.65
150.39
137.89
132.82
129.61
127.52
126.51
126.17
124.53
124.26
118.33
112.26
112.00
111.45
70.72
70.19
70.02
32.31
32.24
32.19
32.15
30.09
29.87
29.59
26.51
26.43
26.28
23.30
23.26
23.24
23.20
14.44
14.41
14.38
200
180
160
140
120
100
80
60
40
20
0
ppm

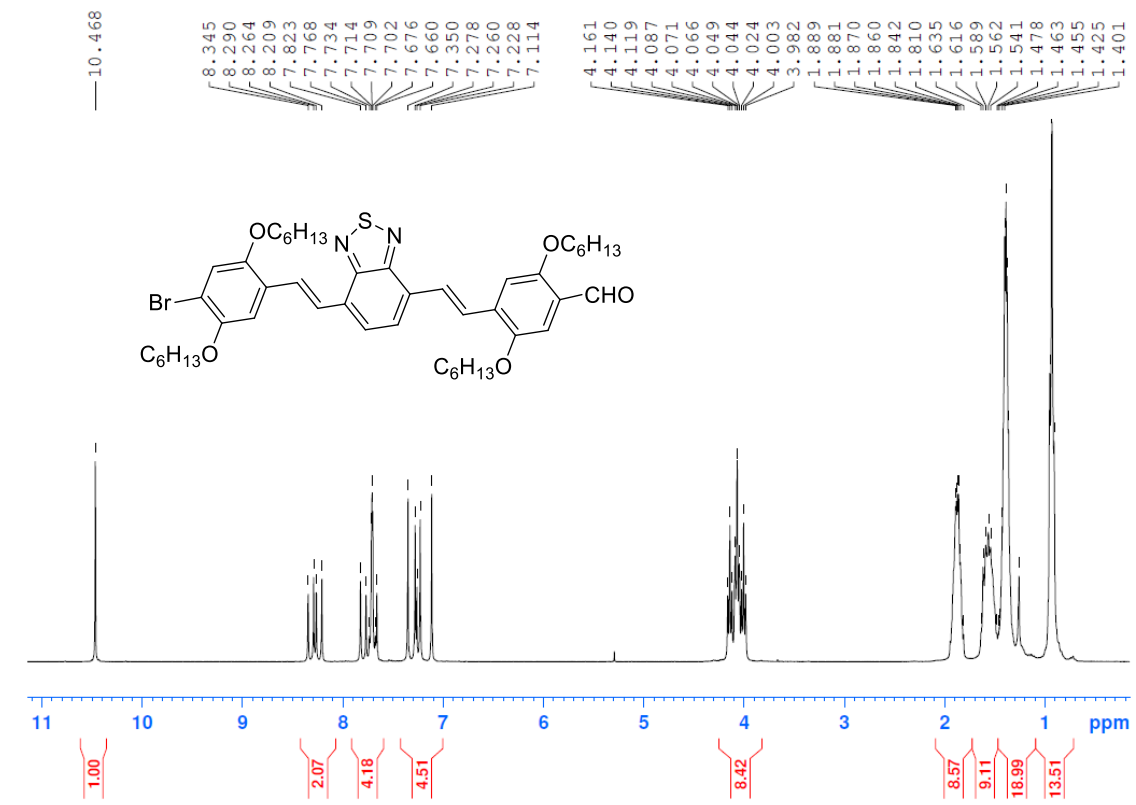
10.468
8.345
8.290
8.264
8.209
7.823
7.768
7.734
7.714
7.709
7.702
7.676
7.660
7.350
7.278
7.260
7.228
7.114
4.161
4.140
4.119
4.087
4.071
4.066
4.049
4.044
4.024
4.003
3.982
1.889
1.881
1.870
1.860
1.842
1.810
1.635
1.616
1.589
1.562
1.541
1.478
1.463
1.455
1.425
1.401
OC6H13
N
S
N
OC6H13
Br
CHO
C6H13O
C6H13O
11
10
9
8
7
6
5
4
3
2
1
ppm
1.00
2.07
4.18
4.51
8.42
8.57
9.11
18.99
13.51

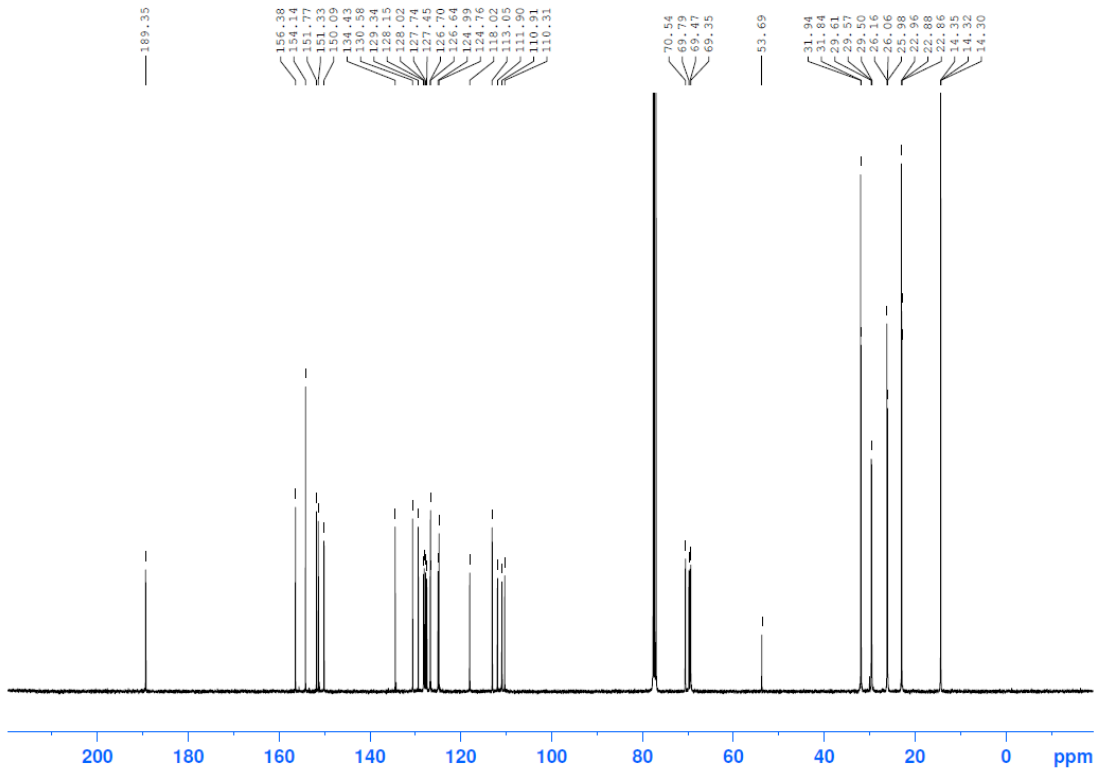
189.35
156.38
154.14
151.77
151.33
150.09
134.43
130.58
129.34
128.15
128.02
127.74
127.45
126.70
126.64
124.99
124.76
118.02
113.05
111.90
110.91
110.31
70.54
69.79
69.47
69.35
53.69
31.94
31.84
29.61
29.57
29.50
26.16
26.06
25.98
22.96
22.88
22.86
14.35
14.32
14.30
200
180
160
140
120
100
80
60
40
20
0
ppm

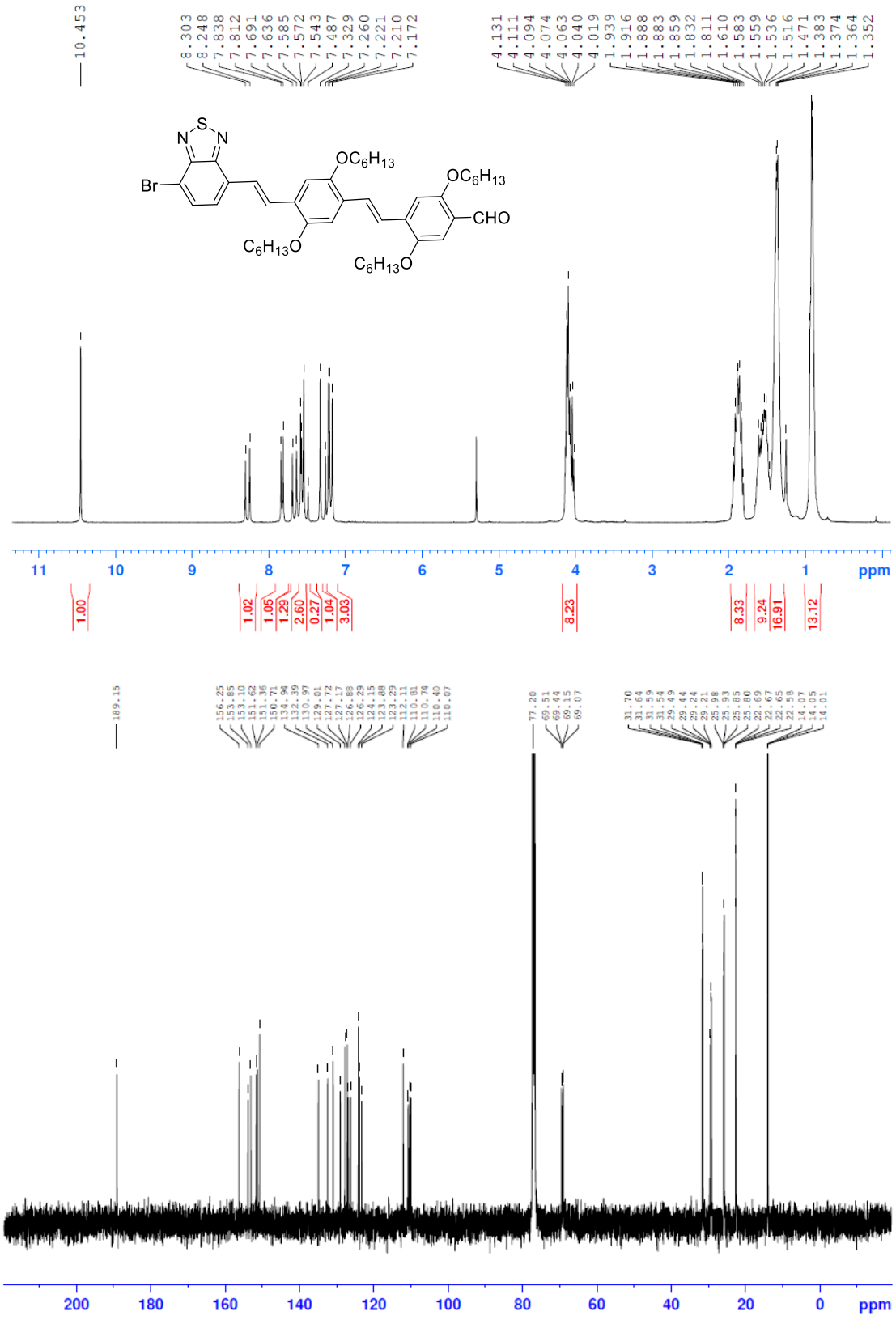
10.453
8.303
8.248
7.838
7.812
7.691
7.636
7.585
7.572
7.543
7.487
7.329
7.260
7.221
7.210
7.172
4.131
4.111
4.094
4.074
4.063
4.040
4.019
1.939
1.916
1.888
1.883
1.859
1.832
1.811
1.610
1.583
1.559
1.536
1.516
1.471
1.383
1.374
1.364
1.352
Br
OC6H13
OC6H13
CHO
C6H13O
C6H13O
11
10
9
8
7
6
5
4
3
2
1
ppm
1.00
1.02
1.05
1.29
2.60
0.27
1.04
3.03
8.23
8.33
9.24
16.91
13.12
189.15
156.25
153.85
153.10
151.62
151.36
150.71
134.94
134.39
130.97
129.01
127.72
127.17
126.88
126.29
124.15
123.88
123.29
112.11
110.81
110.74
110.40
110.07
77.20
69.31
69.44
69.15
69.07
31.70
31.64
31.59
31.54
29.49
29.44
29.24
29.21
25.98
25.83
25.65
25.60
22.69
22.67
22.65
22.58
14.07
14.05
14.01
200
180
160
140
120
100
80
60
40
20
0
ppm

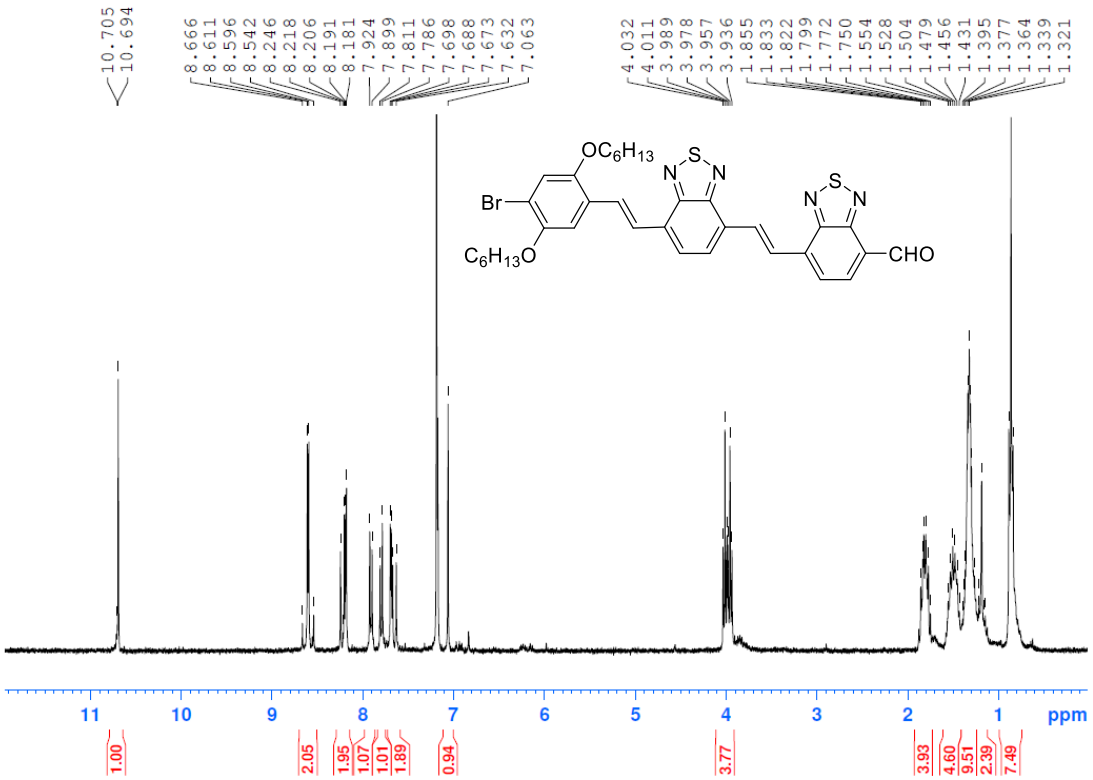
10.705
10.694
8.666
8.611
8.596
8.542
8.246
8.218
8.206
8.191
8.181
7.924
7.899
7.811
7.786
7.698
7.688
7.673
7.632
7.063
4.032
4.011
3.989
3.978
3.957
3.936
1.855
1.833
1.822
1.799
1.772
1.750
1.554
1.528
1.504
1.479
1.456
1.431
1.395
1.377
1.364
1.339
1.321
OC6H13
Br
C6H13O
CHO
11
10
9
8
7
6
5
4
3
2
1
ppm
1.00
2.05
1.95
1.07
1.01
1.89
0.94
3.77
3.93
4.60
9.51
2.39
7.49

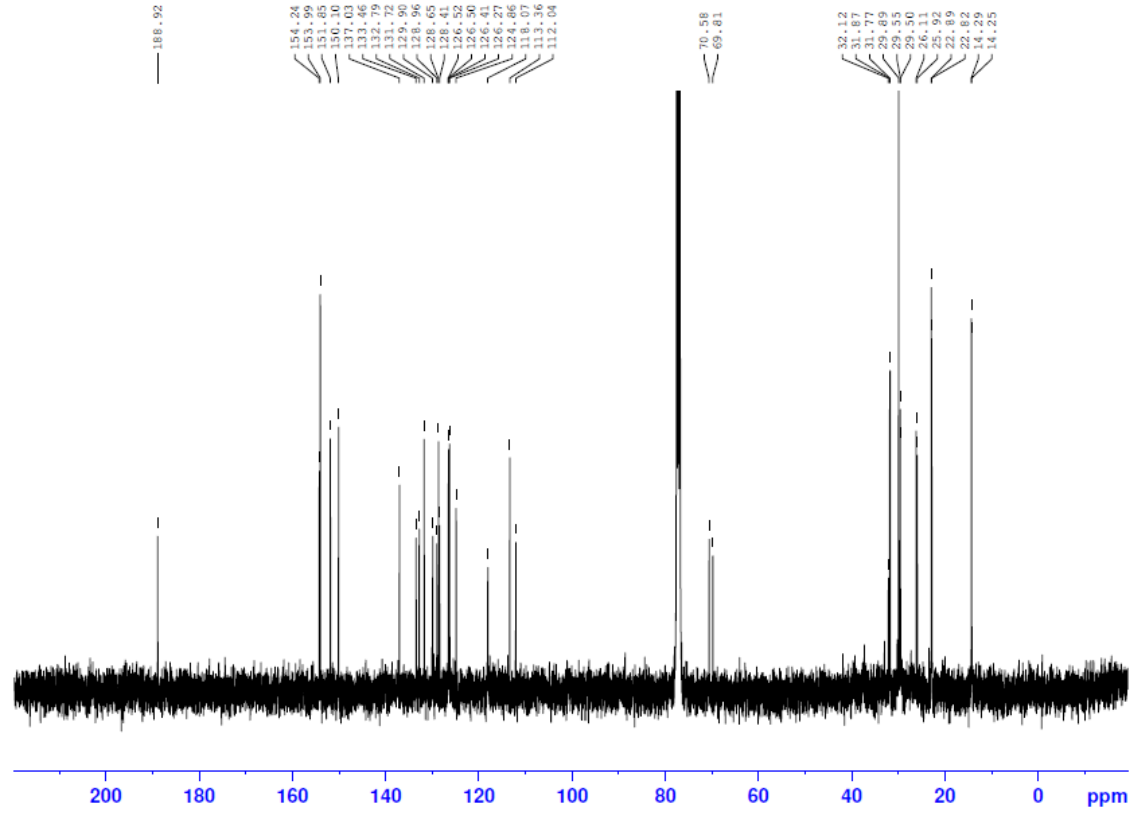
188.92
154.24
153.99
151.85
150.10
137.03
133.46
132.79
131.72
129.90
128.96
128.65
128.41
126.52
126.50
126.41
126.27
124.86
118.07
113.36
112.04
70.58
69.81
32.12
31.67
31.77
29.89
29.55
29.50
26.11
25.92
22.89
22.82
14.29
14.25
200
180
160
140
120
100
80
60
40
20
0
ppm

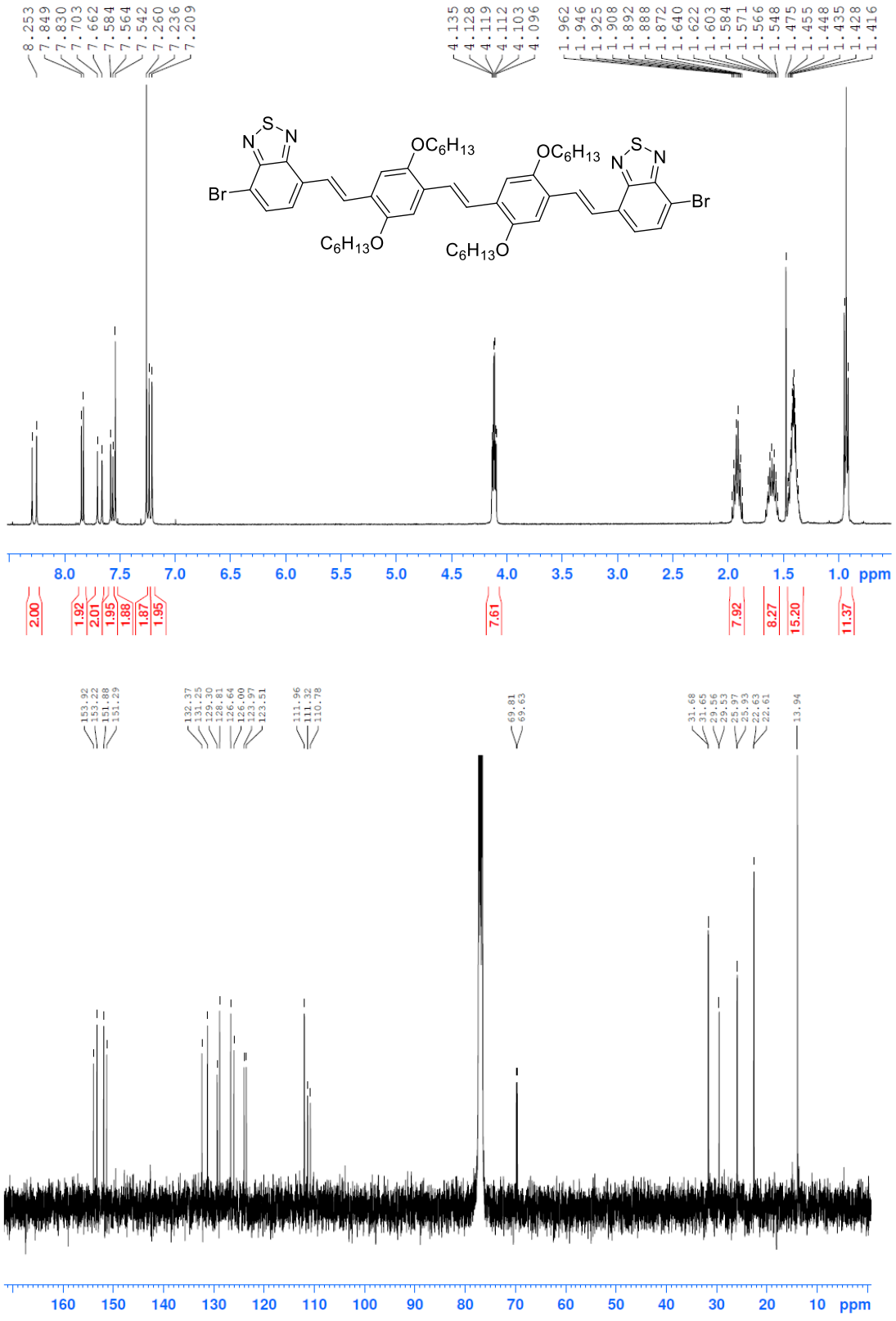
8.253
7.849
7.830
7.703
7.662
7.584
7.564
7.542
7.260
7.236
7.209
4.135
4.128
4.119
4.112
4.103
4.096
1.962
1.946
1.925
1.908
1.892
1.888
1.872
1.640
1.622
1.603
1.584
1.571
1.566
1.548
1.475
1.455
1.448
1.435
1.428
1.416
Br
OC6H13
OC6H13
Br
C6H13O
C6H13O
8.0
7.5
7.0
6.5
6.0
5.5
5.0
4.5
4.0
3.5
3.0
2.5
2.0
1.5
1.0
ppm
2.00
1.92
2.01
1.95
1.88
1.87
1.95
7.61
7.92
8.27
15.20
11.37
153.92
153.22
151.88
151.29
132.37
131.25
129.30
128.81
126.64
126.00
123.97
123.51
111.96
111.32
110.78
69.81
69.63
31.68
31.65
29.56
29.53
25.97
25.93
22.63
22.61
13.94
160
150
140
130
120
110
100
90
80
70
60
50
40
30
20
10
ppm

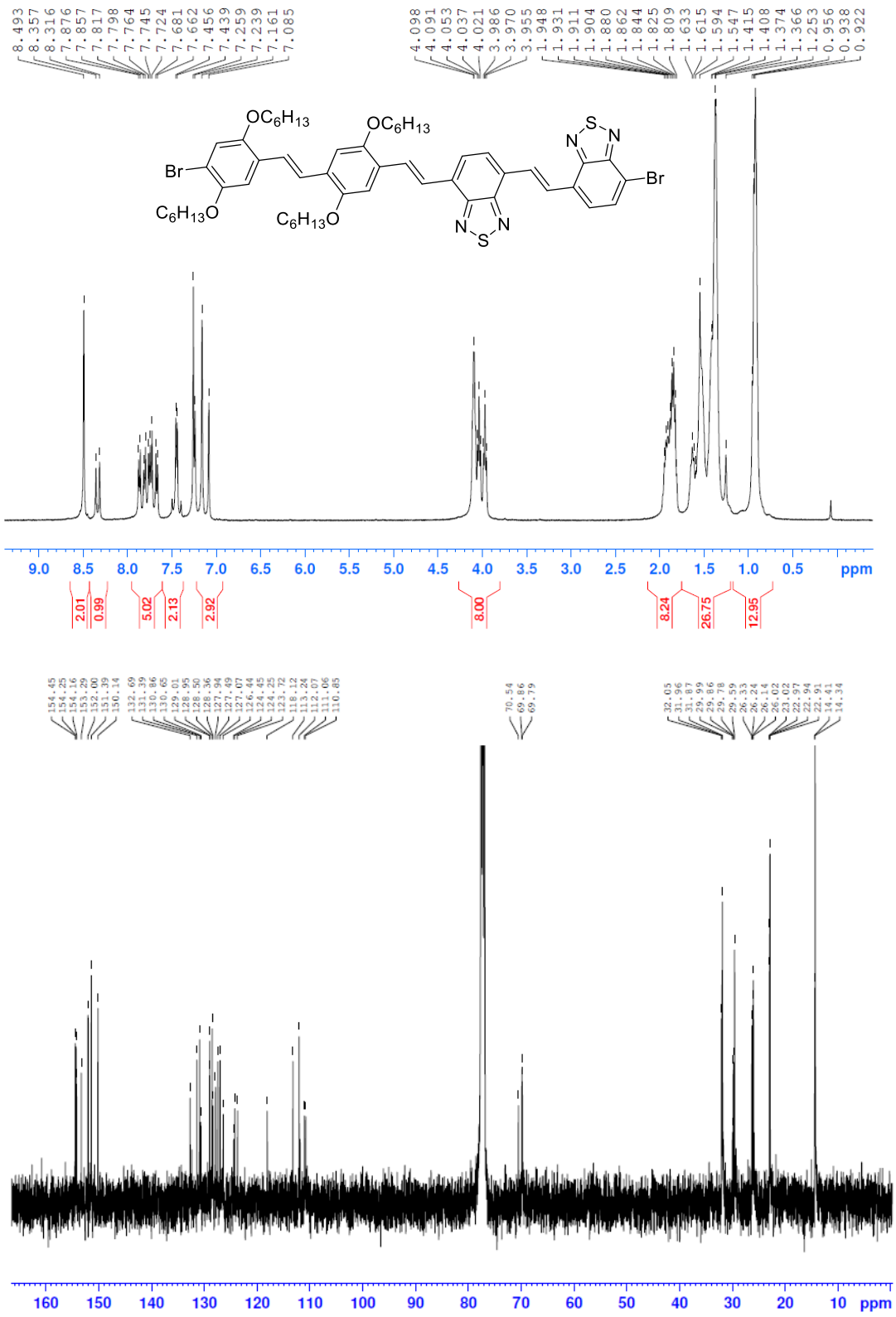
8.493
8.357
8.316
7.876
7.857
7.817
7.798
7.764
7.745
7.724
7.681
7.662
7.456
7.439
7.259
7.239
7.161
7.085
4.098
4.091
4.053
4.037
4.021
3.986
3.970
3.955
1.948
1.931
1.911
1.904
1.880
1.862
1.844
1.825
1.809
1.633
1.615
1.594
1.547
1.415
1.408
1.374
1.366
1.253
0.956
0.938
0.922
OC6H13
OC6H13
Br
C6H13O
C6H13O
N
S
N
N
S
N
Br
9.0
8.5
8.0
7.5
7.0
6.5
6.0
5.5
5.0
4.5
4.0
3.5
3.0
2.5
2.0
1.5
1.0
0.5
ppm
2.01
0.99
5.02
2.13
2.92
8.00
8.24
26.75
12.95
154.45
154.25
154.16
153.29
152.00
151.39
150.14
132.69
131.39
130.86
130.65
129.01
128.95
128.50
128.36
127.94
127.49
127.07
126.44
124.45
124.25
123.72
118.12
113.24
112.07
111.06
110.85
70.54
69.86
69.79
32.05
31.96
31.87
29.99
29.86
29.78
29.59
26.33
26.24
26.14
26.02
23.02
22.97
22.94
22.91
14.41
14.34
160
150
140
130
120
110
100
90
80
70
60
50
40
30
20
10
ppm

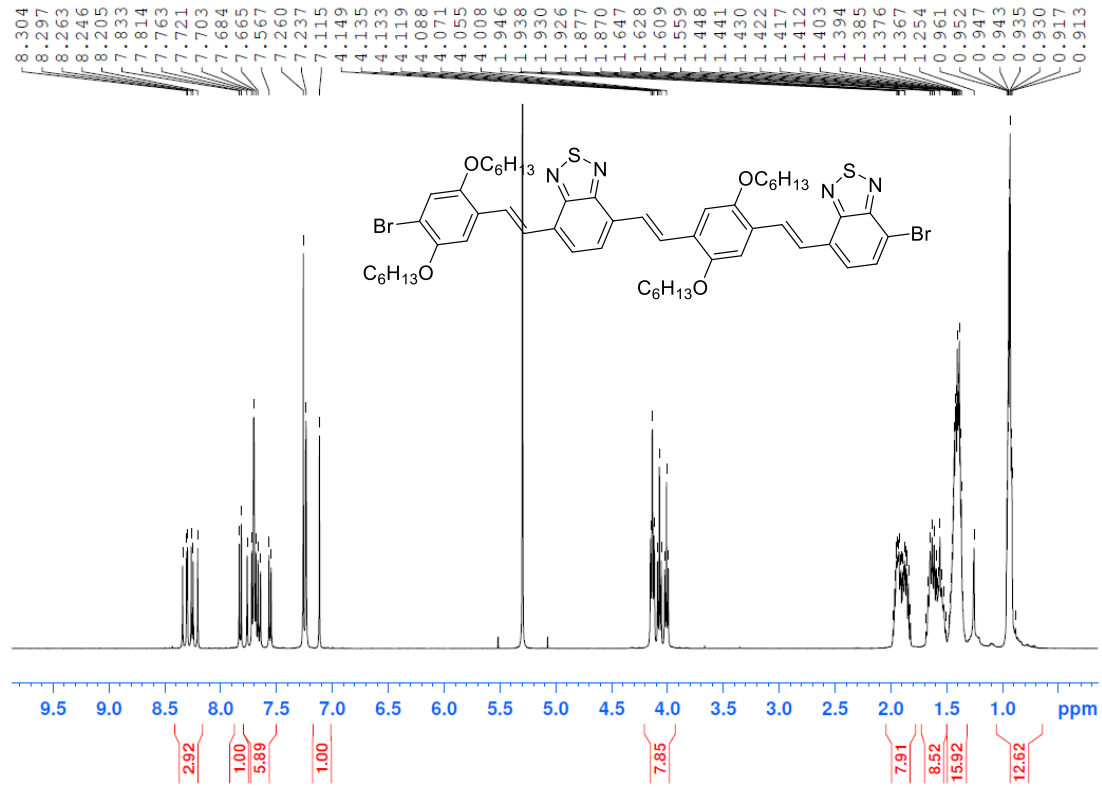
8.304
8.297
8.263
8.246
8.205
7.833
7.814
7.763
7.721
7.703
7.684
7.665
7.567
7.260
7.237
7.115
4.149
4.135
4.133
4.119
4.088
4.071
4.055
4.008
1.946
1.938
1.930
1.926
1.877
1.870
1.647
1.628
1.609
1.559
1.448
1.441
1.430
1.422
1.417
1.412
1.403
1.394
1.385
1.376
1.367
1.254
0.961
0.952
0.947
0.943
0.935
0.930
0.917
0.913
OC6H13
Br
C6H13O
OC6H13
Br
C6H13O
9.5 9.0 8.5 8.0 7.5 7.0 6.5 6.0 5.5 5.0 4.5 4.0 3.5 3.0 2.5 2.0 1.5 1.0 ppm
2.92
1.00
5.89
1.00
7.85
7.91
8.52
15.92
12.62

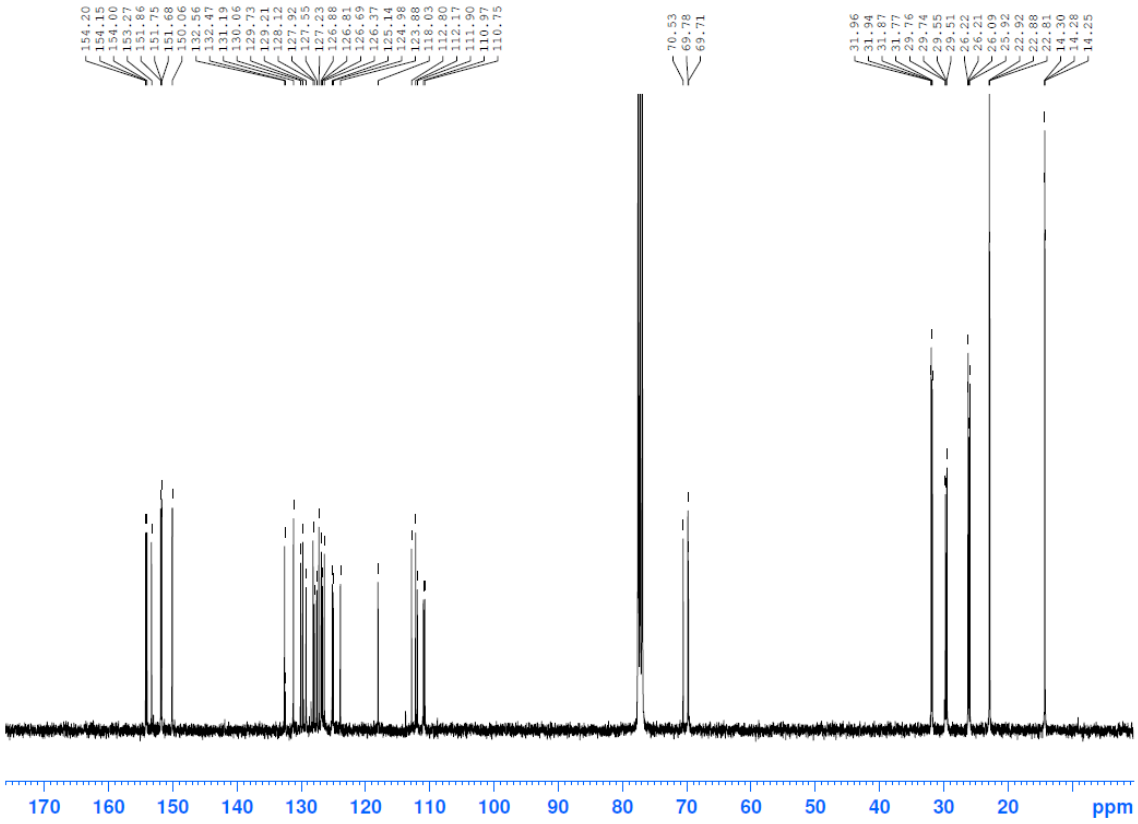
154.20
154.15
154.00
153.27
151.86
151.75
151.68
150.06
132.56
132.47
131.19
130.96
129.73
129.21
128.12
127.92
127.55
127.23
126.88
126.81
126.69
126.37
125.14
124.98
123.88
118.03
112.80
112.17
111.90
110.97
110.75
70.53
69.78
69.71
31.96
31.94
31.87
31.77
29.74
29.55
29.51
26.22
26.21
26.09
25.92
22.88
22.81
14.30
14.28
14.25
170 160 150 140 130 120 110 100 90 80 70 60 50 40 30 20 ppm

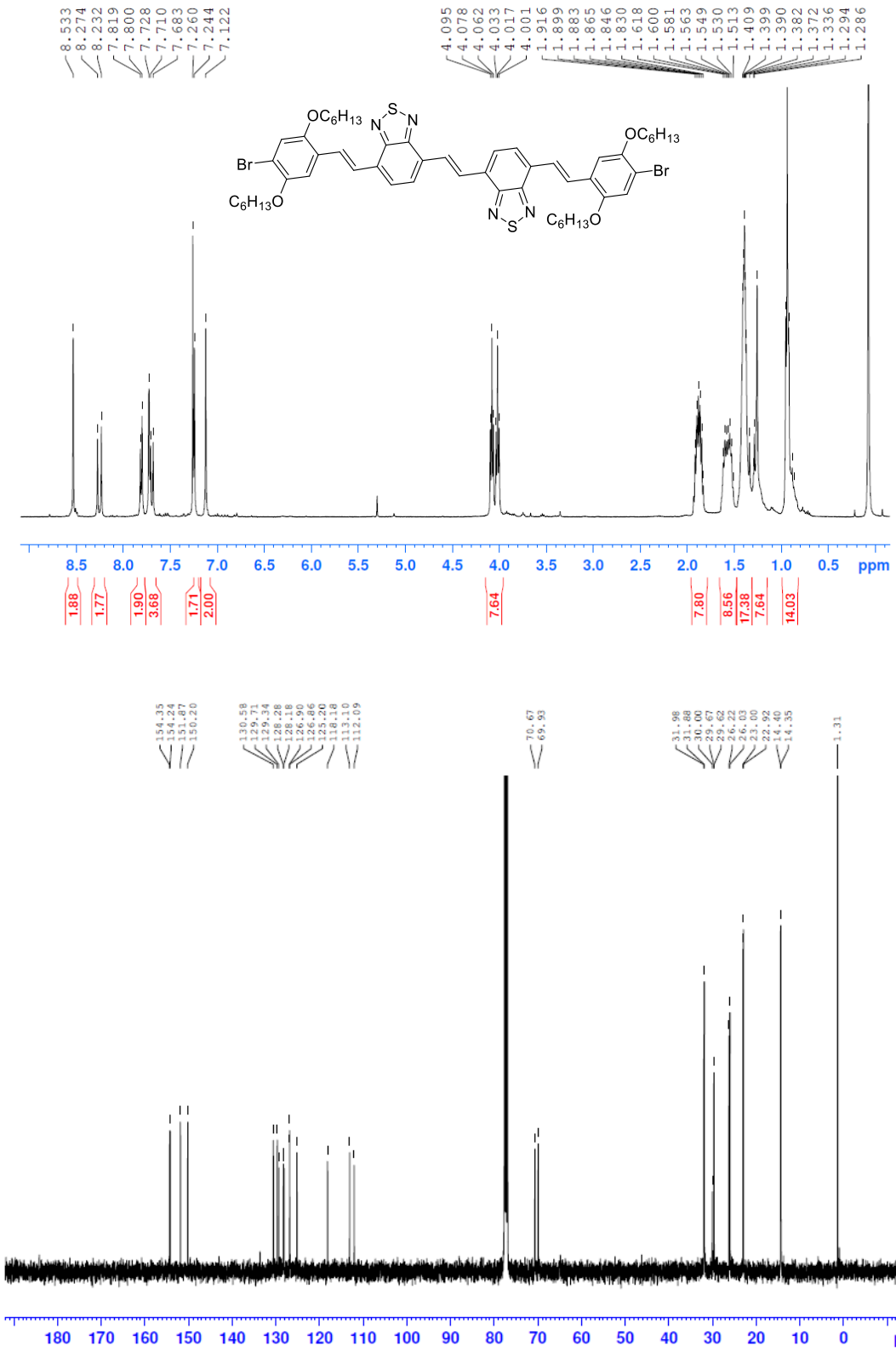
8.533
8.274
8.232
7.819
7.800
7.728
7.710
7.683
7.260
7.244
7.122
4.095
4.078
4.062
4.033
4.017
4.001
1.916
1.899
1.883
1.865
1.846
1.830
1.618
1.600
1.581
1.563
1.549
1.530
1.513
1.409
1.399
1.390
1.382
1.372
1.336
1.294
1.286
OC6H13
Br
C6H13O
N
S
OC6H13
Br
C6H13O
8.5 8.0 7.5 7.0 6.5 6.0 5.5 5.0 4.5 4.0 3.5 3.0 2.5 2.0 1.5 1.0 0.5 ppm
1.88
1.77
1.90
3.68
1.71
2.00
7.64
7.80
8.56
17.38
7.64
14.03
154.35
154.24
151.87
150.20
130.58
129.71
129.34
128.28
128.18
126.90
126.86
125.20
118.18
113.10
112.09
70.67
69.93
31.98
31.88
30.00
29.67
29.62
26.22
26.03
23.00
22.92
14.40
14.35
1.31
180 170 160 150 140 130 120 110 100 90 80 70 60 50 40 30 20 10 0 ppm

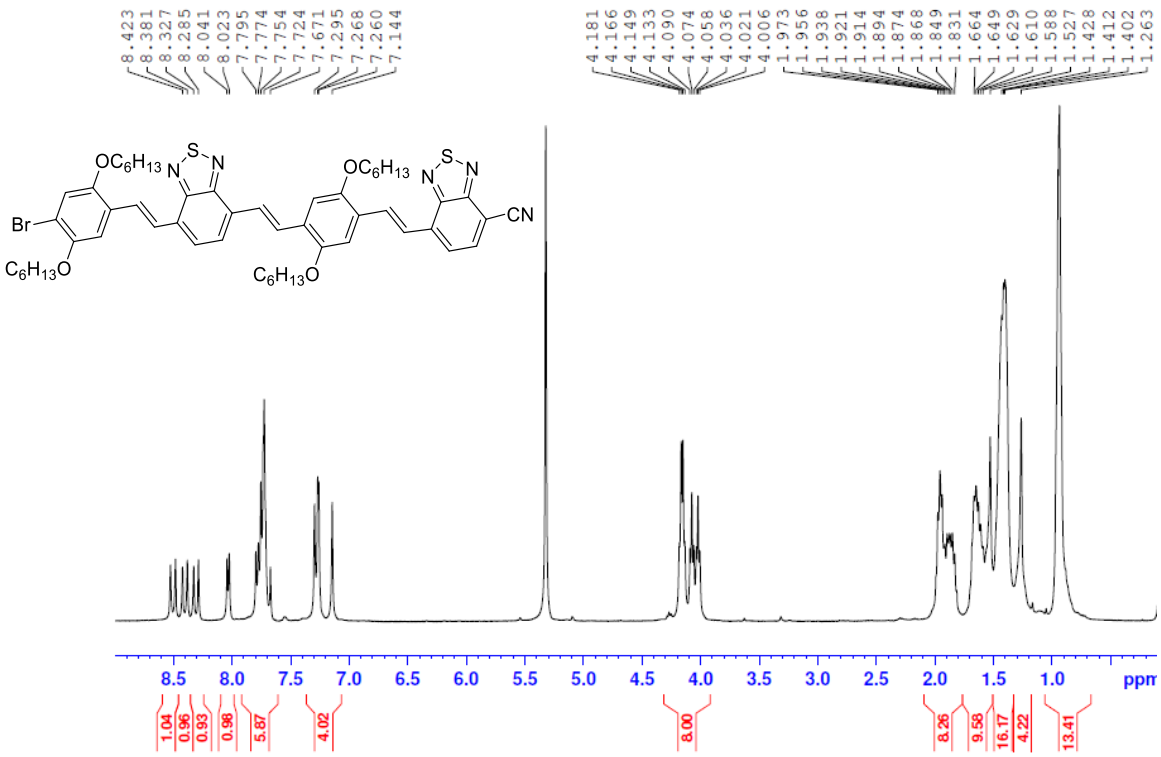
8.423
8.381
8.327
8.285
8.041
8.023
7.795
7.774
7.754
7.724
7.671
7.295
7.268
7.260
7.144
4.181
4.166
4.149
4.133
4.090
4.074
4.058
4.036
4.021
4.006
1.973
1.956
1.938
1.921
1.914
1.894
1.874
1.868
1.849
1.831
1.664
1.649
1.629
1.610
1.588
1.527
1.428
1.412
1.402
1.263
OC6H13
N
S
N
OC6H13
N
S
N
Br
CN
C6H13O
C6H13O
8.5
8.0
7.5
7.0
6.5
6.0
5.5
5.0
4.5
4.0
3.5
3.0
2.5
2.0
1.5
1.0
ppm
1.04
0.96
0.93
0.98
5.87
4.02
8.00
8.26
9.58
16.17
4.22
13.41

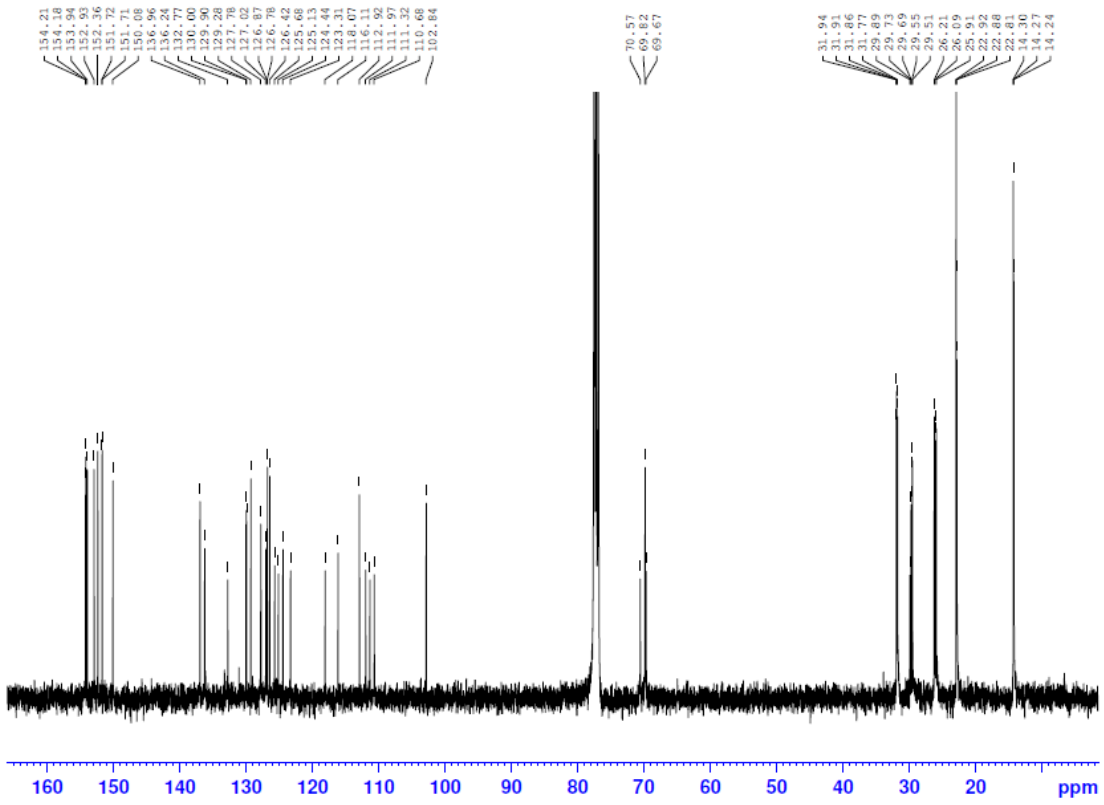
154.21
154.18
153.94
153.93
152.36
151.72
151.71
150.08
136.96
136.24
132.77
130.00
129.90
129.28
127.78
127.02
126.87
126.78
126.42
125.68
125.13
124.44
123.31
118.07
116.11
112.92
111.97
111.32
110.68
102.84
70.57
69.82
69.67
31.94
31.91
31.86
31.77
29.89
29.73
29.69
29.55
29.51
26.21
26.09
25.91
22.92
22.88
22.81
14.30
14.27
14.24
160
150
140
130
120
110
100
90
80
70
60
50
40
30
20
ppm

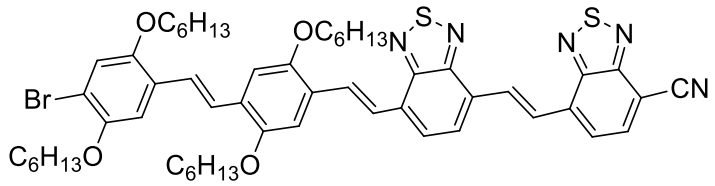
OC6H13
OC6H13
N
S
N
N
S
N
Br
CN
C6H13O
C6H13O

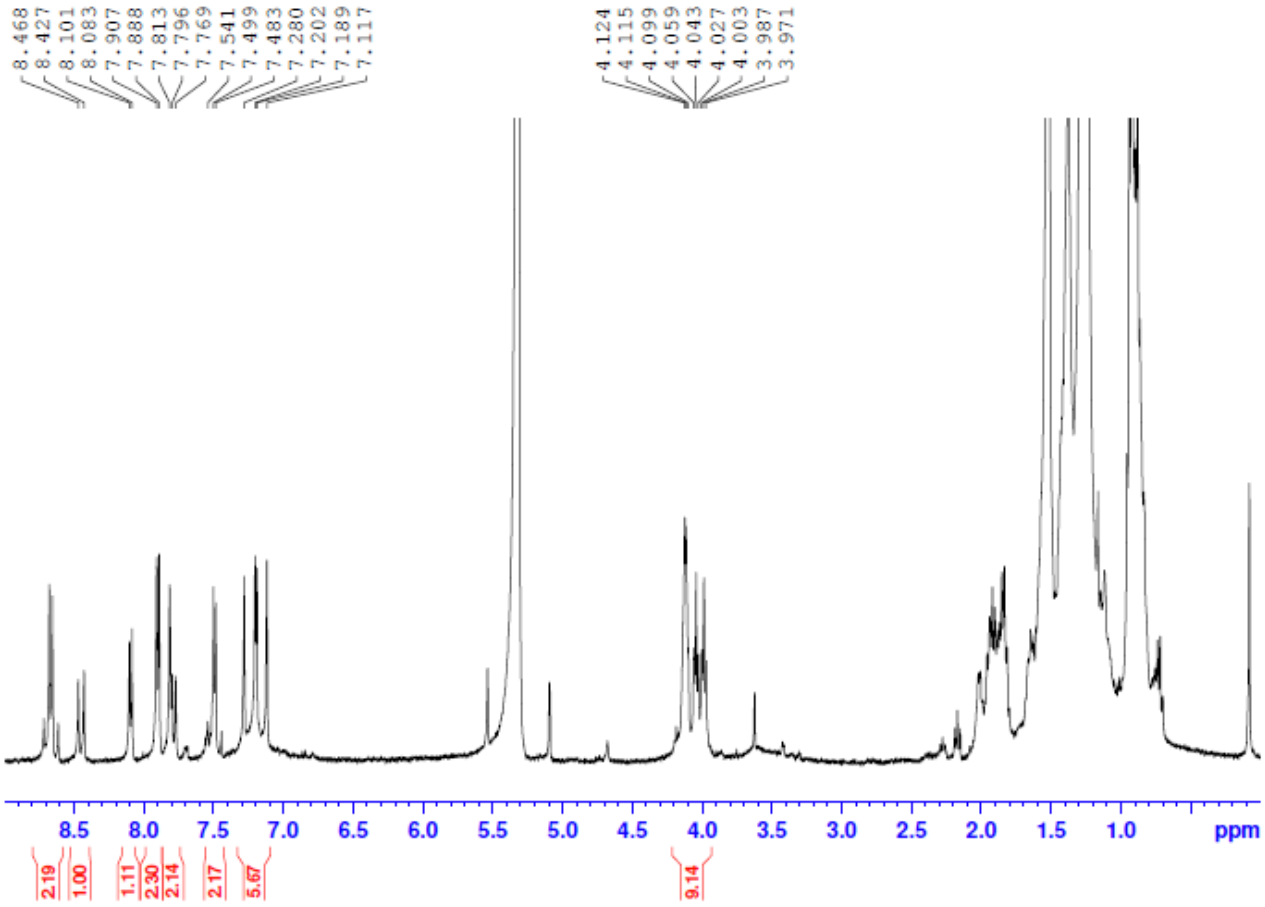
8.468
8.427
8.101
8.083
7.907
7.888
7.813
7.796
7.769
7.541
7.499
7.483
7.280
7.202
7.189
7.117
4.124
4.115
4.099
4.059
4.043
4.027
4.003
3.987
3.971
8.5
8.0
7.5
7.0
6.5
6.0
5.5
5.0
4.5
4.0
3.5
3.0
2.5
2.0
1.5
1.0
ppm
2.19
1.00
1.11
2.30
2.14
2.17
5.67
9.14

B.2 CYCLIC AND DIFFERENTIAL PULSE VOLTAMMOGRAMS OF OLIGOMERS

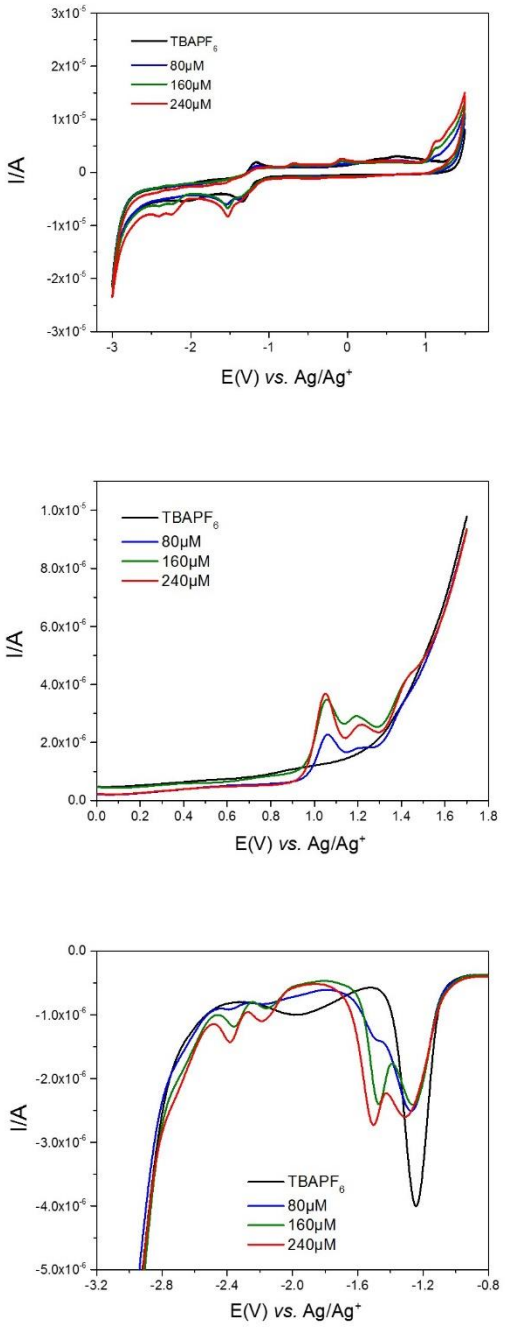

Figure 75. Top: cyclic voltammograms of **Br-PB-Br** in THF. Differential pulse voltammograms of **Br-PB-Br** in THF; Middle: oxidation; Bottom: reduction.

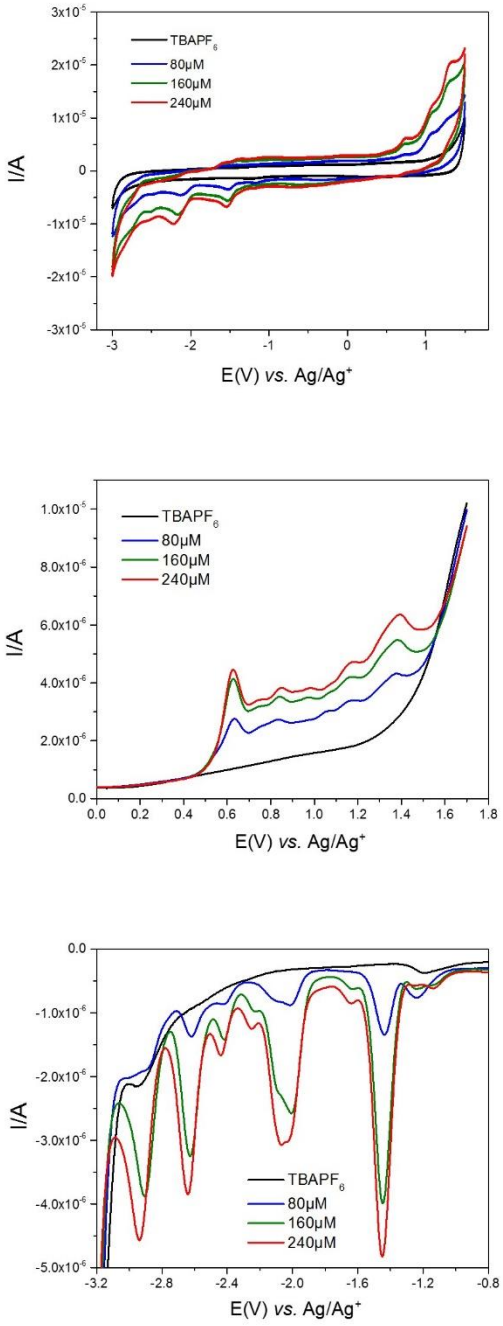

Figure 76. Top: cyclic voltammograms of **Br-PBP-Br** in THF. Differential pulse voltammograms of **Br-PBP-Br** in THF; Middle: oxidation; Bottom: reduction.

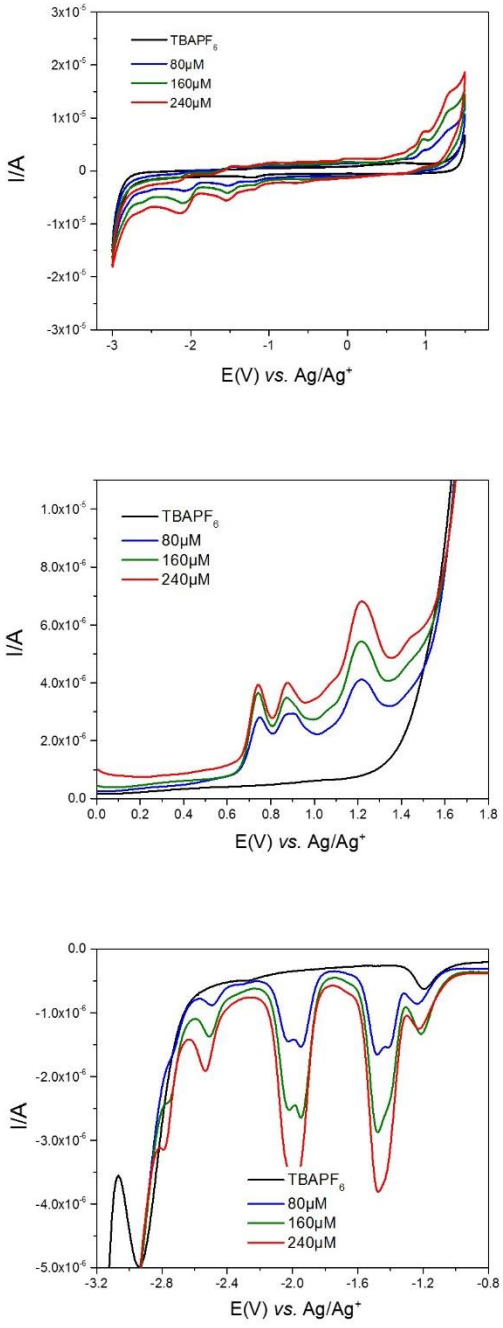

Figure 77. Top: cyclic voltammograms of **Br-BPP-Br** in THF. Differential pulse voltammograms of **Br-PPB-Br** in THF; Middle: oxidation; Bottom: reduction.

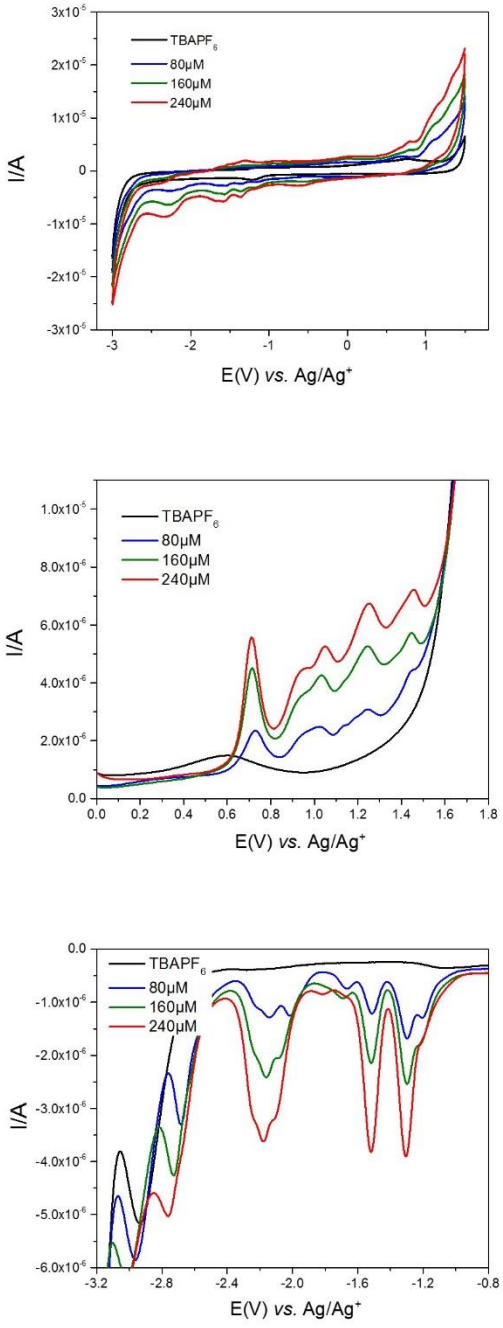

Figure 78. Top: cyclic voltammograms of **Br-BPPB-Br** in THF. Differential pulse voltammograms of **Br-BPPB-Br** in THF; Middle: oxidation; Bottom: reduction.

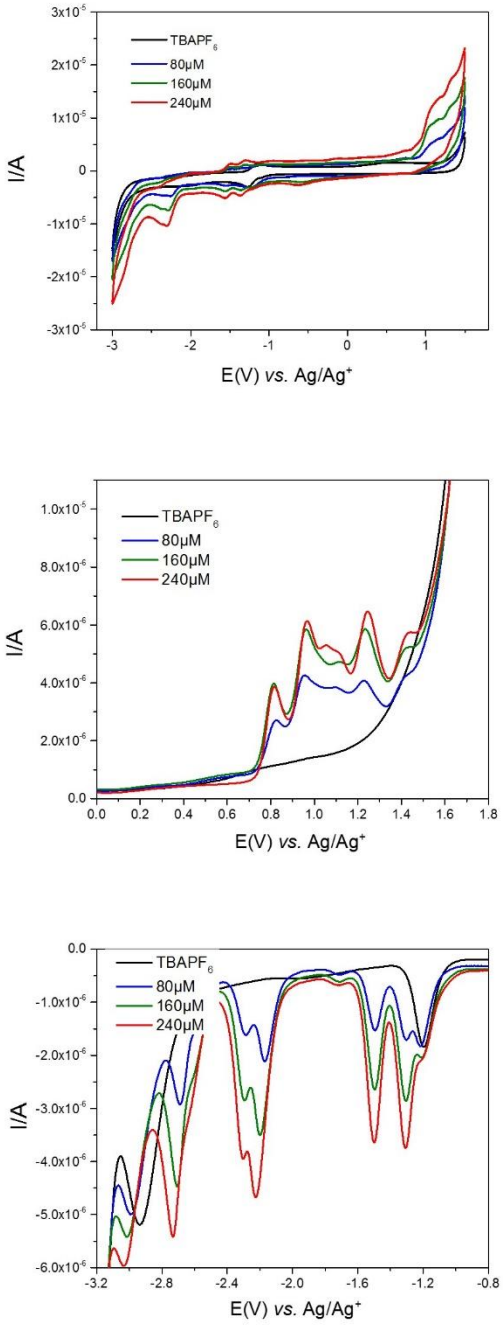

Figure 79. Top: cyclic voltammograms of **Br-PBBP-Br** in THF. Differential pulse voltammograms of **Br-BPPB-Br** in THF; Middle: oxidation; Bottom: reduction.

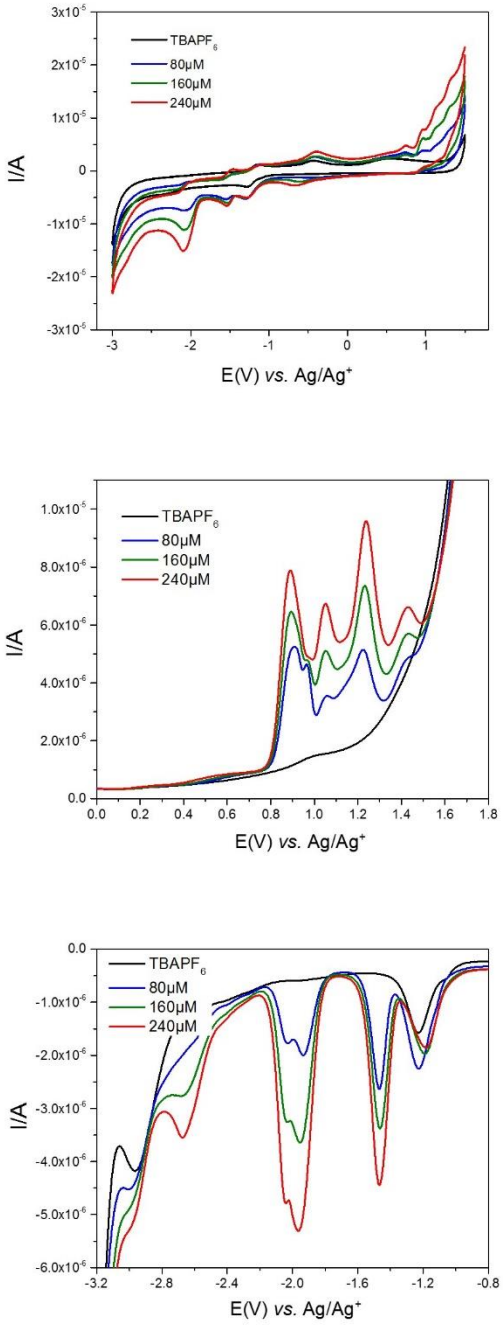

Figure 80. Top: cyclic voltammograms of **Br-PBPB-Br** in THF. Differential pulse voltammograms of **Br-PBPB-Br** in THF; Middle: oxidation; Bottom: reduction.

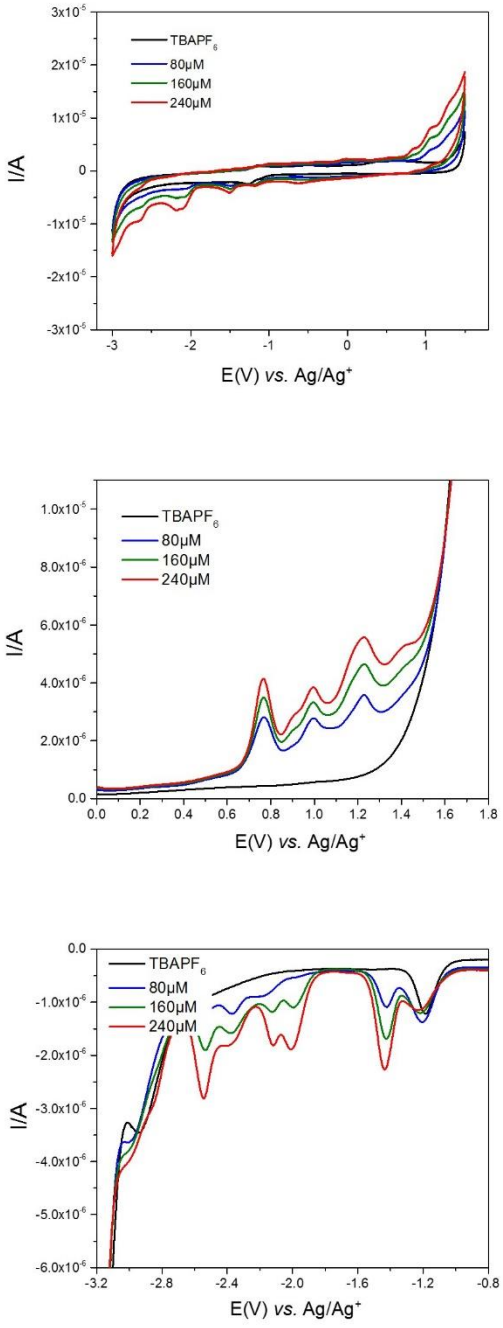

Figure 81. Top: cyclic voltammograms of **Br-PPBB-Br** in THF. Differential pulse voltammograms of **Br-PPBB-Br** in THF; Middle: oxidation; Bottom: reduction.

B.3 ABSORPTION SPECTRA OF SEQUENCED OLIGOMERS

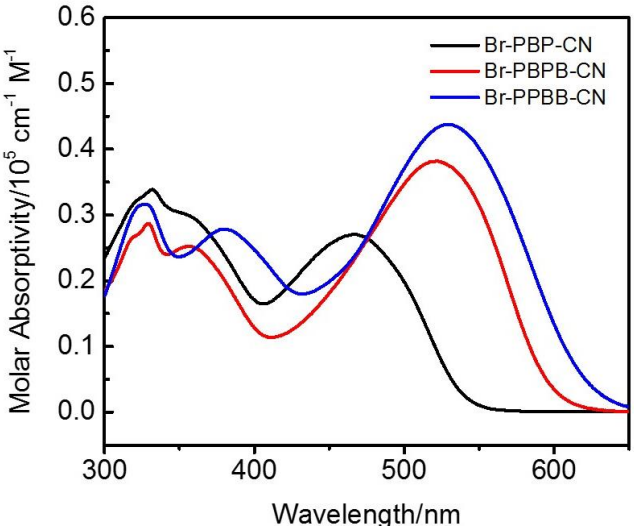

Figure 82. Absorption spectra of selected trimers and tetramers in $CHCl_3$ (1.0×10^{-5} M).

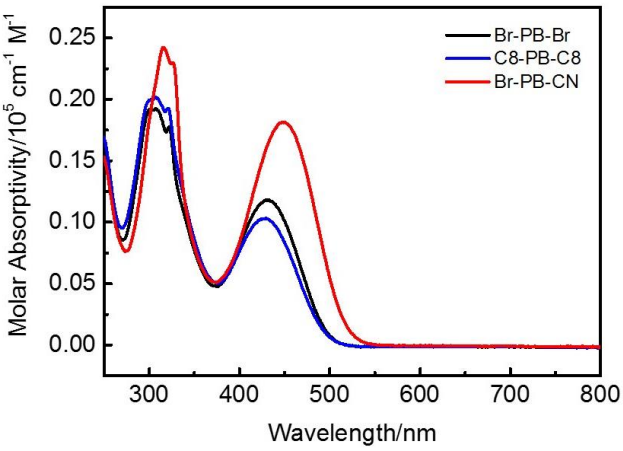

Figure 83. Absorption spectra of dimers in $CHCl_3$ (1.0×10^{-5} M).

B.4 EMISSION SPECTRA OF SEQUENCED OLIGOMERS

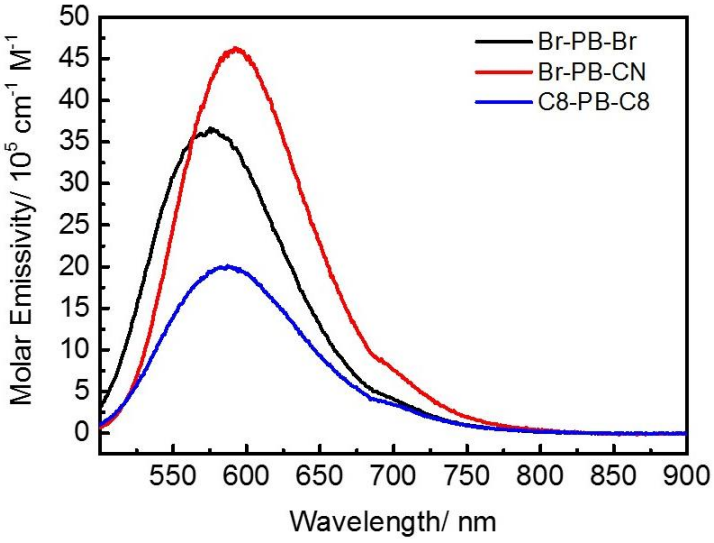

Figure 84. Emission spectra of selected dimers in $CHCl_3$ (1.0×10^{-5} M).

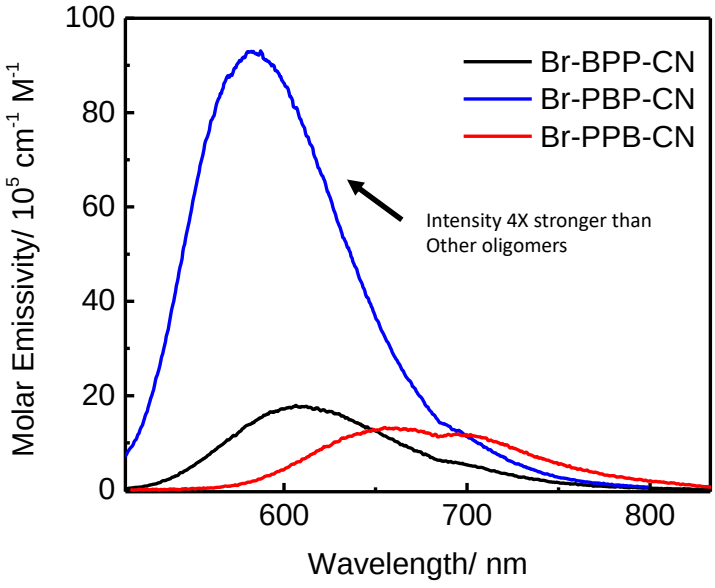

Figure 85. Emission spectra of selected trimers in $CHCl_3$ (1.0×10^{-5} M).

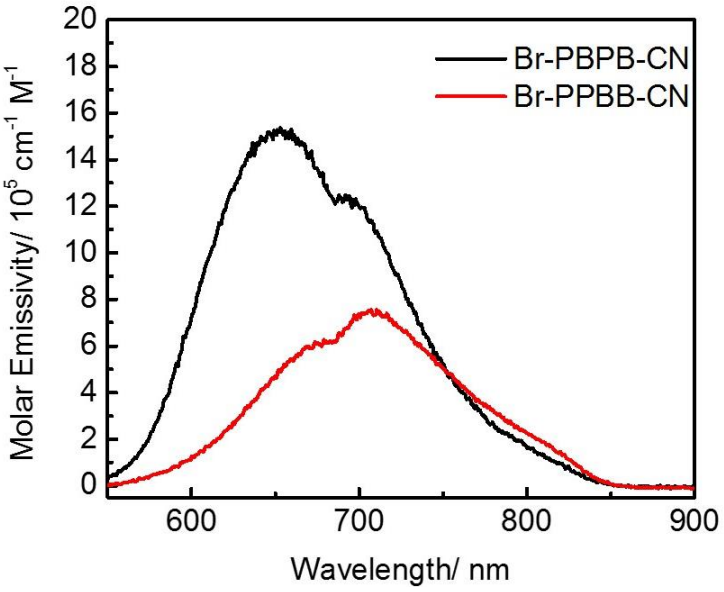

Figure 86. Emission spectra of selected tetramers in $CHCl_3$ (1.0×10^{-5} M).

APPENDIX C

CHAPTER 4 SEQUENCE EFFECTS IN CONJUGATED DONOR-ACCEPTOR POLYMERS

C.1 NMR SPECTRA

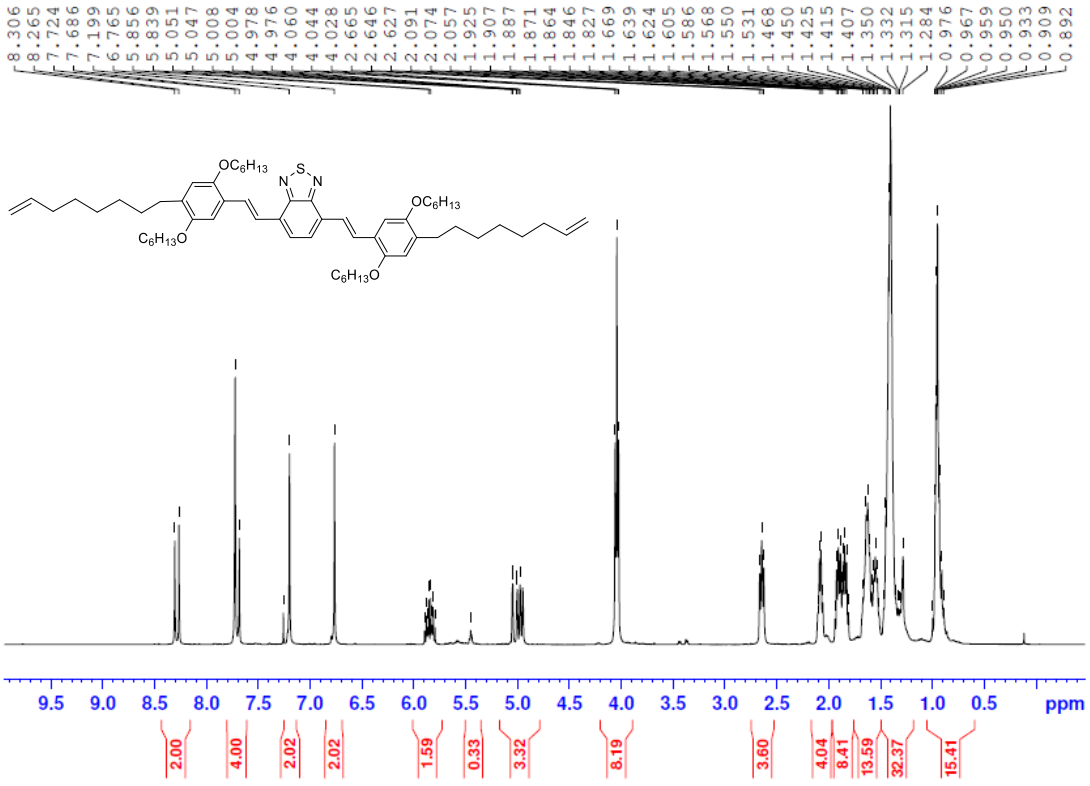

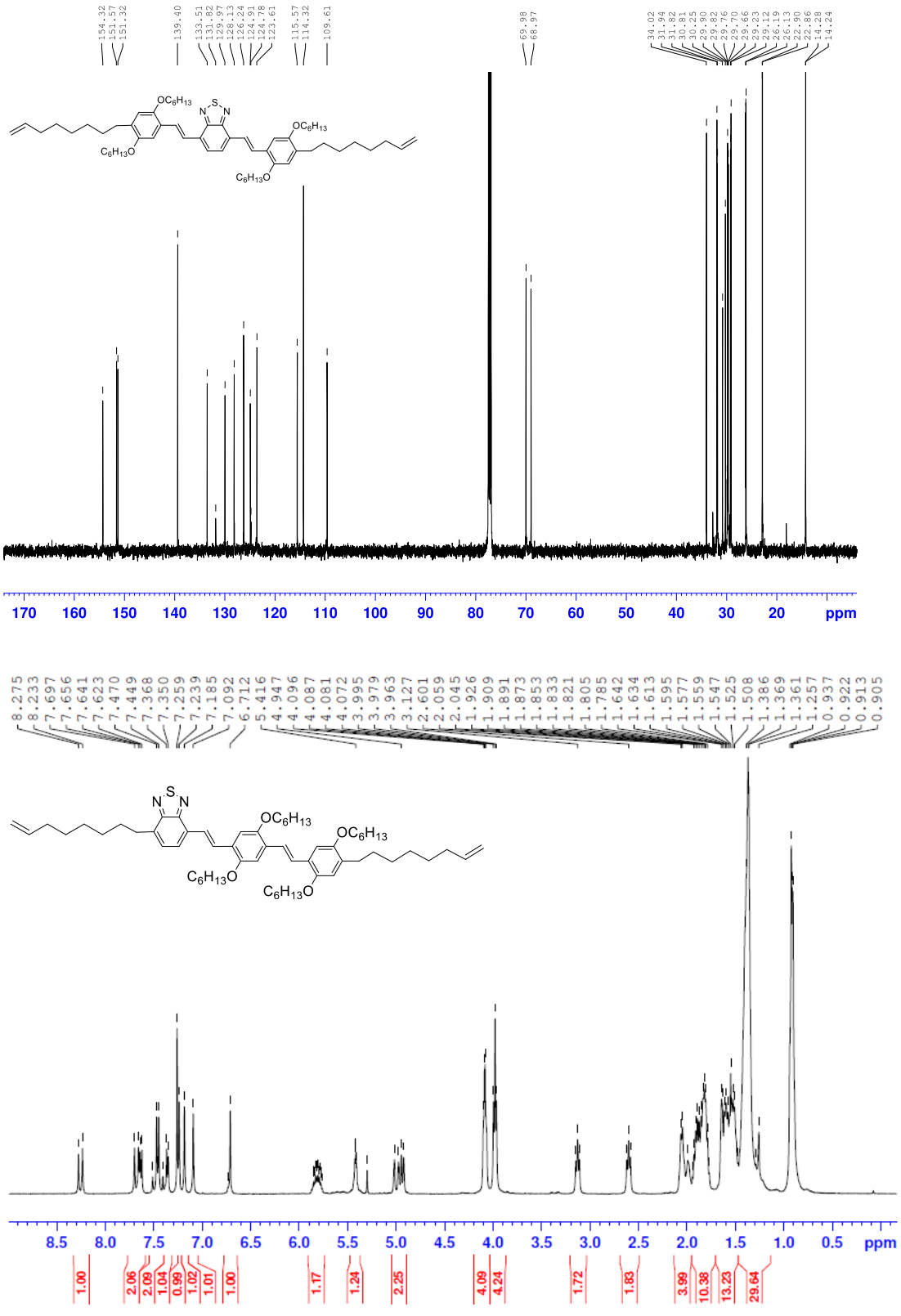
154.32
151.57
151.32
139.40
133.51
131.82
129.97
128.13
126.24
124.91
124.78
123.61
115.57
114.32
109.61
69.98
68.97
34.02
31.94
31.82
30.81
30.25
29.80
29.82
29.76
29.70
29.66
29.23
29.12
26.19
26.13
22.90
22.86
14.28
14.24
OC8H13
C6H13O
OC6H13
C6H13O
170 160 150 140 130 120 110 100 90 80 70 60 50 40 30 20 ppm
8.275
8.233
7.697
7.656
7.641
7.623
7.470
7.449
7.368
7.350
7.259
7.239
7.185
7.092
6.712
5.416
4.947
4.096
4.087
4.081
4.072
3.995
3.979
3.963
3.127
2.601
2.059
2.045
1.926
1.909
1.891
1.873
1.853
1.833
1.821
1.805
1.785
1.642
1.634
1.613
1.595
1.577
1.559
1.547
1.525
1.508
1.386
1.369
1.361
1.257
0.937
0.922
0.913
0.905
OC6H13
OC6H13
C6H13O
C6H13O
8.5 8.0 7.5 7.0 6.5 6.0 5.5 5.0 4.5 4.0 3.5 3.0 2.5 2.0 1.5 1.0 0.5 ppm
1.00
2.06
2.09
1.04
0.99
1.02
1.01
1.00
1.17
1.24
2.25
4.09
4.24
1.72
1.83
3.99
10.38
13.23
29.64

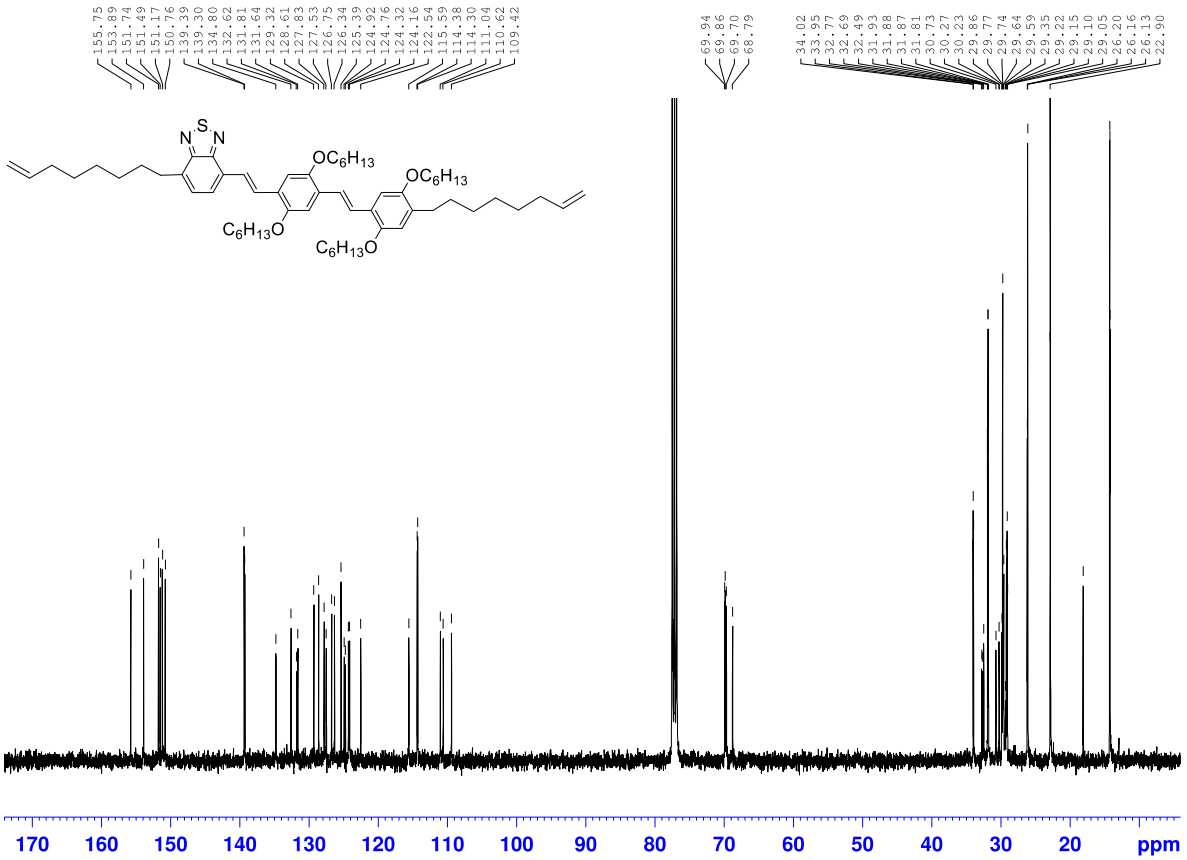
155.75
153.89
151.74
151.49
151.17
150.76
139.39
139.30
134.80
132.62
131.81
131.64
129.32
128.61
127.83
127.53
126.75
126.34
125.39
124.92
124.76
124.32
124.16
122.54
115.59
114.38
114.30
111.04
110.62
109.42
69.94
69.86
69.70
68.79
34.02
33.95
32.77
32.69
32.49
31.93
31.88
31.87
31.81
30.73
30.27
30.23
29.86
29.77
29.74
29.64
29.59
29.35
29.22
29.15
29.10
29.05
26.20
26.16
26.13
22.90
OC6H13
OC6H13
C6H13O
C6H13O
170
160
150
140
130
120
110
100
90
80
70
60
50
40
30
20
ppm

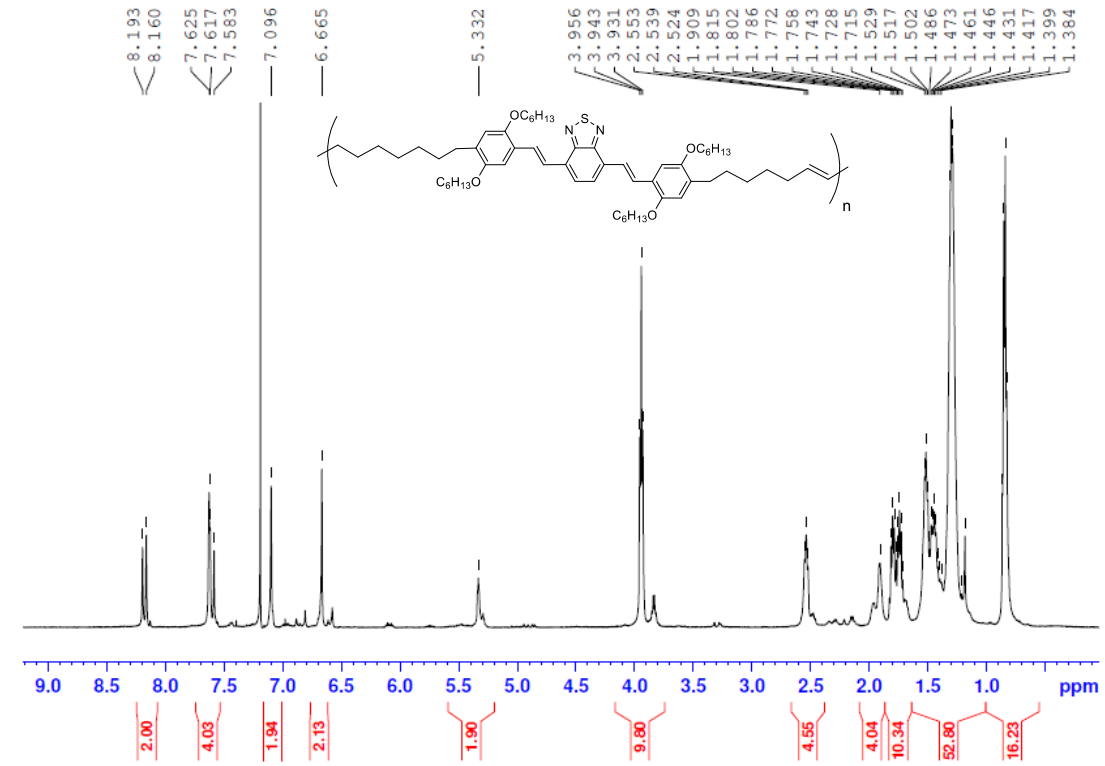
8.193
8.160
7.625
7.617
7.583
7.096
6.665
5.332
3.956
3.943
3.931
2.553
2.539
2.524
1.909
1.815
1.802
1.786
1.772
1.758
1.743
1.728
1.715
1.529
1.517
1.502
1.486
1.473
1.461
1.446
1.431
1.417
1.399
1.384
OC6H13
C6H13O
OC6H13
C6H13O
n
9.0
8.5
8.0
7.5
7.0
6.5
6.0
5.5
5.0
4.5
4.0
3.5
3.0
2.5
2.0
1.5
1.0
ppm
2.00
4.03
1.94
2.13
1.90
9.80
4.55
4.04
10.34
52.80
16.23

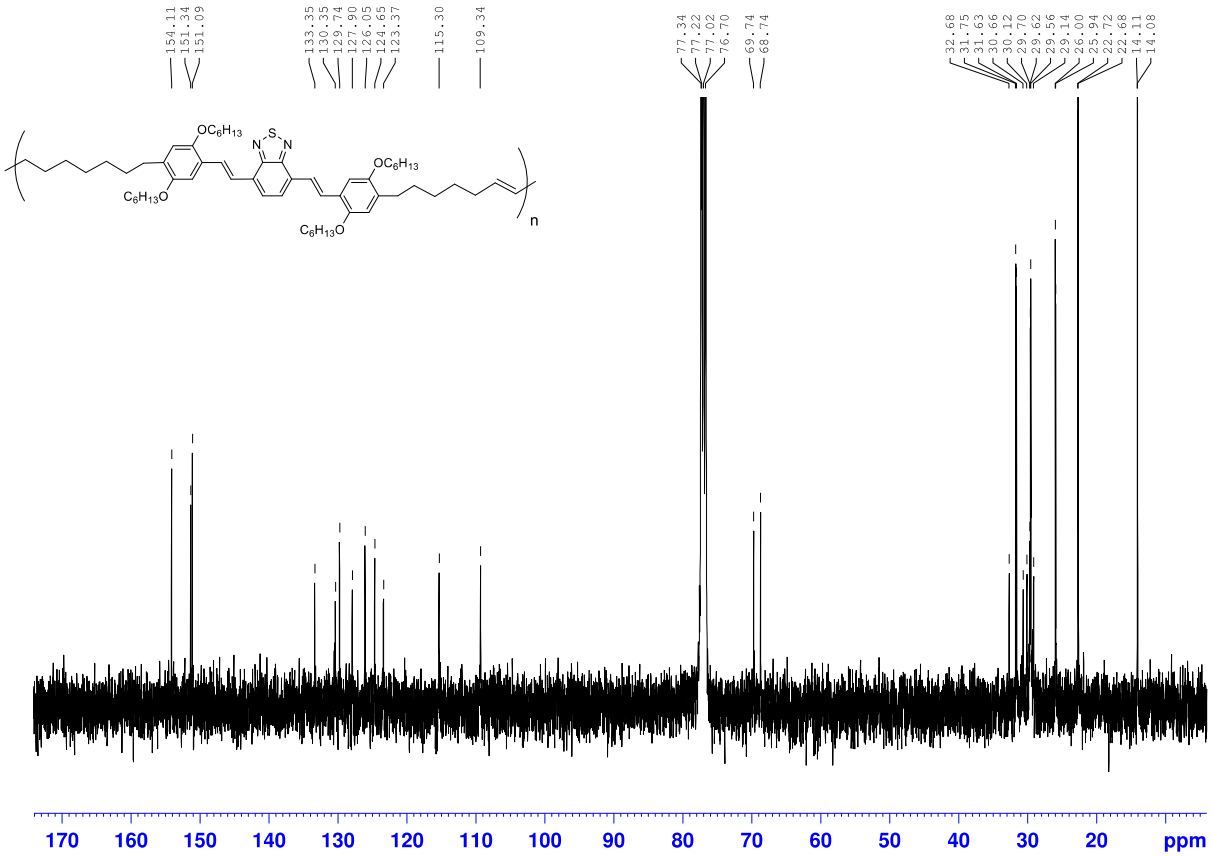
154.11
151.34
151.09
133.35
130.35
129.74
127.90
126.05
124.65
123.37
115.30
109.34
77.34
77.22
77.02
76.70
69.74
68.74
32.68
31.75
31.63
30.66
30.12
29.70
29.62
29.56
29.14
26.00
25.94
22.72
22.68
14.11
14.08
OC6H13
C6H13O
n
170
160
150
140
130
120
110
100
90
80
70
60
50
40
30
20
ppm

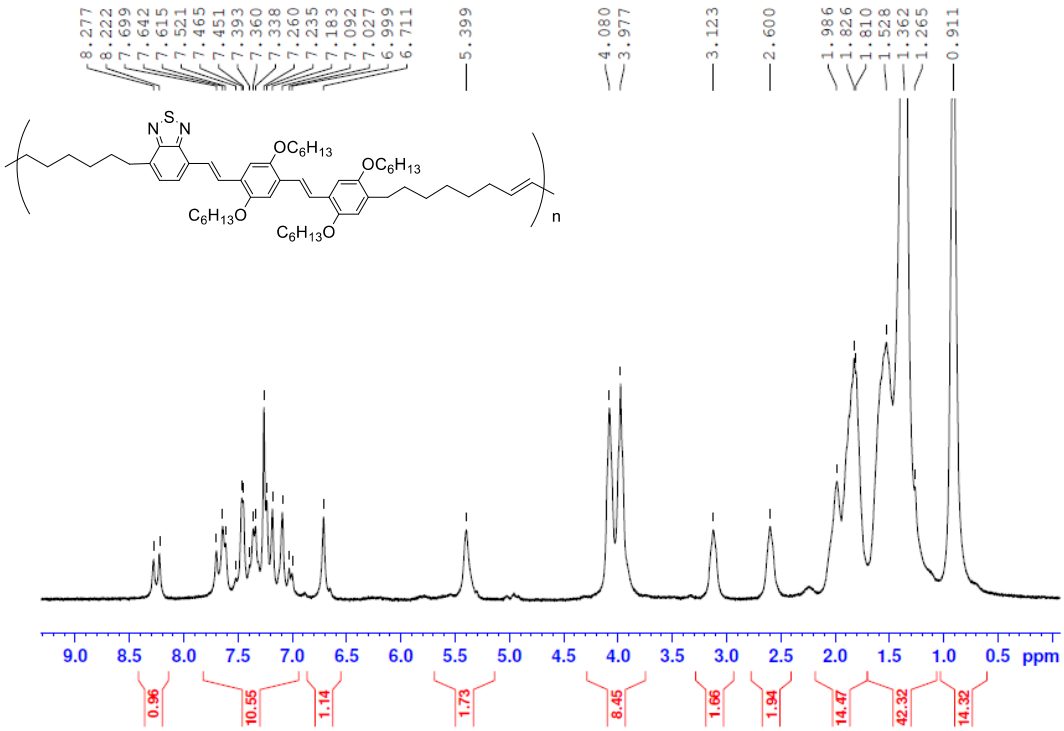
8.277
8.222
7.699
7.642
7.615
7.521
7.465
7.451
7.393
7.360
7.338
7.260
7.235
7.183
7.092
7.027
6.999
6.711
5.399
4.080
3.977
3.123
2.600
1.986
1.826
1.810
1.528
1.362
1.265
0.911
OC6H13
C6H13O
n
9.0
8.5
8.0
7.5
7.0
6.5
6.0
5.5
5.0
4.5
4.0
3.5
3.0
2.5
2.0
1.5
1.0
0.5
ppm
0.96
10.55
1.14
1.73
8.45
1.66
1.94
14.47
42.32
14.32

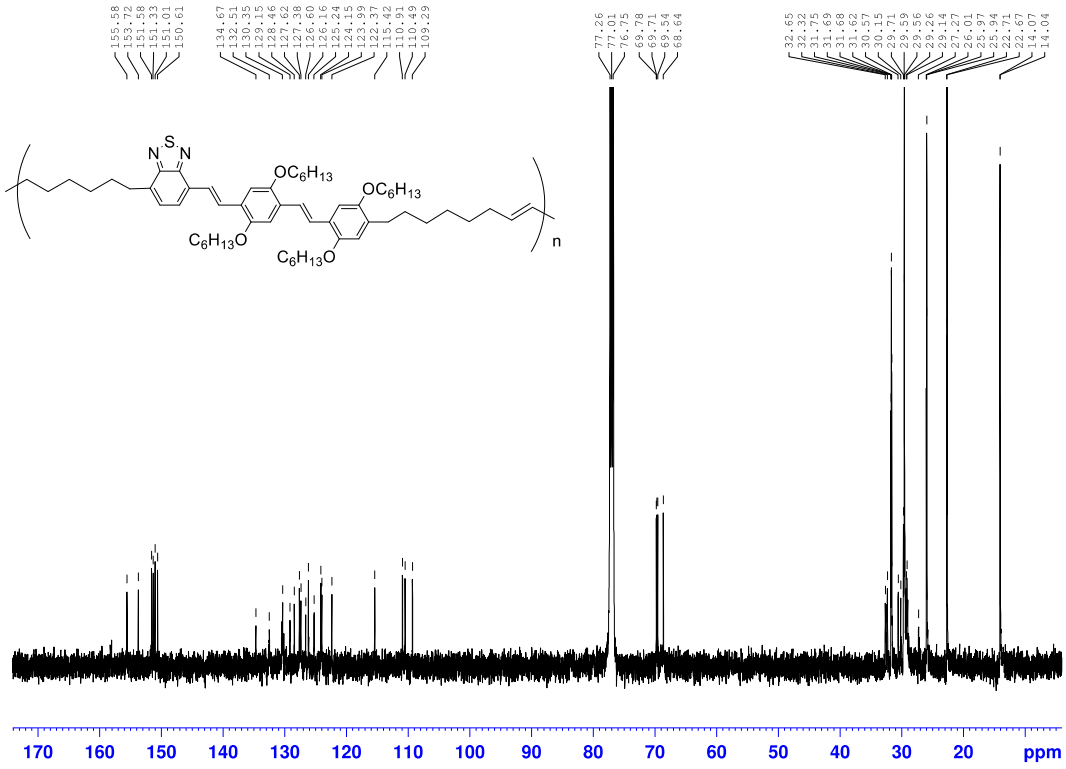
155.58
153.72
151.58
151.33
151.01
150.61
134.67
132.51
130.35
129.15
128.46
127.62
127.38
126.60
126.16
125.24
124.15
123.99
122.37
115.42
110.91
110.49
109.29
77.26
77.01
76.75
69.78
69.71
69.54
68.64
32.65
32.22
31.75
31.69
31.68
31.62
30.57
30.15
29.71
29.59
29.56
29.26
29.14
27.27
27.01
25.97
25.94
22.71
22.67
14.07
14.04
S
N
N
OC6H13
OC6H13
C6H13O
C6H13O
n
170
160
150
140
130
120
110
100
90
80
70
60
50
40
30
20
ppm

C.2 CYCLIC AND DIFFERENTIAL PULSE VOLTAMMOGRAMS

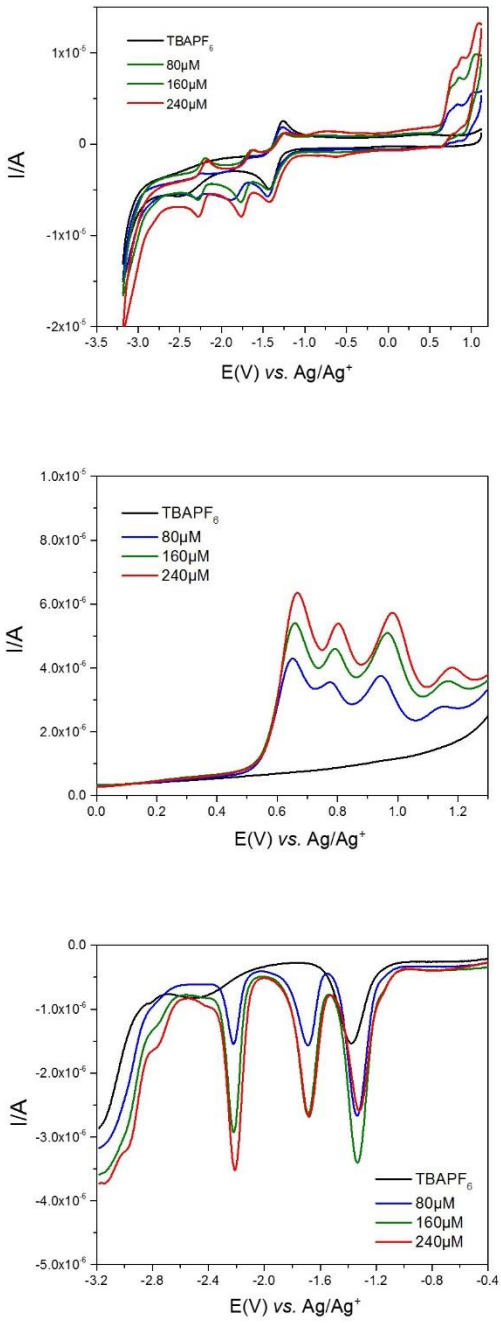

Figure 87. Top: cyclic voltammograms of **PBP** macromonomer in THF. Differential pulse voltammograms of **PBP** in THF; Middle: oxidation; Bottom: reduction.

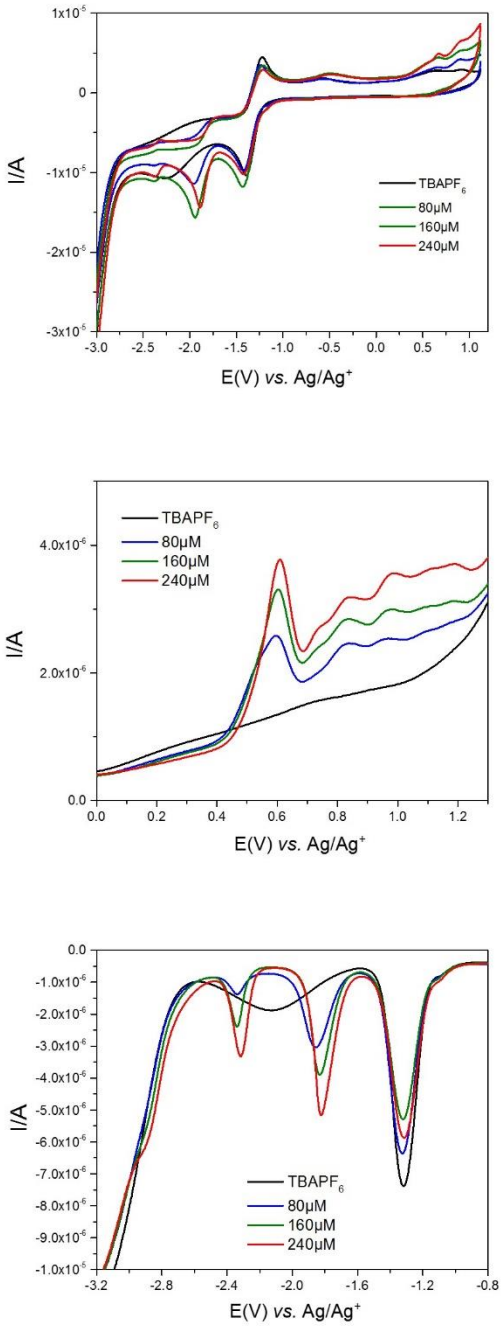

Figure 88. Top: cyclic voltammograms of **BPP** macromonomer in THF. Differential pulse voltammograms of **BPP** in THF; Middle: oxidation; Bottom: reduction.

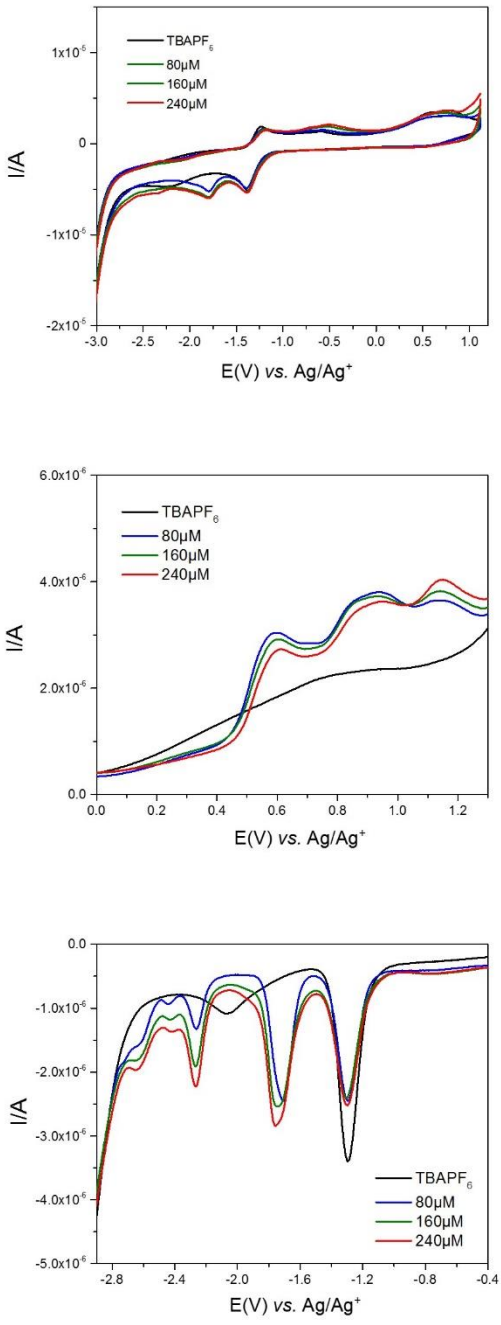

Figure 89. Top: cyclic voltammograms of **PolyBPP** in THF. Differential pulse voltammograms of **PolyPBP** in THF; Middle: oxidation; Bottom: reduction.

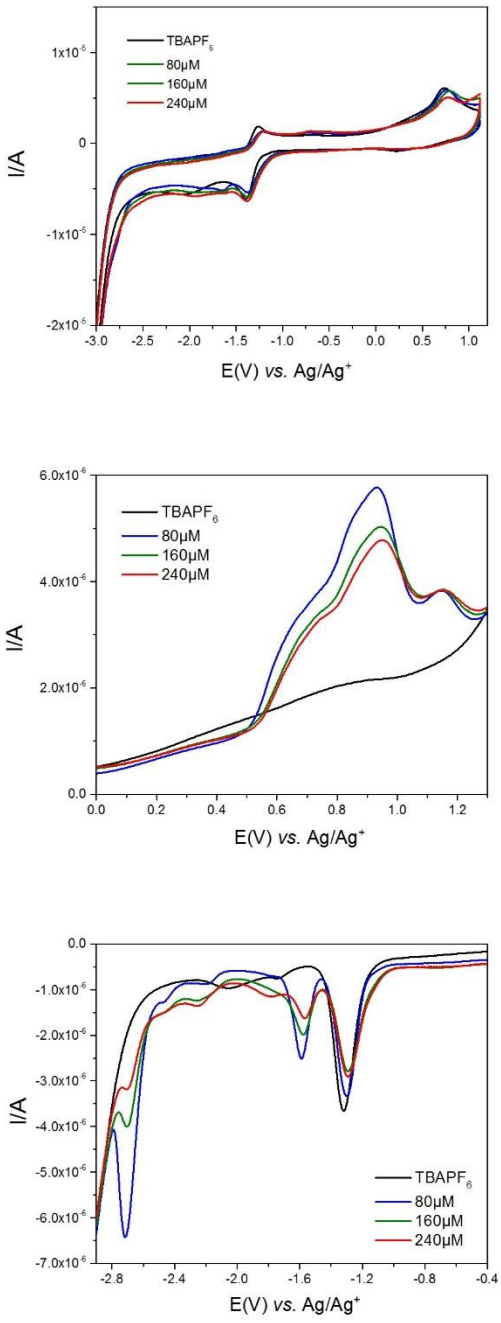

Figure 90. Top: cyclic voltammograms of **PolyPBP** in THF. Differential pulse voltammograms of **PolyPBP** in THF; Middle: oxidation; Bottom: reduction.

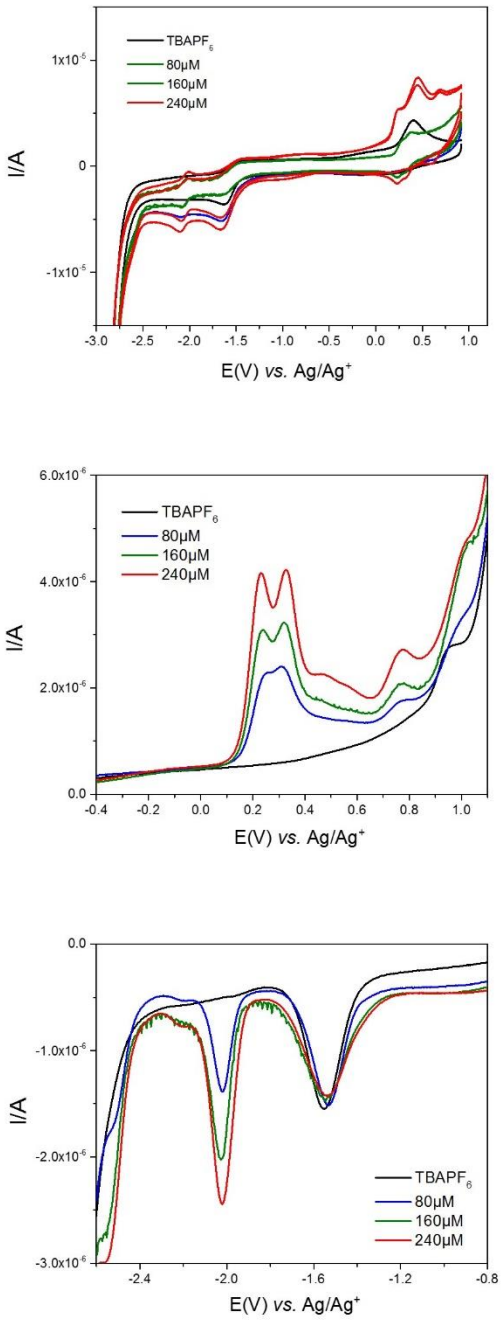

Figure 91. Top: cyclic voltammograms of **PBP** in methylene chloride. Differential pulse voltammograms of **PBP** in methylene chloride; Middle: oxidation; Bottom: reduction.

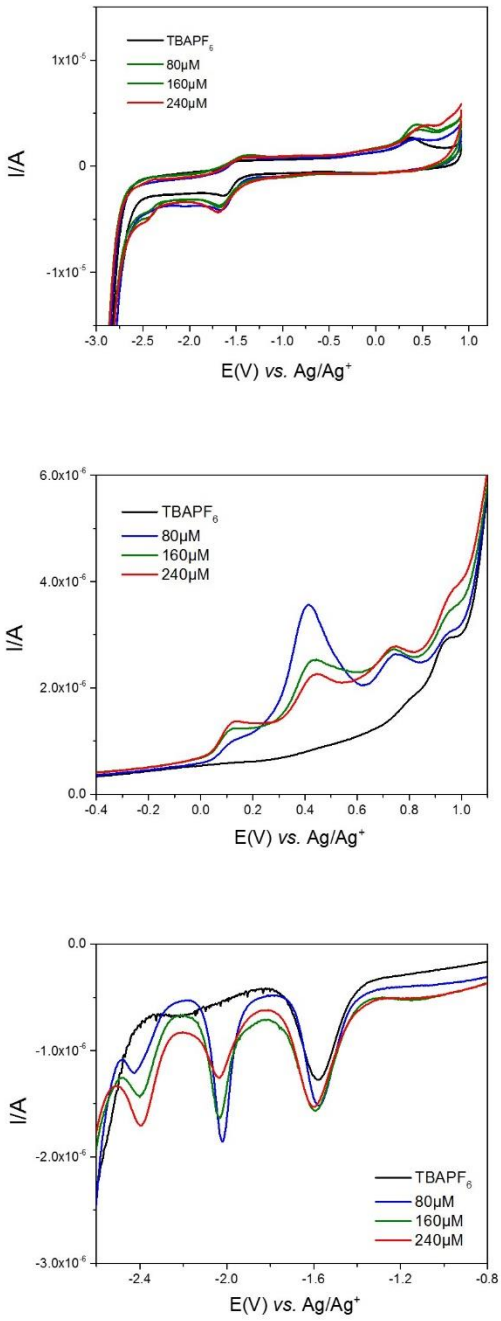

Figure 92. Top: cyclic voltammograms of **PolyPBP** in methylene chloride. Differential pulse voltammograms of **PolyPBP** in methylene chloride; Middle: oxidation; Bottom: reduction.

C.3 DIFFERENTIAL SCANNING CALORIMETRY OF MACROMONOMERS

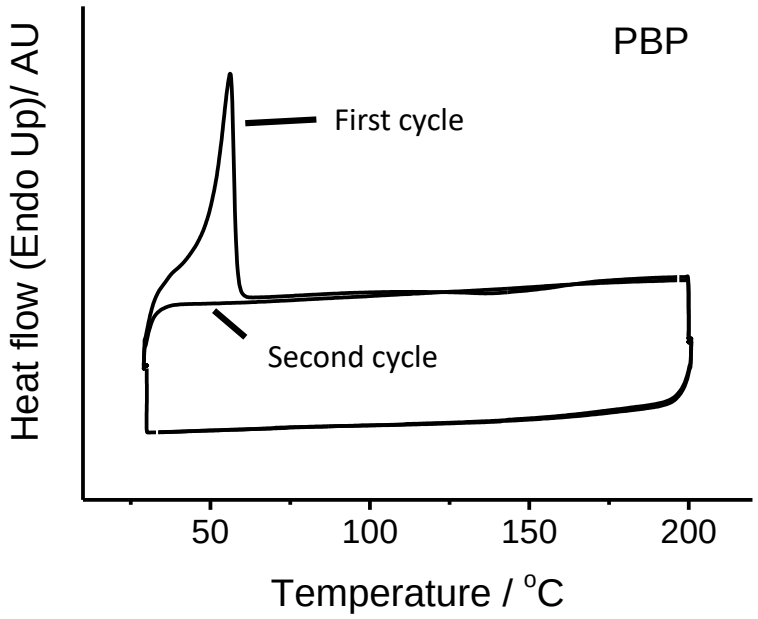

Figure 93. DSC thermograms of **PBP** macromonomer

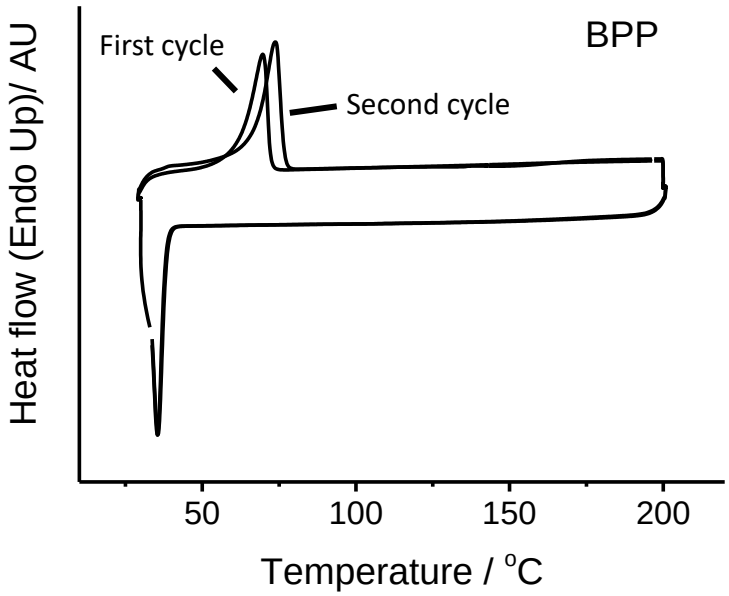

Figure 94. DSC thermograms of **BPP** macromonomer